Volume 72,2024

Neutrosophic Sets and Systems

An International Journal in Information Science and Engineering

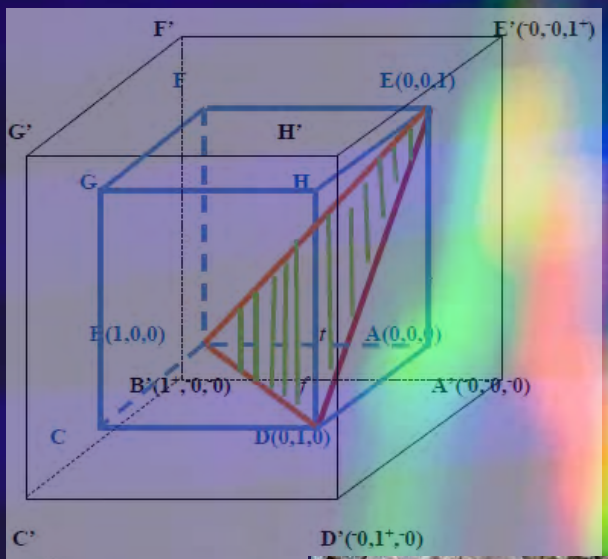

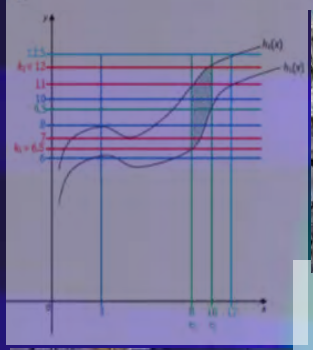

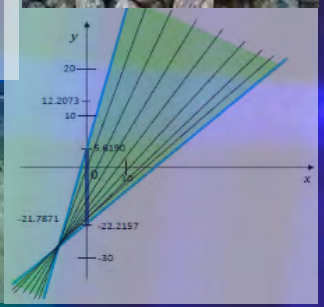

Florentin Smarandache . Mohamed Abdel-Basset . Said Broumi
Editors-in-Chief

ISSN 2331-6055 (Print)
ISSN 2331-608X (Online)

Neutrosophic Science
International Association (NSIA)

ISSN 2331-6055 (print) *ISSN 2331-608X (online)*

Neutrosophic Sets and Systems

An International Journal in Information Science and Engineering

University of New Mexico

ISSN 2331-6055 (print) ISSN 2331-608X (online)

University of New Mexico

Neutrosophic Sets and Systems

An International Journal in Information Science and Engineering

Copyright Notice

Copyright @ Neutrosophics Sets and Systems

All rights reserved. The authors of the articles do hereby grant Neutrosophic Sets and Systems non-exclusive, worldwide, royalty-free license to publish and distribute the articles in accordance with the Budapest Open Initiative: this means that electronic copying, distribution and printing of both full-size version of the journal and the individual papers published therein for non-commercial, academic or individual use can be made by any user without permission or charge. The authors of the articles published in Neutrosophic Sets and Systems retain their rights to use this journal as a whole or any part of it in any other publications and in any way they see fit. Any part of Neutrosophic Sets and Systems howsoever used in other publications must include an appropriate citation of this journal.

Information for Authors and Subscribers

*"*Neutrosophic Sets and Systems*"* has been created for publications on advanced studies in neutrosophy, neutrosophic set, neutrosophic logic, neutrosophic probability, neutrosophic statistics that started in 1995 and their applications in any field, such as the neutrosophic structures developed in algebra, geometry, topology, etc.

The submitted papers should be professional, in good English, containing a brief review of a problem and obtained results.

Neutrosophy is a new branch of philosophy that studies the origin, nature, and scope of neutralities, as well as their interactions with different ideational spectra.

This theory considers every notion or idea <A> together with its opposite or negation <antiA> and with their spectrum of neutralities <neutA> in between them (i.e. notions or ideas supporting neither <A> nor <antiA>). The <neutA> and <antiA> ideas together are referred to as <nonA>.

Neutrosophy is a generalization of Hegel's dialectics (the last one is based on <A> and <antiA> only).

According to this theory every idea <A> tends to be neutralized and balanced by <antiA> and <nonA> ideas - as a state of equilibrium.

In a classical way <A>, <neutA>, <antiA> are disjoint two by two. But, since in many cases the borders between notions are vague, imprecise, Sorites, it is possible that <A>, <neutA>, <antiA> (and <nonA> of course) have common parts two by two, or even all three of them as well.

Neutrosophic Set and *Neutrosophic Logic* are generalizations of the fuzzy set and respectively fuzzy logic (especially of intuitionistic fuzzy set and respectively intuitionistic fuzzy logic). In neutrosophic logic a proposition has a degree of truth (*T*), a degree of indeterminacy (*I*), and a degree of falsity (*F*), where *T, I, F* are standard or non-standard subsets of $]^{-}0, 1^{+}[$.

Neutrosophic Probability is a generalization of the classical probability and imprecise probability.

Neutrosophic Statistics is a generalization of the classical statistics.

What distinguishes the neutrosophics from other fields is the <neutA>, which means neither <A> nor <antiA>.

<neutA>, which of course depends on <A>, can be indeterminacy, neutrality, tie game, unknown, contradiction, ignorance, imprecision, etc.

All submissions should be designed in MS Word format using our template file:

http://fs.unm.edu/NSS/NSS-paper-template.doc.

A variety of scientific books in many languages can be downloaded freely from the Digital Library of Science:

http://fs.unm.edu/ScienceLibrary.htm.

To submit a paper, mail the file to the Editor-in-Chief. To order printed issues, contact the Editor-in-Chief. This journal is non-commercial, academic edition. It is printed from private donations.

Information about the neutrosophics you get from the UNM website:

http://fs.unm.edu/neutrosophy.htm. The

home page of the journal is accessed on

http://fs.unm.edu/NSS.

ISSN 2331-6055 (print) ISSN 2331-608X (online)

University of New Mexico

NSS

Neutrosophic Sets and Systems

An International Journal in Information Science and Engineering

**** NSS has been accepted by SCOPUS. Starting with Vol. 19, 2018, the NSS articles are indexed in Scopus.**

NSS ABSTRACTED/INDEXED IN
SCOPUS,
Google Scholar,
Google Plus,
Google Books,
EBSCO,
Cengage Thompson Gale (USA),
Cengage Learning (USA),
ProQuest (USA),
Amazon Kindle (USA),
University Grants Commission (UGC) - India,
DOAJ (Sweden),
International Society for Research Activity (ISRA),
Scientific Index Services (SIS),
Academic Research Index (ResearchBib),
Index Copernicus (European Union),
CNKI (Tongfang Knowledge Network Technology Co.,
Beijing, China),
Baidu Scholar (China),
Redalyc - Universidad Autonoma del Estado de Mexico (IberoAmerica),
Publons,
Scimago, etc.

Google Dictionaries have translated the neologisms "**neutrosophy**" (1) and"**neutrosophic**" (2), coined in 1995 for the first time, into about 100 languages.
FOLDOC Dictionary of Computing (**1, 2**), Webster
Dictionary (**1, 2**), Wordnik (**1**),Dictionary.com, The Free
Dictionary (**1**), Wiktionary (**2**), YourDictionary (**1, 2**),OneLook Dictionary (**1, 2**), Dictionary / Thesaurus (**1**), Online Medical Dictionary (**1,2**), Encyclopedia (**1, 2**), Chinese Fanyi Baidu Dictionary (**2**), Chinese Youdao Dictionary (**2**) etc. have included these scientific neologisms.

Copyright © Neutrosophic Sets and Systems, 2024

ISSN 2331-6055 (print) NSS **Editorial Board** *ISSN 2331-608X (online)*

University of New Mexico

Editors-in-Chief

Prof. Emeritus Florentin Smarandache, PhD, Postdoc, Mathematics, Physical and Natural Sciences Division, University of New Mexico, Gallup Campus, NM 87301, USA, Email: smarand@unm.edu.
Dr. Mohamed Abdel-Baset, Head of Department of Computer Science, Faculty of Computers and Informatics, Zagazig University, Egypt, Email: mohamedbasset@ieee.org.
Dr. Said Broumi, Laboratory of Information Processing, Faculty of Science Ben M'Sik, University of Hassan II, Casablanca, Morocco, Email: s.broumi@flbenmsik.ma.

Associate Editors

Assoc. Prof. Alok Dhital, Mathematics, Physical and Natural Sciences Division, University of New Mexico, Gallup Campus, NM 87301, USA, Email: adhital@unm.edu.
Dr. S. A. Edalatpanah, Department of Applied Mathematics, Ayandegan Institute of Higher Education, Tonekabon, Iran, Email: saedalatpanah@gmail.com.
Charles Ashbacker, Charles Ashbacher Technologies, Box 294, 118 Chaffee Drive, Hiawatha, IA 52233, United States, Email: cashbacher@prodigy.net.
Prof. Dr. Xiaohong Zhang, Department of Mathematics, Shaanxi University of Science &Technology, Xian 710021, China, Email: zhangxh@shmtu.edu.cn.
Prof. Dr. W. B. Vasantha Kandasamy, School of Computer Science and Engineering, VIT, Vellore 632014, India, Email: vasantha.wb@vit.ac.in.

Editors

Yanhui Guo, University of Illinois at Springfield, One University Plaza, Springfield, IL 62703, United States,Email: yguo56@uis.edu.
Giorgio Nordo, MIFT - Department of Mathematical and Computer Science, Physical Sciences and Earth Sciences, Messina University, Italy,Email: giorgio.nordo@unime.it.
Mohamed Elhoseny, American University in the Emirates,Dubai,UAE,
Email: mohamed.elhoseny@aue.ae.
Le Hoang Son, VNU Univ. of Science, Vietnam National Univ. Hanoi, Vietnam, Email: sonlh@vnu.edu.vn.
Huda E. Khalid, Head of Scientific Affairs and Cultural Relations Department, Nineveh Province, Telafer University, Iraq, Email: dr.huda-ismael@uotelafer.edu.iq.
A. A. Salama, Dean of the Higher Institute of Business and Computer Sciences, Arish, Egypt, Email: ahmed_salama_2000@sci.psu.edu.eg.
Young Bae Jun, Gyeongsang National University, South Korea, Email: skywine@gmail.com.
Yo-Ping Huang, Department of Computer Science and Information, Engineering National Taipei University, New Taipei City, Taiwan, Email: yphuang@ntut.edu.tw.
Tarek Zayed, Department of Building and Real Estate, The Hong Kong Polytechnic University, Hung Hom, 8 Kowloon, Hong Kong, China, Email: tarek.zayed@polyu.edu.hk.
Vakkas Ulucay, Kilis 7 Aralık University, Turkey, Email: vulucay27@gmail.com.
Peide Liu, Shandong University of Finance and Economics, China, Email: peide.liu@gmail.com.
Jun Ye, Ningbo University, School of Civil and Environmental Engineering, 818 Fenghua Road, Jiangbei District, Ningbo City, Zhejiang Province, People's Republic of China, Email: yejun1@nbu.edu.cn.
Memet Şahin, Department of Mathematics, Gaziantep University, Gaziantep 27310, Turkey, Email: mesahin@gantep.edu.tr.
Muhammad Aslam & Mohammed Alshumrani, King Abdulaziz Univ., Jeddah, Saudi Arabia, Emails magmuhammad@kau.edu.sa, maalshmrani @kau.edu.sa.
Mutaz Mohammad, Department of Mathematics, Zayed University, Abu Dhabi 144534, United Arab Emirates. Email: Mutaz.Mohammad@zu.ac.ae.
Abdullahi Mohamud Sharif, Department of Computer Science, University of Somalia, Makka Al-mukarrama Road, Mogadishu, Somalia, Email: abdullahi.shariif@uniso.edu.so.

Copyright © Neutrosophic Sets and Systems, 2024

Katy D. Ahmad, Islamic University of Gaza, Palestine,Email: katyon765@gmail.com.
NoohBany Muhammad, American University of Kuwait,Kuwait,Email: noohmuhammad12@gmail .com.
Soheyb Milles, Laboratory of Pure and Applied Mathematics, University of Msila, Algeria, Email: soheyb.milles@univ-msila.dz.
Pattathal Vijayakumar Arun, College of Science and Technology,Phuentsholing,Bhutan,
Email: arunpv2601@gmail.com.
Endalkachew Teshome Ayele, Department of Mathematics, Arbaminch University, Arbaminch, Ethiopia,Email: endalkachewteshome83@yahoo. com.
A. Al-Kababji, College of Engineering, Qatar University,Doha,Qatar,
Email: ayman.alkababji@ieee.org.
Xindong Peng, School of Information Science and Engineering, Shaoguan University, Shaoguan 512005, China, Email: 952518336@qq.com.
Xiao-Zhi Gao, School of Computing, University of Eastern Finland, FI-70211 Kuopio, Finland, xiao-zhi.gao@uef.fi.
Madad Khan, Comsats Institute of Information Technology,Abbottabad,Pakistan,
Email: madadmath@yahoo.com.
G. Srinivasa Rao, Department of Statistics, The University of Dodoma, Dodoma, PO. Box: 259, Tanzania,Email: gaddesrao@gmail.com.
Ibrahim El-henawy, Faculty of Computers and Informatics,ZagazigUniversity,Egypt,
Email: henawy2000@yahoo.com.
Muhammad Saeed, Department of Mathematics, University of Management and Technology, Lahore, Pakistan,
Email: muhammad.saeed@umt.edu.pk.
A. A. A. Agboola, Federal University of Agriculture, Abeokuta, Nigeria,
Email: agboolaaaa@funaab.edu.ng.
Abduallah Gamal, Faculty of Computers and Informatics, Zagazig University, Egypt,
Email: abduallahgamal@zu.edu.eg.
Ebenezer Bonyah, Department of Mathematics Education, Akenten Appiah-Menka University of Skills Training and Entrepreneurial Development, Kumasi 00233, Ghana,
Email: ebbonya@gmail.com.
Roan Thi Ngan, Hanoi University of Natural Resources and Environment, Hanoi, Vietnam,
Email: rtngan@hunre.edu.vn.
Sol David Lopezdomínguez Rivas, Universidad Nacional de Cuyo, Argentina.
Email: sol.lopezdominguez@fce.uncu.edu.ar.
Maikel Yelandi Leyva Vázquez, Universidad Regional Autónoma de los Andes (UNIANDES), Avenida Jorge Villegas, Babahoyo, Los Ríos, Ecuador,
Email: ub.c.investigacion@uniandes.edu.ec.
Arlen Martín Rabelo, Exxis, Avda. Aviadores del Chaco N° 1669 c/ San Martin, Edif. Aymac I, 4to. piso, Asunción, Paraguay,
Email: arlen.martin@exxis-group.com.
Carlos Granados, Estudiante de Doctorado en Matematicas, Universidad del Antioquia, Medellın, Colombia,
Email: carlosgranadosortiz@outlook.es.
Tula Carola Sanchez Garcia, Facultad de Educacion de la Universidad Nacional Mayor de San Marcos, Lima, Peru,
Email: tula.sanchez1@unmsm.edu.pe.
Carlos Javier Lizcano Chapeta, Profesor - Investigador de pregrado y postgrado de la Universidad de Los Andes, Mérida 5101, Venezuela, Email: lizcha_4@hotmail.com.
Noel Moreno Lemus, Procter & Gamble International Operations S.A., Panamá,
Email: nmlemus@gmail.com.
Asnioby Hernandez Lopez, Mercado Libre, Montevideo, Uruguay.
Email: asnioby.hernandez@mercadolibre.com.
Muhammad Akram, University of the Punjab, New Campus, Lahore, Pakistan,
Email: m.akram@pucit.edu.pk.
Tatiana Andrea Castillo Jaimes, Universidad de Chile, Departamento de Industria, Doctorado en Sistemas de Ingeniería, Santiago de Chile, Chile,
Email: tatiana.a.castillo@gmail.com.
Irfan Deli, Muallim Rifat Faculty of Education, Kilis 7 Aralik University, Turkey,
Email: irfandeli@kilis.edu.tr.
Ridvan Sahin, Department of Mathematics, Faculty of Science, Ataturk University, Erzurum 25240, Turkey, Email: mat.ridone@gmail.com.
Ibrahim M. Hezam, Department of computer, Faculty of Education, Ibb University, Ibb City,

Yemen, Email: ibrahizam.math@gmail.com.
Moddassir khan Nayeem, Department of Industrial and Production Engineering, American International University-Bangladesh, Bangladesh; nayeem@aiub.edu.
Aiyared Iampan, Department of Mathematics, School of Science, University of Phayao, Phayao 56000, Thailand, Email: aiyared.ia@up.ac.th.
Ameirys Betancourt-Vázquez, 1 Instituto Superior Politécnico de Tecnologias e Ciências (ISPTEC), Luanda, Angola, Email: ameirysbv@gmail.com.
H. E. Ramaroson, University of Antananarivo, Madagascar, Email: erichansise@gmail.com.
G. Srinivasa Rao, Department of Mathematics and Statistics, The University of Dodoma, Dodoma PO. Box: 259, Tanzania.
Onesfole Kuramaa, Department of Mathematics, College of Natural Sciences, Makerere University, P.O Box 7062, Kampala, Uganda, Email: onesfole.kurama@mak.ac.ug.
Karina Pérez-Teruel, Universidad Abierta para Adultos (UAPA), Santiago de los Caballeros, República Dominicana, Email: karinaperez@uapa.edu.do.
Neilys González Benítez, Centro Meteorológico Pinar del Río, Cuba, Email: neilys71@nauta.cu.
Jesus Estupinan Ricardo, Centro de Estudios para la Calidad Educativa y la Investigation Cinetifica, Toluca,Mexico,Email: jestupinan2728@gmail.com
Victor Christianto, Malang Institute of Agriculture (IPM), Malang, Indonesia, Email: victorchristianto@gmail.com.
Wadei Al-Omeri, Department of Mathematics, Al-Balqa Applied University, Salt 19117, Jordan, Email: wadeialomeri@bau.edu.jo.
Ganeshsree Selvachandran, UCSI University, Jalan Menara Gading, Kuala Lumpur, Malaysia, Email: Ganeshsree@ucsiuniversity.edu.my.
Ilanthenral Kandasamy, School of Computer Science and Engineering (SCOPE), Vellore Institute of Technology (VIT), Vellore 632014, India, Email: ilanthenral.k@vit.ac.in
Kul Hur, Wonkwang University, Iksan, Jeollabukdo, South Korea, Email: kulhur@wonkwang.ac.kr.
Kemale Veliyeva & Sadi Bayramov, Department of Algebra and Geometry, Baku State University, 23 Z. Khalilov Str., AZ1148, Baku, Azerbaijan, Email: kemale2607@mail.ru,
Email: baysadi@gmail.com.
Irma Makharadze & Tariel Khvedelidze, Ivane Javakhishvili Tbilisi State University, Faculty of Exact and Natural Sciences, Tbilisi, Georgia.
Inayatur Rehman, College of Arts and Applied Sciences, Dhofar University Salalah, Oman, Email: irehman@du.edu.om.
Mansour Lotayif, College of Administrative Sciences, Applied Science University, P.O. Box 5055, East Al-Ekir, Kingdom of Bahrain.
Riad K. Al-Hamido, Math Department, College of Science, Al-Baath University, Homs, Syria, Email: riad-hamido1983@hotmail.com.
Saeed Gul, Faculty of Economics, Kardan University, Parwan-e- Du Square, Kabil, Afghanistan, Email: s.gul@kardan.edu.af.
Faruk Karaaslan, Çankırı Karatekin University, Çankırı, Turkey, Email: fkaraaslan@karatekin.edu.tr.
Morrisson Kaunda Mutuku, School of Business, Kenyatta University, Kenya
Surapati Pramanik, Department of Mathematics, Nandalal Ghosh B T College, India, Email: drspramanik@isns.org.in.
Suriana Alias, Universiti Teknologi MARA (UiTM) Kelantan, Campus Machang, 18500 Machang, Kelantan, Malaysia, Email: suria588@kelantan.uitm.edu.my.
Arsham Borumand Saeid, Dept. of Pure Mathematics, Faculty of Mathematics and Computer, Shahid Bahonar University of Kerman, Kerman, Iran, Email: arsham@uk.ac.ir.
Ahmed Abdel-Monem, Department of Decision support, Zagazig University, Egypt, Email: aabdelmounem@zu.edu.eg.
Çağlar Karamasa, Anadolu University, Faculty of Business,
Turkey, Email: ckaramasa@anadolu.edu.tr.
Mohamed Talea, Laboratory of Information Processing, Faculty of Science Ben M'Sik, Morocco, Email: taleamohamed@yahoo.fr.
Assia Bakali, Ecole Royale Navale, Casablanca, Morocco, Email: assiabakali@yahoo.fr.
V.V. Starovoytov, The State Scientific Institution «The United Institute of Informatics Problems of the National Academy of Sciences of Belarus»,

Minsk, Belarus, Email: ValeryS@newman.bas-net.by.
E.E. Eldarova, L.N. Gumilyov Eurasian National University, Nur-Sultan, Republic of Kazakhstan, Email: Doctorphd_eldarova@mail.ru. Mukhamed iyeva Dilnoz Tulkunovna & Egamberdiev Nodir Abdunazarovich, Science and innovation center for information and communication technologies, Tashkent University of Information Technologies (named after Muhammad Al-Khwarizmi), Uzbekistan.
Mohammad Hamidi, Department of Mathematics, Payame Noor University (PNU), Tehran, Iran. Email: m.hamidi@pnu.ac.ir.
Lemnaouar Zedam, Department of Mathematics, Faculty of Mathematics and Informatics, University Mohamed Boudiaf, M'sila, Algeria, Email: l.zedam@gmail.com.
M. Al Tahan, Department of Mathematics, Lebanese International University, Bekaa, Lebanon, Email: madeline.tahan@liu.edu.lb.
Mohammad Abobala, Tishreen University, Faculty of Science, Department of Mathematics, Lattakia, Syria,Email" mohammad.abobala@tishreen.edu.sy
Rafif Alhabib, AL-Baath University, College of Science, Mathematical Statistics Department, Homs, Syria, Email: ralhabib@albaath-univ.edu.sy.
R. A. Borzooei, Department of Mathematics, Shahid Beheshti University, Tehran, Iran, borzooei@hatef.ac.ir.
Selcuk Topal, Mathematics Department, Bitlis Eren University, Turkey, Email: s.topal@beu.edu.tr.
Qin Xin, Faculty of Science and Technology, University of the Faroe Islands, Tórshavn, 100, Faroe Islands.
Sudan Jha, Pokhara University,Kathmandu, Nepal, Email: jhasudan@hotmail.com.
Mimosette Makem and Alain Tiedeu, Signal, Image and Systems Laboratory, Dept. of Medical and Biomedical Engineering, Higher Technical Teachers' Training College of EBOLOWA, PO Box 886, University of Yaoundé, Cameroon, E-mail: alain_tiedeu@yahoo.fr.
Mujahid Abbas, Department of Mathematics and Applied Mathematics, University of Pretoria Hatfield 002, Pretoria, South Africa, Email: mujahid.abbas@up.ac.za.
Željko Stević, Faculty of Transport and Traffic Engineering Doboj, University of East Sarajevo, Lukavica, East Sarajevo, Bosnia and Herzegovina, Email: zeljko.stevic@sf.ues.rs.ba.
Michael Gr. Voskoglou, Mathematical Sciences School of Technological Applications, Graduate Technological Educational Institute of Western Greece, Patras, Greece, Email: voskoglou@teiwest.gr.
Saeid Jafari, College of Vestsjaelland South, Slagelse, Denmark, Email: sj@vucklar.dk.
Angelo de Oliveira, Ciencia da Computacao, Universidade Federal de Rondonia, Porto Velho - Rondonia, Brazil, Email: angelo@unir.br.
Valeri Kroumov, Okayama University of Science, Okayama, Japan, Email: val@ee.ous.ac.jp.
Rafael Rojas, Universidad Industrial de Santander, Bucaramanga, Colombia, Email: rafael2188797@correo.uis.edu.co.
Walid Abdelfattah, Faculty of Law, Economics and Management, Jendouba, Tunisia, Email: abdelfattah.walid@yahoo.com.
Akbar Rezaei, Department of Mathematics, Payame Noor University, P.O.Box 19395-3697, Tehran, Iran, Email: rezaei@pnu.ac.ir.
John Frederick D. Tapia, Chemical Engineering Department, De La Salle University - Manila, 2401 Taft Avenue, Malate, Manila, Philippines, Email: john.frederick.tapia@dlsu.edu.ph.
Darren Chong, independent researcher, Singapore, Email: darrenchong2001@yahoo.com.sg.
Galina Ilieva, Paisii Hilendarski, University of Plovdiv, 4000 Plovdiv, Bulgaria, Email: galili@uni-plovdiv.bg.
Paweł Pławiak, Institute of Teleinformatics, Cracow University of Technology, Warszawska 24 st., F-5, 31-155 Krakow, Poland, Email: plawiak@pk.edu.pl.
E. K. Zavadskas, Vilnius Gediminas Technical University, Vilnius, Lithuania, Email: edmundas.zavadskas@vgtu.lt.
Darjan Karabasevic, University Business Academy, Novi Sad, Serbia, Email: darjan.karabasevic@mef.edu.rs.
Dragisa Stanujkic, Technical Faculty in Bor, University of Belgrade, Bor, Serbia, Email: dstanujkic@tfbor.bg.ac.rs.
Katarina Rogulj, Faculty of Civil Engineering,

Architecture and Geodesy, University of Split, Matice Hrvatske 15, 21000 Split, Croatia; Email: katarina.rogulj@gradst.hr.
Luige Vladareanu, Romanian Academy, Bucharest, Romania, Email: luigiv@arexim.ro.
Hashem Bordbar, Center for Information Technologies and Applied Mathematics, University of Nova Gorica, Slovenia, Email: Hashem.Bordbar@ung.si.
N. Smidova, Technical University of Kosice, SK 88902, Slovakia, Email: nsmidova@yahoo.com.
Quang-Thinh Bui, Faculty of Electrical Engineering and Computer Science, VŠB-Technical University of Ostrava, Ostrava-Poruba, Czech Republic, Email: qthinhbui@gmail.com.
Mihaela Colhon & Stefan Vladutescu, University of Craiova, Computer Science Department, Craiova, Romania,Emails: colhon.mihaela@ucv.ro, vladutescu.stefan@ucv.ro.
Philippe Schweizer, Independent Researcher, Av. de Lonay 11, 1110 Morges, Switzerland, Email: flippe2@gmail.com.
Madjid Tavanab, Business Information Systems Department, Faculty of Business Administration and Economics University of Paderborn, D-33098 Paderborn, Germany, Email: tavana@lasalle.edu.
Rasmus Rempling, Chalmers University of Technology, Civil and Environmental Engineering, Structural Engineering, Gothenburg, Sweden.
Fernando A. F. Ferreira, ISCTE Business School, BRU-IUL, University Institute of Lisbon, Avenida das Forças Armadas, 1649-026 Lisbon, Portugal, Email: fernando.alberto.ferreira@iscte-iul.pt.
Julio J. Valdés, National Research Council Canada, M-50, 1200 Montreal Road, Ottawa, Ontario K1A 0R6, Canada, Email: julio.valdes@nrc-cnrc.gc.ca.
Tieta Putri, College of Engineering Department of Computer Science and Software Engineering, University of Canterbury, Christchurch, New Zeeland.
Phillip Smith, School of Earth and Environmental Sciences, University of Queensland, Brisbane, Australia, phillip.smith@uq.edu.au.
Sergey Gorbachev, National Research Tomsk State University, 634050 Tomsk, Russia, Email: gsv@mail.tsu.ru.
Sabin Tabirca, School of Computer Science, University College Cork, Cork, Ireland, Email: tabirca@neptune.ucc.ie.
Umit Cali, Norwegian University of Science and Technology, NO-7491 Trondheim, Norway, Email: umit.cali@ntnu.no.
Willem K. M. Brauers, Faculty of Applied Economics, University of Antwerp, Antwerp, Belgium, Email: willem.brauers@uantwerpen.be.
M. Ganster, Graz University of Technology, Graz, Austria, Email: ganster@weyl.math.tu-graz.ac.at.
Ignacio J. Navarro, Department of Construction Engineering, Universitat Politècnica de València, 46022 València, Spain, Email: ignamar1@cam.upv.es.
Francisco Chiclana, School of Computer Science and Informatics, De Montfort University, The Gateway, Leicester, LE1 9BH, United Kingdom, Email: chiclana@dmu.ac.uk.
Jean Dezert, ONERA, Chemin de la Huniere, 91120 Palaiseau, France, Email: jean.dezert@onera.fr.

.

Copyright © Neutrosophic Sets and Systems, 2024

ISSN 2331-6055 (print) NSS ISSN 2331-608X (online)
University of New Mexico

Contents

Mona Mohamed, Alaa Elmor and Florentin Smarandache, Ahmed A. Metwaly, An Efficient SuperHyperSoft Framework for Evaluating LLMs-based Secure Blockchain Platforms……..…….1-21
Yaser Ahmad Alhasan, Suliman Sheen, Qusay Ahassan, and Raja Abdullah Abdulfatah, The 2-refined neutrosophic fraction function and its integrals…….22-40
S. Bhuvaneshwari, C. Antony Crispin Sweety, Akanksha Singh, Said Broumi, Mohamed Talea, Prasanta Kumar Raut, A Novel and an Efficient CODAS Technique to Solve Real-Life MAGDM Problems in Fermatean Neutrosophic Environment…….41-59
A. A. Salama, Huda E. Khalid, Ahmed G. Mabrouk, The Cubic Bipolar Neutrosophic Sets theory and Uncertainty Management in Environmental Data Analysis…….60-133
Ramazan Yasar, and Ahmed Hatip, The Structure of The Binary Two Fold Algebra Based On Intuitionistic Fuzzy Groups……..…….134-141
Yaser Ahmad Alhasan, Florentin Smarandache, Abuobida Alfahal and Raja Abdullah Abdulfatah, The extended study of 2-refined neutrosophic numbers……...142-153
Ahmed Z.M. Elsherif, A. A. Salama, O. M. Khaled, Mostafa Herajy, E. I. Elsedimy, Huda E. Khalid, Ahmed K. Essa, Unveiling Big Data Insights: A Neutrosophic Classification Approach for Enhanced Prediction with Machine Learning……154-172
Aysegul Caksu Guler, Introduction to neutrosophic soft ideal topological spaces…….173-185
M. Kaviyarasu, Hossein Rashmanlou, Saeed Kosari, Said Broumi, R. Venitha, M. Rajeshwari and Farshid Mofidnakhaei, Circular Economy Strategies to Promote Sustainable Development using t-Neutrosophic Fuzzy graph……186-210
Kianoosh Polvan, On Extension of Metricspace to Neutro Hypermetricspace……...211-221
A. A. Salama, Huda E. Khalid, Ahmed G. Mabrouk, Unveiling Uncertainty: Neutrosophic Set-Based Algorithms for Robust Decision-Making…….222-243
Florentin Smarandache, The Principles of (Partial Locality, Partial Indeterminacy, Partial NonLocality) and (Multi Locality, Multi Indeterminacy, Multi NonLocality)……..…….244-255
S. krishna Prabha, Said Broumi, Souhail Dhouib, Mohamed Talea, Implementation of Circle-Breaking Algorithm on Fermatean Neutrosophic Graph to discover Shortest Path……..256-271
R.Narmada Devi and Yamini Parthibanm, Exploring Neutrosophic Over Supra Exterior Modal Topological Structure: Theory and Application in Healthcare Decision-Making……272-285
Debapriya Mondal, Totan Garai, Gopal Chandra Roy, and Shariful Alam, Evaluating the nuclear power plant safety system under neutrosophic environment……...286-303
Madeleine Al Tahan, Saba Al-Kaseasbeh, and Bijan Davvaz, Neutrosophic Quadruple Hv-modules and their fundamental module……...304-325
Nouran Ajabnoor, Evaluation of Distributed Leadership in Education Using Neutrosophic HyperSoft Set…….326-340
Siti Nur Idara Rosli and Mohammad Izat Emir Zulkifly, Deneutrosophication of Neutrosophic Bézier Surface Approximation Model…….341-356
G. Vetrivel, M. Mullai and G. Rajchakit, Product Operations on Pythagorean Co-Neutrosophic Graphs and its Application……..……357-380
A. Mohammed shapique and E. Mathivadhana, Modified Non-Linear Triangular Neutrosophic Numbers: Theory and Applications in Integral Equation……..381-407
Sangeeta K Siri, S Pramod Kumar, Mrityunjaya V. Latte, A Novel Medical Image Segmentation Using Neutrosophic Sets with Slope Variation……...408-430
Fuad S. Al-Duais, Neutrosophic Log-Gamma Distribution and its Applications to Industrial Growth….431-445
Mohamed G. Mahdi, Ahmed Sleem, Ibrahim M. Elhenawy, and Soha Safwat, Hybrid Neutrosophic Deep Learning Model for Enhanced Arabic Handwriting Recognition……446-465

Copyright © Neutrosophic Sets and Systems, 2024

NSS
Neutrosophic Sets and Systems, Vol. 72, 2024
University of New Mexico

An Efficient SuperHyperSoft Framework for Evaluating LLMs-based Secure Blockchain Platforms

Mona Mohamed [1], Alaa Elmor [2] and Florentin Smarandache[3], Ahmed A. Metwaly[4]
[1]Higher Technological Institute, 10th of Ramadan City 44629, Egypt
Email: Mona.fouad@hti.edu.eg;
[2,4]Zagazig University, 44519 Zagazig, Egypt
Email: alaaelmor@zu.edu.eg; a.metwaly23@fci.zu.edu.eg
[3]University of New Mexico, 705 Gurley Ave., Gallup, NM 87301, USA
Email: smarand@unm.edu.

* Correspondence: Mona.fouad@hti.edu.eg;

Abstract: In the age of modern technology, the use of the internet has become imperative. However, this widespread access presents a double-edged sword and opens doors for hackers and scammers to exploit vulnerabilities and engage in illegal activities. Accordingly, scholars and stakeholders are attempting to solve this matter. Large Language Models (LLMs) have provided highly effective methodologies and solutions in various cybersecurity sectors. Hence, we exhibited the efficacy of LLMs in several information and communication technologies (ICT) such as the Internet of Things (IoT), cloud computing, blockchain technology (BCT)…etc which are attacked and threatened. Accordingly, the objective of our study is to illustrate how LLMs are supporting ICT, especially BC to be secure against attacks. Another study's objective is to aid the stakeholders and enterprises that seek resilience and sustainability by recommending the most secure BC platform to adopt in critical sectors. Wherein, LLMs support BC in many directions as developing secure smart contracts and scanning the smart contract to protect it from any subversive acts by identifying anomalous activities. Hence, we suggested a soft opting model to rank the alternatives of BC platforms and recommend optimal BC. Also, the process of constructing this model requires leveraging several techniques. We applied for the first time SuperHyperSoft (SHS) as an extension of Hypersoft to treat various attributes and sub-attributes for BC based on LLMs. Multi-criteria decision-making (MCDM)techniques are utilized for their ability to treat conflicting sub-attributes. Hence, entropy and multi-objective optimization based on simple ratio analysis (MOOSRA) are utilized as techniques of MCDM. These techniques are working under the authority of the Single Value Neutrosophic (SVN) technique to support MCDM techniques in ambiguous situations.

Keywords: Large Language Models (LLMs); SuperHyperSoft; Blockchain; Cybersecurity; Multi-Criteria Decision Making (MCDM); Single Value Neutrosophic (SVN)

1. Introduction

The desire for sustainability and development on a global scale is seen as the driving force behind change and the growing rate of technological advancement. Indeed, in the recent interval, a new phenomenon dubbed Industry 4.0 [1] and eventually, Industry 5.0 has evolved.

These digital transformations permit devices and humans to communicate by utilizing smart devices as sensors in the Industrial Internet of Things (IIoT)[2] to collect data and process it through big data analytical (BDA) and store it in blockchain technology (BCT). Despite the importance of the technologies of Industry 4.0 in transferring and exchanging data, it is vulnerable to attacks. Accordingly, [3] indicated that the usage of cutting-edge technologies has expanded over the past several decades, leading to a significant increase in cyber-attacks and threats. This issue affects all stakeholders who utilize IoT systems, either directly or indirectly. Malicious assaults may cause enormous financial difficulties and incalculable losses, including data corruption, system breakdowns, privacy breaches, reputational damage, lost customers, dependability, and market share, especially for large enterprises. Wherein [4] claimed that only 16% of experts believe that their business is well-prepared to handle cybersecurity threats, even though 75% see cybersecurity as a priority.

Hence, [5] stated that it becomes imperative to have sophisticated and efficient detecting techniques. Similarly[6], as cyber threats evolve, the cybersecurity field can also benefit from state-of-the-art tools. These tools can support cybersecurity practitioners who are always looking for ways to apply new regulations or fortify technological defenses against the leakage of private data, illegal access, and other types of data abuse. According to the perspective of [7], it is imperative to develop proactiv5[5[5e technology for cyber defense. Wherein the defense is represented in harnessing various cutting-edge technologies such as Machine Learning (ML) techniques [5] and deep learning (DL) techniques [8] which are capable of automatically identifying, thwarting, also responding to various cyberattacks[9]. As well the new developments in transformers and large language models (LLMs)[10], which have demonstrated remarkable capabilities in natural language understanding, generation, and reasoning, have made significant strides in several security tasks, including threat detection, automated vulnerability analysis, intelligent defense mechanisms [11]. LLMs have a number of advantages, from customization and transparency to cutting-edge performance. LLMs are classified into open-source models like Llama [12] and Mixtral [13] or closed-source models like ChatGPT and Gemini[14]. They do, however, all have their limitations. Code-based LLMs, such as CodeLlama [15] and StarCoder [16, 17], are especially useful for tasks including automated code review, secure code development, and bug discovery. Their use in threat intelligence, binary analysis, IT operations, vulnerability detection, program repair, and anomaly detection highlights their revolutionary influence on cybersecurity.

1.1 Journey of Language Models Toward Large Language Models: Provenance

Contemporary techniques of artificial intelligence and machines have amalgamated to learn how to comprehend and communicate through human language [18] where a term of language modeling (LM) is the consequence of this amalgamation. This term has appeared in many

studies as [19] LM predominantly strives to forecast the probability of future or omitted tokens by modeling the generative probability of word sequences. As well [20] described the language model's evolution phases. The first phase formed in **statistical language models (SLMs)** [21]this model was initially introduced in the 1990s, and as it was constructed using the Markov assumption, its goal was to anticipate the next word based on the most recent context. The other side of it is bigram and trigram language models [19] where SLMs with a predetermined context length n that's why it's called n-gram language models. Generally, this is not a sufficient model, but newer versions have appeared due to some problems that this model suffered from. Worthwhile[22], neural networks (NNs) serve to predict the probability distribution of the following word in a sequence given the words that came before it as manner in phase two of **Neural Language Models (NLMs).** Wherein, the models of NLs are employed in this phase as multi-layer perceptron (MLP), Recurrent neural networks (RNNs), and (LSTM) [23]to provide a cohesive, comprehensive solution for different NLP. Phase three entails building what are known as **pre-trained language models (PLMs)** [24], which are contextualized word embeddings that seek to capture the meaning and context of words in a phrase or text. Nonetheless, several investigations have [25] examined the performance limitations PLMs encounter when training progressively broader PLMs. Thereby, Generative Pre-Trained Transformer -3 (GPT-3) and Generative Pre-Trained Transformer -4 (GPT-4) were developed to address the deficiencies in phase three. Due to[26], these models can be refined for certain downstream tasks, such as question answering or language translation, after being trained on vast volumes of text data. Accordingly, such models belong to **transformer language models [19]**, in another formula LLMs are considered motivators for phase four. Due to its ability to comprehend natural language and complete challenging tasks.

1.2 Motivations and incentives of study

Each phase finds a way to address the faults of the one before it, based on the discussion from the preceding subsection. In the final phase of LMs, GPT-3 as the model belongs to LLMs can solve a series of complex tasks that GPT-2 can't solve[27]. One of PLM's drawbacks[28], is it cannot generalize to unseen activities without task-specific training, although LLMs can do so without the need for task-specific training. As a result, LLMs serve as the study's focal point and foundation; further motivations will be covered.

A. **First incentive:** we conducted bibliometric analysis for various LMs. This analysis has been conducted on the Web of Science (WoS) database for various published studies from 2020 until 2024. Hence, we conducted a set of queries. Wherein these queries entailed the various techniques for different phases of LMs that were utilized in published studies.

B. These queries were conducted as in Fig 1

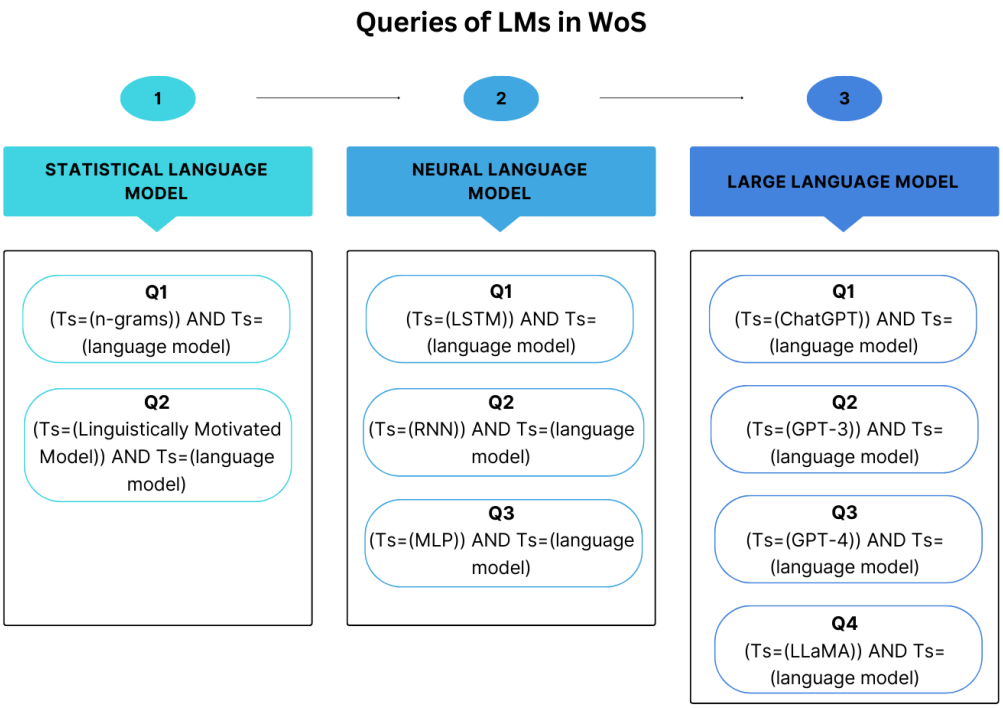

Fig 1. Methodologies of Techniques of Language Models Queries

The findings of conducted queries are illustrated in Fig 2 which comprises the queries' conclusions. This Fig indicated that the techniques of LLMs are constantly increasing over the years. In confirmation of this, in 2024 these techniques achieved the highest use in publishing studies compared to the other models of LMs.

A. Second incentive: business environment and its chain, other domains such as healthcare, transportation, education…etc. are transforming their traditional strategies, planning, and operations into digital. In this light, [29] demonstrated that the urgency for effective security precautions has increased as individuals and enterprises depend on digital technology for essential infrastructure, interactions, and business. Thereby [30] stated that it is challenging for security practitioners to successfully identify, locate, and protect against them due to the magnitude and diversity of cyber threats. To address these issues, [31] suggested LLMs and [5] confirmed that LLMs help to swiftly find relevant threat intelligence, allowing consultants to decide on actions. Accordingly, [32]discussed various roles and contributions of LLMs in cybersecurity. Also [33] suggested Bidirectional Encoder Representations from Transformers (BERT) as an intrusion detection model and BERT outperforms other ML techniques in attack detection on a reputable dataset.

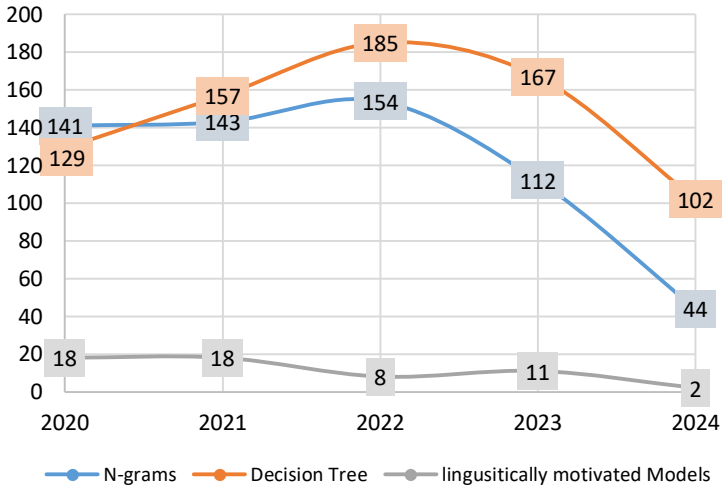

(a) Techniques of Statistical Language Models

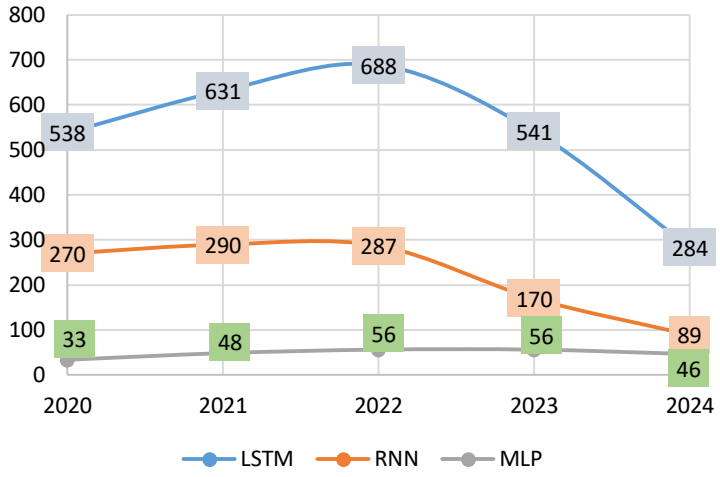

(b) Techniques of Neural Language Model

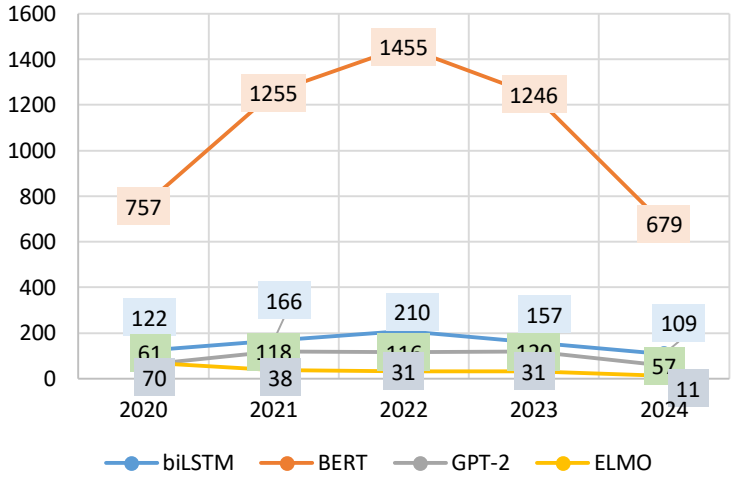

(c) Techniques of Pretrained Language Model

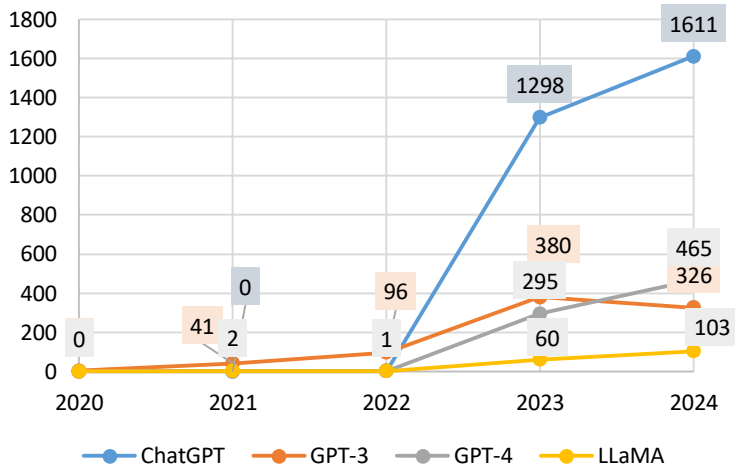

(d) Techniques of Large Language Model

Fig 2. Queries' Findings for Language Models since 2020-2024

1.3 Scientific Contributions and Novelty:

This study attempts to solve the issue of cybersecurity by covering certain aspects as the following:

Theoretically: we conducted surveys in previous studies that related to our scope. We are trying to discuss and determine the main issues of security that threaten the enterprises economically and personally. Accordingly, we are studying the extent to which methods can solve this matter. The findings of our study are deployed in the next aspect (i.e. scientifically).

Scientifically: the findings of surveys are discussed by exhibiting the importance of generative artificial intelligence (AI)-LLMs for securing ICT technologies, especially BC. Also, evaluating the BC that adopting the models of LL is vital. Therefore, we proposed a soft opting model to evaluate these BC.

Practically: we applied the constructed model for two objectives. The first objective is aiding decision makers (DMs) and stakeholders at a loss to choose the secure BC by recommending secure BC based on LLMs. The second objective is to validate the accuracy of our model.

2. Empowering ICT technologies in the realm of LLMs

This section exhibits the role of LLMs in ICT technologies as security tools in various forms.

2.1 Cloud Computing Paradigm and IoT

Many scholars as[34, 35] described cloud computing (CC) as the multi-service paradigm for storing and retrieving data, computational capacity, and applications, such as internet-based on-demand services. CC has been harnessed successfully in several contexts Given that it offers a wide range of services such as control and management through various methodologies such as Infrastructure as a Service (IaaS), Platform as a Service (PaaS), and Software as a Service (SaaS).

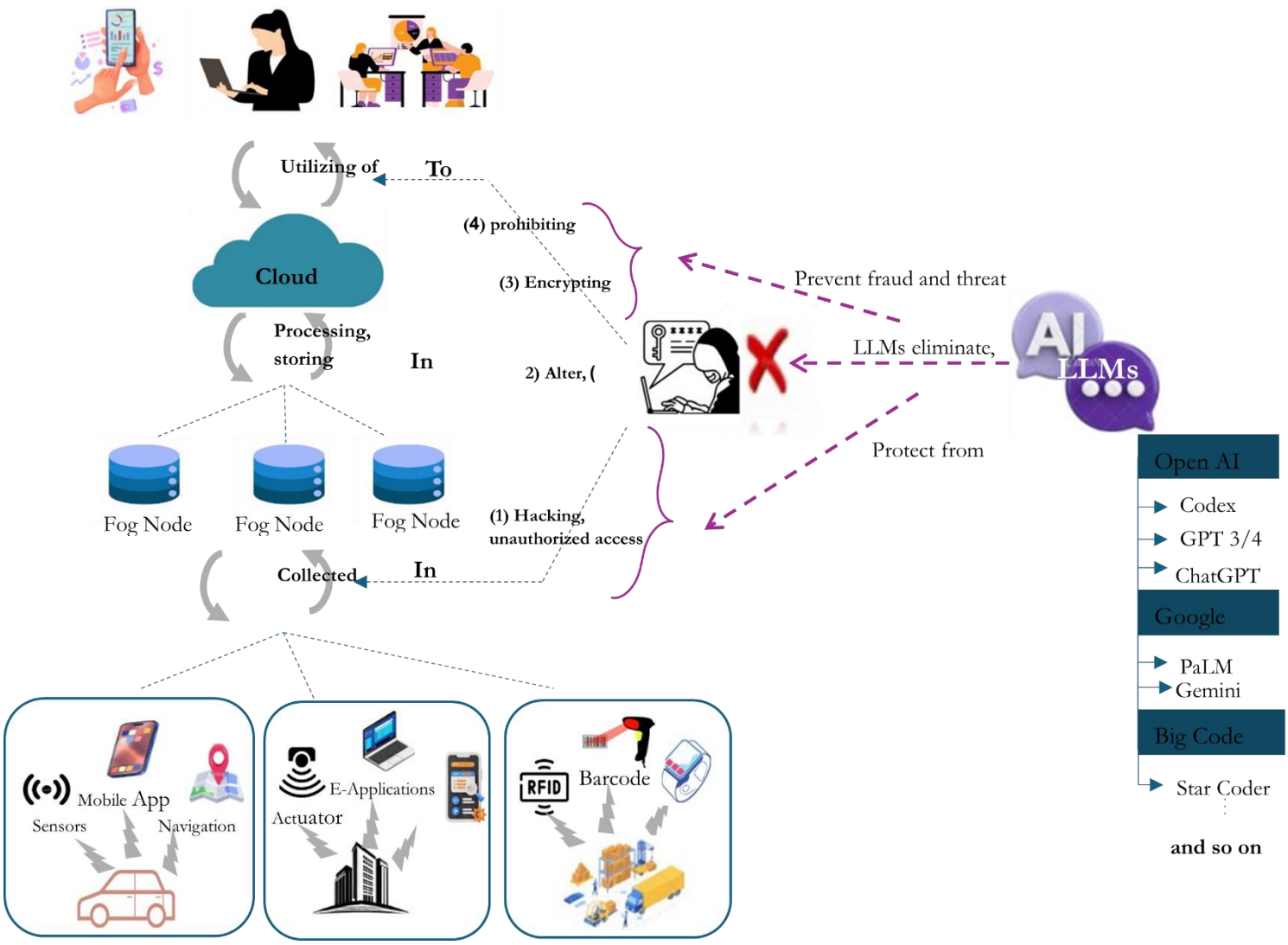

Fig 3. Role of Large Language Model in Securing Cloud-IoT against Threat

This paradigm integrated with other Contemporary technologies such as machine learning (ML) [36]to enhance the privacy, trust, and security of the cloud paradigm. But Cao et al., [37]had an alternative viewpoint and demonstrated that ML techniques are restricted to vulnerability analysis and categorization. Accordingly, the authors in [37] proposed LLMs as solvers for vulnerabilities of ML for securing the cloud. In the same vein [38] harnessed the CC paradigm in the internet of Vehicles (IoV) to store and process data collected from smart equipment as sensors in the Cloud paradigm and vice versa for retrieving data from the cloud. Wherein, LLMs play an important role as cybersecurity tools to countermeasure any threats and through [39] LLMs preserve resilience by facing hostile assaults, illegal access attempts, and data leaks. Fig 3 exhibits the role of LLMs which is discussed in [11] in securing data collected from IoT equipment and preventing hackers and spoofers from intrusion of information through unauthorized access. Also, LLMs are protecting information from encrypting, losing, and fraudulent vital information.

2.2 Blockchain Technology

Latterly, BCT is growing in popularity as a technology for promoting different domains[40]. As well, [41] indicated that Financial institutions brought in BCT to bolster their cybersecurity and investments. Distributed ledger (DL) technology allows BC to store transactions immutably. As stated by [42], BC security is an elaborate process that aims to protect the availability, integrity, and confidentiality of data processed and stored inside a blockchain network. Nevertheless, [43]admitted that the integrity and responsibilities of BC are in danger from several security flaws and threats. These threats formed in various forms as in [44] (see Fig 4) that exhibit vulnerabilities that jeopardize BC security.

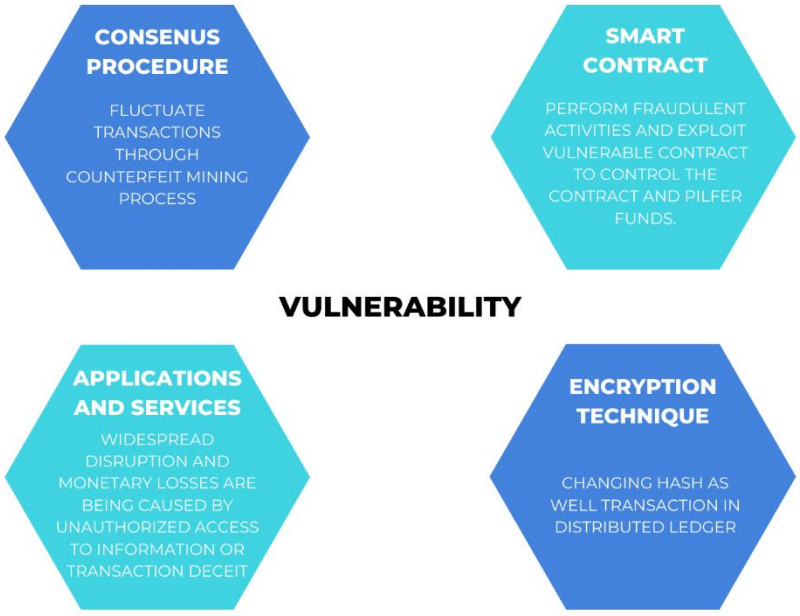

Fig 4. Blockchain Vulnerabilities

To eliminate and avoid the issues of vulnerability that jeopardize BC security, LLMs such as GPTScan [45], and AuditGPT [46] are introduced as auditors in smart contracts to detect and recognize vulnerabilities. As well, LLMs were introduced as detectors for unusual transactions and deceitful actions via leveraging BLOCKGPT[47].

3. Methodology

According to the influential role of LLMs as protectors against threats and risks, the evaluation of their roles in contemporary technology to be a secure technology is an important process. Accordingly, choosing the most secure technology amongst the set of alternatives to other technologies to serve the enterprises' objectives is crucial. This process requires prioritizing between the alternatives based on a set of conflicting criteria. Hence, MCDM techniques have been harnessed in this process due to their ability to treat such problems [48]. Yet experts may run into the issue of being unable to cope with uncertainties when using MCDM techniques, which prevents experts from being able to make an appropriate decision. To avert this issue, the SuperHyperSoft (SHs) technique is integrated with SVNSs to support experts when using MCDM techniques during the evaluation process amongst alternatives. Another impulse for this integration is to serve the study's objectives by constructing a soft opting model. These objectives entailed selecting and recommending the most secure BC platform that deploys LLMs as ChatGPT for developing smart contracts. The accuracy and security of smart contracts, which implement agreements without the need for middlemen, are crucial in BC.
Overall, the procedures of recommending a secure BC platform based on a soft opting model are conducted through the following subsections.
laying forth the assessment process's aspects

3.1 Laying forth the assessment process's main aspects

1. The alternatives of BC platforms are determined to be nominated in the evaluation process.
2. The main attributes and sub-attributes are determined to evaluate BC platforms based on them.
3. The expert panel is forming to contribute to the evaluation process for BC platforms based on attributes and sub-attributes.

3.2 Generative of attributes and sub-attributes weights: SVNSs-Entropy

The objective of this procedure is to generate weights for BC platforms' attributes and sub-attributes. Hence, the entropy of MCDM techniques is combined with SVNSs to generate weights. The generated weights are harassing in the next procedure of alternatives ranking. We implement a series of phases to accomplish the objective.

4. Transforming the utilized linguistic terms of DMs into Neutrosophic values based on the SVN scale which is mentioned in [49]. Thereby, Neutrosophic decision matrices are constructed based on the rating of DMs.
5. The score function in Eq.(1) is embraced for converting the constructed matrices into crisp matrices.

$$\boldsymbol{s}(\sigma_{ij}) = \frac{(2+ \alpha - \beta - \theta)}{3} \quad (1)$$

Where α, β, θ refer to truth, false, and indeterminacy respectively.

6. Aggregate the crisp matrices into a compiled matrix based on Eq.(2).

$$\wp_{ij} = \frac{(\sum_{j=1}^{N} \sigma_{ij})}{Z} \quad (2)$$

Where σ_{ij} refers to the value of the criterion in the matrix, and Z refers to the number of decision-makers.

7. Eq.(3) is utilized in the compiled matrix to normalize it to construct a normalized matrix.

$$\mathbb{N}or_{ij} = \frac{\wp_{ij}}{\sum_{j=1}^{m} \wp_{ij}} \quad (3)$$

Where $\sum_{j=1}^{m} \wp_{ij}$ indicates the sum of each criterion in the compiled matrix per column.

8. Eq.s(4),(5) are contributed to compute entropy.

$$En_{j=-h\sum_{i=1}^{m} \mathbb{N}or_{ij}} \ln \mathbb{N}or_{ij} \quad (4)$$

where,

$$h = \frac{1}{\ln(N)} \quad (5)$$

N refers to utilized alternatives

9. Finally, the weights of attributes are generated by employing Eq. (6)

$$\omega_j = \frac{1 - En_j}{\sum_{j=1}^{n}(1 - En_j)} \quad (6)$$

3.3 Recommending the most secure BC platform: SuperHyperSoft and SVNSs-MOOSRA

Herein, three techniques are integrated to rank BC platforms. Each technique plays a vital role in solving the problem of selection. SHS is utilized to determine and employ a power set of attributes to obtain the most secure and appropriate BC platform. While SVNSs are harnessed for supporting MOOSRA in uncertain environments and ambiguity of information during the ranking process.

3.3.1 SuperHyperSoft (SHS)

SHs introduced by Smarandache [50] this technique is considered an extension of HyperSoft and consists of several HyperSoft Sets. SHS was utilized in this study as the methodology for representing the determined attributes and sub-attributes for selecting the secure BC platform based on the selected attributes and sub-attributes.

- Suppose the universe set $\mathfrak{R}$= { BC_1, BC_2,… BC_n} which was determined in the previous procedure. Moreover, P ($\mathfrak{R}$) is the powerset of $\mathfrak{R}$. As well, A_1, A_2, A_3 are utilized attributes where BC platforms have been evaluated over these attributes. Hence, P(A_1), P(A_2), and P(A_3) are powersets of A_1, A_2, A_3.
- Let F: P(A_1) × P(A_2) × P(A_3) → P($\mathfrak{R}$), where × indicates to Cartesian product. Hence, this is called SHs over $\mathfrak{R}$.
- In this study Cartesian product for attributes and sub−attributes formed as

$$\mathrm{P}(\mathrm{A}_1)\times\mathrm{P}(\mathrm{A}_2)\times\mathrm{P}(\mathrm{A}_3)=\Big\{\big\{\{\mathrm{A}_{11}\},\{\mathrm{A}_{12}\},\{\mathrm{A}_{11},\mathrm{A}_{12}\}\big\}\times$$
$$\big\{\{\mathrm{A}_{21}\},\{\mathrm{A}_{22}\},\{\mathrm{A}_{21},\mathrm{A}_{22}\},\big\}\times$$
$$\big\{\{\mathrm{A}_{31}\},\{\mathrm{A}_{32}\},\{\mathrm{A}_{33}\},\{\mathrm{A}_{31},\mathrm{A}_{32}\},\{\mathrm{A}_{31},\mathrm{A}_{33}\},\{\mathrm{A}_{32},\mathrm{A}_{33}\},\{\mathrm{A}_{31},\mathrm{A}_{32},\mathrm{A}_{33}\}\big\}\Big\}.$$

  - According to Eq. (7), $\mathrm{P}(\mathrm{A}_1)\times\mathrm{P}(\mathrm{A}_2)\times\mathrm{P}(\mathrm{A}_3)=$

$$\left\{\begin{array}{c}\widetilde{s_1}\ (A_{11},A_{21},A_{31});\widetilde{s_2}\ (A_{11},A_{21},A_{32});\widetilde{s_3}\ (A_{11},A_{21},A_{33});\\ \widetilde{s_4}\ (A_{11},A_{21},\{A_{31},A_{32}\});\widetilde{s_5}\ (A_{11},A_{21},\{A_{31},A_{33}\});\widetilde{s_6}\ (A_{11},A_{21},\{A_{32},A_{33}\});\\ \widetilde{s_7}\ (A_{11},A_{21},\{A_{31},A_{32},A_{33}\});\widetilde{s_8}\ (A_{11},A_{22},A_{31});\dots\widetilde{s_{14}}\ (A_{11},A_{22},\{A_{31},A_{32},A_{33}\});\\ \widetilde{s_{15}}\ (A_{11},\{A_{21},A_{22}\},A_{31});\dots\widetilde{s_{21}}\ (A_{11},\{A_{21},A_{22}\},\{A_{31},A_{32},A_{33}\});\widetilde{s_{22}}\ (A_{12},A_{21},A_{31});\cdots\\ \widetilde{s_{28}}\ (A_{12},A_{21},\{A_{31},A_{32},A_{33}\});\widetilde{s_{29}}\ (A_{12},A_{22},A_{31});\cdots\widetilde{s_{35}}\ (A_{12},A_{22},\{A_{31},A_{32},A_{33}\});\\ \widetilde{s_{36}}\ (A_{12},\{A_{21},A_{22}\},A_{31});\ \cdots\widetilde{s_{42}}\ (A_{12},\{A_{21},A_{22}\},\{A_{31},A_{32},A_{33}\});\widetilde{s_{43}}\ (\{A_{11},A_{12}\},A_{21},A_{31});\cdots\\ \widetilde{s_{49}}\ (\{A_{11},A_{12}\},A_{21},\{A_{31},A_{32},A_{33}\});\widetilde{s_{50}}\ (\{A_{11},A_{12}\},A_{22},A_{31});\cdots\widetilde{s_{56}}\ (\{A_{11},A_{12}\},A_{22},\{A_{31},A_{32},A_{33}\});\\ \widetilde{s_{57}}\ (\{A_{11},A_{12}\},\{A_{21},A_{22}\},A_{31});\cdots\widetilde{s_{63}}\ (\{A_{11},A_{12}\},\{A_{21},A_{22}\},\{A_{31},A_{32},A_{33}\}).\end{array}\right\}$$

(7)

3.3.2 SVNSs-MOOSRA

Multi-objective optimization based on simple ratio analysis (MOOSRA)[51] is implemented under the authority of SVNSs based on SHS for ranking BC platforms that adopt ChatGPT-LLMs for developing secured smart contracts. After that recommend the most secure BC platform which implements the secured smart contract. Overall, the ranking procedures have been conducted as follows:

10. Constructing Neutrosophic decision matrices for each DM to evaluate BC platforms based on sub-attributes determined by SHS.
11. Transforming Neutrosophic decision matrices into de-neutrosophic decision matrices through using Eq.(1).
12. Eq.(2) is utilized for the second time to aggregate these matrices into an aggregated matrix.
13. Normalizing the aggregated matrix based on Eq.(8).

$$\mathrm{Nor}_{ij} = \frac{\wp_{ij}}{\left[\sum_{j}^{m} \wp_{ij}\right]^{1/2}} \quad (8)$$

14. Compute a weighted decision matrix based on Eq.(9).

$$\mathrm{weighted-matrix}_{ij=}\mathrm{Nor}_{ij} * \omega_j \quad (9)$$

15. Calculating ratio as in Eq.(10) to obtain final rank for alternatives.

$$\mathrm{Ratio} = \frac{\sum_{j=1}^{B} \mathrm{Nor}_{ij}}{\sum_{j=1}^{NB} \mathrm{Nor}_{ij}} \quad (10)$$

4. Implementation of the constructed soft opting model: Case-study

Herein we implemented our constructed soft opting model in realistic to validate the efficacy of the constructed model.

4.1 Problem Description

We exhibit the problem that our constructed model is supposed to be applied through the following scenario.

Scenario 1
One of the most significant technologies being utilized right now across a variety of sectors in BC, particularly in sectors with a long history and significant consumer data. This is because of the utilization of robust encryption techniques such as hash. Yet, because of the extensive usage of the Internet and its applications, hackers may now easily forge hash mining to alter and steal data, as well as smart contracts that expose the money and data of consumers to jeopardy. Hence, the business sectors exploit generative AI capabilities as LLMs to bolster the efficiency of BC as ChatGPT, PaLM…etc. these models of LLM support enterprises to be proactive and become resilient. Therefore, any business aiming for sustainability and resilience must

implement the strongest BC practices involving LLMs. Accordingly, businesses may face the problem of applying the strongest and most secure BC platform. We exhibit the problem of four enterprises that need to make accurate decisions for selecting the most secured BC platform based on LLMs amongst five alternatives of BC platforms.

Action: the businesses should follow the methodology for selecting the optimal and most secured BC which deploys the robust security models based on LLM. Herein, this methodology entails implementing the constructed soft opting model to aid stakeholders in deciding the optimal decision with various propositions toward securing businesses based on robust BC.

4.2 Toward Most Secure BC platform-based LLMs: Procedures

Herein, the process of recommending optimal BC has been conducted into two subsections for generating attributes' weights. These weights are used in another subsection to recommend optimal BC platforms.

4.1.1 Generating attributes' weights

Entropy based on SVNSs is implemented to serve the target of this subsection.

1. Three Neutrosophic decision matrices are constructed based on members of the panel to evaluate five BC platforms based on four attributes (see Fig 4). These matrices are transformed into de-neutrosophic matrices based on Eq.(1).
2. These matrices aggregated into the single matrix is an aggregated matrix as listed in Table 1 based on Eq.(2).
3. Table 2 exhibits the normalized matrix which is calculated based on Eq.(3).
4. Eq.(4) is implemented to compute entropy.
5. The final attributes' weights are obtained in Fig5 through executing Eq.(6) which indicates that A2 has the highest weight otherwise, A1 has the lowest value.

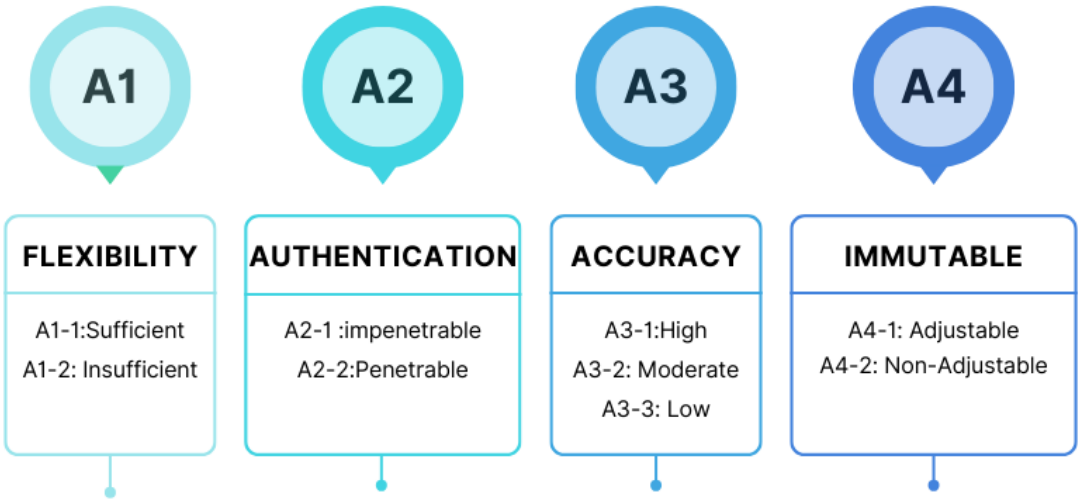

Fig 4. Attributes and Sub-attributes of BC based on LLMs

Table 1. Aggregated decision matrix

	A1	A2	A3	A4
BC1	0.604444444	0.5722222	0.42666667	0.672222222
BC2	0.816666667	0.5777778	0.71666667	0.9
BC3	0.538888889	0.38	0.5	0.537777778
BC4	0.705555556	0.8055556	0.65	0.816666667
BC5	0.644444444	0.7111111	0.81666667	0.838888889

Table 2. Normalized matrix

	A1	A2	A3	A4
BC1	0.182611615	0.18781911	0.137191854	0.178518737
BC2	0.24672709	0.189642597	0.230439443	0.239008557
BC3	0.162806311	0.124726477	0.160771704	0.14281499
BC4	0.213158778	0.264405543	0.209003215	0.216878135
BC5	0.194696207	0.233406273	0.262593783	0.222779581

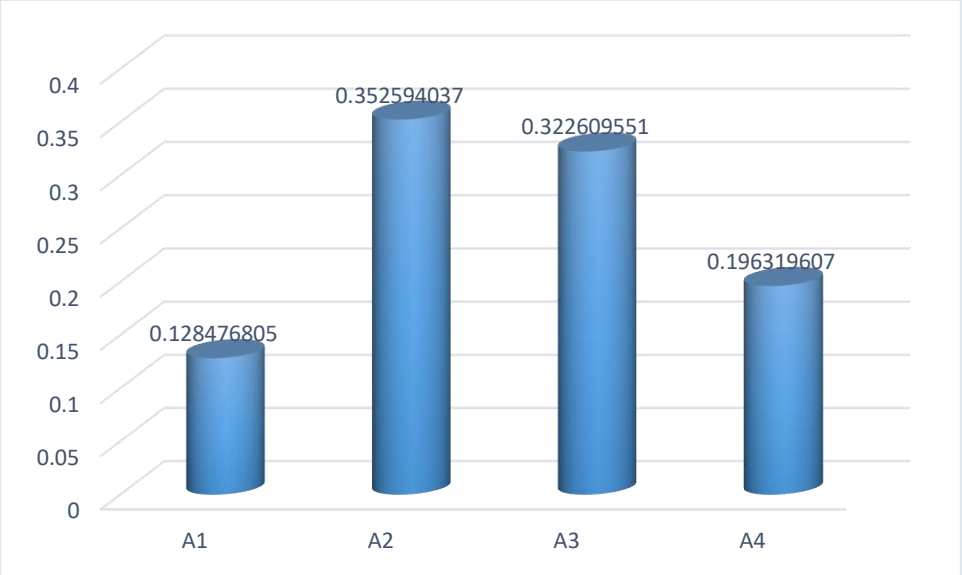

Fig 5. Attributes weights

4.2.2 Ranking BC Platforms

Based on the methodology of SHS we can suppose a set of propositions for sub-attributes to rank BC based on LLMs :

- let F({Sufficient, Non-sufficient}, {Impenetrable, Penetrable},{Low},{Non-Adjustable}).
- According to Eq.(7), there are four propositions for sub-attributes. in other words, there are four hypersofts:

proposition 1: Sufficient, Impenetrable, Low, Non-Adjustable.
proposition 2: Sufficient, Penetrable, Low, Non-Adjustable
proposition 3: Non-sufficient, Impenetrable, Low, Non-Adjustable
proposition 4: Non-sufficient, Penetrable, Low, Non-Adjustable

After that, we can implement SVNSs-MOOSRA to rank BC platforms and obtain the most secure BC.

According to Proposition 1:

- Three neutrosophic decision matrices are constructed for evaluating BC platforms based on sub-attributes according to the proposition.
- deneutrosophic these matrices based on Eq.(1).
- Aggregated these matrices into an aggregated matrix based on Eq.(2) as in Table 3.
- Table 4 represents the normalized matrix according to Eq.(8).
- Table 5 for the weighted normalized matrix is generated based on Eq.(9).

The final ranking for BC platforms is exhibited in Fig 6 which indicates that BC4 is the most secure platform.

Table 3. Aggregated matrix

	A11	A21	A31	A42
BC1	0.644444	0.56	0.353333	0.605556
BC2	0.498889	0.76	0.386667	0.777778
BC3	0.42	0.498889	0.538889	0.666667
BC4	0.598889	0.877778	0.732222	0.458889
BC5	0.565556	0.665556	0.632222	0.671111

Table 4. Normalized matrix.

	A11	A21	A31	A41
BC1	0.522865	0.365028	0.288437	0.420175
BC2	0.40477	0.495395	0.315648	0.539675
BC3	0.340764	0.325194	0.439911	0.462578
BC4	0.485904	0.572167	0.597735	0.318408
BC5	0.458859	0.433833	0.516102	0.465662

Table 5. Weighted Normalized matrix

	A11	A21	A31	A42
BC1	0.040783461	0.095272375	0.04384238	0.050421043
BC2	0.031572024	0.129298223	0.047978453	0.064760973
BC3	0.026579566	0.084875588	0.066866523	0.055509405
BC4	0.037900492	0.149335667	0.090855749	0.038208974
BC5	0.035791003	0.113230461	0.078447529	0.055879468

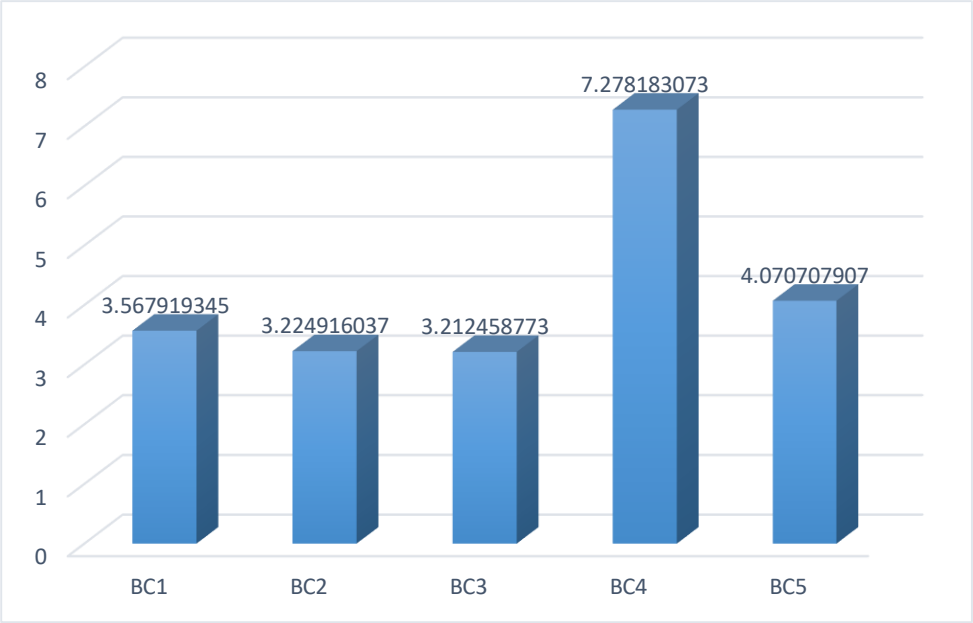

Fig 6. Final ranking for BC platforms

According to Proposition 2:

- Table 6 represents the normalized matrix according to Eq.(8).
- Table 7 for the weighted normalized matrix is generated based on Eq.(9).

Table 6. Normalized matrix

	A11	A22	A31	A42
BC1	0.404239135	0.452016567	0.288436709	0.420175361
BC2	0.546168684	0.518707536	0.315647719	0.539674775
BC3	0.360397023	0.44460646	0.439911333	0.462578379
BC4	0.471860019	0.358649211	0.597735192	0.318408118
BC5	0.430990254	0.447570503	0.516102162	0.465662235

Table 7. Weighted Normalized matrix

	A11	A22	A31	A42
BC1	0.031530653	0.041585524	0.04384238	0.050421043
BC2	0.042601157	0.047721093	0.047978453	0.064760973
BC3	0.028110968	0.040903794	0.066866523	0.055509405
BC4	0.036805082	0.032995727	0.090855749	0.038208974
BC5	0.03361724	0.041176486	0.078447529	0.055879468

According to Proposition 3:

- Table 8 represents the normalized matrix according to Eq.(8).

- Table 9 for the weighted normalized matrix is generated based on Eq.(9).

Table 8. Normalized matrix

	A12	A21	A31	A42
BC1	0.159831631	0.365028256	0.288436709	0.420175361
BC2	0.409092866	0.49539549	0.315647719	0.539674775
BC3	0.513744529	0.325193823	0.439911333	0.462578379
BC4	0.570827254	0.572167306	0.597735192	0.318408118
BC5	0.466175591	0.433833185	0.516102162	0.465662235

Table 9. Weighted Normalized matrix

	A12	A21	A31	A42
BC1	0.008151413	0.0335826	0.04384238	0.050421043
BC2	0.020863736	0.045576385	0.047978453	0.064760973
BC3	0.026200971	0.029917832	0.066866523	0.055509405
BC4	0.02911219	0.052639392	0.090855749	0.038208974
BC5	0.023774955	0.039912653	0.078447529	0.055879468

According to Proposition 4:

- Table 10 represents the normalized matrix according to Eq.(8).

- Table 11 for the weighted normalized matrix is generated based on Eq.(9).

Table 10. Normalized matrix

	A12	A22	A31	A42
BC1	0.159831631	0.452016567	0.288436709	0.420175361
BC2	0.409092866	0.518707536	0.315647719	0.539674775
BC3	0.513744529	0.44460646	0.439911333	0.462578379
BC4	0.570827254	0.358649211	0.597735192	0.318408118
BC5	0.466175591	0.447570503	0.516102162	0.465662235

Table 11. Weighted Normalized matrix

	A12	A22	A31	A42
BC1	0.008151413	0.041585524	0.04384238	0.050421043
BC2	0.020863736	0.047721093	0.047978453	0.064760973
BC3	0.026200971	0.040903794	0.066866523	0.055509405
BC4	0.02911219	0.032995727	0.090855749	0.038208974
BC5	0.023774955	0.041176486	0.078447529	0.055879468

- After we applied the four propositions or four hypersoftsets, we concluded that BC5 is the most secure and appropriate for utilizing against any attack as shown in Fig 7.

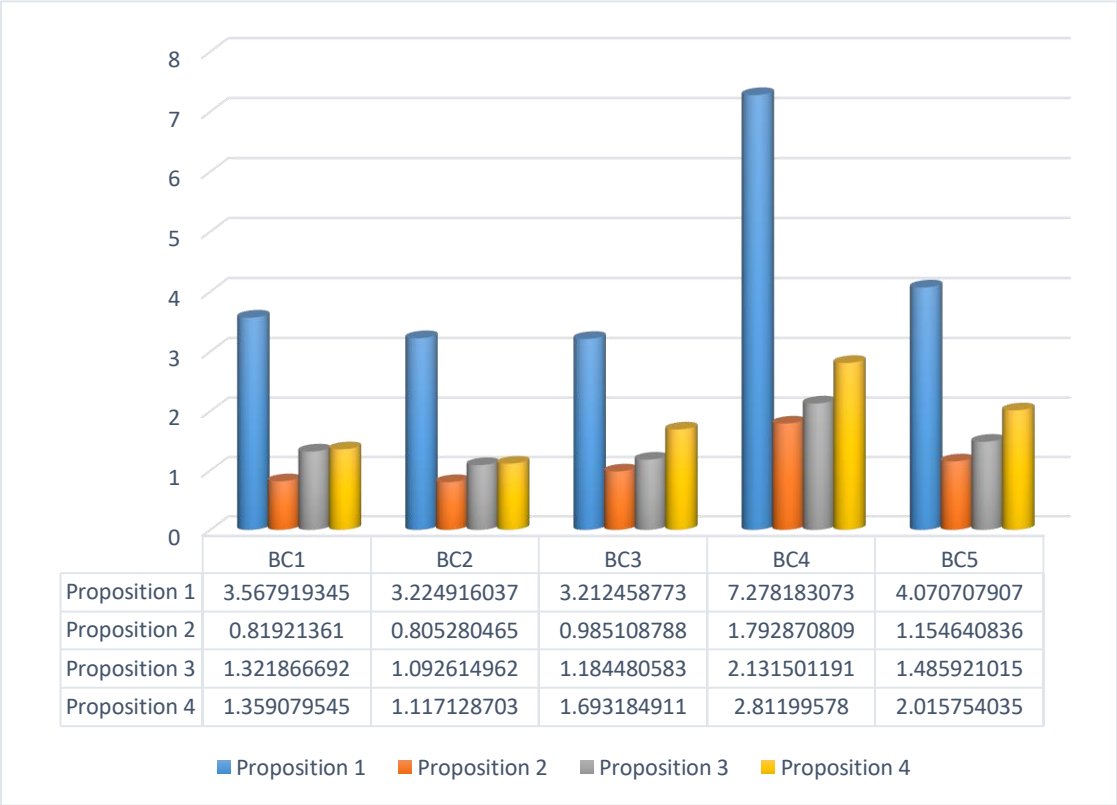

	BC1	BC2	BC3	BC4	BC5
Proposition 1	3.567919345	3.224916037	3.212458773	7.278183073	4.070707907
Proposition 2	0.81921361	0.805280465	0.985108788	1.792870809	1.154640836
Proposition 3	1.321866692	1.092614962	1.184480583	2.131501191	1.485921015
Proposition 4	1.359079545	1.117128703	1.693184911	2.81199578	2.015754035

Fig 7. Final ranking for BC platforms based on various propositions

5 Conclusion

In this study, we attempt to solve the problem of attacks and exploiting vulnerabilities, especially in digital technologies. Hence, we focused on BC as one of the important technologies for many sectors Especially financial sectors and transactions that require customer information. Thus, fraudulent and dubious actions endanger financial establishments as well as people by corrupting and leaking data through encryption. Accordingly, LLMs can be harnessed to protect transactions and DL from any manipulation. through applying PaLM, BLOCKGPT, GPTu-tor….etc to scan smart contracts, detecting and recognizing unusual and abnormal activities as well, these models can develop secured smart contracts. Hence, we exhibit the importance of adopting LLMs in BC to make any business proactive and resilient against any crisis that is facing any sector.

Yet, stakeholders may face the problem of which BC platform can use. Hence, we constructed a soft opting model to aid them in recommending the most appropriate and secure BC. In these models, we applied for the first time SHS for supporting a set of propositions of sub-attributes.

Entropy is applied to generate weights for attributes and sub-attributes which are proposed by SHS to utilize in MOOSRA for recommending optimal BC based on LLMs.

The findings of a soft opting model indicated that BC 4 is the most secure platform to adopt in enterprises.

References

1. Ustundag, A., et al., *Overview of cyber security in the industry 4.0 era.* Industry 4.0: managing the digital transformation, 2018: p. 267-284.
2. Toussaint, M., S. Krima, and H. Panetto, *Industry 4.0 data security: A cybersecurity frameworks review.* Journal of Industrial Information Integration, 2024: p. 100604.
3. Weber, R.H. and E. Studer, *Cybersecurity in the Internet of Things: Legal aspects.* Computer Law & Security Review, 2016. **32**(5): p. 715-728.
4. Pandey, S., et al., *Cyber security risks in globalized supply chains: conceptual framework.* Journal of Global Operations and Strategic Sourcing, 2020. **13**(1): p. 103-128.
5. Ferrag, M.A., et al., *Revolutionizing cyber threat detection with large language models: A privacy-preserving bert-based lightweight model for iot/iiot devices.* IEEE Access, 2024.
6. Kaur, R., D. Gabrijelčič, and T. Klobučar, *Artificial intelligence for cybersecurity: Literature review and future research directions.* Information Fusion, 2023. **97**: p. 101804.
7. Hassanin, M. and N. Moustafa, *A Comprehensive Overview of Large Language Models (LLMs) for Cyber Defences: Opportunities and Directions.* arXiv preprint arXiv:2405.14487, 2024.
8. Salim, S., et al., *Deep federated learning-based threat detection model for extreme satellite communications.* IEEE Internet of Things Journal, 2023.
9. Farah, J.C., et al. *Impersonating chatbots in a code review exercise to teach software engineering best practices*. in *2022 IEEE Global Engineering Education Conference (EDUCON)*. 2022. IEEE.
10. Wu, J., *Literature review on vulnerability detection using NLP technology. arXiv 2021.* arXiv preprint arXiv:2104.11230, 2021.
11. Zhang, J., et al., *When llms meet cybersecurity: A systematic literature review.* arXiv preprint arXiv:2405.03644, 2024.
12. Touvron, H., et al., *Llama: Open and efficient foundation language models.* arXiv preprint arXiv:2302.13971, 2023.
13. Jiang, A.Q., et al., *Mixtral of experts.* arXiv preprint arXiv:2401.04088, 2024.
14. Team, G., et al., *Gemini: a family of highly capable multimodal models.* arXiv preprint arXiv:2312.11805, 2023.
15. Roziere, B., et al., *Code llama: Open foundation models for code.* arXiv preprint arXiv:2308.12950, 2023.
16. Li, R., et al., *Starcoder: may the source be with you!* arXiv preprint arXiv:2305.06161, 2023.
17. Lozhkov, A., et al., *Starcoder 2 and the stack v2: The next generation.* arXiv preprint arXiv:2402.19173, 2024.
18. Mao, Y., et al., *A Survey on LoRA of Large Language Models.* arXiv preprint arXiv:2407.11046, 2024.

19. Zhao, W.X., et al., *A survey of large language models.* arXiv preprint arXiv:2303.18223, 2023.
20. Hadi, M.U., et al., *A survey on large language models: Applications, challenges, limitations, and practical usage.* Authorea Preprints, 2023.
21. Gao, J. and C.-Y. Lin, *Introduction to the special issue on statistical language modeling*. 2004, ACM New York, NY, USA. p. 87-93.
22. Bengio, Y., R. Ducharme, and P. Vincent, *A neural probabilistic language model.* Advances in neural information processing systems, 2000. **13**.
23. Kombrink, S., et al. *Recurrent Neural Network Based Language Modeling in Meeting Recognition*. in *Interspeech*. 2011.
24. Vaswani, A., *Attention is all you need.* arXiv preprint arXiv:1706.03762, 2017.
25. Kaplan, J., et al., *Scaling laws for neural language models.* arXiv preprint arXiv:2001.08361, 2020.
26. Yang, J., et al., *Harnessing the power of llms in practice: A survey on chatgpt and beyond.* ACM Transactions on Knowledge Discovery from Data, 2024. **18**(6): p. 1-32.
27. Wei, J., et al., *Chain-of-thought prompting elicits reasoning in large language models.* Advances in neural information processing systems, 2022. **35**: p. 24824-24837.
28. Kalyan, K.S., *A survey of GPT-3 family large language models including ChatGPT and GPT-4.* Natural Language Processing Journal, 2023: p. 100048.
29. Sarker, I.H., et al., *Multi-aspect rule-based AI: Methods, taxonomy, challenges and directions toward automation, intelligence and transparent cybersecurity modeling for critical infrastructures.* Internet of Things, 2024: p. 101110.
30. Ferrag, M.A., et al., *Generative AI and Large Language Models for Cyber Security: All Insights You Need.* arXiv preprint arXiv:2405.12750, 2024.
31. Yao, Y., et al., *A survey on large language model (llm) security and privacy: The good, the bad, and the ugly.* High-Confidence Computing, 2024: p. 100211.
32. Liu, Z. *A review of advancements and applications of pre-trained language models in cybersecurity*. in *2024 12th International Symposium on Digital Forensics and Security (ISDFS)*. 2024. IEEE.
33. Devlin, J., et al., *BERT: Pre-training of deep bidirectional transformers for language understanding. NAACL HLT. 2019*. 1810.
34. Putzier, M., et al., *Implementation of cloud computing in the German healthcare system.* NPJ Digital Medicine, 2024. **7**(1): p. 12.
35. Gharib, M., F. Smarandache, and M. Mohamed, *CSsEv: Modelling QoS Metrics in Tree Soft Toward Cloud Services Evaluator based on Uncertainty Environment*. 2024: Infinite Study.
36. Ayyadapu, A.K.R., *Secure Cloud Infrastructures: A Machine Learning Perspective.* International Neurourology Journal, 2022. **26**(4): p. 22-29.
37. Cao, D. and W. Jun. *LLM-CloudSec: Large Language Model Empowered Automatic and Deep Vulnerability Analysis for Intelligent Clouds*. in *IEEE INFOCOM 2024-IEEE Conference on Computer Communications Workshops (INFOCOM WKSHPS)*. 2024. IEEE.
38. Desai, B. and K. Patil, *Secure and Scalable Multi-Modal Vehicle Systems: A Cloud-Based Framework for Real-Time LLM-Driven Interactions.* Innovative Computer Sciences Journal, 2023. **9**(1): p. 1− 11-1− 11.

39. Pal, S., et al., *A domain-specific next-generation large language model (LLM) or ChatGPT is required for biomedical engineering and research.* Annals of biomedical engineering, 2024. **52**(3): p. 451-454.
40. Smarandache, F., M. Mohamed, and M. Voskoglou, *Evaluating Blockchain Cybersecurity Based on Tree Soft and Opinion Weight Criteria Method under Uncertainty Climate.* HyperSoft Set Methods in Engineering, 2024. **1**: p. 1-10.
41. Peters, G.W. and E. Panayi, *Understanding modern banking ledgers through blockchain technologies: Future of transaction processing and smart contracts on the internet of money*. 2016: Springer.
42. He, Z., et al., *NURGLE: Exacerbating Resource Consumption in Blockchain State Storage via MPT Manipulation.* arXiv preprint arXiv:2406.10687, 2024.
43. Berdik, D., et al., *A survey on blockchain for information systems management and security.* Information Processing & Management, 2021. **58**(1): p. 102397.
44. Xu, H., et al., *Large language models for cyber security: A systematic literature review.* arXiv preprint arXiv:2405.04760, 2024.
45. Sun, Y., et al. *Gptscan: Detecting logic vulnerabilities in smart contracts by combining gpt with program analysis*. in *Proceedings of the IEEE/ACM 46th International Conference on Software Engineering*. 2024.
46. Xia, S., et al., *AuditGPT: Auditing Smart Contracts with ChatGPT.* arXiv preprint arXiv:2404.04306, 2024.
47. Gai, Y., et al., *Blockchain large language models.* arXiv preprint arXiv:2304.12749, 2023.
48. Sahoo, S.K. and S.S. Goswami, *A comprehensive review of multiple criteria decision-making (MCDM) Methods: advancements, applications, and future directions.* Decision Making Advances, 2023. **1**(1): p. 25-48.
49. El-Henawy, I., et al., *Modeling Influenced Criteria in Classifiers' Imbalanced Challenges Based on TrSS Bolstered by The Vague Nature of Neutrosophic Theory*. 2024: Infinite Study.
50. Smarandache, F., *Foundation of the SuperHyperSoft Set and the Fuzzy Extension SuperHyperSoft Set: A New Vision.* Neutrosophic Systems with Applications, 2023. **11**: p. 48-51.
51. Feizi, F., A.A. Karbalaei-Ramezanali, and S. Farhadi, *FUCOM-MOORA and FUCOM-MOOSRA: new MCDM-based knowledge-driven procedures for mineral potential mapping in greenfields.* SN Applied Sciences, 2021. **3**: p. 1-19.

Received: April 1, 2024. Accepted: Aug 25, 2024

Neutrosophic Sets and Systems, Vol. 72, 2024
University of New Mexico

The 2-refined neutrosophic fraction function and its integrals

Yaser Ahmad Alhasan[1],*, Suliman Sheen[2] Qusay Ahassan[3] and Raja Abdullah Abdulfatah[4]

[1]Deanship of the Preparatory Year, Prince Sattam bin Abdulaziz University, KSA; y.alhasan@psau.edu.sa
[2]Deanship the Preparatory Year, Prince Sattam bin Abdulaziz University, Alkharj Saudi Arabia; S.almleh@psau.edu.sa
[3]Faculty of Informatics Engineering, Cordoba Private University, Syria; qusayalhassan77@gmail.com
[4]Deanship of the Preparatory Year, Prince Sattam bin Abdulaziz University, Alkharj, Saudi Arabia; ra.raj.1960@hotmail.com

***Corresponding author:** y.alhasan@psau.edu.sa

Abstract: The goal of this article is to study the 2-refined neutrosophic fraction function and its integrals. We were defining the 2-refined neutrosophic fraction function and discussing Algorithm for finding the integral of the 2-refined neutrosophic proper rational function and introduce the integral of the 2-refined neutrosophic improper rational functions. Where each case was explained by given specific examples.

Keywords: 2-refined neutrosophic; partial fraction; proper rational function; integrals.

1. Introduction and Preliminaries

As an alternative to the existing logics, Smarandache proposed the neutrosophic Logic to characterize a mathematical model of uncertainty, vagueness, ambiguity, imprecision, undefined, unknown, incompleteness, inconsistency, redundancy, and contradiction. Refined neutrosophic numbers were made available by Smarandache in the following format: $(a, b_1I_1, b_2I_2, \dots, b_nI_n)$ where $a, b_1, b_2, \dots, b_n \in R \text{ or } C$ [1].

The notion of refined neutrosophic algebraic structures was first proposed by Agboola[2]. Furthermore, paper [3] examined the refined neutrosophic rings I, assuming that they divide into two indeterminacies I_1 [contradiction (true (T) and false (F))] and I_2 [ignorance (true (T) or false (F))]. It then follows logically that: [3]

$$I_1I_1 = {I_1}^2 = I_1 \qquad (1)$$

$$I_2I_2 = {I_2}^2 = I_2 \qquad (2)$$

$$I_1I_2 = I_2I_1 = I_1 \qquad (3)$$

Furthermore, a large number of papers [4-5-6-7-8-12-13-14-15] present research on revised neutrosophic numbers. A study on the refined ah-isometry and its applications in refined neutrosophic surfaces was given by Mehmet Celik and Ahmed Hatip. Smarandache talked about neutrosophic indefinite integral [11]. Additionally, Alhasan gave multiple calculus presentations in

which he covered neutrosophic definite and indefinite integrals. Also, he demonstrated the most significant uses of definite integrals in neutrosophic logic [9–10].

This work included several of subjects: the first part provided an introduction and background material, while the main discussion section covered the 2-refined neutrosophic integrals by partial fraction. The last portion contains the conclusion.

Main Discussion

2. The 2-refined neutrosophic fraction function

Definition3.1

A polynomial whose coefficients are 2-refined neutrosophic numbers call 2-refined neutrosophic real polynomials:

$$Q(x,I_1,I_2) = (a_0 + b_0I_1 + c_0I_2) + (a_1 + b_1I_1 + c_1I_2)x + (a_2 + b_2I_1 + c_2I_2)x^2 + \cdots + (a_n + b_nI_1 + c_nI_2)x^n$$

Where $a_0, b_0, c_0, a_1, b_1, c_1, a_2, b_2, c_2, \dots, a_n, b_n, c_n$ are real numbers, I_1, I_2 represent indeterminacy and n is positive integer.

Definition3.2

2-Refined neutrosophic fraction function takes the formula:

$$f(x,I_1,I_2) = \frac{Q_1(x,I_1,I_2)}{Q_2(x,I_1,I_2)}$$

Where $Q_1(x,I_1,I_2)$, $Q_2(x,I_1,I_2)$ are 2-refined neutrosophic real polynomials and $Q_2(x,I_1,I_2) \neq 0$, at least the numerator or denominator is a 2-refined neutrosophic real polynomials.

Example 1

1) $f(x,I_1,I_2) = \dfrac{(-4 + 5I_1 + I_2)x^2 + (7I_1 + 8I_2)x - 2I_2}{8I_2x - 7 + 4I_1 + 2I_2}$

2) $f(x,I_1,I_2) = \dfrac{(6 - 7I_1 + 14I_2)x}{(I_1 + I_2)x^2 - 11I_2x - 5 - I_1}$

3) $f(x,I_1,I_2) = \dfrac{1}{(2I_1 + 3I_2)x^2 - 1 + 2I_1}$

Remark 1

- If degree of $Q_1(x,I_1,I_2)$ is less than degree of $Q_2(x,I_1,I_2)$, then:

  $$f(x,I_1,I_2) = \frac{Q_1(x,I_1,I_2)}{Q_2(x,I_1,I_2)}$$

  Is a 2-refined neutrosophic proper rational function.

- If degree of $Q_1(x,I_1,I_2)$ is greater than degree of $Q_2(x,I_1,I_2)$, then:

  $$f(x,I_1,I_2) = \frac{Q_1(x,I_1,I_2)}{Q_2(x,I_1,I_2)}$$

  Is a 2-refined neutrosophic improper rational function.

2.1. Integral of the 2-refined neutrosophic proper rational functions

2.1.1 Cases of the 2-refined neutrosophic proper rational function

- State 1: when it is possible to express the denominator as the product of linear factors that non-repeated.

Let $Q_2(x,I_1,I_2)=\big((a_1+b_1I_1+c_1I_2)x+d_1+s_1I_1+t_1I_2\big)\big((a_2+b_2I_1+c_2I_2)x+d_2+s_2I_1+t_2I_2\big)\dots\big((a_n+b_nI_1+c_nI_2)x+d_n+s_nI_1+t_nI_2\big)$
Where $a_1,b_1,c_1,d_1,s_1,t_1,a_2,b_2,c_2,d_2,s_2,t_2,\dots,a_n,b_n,c_n,d_ns_n,t_n$ are real numbers, then:

$$\frac{Q_1(x,I_1,I_2)}{Q_2(x,I_1,I_2)}=\frac{A_1}{(a_1+b_1I_1+c_1I_2)x+d_1+s_1I_1+t_1I_2}+\frac{A_2}{(a_2+b_2I_1+c_2I_2)x+d_2+s_2I_1+t_2I_2}+\cdots+\frac{A_n}{(a_n+b_nI_1+c_nI_2)x+d_n+s_nI_1+t_nI_2}$$

The values of the constants $A_1,A_2,\dots,A_n$ are to be determined.

- State 2: when it is possible to express the denominator as the product of linear factors that repeated.

Let $Q_2(x,I_1,I_2)=\big((a_1+b_1I_1+c_1I_2)x+d_1+s_1I_1+t_1I_2\big)\big((a_1+b_1I_1+c_1I_2)x+d_1+s_1I_1+t_1I_2\big)\dots\big((a_1+b_1I_1+c_1I_2)x+d_1+s_1I_1+t_1I_2\big)$
$=\big((a_1+b_1I_1+c_1I_2)x+d_1+s_1I_1+t_1I_2\big)^n$

Where a_1,b_1,c_1,d_1,s_1,t_1 are real numbers and n is `positive integer`, then:

$$\frac{Q_1(x,I_1,I_2)}{Q_2(x,I_1,I_2)}=\frac{A_1}{(a+bI_1+cI_2)x+d+sI_1+tI_2}+\frac{A_2}{\big((a+bI_1+cI_2)x+d+sI_1+tI_2\big)^2}+\cdots+\frac{A_n}{\big((a+bI_1+cI_2)x+d+sI_1+tI_2\big)^n}$$

The values of the constants $A_1,A_2,\dots,A_n$ are to be determined.

- State 3: When the denominator can be express as the product of repeated and non-repeated linear factors.

Let $Q_2(x,I_1,I_2)=\big((a_1+b_1I_1+c_1I_2)x+d_1+s_1I_1+t_1I_2\big)\big((a_2+b_2I_1+c_2I_2)x+d_2+s_2I_1+t_2I_2\big)\dots\big((a_n+b_nI_1+c_nI_2)x+d_n+s_nI_1+t_nI_2\big)\big((a+bI_1+cI_2)x+d+sI_1+tI_2\big)^m$

Where $a_1,b_1,c_1,d_1,s_1,t_1,a_2,b_2,c_2,d_2,s_2,t_2,\dots,a_n,b_n,c_n,d_n,s_n,t_n,a,b,c,d,s,t$ are real numbers and n,m is `positive integer`, then we can write:

$$\frac{Q_1(x,I_1,I_2)}{Q_2(x,I_1,I_2)}=\frac{A_1}{(a_1+b_1I_1+c_1I_2)x+d_1+s_1I_1+t_1I_2}+\frac{A_2}{(a_2+b_2I_1+c_2I_2)x+d_2+s_2I_1+t_2I_2}+\cdots+\frac{A_n}{(a_n+b_nI_1+c_nI_2)x+d_n+s_nI_1+t_nI_2}+\frac{B_1}{(a+bI_1+cI_2)x+d+sI_1+tI_2}+\frac{B_2}{\big((a+bI_1+cI_2)x+d+sI_1+tI_2\big)^2}+\cdots+\frac{B_m}{\big((a+bI_1+cI_2)x+d+sI_1+tI_2\big)^m}$$

The values of the constants $A_1,A_2,\dots,A_n,\ B_1,B_2,\dots,B_m$ are to be determined.

- State 4: When the denominator can be express as the product of non-repeated quadratic factors, which cannot be further factorize to linear factors.

Let: $Q_2(x, I_1, I_2) = \big((a_1 + b_1I_1 + c_1I_2)x^2 + d_1 + s_1I_1 + t_1I_2)x + e_1 + k_1I_1 + r_1I_2\big)\big((a_2 + b_2I_1 + c_2I_2)x^2 + d_2 + s_2I_1 + t_2I_2)x + e_2 + k_2I_1 + r_2I_2\big) \dots \big((a_n + b_nI_1 + c_nI_2)x^2 + d_n + s_nI_1 + t_nI_2)x + e_n + k_nI_1 + r_nI_2\big)$

Where $a_1, b_1, c_1, d_1, s_1, t_1, e_1, k_1, r_1, a_2, b_2, c_2, d_2, s_2, t_2, e_2, k_2, r_2 \dots, a_n, b_n, c_n, d_n, s_n, t_n, e_n, k_n, r_n$ are real numbers and n, m is `positive integer`, then we can write:

Then we can write:

$$\frac{Q_1(x, I_1, I_2)}{Q_2(x, I_1, I_2)} = \frac{A_1x + B_1}{(a_1 + b_1I_1 + c_1I_2)x^2 + d_1 + s_1I_1 + t_1I_2)x + e_1 + k_1I_1 + r_1I_2} + \frac{A_2x + B_2}{(a_2 + b_2I_1 + c_2I_2)x^2 + d_2 + s_2I_1 + t_2I_2)x + e_2 + k_2I_1 + r_2I_2} + \cdots + \frac{A_nx + B_n}{(a_n + b_nI_1 + c_nI_2)x^2 + d_n + s_nI_1 + t_nI_2)x + e_n + k_nI_1 + r_nI_2}$$

Where $A_1, A_2, \dots, A_n,\ B_1, B_2, \dots, B_n$ are constants whose values are to be determined.

2.1.2 Algorithm for finding Integral of the 2-refined neutrosophic proper rational functions

To evaluate $\int \frac{Q_1(x,I_1,I_2)}{Q_2(x,I_1,I_2)}$ we follow the following steps:

1) Reformulate the form of the function in one of the previous four cases according to the form of the denominator as sum of 2-refined neutrosophic partial fractions.
2) Integrate both sides.

Example 2

Evaluate:

$$\int \frac{dx}{(x + 3 - I_1 + 2I_2)(x + 1 + I_1 + I_2)}$$

Solution:

$$\frac{1}{(x + 3 - I_1 + 2I_2)(x + 1 + I_1 + I_2)} = \frac{A}{x + 3 - I_1 + 2I_2} + \frac{B}{x + 1 + I_1 + I_2} \qquad (*)$$

let's multiply both sides $(*)$ by $(x + 3 - I_1 + 2I_2)$ to find value of A:

$$\frac{1}{x + 1 + I_1 + I_2} = A + \frac{(x + 3 - I_1 + 2I_2)B}{x + 1 + I_1 + I_2} \qquad (1)$$

By substituting $x = -3 + I_1 - 2I_2$ in (1), we get:

$$A = \frac{1}{-3 + I_1 - 2I_2 + 1 + I_1 + I_2} = \frac{1}{-2 + 2I_1 - I_2}$$

let's multiply both sides $(*)$ by $(x + 1 + I_1 + I_2)$ to find value of B:

$$\frac{1}{x + 3 - I_1 + 2I_2} = \frac{(x + 1 + I_1 + I_2)A}{x + 3 - I_1 + 2I_2} + B \qquad (2)$$

By substituting $x = -1 - I_1 - I_2$ in (2), we get:

$$B = \frac{1}{-1 - I_1 - I_2 + 3 - I_1 + 2I_2} = \frac{1}{2 - 2I_1 + I_2}$$

By substituting in (*) we get:

$$\frac{1}{(x + 3 - I_1 + 2I_2)(x + 1 + I_1 + I_2)} = \frac{\frac{1}{-2 + 2I_1 - I_2}}{x + 3 - I_1 + 2I_2} + \frac{\frac{1}{2 - 2I_1 + I_2}}{x + 1 + I_1 + I_2}$$

$$\Rightarrow \int \frac{dx}{(x + 3 - I_1 + 2I_2)(x + 1 + I_1 + I_2)} dx = \int \left(\frac{\frac{1}{-2 + 2I_1 - I_2}}{x + 3 - I_1 + 2I_2} + \frac{\frac{1}{2 - 2I_1 + I_2}}{x + 1 + I_1 + I_2} \right) dx$$

$$= \frac{1}{-2 + 2I_1 - I_2} ln|x + 3 - I_1 + 2I_2| + \frac{1}{2 - 2I_1 + I_2} ln|x + 1 + I_1 + I_2|$$

$$= \frac{1}{-2 + 2I_1 - I_2} (ln|x + 3 - I_1 + 2I_2| - ln|x + 1 + I_1 + I_2|)$$

$$= \frac{1}{-2 + 2I_1 - I_2} ln \left| \frac{x + 3 - I_1 + 2I_2}{x + 1 + I_1 + I_2} \right|$$

$$= \left(-\frac{1}{2} - \frac{2}{3} I_1 + \frac{1}{6} I_2 \right) ln \left| \frac{x + 3 - I_1 + 2I_2}{x + 1 + I_1 + I_2} \right| + C$$

Whereas $C = a + bI_1 + cI_2$ and a, b, c are real numbers.

Let's check the answer:

$$\frac{d}{dx} \left[\left(-\frac{1}{2} - \frac{2}{3} I_1 + \frac{1}{6} I_2 \right) ln \left| \frac{x + 3 - I_1 + 2I_2}{x + 1 + I_1 + I_2} \right| + C \right]$$

$$= \frac{d}{dx} \left[\left(-\frac{1}{2} - \frac{2}{3} I_1 + \frac{1}{6} I_2 \right) (ln|x + 3 - I_1 + 2I_2| - ln|x + 1 + I_1 + I_2|) + C \right]$$

$$= \left(-\frac{1}{2} - \frac{2}{3} I_1 + \frac{1}{6} I_2 \right) \left(\frac{1}{x + 3 - I_1 + 2I_2} - \frac{1}{x + 1 + I_1 + I_2} \right)$$

$$= \left(-\frac{1}{2} - \frac{2}{3} I_1 + \frac{1}{6} I_2 \right) \left(\frac{x + 1 + I_1 + I_2 - x - 3 + I_1 - 2I_2}{(x + 3 - I_1 + 2I_2)(x + 1 + I_1 + I_2)} \right)$$

$$= \left(-\frac{1}{2} - \frac{2}{3} I_1 + \frac{1}{6} I_2 \right) \left(\frac{-2 + 2I_1 - I_2}{(x + 3 - I_1 + 2I_2)(x + 1 + I_1 + I_2)} \right) = \frac{\left(-\frac{1}{2} - \frac{2}{3} I_1 + \frac{1}{6} I_2 \right) (-2 + 2I_1 - I_2)}{(x + 3 - I_1 + 2I_2)(x + 1 + I_1 + I_2)}$$

$$= \frac{1}{(x + 3 - I_1 + 2I_2)(x + 1 + I_1 + I_2)}$$

The same integral function.

Example 3

Evaluate:

$$\int \frac{2+I_1+I_2}{((4+I_1+I_2)x+4-I_1-I_2)((1+2I_1+I_2)x+4+2I_1+I_2)}dx$$

Solution:

$$\frac{2+I_1+I_2}{((4+I_1+I_2)x+4-I_1-I_2)((1+2I_1+I_2)x+4+2I_1+I_2)} = \frac{A}{(4+I_1+I_2)x+4-I_1-I_2}+\frac{B}{(1+2I_1+I_2)x+4+2I_1+I_2} \qquad (*)$$

To find value of A, we multiply both sides of $(*)$ by $((4+I_1+I_2)x+4-I_1-I_2)$:

$$\frac{2+I_1+I_2}{(1+2I_1+I_2)x+4+2I_1+I_2} = A+\frac{((4+I_1+I_2)x+4-I_1-I_2)B}{(1+2I_1+I_2)x+4+2I_1+I_2} \qquad (1)$$

By substituting

$$x=\frac{-4+I_1+I_2}{4+I_1+I_2}=-1+\frac{4}{15}I_1+\frac{2}{5}I_2$$

in (1), we get:

$$A=\frac{2+I_1+I_2}{(1+2I_1+I_2)\left(-1+\frac{4}{15}I_1+\frac{2}{5}I_2\right)+4+2I_1+I_2}=\frac{2+I_1+I_2}{3+\frac{28}{15}I_1+\frac{4}{5}I_2}=\frac{2}{3}-\frac{27}{323}I_1+\frac{7}{57}I_2$$

To find value of B, we multiply both sides $(*)$ by $((1+2I_1+I_2)x+4+2I_1+I_2)$:

$$\frac{2+I_1+I_2}{(4+I_1+I_2)x+4-I_1-I_2}=\frac{((1-2I_1+I_2)x+4+2I_1+I_2)A}{(4+I_1+I_2)x+4-I_1-I_2}+B \qquad (2)$$

By substituting

$$x=\frac{-4-2I_1-I_2}{1+2I_1+I_2}=-4+\frac{3}{4}I_1+\frac{3}{2}I_2$$

in (2), we get:

$$B=\frac{2+I_1+I_2}{(4+I_1+I_2)\left(-4+\frac{3}{4}I_1+\frac{3}{2}I_2\right)+4-I_1-I_2}=\frac{2+I_1+I_2}{-12+I_1+\frac{5}{2}I_2}=-\frac{1}{6}-\frac{50}{323}I_1-\frac{17}{114}I_2$$

By substituting in (*) we get:

$$\frac{2+I_1+I_2}{\left((4+I_1+I_2)x+4-I_1-I_2\right)\left((1+2I_1+I_2)x+4+2I_1+I_2\right)}$$

$$=\frac{\frac{2}{3}-\frac{27}{323}I_1+\frac{7}{57}I_2}{(4+I_1+I_2)x+4-I_1-I_2}+\frac{-\frac{1}{6}-\frac{50}{323}I_1-\frac{17}{114}I_2}{(1+2I_1+I_2)x+4+2I_1+I_2}$$

$$\Rightarrow \quad \int \frac{2+I_1+I_2}{\left((4+I_1+I_2)x+4-I_1-I_2\right)\left((1+2I_1+I_2)x+4+2I_1+I_2\right)}$$

$$=\int\left(\frac{\frac{2}{3}-\frac{27}{323}I_1+\frac{7}{57}I_2}{(4+I_1+I_2)x+4-I_1-I_2}+\frac{-\frac{1}{6}-\frac{50}{323}I_1-\frac{17}{114}I_2}{(1+2I_1+I_2)x+4+2I_1+I_2}\right)dx$$

$$= \frac{\frac{2}{3} - \frac{27}{323}I_1 + \frac{7}{57}I_2}{4 + I_1 + I_2} ln|(4 + I_1 + I_2)x + 4 - I_1 - I_2| + \frac{-\frac{1}{6} - \frac{50}{323}I_1 - \frac{17}{114}I_2}{1 + 2I_1 + I_2} ln|(1 + 2I_1 + I_2)x + 4 + 2I_1 + I_2|$$

$$= \left(\frac{1}{6} - \frac{13}{323}I_1 - \frac{1}{114}I_2\right) ln|(4 + I_1 + I_2)x + 4 - I_1 - I_2| + \left(-\frac{1}{6} + \frac{13}{323}I_1 + \frac{1}{114}I_2\right) ln|(1 + 2I_1 + I_2)x + 4 + 2I_1 + I_2|$$

$$= \left(\frac{1}{6} - \frac{13}{323}I_1 - \frac{1}{114}I_2\right)(ln|(4 + I_1 + I_2)x + 4 - I_1 - I_2| - ln|(1 + 2I_1 + I_2)x + 4 + 2I_1 + I_2|)$$

$$= \left(\frac{1}{6} - \frac{13}{323}I_1 - \frac{1}{114}I_2\right) ln\left|\frac{(4 + I_1 + I_2)x + 4 - I_1 - I_2}{(1 + 2I_1 + I_2)x + 4 + 2I_1 + I_2}\right| + C$$

Whereas $C = a + bI_1 + cI_2$ *and* a, b, c are real numbers.

Example 4

Evaluate:

$$\int \frac{2x - 3I_1 + I_2}{(x + 2 + 2I_1)^2(x - 1)} dx$$

Solution:

$$\frac{2x - 3I_1 + I_2}{(x + 2 + 2I_1)^2(x - 1)} = \frac{A}{x + 2 + 2I_1} + \frac{B}{(x + 2 + 2I_1)^2} + \frac{D}{x - 1} \qquad (*)$$

To find value of D, We multiply both sides $(*)$ by $(x - 1)$:

$$\frac{2x - 3I_1 + I_2}{(x + 2 + 2I_1)^2} = \frac{(x - 1)A}{x + 2 + 2I_1} + \frac{(x - 1)B}{(x + 2 + 2I_1)^2} + D \qquad (1)$$

By substituting $x = 1$ in (1), we get:

$$D = \frac{2(1) - 3I_1 + I_2}{(3 + 2I_1)^2} = \frac{2 - 3I_1 + I_2}{9 + 16I_1}$$

$$\Longrightarrow \qquad D = \frac{2}{9} - \frac{1}{3}I_1 + \frac{1}{9}I_2$$

To find value of B, We multiply both sides $(*)$ by $(x + 2 + 2I_1)^2$:

$$\frac{2x - 3I_1 + I_2}{x - 1} = \frac{(x + 2 + 2I_1)^2 A}{x + 2 + 2I_1} + B + \frac{(x + 2 + 2I_1)^2 D}{x - 1} \qquad (2)$$

By substituting $x = -2 - 2I_1$ in (2), we get:

$$B = \frac{2(-2 - 2I_1) - 3I_1 + I_2}{-2 - 2I_1 - 1} = \frac{-4 - 7I_1 + I_2}{-3 - 2I_1}$$

$$\Rightarrow \qquad B = \frac{4}{3} + I_1 - \frac{1}{3}I_2$$

To find value of A, we substitute value of B, D and $x = -1$ in (*), we get:

$$\frac{-2 - 3I_1 + I_2}{(-1 + 2 + 2I_1)^2(-1 - 1)} = \frac{A}{-1 + 2 + 2I_1} + \frac{\frac{4}{3} + I_1 - \frac{1}{3}I_2}{(-1 + 2 + 2I_1)^2} + \frac{\frac{2}{9} - \frac{1}{3}I_1 + \frac{1}{9}I_2}{-1 - 1}$$

$$\frac{-2 - 3I_1 + I_2}{-2 - 16I_1} = \frac{A}{1 + 2I_1} + \frac{\frac{4}{3} + I_1 - \frac{1}{3}I_2}{1 + 8I_1} - \frac{1}{9} + \frac{1}{6}I_1 - \frac{1}{18}I_2$$

$$1 - \frac{5}{18}I_1 - \frac{1}{2}I_2 = \frac{A}{1 + 2I_1} + \frac{4}{3} - \frac{7}{9}I_1 - \frac{1}{3}I_2 - \frac{1}{9} + \frac{1}{6}I_1 - \frac{1}{18}I_2$$

$$\frac{A}{1 + 2I_1} = 1 - \frac{5}{18}I_1 - \frac{1}{2}I_2 - \frac{4}{3} + \frac{7}{9}I_1 + \frac{1}{3}I_2 + \frac{1}{9} - \frac{1}{6}I_1 + \frac{1}{18}I_2$$

$$A = (1 + 2I_1)\left(-\frac{2}{9} + \frac{1}{3}I_1 - \frac{1}{9}I_2\right) = -\frac{2}{9} + \frac{1}{3}I_1 - \frac{1}{9}I_2 - \frac{4}{9}I_1 + \frac{2}{3}I_1 - \frac{2}{9}I_1$$

$$\Rightarrow \qquad A = -\frac{2}{9} + \frac{1}{3}I_1 - \frac{1}{9}I_2$$

By substituting in (*) we get:

$$\frac{2x - 3I_1 + I_2}{(x + 2 + 2I_1)^2(x - 1)} = \frac{-\frac{2}{9} + \frac{1}{3}I_1 - \frac{1}{9}I_2}{x + 2 + 2I_1} + \frac{\frac{4}{3} + I_1 - \frac{1}{3}I_2}{(x + 2 + 2I_1)^2} + \frac{\frac{2}{9} - \frac{1}{3}I_1 + \frac{1}{9}I_2}{x - 1}$$

$$\Rightarrow \int \frac{2x - 3I_1 + I_2}{(x + 2 + 2I_1)^2(x - 1)}dx = \int \left(\frac{-\frac{2}{9} + \frac{1}{3}I_1 - \frac{1}{9}I_2}{x + 2 + 2I_1} + \frac{\frac{4}{3} + I_1 - \frac{1}{3}I_2}{(x + 2 + 2I_1)^2} + \frac{\frac{2}{9} - \frac{1}{3}I_1 + \frac{1}{9}I_2}{x - 1} \right) dx$$

$$= \left(-\frac{2}{9} + \frac{1}{3}I_1 - \frac{1}{9}I_2\right) ln|x + 2 + 2I_1| - \left(\frac{4}{3} + I_1 - \frac{1}{3}I_2\right)\frac{1}{x + 2 + 2I_1} + \left(\frac{2}{9} - \frac{1}{3}I_1 + \frac{1}{9}I_2\right) ln|x - 1| + C$$

$$= \left(-\frac{2}{9} + \frac{1}{3}I_1 - \frac{1}{9}I_2\right)(ln|x + 2 + 2I_1| - ln|x - 1|) - \left(\frac{4}{3} + I_1 - \frac{1}{3}I_2\right)\frac{1}{x + 2 + 2I_1} + C$$

$$= \left(-\frac{2}{9} + \frac{1}{3}I_1 - \frac{1}{9}I_2\right) ln\left|\frac{x + 2 + 2I_1}{x - 1}\right| - \left(\frac{4}{3} + I_1 - \frac{1}{3}I_2\right)\frac{1}{x + 2 + 2I_1} + C$$

Whereas $C = a + bI_1 + cI_2$ *and* a, b, c are real numbers.

Example 5

Evaluate:

$$\int \frac{I_1 + I_2}{x^2 - 16 - 11I_1 - 9I_2}dx$$

Solution:
to find the denominator factors

$$x^2 - 16 - 11I_1 - 9I_2 = x^2 - \left(\sqrt{16 + 11I_1 + 9I_2}\right)^2$$

Let's find: $\sqrt{16+11I_1+9I_2}$

$$\sqrt{16+11I_1+9I_2}=x+yI_1+zI_2$$
$$16+11I_1+9I_2=(x+yI_1+zI_2)^2$$

$$16+11I_1+9I_2=(x+yI_1)^2+2(x+yI_1)(zI_2)+(zI_2)^2$$

$$16+11I_1+9I_2=x^2+2xyI_1+(yI_1)^2+2(x+yI_1)(zI_2)+(zI_2)^2$$

$$16+11I_1+9I_2=x^2+2xyI_1+y^2I_1+2xzI_2+2yzI_1+z^2I_2$$

$$16+11I_1+9I_2=x^2+(y^2+2xy+2yz)I_1+(z^2+2xz)I_2$$

Whence:

$$\begin{cases} x^2=16 \\ y^2+2xy+2yz=11 \\ z^2+2xz=9 \end{cases}$$

$$\Rightarrow \begin{cases} x=\pm 4 \\ y^2+2xy+2yz=11 \\ z^2+2xz=9 \quad (2) \end{cases} \qquad (1)$$

Case1: $x=4$ by substituting in (2)

$$z^2+8z-9=0$$
$$(z-1)(z+9)=0$$

Then:

$$\begin{cases} z=1 \\ z=-9 \end{cases}$$

For $z=1$ we substitute in (1)

$$y^2+10y-11=0$$
$$(y+11)(y-1)=0$$

Then:

$$\begin{cases} y=1 \\ y=-11 \end{cases}$$

Hence:

$\sqrt{16+11I_1+9I_2}=4+I_1+I_2$

Or:

$$=4-11I_1+I_2$$

For $z=-9$ we substitute in (1)

$$y^2-10y-11=0$$
$$(y-11)(y+1)=0$$

Then:

$$\begin{cases} y=11 \\ y=-1 \end{cases}$$

Hence:

$\sqrt{16+11I_1+9I_2}=4+11I_1-9I_2$

Or:

$$=4-I_1-9I_2$$

Case2: $x=-4$ by substituting in (2)

$$z^2 - 8z - 9 = 0$$
$$(z-9)(z+1) = 0$$

Then:

$$\begin{cases} z = 9 \\ z = -1 \end{cases}$$

For $z = 9$ we substitute in (1)

$$y^2 + 10y - 11 = 0$$
$$(y-1)(y+11) = 0$$

Then:

$$\begin{cases} y = 1 \\ y = -11 \end{cases}$$

Hence:

$\sqrt{16 + 11I_1 + 9I_2} = -4 + I_1 + 9I_2$

Or:

$$= -4 - 11I_1 + 9I_2$$

For $z = -1$ we substitute in (1)

$$y^2 - 10y - 11 = 0$$
$$(y-11)(y+1) = 0$$
$$\begin{cases} y = 11 \\ y = -1 \end{cases}$$

Hence:

$\sqrt{16 + 11I_1 + 9I_2} = -4 + 11I_1 - I_2$

Or:

$$= -4 - I_1 - I_2$$

Hence, we got eight 2-refined neutrosophic solutions:

$$\sqrt{16 + 11I_1 + 9I_2} = 4 + I_1 + I_2$$

Or:

$$= 4 - 11I_1 + I_2$$

Or:

$$= 4 + 11I_1 - 9I_2$$

Or:

$$= 4 - I_1 - 9I_2$$

Or:

$$= -4 + I_1 + 9I_2$$

Or:

$$= -4 - 11I_1 + 9I_2$$

Or:

$$= -4 + 11I_1 - I_2$$

Or:

$$= -4 - I_1 - I_2$$

First 2-refined neutrosophic factoring:

$$x^2 - 16 - 11I_1 - 9I_2 = (x - 4 - I_1 - I_2)(x + 4 + I_1 + I_2)$$

Second 2-refined neutrosophic factoring:

$$x^2 - 16 - 11I_1 - 9I_2 = (x - 4 + 11I_1 - I_2)(x + 4 - 11I_1 + I_2)$$

Third 2-refined neutrosophic factoring:

$$x^2 - 16 - 11I_1 - 9I_2 = (x - 4 - 11I_1 + 9I_2)(x + 4 + 11I_1 - 9I_2)$$

Fourth 2-refined neutrosophic factoring:

$$x^2 - 16 - 11I_1 - 9I_2 = (x - 4 + I_1 + 9I_2)(x + 4 - I_1 - 9I_2)$$

Thus, the denominator factors can be write in four cases:
Case1:

$$x^2 - 16 - 11I_1 - 9I_2 = (x - 4 - I_1 - I_2)(x + 4 + I_1 + I_2)$$

$$\frac{I_1 + I_2}{x^2 - 16 - 11I_1 - 9I_2} = \frac{I_1 + I_2}{(x - 4 - I_1 - I_2)(x + 4 + I_1 + I_2)}$$

$$\frac{I_1 + I_2}{(x - 4 - I_1 - I_2)(x + 4 + I_1 + I_2)} = \frac{A}{x - 4 - I_1 - I_2} + \frac{B}{x + 4 + I_1 + I_2} \qquad (*)$$

To find value of A, We multiply both sides $(*)$ by $(x - 4 - I_1 - I_2)$:

$$\frac{I_1 + I_2}{x + 4 + I_1 + I_2} = A + \frac{(x - 4 - I_1 - I_2)B}{x + 4 + I_1 + I_2} \qquad (1)$$

By substituting $x = 4 + I_1 + I_2$ in (1), we get:

$$A = \frac{I_1 + I_2}{8 + 2I_1 + 2I_2} = \frac{1}{15}I_1 + \frac{1}{10}I_2$$

To find value of A, We multiply both sides $(*)$ by $(x + 4 + I_1 + I_2)$:

$$\frac{I_1 + I_2}{x - 4 - I_1 - I_2} = \frac{(x + 4 + I_1 + I_2)A}{x - 4 - I_1 - I_2} + B \qquad (2)$$

By substituting $x = -4 - I_1 - I_2$ in (2), we get:

$$B = \frac{I_1 + I_2}{-8 - 2I_1 - 2I_2} = -\frac{1}{15}I_1 - \frac{1}{10}I_2$$

By substituting in (*) we get:

$$\frac{I_1 + I_2}{(x - 4 - I_1 - I_2)(x + 4 + I_1 + I_2)} = \frac{\frac{1}{15}I_1 + \frac{1}{10}I_2}{x - 4 - I_1 - I_2} + \frac{-\frac{1}{15}I_1 - \frac{1}{10}I_2}{x + 4 + I_1 + I_2}$$

$$\Rightarrow \int \frac{I_1 + I_2}{(x - 4 - I_1 - I_2)(x + 4 + I_1 + I_2)}dx = \int \left(\frac{\frac{1}{15}I_1 + \frac{1}{10}I_2}{x - 4 - I_1 - I_2} + \frac{-\frac{1}{15}I_1 - \frac{1}{10}I_2}{x + 4 + I_1 + I_2} \right) dx$$

$$= \left(\frac{1}{15}I_1 + \frac{1}{10}I_2\right) ln|x - 4 - I_1 - I_2| + \left(-\frac{1}{15}I_1 - \frac{1}{10}I_2\right) ln|x + 4 + I_1 + I_2|$$

$$= \left(\frac{1}{15}I_1 + \frac{1}{10}I_2\right) (ln|x - 4 - I_1 - I_2| - ln|x + 4 + I_1 + I_2|)$$

$$= \left(\frac{1}{15}I_1 + \frac{1}{10}I_2\right) ln\left|\frac{x - 4 - I_1 - I_2}{x + 4 + I_1 + I_2}\right| + C$$

Case2:

$$x^2 - 16 - 11I_1 - 9I_2 = (x - 4 + 11I_1 - I_2)(x + 4 - 11I_1 + I_2)$$

$$\frac{I_1+I_2}{x^2-16-11I_1-9I_2}=\frac{I_1+I_2}{(x-4+11I_1-I_2)(x+4-11I_1+I_2)}$$

$$\frac{I_1+I_2}{(x-4+11I_1-I_2)(x+4-11I_1+I_2)}=\frac{A}{x-4+11I_1-I_2}+\frac{B}{x+4-11I_1+I_2} \qquad (*)'$$

To find value of A, We multiply both sides $(*)'$ by $(x-4+11I_1-I_2)$:

$$\frac{I_1+I_2}{x+4-11I_1+I_2}=A+\frac{(x-4+11I_1-I_2)B}{x+4-11I_1+I_2} \qquad (1)'$$

By substituting $x=4-11I_1+I_2$ in $(1)'$, we get:

$$A=\frac{I_1+I_2}{8-22I_1+2I_2}=-\frac{4}{15}I_1+\frac{1}{10}I_2$$

To find value of A, We multiply both sides $(*)'$ by $(x+4-11I_1+I_2)$:

$$\frac{I_1+I_2}{x-4+11I_1-I_2}=\frac{(x+4-11I_1+I_2)A}{x-4+11I_1-I_2}+B \qquad (2)'$$

By substituting $x=-4+11I_1-I_2$ in $(2)'$, we get:

$$B=\frac{I_1+I_2}{-8+22I_1-2I_2}=\frac{4}{15}I_1-\frac{1}{10}I_2$$

By substituting in $(*)'$ we get:

$$\frac{I_1+I_2}{(x-4+11I_1-I_2)(x+4-11I_1+I_2)}=\frac{-\frac{4}{15}I_1+\frac{1}{10}I_2}{x-4+11I_1-I_2}+\frac{\frac{4}{15}I_1-\frac{1}{10}I_2}{x+4-11I_1+I_2}$$

$$\Rightarrow\int\frac{I_1+I_2}{(x-4+11I_1-I_2)(x+4-11I_1+I_2)}dx=\int\left(\frac{-\frac{4}{15}I_1+\frac{1}{10}I_2}{x-4+11I_1-I_2}+\frac{\frac{4}{15}I_1-\frac{1}{10}I_2}{x+4-11I_1+I_2}\right)dx$$

$$=\left(-\frac{4}{15}I_1+\frac{1}{10}I_2\right)ln|x-4+11I_1-I_2|+\left(\frac{4}{15}I_1-\frac{1}{10}I_2\right)ln|x+4-11I_1+I_2|$$

$$=\left(-\frac{4}{15}I_1+\frac{1}{10}I_2\right)(ln|x-4+11I_1-I_2|-ln|x+4-11I_1+I_2|)$$

$$=\left(-\frac{4}{15}I_1+\frac{1}{10}I_2\right)ln\left|\frac{x-4+11I_1-I_2}{x+4-11I_1+I_2}\right|+C$$

Case3:

$$x^2-16-11I_1-9I_2=(x-4-11I_1+9I_2)(x+4+11I_1-9I_2)$$

$$\frac{I_1+I_2}{x^2-16-11I_1-9I_2}=\frac{I_1+I_2}{(x-4-11I_1+9I_2)(x+4+11I_1-9I_2)}$$

$$\frac{I_1+I_2}{(x-4-11I_1+9I_2)(x+4+11I_1-9I_2)}=\frac{A}{x-4-11I_1+9I_2}+\frac{B}{x+4+11I_1-9I_2} \qquad (**)$$

To find value of A, We multiply both sides $(**)$ by $(x-4-11I_1+9I_2)$:

$$\frac{I_1+I_2}{x+4+11I_1-9I_2}=A+\frac{(x-4-11I_1+9I_2)B}{x+4+11I_1-9I_2} \qquad (1)''$$

By substituting $x=4+11I_1-9I_2$ in $(1)''$, we get:

$$A=\frac{I_1+I_2}{8+22I_1-18I_2}=\frac{4}{15}I_1-\frac{1}{10}I_2$$

To find value of A, We multiply both sides $(**)$ by $(x+4+11I_1-9I_2)$:

$$\frac{I_1+I_2}{x-4-11I_1+9I_2}=\frac{(x+4+11I_1-9I_2)A}{x-4-11I_1+9I_2}+B \qquad (2)''$$

By substituting $x=-4-11I_1+9I_2$ in $(2)''$, we get:

$$B=\frac{I_1+I_2}{-8-22I_1+18I_2}=-\frac{4}{15}I_1+\frac{1}{10}I_2$$

By substituting in $(**)$ we get:

$$\frac{I_1+I_2}{(x-4-11I_1+9I_2)(x+4+11I_1-9I_2)}=\frac{A}{x-4-11I_1+9I_2}+\frac{B}{x+4+11I_1-9I_2}$$

$$\Rightarrow\int\frac{I_1+I_2}{(x-4-11I_1+9I_2)(x+4+11I_1-9I_2)}dx=\int\left(\frac{\frac{4}{15}I_1-\frac{1}{10}I_2}{x-4-11I_1+9I_2}+\frac{-\frac{4}{15}I_1+\frac{1}{10}I_2}{x+4+11I_1-9I_2}\right)dx$$

$$=\left(\frac{4}{15}I_1-\frac{1}{10}I_2\right)ln|x-4-11I_1+9I_2|+\left(-\frac{4}{15}I_1+\frac{1}{10}I_2\right)ln|x+4+11I_1-9I_2|$$

$$=\left(\frac{4}{15}I_1-\frac{1}{10}I_2\right)(ln|x-4-11I_1+9I_2|-ln|x+4+11I_1-9I_2|)$$

$$=\left(\frac{4}{15}I_1-\frac{1}{10}I_2\right)ln\left|\frac{x-4-11I_1+9I_2}{x+4+11I_1-9I_2}\right|+C$$

Case4:

$$x^2-16-11I_1-9I_2=(x-4+I_1+9I_2)(x+4-I_1-9I_2)$$

$$\frac{I_1+I_2}{x^2-16-11I_1-9I_2}=\frac{I_1+I_2}{(x-4+I_1+9I_2)(x+4-I_1-9I_2)}$$

$$\frac{I_1+I_2}{(x-4+I_1+9I_2)(x+4-I_1-9I_2)}=\frac{A}{x-4+I_1+9I_2}+\frac{B}{x+4-I_1-9I_2} \qquad (**)'$$

To find value of A, We multiply both sides $(**)'$ by $(x-4+I_1+9I_2)$:

$$\frac{I_1+I_2}{x+4-I_1-9I_2}=A+\frac{(x-4+I_1+9I_2)B}{x+4-I_1-9I_2} \qquad (1)'''$$

By substituting $x=-4+I_1+9I_2$ in $(1)'''$, we get:

$$A = \frac{I_1 + I_2}{8 - 2I_1 - 18I_2} = -\frac{1}{15}I_1 - \frac{1}{10}I_2$$

To find value of A, We multiply both sides $(**)'$ by $(x + 4 - I_1 - 9I_2)$:

$$\frac{I_1 + I_2}{x - 4 + I_1 + 9I_2} = \frac{(x + 4 - I_1 - 9I_2)A}{x - 4 - 11I_1 + 9I_2} + B \qquad (2)'''$$

By substituting $x = -4 + I_1 + 9I_2$ in $(2)'''$, we get:

$$B = \frac{I_1 + I_2}{-8 + 2I_1 + 18I_2} = \frac{1}{15}I_1 + \frac{1}{10}I_2$$

By substituting in $(**)'$ we get:

$$\frac{I_1 + I_2}{(x - 4 + I_1 + 9I_2)(x + 4 - I_1 - 9I_2)} = \frac{A}{x - 4 + I_1 + 9I_2} + \frac{B}{x + 4 - I_1 - 9I_2}$$

$$\Rightarrow \int \frac{I_1 + I_2}{(x - 4 + I_1 + 9I_2)(x + 4 - I_1 - 9I_2)}dx = \int \left(\frac{-\frac{1}{15}I_1 - \frac{1}{10}I_2}{x - 4 + I_1 + 9I_2} + \frac{\frac{1}{15}I_1 + \frac{1}{10}I_2}{x + 4 - I_1 - 9I_2} \right) dx$$

$$= \left(-\frac{1}{15}I_1 - \frac{1}{10}I_2\right) ln|x - 4 + I_1 + 9I_2| + \left(\frac{1}{15}I_1 + \frac{1}{10}I_2\right) ln|x + 4 - I_1 - 9I_2|$$

$$= \left(-\frac{1}{15}I_1 - \frac{1}{10}I_2\right) (ln|x - 4 + I_1 + 9I_2| - ln|x + 4 - I_1 - 9I_2|)$$

$$= \left(-\frac{1}{15}I_1 - \frac{1}{10}I_2\right) ln\left|\frac{x - 4 + I_1 + 9I_2}{x + 4 - I_1 - 9I_2}\right| + C$$

Hence:

$$\int \frac{5I}{x^2 - 4 + 3I}dx = \begin{cases} \left(\frac{1}{15}I_1 + \frac{1}{10}I_2\right) ln\left|\frac{x - 4 - I_1 - I_2}{x + 4 + I_1 + I_2}\right| + C \\ \left(-\frac{4}{15}I_1 + \frac{1}{10}I_2\right) ln\left|\frac{x - 4 + 11I_1 - I_2}{x + 4 - 11I_1 + I_2}\right| + C \\ \left(\frac{4}{15}I_1 - \frac{1}{10}I_2\right) ln\left|\frac{x - 4 - 11I_1 + 9I_2}{x + 4 + 11I_1 - 9I_2}\right| + C \\ \left(-\frac{1}{15}I_1 - \frac{1}{10}I_2\right) ln\left|\frac{x - 4 + I_1 + 9I_2}{x + 4 - I_1 - 9I_2}\right| + C \end{cases}$$

Whereas $C = a + bI_1 + cI_2 \ \ and \ \ a, b, c$ are real numbers.

Example 6

Evaluate:

$$\int \frac{4 + I_1 + 2I_2}{(x + 1 + I_1 + 2I_2)(x^2 + 4 + I_2)}dx$$

Solution:

We note that $(x^2 + 4 + I_2)$ cannot be analyzing, because:

$$x^2 + 4 + I_2 = x^2 - \left(\sqrt{-4 - I_2}\right)^2$$

Let's find $\sqrt{-4 - I_2}$

$$\sqrt{-4 - I_2} = \alpha + \beta I_2 + \gamma I_2$$

$$-4-I_2=\alpha^2+(\beta^2+2\alpha\beta+2\beta\gamma)I_1+(\gamma^2+2\alpha\gamma)I_2$$

then:

$$\alpha^2=-4 \text{ (Impossible in real number)}$$

So:

$$\frac{4+I_1+2I_2}{(x+1+I_1+2I_2)(x^2+4+I_2)}=\frac{A}{x+1+I_1+2I_2}+\frac{Bx+D}{x^2+4+I_2} \qquad (*)$$

To find value of A, We multiply both sides $(*)$ by $(x+1+I_1+2I_2)$:

$$\frac{4+I_1+2I_2}{x^2+4+I_2}=A+\frac{(x+1+I_1+2I_2)(Bx+D)}{x^2+4+I_2} \qquad (1)$$

by substituting $x=-1-I_1-2I_2$ in (1), we get:

$$A=\frac{4+I_1+2I_2}{(-1-I_1-2I_2)^2+4+I_2}=\frac{4+I_1+2I_2}{5+7I_1+9I_2}$$

$$\Rightarrow \qquad A=\frac{4}{5}-\frac{2}{21}I_1-\frac{13}{35}I_2$$

To find value of B, We multiply both sides $(*)$ by x:

$$\frac{(4+I_1+2I_2)x}{(x+1+I_1+2I_2)(x^2+4+I_2)}=\frac{Ax}{x+1+I_1+2I_2}+\frac{Bx^2+D}{x^2+4+I_2} \qquad (2)$$

By take limit both sides in (2), when $x\longrightarrow\infty$, we get:

$$A+B=0 \quad \Rightarrow \quad B=-A=-\frac{4}{5}+\frac{2}{21}I_1+\frac{13}{35}I_2$$

To find value of D, we substitute value of A,B and let be $x=0$, in (*), we get:

$$\frac{4+I_1+2I_2}{(0+1+I_1+2I_2)(0^2+4+I_2)}=\frac{\frac{4}{5}-\frac{2}{21}I_1-\frac{13}{35}I_2}{0+1+I_1+2I_2}+\frac{\left(-\frac{4}{5}+\frac{2}{21}I_1+\frac{13}{35}I_2\right)(0)+D}{0^2+4+I_2}$$

$$\frac{4+I_1+2I_2}{4+5I_1+11I_2}=\frac{\frac{4}{5}-\frac{2}{21}I_1-\frac{13}{35}I_2}{1+I_1+2I_2}+\frac{D}{4+I_2}$$

$$1-\frac{1}{20}I_1-\frac{3}{5}I_2=\frac{4}{5}-\frac{5}{84}I_1-\frac{23}{35}I_2+\frac{D}{4+I_2}$$

$$\frac{D}{4+I_2}=\frac{1}{5}+\frac{1}{105}I_1+\frac{2}{35}I_2$$

$$D=\frac{4}{5}+\frac{1}{21}I_1+\frac{17}{35}I_2$$

By substituting in (*) we get:

$$\frac{4+I_1+2I_2}{(x+1+I_1+2I_2)(x^2+4+I_2)}=\frac{\frac{4}{5}-\frac{2}{21}I_1-\frac{13}{35}I_2}{x+1+I_1+2I_2}+\frac{\left(-\frac{4}{5}+\frac{2}{21}I_1+\frac{13}{35}I_2\right)x+\frac{4}{5}+\frac{1}{21}I_1+\frac{17}{35}I_2}{x^2+4+I_2}$$

$$\Rightarrow \int \frac{4+I_1+2I_2}{(x+1+I_1+2I_2)(x^2+4+I_2)}dx$$

$$= \int \left(\frac{\frac{4}{5}-\frac{2}{21}I_1-\frac{13}{35}I_2}{x+1+I_1+2I_2} + \frac{\left(-\frac{4}{5}+\frac{2}{21}I_1+\frac{13}{35}I_2\right)x+\frac{4}{5}+\frac{1}{21}I_1+\frac{17}{35}I_2}{x^2+4+I_2} \right) dx$$

$$= \int \frac{\frac{4}{5}-\frac{2}{21}I_1-\frac{13}{35}I_2}{x+1+I_1+2I_2}dx + \int \frac{\left(-\frac{4}{5}+\frac{2}{21}I_1+\frac{13}{35}I_2\right)x}{x^2+4+I_2}dx + \int \frac{\frac{4}{5}+\frac{1}{21}I_1+\frac{17}{35}I_2}{x^2+4+I_2}dx$$

$$= \left(\frac{4}{5}-\frac{2}{21}I_1-\frac{13}{35}I_2\right) ln|x+1+I_1+2I_2| - \left(\frac{2}{5}-\frac{1}{21}I_1-\frac{13}{70}I_2\right) ln|x^2+4+I_2| + \int \frac{\frac{4}{5}+\frac{1}{21}I_1+\frac{17}{35}I_2}{x^2+\left(\sqrt{4+I_2}\right)^2}dx$$

$$= \left(\frac{4}{5}-\frac{2}{21}I_1-\frac{13}{35}I_2\right) ln|x+1+I_1+2I_2| - \left(\frac{2}{5}-\frac{1}{21}I_1-\frac{13}{70}I_2\right) ln|x^2+4+I_2| + \int \frac{\frac{4}{5}+\frac{1}{21}I_1+\frac{17}{35}I_2}{x^2+\left(2+(\sqrt{5}-2)I_2\right)^2}dx$$

$$= \left(\frac{4}{5}-\frac{2}{21}I_1-\frac{13}{35}I_2\right) ln|x+1+I_1+2I_2| - \left(\frac{2}{5}-\frac{1}{21}I_1-\frac{13}{70}I_2\right) ln|x^2+4+I_2| + \left(\frac{\frac{4}{5}+\frac{1}{21}I_1+\frac{17}{35}I_2}{2+(\sqrt{5}-2)I_2}\right) tan^{-1}\left(\frac{x}{2+(\sqrt{5}-2)I_2}\right)$$

$$= \left(\frac{4}{5}-\frac{2}{21}I_1-\frac{13}{35}I_2\right) ln|x+1+I_1+2I_2| - \left(\frac{2}{5}-\frac{1}{21}I_1-\frac{13}{70}I_2\right) ln|x^2+4+I_2| + \left(\frac{2}{5}+\frac{\sqrt{5}}{105}I_1+\left(\frac{9}{7\sqrt{5}}-\frac{2}{5}\right)I_2\right) tan^{-1}\left(\frac{1}{2}+\left(-\frac{1}{2}+\frac{1}{\sqrt{5}}\right)I_2\right)x + C$$

Whereas $\sqrt{4+I_2} = \sqrt{4}+\left(-\sqrt{5}+\sqrt{5}\right)I_1+\left(-\sqrt{4}+\sqrt{5}\right)I_2 = 2+(\sqrt{5}-2)I_2$ and $C = a+bI_1+cI_2$ *and* a,b,c are real numbers.

2.2. Integral of the 2- refined neutrosophic improper rational functions

To facilitate the integration process, we can apply the long division method or the synthetic division method if the degree of the numerator is higher than the degree of the denominator.

Example 7

$$\int \frac{x^3+(1+I_1+2I_2)x^2+(2+I_2)x-3+2I_1-4I_2}{x-5-I_1-6I_2}dx$$

By using synthetic division method, we get:

$5+I_1+6I_2$	1	$1+I_1+2I_2$	$2+I_2$	$-3+2I_1-4I_2$
		$5+I_1+6I_2$	$30+38I_1+124I_2$	$160+613I_1+1567I_2$
	1	$6+2I_1+8I_2$	$32+38I_1+125I_2$	$157+615I_1+1563I_2$

Then:

$$\frac{x^3+(1+I_1+2I_2)x^2+(2+I_2)x-3+2I_1-4I_2}{x-5-I_1-6I_2}$$

$$=x^2+(6+2I_1+8I_2)x+(32+38I_1+125I_2)+\frac{157+615I_1+1563I_2}{x-5-I_1-6I_2}$$

$$\Rightarrow \int\frac{x^3+(1+I_1+2I_2)x^2+(2+I_2)x-3+2I_1-4I_2}{x-5-I_1-6I_2}dx$$

$$=\int\left(x^2+(6+2I_1+8I_2)x+(32+38I_1+125I_2)+\frac{157+615I_1+1563I_2}{x-5-I_1-6I_2}\right)dx$$

$$=\frac{x^3}{3}+(3+I_1+4I_2)x^2+(32+38I_1+125I_2)x+(157+615I_1+1563I_2)ln|x-5-I_1-6I_2|+C$$

Whereas $C=a+bI_1+cI_2$ and a,b,c are real numbers.

Example 8

Evaluate:

$$\int\frac{(5+I_1-3I_2)x^2+(-4-24I_1-10I_2)x-6-12I_1-10I_2}{x-1-6I_1-7I_2}dx$$

By using synthetic division method, we get:

$1+6I_1+7I_2$	$5+I_1-3I_2$	$-4-24I_1-10I_2$	$-6-12I_1-10I_2$
		$5+26I_1+11I_2$	$1+40I_1+15I_2$
	$5+I_1-3I_2$	$1+2I_1+I_2$	$-5+28I_1+5I_2$

Then:

$$\frac{(5+I_1-3I_2)x^2+(-4-24I_1-10I_2)x-6-12I_1-10I_2}{x-1-6I_1-7I_2}$$

$$=(5+I_1-3I_2)x+(1+2I_1+I_2)+\frac{-5+28I_1+5I_2}{x-1-6I_1-7I_2}$$

$$\Rightarrow \int\frac{(5+I_1-3I_2)x^2+(-4-24I_1-10I_2)x-6-12I_1-10I_2}{x-1-6I_1-7I_2}dx$$

$$=\int\left((5+I_1-3I_2)x+(1+2I_1+I_2)+\frac{-5+28I_1+5I_2}{x-1-6I_1-7I_2}\right)dx$$

$$=\left(\frac{5}{2}+\frac{1}{2}I_1-\frac{3}{2}I_2\right)x^2+(1+2I_1+I_2)x+(-5+28I_1+5I_2)ln|x-1-6I_1-7I_2|+C$$

Whereas $C = a + bI_1 + cI_2 \ \ and \ \ a, b, c$ are real numbers.

4. Conclusions

The 2-refined neutrosophic partial fraction is important in neutrosophic logic. We searched for a way to integrate it by discussing all the cases using the division of 2-refined neutrosophic numbers, and we obtained accurate results that were verified. In addition, illustrated through a set of examples.

Acknowledgments "This study is supported via funding from Prince sattam bin Abdulaziz University project number (PSAU/2024/R/1445)".

References

[1] Smarandache, F; "(T,I,F)- Neutrosophic Structures", Neutrosophic Sets and Systems, Volume8, PP:3-10, 2015.

[2] Agboola,A.A.A; On Refined Neutrosophic Algebraic Structures. Neutrosophic Sets and Systems, Volume10, PP: 99-101, 2015.

[3] Adeleke, E.O., Agboola, A.A.A.,and Smarandache, F; Refined Neutrosophic Rings I. International Journal of Neutrosophic Science, Volume 2, Issue 2, PP:77-81, 2020.

[4] Smarandache, F; n-Valued Refined Neutrosophic Logic and Its Applications in Physics. Progress in Physics, USA, Volume 4, PP: 143-146, 2013.

[5] Vasantha Kandasamy,W.B; Smarandache,F; Neutrosophic Rings" Hexis, Phoenix, Arizona, http://fs.gallup.unm.edu/NeutrosophicRings.pdf, 2006.

[6] Zeina, M., Abobala, M; On The Refined Neutrosophic Real Analysis Based on Refined Neutrosophic Algebraic AH-Isometry", Neutrosophic Sets and Systems, Volume 54, PP: 158-168, 2023.

[7] Agboola, A.A.A.; Akinola, A.D; Oyebola, O.Y; Neutrosophic Rings I. Int. J. of Math. Comb, Volume 4, PP:1-14, 2011.

[8] Celik, M., and Hatip, A; On the Refined AH-Isometry and Its Applications in Refined Neutrosophic Surfaces. Galoitica Journal of Mathematical Structures and Applications, 2022.

[9] Alhasan, Y; The neutrosophic integrals and integration methods. Neutrosophic Sets and Systems, Volume 43, PP: 290-301, 2021.

[10] Alhasan, Y; The definite neutrosophic integrals and its applications. Neutrosophic Sets and Systems, Volume 49, PP: 277-293, 2022.

[11] Smarandache, F; Neutrosophic Precalculus and Neutrosophic Calculus. Book, 2015.

[12] Celik, M., and Hatip, A; On the Refined AH-Isometry and Its Applications in Refined Neutrosophic Surfaces. International Journal of Neutrosophic Science, Volume 2, Issue 1, PP: 21-28, 2022.

[13] Alhasan, Y; Ahmed, M; Abdulfatah, R; Sheen, S; The refined indefinite neutrosophic integral, Neutrosophic Sets and Systems, Vol. 67, 127- 134, 2024.

[14] Alhasan, Y; Mohamed, M; Abdulfatah, R; The limits of 2- refined neutrosophic, Neutrosophic Sets and Systems, Vol. 68, 39-49, 2024.

[15] Smarandache, F; Abobala, M; Operations with n-Refined Literal Neutrosophic Numbers using the Identification Method and the n-Refined AH-Isometry, Neutrosophic Sets and Systems, Vol. 70, 350-358, 2024.

Received: April 10, 2024. Accepted: Aug 24, 2024

Neutrosophic Sets and Systems, Vol.72, 2024
University of New Mexico

A Novel and an Efficient CODAS Technique to Solve Real-Life MAGDM Problems in Fermatean Neutrosophic Environment

S. Bhuvaneshwari[1], C. Antony Crispin Sweety[2], Akanksha Singh[3], Said Broumi [4,5,*], Mohamed Talea[4], Prasanta Kumar Raut[6]

[1,2] Avinashilingam Institute for Home Science and Higher Education for Women, Coimbatore, Tamil Nadu, India. [1]bhuvaneswari_maths@avinuty.ac.in, [2]riosweety@gmail.com

[3] Department of Mathematics, UIS, Chandigarh University, Gharuan, Mohali, India, akanksha.e10462@cumail.in

[4] Laboratory of Information Processing, Faculty of Science Ben M'Sik, University of Hassan II, Casablanca, Morocco. broumisaid78@gmail.com

[5] STIE team, Regional Center for the Professions of Education and Training (C.R.M.E.F), Casablanca- Settat, Morocco.

[6] Trident Academy of Technology, Bhubaneswar, Odisha, India. prasantaraut95@gmail.com

***** broumisaid78@gmail.com

Abstract: As a generalization of fuzzy sets and intuitionistic fuzzy sets, neutrosophic sets, and their combinations have been developed to represent uncertain, imprecise, incomplete, and inconsistent information existing in the real world. A neutrosophic set has the potential to be a general framework for uncertainty analysis in various spectra. On the other hand, the idea of Fermatean neutrosophic sets (FNSs) is the hybrid model of Fermatean fuzzy sets and neutrosophic sets, developed to enable the analytical management of ambiguous data from relatively typical real-world decision-making scenarios. In this work, we develop an algorithm to compare the Fermatean neutrosophic set and the neutrosophic set, Fermatean Neutrosophic Weighted Arithmetic Mean (FNWAM) and Fermatean Neutrosophic Weighted Geometric Mean (FNWGM) operators as an accuracy function in addition to the conventional aggregating operators are designed. Further, the CODAS technique for Multiple Attribute Group Decision Making (MAGDM) problems according to the defined operators is proposed. Additionally, to make a clear understanding of the presented study, a university faculty selection problem is studied to illustrate the proposed methodology. Finally, the results of the above two sets prove the authenticity of this study.

Keywords: Fermatean Neutrosophic Set (FNS); Multi-Criteria Decision Making (MCDM); Multiple Attribute Group Decision Making ; Decision Matrix (D-Mx); Negative Ideal Solution (NIS); Positive Ideal Solution (PIS); FNWAM; FNWGM; Score function (SF); Accuracy Function (AF).

1. Introduction

Zadeh proposed his remarkable theory of fuzzy sets (FSs) in 1965 [22] to encounter different types of uncertainties. This novel concept is used successfully in modeling uncertainty in many fields of real life. A fuzzy set is characterized by a membership function μ with the range [0,1]. Further generalization of this fuzzy set was made by K. Atanassov [2] in 1986, which is known as Intuitionistic fuzzy sets (IFS). In IFS, instead of one membership grade, there is also a non-membership grade attached to each element. Further, there is a restriction that the sum of these two grades is less or equal to unity. In IFS the degree of non-belongingness is not independent but it is

dependent on the degree of belongingness. IFS can handle imprecise data both complete and incomplete.

Recently a new theory has been introduced which is known as neutrosophic logic and sets. The term neutrosophy means knowledge of neutral thought and this neutral represents the main distinction between fuzzy and intuitionistic fuzzy logic and set. Neutrosophic logic was introduced by Florentin Smarandache [17]. It is a logic in which each proposition is estimated to have a degree of truth (T), a degree of indeterminacy (I), and a degree of falsity (F). A Neutrosophic set is a set where each element of the universe has a degree of truth, indeterminacy, and falsity respectively, and which lies between [0, 1], the non-standard unit interval. Neutrosophic sets have been successfully applied in different fields, including decision-making problems [9-10]. In the extent of natural science, operations research, economics, management science, military affairs, and urban planning, NSs have a broad application. They also can be applied to decision-making problems when the ambiguity and complexity of the attributes make the problems impossible to express or value with real numbers.

Since the neutrosophic set is difficult to be directly used in real-life applications. In 2005, Smarandache and Wang et al. [19], proposed the concept of a single-valued neutrosophic set. Here the degree of truth, indeterminacy, and falsity respectively of any element of a neutrosophic set lies in the standard unit interval [0, 1]. The single-valued neutrosophic set is a generalization of the classical set, fuzzy set, intuitionistic fuzzy set paraconsistent sets, etc. and hence has many broad perspectives for dealing with the real-world problems. Singh et.al. have solved many real-life problems in neutrosophic environment that delas with neutrosophic transportation linear programming problems [15], neutrosophic non-linear programming problems [12], fully neutrosophic linear programming problems [16]. Singh and Bhat have proposed novel score and accuracy functions for neutrosophic sets [14]. Also, Singh [13] has proposed a novel Dijkstra algorithm for finding shortest route problem.

In 2020, Senapati and Yager [11] established a new extension of fuzzy sets named Fermatean fuzzy sets. Some important studies on Fermatean fuzzy sets for Multi-Criteria Decision Making (MCDM) problems have been conducted by various researchers like Chinnadurai et.al. [6] used complex Fermatean fuzzy sets to solve MCDM problems, Ganie [7] has solved MCDM problems using distance and knowledge measure in Fermatean fuzzy sets environment. Xu and Shen [20] solved MCDM problems by using similarity measures of Fermatean fuzzy sets for pattern recognition. By extending Fermatean fuzzy sets, Antony and R. Jansi [1] presented the concept of FNSs. FNSs are specific types of neutrosophic sets that are used to model uncertainty, indeterminacy, and incomplete information in decision-making processes [3-5]. It also presents a thorough comparison of the Fermatean neutrosophic set with the neutrosophic sets.

Some significant Highlights of the work

- In addition to the standard aggregating operators, FNWGM and FNWAM operations are created as accuracy functions.
- It is suggested to use the CODAS approach for the Multiple Attribute Group Decision Making issue using the described operators.
- To demonstrate the suggested methods, a faculty selection problem at a university is examined. Ultimately, the findings from the first two sets demonstrate the validity of this research.
- The outcome leads us to the conclusion that, in comparison to neutrosophic sets, FNSs yield more accurate results.

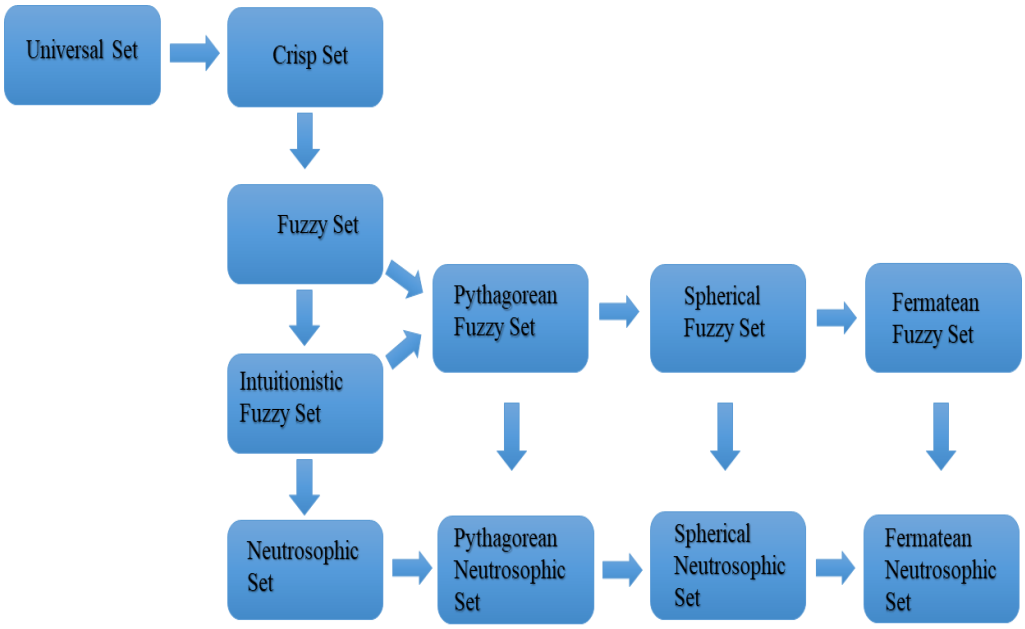

Fig.1 Extensions of FNSs

2. Preliminaries

Some basic definitions are required for better understanding of the proposed work so are presented as follows:

Definition 2.1 [22]: Let X be a nonempty set. A fuzzy set A drawn from X is defined as$A = \{\langle x, \mu_A(x)\rangle | x \in X\}$ where $\mu_A: X \to [0,1]$ is the membership function of the fuzzy set A.

Definition 2.2 [2]: Let X be a universe. An intuitionistic fuzzy set A on X can be defined as follows: $A = \{\langle x, \mu_A(x), \nu_A(x)\rangle | x \in X\}$, where $\mu_A: X \to [0,1]$ is the degree of membership and and $\nu_A: X \to [0,1]$ is the degree of non- membership of the element x such that $0 \leq \mu_A(x) + \nu_A(x) \leq 1$ for any $x \in X$.

Definition 2.3 [17]: Let X be a universe set. A Neutrosophic Set (NS) A in X is characterized by a truth membership functionT_A, an indeterminacy membership function I_A and a falsity membership function $F_A$where T_A , I_A and F_A are real standard elements of [0,1]. It can be written as $A = \{\langle X, (T_A(x)) + (I_A(x)) + (F_A(x))\rangle : x \in E, T_A, I_A, F_A \in]^-0, 1^+[\}$. There is no restriction on the sum of $(T_A(x)), (I_A(x))$and $(F_A(x))$ as $0^- \leq (T_A(x)) + (I_A(x)) + (F_A(x)) \leq 3^+$.

Definition 2.4 [18]: Let $A = \{\langle x, T_A(x), I_A(x), F_A(x)\rangle | x \in X\}$, and $B = \{\langle x, T_B(x), I_B(x), F_B(x)\rangle | x \in X\}$ are any two neutrosophic sets of a not empty (universe) X on which axioms are defined as follows:

a. $(A) \subseteq (B) iff T_A(x) \leq T_B(x); I_A(x) \leq I_B(x); and F_A(x) \geq F_B(x)$
b. $(A) = (B) iff T_A(x) = T_B(x); I_A(x) = I_B(x); and F_A(x) = F_B(x) \forall x \in X$
c. $A \cap B = \{\langle x, T_{A\cap B}(x), I_{A\cap B}(x), F_{A\cap B}(x)\rangle | x \in X\}$ where,
   i. $T_{A\cap B}(x) = min\{T_A(x), T_B(x)\}$
   ii. $I_{A\cap B}(x) = min\{I_A(x), I_B(x)\}$
   iii. $F_{A\cap B}(x) = max\{F_A(x), F_B(x)\}$
d. $A \cup B = \{\langle x, T_{A\cup B}(x), I_{A\cup B}(x), F_{A\cup B}(x)\rangle | x \in X\}$ where,
   i. $T_{A\cup B}(x) = max\{T_A(x), T_B(x)\}$
   ii. $I_{A\cup B}(x) = max\{I_A(x), I_B(x)\}$
   iii. $F_{A\cup B}(x) = min\{F_A(x), F_B(x)\}$

Let $A = \{\langle x, T_A(x), I_A(x), F_A(x)\rangle | x \in X\}$ be a neutrosophic set on X , then the complement of the set A ($C(A)$ for short), maybe defined as $C(A) = \{\langle x, F_A(x), 1 - I_A(x), T_A(x)\rangle | x \in X\}$.

Definition 2.5.[19]: Consider X be a set that is not empty (universe). A single-valued neutrosophic set (SVNS) A in X is a neutrosophic set which is of the form

$$A = \{\langle x: (T_A(x)) + (I_A(x)) + (F_A(x))\rangle, x \in X\}$$

that is characterized by the degree of membership (namely $(T_A(x))$, the degree of indeterminacy (namely $(I_A(x))$ and the degree of non-membership (namely $(F_A(x))$, where $T_A(x), I_A(x), F_A(x) \in [0,1]$ such that $0 \leq (T_A(x)) + (I_A(x)) + (F_A(x)) \leq 3$, for all $x \in X$, respectively. For X, $SVNS(X)$ denotes the collection of all single valued neutrosophic sets of X.

Definition 2.6. [21]: Let X be a non-empty set (universe). A Pythagorean set A on X is defined as $A = \{\langle x, T_A(x), I_A(x), F_A(x)\rangle | x \in X\}$, where $T_A(x), I_A(x), F_A(x) \in [0,1]$, $0 \leq T_A(x) + I_A(x) + F_A(x) \leq 2$, for every x in X. $T_A(x)$ is the degree of membership, $I_A(x)$ is the degree of indeterminacy and $F_A(x)$ is the degree of non-membership. Here $T_A(x)$ *and* $F_A(x)$ are dependent components and $I_A(x)$ is an independent component.

Definition 2.7. [8]: Consider X be a set that is not empty (universe). A Pythagorean Neutrosophic Set (PNS) A on X is defined as $A = \{\langle x, T_A(x), I_A(x), F_A(x)\rangle | x \in X\}$, where $T_A(x)$ is the degree of membership, $I_A(x)$ is the degree of indeterminacy, $F_A(x)$ is the degree of non- membership, and $T_A(x), I_A(x), F_A(x) \in [0,1]$, $0 \leq (T_A(x))^2 + (I_A(x))^2 + (F_A(x))^2 \leq 2$, for every $x \in X$. Here $T_A(x)$ *and* $F_A(x)$ are dependent components and $I_A(x)$ is an independent.

3. Fermatean Neutrosophic set (FNS) [11]

The cube sum of the parameters in FNS can range between 0 and 2, and it is possible to define each of them individually between 0 and 1 independently. In this section, the explanation of FNS and overview of Fermatean distance measurement, arithmetic operation and aggregation and de-neutrosophication processes are provided.

Definition 3.1: Let X be a non-empty set (universe). A Fermatean neutrosophic set (FNS) $\tilde{S}$ on X is an object of the form:

$\tilde{S} = \{< s, (T_{\tilde{S}}(s), I_{\tilde{S}}(s), F_{\tilde{S}}(s)) > | s \in X\}$ (1) where,

$T_{\tilde{S}}(s), I_{\tilde{S}}(s), F_{\tilde{S}}(s): X \to [0,1]$, $0 \leq {T_{\tilde{S}}}^3(s) + {F_{\tilde{S}}}^3(s) \leq 1, 0 \leq {I_{\tilde{S}}}^3(s) \leq 1$ then

$0 \leq {T_{\tilde{S}}}^3(s) + {I_{\tilde{S}}}^3(s) + {F_{\tilde{S}}}^3(s) \leq 2 \; \forall \; s \in X$ (2)

and $T_{\tilde{S}}(s)$ is the degree of membership, $I_{\tilde{S}}(s)$ is the degree of inderminancy and $F_{\tilde{S}}(s)$ is the degree of non-membership. Here $T_{\tilde{S}}(s)$ and $F_{\tilde{S}}(s)$ are dependent components and $I_{\tilde{S}}(s)$ is an independent component.

Definition 3.2. Let $\tilde{A} = \{\langle x, T_{\tilde{A}}(x), I_{\tilde{A}}(x), F_{\tilde{A}}(x)\rangle | x \in X\}$ and $\tilde{B} = \{\langle x, T_{\tilde{B}}(x), I_{\tilde{B}}(x), F_{\tilde{B}}(x)\rangle | x \in X\}$ are any two Fermatean neutrosophic sets (FNSs). The basic operational laws of FNSs are defined below:

$$\tilde{A} \oplus \tilde{B} = \left\{ \left({T_{\tilde{A}}}^3 + {T_{\tilde{B}}}^3 - {T_{\tilde{A}}}^3 {T_{\tilde{B}}}^3 \right)^{\frac{1}{3}}, I_{\tilde{A}} I_{\tilde{B}}, \left(\left(1 - {T_{\tilde{B}}}^3\right) {F_{\tilde{A}}}^3 + \left(1 - {I_{\tilde{A}}}^3\right) {F_{\tilde{B}}}^3 - {F_{\tilde{A}}}^3 {F_{\tilde{B}}}^3 \right)^{\frac{1}{3}} \right\} \quad (3)$$

$$\tilde{A} \otimes \tilde{B} = \left\{ (T_{\tilde{A}} T_{\tilde{B}}), \left(I_{\tilde{A}}^3 + I_{\tilde{B}}^3 - I_{\tilde{A}}^3 I_{\tilde{B}}^3 \right)^{\frac{1}{3}}, \left(\left(1 - I_{\tilde{B}}^3\right) F_{\tilde{A}}^3 + \left(1 - I_{\tilde{A}}^3\right) F_{\tilde{B}}^3 - F_{\tilde{A}}^3 F_{\tilde{B}}^3 \right)^{\frac{1}{3}} \right\} \quad (4)$$

$$\lambda \bullet \tilde{A} = \left\{ \left(1 - \left(1 - {T_{\tilde{A}}}^3\right)^{\lambda} \right)^{\frac{1}{3}}, {I_{\tilde{A}}}^{\lambda}, \left(\left(1 - {T_{\tilde{A}}}^3\right)^{\lambda} - \left(1 - {T_{\tilde{A}}}^3 - {F_{\tilde{A}}}^3\right)^{\lambda} \right)^{\frac{1}{3}} \right\} \quad (5)$$

$$\tilde{A}^{\lambda} = \left\{ {T_{\tilde{A}}}^{\lambda}, \left(1 - \left(1 - {I_{\tilde{A}}}^3\right)^{\lambda} \right)^{\frac{1}{3}}, \left(\left(1 - {I_{\tilde{A}}}^3\right)^{\lambda} - \left(1 - {I_{\tilde{A}}}^3 - {F_{\tilde{A}}}^3\right)^{\lambda} \right)^{\frac{1}{3}} \right\} \lambda \geq 0 \quad (6)$$

Definition 3.3. For any two FNSa $\tilde{M} = (T_{\tilde{M}}, I_{\tilde{M}}, F_{\tilde{M}})$and $\tilde{N} = (T_{\tilde{N}}, I_{\tilde{N}}, F_{\tilde{N}})$, some scalar operational laws are defined. Let $\lambda, \lambda_1, \lambda_2 > 0$are some scalars, the operational laws are as follows:

1. $\tilde{M} \oplus \tilde{N} = \tilde{N} \oplus \tilde{M}$ (7)
2. $\tilde{M} \otimes \tilde{N} = \tilde{M} \otimes \tilde{N}$ (8)
3. $\lambda(\tilde{M} \oplus \tilde{N}) = \lambda\tilde{M} \oplus \lambda\tilde{N}$ (9)
4. $\lambda_1\tilde{M} \oplus \lambda_2\tilde{M} = (\lambda_1 + \lambda_2)\tilde{M}$ (10)
5. $\left(\tilde{M} \otimes \tilde{N}\right)^{\lambda} = \tilde{M}^{\lambda} \otimes \tilde{N}^{\lambda}$ (11)
6. $\tilde{M}^{\lambda_1} \otimes \tilde{M}^{\lambda_2} = \tilde{M}^{\lambda_1 + \lambda_2}$ (12)

Definition 3.4. Let $\tilde{A}$ be a set defined on universe X for the weight vector, $= (z_1, z_2, z_3, \ldots . z_n)$; $z_j \in [0,1]; \sum_{j=1}^{n} z_j \leq 2$. A Fermatean neutrosophic weighted arithmetic mean

(FNWAM) is defined as:

$$FNWAM_z(\tilde{A}_1, \tilde{A}_2, \dots \tilde{A}_n) = z_1\tilde{A}_1 + z_2\tilde{A}_2 + z_3\tilde{A}_3 + \dots + z_n\tilde{A}_n$$
$$\left\{\left[1 - \prod_{j=1}^{n}\left(1 - T_{\tilde{A}}{}^3\right)^{z_j}\right]^{\frac{1}{3}}, \left[\prod_{j=1}^{n}(I_{\tilde{A}})^{z_j}\right]^{\frac{1}{3}}, \left[\prod_{j=1}^{n}\left(1 - T_{\tilde{A}}{}^3\right)^{z_j} - \prod_{j=1}^{n}\left(1 - T_{\tilde{A}}{}^3 - F_{\tilde{A}}{}^3\right)^{z_j}\right]^{\frac{1}{3}}\right\} \quad (13)$$

Definition 3.5. Let $\tilde{A}$ be a set defined on universe X for the weight vector, $= (z_1, z_2, z_3, \dots . z_n)$; $z_j \in [0,1]; \sum_{j=1}^{n} z_j \leq 2$. A Fermatean neutrosophic weighted geometric mean (FNWGM) is defined as

$$FNWGM_z(\tilde{A}_1, \tilde{A}_2, \dots \tilde{A}_n) = \tilde{A}_1{}^{z_1} + \tilde{A}_2{}^{z_2} + \tilde{A}_3{}^{z_3} + \dots + \tilde{A}_n{}^{z_n}$$
$$\left\{\prod_{j=1}^{n} T_{\tilde{A}}{}^{z_j}, \left[1 - \prod_{j=1}^{n}\left(1 - I_{\tilde{A}}{}^3\right)^{z_j}\right]^{\frac{1}{3}}, \prod_{j=1}^{n}\left(1 - I_{\tilde{A}}{}^3\right)^{z_j} - \prod_{j=1}^{n}\left(1 - I_{\tilde{A}}{}^3 - F_{\tilde{A}}{}^3\right)^{z_j}\right\} \quad (14)$$

Definition 3.6. Let $\tilde{S} = \{\langle x, T_{\tilde{S}}(x), I_{\tilde{S}}(x), F_{\tilde{S}}(x)\rangle | s \in X\}$ on X be any FNS, then a score function (SF) and accuracy function (AF) for FNS classification are defined as:

$$Score(\tilde{S}) = \left(T_{ijw} - F_{ijw}\right)^3 - \left(I_{ijw} - F_{ijw}\right)^3 \quad (15)$$

$$Accuracy(\tilde{S}) = T_{\tilde{S}}{}^3 + I_{\tilde{S}}{}^3 + F_{\tilde{S}}{}^3 \quad (16)$$

Definition 3.7. Let $\tilde{A} = \{\langle x, T_{\tilde{A}}(x), I_{\tilde{A}}(x), F_{\tilde{A}}(x)\rangle | x \in X\}$ and $\tilde{B} = \{\langle x, T_{\tilde{B}}(x), I_{\tilde{B}}(x), F_{\tilde{B}}(x)\rangle | x \in X\}$ are any two FNSs. For comparing any two FNSs, a comparison method is developed as follows:

- If $Score(\tilde{S})_{\tilde{A}} < Score(\tilde{S})_{\tilde{B}}$ then $\tilde{A} < \tilde{B}$
- If $Score(\tilde{S})_{\tilde{A}} > Score(\tilde{S})_{\tilde{B}}$ then $\tilde{A} > \tilde{B}$

If $Score(\tilde{S})_{\tilde{A}} = Score(\tilde{S})_{\tilde{B}}$ then check $Accuracy(\tilde{S})$ in the next step (17)

- If $Accuracy(\tilde{S})_{\tilde{A}} > Accuracy(\tilde{S})_{\tilde{B}}$ then $\tilde{A} > \tilde{B}$
- If $Accuracy(\tilde{S})_{\tilde{A}} < Accuracy(\tilde{S})_{\tilde{B}}$ then $\tilde{A} < \tilde{B}$
- If $Accuracy(\tilde{S})_{\tilde{A}} = Accuracy(\tilde{S})_{\tilde{B}}$ then $\tilde{A} = \tilde{B}$

4. Proposed CODA'S technique for MAGDM

A Decision Matrix (D-Mx) with entries that represent the assessment scores of every choice in relation to every criterion in a neutrosophic environment can be used to represent a multi-criteria decision making (MCDM) problem. Suppose that $S = \{s_1, s_2, s_3, \dots . s_m\} (m \geq 2)$ represents distinct collection of m possible options, and $K = \{K_1, K_2, K_3, \dots . K_n\}$ be the weight vector derived from every requirement that meet $0 \leq z_j \leq 1$ and $\sum_{j=1}^{n} z_j \leq 2$.

Step 1. Let D-Mx s use the linguistic terms (LT) listed in Table 1 to complete the assessment matrices for decisions and criteria.

Table 1. Terms used in linguistics and their associated Spherical Neutrosophic Number

LT		**(T, I, F)**
Probably More Significant	PMS	(0.95, 0.9, 0.4)
Extremely Significant	ES	(0.9, 0.8, 0.4)
High Priority	HP	(0.8, 0.9, 0.5)
Relatively Greater Significance	RGS	(0.7, 0.9, 0.6)
Equally Important	EI	(0.6, 0.8, 0.6)
Very Minimal Significance	VMS	(0.6, 0.8, 0.7)
Low Priority	LP	(0.5, 0.7, 0.8)

extremely low significant	ELS	(0.5, 0.5, 0.9)
Definitely Not Important	DNI	(0.4, 0.5, 0.95)

Step 2. Aggregate the outcomes reached by D-Mx using FNWAM. Aggregate the DMs' Fermatean Neutrosophic linguistic judgements of the selection criteria. Assemble neutrosophic D-Mx based on Decision Makers' views. Indicate the alternative's evaluation value $S_i(i = 1,2,\dots m)$ with respect to criterion $K_j(j = 1,2\dots n)$ by $K_j(\tilde{S}_i) = (T_{ij}, I_{ij}, F_{ij})$ and $D = \left(K_j(\tilde{S}_i)\right)_{m\times n}$ is a Fermatean Neutrosophic Decision Matrix (FN D-Mx). D-Mx for MCDM problem using FNS, $D = \left(K_j(\tilde{S}_i)\right)_{m\times n}$ must be put together as shown in equation (18).

$$D = \left(K_j(\tilde{S}_i)\right)_{m\times n} = \begin{pmatrix} (\tilde{T}_{11}, \tilde{I}_{11}, \tilde{F}_{11}) & (\tilde{T}_{12}, \tilde{I}_{12}, \tilde{F}_{12}) & \dots & (\tilde{T}_{1n}, \tilde{I}_{1n}, \tilde{F}_{1n}) \\ (\tilde{T}_{21}, \tilde{I}_{21}, \tilde{F}_{21}) & (\tilde{T}_{22}, \tilde{I}_{22}, \tilde{F}_{22}) & \dots & (\tilde{T}_{2n}, \tilde{I}_{2n}, \tilde{F}_{2n}) \\ \vdots & \vdots & \dots & \vdots \\ (\tilde{T}_{m1}, \tilde{I}_{m1}, \tilde{F}_{m1}) & (\tilde{T}_{m2}, \tilde{I}_{m2}, \tilde{F}_{m2}) & \dots & (\tilde{T}_{mn}, \tilde{I}_{mn}, \tilde{F}_{mn}) \end{pmatrix} \quad (18)$$

Step 3. Following the determination of the alternative ratings and the weights assigned to the criteria, the aggregated weighted FN D-Mx is built using multiplication equation and then the aggregated weighted FN D-Mx can be defined as follows:

$$D = \left(K_j(\tilde{S}_{iz})\right)_{m\times n} = \begin{pmatrix} (T_{11z}, I_{11z}, F_{11z}) & (T_{12z}, I_{12z}, F_{12z}) & \dots & (T_{1nz}, I_{1nz}, F_{1nz}) \\ (T_{21z}, I_{21z}, F_{21z}) & (T_{22z}, I_{22z}, F_{22z}) & \dots & (T_{2nz}, I_{2nz}, F_{2nz}) \\ \vdots & \vdots & \dots & \vdots \\ (T_{m1z}, I_{m1z}, F_{m1z}) & (T_{m2z}, I_{m2z}, F_{m2z}) & \dots & (T_{mnz}, I_{mnz}, F_{mnz}) \end{pmatrix} \quad (19)$$

Step 4. De-neutrosophication of the aggregated weighted D-Mx is done by utilizing below given equation,

$$Score\left(K_j(\tilde{S}_{iz})\right) = \left(T_{ijz} - F_{ijz}\right)^3 - \left(I_{ijz} - F_{ijz}\right)^3 \quad (20)$$

de-neutrosophication of the aggregated weighted D-Mx is done.

Step 5. Using SF acquired in Step 4, find the Fermatean Neutrosophic positive ideal solution (FN-PIS) as follows:

$$S^* = \left\{K_j, \max_i \left\langle Score\left(K_j(S_{iz})\right)\right\rangle | j = 1,2,\dots n\right\} \quad (21)$$

$$S^* = \{\langle K_1, (T_1{}^*, I_1{}^*, F_1^*)\rangle, \langle K_2, (T_2{}^*, I_2{}^*, F_2^*)\rangle, \dots \langle K_n, (T_n{}^*, I_n{}^*, F_n^*)\rangle\}$$

and Fermatean Neutrosophic negative ideal solution (FN-NIS) as follows:

$$S^- = \left\{K_j, \min_i \left\langle Score\left(K_j\left(S_{iz}\right)\right)\right\rangle | \ j = 1,2,\dots n\right\} \quad (22)$$

$$S^- = \{\langle K_1, (T_1{}^-, I_1{}^-, F_1^-)\rangle, \langle K_2, (T_2{}^-, I_2{}^-, F_2^-)\rangle, \dots \langle K_n, (T_n{}^-, I_n{}^-, F_n^-)\rangle\}$$

Step 6. The distances between alternative S_i, FN-NIS, and FN-PIS is calculated, accordingly.
For the FN-NIS:

$$D(S_i, S^-) = \sqrt{\frac{1}{3}\sum_{i=1}^{n}\left(\left(T_{S_i}{}^3 - T_{S^-}{}^3\right)^2 + \left(I_{S_i}{}^3 - I_{S^-}{}^3\right)^2 + \left(F_{S_i}{}^3 - F_{S^-}{}^3\right)^2\right)} \quad (23)$$

For the FN-PIS:

$$D(S_i, S^*) = \sqrt{\frac{1}{3}\sum_{i=1}^{n}\left(\left({T_{S_i}}^3 - {T_{S^*}}^3\right)^2 + \left({I_{S_i}}^3 - {I_{S^*}}^3\right)^2 + \left({F_{S_i}}^3 - {F_{S^*}}^3\right)^2\right)} \quad (24)$$

Step 7. Calculate the minimum and maximum distances to the FN-NIS and FN-PIS, respectively.

$$D_{max}(S_i, S^-) = \max_{i \le i \le m}(S_i, S^-) \quad (25)$$

$$D_{min}(S_i, S^*) = \min_{i \le i \le m}(S_i, S^*). \quad (26)$$

Step 8. Compute the revised proximity ratio using equation given below:

$$\xi(S_i) = \frac{D(S_i, S^-)}{D_{max}(S_i, S^-)\frac{D(S_i, S^*)}{D_{min}(S_i, S^*)}} \quad (27)$$

In equation (27) the subtraction's second element must be at least equal to its first element, then only the result is zero or negative. So, Equation (27) is altered to Equation (28) to obtain result as zero

$$\xi(S_i) = \frac{D(S_i, S^*)}{D_{min}(S_i, S^*)\frac{D(S_i, S^-)}{D_{max}(S_i, S^-)}} \quad (28)$$

Step 9. Determine the best solution by rating the alternatives in the best possible order. The alternatives are organized according to the rising closeness ratio.

5. Application on Fermatean Neutrosophic set

Consider the evaluation of university professors for tenure and promotions. The criteria used at some universities are teaching, research, service and social participation. Weights must be determined for these criteria, and the candidates must also be evaluated with regard to each criterion. Let us consider any four criteria, say Teaching ($K1$), Research ($K2$), Service ($K3$), Social Participation ($K4$), and ten faculty members ($S1$, $S2$, $S3$, $S4$, $S5$, $S6$, $S7$, $S8$, $S9$, $S10$). Let an evaluation committee of 03 decision makers (ĐM1, ĐM2, and ĐM3) is constituted who has an experience with the university faculty selection. The weights of the D-Mx, are considered as 0.4, 0.5 and 0.3 representing their level of experience respectively.

Firstly, the judgements made by the decision-makers with regard to the objective are compiled using the language phrases as presented in Section 4, Step-1, then onwards every decision is rendered from Tables 2 to Table 4, as given below:

Table 2. Decisions of ĐM1

ĐM1	(K_1)	(K_2)	(K_3)	(K_4)
S_1	ES	HP	EI	RGS
S_2	PMS	ES	HP	EI
S_3	LP	VMS	ES	ELS
S_4	EI	ELS	LP	DNI
S_5	VMS	ELS	HP	HP
S_6	LP	EI	ES	HP
S_7	HP	RGS	RGS	ELS
S_8	VMS	LP	HP	EI
S_9	LP	VMS	HP	PMS
S_{10}	PMS	RGS	HP	VMS

Table 3. Decisions of ĐM2

ĐM2	(K_1)	(K_2)	(K_3)	(K_4)
S_1	PMS	HP	LP	PMS
S_2	VMS	LP	HP	EI
S_3	HP	RGS	RGS	ELS
S_4	ELS	EI	LP	ES
S_5	ES	HP	EI	RGS
S_6	PMS	ES	HP	EI
S_7	VMS	ELS	HP	HP
S_8	LP	EI	ES	HP
S_9	LP	VMS	HP	ELS
S_{10}	VMS	ES	ELS	DNI

Table 4. Decisions of ĐM3

ĐM3	(K_1)	(K_2)	(K_3)	(K_4)
S_1	HP	ES	PMS	RGS

S_2	VMS	PMS	ES	VMS
S_3	VMS	ELS	HP	HP
S_4	LP	EI	ES	HP
S_5	VMS	LP	HP	EI
S_6	LP	VMS	HP	PMS
S_7	HP	RGS	RGS	ELS
S_8	ELS	EI	LP	ES
S_9	ES	HP	EI	RGS
S_{10}	PMS	ES	HP	EI

The significance levels of the DMs are considered when combining these judgements utilizing the FNWAM and FNWGM operators. The decision matrices shown in Tables 5 and 6 are obtained.

Table 5. FND-Mx by using FNWAM operator

Alternatives	(K_1)	(K_2)	(K_3)	(K_4)
S_1	0.27312 0.8406786 0.4130087	0.864289 0.850639 0.47017	0.807666 0.74141 0.629188	0.87753 0.88123 0.5294
S_2	0.20744 0.8019901 0.5747402	0.883933 0.741409 0.54257	0.864289 0.85064 0.470173	0.63267 0.76508 0.69
S_3	0.12813 0.7692854 0.6704603	0.664564 0.704771 0.75931	0.849157 0.84068 0.502306	0.65805 0.51921 0.853
S_4	0.07608 0.735039 0.7249439	0.603416 0.633957 0.78606	0.73719 0.67845 0.704012	0.83928 0.65676 0.6858
S_5	0.18699 0.765082 0.567264	0.713852 0.646009 0.75498	0.774253 0.83083 0.548577	0.68754 0.85064 0.6477
S_6	0.21868 0.7390773 0.5906023	0.824727 0.765082 0.53741	0.87323 0.84068 0.460059	0.85704 0.83083 0.5568
S_7	0.15471 0.8308349 0.5935959	0.671578 0.656833 0.78389	0.782646 0.88123 0.565592	0.71385 0.58398 0.8056
S_8	0.07036 0.7156687 0.7658741	0.603416 0.725289 0.70888	0.854821 0.7705 0.533136	0.82992 0.81149 0.545
S_9	0.13354 0.6784459 0.7040125	0.706234 0.792599 0.66539	0.80032 0.85064 0.529397	0.83358 0.65683 0.7063
S_{10}	0.25783 0.8308349 0.4856471	0.888984 0.80199 0.45308	0.757056 0.65683 0.723123	0.56883 0.60485 0.8754

Table 6. FN D-Mx by using FNWGM operator

Alternatives	(K_1)	(K_2)	(K_3)	(K_4)

S_1	0.8739484 0.9167447 0.0386399	0.7925994 0.92232 0.0145842	0.5676264 0.949417 0.36485	0.7593298 0.9369043 0.2109124
S_2	0.6510442 0.8480513 0.1041311	0.6675735 0.8557976 0.0717245	0.7925994 0.9734057 0.2443212	0.5417283 0.8362945 0.3582132
S_3	0.5815384 0.8638603 0.0528844	0.5539882 0.8515889 0.0591803	0.750193 0.9714403 0.1814646	0.5930127 0.8901439 0.2742413
S_4	0.4682055 0.7684854 0.1290153	0.503627 0.8087295 0.0814144	0.5192132 0.9249037 0.4498819	0.6149959 0.8301354 0.4744039
S_5	0.6634789 0.874405 0.6335135	0.5505845 0.8266696 0.6951435	0.6625804 0.8962461 0.5247078	0.4962624 0.9089642 0.559875
S_6	0.5999856 0.8874495 0.6464972	0.6634789 0.8326255 0.590631	0.8019901 0.9028368 0.4818561	0.6976357 0.8962461 0.5059124
S_7	0.6625804 0.9219875 0.5657301	0.5508757 0.8549678 0.6874469	0.6968088 0.9249327 0.5412399	0.5505845 0.8071637 0.7209706
S_8	0.494528 0.8460034 0.7318585	0.503627 0.8061146 0.679085	0.7047714 0.8593818 0.5812094	0.7064448 0.8814948 0.5187233
S_9	0.5192132 0.822129 0.7468214	0.5905588 0.8642892 0.634654	0.701821 0.9089642 0.5055983	0.5262504 0.8549678 0.6617572
S_{10}	0.7472779 0.9219875 0.5356048	0.7969539 0.8732296 0.5607912	0.6048504 0.8549678 0.6508325	0.4423193 0.7570557 0.8065158

Now, to display the important weights of the language phrases used to express the criteria determined by DMs are given below in the Table 7

Table 7. The weights assigned to each criterion

Criteria	DM1	DM2	DM3
(K_1)	LP	VMS	HP
(K_2)	RGS	EI	RGS
(K_3)	PMS	RGS	HP
(K_4)	HP	HP	VMS

As the weights assigned to the criteria and evaluations of the substitutions have been determined, then the aggregated weighted Frematean Neutrosophic choice matrices are constructed using Equation (4), as illustrated in Tables 8 and 9 given below:

Table 8. Weighted FN D-Mx according to FNWAM operator

Alternatives	(K_1)	(K_2)	(K_3)	(K_4)
S_1	0.599732 0.9696	0.5532716 0.97272	0.50402 0.9661945	0.4858238 0.9798257

	0.2378533	0.2228067	0.2522586	0.1877903
S_2	0.446768 0.9593 0.2620644	0.4659976 0.95282 0.2926157	0.7037833 0.9803937 0.1935042	0.4335559 0.9566684 0.2858825
S_3	0.399071 0.9577 0.2640716	0.3867098 0.95739 0.2639464	0.6661288 0.9791279 0.1960074	0.4011101 0.9347745 0.3467808
S_4	0.351964 0.9409 0.3182602	0.3515553 0.93619 0.3394726	0.4610319 0.9525171 0.2989162	0.4921935 0.9537692 0.2893229
S_5	0.128316 0.9052 0.4315658	0.4983021 0.90528 0.425867	0.6874925 0.9647806 0.2634483	0.5502502 0.9610388 0.2674005
S_6	0.150066 0.8958 0.4516889	0.5756981 0.93358 0.3706279	0.7753783 0.9666839 0.2596971	0.6859033 0.956238 0.2925744
S_7	0.106169 0.9301 0.3636541	0.4687926 0.90769 0.4157295	0.6949454 0.9747206 0.2182882	0.5713099 0.9043526 0.4271843
S_8	0.048287 0.8875 0.4542645	0.4212124 0.92369 0.3804751	0.7590325 0.9535271 0.306038	0.6642016 0.9516355 0.3096972
S_9	0.091641 0.8746 0.487558	0.4929843 0.94067 0.3318198	0.7106386 0.9686287 0.24833	0.6671278 0.9180629 0.3994349
S_{10}	0.176931 0.9301 0.3733505	0.6205529 0.94313 0.3482501	0.6722225 0.9343263 0.3579231	0.4552487 0.9081359 0.4132314

Table 9. Weighted FN D-Mx according to FNWGM operator

Alternatives	(K_1)	(K_2)	(K_3)	(K_4)
S_1	0.599732 0.9696 0.2378533	0.5532716 0.97272 0.2228067	0.50402 0.9661945 0.2522586	0.4858238 0.9798257 0.1877903
S_2	0.446768 0.9593 0.2620644	0.4659976 0.95282 0.2926157	0.7037833 0.9803937 0.1935042	0.4335559 0.9566684 0.2858825
S_3	0.399071 0.9577 0.2640716	0.3867098 0.95739 0.2639464	0.6661288 0.9791279 0.1960074	0.4011101 0.9347745 0.3467808
S_4	0.351964 0.9409 0.3182602	0.3515553 0.93619 0.3394726	0.4610319 0.9525171 0.2989162	0.4921935 0.9537692 0.2893229
S_5	0.455301 0.9474 0.3038595	0.3843338 0.9497 0.2936334	0.5883338 0.9777741 0.2052041	0.3971687 0.9756863 0.2079718
S_6	0.41173 0.9526 0.2826554	0.4631394 0.95131 0.3033269	0.7121217 0.9791279 0.2004881	0.5583317 0.9724287 0.2288113

S_7	0.454685 0.9668 0.2342095	0.3845371 0.95743 0.2624053	0.6187267 0.983725 0.169682	0.4406437 0.9506175 0.3007638
S_8	0.339362 0.9361 0.3291924	0.3515553 0.94422 0.3171253	0.625797 0.9703515 0.2379528	0.5653818 0.9686945 0.2450548
S_9	0.356301 0.9268 0.3560827	0.4122377 0.96002 0.2602199	0.6231772 0.9803937 0.1920993	0.4211687 0.9621 0.2618756
S_{10}	0.512807 0.9668 0.2385146	0.5563112 0.96252 0.2609107	0.5370728 0.9694799 0.2376378	0.3539969 0.939153 0.3321644

Now, the SF for the Tables 8 and Table 9, are calculated using Equation (19), and are illustrate below in Tables 10 and 11:

Table 10. SF according to FNWAM operator

Alternatives	(K_1)	(K_2)	(K_3)	(K_4)
S_1	-0.102696624	-0.0970618	-0.07354798	-0.1199294
S_2	-0.108987271	-0.0440079	-0.12045131	-0.0528184
S_3	-0.152202584	-0.0254067	-0.11598152	-0.0127956
S_4	-0.203787216	-0.0242385	-0.05676854	-0.0322167
S_5	-0.116205997	-0.018027	-0.12084457	-0.0906297
S_6	-0.106870937	-0.0514848	-0.11371195	-0.0901128
S_7	-0.130865281	-0.0199341	-0.14220281	-0.0168308
S_8	-0.227415649	-0.0339416	-0.08437937	-0.0856538
S_9	-0.177373815	-0.0485612	-0.12900768	-0.0305925
S_{10}	-0.1011057	-0.0712032	-0.05027061	-0.0208083

Table 11. SF according to FNWGM operator

Alternatives	(K_1)	(K_2)	(K_3)	(K_4)
S_1	-0.132904692	-0.1490711	-0.11516239	-0.1799611
S_2	-0.077655645	-0.0714967	-0.17934191	-0.0863273
S_3	-0.071635948	-0.0738806	-0.16560057	-0.0407079
S_4	-0.050781853	-0.0501121	-0.06871214	-0.0640134
S_5	-0.053462748	-0.0610407	-0.18135355	-0.1538215
S_6	-0.061277311	-0.0732582	-0.17167781	-0.1544827
S_7	-0.102629021	-0.0730339	-0.1970089	-0.0607866

S_8	-0.048977168	-0.0596674	-0.13723765	-0.1384089
S_9	-0.041574044	-0.0845966	-0.19297989	-0.0903405
S_{10}	-0.10844757	-0.10184	-0.121563	-0.0490283

The FN-PIS and FN-NIS corresponding to the highest and worst scores are shown in Tables 12 and 13.

Table 12. FN-PIS and FN-NIS according to FNWAM operator

Alternatives	(K_1)	(K_2)	(K_3)	(K_4)
S^* (Best)	0.176931 0.9103 0.5100636	0.4983021 0.88301 0.633333	0.6722225 0.9180678 0.5439011	0.5266505 0.8747414 0.6542648
S^- (Worst)	0.048287 0.8596 0.6503624	0.6033144 0.94205 0.4795027	0.6949454 0.9656181 0.4191644	0.7023054 0.9577875 0.4414136

Table 13. FN-PIS and FN-NIS according to FNWGM operator

Alternatives	(K_1)	(K_2)	(K_3)	(K_4)
S^* (Great)	0.356301 0.9062 0.6296002	0.3515553 0.91746 0.5813109	0.4610319 0.9381152 0.529159	0.4011101 0.9163859 0.5938768
S^- (Poor)	0.599732 0.9603 0.4452952	0.5532716 0.96327 0.4308737	0.6231772 0.9730824 0.3814316	0.4858238 0.9725006 0.407416

Based on Equations (23) and Equation (24), the distance between the option S_i from both the FN-PIS and FN-NIS can be determined and hence are presented in the Tables 14 and in Table 15 respectively.

Table 14. Distance to PIS and NIS according to FNWAM operator

Alternatives	$D(S_i, S^*)$	$D(S_i, S^-)$
S_1	-0.0001984	-0.000719
S_2	0.0001634	-0.0021034
S_3	0.0001311	-0.0001512
S_4	0.0009971	4.081E-05
S_5	-0.0006797	-0.0009046
S_6	0.0004388	0.0002226
S_7	-0.0001534	4.069E-05
S_8	0.0005392	-0.0007033
S_9	0.0008378	5.726E-05
S_{10}	-3.289E-05	-0.0026617

Table 15. Distance to PIS and NIS according to FNWGM operator

Alternatives	$D(S_i, S^*)$	$D(S_i, S^-)$
S_1	0.0385384	-0.0003446
S_2	0.0845744	-0.0003869
S_3	0.062182	-0.000897
S_4	0.0256772	-0.0024915
S_5	0.0197199	-0.0008921
S_6	0.0905429	-0.0006766
S_7	0.0296447	-0.0008057
S_8	0.0451872	-0.0022975
S_9	0.0396455	-0.0012789
S_{10}	0.0401722	0.0004508

Using Tables 14 and Table 15, the maximum and minimum distances is evaluated to the FN-NIS and FN-PIS, respectively, and the closeness ratios are computed using Equation (28), as shown in Tables 16 and 17. Also, the aggregation operators determine how the ranks differ. So, according to the FNWAM operator, the closeness ratio for each alternative shows that the best option is $S7$, and over all ranking is $S7 > S3 > S9 > S4 >$S4>S8>S1>S5>S2>S10 as shown in Table 16.

Table 16. Every alternative's closeness ratio according to the FNWAM operator

Alternatives	Closeness Ratio	Rank
S_1	3.5219025	7
S_2	9.2088361	9
S_3	0.4863661	2
S_4	1.6503041	5
S_5	5.0637916	8
S_6	1.6455789	4
S_7	0.0428936	1
S_8	2.3661877	6
S_9	1.4898353	3
S_{10}	12.005712	10

And, the closest alternative, according to the proximity ratios based on the FNWGM operator, $S10$, and overall ranking is $S10 > S1 > S5 > S7 >$S9>S2>S3>S6>S4>S8, as shown in the Table 17.

Table 17. Closeness ratio of each alternative according to FNWGM operator

Alternatives	Closeness Ratio	Rank
S_1	2.7187086	2
S_2	5.1470364	6
S_3	5.1430573	7
S_4	6.828937	9
S_5	2.9789264	3
S_6	6.0923355	8
S_7	3.2905556	4
S_8	7.3879469	10
S_9	4.8473876	5
S_{10}	1.0371401	1

6. Comparative analysis among NS and FNS

In this section, comparison between the Neutrosophic set and Fermatean neutrosophic set is presented. Here, initially linguistics values are considered for neutrosophic set which are related to Fermatean neutrosophic value that is truth and indeterminacy values are same and false values are different form Fermatean neutrosophic set.

Table 18. Terms used in linguistics and their associated Neutrosophic Number

LT		(T, I, F)
Probably More Significant	PMS	(0.95, 0.9, 0.05)
Extremely Significant	ES	(0.9, 0.8, 0.1)
High Priority	HP	(0.8, 0.9, 0.2)
Relatively Greater Significance	RGS	(0.7, 0.9, 0.3)
Equally Important	EI	(0.6,0.8, 0.4)
Very Minimal Significance	VMS	(0.6,0.7,0.4)
Low Priority	LP	(0.5, 0.7,0.5)
Extremely Low Significant	ELS	(0.5,0.6, 0.5)
Definitely Not Important	DNI	(0.4, 0.5, 0.6)

Using the proposed algorithm of Section 4, closeness ratio of each alternative is computed according to the Neutrosophic Weighted Arithmetic Mean and Neutrosophic Weighted Geometric Mean operator, and then the maximum and minimum distances to the Neutrosophic Negative Ideal Solutions and Neutrosophic Positive Ideal Solutions, and the closeness ratios are computed using Equation (28), as shown in Tables 19 and 20 below:

Table 19. Every alternative's closeness ratio according to the NWAM operator

Alternatives	Closeness Ratio	Rank
S_1	7.814948	5
S_2	0.328438	1
S_3	9.972041	7
S_4	28.63632	10
S_5	6.517592	3
S_6	6.972054	4
S_7	9.011573	6
S_8	25.02782	9
S_9	21.91097	8
S_{10}	1.034024	2

Table 20. Closeness ratio of each alternative according to NWGM operator

Alternatives	Closeness Ratio	Rank
S_1	0.1892229	2
S_2	0.5188592	4
S_3	1.3105063	7
S_4	2.122334	10
S_5	1.4066268	9
S_6	0.2431025	3
S_7	1.1300182	6
S_8	1.3662806	8
S_9	1.0490239	5
S_{10}	0.1534107	1

7. Results and Discussions

In the Fermatean Neutrosophic CODAS approach, the outputs tend to be closer together compared to those produced by traditional neutrosophic logic. Here, the role of the false membership function is minimal. In the linguistic table, FNS contains a greater variety of values in the falsity function. This diversity in the falsity function alters the priority of selection. In contrast, in neutrosophic sets, truth and false functions are interdependent, restricting the sum of truth and false functions to be less than or equal to

one. Consider a faculty selection problem where a candidate has ten years of teaching service, but only at the college level. For university-level teaching, they might face challenges. In this case, truth value of 0.8 and a false value of 0.4 is assigned to the lack of teaching service. Such nuanced evaluations are possible within FNSs. These adjustments can significantly impact ranking in the selection process. This method proves particularly useful and yields accurate results, especially in the medical field. In the comparison below, the assessment of the Neutrosophic Weighted Arithmetic Mean (NWAM) and Neutrosophic Weighted Geometric Mean (NWGM) against the FNWAM and FNWGM are presented.

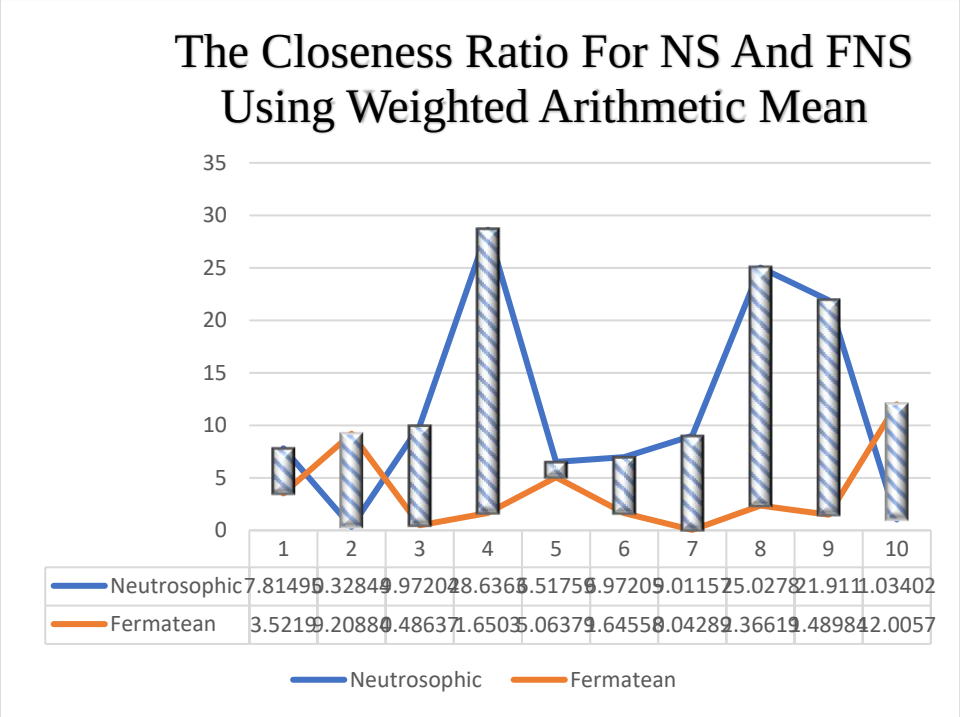

Fig.3 The closeness ratio for NS and FNS using Weighted Arithmetic Mean

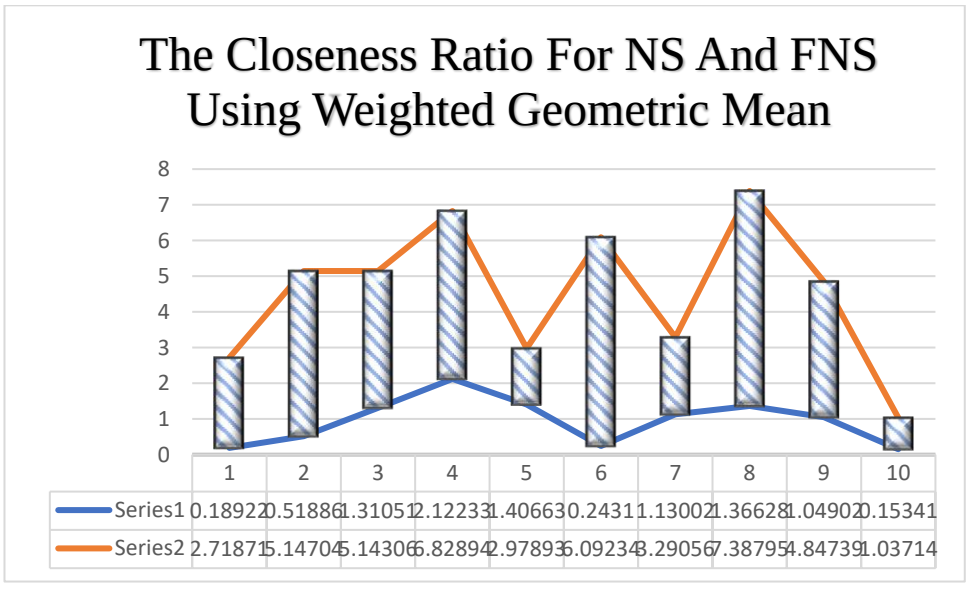

Fig.4 The closeness ratio for NS and FNS using Weighted Geometric Mean

8. Conclusions

This paper clearly states that the proposed technique helps to understand that while both types of sets-NS and FNS, address uncertainty, though they differ in their representation, conditions, and applications. On applying the proposed CODAS technique on a real-life problem, it is concluded that the Fermatean neutrosophic technique are providing more reliable results when compared to neutrosophic set in particular cases. This can be inferred from the obtained results that the neutrosophic sets are more general, while FNSs offer a more structured approach to handling uncertainty with specific constraints and functions. Furthermore, it is believed that these FNSs can be readily applied to real-life problems to determine the optimal solutions.

Funding: This research received no external funding.

Acknowledgments: The author is grateful to the editorial and reviewers, as well as the correspondent author, who offered assistance in the form of advice, assessment, and checking during the study period.

Conflicts of Interest: The authors declare no conflict of interest.

References:

[1] Antony Crispin Sweety, C., & Jansi, R. (2021). Fermatean Neutrosophic Sets. *International Journal of Advanced Research in Computer and Communication Engineering*, 10(6), 24-27.

[2] Atanassov, K. T. (1986). Intuitionistic Fuzzy Sets. *Fuzzy Sets and Systems*, 20, 87-96.

[3] Broumi, S., Mohanaselvi, S., Witczak, T., Talea, M., Bakali, A., & Smarandache, F. (2023). Complex fermatean neutrosophic graph and application to decision making. *Applications in Management and Engineering*, 6(1), 474-501.

[4] Broumi, S., Sundareswaran, R., Shanmugapriya, M., Bakali, A. & Talea, M. (2022). Theory and Applications of Fermatean Neutrosophic Graphs. *Neutrosophic Sets and Systems*, 50, 248-286.

[5] Broumi, S., Sundareswaran, R., Shanmugapriya, M., Nordo, G., Talea, M., Bakali, A. & Smarandache, F. (2022). Interval-valued fermatean neutrosophic graphs. Collected Papers. Volume XIII: On various scientific topics, 496.

[6] Chinnadurai, V., Thayalan, S., & Bobin, A. (2021). Multi-criteria decision-making in complex Fermatean fuzzy environment. *Journal of Mathematical and Computational Science*, 11(6), 7209-7227.

[7] Ganie, A. H. (2022). Multicriteria decision-making based on distance measures and knowledge measures of Fermatean fuzzy sets. *Granular Computing*, 7(4), 979-998.

[8] Jansi, R., Mohana, K., & Smarandache, F. (2019). Correlation measure for Pythagorean neutrosophic sets with T and F as dependent neutrosophic components. *Neutrosophic Sets and Systems*, vol. 30, 2019.

[9] Karak, M., Mahata, A., Rong, M., Mukherjee, S., Mondal, S. P., Broumi, S., & Roy, B. (2023). A solution technique of transportation problem in neutrosophic environment. *Neutrosophic Systems with Applications*, 3, 17-34.

[10] Martin, N., Broumi, S., Sudha, S., & Priya, R. (2023). Neutrosophic MARCOS in Decision Making on Smart Manufacturing System. *Neutrosophic Systems with Applications*, 4, 12-32.

[11] Senapati, T., & Yager, R. R. (2020). Fermatean fuzzy sets. *Journal of ambient intelligence and humanized computing*, 11, 663-674.

[12] Singh, A. (2018). Modified method for solving non-linear programming for multi-criteria decision making problems under interval neutrosophic set environment. *Mathematical Sciences International reserach Journal*, 7, 41-52.

[13] Singh, A. (2022, December). A Novel Shortest Path Problem using Dijkstra Algorithm in Interval-Valued Neutrosophic Environment. In *2022 International Conference on Smart Generation Computing, Communication and Networking (SMART GENCON)* (pp. 1-6). IEEE.

[14] Singh, A., & Bhat, S. A. (2021). A novel score and accuracy function for neutrosophic sets and their real-world applications to multi-criteria decision-making process. *Neutrosophic Sets and Systems*, 41, 168-197.

[15] Singh, A., Kumar, A., & Appadoo, S. S. (2017). Modified approach for optimization of real life transportation problem in neutrosophic environment. *Mathematical Problems in Engineering*, 2017 (Aug, 2017), Article ID 2139791, 9 pages.

[16] Singh, A., Kumar, A., & Appadoo, S. S. (2019). A novel method for solving the fully neutrosophic linear programming problems: Suggested modifications. *Journal of intelligent & fuzzy systems*, 37(1), 885-895.

[17] Smarandache F. A. (1999). Unifying Field in Logics. Neutrosophy: Neutrosophic Probability, Set and Logic. Rehoboth: American Research Press.

[18] Smarandache, F. (2005). Neutrsosophic Set, a generalization of the inutitionistic fuzzy sets. *International Journal of Pure Applied Mathematics*, 24, 287-297.

[19] Wang, H., Smarandache, F., Zhang, Y., & Sunderraman, R. (2010). Single valued neutrosophic sets. Infinite study, 12, 20110.

[20] Xu, C., & Shen, J. (2021). Multi-criteria decision making and pattern

recognition based on similarity measures for Fermatean fuzzy sets. *Journal of Intelligent & Fuzzy Systems*, 41(6), 5847-5863.

[21] Yager, R. R. (2013, June). Pythagorean fuzzy subsets. *In 2013 joint IFSA world congress and NAFIPS annual meeting (IFSA/NAFIPS) (pp. 57-61)*. IEEE.

[22] Zadeh, L. A. (1965). Fuzzy sets. *Information and control*, 8(3), 338-353.

Received: April 13, 2024. Accepted: Aug 20, 2024

Neutrosophic Sets and Systems, Vol. 72, 2024
University of New Mexico

The Cubic Bipolar Neutrosophic Sets theory and Uncertainty Management in Environmental Data Analysis

A. A. Salama[1], Huda E. Khalid[2] , Ahmed G. Mabrouk[3]

[1] Dept. of Math and Computer Sci., Faculty of Science, Port Said Univ., Egypt

[1]Dean of higher Institute of Computer Science and Information Systems, October City, Ministry of Higher Education; Egypt *drsalama44@gmail.com ahmed_salama_2000@sci.psu.edu.eg*

[2]Telafer University, The Administration Assistant for the President of the Telafer University, Telafer, Iraq; https://orcid.org/0000-0002-0968-5611 , dr.huda-ismael@uotelafer.edu.iq

[3]Higher Institute of Computer Science and Information Systems, October City, Ministry of Higher Education; Egypt ***agaber2008@csi.edu.eg***

*Correspondence: dr.huda-ismael@uotelafer.edu.iq

Abstract: Environmental data analysis often faces uncertainties in measurements. Cubic Bipolar Neutrosophic Sets (CBN Sets) provide a powerful framework to address this challenge. This paper explores the mathematical foundations of CBN Sets and highlights their practical applications through illustrative examples. We demonstrate how CBN Sets effectively capture varying degrees of certainty, possibility, and impermanence in environmental parameters. The concept of inclusion relations facilitates comparisons and information fusion. Fundamental set operations (intersection, union, complement) are explored for manipulating and analyzing uncertain environmental data. We present the application of CBN Sets in water quality assessment, highlighting their ability to analyze parameters while accounting for measurement uncertainties. The potential for air quality monitoring using CBN Sets is also discussed. Finally, distance measures and similarity coefficients are introduced to quantify relationships between air quality characteristics from different stations. By leveraging CBN Sets and their associated operations, researchers can gain a more nuanced understanding of environmental data, enabling informed decision-making for a healthier planet.

Keywords: Cubic Bipolar Neutrosophic Sets (CBN Sets), Uncertainty Management, Environmental Data Analysis, Water Quality Assessment, Air Quality Monitoring, Set Operations, Distance Measures, Similarity Coefficients

1. Introduction

Environmental data analysis plays a crucial role in understanding and managing our planet's health. However, real-world measurements are often subject to inherent uncertainties due to sensor limitations, natural variations, and other factors. Traditional binary approaches that rely on strict classifications can struggle to capture these nuances (e.g., [10]).

This paper introduces Cubic Bipolar Neutrosophic Sets (CBN Sets) as a powerful tool for representing and managing uncertainty in environmental data analysis. CBN Sets extend beyond traditional set theory by incorporating multiple levels of certainty, possibility, and impermanence. This builds upon the concepts of neutrosophic sets, which generalize intuitionistic fuzzy sets by allowing independent truth, falsity and indeterminacy memberships [1]. CBN Sets further enhance this framework by incorporating bipolarity and cubic elements, providing a richer framework for capturing the multifaceted nature of environmental data [2, 3]. The following sections of this paper will explore the mathematical foundation of CBN Sets, delve into their practical applications through illustrative examples, and demonstrate their effectiveness in managing uncertainty within environmental data analysis. We will explore how CBN Sets can be used in various environmental applications, such as water quality assessment and air quality monitoring. By leveraging this innovative approach, researchers and environmental scientists can gain a richer understanding of our environment, leading to more informed decision-making for a sustainable future. In addition to many references in [7-25]

2. Related Work

Environmental data analysis is crucial for understanding and managing our planet's health. However, inherent uncertainties due to sensor limitations, natural variations, and sampling limitations can hinder accurate data interpretation. Traditional binary classifications often struggle to capture these nuances. Here, we explore various techniques used to manage uncertainty in environmental data analysis:

1. **Fuzzy Set Theory:**

A well-established approach, fuzzy set theory allows for gradual membership within a set, reflecting the possibility of belongingness. This provides a more nuanced representation of uncertainty compared to crisp sets. For instance, Liu et al. (2012) applied fuzzy logic to environmental impact assessment, incorporating uncertainty analysis [1].

2. **Interval Type Methods:**

These methods represent uncertainty by specifying a range of possible values for an environmental parameter. This approach is useful when precise measurement is challenging. Mustafa et al. (2018)

demonstrates the application of a Time Monte Carlo method for addressing uncertainty in land-use change models [2].

3. Probability and Statistics:

Probabilistic and statistical methods quantify uncertainty by assigning probabilities to different possible outcomes. This allows for risk calculation and estimation of confidence intervals for environmental measurements. Jain et al. (1999) provides a comprehensive review of data clustering techniques, which are often used in conjunction with probabilistic approaches [3].

4. Dempster-Shafer Theory (DST):

DST is a mathematical framework for reasoning with uncertainty. It allows for the representation of belief functions that assign probabilities to sets of possible outcomes, rather than individual values. Dezert (2009) offers a collection of works exploring advanced applications of DST [4].

5. Neutrosophic Logic Extensions:

Recent studies explore neutrosophic set extensions like bipolar neutrosophic sets and neutrosophic cubic sets for decision-making problems. While not directly applied to environmental data analysis yet, these works, like Al Shumrani et al. (2020), demonstrate the potential of neutrosophic logic for uncertainty management [5].

6. Similarity Measures and Distance Metrics:

Defining appropriate similarity measures and distance metrics is crucial for comparing and analyzing environmental data with uncertainty. These techniques are often combined with the aforementioned methods. Ulucay et al. (2018) explored similarity measures for bipolar neutrosophic sets applicable to multi-criteria decision-making [6].

This overview provides a foundation for understanding existing methods for managing uncertainty in environmental data analysis. By comparing and contrasting these approaches with CBN Sets, the subsequent sections of this paper can highlight the unique advantages and potential applications of CBN Sets for environmental data analysis tasks.

3. Cubic Bipolar Neutrosophic Sets (CBN Sets)

3.1. Cubic Bipolar Neutrosophic Sets: A Formal Definition and Exploration of Uncertainty Representation

CBN Sets provide a powerful framework for representing uncertainty by incorporating various degrees of truth membership, falsity membership, and indeterminacy membership. To formally define a CBN Set, we introduce the concept of a 12-tuple.

Definition: A Cubic Bipolar Neutrosophic Set (CBN Set) M in a universe of discourse U is characterized by:

$M = < \{T^{+1}(x)\}, \{T^{+2}(x)\}, \{T^{-1}(x)\}, \{T^{-2}(x)\}, \{I^{+1}(x)\}, \{I^{+2}(x)\}, \{I^{-1}(x)\}, \{I^{-2}(x)\}, \{F^{+1}(x)\}, \{F^{+2}(x)\}, \{F^{-1}(x)\}, \{F^{-2}(x)\} >$

where:

- $x \in U$: x is an element in the universe of discourse U.
- $T^{+1}(x)$, $T^{+2}(x)$: represent the truth membership degrees of x belonging to M with positive certainty (strongly true and somewhat true, respectively).
- $T^{-1}(x)$, $T^{-2}(x)$: represent the truth membership degrees of x not belonging to M with positive certainty (strongly false and somewhat false, respectively).
- $I^{+1}(x)$, $I^{+2}(x)$: represent the indeterminacy membership degrees of x possibly belonging to M (highly indeterminate and somewhat indeterminate, respectively).
- $I^{-1}(x)$, $I^{-2}(x)$: represent the indeterminacy membership degrees of x possibly not belonging to M (highly indeterminate and somewhat indeterminate, respectively).
- $F^{+1}(x)$, $F^{+2}(x)$: represent the falsity membership degrees of x belonging to M with negative certainty (strongly false and somewhat false, respectively).
- $F^{-1}(x)$, $F^{-2}(x)$: represent the falsity membership degrees of x not belonging to M with negative certainty (strongly true and somewhat true, respectively).

Each membership degree is a value between 0 and 1, with 0 representing complete absence and 1 representing complete membership. The superscripts (+/-) indicate positive/negative certainty, while the subscripts ($^{1}/_{2}$) indicate strong/somewhat certainty or indeterminacy/falsity.

3.2. Unveiling the Power of CBN Sets: Hands-on Exploration with Numerical Examples

Cubic Bipolar Neutrosophic Sets (CBN Sets) offer a powerful tool for representing and managing uncertainty in environmental data analysis. Unlike traditional set theory, CBN Sets go beyond simple membership (in or out) to capture varying degrees of certainty (T), possibility (I), and impermanence (F) associated with environmental data. This hands-on exploration will delve into CBN Sets through illustrative examples, demonstrating their practical application in environmental assessments.

Example 1: Representing "Tallness" with CBN Sets

Traditional set theory often struggles to capture the nuances of real-world classifications. For instance, classifying someone as "tall" or "short" can be subjective and depend on context. CBN Sets offer a powerful alternative by incorporating varying degrees of certainty, possibility, and indeterminacy.

Here is how we can represent the concept of "tallness" in humans using a CBN Set:

- **Universe of Discourse (U):** Set of all human heights in centimeters (cm).

We can define a CBN Set (M) that captures the "tallness" of a person with different membership degrees:

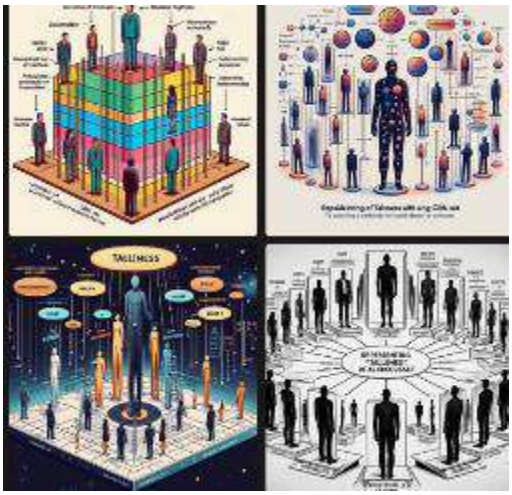

Fig.1: Cloud of Uncertainty: Representing "Tallness" with CBN Sets

Fig.1: depicts a CBN Set representing the concept of "tallness" in humans. It assigns membership degrees to different height ranges, capturing the uncertainty associated with classifying someone as "tall" or "short".

Table 1: CBN Set for Representing "Tallness" in Humans (150 cm)

Height (cm)	Category	Truth Value
150	T^{+1} (Strongly Tall)	0.1
150	T^{+2} (Somewhat Tall)	0.2
150	T^{-1} (Strongly Short)	0.8
150	T^{-2} (Somewhat Short)	0.7
150	I^{+1} (Possibly Tall)	0.3
150	I^{+2} (Somewhat Indeterminate)	0.2
150	I^{-1} (Possibly Short)	0.1
150	I^{-2} (Somewhat Indeterminate)	0.0
150	F^{+1} (Strongly Short)	0.0
150	F^{+2} (Somewhat Short)	0.0
150	F^{-1} (Strongly Tall)	0.9

Height (cm)	Category	Truth Value
150	F^{-2} (Somewhat Tall)	0.8

This table provides a structured view of the data with the height categories, specific categories, and corresponding truth-values. Let me know if you need any further assistance or if you have more data to analyze.

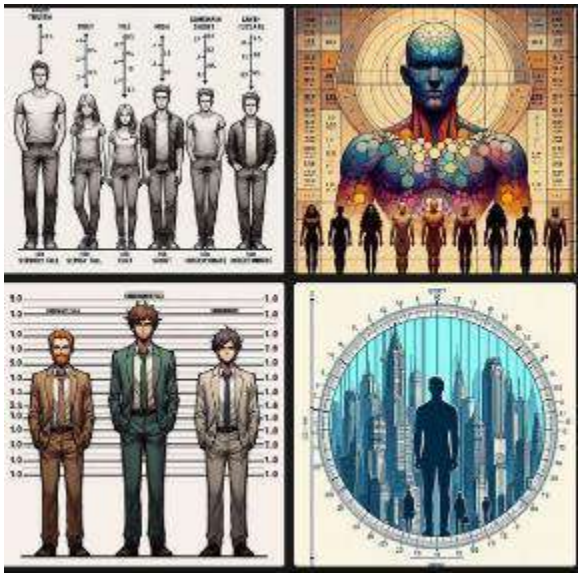

Fig.2: Representing Tallness with single CBN set

Explanation: Table 1: This table displays the membership truth values for different object heights. You can expand this table to include more height ranges and corresponding membership degrees to depict a wider range of "tallness" classifications.

- A person of 150 cm is considered "short" with strong negative certainty ($F^{-1} = 0.9$) and somewhat negative certainty ($F^{-2} = 0.8$). This indicates a high likelihood of being short.
- There is a slight possibility ($I^{+1} = 0.3$) of being somewhat indeterminate ($I^{+2} = 0.2$) in terms of height classification. This could be due to factors like posture or rounding measurements.
- The positive truth memberships (T^{+1}) and (T^{+2}) are relatively low for this height, reflecting the low certainty of being tall.

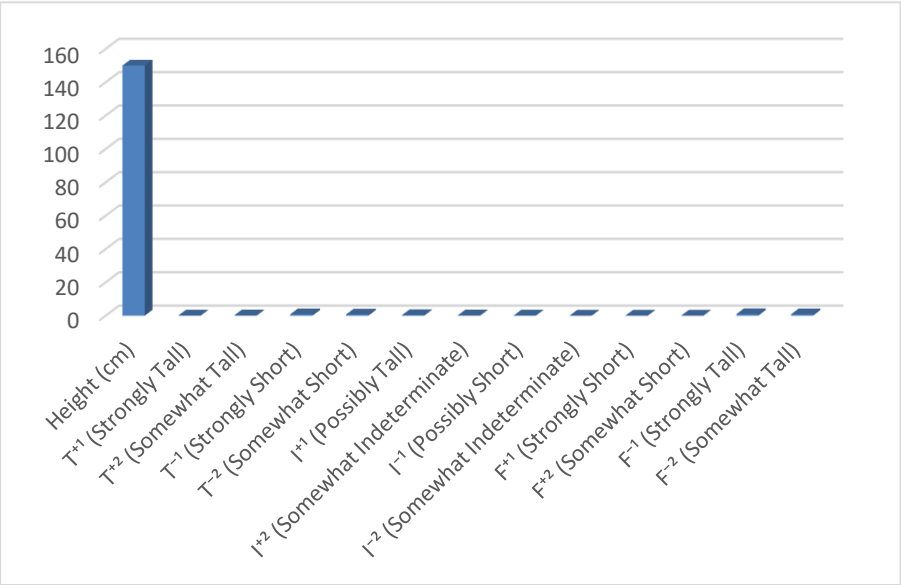

Graph 1: Membership Function for Tallness with CBN Sets

Visualizing Certainty and Possibility (Optional: Graph 1):

A graph can be a helpful tool to visually represent the certainty and possibility of being tall for each height range. The x-axis could represent height ranges (e.g., 140-150 cm, 150-160 cm, etc.), and the y-axis could represent the membership degree values (0 to 1). Separate lines can be plotted for positive truth memberships (T^{+1}, T^{+2}), negative truth memberships (T^{-1}, T^{-2}), and indeterminacy memberships (I^{+1}, I^{+2}, I^{-1}, I^{-2}). This visualization can provide a clearer understanding of how certainty and possibility change across different height ranges.

By utilizing CBN Sets, we can move beyond binary classifications (tall/short) and represent the multifaceted nature of height perception in humans. This approach can be beneficial in various applications, such as ergonomics studies or clothing size recommendations, where considering uncertainties in height measurements can be crucial.

- **Beyond Binary: CBN Sets in Image Processing**

Traditional image processing techniques often rely on crisp classifications for pixel values, which can be limiting when dealing with real-world satellite imagery. Sensor limitations, atmospheric conditions, and inherent variations in the environment can introduce uncertainty in pixel classification. CBN Sets offer a powerful approach to address these uncertainties.

Example 2: Classifying Pixels in Satellite Images

Consider a satellite image where we want to classify pixels based on their color (e.g., green vegetation, blue water) and spectral signature (unique reflectance pattern of materials). Here is how CBN Sets can be used to account for uncertainty:

- **Universe of Discourse (U):** Set of all possible color and spectral signature values captured by the satellite sensor.

Color Classification:

We can define a CBN Set (M_color) to represent the membership degrees of a pixel belonging to a specific color class (e.g., green):

This table displays the membership degrees assigned to different categories within a CBN Set (M_color). The CBN Set represents the likelihood of a pixel belonging to a specific color class, such as green, in an image.

Table 1: Membership Degrees in a CBN Set for Pixel Color Classification (M_color)

Category	Truth Value	Description	Color Association
T^{+1} (Green)	0.8	Strongly Green	Dark Green
T^{+2} (Somewhat Green)	0.2	Moderately Green	Light Green
T^{-1} (Not Green)	0.1	Strongly Not Green	No Green
T^{-2} (Somewhat Not Green)	0.0	Slightly Not Green	Very Light Green
I^{+1} (Possibly Green)	0.3	Possible Green	Light Green Tint
I^{+2} (Somewhat Indeterminate)	0.2	Uncertain Classification	Gray
I^{-1} (Possibly Not Green)	0.1	Possible Not Green	Light Green Tint
I^{-2} (Somewhat Indeterminate)	0.0	Uncertain Classification	Gray

F^{+1} (Not Green)	**0.0**	**Strongly Not Green**	**No Green**
F^{+2} (Somewhat Not Green)	**0.0**	**Slightly Not Green**	**Very Light Green**
F^{-1} (Green)	**0.7**	**Strongly Green**	**Dark Green**
F^{-2} (Somewhat Green)	**0.2**	**Moderately Green**	**Light Green**

Fig.3: The Color Association of Green".

Fig.3: is a green with different shades. Here is a breakdown of the color associations provided:

* Strongly Green (T^{1+}): Dark Green (0.8)

* Moderately Green (T^{+2}): Light Green (0.2)

* Possible Green (I^{+1}): Light Green Tint (0.3)

* Strongly Green (F^{-1}): Dark Green (0.7)

* Moderately Green (F^{-2}): Light Green (0.2)

Explanation:

- The table.1: categorizes the membership degrees along with a brief description and corresponding color association.
- The Truth Value column represents the degree of membership in each category. A value closer to 1 indicates stronger membership, while a value closer to 0 indicates weaker membership.
- The Color Association column suggests the visual representation for each category. Dark Green corresponds to high confidence in "Green," while No Green indicates low confidence. Light Green tints are used for "Possibly Green" and "Possibly Not Green" categories to represent some level of possibility. Gray is used for "Somewhat Indeterminate" categories to signify uncertainty.

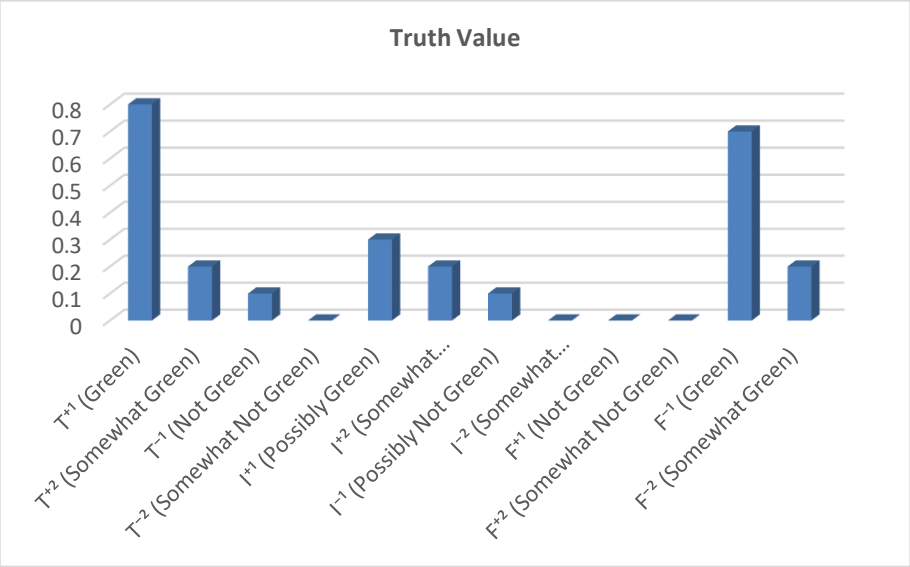

Graph 2: The Color Association of Green".

- **Spectral Signature Classification with CBN Sets**

In remote sensing applications, classifying the materials present in an image pixel often relies on analyzing its spectral signature. A spectral signature is a unique pattern of electromagnetic radiation reflected by a material across various wavelengths. CBN Sets (Certainty-Possibility-Fuzzy Sets) offer a powerful tool to represent the varying degrees of membership a pixel's spectral signature has for belonging to a specific material class.

Fig.4: Spectral Signature Classification with CBN Sets"

Example1 : Classifying Vegetation

Consider a scenario where we want to classify pixels in a satellite image as "vegetation" or "not vegetation" based on their spectral signatures. We can define a CBN Set (M_spectral) to represent the membership degrees for each pixel:

Table 2: Membership Degrees in a CBN Set for Spectral Signature Classification (M_spectral)

Spectral Signature Range	Truth Value	Description
T^{+1} (Vegetation)	0.7	Strongly Matches Vegetation Signature
T^{+2} (Somewhat Vegetation)	0.3	Moderately Matches Vegetation Signature
T^{-1} (Not Vegetation)	0.1	Strongly Deviates from Vegetation Signature

T^{-2} (Somewhat Not Vegetation)	0.0	Slightly Deviates from Vegetation Signature
I^{+1} (Possibly Vegetation)	0.2	Possible Vegetation Signature
I^{+2} (Somewhat Indeterminate)	0.1	Uncertain Classification
I^{-1} (Possibly Not Vegetation)	0.2	Possible Not Vegetation Signature
I^{-2} (Somewhat Indeterminate)	0.0	Uncertain Classification
F^{+1} (Not Vegetation)	0.0	Strongly Deviates from Vegetation Signature
F^{+2} (Somewhat Not Vegetation)	0.0	Slightly Deviates from Vegetation Signature
F^{-1} (Vegetation)	0.8	Strongly Matches Vegetation Signature
F^{-2} (Somewhat Vegetation)	0.2	Moderately Matches Vegetation Signature

Figure 5: CBN Sets for Vegetation Classification

Figure 5: incorporates the concept of CBN Sets for vegetation classification:

Explanation:

- The table categorizes the membership degrees for a pixel's spectral signature matching a vegetation signature.
- **Truth Value (0-1):** Represents the degree of membership in each category. A higher value indicates stronger membership.
- **Description:** Provides a brief explanation of each category.
- In this example, a pixel with a membership degree of 0.7 in T^{+1} (Vegetation) has a strong spectral signature match for vegetation.
- Conversely, a membership degree of 0.1 in T^{-1} (Not Vegetation) suggests the spectral signature deviates from vegetation.
- The "Possibly" and "Somewhat Indeterminate" categories (I^{+1}, I^{+2}, I^{-1}, I^{-2}) capture uncertainty in the classification.

Benefits of CBN Sets:

- **Uncertainty Representation:** CBN Sets effectively handle the inherent uncertainties in spectral signature analysis.
- **Detailed Classification:** They provide a more nuanced classification compared to simple "vegetation" or "not vegetation" labels.
- **Flexibility:** The concept can be extended to classify various materials by defining appropriate CBN Sets.

Spectral Signature Classification using CBN Sets allows for a more robust and informative approach to analyzing remote sensing data.

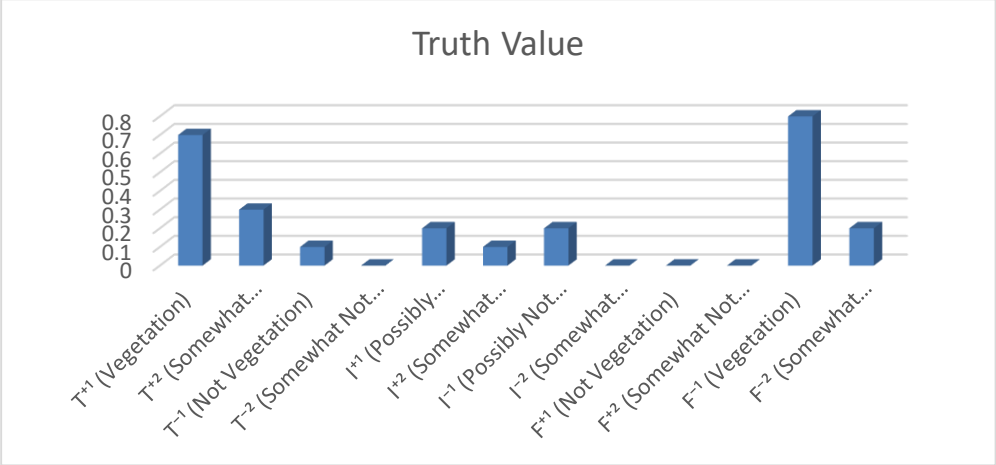

Graph 3: Vegetation Classification:

Graph 3: represent various classifications (T^{+1}, T^{-1}, etc.) along with their truth-values. For instance, the dark green bar at 0.8 on the y-axis corresponds to "T^{+1} (Vegetation)", indicating a high confidence that a pixel's spectral signature strongly matches vegetation.

- **Visualizing Membership Degrees**

There are several ways to visualize membership degrees in CBN Sets for Spectral Signature Classification:

Fig.6: Visualizing Membership Degrees in CBN Sets for Spectral Signature Classification

Fig.6: shows four different ways to visualize membership degrees in CBN sets for spectral signature classification. These visualizations likely correspond to different techniques used to represent the data.

1. Color-Coded Images:

- Assign a unique color to each membership degree category (T^{+1}, T^{+2}, etc.) in the CBN Set (M_spectral).
- Overlay this color map onto the original satellite image, where each pixel's color represents its corresponding membership degree for "vegetation."
- This approach provides a quick visual overview of the spatial distribution of vegetation within the image.
- Example: Dark green for strong vegetation membership (T^{+1}), light green for somewhat vegetation (T^{+2}), and red for strong non-vegetation (F^{-1}).

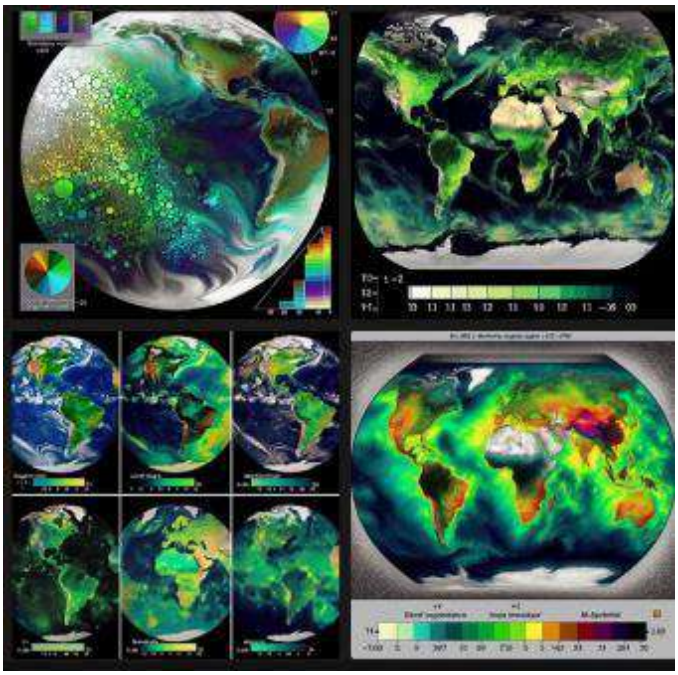

Fig.7: Color-Coded Images: Vegetation Distribution

Fig.7: incorporates the key information: **Color-Coded Images**: This refers to the method used to create the image, which assigns colors to represent different membership degrees.

__Vegetation Distribution__: This refers to what the image is showing, which is the spatial distribution of vegetation within the satellite image.

2. Stacked Bar Charts:

- Generate a stacked bar chart for each pixel in the image.
- Each bar in the stack represents a membership degree category (T^{+1}, T^{+2}, etc.) and its corresponding value.
- The height of each bar segment reflects the strength of membership.
- This method allows for detailed inspection of the membership degree distribution for individual pixels.

- While informative, it can be overwhelming for large images with many pixels.

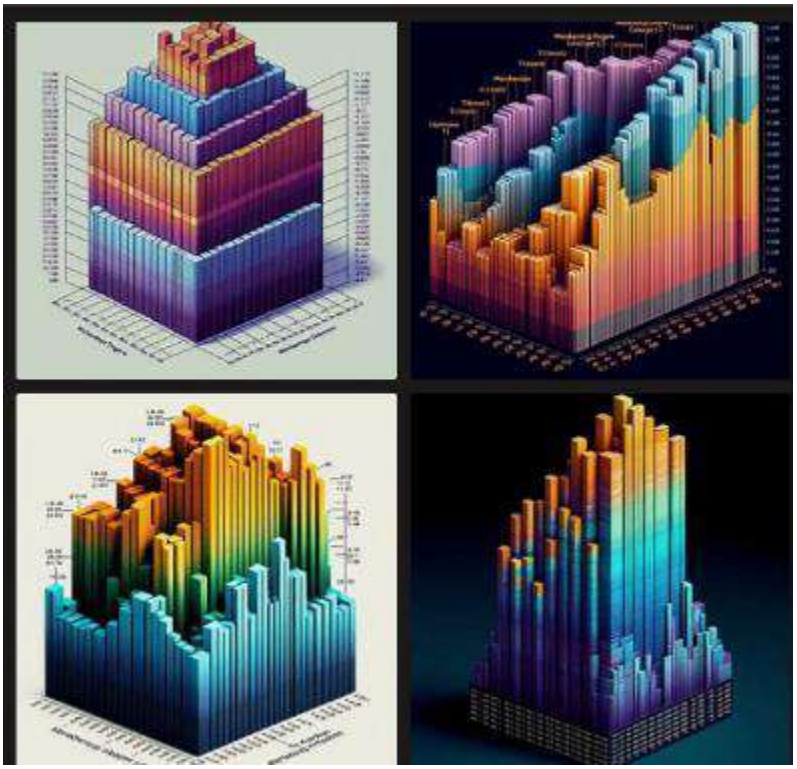

Fig.8: Pixel Membership in Vegetation Classification (Stacked Bar Chart)

Fig.8: has a stacked bar chart showing its membership degrees in various categories (vegetation, somewhat vegetation, not vegetation, etc.) The height of each bar segment represents the strength of the pixel's membership in that category.

3. 3 D Surface Plots:

- Create a 3D surface plot where the x and y axes represent the image spatial coordinates, and the z-axis represents the dominant membership degree value for each pixel.
- This approach provides a visualization of the overall "vegetation landscape" within the image.
- It can be helpful for identifying areas with high vegetation concentration or areas with mixed signatures.

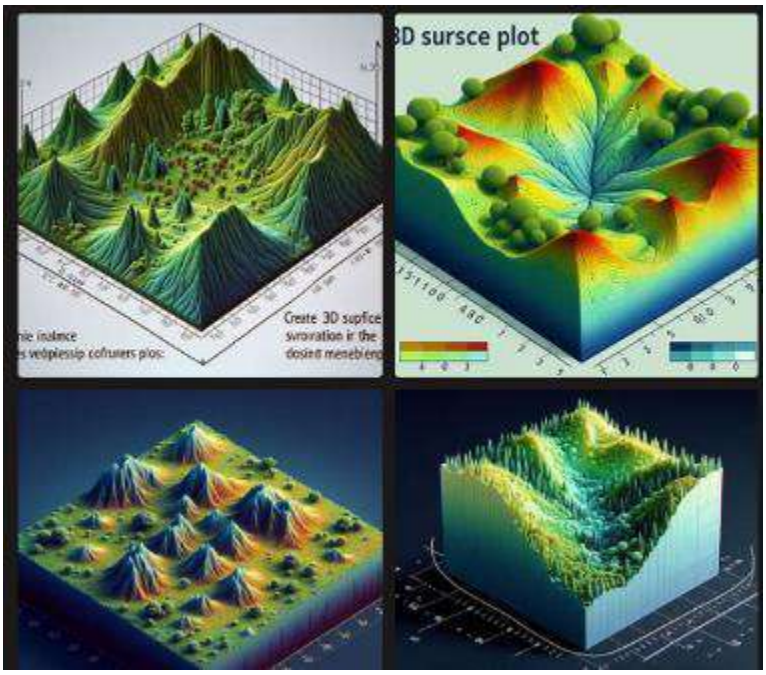

Fig.9: 3D Visualization of Vegetation Landscape

Fig.9: describes the image is a 3D surface plot where the x and y axes represent the image's spatial coordinates (location of each pixel) and the z-axis represents the dominant membership degree value for each pixel (how strongly each pixel is classified as vegetation).

3.4. Interactive Visualization Tools:

- Develop interactive web-based or desktop applications that allow users to explore the membership degrees.
- Users can hover over specific pixels to view detailed membership degree breakdowns.
- This approach offers greater flexibility and can be customized to specific user needs.

Fig.10: is "Interactive Visualization Tools: Explore Membership Degrees". Choosing the Best Visualization:

The most suitable visualization method depends on the specific application and the desired level of detail.

- For a quick overview, color-coded images are effective.
- Stacked bar charts offer detailed information but can be overwhelming for large datasets.
- 3D surface plots provide a good overall picture but might require additional exploration for specific locations.
- Interactive tools offer the most flexibility but require more development effort.

Problem: GPS data used for tracking objects has inherent uncertainties due to various factors. Traditional methods treat this data as deterministic, leading to inaccurate location estimates.

Solution: CBN Sets offer a powerful approach to capture and manage these uncertainties.

Fig.11: Overcoming GPS Inaccuracy

Fig.11: Describes how traditional methods for tracking objects with GPS data are inaccurate due to uncertainties.

Example: Tracking a Car's Location

- We define the Universe of Discourse (U) as all possible latitude and longitude values within the relevant geographic region.
- Two CBN Sets are used:
  - M_latitude: Represents membership degrees for the car's actual latitude within a specific range.
  - M_longitude: Represents membership degrees for the car's actual longitude within a specific range.

Absolutely, here is Table 3 again:

This table presents the CBN Sets (Certainty-Possibility-Fuzzy Sets) for representing the membership degrees of the car's location in terms of latitude and longitude.

Table 3: CBN Sets for Car Location (Latitude and Longitude)

Latitude/Longitude Range	Truth Value	Description
Latitude (Current Latitude ± Error Margin)		
T^{+1} (Correct Latitude)	0.8	Strongly Matches Current Latitude

T^{+2} (Somewhat Correct)	0.1	Moderately Matches Current Latitude
T^{-1} (Incorrect Latitude)	0.05	Strongly Deviates from Current Latitude
T^{-2} (Somewhat Incorrect)	0.0	Slightly Deviates from Current Latitude
I^{+1} (Possible Latitude)	0.05	Possible Current Latitude
I^{+2} (Somewhat Indeterminate)	0.0	Uncertain Classification
I^{-1} (Possible Incorrect Latitude)	0.0	Possible Not Current Latitude
I^{-2} (Somewhat Indeterminate)	0.0	Uncertain Classification
F^{+1} (Incorrect Latitude)	0.05	Strongly Deviates from Current Latitude
F^{+2} (Somewhat Incorrect)	0.0	Slightly Deviates from Current Latitude
F^{-1} (Correct Latitude)	0.9	Strongly Matches Current Latitude
F^{-2} (Somewhat Correct)	0.1	Moderately Matches Current Latitude

Note: This table represents the CBN Sets for latitude. A similar table can be created for longitude using the same categories and descriptions.

- High positive truth membership (T^{+1}) for being within the reported latitude range.
- Slight possibility (I^{+1}) of being outside this range due to GPS error.
- Similar membership degrees can be defined for longitude (separate table).

Fig.12: Tracking a Car's Location with CBN Sets

Fig.12: explains how CBN sets are used to represent the membership degrees for a car's location in terms of latitude and longitude. The table (Table 3) provides details on these CBN sets.

- **Visualizing Membership Degrees:**

A graph can be created to visualize the membership degrees for both latitude and longitude. This would help understand how the certainty of location changes within the specified range.

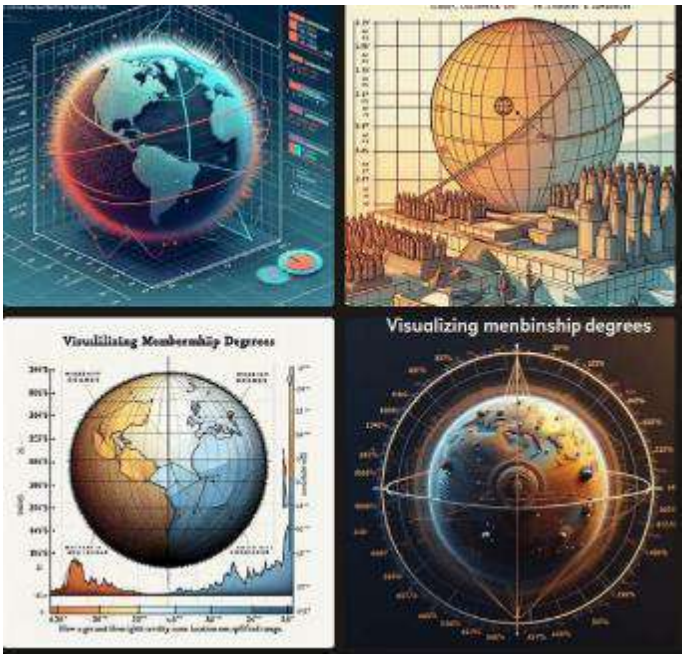

Fig. 13: Visualization of Car Location Uncertainty with CBN Sets

Fig.13: describes visualize the membership degrees for both latitude and longitude, helping to understand how certain the car's location is within a specified range.

- **Benefits of Using CBN Sets:**

- Captures and manages uncertainties in location data.
- Provides a more nuanced representation compared to "correct" or "incorrect" labels.
- Enables development of more robust tracking algorithms.
- Leads to more accurate and reliable location estimates.

Overall, this example effectively demonstrates how CBN Sets can be a valuable tool for dealing with uncertainty in location data for moving objects.

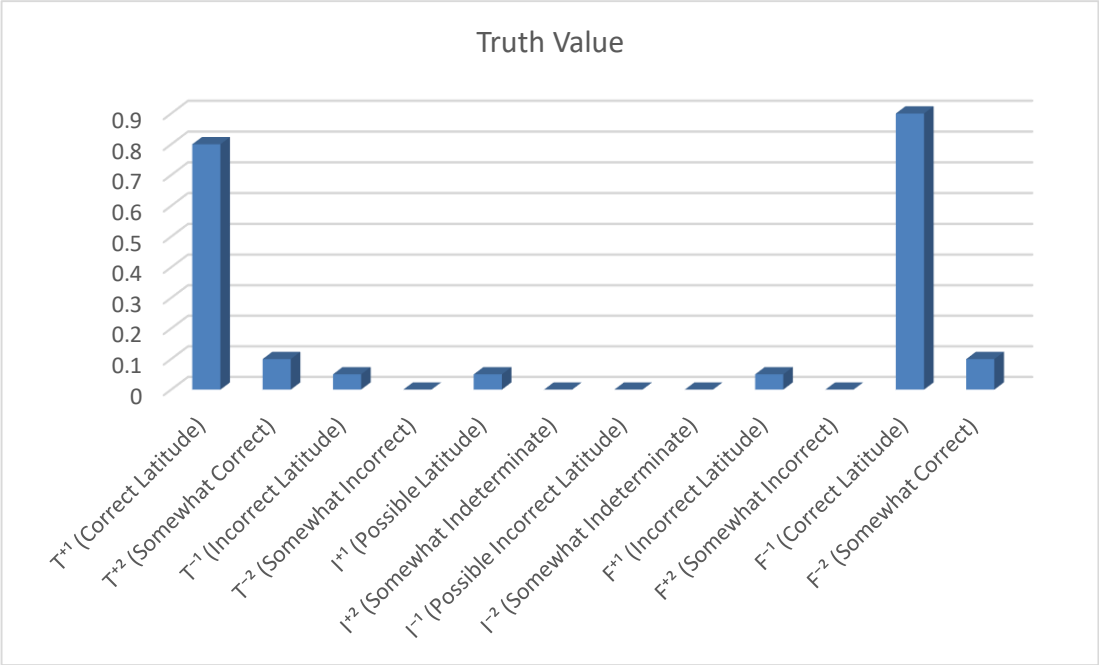

Graph 4: Truth Value of Latitude Estimates

4. Ordering and Comparing Uncertainty: Inclusion Relations for Cubic Bipolar Neutrosophic Sets (CBN Sets)

Having explored the mathematical foundation and applications of CBN Sets, this section delves into the concept of inclusion relations. Inclusion relations play a crucial role in comparing and manipulating CBN Sets, allowing us to refine information, generalize knowledge, and perform set operations effectively within the context of environmental data analysis.

4.1 Defining Inclusion Relations

An inclusion relation between two CBN Sets (M_1 and M_2) in the same universe of discourse (U) is established when the membership degrees of M_1 are consistently less than or equal to the corresponding membership degrees of M_2. Mathematically, this can be represented as follows:

$M_1 \leq M_2$ if and only if:

- $T^{+1}(x)$ in $M_1 \leq T^{+1}(x)$ in M_2 for all $x \in U$
- $T^{+2}(x)$ in $M_1 \leq T^{+2}(x)$ in M_2 for all $x \in U$
- ... (similarly for all other membership degrees: T^{-1}, T^{-2}, I^{+1}, I^{+2}, etc.)

Intuitively, this implies that M_1 possesses less or equal certainty, possibility, and indeterminacy compared to M_2 for every element (x) within the universe of discourse.

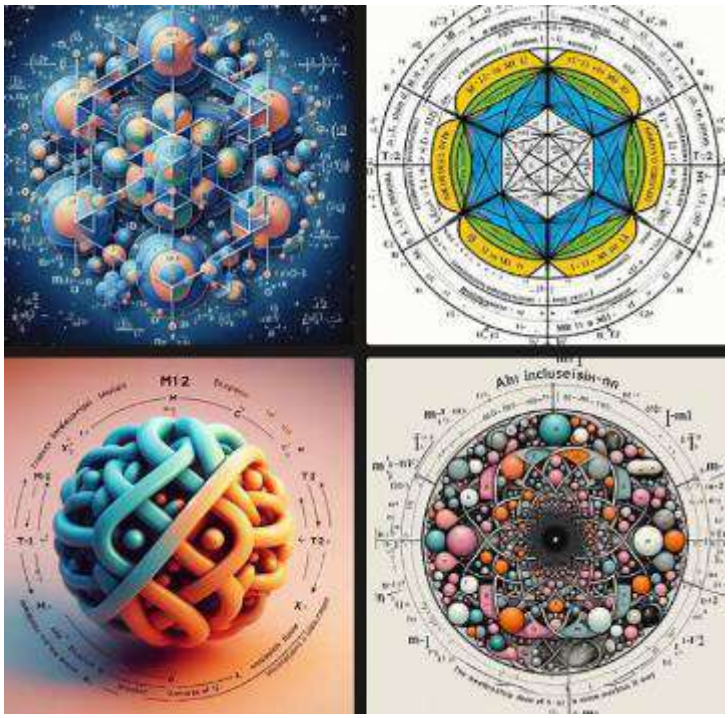

Fig. 14: Defining Inclusion Relations in CBN Sets

- **Some numerical examples for defining inclusion relations between two CBN Sets (M_1 and M_2) within the same universe of discourse (U):**

Example 1: Inclusion Relation

Consider two CBN Sets representing the weather forecast for rain tomorrow:

- **M_1 (Cloudy):** Represents the membership degrees for the possibility of rain if the forecast is cloudy.
- **M_2 (Rainy):** Represents the membership degrees for the possibility of rain if it's explicitly mentioned as rainy.

Universe of Discourse (U): {Rain, No Rain}

Table 4: CBN Sets for Rain Forecast (Cloudy vs. Rainy)".

Category	M_1 (Cloudy)	M_2 (Rainy)	Inclusion Relation
T^{+1} (Rain)	0.3	1.0	$M_1 \leq M_2$
T^{+2} (Somewhat Rain)	0.2	0.0	$M_1 \leq M_2$

T^{-1} (No Rain)	0.4	0.0	$M_1 \leq M_2$
T^{-2} (Somewhat No Rain)	0.1	0.0	$M_1 \leq M_2$
I^{+1} (Possible Rain)	0.0	0.0	$M_1 \leq M_2$
I^{+2} (Somewhat Indeterminate)	0.0	0.0	$M_1 \leq M_2$
I^{-1} (Possible No Rain)	0.0	0.0	$M_1 \leq M_2$
I^{-2} (Somewhat Indeterminate)	0.0	0.0	$M_1 \leq M_2$
F^{+1} (No Rain)	0.0	0.0	$M_1 \leq M_2$
F^{+2} (Somewhat No Rain)	0.0	0.0	$M_1 \leq M_2$
F^{-1} (Rain)	0.7	1.0	$M_1 \leq M_2$
F^{-2} (Somewhat Rain)	0.3	0.0	$M_1 \leq M_2$

Explanation:

- In this example, M_1 (Cloudy) represents a less certain forecast compared to M_2 (Rainy).
- For every category (T^{+1}, T^{-1}, etc.), the membership degree in M_1 is less than or equal to the corresponding degree in M_2.
- Therefore, $M_1 \leq M_2$, indicating an inclusion relation.

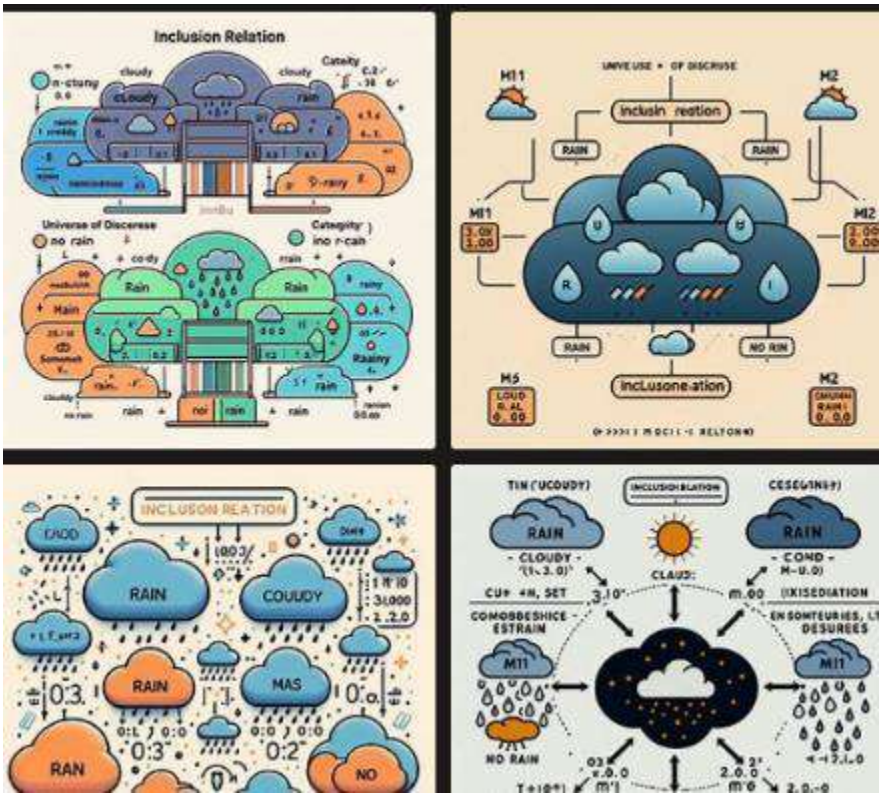

Fig. 15: Inclusion Relation between Cloudy and Rainy Weather

Example 2: No Inclusion Relation

Consider two CBN Sets representing the size of a house:

- **M_1 (Large):** Represents the membership degrees for a house being considered "large."
- **M_2 (Spacious):** Represents the membership degrees for a house being considered "spacious."

Universe of Discourse (U): {Very Small, Small, Medium, Large, Very Large}

Table 5: CBN Sets for House Size (Large vs. Spacious)".

Category	M_1 (Large)	M_2 (Spacious)	Inclusion Relation
T^{+1} (Large)	0.8	0.6	No Relation
T^{+2} (Somewhat Large)	0.1	0.2	No Relation
T^{-1} (Small)	0.05	0.1	No Relation
T^{-2} (Somewhat Small)	0.0	0.0	No Relation

I^{+1} (Possibly Large)	0.0	0.1	No Relation
I^{+2} (Somewhat Indeterminate)	0.05	0.0	No Relation
I^{-1} (Possibly Small)	0.0	0.0	No Relation
I^{-2} (Somewhat Indeterminate)	0.0	0.0	No Relation
F^{+1} (Small)	0.0	0.0	No Relation
F^{+2} (Somewhat Small)	0.0	0.0	No Relation
F^{-1} (Large)	0.9	0.8	No Relation
F^{-2} (Somewhat Large)	0.05	0.2	No Relation

Fig. 16: CBN Sets for House Size (Large vs. Spacious)

Explanation:

- Here, M_1 and M_2 represent different aspects of house size - largeness and spaciousness.
- There's no consistent relationship between the membership degrees. For example, M_1 has a higher degree in T^{+1} (Large) compared to M_2 but a lower degree in I^{+1} (Possibly Large).
- Therefore, there's no inclusion relation between M_1 and M_2.

These examples highlight how to evaluate inclusion relations between CBN Sets based on

4.2 Ordering Membership Degrees

Inclusion relations rely on establishing an order for each type of membership degree within a CBN Set. Here's a breakdown of the ordering for positive certainty (T^{+1} and T^{+2}), negative certainty (T^{-1} and T^{-2}), indeterminacy (I^{+1} and I^{+2}, I^{-1} and I^{-2}), and falsity (F^{+1} and F^{+2}, F^{-1} and F^{-2}):

- **Positive Certainty ($T^{+1} \geq T^{+2}$)**: A higher T^{+1} value indicates stronger truth membership compared to T^{+2}.
- **Negative Certainty ($T^{-1} \geq T^{-2}$)**: A higher T^{-1} value indicates stronger falsehood membership compared to T^{-2}.
- **Indeterminacy ($I^{+1} \geq I^{+2}$, $I^{-1} \geq I^{-2}$)**: Higher I^{+1} and I^{-1} values represent greater indeterminacy (possibility of belonging or not belonging).
- **Falsity ($F^{+1} \geq F^{+2}$, $F^{-1} \geq F^{-2}$)**: Higher F^{+1} and F^{-1} values indicate stronger falsity membership.

By following this ordering principle, we can compare the overall level of uncertainty between two CBN Sets using inclusion relations.

- **some numerical examples for ordering membership degrees within a CBN Set, following the principles you outlined:**

Example 1: Ordering Membership Degrees in a Weather Forecast

Consider a CBN Set (M) representing the possibility of rain tomorrow:

- **Universe of Discourse (U):** {Rain, No Rain}

Table 6: CBN Set for Rain Forecast (Ordered Membership Degrees)".

Category	Description	Example Value	Ordering
T^{+1} (Rain)	Strongly Likely Rain	0.8	$T^{+1} \geq T^{+2}$

T^{+2} (Somewhat Likely Rain)	Moderately Likely Rain	0.2	
T^{-1} (Not Rain)	Strongly Unlikely Rain	0.0	$T^{-1} \geq T^{-2}$
T^{-2} (Somewhat Unlikely Rain)	Slightly Unlikely Rain	0.0	
I^{+1} (Possible Rain)	Possible Rain, but Uncertain	0.0	$I^{+1} \geq I^{+2}$ (Can be adjusted based on scenario)
I^{+2} (Somewhat Indeterminate)	More Uncertain about Rain Possibility	0.0	
I^{-1} (Possible No Rain)	Possible No Rain, but Uncertain	0.0	$I^{-1} \geq I^{-2}$ (Can be adjusted based on scenario)
I^{-2} (Somewhat Indeterminate)	More Uncertain about No Rain Possibility	0.0	
F^{+1} (Not Rain)	Definitely No Rain	0.0	$F^{+1} \geq F^{+2}$
F^{+2} (Somewhat Not Rain)	Slightly Leaning Towards No Rain	0.0	
F^{-1} (Rain)	Definitely Rain	1.0	$F^{-1} \geq F^{-2}$

F^{-2} (Somewhat Rain)	Slightly Leaning Towards Rain	0.0	

Explanation:

- This example displays a clear ordering within each category pair (T^{+1}, T^{+2}), (T^{-1}, T^{-2}), etc., following the established principles.
- The values (0.8, 0.2, etc.) are for illustrative purposes and can vary depending on the specific scenario.

Example 2: Ordering Membership Degrees in Car Speed Estimation

Consider a CBN Set (M) representing the estimated speed of a car:

- **Universe of Discourse (U):** {0 km/h, 20 km/h, 40 km/h, 60 km/h, 80 km/h, 100 km/h}

Table 6: CBN Set for Car Speed Estimation (Ordered Membership Degrees)".

Category	Description	Example Value	Ordering
T^{+1} (60 km/h)	Strongly Matches Recorded Speed of 60 km/h	0.7	$T^{+1} \geq T^{+2}$
T^{+2} (Somewhat Likely 60 km/h)	Moderately Likely Speed is 60 km/h	0.2	
T^{-1} (Not 40 km/h)	Strongly Deviates from 40 km/h Speed	0.05	$T^{-1} \geq T^{-2}$
T^{-2} (Somewhat Not 40 km/h)	Slightly Deviates from 40 km/h Speed	0.0	
I^{+1} (Possible 80 km/h)	Possible Speed is 80 km/h, but Uncertain	0.03	$I^{+1} \geq I^{+2}$ (Can be adjusted based on sensor data)

I^{+2} (Somewhat Indeterminate)	More Uncertain about the Speed Being 80 km/h	0.0	
I^{-1} (Possible Not 20 km/h)	Possible Speed is Not 20 km/h, but Uncertain	0.02	$I^{-1} \geq I^{-2}$ (Can be adjusted based on sensor data)
I^{-2} (Somewhat Indeterminate)	More Uncertain about the Speed Not Being 20 km/h	0.0	
F^{+1} (Not 60 km/h)	Definitely Not 60 km/h Speed	0.0	$F^{+1} \geq F^{+2}$
F^{+2} (Somewhat Not 60 km/h)	Slightly Leaning Away from 60 km/h Speed	0.0	
F^{-1} (Exactly 60 km/h)	Confirmed Speed is 60 km/h (unlikely in real-world scenarios)	0.0	$F^{-1} \geq F^{-2}$
F^{-2} (Somewhat Likely 60 km/h)	Slightly Leaning Towards 6		

4.3 Benefits of Inclusion Relations

Inclusion relations offer several advantages in environmental data analysis using CBN Sets:

- **Refining Information:** By comparing CBN Sets, we can identify areas with higher certainty or lower uncertainty. This allows us to focus on more reliable data points and refine our understanding of environmental phenomena.
- **Generalizing Information:** Inclusion relations can help establish general trends across environmental data. For instance, we might compare CBN Sets representing water quality parameters from different locations to identify similarities or overarching patterns.

- **Performing Set Operations:** Inclusion relations form the foundation for performing set operations (intersection, union, complement) on CBN Sets. These operations allow us to manipulate and analyze environmental data while accounting for inherent uncertainties.

In the following section, we will explore how set operations based on inclusion relations can be utilized for effective uncertainty management in environmental data analysis.

- **Numerical Examples for Benefits of Inclusion Relations in Environmental Data Analysis with CBN Sets**

Here are some numerical examples displaying the benefits of inclusion relations in environmental data analysis using CBN Sets:

Example 1: Refining Information - Air Quality Monitoring

Imagine a scenario where two air quality monitoring stations (Station A and Station B) measure ozone levels (in parts per million, ppm) using CBN Sets (M_A and M_B) to account for measurement uncertainties.

- **Universe of Discourse (U):** {0 ppm, 0.02 ppm, 0.04 ppm, ..., 0.1 ppm} (incremented by 0.02 ppm)

Table 7: Refined Air Quality Data with CBN Sets (Station A vs. B)

Ozone Level (ppm)	M_A (Station A)	M_B (Station B)	Inclusion Relation	Interpretation
0.04 ppm	T^{+1} (0.8)	T^{+1} (0.9)	M_B ≤ M_A	Station A's data has higher certainty for 0.04 ppm ozone level.
0.06 ppm	T^{+2} (0.3)	T^{+1} (0.7)	M_B ≤ M_A	Station A's data is more reliable for 0.06 ppm ozone level.
0.08 ppm	I^{+1} (0.2)	T^{+2} (0.5)	No Relation	Both stations have some uncertainty, but Station B shows a stronger possibility of 0.08 ppm.

Explanation:

- By comparing the membership degrees, we can identify that Station A's data has higher certainty (higher T^{+1} values) for ozone levels of 0.04 ppm and 0.06 ppm.
- This allows us to focus on Station A's data for these specific levels, refining our understanding of the local air quality.

Example 2: Generalizing Information - Soil Moisture Analysis

Consider a study analyzing soil moisture content (%) at two different depths (Depth 1 and Depth 2) using CBN Sets (M_d1 and M_d2).

- **Universe of Discourse (U):** {0%, 10%, 20%... 50%} (incremented by 10%)

Table 8: Soil Moisture Analysis with CBN Sets (Depth Comparison)".

Soil Moisture (%)	M_d1 (Depth 1)	M_d2 (Depth 2)	Inclusion Relation	Interpretation
20%	T^{+1} (0.7)	T^{+2} (0.5)	M_d2 ≤ M_d1	Depth 1 has a stronger indication of 20% moisture content.
30%	T^{+2} (0.2)	T^{+1} (0.8)	M_d1 ≤ M_d2	Depth 2 has a clearer signal for 30% moisture content.
40%	I^{+1} (0.1)	I^{+2} (0.3)	No Relation	Both depths have some possibility of 40% moisture, but the evidence is weak.

Explanation:

- Here, the inclusion relations help identify general trends. While Depth 1 has a stronger signal for lower moisture levels (20%), Depth 2 shows a higher certainty for a higher moisture level (30%).
- This suggests a potential moisture content gradient with depth, providing valuable insights into soil hydrology.

These examples demonstrate how inclusion relations enable us to:

- Refine information by focusing on data points with higher certainty within a CBN Set.

- Generalize information by identifying trends and patterns across different CBN Sets representing environmental data.

By leveraging inclusion relations, we can effectively manage uncertainties and gain a more nuanced understanding of environmental phenomena.

5. Harnessing the Power of Cubic Bipolar Neutrosophic Sets (CBN Sets) for Effective Uncertainty Management in Environmental Data Analysis

Environmental data analysis is fundamental for understanding and managing our planet's health. However, real-world measurements are often subject to inherent uncertainties due to sensor limitations, natural variations, and other factors. Traditional binary approaches that rely on strict classifications can struggle to capture these nuances. CBN Sets offer a powerful framework for representing and managing uncertainty, enabling more robust and informative environmental data analysis.

5.1 Manipulating Uncertainty with CBN Sets: Intersection, Union, and Complement

Building upon the concept of inclusion relations, we can now explore fundamental set operations for CBN Sets: intersection, union, and complement. These operations allow us to manipulate and analyze environmental data while accounting for the inherent uncertainties represented by the membership degrees.

- **Intersection ($M_1 \cap M_2$):** This operation identifies elements that belong to both CBN Sets (M_1 and M_2) with a certain degree of certainty, possibility, and indeterminacy. The resulting membership degrees in the intersection set are calculated as the minimum of the corresponding membership degrees in M_1 and M_2.

  For example, consider two CBN Sets representing water quality parameters at a location. The intersection can reveal areas where both sets agree on the "cleanliness" of the water with a specific certainty level.

- **Union ($M_1 \cup M_2$):** This operation captures elements that belong to either M_1 or M_2 or possibly to both sets. The resulting membership degrees in the union set are calculated as the maximum of the corresponding membership degrees in M_1 and M_2.

  The union can be helpful in environmental studies to identify regions where either set indicates potential environmental concerns, even if the certainty levels differ.

- **Complement (M^{1c}):** This operation produces a new CBN Set that includes elements that do not belong to the original set (M_1). The membership degrees in the complement are calculated as 1 minus the corresponding membership degrees in M_1.

  The complement can be used to identify areas where environmental parameters deviate from expected values or established thresholds, even with some degree of uncertainty.

By effectively utilizing these set operations on CBN Sets, researchers can achieve a more comprehensive understanding of environmental data while acknowledging the inherent uncertainties associated with measurements.

- **Numerical Examples for Manipulating Uncertainty with CBN Sets: Intersection, Union, and Complement**

Here are some numerical examples demonstrating how set operations on CBN Sets (intersection, union, and complement) can be used to manipulate and analyze environmental data while accounting for uncertainties:

Scenario: We are monitoring water quality parameters (temperature, pH, etc.) at two locations (Lake A and River B) using CBN Sets (M_lake and M_river) due to potential pollution concerns.

- **Universe of Discourse (U):** {Ideal, Slightly Polluted, Moderately Polluted, Heavily Polluted}

1. Intersection (M_lake ∩ M_river): Identifying Areas with Consistent Water Quality

Table 9: "Water Quality Analysis: Intersection of Lake and River Data (M_lake ∩ M_river)"

Parameter	M_lake (Lake A)	M_river (River B)	M_lake ∩ M_river (Intersection)	Interpretation
Temperature	T^{+1} (0.8)	T^{+2} (0.6)	T^{+1} (min(0.8, 0.6)) = 0.6	Both locations have a moderate certainty (0.6) of ideal temperature.
pH	I^{+1} (0.2)	T^{-1} (0.7)	Ø (Empty Set)	No overlap in membership degrees. Lake A might have slightly high pH (I^{+1}), while River B shows a strong possibility (T^{-1}) of being slightly acidic.

This table analyzes the water quality of a lake (M_lake) and a river (M_river) using the intersection (∩) of their respective CBN Sets. The intersection identifies areas where both water bodies share similar characteristics.

Parameters:

The table focuses on two key water quality parameters: temperature and pH.

Interpretation:

- **Temperature:**
  - M_lake (Lake A): T^{+1} (0.8) indicates a strong certainty (80%) of ideal temperature in the lake.
  - M_river (River B): T^{+2} (0.6) indicates a moderate certainty (60%) of ideal temperature in the river.
  - M_lake ∩ M_river (Intersection): The intersection considers the minimum certainty level (min(0.8, 0.6)) resulting in T^{+1} (0.6). This means there's a moderate certainty (60%) of ideal temperature in areas where the lake and river water mix.
- **pH:**
  - M_lake (Lake A): I^{+1} (0.2) suggests a slight possibility (20%) of the lake having a slightly high pH.
  - M_river (River B): T^{-1} (0.7) indicates a strong possibility (70%) of the river being slightly acidic.
  - M_lake ∩ M_river (Intersection): The intersection results in the empty set (Ø) because there's no overlap in membership degrees for pH. The lake might have a slightly high pH, while the river shows a strong possibility of being slightly acidic, indicating no areas where both characteristics intersect.

2. Union (M_lake ∪ M_river): Identifying Areas with Potential Water Quality Issues

While the intersection of CBN Sets focuses on overlapping areas of similarity, the union (U) considers areas where **either** water body might have a water quality issue. This can be helpful for identifying potential problems that require further investigation.

Table 10: Water Quality Analysis: Union of Lake and River Data (M_lake ∪ M_river)

Parameter	M_lake (Lake A)	M_river (River B)	M_lake ∪ M_river (Union)	Interpretation
Temperature	T^{+1} (0.8)	T^{+2} (0.6)	T^{+1} (max(0.8, 0.6)) = 0.8	Strong certainty (0.8) of ideal temperature (from Lake A) or moderate certainty (0.6) (from River B).
pH	I^{+1} (0.2)	T^{-1} (0.7)	T^{-1} (max(0.2, 0.7)) = 0.7	Strong possibility (0.7) of slightly acidic water (from River B), or slight possibility (0.2) of slightly high pH (from Lake A).

This table analyzes the potential water quality issues in Lake A and River B using the union (U) of their respective CBN Sets. The union identifies areas where **at least one location (or potentially both)** might exceed optimal water quality conditions for a specific parameter.

Parameters:

The table focuses on two key parameters: temperature and pH.

Interpretation:

- **Temperature:**
  - M_lake (Lake A): T^{+1} (0.8) indicates a strong certainty (80%) of ideal temperature in the lake.
  - M_river (River B): T^{+2} (0.6) indicates a moderate certainty (60%) of ideal temperature in the river.
  - M_lake ∪ M_river (Union): The union considers the **maximum** membership degree (max(0.8, 0.6)) resulting in T^{+1} (0.8). This signifies a **strong overall certainty (80%)** that at least one location (lake or river, or potentially both) has ideal temperature. However, the union itself doesn't pinpoint the exact locations.
- **pH:**
  - M_lake (Lake A): I^{+1} (0.2) suggests a slight possibility (20%) of the lake having a slightly high pH.
  - M_river (River B): T^{-1} (0.7) indicates a strong possibility (70%) of the river being slightly acidic.
  - M_lake ∪ M_river (Union): The union considers the maximum membership degree (max(0.2, 0.7)) resulting in T^{-1} (0.7). This highlights a **strong possibility (70%)** that at least one location (lake or river) deviates from the optimal pH range. The source (lake or river) cannot be determined solely based on the union.

3. Complement (M_lake^{1c} and M_river^{1c}): Identifying Deviations from Expected Values

The concept of the complement in CBN Sets allows us to identify areas where the environmental data significantly deviates from the expected values for a specific parameter. Let us explore how this works for lakes and rivers:

This table analyzes deviations from expected water quality values in Lake A using the complement (M_lake^{1c}) of its CBN Set. The complement identifies areas where the environmental data might deviate from the ideal or optimal ranges.

Table 11: Water Quality Analysis: Deviations from Expected Values (Lake A)"

Parameter	M_lake (Lake A)	M_lake^{1c} (Complement)	Interpretation
Temperature	T^{+1} (0.8)	F^{+1} (1 - 0.8) = 0.2	Areas with a certainty level of 0.2 for deviating from the ideal temperature range.
pH	I^{+1} (0.2)	F^{+1} (1 - 0.2) = 0.8	Areas with a certainty level of 0.8 for deviating from the expected pH range (due to the possibility of slightly high pH).

The complement of Lake A's CBN Set (M_lake^{1c}) identifies areas with a certainty level of 0.2 for deviating from the expected ideal temperature range. This certainty level (0.2) is calculated by subtracting the membership degree in M_lake (0.8) from 1 (representing complete certainty).

Important Note: This 0.2 certainty level does not necessarily indicate a confirmed problem, but rather the degree to which the data deviates from the ideal range. It could be due to:

- **Instrument limitations:** Measurement errors can introduce slight variations in the data.
- **Natural variations within the lake:** Temperature might fluctuate slightly across different areas of the lake.

These examples showcase the power of set operations on CBN Sets:

- **Identifying Consistent or Potentially Problematic Water Quality:** The intersection (∩) helps identify areas where both locations share similar characteristics (e.g., ideal temperature in overlapping zones). The union (U) helps us flag areas where either location might have a water quality concern, even if the certainty levels differ.
- **Capturing the Overall Picture:** By analyzing both intersection and union, we gain a broader understanding of potential water quality issues across different areas, even if the certainty levels vary.
- **Highlighting Deviations with Acknowledged Uncertainty:** The complement (^{1}) focuses on areas where the data deviates from expected values, prompting further investigation while acknowledging the inherent uncertainties in environmental data.

Overall, these set operations provide a comprehensive framework for analyzing water quality data, allowing us to identify areas requiring further monitoring and develop better environmental management strategies.

5.2 Applying CBN Sets to Environmental Applications (Focus on Water Quality Assessment) with Numerical Examples

*** Water Quality Parameters as CBN Sets:**

Let us consider a scenario where we are monitoring two key water quality parameters: pH and dissolved oxygen (DO) in a lake. We will use CBN Sets to represent these parameters, accounting for measurement uncertainties.

Universe of Discourse:

- **pH:** {< 6 (Strongly Acidic), 6-6.5 (Somewhat Acidic), 6.5-8 (Neutral), 8-8.5 (Somewhat Basic), > 8.5 (Strongly Basic)}
- **DO (mg/L):** {< 4 (Critically Low), 4-5 (Low), 5-8 (Optimal), 8-10 (High), > 10 (Supersaturated)}

Example 1: Representing pH with CBN Sets

Imagine a measured pH value of 7.3. Here is a possible CBN Set representing this data:

Table 12: CBN Set Representation of Measured pH (7.3)

Category	Description	Membership Degree
T^{+1} (Neutral)	Strongly Matches Optimal pH Range (6.5-8)	0.7
T^{+2} (Somewhat Basic)	Moderately Leans Towards Slightly High pH	0.2
I^{+1} (Possibly Somewhat Acidic)	Slight Possibility of Being Below Optimal Range	0.1
F^{+1} (Strongly Acidic)	Negligible Certainty of Being Strongly Acidic	0.0
F^{+2} (Somewhat Acidic)	Very Low Certainty of Being Moderately Low pH	0.0
F^{-1} (Strongly Basic)	Negligible Certainty of Being Strongly Basic	0.0

F^{-2} (Somewhat Basic)	Very Low Certainty of Being Moderately High pH (beyond Somewhat Basic)	0.0

This table depicts a CBN Set representing a measured pH of 7.3. Here is an explanation for each category and its corresponding membership degree:

- **T^{+1} (Neutral) (0.7):** This category captures the high certainty (0.7) of the pH being within the ideal or optimal range (6.5-8) for the specific environment. The measured value (7.3) falls relatively close to the center of this range.
- **T^{+2} (Somewhat Basic) (0.2):** This category indicates a moderate certainty (0.2) that the pH leans slightly towards the basic side (higher than ideal). However, the value is still somewhat close to the ideal range.
- **I^{+1} (Possibly Somewhat Acidic) (0.1):** The slight possibility (0.1) in this category reflects the fact that the measured pH is not perfectly centered in the ideal range and could be edging slightly towards the acidic side.
- **F^{+1} (Strongly Acidic) (0.0): Ø (Empty Set):** These categories represent extremely acidic conditions. Since the measured value is nowhere near this range, the membership degrees are zero (0), indicating negligible certainty.
- **F^{+2} (Somewhat Acidic) (0.0):** This category reflects a very low certainty (0) of the pH being moderately acidic. The measured value is closer to the ideal range than moderately acidic.
- **F^{-1} (Strongly Basic) (0.0): F^{-2} (Somewhat Basic) (0.0):** Similar to the strongly acidic categories, these categories for extremely basic or moderately high basic pH have zero membership degrees due to the measured value being far from these ranges.

Example 2: Utilizing Set Operations for Water Quality Analysis

Suppose we have CBN Sets for both pH and DO measured at different locations in the lake. We can use set operations to analyze the data:

- **Intersection:** This identifies areas where both pH and DO meet acceptable water quality standards simultaneously. A high intersection value indicates a location with a strong likelihood of good overall water quality.

For instance, if another location has a CBN Set for DO with a high T^{+1} (Optimal) membership degree, the intersection of the pH and DO sets might reveal a location with a strong certainty of having both optimal pH and DO levels.

- **Union:** This highlights regions where either pH or DO (or potentially both) might fall outside the acceptable range, even with some uncertainty. A high union value suggests a potential water quality concern that needs further investigation.

Imagine a location's DO CBN Set has a high I^{+1} (Low) membership degree. The union with the previous pH CBN Set might indicate a location with a good pH level but a possibility of low DO, requiring attention.

- **Complement:** This helps pinpoint areas where any parameter deviates from optimal values. A high complement value for a specific category (e.g., Strongly Acidic for pH) suggests a location where that parameter might be a concern, even if the overall intersection or union values do not show a critical issue.

For example, the complement of the pH CBN Set (considering only Strongly Acidic and Somewhat Acidic categories) might reveal areas with a slight possibility of deviating from the optimal range, even though the intersection with DO might still be high.

By analyzing combinations of CBN Sets for various water quality parameters, researchers can gain a more comprehensive understanding of the spatial variability and potential water quality issues across the lake. This information can be crucial for targeted water management strategies.

6. Manipulating Uncertainty with CBN Sets: Intersection, Union, and Complement

6.1. Demystifying CBN Set Operations: Intersection, Union, and Complement Explained

Having established inclusion relations for comparing CBN Sets, we can now delve into fundamental set operations: intersection, union, and complement. These operations allow us to analyze and manipulate environmental data while accounting for the inherent uncertainties represented by the membership degrees within CBN Sets.

- **Intersection ($M_1 \cap M_2$):** This operation identifies elements that belong to **both** CBN Sets (M_1 and M_2) with a certain degree of certainty, possibility, and indeterminacy. It essentially finds the overlapping area between the two sets, considering the membership degrees.

Calculation: The resulting membership degrees in the intersection set ($M_1 \cap M_2$) are calculated as the **minimum** of the corresponding membership degrees in M_1 and M_2.

Example:

Consider two CBN Sets representing water quality parameters (e.g., pH and dissolved oxygen) at a specific location. Let M_1 represent pH and M_2 represent dissolved oxygen. The intersection ($M_1 \cap M_2$) would reveal areas where both sets agree on the "healthy" range of these parameters with a specific certainty level. For instance, the intersection might show a high positive truth membership (T^{+1}) for "suitable pH" and "adequate dissolved oxygen," indicating a high likelihood of good water quality based on both parameters.

6.2. Demystifying CBN Set Operations: Intersection, Union, and Complement Explained with Numerical Examples

Following the concept of inclusion relations, we can now explore fundamental set operations for CBN Sets: intersection, union, and complement. These operations allow us to analyze and manipulate environmental data while considering the uncertainties within the membership degrees.

1. Intersection ($M_1 \cap M_2$): Identifying Areas with Consistent Quality

- **Concept:** Intersection captures elements that belong to both CBN Sets (M_1 and M_2) with a certain degree of certainty, possibility, and indeterminacy. It finds the overlapping area between the two sets, considering the membership degrees.
- **Calculation:** The resulting membership degrees in the intersection set (M_1 Transcription $\cap$ M_2) are determined by taking the minimum value for each category between the corresponding membership degrees in M_1 and M_2.

Example: Water Quality Assessment

Imagine we are monitoring two water quality parameters: pH (M_1) and dissolved oxygen (DO) (M_2) at a specific location in a lake. The universe of discourse for both is:

- {< Ideal, Slightly Low, Ideal, Slightly High, > Ideal}

Let us say we have the following CBN Sets based on measurements:

Table 13: "CBN Sets for Water Quality Monitoring (pH and Dissolved Oxygen)".

Category	M_1 (pH)	M_2 (DO)
T^{+1} (Ideal)	0.8	0.7
T^{+2} (Somewhat Ideal)	0.1	0.2
I^{+1} (Possible Slightly Low/High)	0.05	0.05
F^{+1} (< Ideal/ > Ideal)	0.0	0.0
F^{+2} (Somewhat Low/High)	0.05	0.05

Intersection ($M_1 \cap M_2$):

Table 14: "Water Quality Analysis: Intersection of pH and Dissolved Oxygen ($M_1 \cap M_2$)"

Category	$M_1 \cap M_2$ (Minimum Membership Degree)	Interpretation
T^{+1} (Ideal)	min(0.8, 0.7) = 0.7	Strong certainty (0.7) of ideal conditions for both pH and DO.
T^{+2} (Somewhat Ideal)	min(0.1, 0.2) = 0.1	Moderate possibility (0.1) of both pH and DO being slightly outside the ideal range.
I^{+1} (Possible Slightly Low/High)	min(0.05, 0.05) = 0.05	Very slight possibility (0.05) of either parameter deviating slightly from ideal.
F^{+1} (< Ideal/ > Ideal)	min(0.0, 0.0) = 0.0	No certainty (0.0) of both parameters being outside the ideal range (since minimum is 0 for both M_1 and M_2).
F^{+2} (Somewhat Low/High)	min(0.05, 0.05) = 0.05	Very slight possibility (0.05) of either parameter being somewhat outside the ideal range.

Interpretation:

The intersection highlights a location with a strong likelihood (0.7) of good water quality based on both pH and DO levels. There's also a moderate possibility (0.1) of them being slightly outside the ideal range, along with very slight chances of more significant deviations.

This example demonstrates how the intersection helps identify areas where multiple water quality parameters meet acceptable standards simultaneously.

6.3. Applications in Decision-Making and Pattern Recognition:

- Identifying areas where multiple environmental parameters meet acceptable standards simultaneously. This can be crucial for pinpointing locations with consistently good environmental conditions.

- Highlighting locations with consistent agreement on specific environmental conditions across different measurements. This can aid in pattern recognition, revealing potential correlations between environmental factors.
- Refining decision-making by focusing on areas with high certainty overlap between multiple CBN Sets. This can help prioritize areas for environmental protection or resource management based on strong evidence.
- **Union ($M_1 \cup M_2$):** This operation captures elements that belong to **either** M_1 or M_2 or possibly to **both sets**. It essentially represents the combined area of both sets, acknowledging the possibility of an element belonging to either set.

  Calculation: The resulting membership degrees in the union set ($M_1 \cup M_2$) are calculated as the **maximum** of the corresponding membership degrees in M_1 and M_2.

  Example:

  Imagine two CBN Sets representing potential air pollution levels at different monitoring stations (M_1 and M_2). The union ($M_1 \cup M_2$) would encompass regions where either station indicates potential air quality concerns, even if the certainty levels differ. For instance, the union might show a high positive truth membership (T^{+1}) for "elevated ozone levels" in M_1 and a high indeterminacy membership (I^{+1}) for "particulate matter" in M_2. This would indicate a potential air pollution issue at the combined location, even if the specific pollutant type might have some uncertainty.

*** Applications in Decision-Making and Pattern Recognition with Numerical Examples**

1. Intersection ($M_1 \cap M_2$):

We already saw how intersection helps identify areas with consistent quality in water quality assessment. Here's another example:

- **Scenario:** Monitoring soil quality using CBN Sets for nutrients (M_1) and heavy metals (M_2).
- **Interpretation:** A high intersection value for "adequate nutrient levels" and "low heavy metal content" across different soil samples would indicate consistently good soil quality for plant growth.

2. Highlighting Consistent Agreements and Pattern Recognition:

- **Scenario:** Monitoring temperature (M_1) and precipitation (M_2) across different regions over time.
- **Example:** Consistent high intersection values for "warm temperatures" in M_1 and "low precipitation" in M_2 across several regions during a specific season might suggest a pattern of drought conditions in those areas. This could be helpful in predicting future droughts and implementing water management strategies.

3. Refining Decision-Making with High Certainty Overlap:

- **Scenario:** Assessing potential risks associated with a new industrial facility.

- **Example:** We can analyze CBN Sets for air quality parameters (M_1) near the facility and potential environmental impact on nearby wildlife (M_2). A high intersection value for "elevated air pollution levels" in M_1 and "high risk to sensitive bird species" in M_2 would indicate a strong need for mitigation measures before construction due to the high certainty overlap.

4. Union ($M_1 \cup M_2$):

- **Concept:** Union captures elements that belong to either M_1 or M_2 (or possibly both) with a certain degree of certainty, possibility, and indeterminacy. It represents the combined area of both sets, acknowledging the possibility of an element belonging to either set.
- **Calculation:** The resulting membership degrees in the union set ($M_1 \cup M_2$) are determined by taking the maximum value for each category between the corresponding membership degrees in M_1 and M_2.

Example: Air Pollution Monitoring:

Imagine we have CBN Sets representing potential air pollution levels at different monitoring stations (M_1 and M_2). The universe of discourse for both could be:

- {Low, Moderate, High, Very High}

Let us say the CBN Sets are based on measurements:

Table 15: Table 15: "CBN Sets for Air Pollution Monitoring (Station M_1 vs. M_2)"

Category	M_1	M_2
T^{+1} (Low)	0.2	0.1
T^{+2} (Moderate)	0.5	0.6
I^{+1} (Possible High)	0.2	0.2
F^{+1} (Very High)	0.0	0.0
F^{+2} (Somewhat High)	0.1	0.1

Union ($M_1 \cup M_2$):

Table 16: Air Pollution Analysis: Union of Monitoring Station Data ($M_1 \cup M_2$)

Category	$M_1 \cup M_2$ (Maximum Membership Degree)	Interpretation
T^{+1} (Low)	max(0.2, 0.1) = 0.2	Low certainty (0.2) of good air quality at either location.
T^{+2} (Moderate)	max(0.5, 0.6) = 0.6	Strong certainty (0.6) of moderate air pollution levels at either station (or possibly both).
I^{+1} (Possible High)	max(0.2, 0.2) = 0.2	Moderate possibility (0.2) of high pollution levels at either location.
F^{+1} (Very High)	max(0.0, 0.0) = 0.0	No certainty (0.0) of very high pollution at either location.
F^{+2} (Somewhat High)	max(0.1, 0.1) = 0.1	Low certainty (0.1) of somewhat high pollution at either location.

The union highlights a potential air quality concern, with a strong possibility (0.6) of moderate pollution at either station or potentially both. There's also a moderate chance (0.2) of even higher pollution levels. This emphasizes the need for further investigation despite uncertainties in specific pollution types.

These examples showcase how CBN set operations can be used for informed decision-making and pattern recognition in environmental applications by considering both the certainties and uncertainties associated with environmental data.

6.4. Applications in Data Analysis:

- Identifying regions where any parameter might exceed acceptable levels, even with some uncertainty. This provides a broader perspective on potential environmental threats across a larger area.

- Creating a broader picture of potential environmental concerns across a larger area. This can be helpful for initial data analysis, highlighting areas that warrant further investigation.
- Informing strategies for environmental monitoring by highlighting areas where further investigation might be necessary. This can optimize resource allocation for environmental monitoring efforts.
- **Complement (M^{1c}):** This operation produces a new CBN Set that includes elements that **do not** belong to the original set (M_1). It essentially flips the membership degrees, reflecting the opposite condition.

  Calculation: The membership degrees in the complement (M^{1c}) are calculated as **1 minus** the corresponding membership degrees in M_1.

  Example:

  Consider a CBN Set (M_1) representing "suitable habitat" for a particular endangered species. The complement (M^{1c}) would represent areas that are **not** suitable habitat. The complement might show a high positive truth membership (T^{+1}) for "unsuitable vegetation" and a high indeterminacy membership (I^{+1}) for "lack of prey availability." This information helps identify areas where the species is unlikely to thrive.

Applications in Data Analysis with Numerical Examples

1. Union ($M_1 \cup M_2$):

We already saw how union helps highlight potential air pollution concerns. Here is another example for data analysis:

- **Scenario:** Monitoring forest health using CBN Sets for insect infestation (M_1) and drought stress (M_2) across a large forest area.
- **Example:** The union might reveal a vast region with a high possibility (from either M_1 or M_2) of experiencing either insect infestation or drought stress. This broader perspective helps identify areas that warrant further investigation for specific threats to forest health.

2. Creating a Broader Picture of Potential Environmental Concerns:

- **Scenario:** Monitoring water quality using multiple parameters (e.g., pH, DO, nitrate levels) represented by different CBN Sets (M_1, M_2, M_3).
- **Example:** Analyzing the union of these sets across a river system can identify stretches with a possibility of exceeding acceptable levels for any of the parameters, even if specific issues are unclear. This helps prioritize areas for more detailed water quality testing.

3. Informing Strategies for Environmental Monitoring:

- **Scenario:** Monitoring potential land degradation using CBN Sets for soil erosion (M_1) and desertification risk (M_2).
- **Example:** The union might highlight a large region with a possibility of facing either soil erosion or desertification. This information can guide resource allocation for deploying environmental monitoring sensors or conducting field studies in these areas to confirm specific threats and take necessary measures.

4. Complement (M^{1c}):

- **Concept:** Complement produces a new CBN Set that includes elements that do not belong to the original set (M_1). It essentially flips the membership degrees, reflecting the opposite condition.
- **Calculation:** The membership degrees in the complement (M^{1c}) are calculated as 1 minus the corresponding membership degrees in M_1.

Example: Habitat Suitability:

Consider a CBN Set (M_1) representing "suitable habitat" for a particular endangered bird species. The universe of discourse could be:

- {Abundant Food, Suitable Nesting Sites, Safe from Predators}

Let us say the CBN Set for suitable habitat is based on data:

Table 17: CBN Set for Suitable Habitat (Endangered Bird Species)

Category	M_1 (Suitable Habitat)
T^{+1} (Abundant Food)	0.8
T^{+2} (Suitable Nesting Sites)	0.7
I^{+1} (Possible Predator Threats)	0.2
F^{+1} (Lack of Food/Nesting Sites)	0.0
F^{+2} (High Predator Risk)	0.0

Complement (M_1^c - unsuitable habitat):

Table 18: Unsuitable Habitat Analysis for Endangered Bird Species (M_1^c)

Category	M_1^c (Complement)	Interpretation
T^{+1} (Lack of Food)	1 - 0.8 = 0.2	Moderate certainty (0.2) of limited food availability.

T^{+2} (Unsuitable Nesting Sites)	1 - 0.7 = 0.3	Strong certainty (0.3) of unsuitable nesting sites.
I^{+1} (Possible Safe from Predators)	1 - 0.2 = 0.8	High possibility (0.8) of being relatively safe from predators (opposite of I^{+1} in M_1).
F^{+1} (Abundant Food/Nesting Sites)	1 - 0.0 = 1.0	Certain (1.0) absence of abundant food or suitable nesting sites (opposite of F^{+1} in M_1).
F^{+2} (Low Predator Risk)	1 - 0.0 = 1.0	Certain (1.0) absence of high predator risk (opposite of F^{+2} in M_1).

Interpretation:

The complement highlights areas unsuitable for the bird species. It confirms the lack of abundant food and suitable nesting sites (certainties of 1.0) while also suggesting a moderate possibility (0.8) of being relatively safe from predators. This information helps identify areas where the species is unlikely to thrive and focus conservation efforts on improving suitable habitat in other areas.

These examples highlight how CBN set operations, particularly union and complement, can be used for broader environmental data analysis. They help create a comprehensive picture of potential environmental concerns across larger areas, informing resource allocation for further investigations and targeted environmental monitoring strategies.

o Applications in Data Analysis and Risk Assessment:

- Pinpointing areas where environmental parameters deviate from expected values or established thresholds, even with some degree of uncertainty. This can be useful for identifying potential environmental issues that require further investigation.
- Identifying areas outside the scope of a particular CBN Set, potentially leading to further investigation or refined set definitions. This can lead to a more comprehensive understanding of the environmental conditions being studied.
- Highlighting potential risks or concerns by focusing on areas outside the desired environmental conditions. This can be crucial for environmental risk assessment and prioritizing areas for mitigation strategies.

By effectively utilizing these set operations on CBN Sets, researchers can achieve a richer understanding

* Applications in Data Analysis and Risk Assessment with Numerical Examples

1. Complement (M^{1c}):

We already saw how complement helps identify unsuitable habitat for endangered species. Here is another example for data analysis and risk assessment:

- **Scenario:** Monitoring potential flood risk using a CBN Set (M_1) for water level at a river station.
- **Universe of Discourse:** {Safe Water Level, Moderate Flood Risk, High Flood Risk, Catastrophic Flood Risk}
- **CBN Set (M_1):** Based on historical data and floodplains, M_1 might show high membership degrees for "safe water level" and very low degrees for other categories.

Complement (M_1^c - Flood Risk):

By analyzing the complement, we can identify areas potentially at risk of flooding:

Table 19: "Flood Risk Analysis Using Habitat Suitability Complement (M_1^c)"

Category	M_1^c (Complement)	Interpretation
T^{+1} (Moderate Flood Risk)	0.1	Low certainty (0.1) of moderate flooding, but highlights a possibility beyond the "safe" category in M_1.
T^{+2} (High Flood Risk)	0.05	Very low certainty (0.05) of high flood risk, but indicates a chance exceeding the "safe" range.
I^{+1} (Possible Catastrophic Flood)	0.0	No possibility of catastrophic flooding based on M_1.
F^{+1} (Safe Water Level)	0.0	Certain (0.0) absence of safe water level (opposite of F^{+1} in M_1).

F^{+2} (Low Flood Risk)	0.85	Certain (0.85) absence of low flood risk (opposite of F^{+2} in M_1 - not relevant for identifying flood risk).

The complement highlights a slight possibility (0.1) of moderate flooding and a very low chance (0.05) of high flood risk. While the certainty levels are low, this information is valuable for risk assessment, prompting further investigation or implementing early warning systems near the river station.

2. Identifying Areas Outside CBN Set Scope:

- **Scenario:** Monitoring air quality using a CBN Set (M_1) for common pollutants (e.g., ozone, PM2.5).
- **Analysis:** If the analysis reveals areas with consistently low membership degrees for all categories in M_1, it might indicate the presence of uncommon pollutants not included in the initial CBN Set definition. This would warrant further investigation to identify the specific pollutants and assess potential risks.

3. Highlighting Potential Risks:

- **Scenario:** Assessing potential risks associated with a new industrial facility.
- **Example:** We can analyze a CBN Set (M_1) for potential air pollution emissions from the facility and a CBN Set (M_2) for the vulnerability of nearby ecosystems. The complement of the intersection $(M_1 \cap M_2)^{1c}$ would highlight areas where the intersection is low (i.e., low certainty of both low emissions and low vulnerability). This indicates potential risk due to a possibility of high emissions impacting a vulnerable ecosystem, even if the exact certainty levels in M_1 or M_2 are unclear.

These examples showcase how CBN set operations, particularly complement and analyzing areas outside the CBN Set scope, can be powerful tools in data analysis and risk assessment. They help identify potential environmental issues beyond the initial focus of the CBN Sets, leading to a more comprehensive understanding of environmental risks and informing the development of mitigation strategies.

○ Applying CBN Sets to Water Quality Assessment: A Detailed Example

Water quality is a critical indicator of ecosystem health and human well-being. Traditional methods for water quality assessment often rely on point measurements, which may not capture the spatial and temporal variability of water quality parameters. Additionally, inherent uncertainties in sensor limitations and natural variations can pose challenges. Cubic Bipolar Neutrosophic Sets (CBN Sets) offer a powerful framework to address these limitations by incorporating uncertainty into the analysis.

- **Applying CBN Sets to Water Quality Assessment: A Detailed Example with Numerical Values**

Scenario: We're monitoring a lake for water quality assessment. We'll use CBN Sets to represent two key parameters: pH and dissolved oxygen (DO).

Universe of Discourse:

- **pH:** {< 6 (Strongly Acidic), 6-6.5 (Somewhat Acidic), 6.5-8 (Neutral), 8-8.5 (Somewhat Basic), > 8.5 (Strongly Basic)}
- **DO (mg/L):** {< 4 (Critically Low), 4-5 (Low), 5-8 (Optimal), 8-10 (High), > 10 (Supersaturated)}

Data Collection and Measurement Uncertainties:

- We take pH and DO measurements at a specific location in the lake. However, inherent uncertainties exist due to sensor limitations or natural fluctuations.

Example: Representing pH with CBN Sets

Measured pH value: 7.3

Table 20: Representing pH with CBN Sets (Measured pH: 7.3)

Category	Description	Membership Degree
T^{+1} (Neutral)	Strongly Matches Optimal pH Range (6.5-8)	0.7
T^{+2} (Somewhat Basic)	Moderately Leans Towards Slightly High pH	0.2
I^{+1} (Possibly Somewhat Acidic)	Slight Possibility of Being Below Optimal Range	0.1
F^{+1} (Strongly Acidic)	Negligible Certainty of Being Strongly Acidic	0.0
F^{+2} (Somewhat Acidic)	Very Low Certainty of Being Moderately Low pH	0.0
F^{-1} (Strongly Basic)	Negligible Certainty of Being Strongly Basic	0.0

F^{-2} (Somewhat Basic)	Very Low Certainty of Being Moderately High pH (beyond Somewhat Basic)	0.0

The measured pH value of 7.3 is effectively represented by this CBN Set (Table 20). Here's a breakdown of each category and its membership degree:

- **T^{+1} (Neutral) (0.7):** This category captures the **strong certainty (0.7)** of the pH being within the ideal or optimal range (6.5-8) for the specific environment. The measured value (7.3) falls relatively close to the center of this range, justifying the high membership degree.
- **T^{+2} (Somewhat Basic) (0.2):** This category indicates a **moderate possibility (0.2)** that the pH leans slightly towards the basic side (higher than ideal). However, the value is still somewhat close to the ideal range as reflected by the lower membership degree compared to T^{+1}.
- **I^{+1} (Possibly Somewhat Acidic) (0.1):** The slight possibility (0.1) in this category reflects the fact that the measured pH is not perfectly centered in the ideal range and could be edging slightly towards the acidic side, although the certainty is low.
- **F^{+1} (Strongly Acidic) (0.0): Ø (Empty Set):** These categories represent extremely acidic conditions. Since the measured value is nowhere near this range, the membership degrees are zero (0), indicating negligible certainty.
- **F^{+2} (Somewhat Acidic) (0.0):** This category reflects a very low certainty (0) of the pH being moderately acidic. The measured value is closer to the ideal range than moderately acidic.
- **F^{-1} (Strongly Basic) (0.0): F^{-2} (Somewhat Basic) (0.0):** Similar to the strongly acidic categories, these categories for extremely basic or moderately high basic pH have zero membership degrees due to the measured value being far from these ranges.

Representing DO with CBN Sets:

Imagine the measured DO value is 6.2 mg/L.

Table 21: Representing DO with CBN Sets (Measured DO: 6.2 mg/L)

Category	Description	Membership Degree
T^{+1} (Optimal)	Strongly Matches Optimal DO Range (5-8 mg/L)	0.8
T^{+2} (Somewhat High)	Moderately Leans Towards Slightly High DO	0.1

I^{+1} (Possible Low)	Slight Possibility of Being Below Optimal Range	0.1
F^{+1} (Critically Low)	Negligible Certainty of Being Critically Low	0.0
F^{+2} (Low)	Very Low Certainty of Being Below Optimal Range (but not critically low)	0.0
F^{-1} (Supersaturated)	Negligible Certainty of Being Supersaturated	0.0
F^{-2} (High)	Very Low Certainty of Being Above Optimal Range (but not supersaturated)	0.0

Table 21 effectively represents the measured Dissolved Oxygen (DO) value of 6.2 mg/L using a CBN Set. Let's break down the categories and membership degrees:

- **T^{+1} (Optimal) (0.8):** This category captures the **strong certainty (0.8)** of the DO concentration being within the ideal or optimal range (5-8 mg/L) for the specific environment. The measured value (6.2 mg/L) falls within this range, justifying the high membership degree.
- **T^{+2} (Somewhat High) (0.1):** This category indicates a **low certainty (0.1)** that the DO concentration leans **slightly** above the optimal range. It is important to note that "Somewhat High" here refers to being slightly above the optimal range, but still within acceptable limits.
- **I^{+1} (Possible Low) (0.1):** The slight possibility (0.1) in this category reflects the fact that the measured DO is closer to the lower limit of the optimal range. However, the certainty of being truly low (below optimal) is also low.

Key Points:

- The measured DO (6.2 mg/L) is within the optimal range, with a strong certainty (0.8) based on the CBN Set.
- There is a slight possibility (0.1) of the DO being slightly lower than the ideal level, but the certainty is also low.
- The remaining categories (F^{+1} to F^{-2}) have zero membership degrees (0.0) because the measured value is far from critically low, low, supersaturated, or high DO conditions.

- **Utilizing Set Operations for Spatial Analysis:**

Now, imagine we have CBN Sets for pH and DO at multiple locations across the lake. We can use set operations to analyze the data spatially:

- **Intersection (M_pH ∩ M_DO):** This identifies areas where both pH and DO meet acceptable water quality standards simultaneously. A high intersection value indicates a location with a strong likelihood of good overall water quality.
- **Union (M_pH ∪ M_DO):** This highlights regions where either pH or DO (or potentially both) might fall outside the acceptable range, even with some uncertainty. A high union value suggests a potential water quality concern that needs further investigation.
- **Complement (M_pH^c or M_DO^c):** This helps pinpoint areas where any parameter deviates from optimal values. A high complement value for a specific category (e.g., Strongly

7. Representing Water Quality Parameters as CBN Sets

Essential water quality parameters like pH, turbidity, and dissolved oxygen can be effectively represented as CBN Sets. Each parameter's set would include membership degrees reflecting the certainty, possibility, and indeterminacy of the measured value falling within acceptable ranges for healthy water quality.

7.1. Example: Representing pH with CBN Sets

A CBN Set for pH might include membership degrees for:

Table 22: "CBN set for pH

Description	Membership Degree
Strongly acidic (low pH)	T^{+1} (Strongly Acidic)
Somewhat acidic (moderately low pH)	T^{+2} (Somewhat Acidic)
Neutral (optimal pH range)	T^{+1} (Neutral)
Somewhat basic (moderately high pH)	T^{+2} (Somewhat Basic)
Strongly basic (high pH)	T^{+1} (Strongly Basic)

The specific values for these membership degrees would be determined based on the measured pH value and established thresholds for optimal water quality. Similar CBN Sets can be created for other parameters like turbidity and dissolved oxygen.

Explanation of how a CBN set can be used to represent pH with membership degrees. Here is a specific numerical example to illustrate the concept further:

We measure the pH of a lake sample and find a value of 7.3.

Universe of Discourse:

- {< 6 (Strongly Acidic), 6-6.5 (Somewhat Acidic), 6.5-8 (Neutral), 8-8.5 (Somewhat Basic), > 8.5 (Strongly Basic)}

Reasoning behind Membership Degrees:

- Since optimal water quality for most aquatic life falls within the 6.5-8 pH range (Neutral), we will assign a higher membership degree (truth membership) to this category.
- We can consider a buffer zone on either side of the optimal range, assigning moderately high membership degrees (T^{+2}) for "Somewhat Acidic" (6-6.5) and "Somewhat Basic" (8-8.5).
- As we move further away from the optimal range, the membership degrees for "Strongly Acidic" (T^{+1}) and "Strongly Basic" (T^{+1}) become negligible (0.0) because these conditions are less likely for healthy water.
- We can also include "possible" categories (I^{+1}) with very low membership degrees to account for slight uncertainties in the measurement or natural fluctuations.

Example CBN set for pH:

This example demonstrates how CBN Sets, with their assigned membership degrees, can capture both the measured value and the inherent uncertainties in environmental data.

Table 23: Example CBN Set for pH

Category	Description	Membership Degree

T^{+1} (Neutral)	Strongly Matches Optimal pH Range (6.5-8)	0.7
T^{+2} (Somewhat Basic)	Moderately Leans Towards Slightly High pH	0.2
I^{+1} (Possibly Somewhat Acidic)	Slight Possibility of Being Below Optimal Range	0.1
F^{+1} (Strongly Acidic)	Negligible Certainty of Being Strongly Acidic	0.0
F^{+2} (Somewhat Acidic)	Very Low Certainty of Being Moderately Low pH	0.0
F^{-1} (Strongly Basic)	Negligible Certainty of Being Strongly Basic	0.0
F^{-2} (Somewhat Basic)	Very Low Certainty of Being Moderately High pH (beyond Somewhat Basic)	0.0

Interpretation:

This CBN Set effectively represents the measured pH value. Here's a breakdown of the information:

- There is a strong likelihood (0.7) of the pH being within the optimal range (6.5-8) for **most freshwater ecosystems**. This suggests a healthy environment for a variety of aquatic life.
- A moderate possibility (0.2) exists that the pH leans slightly towards the basic side. Depending on the specific tolerances of the resident organisms, this might require further investigation.

- A slight chance (0.1) exists that the pH might be slightly below the optimal range (acidic). However, the low certainty indicates minimal concern at this point.
- The very low membership degrees for extreme categories (Strongly Acidic/Basic) indicate negligible certainty of the pH being outside the acceptable range.

7.2. Sample Data Analysis with CBN Sets

Imagine we have CBN Sets representing pH, turbidity, and dissolved oxygen (DO) for three water samples (Table 4).

Here is a breakdown of the sample data analysis with CBN Sets (Table 4) using the provided information:

Table 24: Water Quality Data with CBN Sets

Sample	pH	Turbidity	DO
1	(0.8, 0.1, 0.05, 0.0, 0.05, 0.0, 0.0, 0.0, 0.05, 0.0, 0.9, 0.1)	(0.7, 0.2, 0.0, 0.1, 0.0, 0.0, 0.0, 0.0, 0.3, 0.2, 0.5, 0.0)	(0.9, 0.1, 0.0, 0.0, 0.0, 0.0, 0.0, 0.0, 0.1, 0.0, 0.8, 0.2)
2	(0.6, 0.2, 0.1, 0.0, 0.1, 0.0, 0.0, 0.0, 0.0, 0.0, 1.0, 0.0)	(0.4, 0.3, 0.1, 0.1, 0.1, 0.0, 0.0, 0.0, 0.5, 0.2, 0.4, 0.0)	(0.7, 0.2, 0.0, 0.1, 0.0, 0.0, 0.0, 0.0, 0.3, 0.1, 0.6, 0.0)
3	(0.3, 0.2, 0.4, 0.1, 0.0, 0.0, 0.0, 0.0, 0.7, 0.2, 0.1, 0.0)	(0.2, 0.3, 0.4, 0.1, 0.0, 0.0, 0.0, 0.0, 0.8, 0.5, 0.0, 0.0)	(0.5, 0.3, 0.1, 0.0, **0.1** , 0.0, 0.0, 0.0, 0.4, 0.2, 0.3, 0.0)

Analysis:

- **Sample 1:**
  - **pH:** High certainty (0.8) of being within the optimal range, with a slight possibility (0.05) of being acidic.
  - **Turbidity:** Moderately high possibility (0.7) of being within acceptable limits, with a moderate chance (0.3) of exceeding them.
  - **DO:** Very strong certainty (0.9) of having optimal dissolved oxygen levels.
- **Sample 2:**
  - **pH:** Slightly leans towards the optimal range (0.6) with some uncertainty (0.2 towards acidic and 0.1 towards basic).

- **Turbidity:** High possibility (0.7) of exceeding acceptable turbidity levels.
- **DO:** Similar to Sample 1, with very strong certainty (0.7) of optimal DO levels.

- **Sample 3:**
  - **pH:** Moderately low certainty (0.3) for optimal pH, with significant possibilities (0.4) of being acidic.
  - **Turbidity:** Very high certainty (0.8) of exceeding acceptable turbidity levels.
  - **DO:** Moderate certainty (0.5) of being within the optimal range, but with a slight possibility (0.1) of being low (**highlighted value**).

Interpretation:

This analysis reveals:

- Sample 1 has the most favorable water quality conditions with a high likelihood of optimal pH, moderate turbidity, and very good DO levels.
- Sample 2 has a potential concern with turbidity exceeding acceptable levels, although pH and DO seem to be within a desirable range.
- Sample 3 has the most significant water quality issues. The pH is likely acidic, turbidity is very high, and DO levels show a slight possibility of being low.

Note: These interpretations are based on hypothetical thresholds for optimal water quality. In real-

7.3. Numerical Examples for Air Quality Monitoring with CBN Sets

- **Representing Air Quality Parameters as CBN Sets**

Example: Representing Ozone Levels with CBN Sets

Here is a breakdown of a CBN Set for ozone levels with assigned membership degrees:

Universe of Discourse: Parts per Billion (ppb)

- **Low Ozone (Safe):** T^{+1} (Low Ozone) - Ozone concentration <= healthy threshold (e.g., 50 ppb)
- **Moderately Elevated Ozone Levels:** T^{+2} (Moderately Elevated) - Between healthy and unhealthy thresholds (e.g., 51-70 ppb)
- **High Ozone Levels (Unhealthy):** T^{+1} (High Ozone) - Above unhealthy threshold (e.g., > 70 ppb)
- **Indeterminate Ozone Measurement:** I^{+1} (Indeterminate) - Sensor malfunction, unclear reading, etc.
- **Falsely Low Ozone Reading:** F^{+1} (Falsely Low) - Equipment issue resulting in underestimation of ozone concentration.
- **Assigning Membership Degrees:**

Imagine we measure an ozone concentration of 65 ppb. Here is a possible assignment:

Table 25: Ozone Concentration CBN Set (65 ppb)

Category	Description	Membership Degree
T^{+1} (Low Ozone)	Negligible Certainty (safe)	0.0
T^{+2} (Moderately Elevated)	High Certainty (unhealthy range)	0.8
T^{+1} (High Ozone)	Moderate Certainty (exceeding healthy threshold)	0.2
I^{+1} (Indeterminate)	No Indeterminacy	0.0
F^{+1} (Falsely Low)	Very Low Certainty (unlikely underestimation)	0.0

This table represents a CBN Set for a measured ozone concentration of 65 ppb. Here's a breakdown of the categories and membership degrees:

- **T^{+1} (Low Ozone) (0.0):** This category has a membership degree of 0.0, indicating **negligible certainty** of the ozone concentration being low (safe). Given the measured value (65 ppb) and the descriptions of other categories, this category likely applies to much lower ozone concentrations than 65 ppb.
- **T^{+2} (Moderately Elevated) (0.8):** This category has a high membership degree (0.8), indicating **strong certainty** that the ozone concentration falls within the moderately elevated range. The description can be rephrased to "**Likely in the unhealthy range**" based on the high membership degree.
- **T^{+1} (High Ozone) (0.2):** This category has a moderate membership degree (0.2), indicating **some certainty** that the ozone concentration might be exceeding the healthy threshold and reaching high ozone levels.
- **Sample Data Analysis with CBN Sets**

Table 26: (Example): Air Quality Data with CBN Sets

Station	Ozone (O_3)	PM2.5
1	(0.7, 0.2, 0.0, 0.1, 0.0, 0.0, 0.0, 0.0, 0.3, 0.1, 0.6, 0.0)	(0.8, 0.1, 0.0, 0.0, 0.1, 0.0, 0.0, 0.0, 0.1, 0.0, 0.8, 0.2)
2	(0.4, 0.3, 0.1, 0.1, 0.1, 0.0, 0.0, 0.0, 0.5, 0.2, 0.4, 0.0)	(0.6, 0.2, 0.1, 0.0, 0.0, 0.1, 0.0, 0.0, 0.4, 0.2, 0.5, 0.0)
3	(0.2, 0.1, 0.5, 0.2, 0.0, 0.0, 0.0, 0.0, 0.8, 0.5, 0.0, 0.0)	(0.5, 0.3, 0.1, 0.1, 0.0, 0.0, 0.0, 0.0, 0.5, 0.2, 0.3, 0.0)

Analysis of Table 26: Air Quality Data with CBN Sets

This table presents air quality data for Ozone (O_3) and PM2.5 at three stations, with each station having two sets of CBN membership degrees representing potentially duplicate measurements or different time points. Here's a breakdown of the information and potential interpretations:

Assuming Membership Degrees Represent Categories:

We can analyze the data assuming each set of membership degrees corresponds to specific CBN Set categories (though category descriptions are not provided). Here's a possible interpretation for each station:

- **Station 1:**
  - **Ozone (O_3):**
    - First row: High certainty (0.7) of **low ozone levels (likely safe)** and moderate possibility (0.2) of exceeding the ideal range.
    - Second row: Very high certainty (0.8) of **safe ozone levels** and low certainty (0.1) of exceeding the ideal range.
  - **PM2.5:**
    - Membership degrees are not shown, but the presence of a high value (likely in the T^{+1} category) in both rows suggests **very good air quality** for PM2.5.
- **Station 2:**
  - **Ozone (O_3):**
    - First row: Moderate certainty (0.4) of **moderately elevated ozone levels** and significant possibility (0.3) of exceeding healthy limits.

- Second row: High certainty (0.6) of **ozone levels within the acceptable range** and low certainty (0.1) of exceeding the ideal range.

o **PM2.5:**

- Membership degrees are not shown, but the presence of a moderate value (likely in the T^{+2} category) in both rows suggests **a possibility of PM2.5 exceeding the ideal range, but with moderate certainty**.

- **Station 3:**

o **Ozone (O_3):**

- First row: Low certainty (0.2) of safe ozone levels and **significant possibility (0.5) of exceeding healthy ozone levels**.
- Second row: Moderate certainty (0.5) of **ozone levels exceeding healthy limits** and significant possibility (0.3) of very high ozone levels.

o **PM2.5:**

- Membership degrees are not shown, but the presence of a high value (likely in the T^{+1} category) in the first row suggests good air quality. The second row's membership degrees are needed for a complete picture.

Important Considerations:

- **Missing Information:** The absence of category descriptions for the membership degrees limits a fully detailed analysis. Knowing the specific ranges and descriptions associated with each category (e.g., T^{+1} for ozone - safe vs. moderately elevated) would provide clearer interpretations.
- **Multiple Measurements:** It's unclear if each row represents duplicate measurements or data from different time points. If they are different time points, then the analysis would need to consider the variability within each station.

8. (Enhanced) Air Quality Analysis with CBN Sets: Operations, Distances, and Similarities

8.1. Some numerical examples to illustrate the concepts of set operations, distances, and similarities in air quality analysis using CBN Sets

We can leverage set operations like intersection, union, and complement to gain valuable insights from CBN Sets for air quality analysis.

We have CBN Sets representing ozone (O_3) and PM2.5 levels at three air quality-monitoring stations

Table 27: CBN sets for ozone (O_3) and PM2.5 levels at three stations

Station	Ozone (O_3)	PM2.5

1	(0.7, 0.2, 0.0, 0.1, 0.0, 0.0, 0.0, 0.0, 0.3, 0.1, 0.6, 0.0)	(0.8, 0.1, 0.0, 0.0, 0.1, 0.0, 0.0, 0.0, 0.1, 0.0, 0.8, 0.2)
2	(0.4, 0.3, 0.1, 0.1, 0.1, 0.0, 0.0, 0.0, 0.5, 0.2, 0.4, 0.0)	(0.6, 0.2, 0.1, 0.0, 0.0, 0.1, 0.0, 0.0, 0.4, 0.2, 0.5, 0.0)
3	(0.2, 0.1, 0.5, 0.2, 0.0, 0.0, 0.0, 0.0, 0.8, 0.5, 0.0, 0.0)	(0.5, 0.3, 0.1, 0.1, 0.0, 0.0, 0.0, 0.0, 0.5, 0.2, 0.3, 0.0)

- **Leveraging Set Operations for Air Quality Insights**

Intersection: Let us define acceptable thresholds for ozone (e.g., T^{+1} for "Low Ozone") and PM2.5 (e.g., T^{+1} for "Good PM2.5"). The intersection of CBN Sets for Stations 1 and 2 might be a set with high membership degrees (around 0.7-0.8) for these categories, indicating a good chance of both stations having acceptable air quality.

- **Union:** The union of CBN Sets for ozone across all stations might include membership degrees for "Moderately Elevated" and "High Ozone" due to elevated levels at Stations 2 and 3, highlighting potential air quality concerns in the broader region.
- **Complement:** The complement of the CBN Set representing "Good Air Quality" for Station 3 might have high membership degrees for "High Ozone" and "Moderately High PM2.5" categories, pinpointing potential issues at that location.

8.2. Quantifying Relationships with Distance Measures and Similarity Coefficients

- **Distance Measures:**
    - **Euclidean Distance:** We can calculate the Euclidean distance between the CBN Sets for Stations 1 and 2. This distance considers the differences in membership degrees for all categories (truth, indeterminacy, falsity) and reflects the dissimilarity in their air quality profiles.

Calculating Euclidean Distance:

1. **Square the differences:** For each corresponding membership degree (truth, indeterminacy, falsity) category in the two CBN Sets (Station 1 and Station 2), calculate the squared difference between their membership degrees.

2. **Sum the squared differences:** Add the squared differences obtained in step 1 for all categories.
3. **Take the square root:** Finally, calculate the square root of the sum obtained in step 2. This will be the Euclidean distance between the two CBN Sets.

Interpretation:

A higher Euclidean distance indicates greater dissimilarity between the air quality profiles of the two stations. The membership degrees encode the certainty levels for various air quality conditions (e.g., low ozone, moderately elevated ozone). Therefore, the Euclidean distance captures the overall difference in these certainty levels between the stations.

Example:

Let us consider simplified CBN Sets for Station 1 and Station 2 with only three categories (Low, Moderate, High) and their corresponding membership degrees:

- Station 1: (0.8, 0.1, 0.1) - High certainty (0.8) of low air pollution, low certainty (0.1) each for moderate and high pollution.
- Station 2: (0.2, 0.5, 0.3) - Low certainty (0.2) of low pollution, moderate certainty (0.5) of moderate pollution, and moderate certainty (0.3) of high pollution.

Calculating the distance:

1. Squared differences: [(0.8-0.2)^2, (0.1-0.5)^2, (0.1-0.3)^2] = [0.36, 0.16, 0.04]
2. Sum of squared differences: 0.36 + 0.16 + 0.04 = 0.56
3. Euclidean distance: $\sqrt{0.56} \approx 0.75$

In this example, the Euclidean distance of approximately 0.75 indicates a moderate dissimilarity between the air quality profiles of the two stations. Station 1 has a higher certainty of low pollution, while Station 2 has a higher certainty of moderate and high pollution levels.

By calculating Euclidean distances between CBN Sets for multiple stations, we can identify patterns and potential pollution hotspots that require further investigation.

Manhattan Distance:

1. **Absolute differences:** For each corresponding membership degree category (truth, indeterminacy, falsity) in the two CBN Sets (Stations 2 and 3 in this case), calculate the absolute difference between their membership degrees.
2. **Sum the absolute differences:** Add the absolute differences obtained in step 1 for all categories.

Interpretation:

Similar to Euclidean distance, a higher Manhattan distance indicates greater dissimilarity between the air quality profiles. However, Manhattan distance focuses on the **sum of absolute differences**

rather than squared differences. This means it emphasizes larger discrepancies between membership degrees, potentially giving more weight to significant variations in certainty levels.

Example:

Let us reuse the simplified CBN Sets from the previous example for Station 2: (0.2, 0.5, 0.3) and create a hypothetical CBN Set for Station 3: (0.1, 0.4, 0.5).

Calculating Manhattan distance:

1. Absolute differences: [|0.2-0.1|, |0.5-0.4|, |0.3-0.5|] = [0.1, 0.1, 0.2]
2. Sum of absolute differences: 0.1 + 0.1 + 0.2 = 0.4

In this example, the Manhattan distance is 0.4. Compared to the Euclidean distance of 0.75 between Station 1 and Station 2, this smaller Manhattan distance suggests a potentially **weaker** difference between Stations 2 and 3.

Choosing Between Euclidean and Manhattan Distances:

- **Euclidean distance** might be preferable when emphasizing larger variations in certainty levels between corresponding categories. Squaring the differences magnifies the impact of significant discrepancies.
- **Manhattan distance** is more sensitive to the **number of categories** with non-zero membership degrees. Even small absolute differences can contribute more to the overall distance if there are many categories.

The choice between these distances depends on the specific analysis goals and the importance you place on highlighting substantial variations in membership degrees.

In conclusion, both Euclidean and Manhattan distances offer valuable insights into the dissimilarity between air quality profiles represented by CBN Sets. By considering these distances alongside set operations like intersection and union, we can gain a comprehensive understanding of air quality variations across monitoring stations.

- **Similarity Coefficients:**
    - **Jaccard Similarity for Dissimilarity in Air Quality**

As you mentioned, Jaccard Similarity is a metric that quantifies the similarity between two sets by focusing on the proportion of elements they share. In the case of CBN Sets, these elements represent the membership degrees for various air quality categories (e.g., low ozone, moderate ozone). A lower Jaccard Similarity value indicates a lesser degree of similarity in the air quality profiles of the stations, potentially due to differences in specific parameters like ozone levels.

Calculation Steps:

1. **Intersection:** Find the sum of the **minimum membership degrees** for each corresponding category (truth, indeterminacy, falsity) between the CBN Sets for Stations 1 and 3.
2. **Union:** Find the sum of the **maximum membership degrees** for each corresponding category between the two stations' CBN Sets.

3. **Jaccard Similarity:** Divide the intersection (step 1) by the union (step 2).

Interpretation:

The Jaccard Similarity value will range from 0 to 1:

- **1**: Perfect similarity (both stations have identical CBN Sets).
- **0**: No overlap in membership degrees (completely dissimilar air quality profiles).
- **Values closer to 0**: Lower degree of similarity, potentially due to significant differences in ozone levels or other air quality parameters.

Example (assuming simplified CBN Sets with three categories):

- Station 1: CBN Set (0.8, 0.1, 0.1) - High certainty (0.8) for low ozone, low certainty (0.1) each for moderate and high ozone.
- Station 3: CBN Set (0.2, 0.5, 0.3) - Low certainty (0.2) for low ozone, moderate certainty (0.5) for moderate ozone, and moderate certainty (0.3) for high ozone.

Calculating Jaccard Similarity:

1. Intersection: Minimums = (0.8, min(0.1, 0.5), min(0.1, 0.3)) = (0.8, 0.1, 0.1) ; Sum of minimums = 1.
2. Union: Maximums = (0.8, max(0.1, 0.5), max(0.1, 0.3)) = (0.8, 0.5, 0.3) ; Sum of maximums = 1.6.
3. Jaccard Similarity: 1 (intersection) / 1.6 (union) ≈ 0.625.

Interpretation of the Example:

The Jaccard Similarity of approximately 0.625 indicates a moderate degree of similarity between Stations 1 and 3. While Station 1 has a higher certainty of low ozone levels, there's some overlap in certainty levels for the "Low" and "Moderate" ozone categories between the two stations. This suggests that ozone might not be a major differentiating factor between their air quality profiles.

Jaccard Similarity vs. Other Distances:

It's important to remember that Jaccard Similarity focuses on the **proportion** of shared membership degrees, whereas metrics like Euclidean and Manhattan distances consider the **magnitude** of differences. Jaccard Similarity is a valuable tool when the presence or absence of overlap in membership degrees is more important than the extent of those differences.

By incorporating Jaccard Similarity alongside other analytical techniques, we can gain a comprehensive understanding of similarities and dissimilarities in air quality data represented by CBN Sets at different monitoring stations.

Jaccard Similarity for CBN Sets:

Key Points about Jaccard Similarity:

- **Focuses on Shared Memberships:** Jaccard Similarity emphasizes the **proportion of membership degrees** that two CBN Sets have in common. This considers both categories

where stations share similar certainty levels (overlap) and categories where their certainty levels differ (non-overlap).

- **Interpretation:** The Jaccard Similarity value ranges from 0 to 1.
    - **1**: Indicates perfect similarity (identical CBN Sets).
    - **0**: Indicates no overlap in membership degrees (completely dissimilar air quality profiles).
    - **Values closer to 0**: Suggest a lesser degree of similarity, potentially due to differences in air quality parameters like ozone levels.

Jaccard Similarity Calculation:

1. **Intersection:** Find the sum of the **minimum membership degrees** for each corresponding category (truth, indeterminacy, falsity) between the two CBN Sets.
2. **Union:** Find the sum of the **maximum membership degrees** for each corresponding category between the two CBN Sets.
3. **Jaccard Similarity:** Divide the intersection (step 1) by the union (step 2).

Example:

Consider simplified CBN Sets with three categories (Low, Moderate, High) for Station 1 (0.8, 0.1, 0.1) and Station 3 (0.2, 0.5, 0.3).

Calculating Jaccard Similarity:

- Intersection: Minimums = (0.8, min(0.1,0.5), min(0.1,0.3)) = (0.8, 0.1, 0.1) ; Sum = 1.
- Union: Maximums = (0.8, max(0.1,0.5), max(0.1,0.3)) = (0.8, 0.5, 0.3) ; Sum = 1.6.
- Jaccard Similarity: 1 (intersection) / 1.6 (union) ≈ 0.625.

Interpretation of the Example:

The Jaccard Similarity of 0.625 indicates a moderate degree of similarity between Stations 1 and 3. Even though Station 1 has a higher certainty of low ozone, there's some overlap in certainty levels for the "Low" and "Moderate" categories, suggesting ozone might not be a significant differentiating factor.

Jaccard Similarity vs. Other Distances:

- **Focus on Proportion vs. Magnitude:** Jaccard Similarity focuses on the **proportion** of shared memberships, while Euclidean and Manhattan distances consider the **magnitude** of differences in membership degrees.
- **When to Use Jaccard Similarity:** It's valuable when the presence or absence of overlap in membership degrees is more important than the extent of those differences.

By incorporating Jaccard Similarity alongside other techniques, we can gain a comprehensive understanding of similarities and dissimilarities in air quality data from CBN Sets at various monitoring stations.

9. Calculation:

1. **Intersection:** Find the sum of the minimum membership degrees for each corresponding category (truth, indeterminacy, falsity) between the two CBN Sets (Stations 1 and 3 in this case).
2. **Union:** Find the sum of the maximum membership degrees for each corresponding category between the two CBN Sets.
3. **Jaccard Similarity:** Divide the intersection (step 1) by the union (step 2).

Interpretation:

- The Jaccard Similarity ranges from 0 to 1.
- A value of 1 indicates that the CBN Sets are identical (perfect similarity).
- A value of 0 indicates no overlap in membership degrees (complete dissimilarity).
- Lower values (closer to 0) suggest a lesser degree of similarity, potentially due to differences in specific air quality parameters (like ozone levels in your example).

Example:

Let's again consider simplified CBN Sets with three categories (Low, Moderate, High) for Station 1 (0.8, 0.1, 0.1) and Station 3 (0.2, 0.5, 0.3).

Calculating Jaccard Similarity:

1. Intersection: Minimums = (0.8, min(0.1,0.5), min(0.1,0.3)) = (0.8, 0.1, 0.1) ; Sum of minimums = 1.
2. Union: Maximums = (0.8, max(0.1,0.5), max(0.1,0.3)) = (0.8, 0.5, 0.3) ; Sum of maximums = 1.6.
3. Jaccard Similarity: 1 (intersection) / 1.6 (union) ≈ 0.625.

In this example, the Jaccard Similarity of 0.625 indicates a moderate degree of similarity between the air quality profiles of Stations 1 and 3. While Station 1 has a higher certainty of low pollution, Station 3 has some overlap in certainty levels for the "Low" and "Moderate" categories.

Jaccard Similarity vs. Other Distances:

- Jaccard Similarity focuses on the **proportion** of shared memberships, whereas Euclidean and Manhattan distances consider the **magnitude** of differences.
- It can be useful when the presence or absence of overlap in membership degrees is more important than the extent of those differences.

By incorporating Jaccard Similarity alongside Euclidean and Manhattan distances, we can gain a more nuanced understanding of similarities and dissimilarities between air quality profiles at different stations.

- **Dice Coefficient:** The Dice Coefficient is indeed a strong candidate for highlighting the potential overlap in exceeding acceptable ozone levels between Stations 2 and 3, and it might even be higher than the Jaccard Similarity in this scenario. Here is why:

Dice Coefficient for CBN Sets:

The Dice Coefficient emphasizes **agreements** between CBN Sets more than Jaccard Similarity. It focuses on the **sum of twice the minimum membership degrees** for each corresponding category (truth, indeterminacy, falsity) between the two stations.

Why Might Dice Coefficient be Higher?

- **Emphasis on Overlap:** By doubling the minimum membership degrees, the Dice Coefficient gives more weight to categories where both stations have some level of membership, even if the certainty levels differ.
- **Potential Ozone Level Similarity:** In your example, both Stations 2 and 3 have a possibility of exceeding acceptable ozone levels. This means there might be some overlap in their membership degrees for the "Moderately Elevated" or "High" ozone categories, even if they differ in certainty levels.
- **Higher Weighting:** The Dice Coefficient places more weight on this overlap compared to Jaccard Similarity, potentially leading to a higher value.

Calculation:

1. **Minimum membership degrees:** Find the minimum membership degree for each corresponding category between the two CBN Sets.
2. **Dice Coefficient:** Multiply each minimum membership degree by 2 and add them up.

Interpretation:

- The Dice Coefficient ranges from 0 to 1, similar to Jaccard Similarity.
- **1**: Perfect similarity (identical CBN Sets).
- **0**: No overlap in membership degrees (completely dissimilar air quality profiles).
- **Values closer to 1**: Higher degree of similarity, potentially due to shared possibility of exceeding ozone limits or overlap in other categories.

Example (assuming simplified CBN Sets):

- Station 2: CBN Set (0.4, 0.5, 0.1)
- Station 3: CBN Set (0.2, 0.4, 0.5)

Calculating Dice Coefficient:

1. Minimum membership degrees: (0.4, min(0.5, 0.4), min(0.1, 0.5)) = (0.4, 0.4, 0.1).
2. Dice Coefficient: (2 * 0.4) + (2 * 0.4) + (2 * 0.1) = 1.8.

Note: The Dice Coefficient can be greater than 1 due to the doubling of membership degrees. We often normalize it by dividing by 2, resulting in a value between 0 and 1. In this example, the normalized value would be 0.9.

Comparison with Jaccard Similarity:

We haven't calculated the Jaccard Similarity yet, but because it only sums the minimum membership degrees (without doubling), it's likely to be lower than the Dice Coefficient in this case. The emphasis

on overlap in the Dice Coefficient captures the possibility of both stations exceeding ozone limits, even if their certainty levels differ.

By considering both the Dice Coefficient and Jaccard Similarity, we gain a more nuanced understanding of the similarity between Stations 2 and 3. The Dice Coefficient highlights the potential for exceeding ozone limits at both stations, while Jaccard Similarity provides a broader measure of overall agreement in membership degrees.

Combining Set Operations, Distances, and Similarities:

- **Combining Techniques for Air Quality Analysis:**

2. **Intersection:** Identify Stations of Concern:
    - Define acceptable thresholds for each air quality category (e.g., T^{+1} for "Good PM2.5").
    - The intersection of CBN Sets for multiple stations will reveal stations with membership degrees below these thresholds, potentially indicating air quality concerns. For example, a low membership degree in the "Good" category for Station 3 in your example suggests potential issues.
3. **Distances or Similarities for Spatial Context:**
    - Once you identify stations of concern, calculate the distance or similarity between their CBN Sets and nearby stations.
    - **Distances (Euclidean, Manhattan):**
        - A high distance between a station with air quality concerns (e.g., Station 3) and nearby stations (Stations 1 and 2) might suggest a localized issue. The larger the distance, the greater the dissimilarity in air quality profiles.
    - **Similarities (Jaccard, Dice):**
        - A high similarity between a station with concerns and nearby stations suggests a more widespread issue. The higher the similarity, the more the air quality profiles share characteristics.

Example:

- Station 3 has a low membership degree for "Good Air Quality" (potential concern).
- Stations 1 and 2 have high similarity with Station 3 (based on Jaccard or Dice Coefficient).
- Station 3 has a large Euclidean distance compared to Stations 1 and 2.

Interpretation:

While Stations 1, 2, and 3 share similar air quality characteristics, the large Euclidean distance between Station 3 and the others suggests the issue might be localized to Station 3. The high similarity could indicate a common source of pollution affecting a broader region, but Station 3 experiences it more intensely.

Additional Considerations:

- **Visualizations:** Creating maps with color gradients representing membership degrees or distances can provide a clear spatial understanding of air quality variations.
- **Wind Data:** Wind direction and speed data can be integrated to understand potential pollutant transport and how localized issues might affect nearby areas.

By combining set operations, distances, similarities, and potentially other relevant data, we can gain a comprehensive understanding of air quality patterns, identify areas with potential concerns, and assess the spatial extent of air quality issues.

10. Conclusion

Cubic Bipolar Neutrosophic Sets (CBN Sets) have emerged as a powerful tool for environmental data analysis, particularly in scenarios where uncertainty is inherent. This concluding section summarizes the key takeaways and highlights the potential of CBN Sets in environmental science.

Key Takeaways:

- CBN Sets effectively represent environmental data by incorporating truth, indeterminacy, and falsity membership degrees, acknowledging inherent uncertainties in measurements.
- Set operations (intersection, union, complement) on CBN Sets enable researchers to manipulate and analyze environmental data while considering these uncertainties.
- Distance measures and similarity coefficients quantify the relationships between air quality profiles of different monitoring stations, revealing spatial patterns and potential pollutant sources.

Potential of CBN Sets in Environmental Science:

- **Refined Information:** CBN Sets allow for a more nuanced understanding of environmental phenomena by accounting for uncertainties in data.
- **Improved Decision-Making:** By providing a clearer picture of environmental conditions with associated certainty levels, CBN Sets can inform better decision-making for environmental management and resource allocation.
- **Enhanced Trend Analysis:** Analyzing CBN Sets over time allows for the identification of trends in environmental parameters, facilitating proactive measures to address potential environmental issues.
- **Unified Framework:** CBN Sets offer a versatile framework applicable to various environmental domains beyond water and air quality, including soil contamination analysis, biodiversity monitoring, and climate change studies.

Future Directions:

The application of CBN Sets in environmental science is a burgeoning field. Future research can explore:

- Developing advanced set operations and similarity measures specifically tailored for environmental data analysis.
- Integrating CBN Sets with machine learning algorithms for automated environmental data analysis and pattern recognition.
- Implementing CBN Sets in environmental modeling and simulation for more robust predictions under uncertain conditions.

In conclusion, CBN Sets hold immense potential for revolutionizing environmental data analysis by embracing the inherent uncertainties in environmental measurements. As research and applications in this field continue to evolve, CBN Sets can become a cornerstone for achieving a more comprehensive understanding and improved management of our planet's health.

Acknowledgement

This research is supported by the Neutrosophic Science International Association (NSIA) in both of its headquarters at New Mexico University and its Iraqi branch at Telafer University, for more details about (NSIA) see the URL http://neutrosophicassociation.org/.

Conflicts of Interest: The authors declare no conflict of interest.

References

1. Smarandache, F. (2005). A unifying field in logics: neutrosophic logic. Neutrosophy, neutrosophic set, neutrosophic probability: neutrsophic logic. Neutrosophy, neutrosophic set, neutrosophic probability. Infinite Study.
2. Das, S., Roy, B. K., Kar, M. B., Kar, S., & Pamučar, D. (2020). Neutrosophic fuzzy set and its application in decision-making. Journal of Ambient Intelligence and Humanized Computing, 11, 5017-5029.
3. Zhang, F., Liu, Z., Li, H., Ye, J., & Han, B. (2022). Parameterized soil recognition using normal similarity measures on dynamic neutrosophic cubic sets. International Journal of Fuzzy Systems, 24(3), 1634-1652.
4. Lee, K. M., LEE, K. M., & CIOS, K. J. (2001). Comparison of interval-valued fuzzy sets, intuitionistic fuzzy sets, and bipolar-valued fuzzy sets. In Computing and information technologies: exploring emerging technologies (pp. 433-439).
5. Sokal, R. R. (1961). Distance as a measure of taxonomic similarity. Systematic Zoology, 10(2), 70-79.
6. Gulistan, M., Yaqoob, N., Elmoasry, A., & Alebraheem, J. (2021). Complex bipolar fuzzy sets: an application in a transport's company. Journal of Intelligent & Fuzzy Systems, 40(3), 3981-3997.
7. Zhang, W. R. (1998, May). (Yin)(Yang) bipolar fuzzy sets. In 1998 IEEE international conference on fuzzy systems proceedings. IEEE world congress on computational intelligence (Cat. No. 98CH36228) (Vol. 1, pp. 835-840). IEEE.

8. Kokaly, R. F., Clark, R. N., Swayze, G. A., Livo, K. E., Hoefen, T. M., Pearson, N. C., ... & Klein, A. J. (2017). Usgs spectral library version 7 data: Us geological survey data release. United States Geological Survey (USGS): Reston, VA, USA, 61.
9. Mustafa, A., Saadi, I., Cools, M., & Teller, J. (2018). A Time Monte Carlo method for addressing uncertainty in land-use change models. International Journal of Geographical Information Science, 32(11), 2317-2333.
10. Jain, A. K., Murty, M. N., & Flynn, P. J. (1999). Data clustering: a review. ACM computing surveys
11. Dezert, J. (2009). Advances and applications of DSmt for information fusion: collected works. American Research Press.
12. Al Shumrani, M. A., Gulistan, M., & Khan, S. (2020). The neutro-stability analysis of neutrosophic cubic sets with application in decision making problems. Journal of Mathematics, 2020, 1-16.
13. Ali, M., Son, L. H., Deli, I., & Tien, N. D. (2017). Bipolar neutrosophic soft sets and applications in decision making. Journal of Intelligent & Fuzzy Systems, 33(6), 4077-4087.
14. Ulucay, V., Deli, I., & Şahin, M. (2018). Similarity measures of bipolar neutrosophic sets and their application to multiple criteria decision making. Neural Computing and Applications, 29, 739-748.
15. Kamacı, H., Garg, H., & Petchimuthu, S. (2021). Bipolar trapezoidal neutrosophic sets and their Dombi operators with applications in multicriteria decision making. Soft Computing, 25(13), 8417-8440.
16. Hashim, R. M., Gulistan, M., & Smarandache, F. (2018). Applications of neutrosophic bipolar fuzzy sets in HOPE foundation for planning to build a children hospital with different types of similarity measures. Symmetry, 10(8), 331.
17. Sultana, F., Gulistan, M., Liu, P., Ali, M., Khan, Z., Al-Shamiri, M. M., & Azhar, M. (2022). On Development of Neutrosophic Cubic Graphs with Applications in Decision Sciences. Journal of Function Spaces, 2022.
18. Otay, İ., & Kahraman, C. (2019). A state-of-the-art review of neutrosophic sets and theory. Fuzzy multi-criteria decision-making using neutrosophic sets, 3-24.
19. El Alaoui, M. (2021). Fuzzy TOPSIS: logic, approaches, and case studies. CRC press.
20. Farag, R. M., Shams, M. Y., Aldawody, D. A., Khalid, H. E., El-Bakry, H. M., & Salama, A. A. (2024). Integration between Bioinformatics Algorithms and Neutrosophic Theory. Neutrosophic Sets and Systems, 66, 34-54.
21. Salama, A. A., Shams, M. Y., Khalid, H. E., & Mousa, D. E. (2024). Enhancing Medical Image Quality using Neutrosophic Fuzzy Domain and Multi-Level Enhancement Transforms: A Comparative Study for Leukemia Detection and Classification. Neutrosophic Sets and Systems, 65, 32-56.
22. Salama, A. A., Shams, M. Y., Elseuofi, S., & Khalid, H. E. (2024). Exploring Neutrosophic Numeral System Algorithms for Handling Uncertainty and Ambiguity in Numerical Data: An Overview and Future Directions. Neutrosophic Sets and Systems, 65, 253-295.
23. Alhabib, A., Alhabib, R., Khalid, H. E., & Salama, A. A. (2024). A Neutrosophic Study for the Transmission of Infection with Pathogenic Fungi from Males of Olive Fly Insects to Their Females. Neutrosophic Sets and Systems, 64, 38-45.

24. Salama, A. A., Tarek, Z., Darwish, E. Y., Elseuof, S., & Shams, M. Y. (2024). Neutrosophic Encoding and Decoding Algorithm for ASCII Code System. Neutrosophic Sets and Systems, 63, 105-129.
25. Essa, A. K., Sabbagh, R., Salama, A. A., Khalid, H. E., Aziz, A. A. A., & Mohammed, A. A. (2023). An Overview of Neutrosophic Theory in Medicine and Healthcare. Neutrosophic Sets and Systems, 61(1), 13.

Received: April 20, 2024. Accepted: Aug 22, 2024

The Structure Of The Binary Two Fold Algebra Based On Intuitionistic Fuzzy Groups

Ramazan Yasar
Ankara University, Engineering Faculty, Department of Artificial Intelligence and Data Engineering, Ankara, Turkey**, yasarr@ankara.edu.tr**
Ahmed Hatip
Department of Mathematics, Gaziantep University, Gaziantep, Turkey
Kollnaar5@gmail.com

Abstract:

In this paper, we study the binary two-fold algebra built over intuitionistic fuzzy groups, where the two-fold binary operations and some related substructures such as binary two-fold sub-algebras of intuitionistic fuzzy groups two-fold algebras, binary two-fold centers, binary normality, binary two-fold group products. On the other hand, we illustrate many examples to explain the validity of our discussion.

Keywords: binary two-fold algebra, two-fold intuitionistic fuzzy group, binary operation, two-fold normality.

Introduction

Two-fold algebras was first presented by Smarandache in [1], where he has suggested a connection between neutrosophic sets and algebraic structures combined in a unique algebraic structure called two-fold algebra.

Although this topic is very recent, it has attracted the interest of many researchers due to its importance and generalizability of traditional algebraic structures, and also some neutrosophic structures [6-8].

We now recall some recent results that have been published on Two-fold algebras:

In [2], the concept of two-fold algebra based on a standard fuzzy number theoretical system was introduced with many interesting properties [3].

In [5], the concept of two-fold refined neutrosophic numbers was studied, where many results about these numbers were presented and handled by many theorems and examples. In [4], The concept of two-fold algebraic vector spaces and two-fold algebraic modules was proposed and studied in detail, with many interesting properties about algebraic basis and two-fold linear functions.

These results have motivated us to study for the first time the binary two-fold algebra built over intuitionistic fuzzy groups. We concentrate our study on covering substructures and binary operations on these algebras such as:

the existence of identity, the existence of the inverse, two-fold centers, and normality.

For more details about fuzzy groups, anti-fuzzy groups, and fuzzy algebras, check [9-11].

Main Discussion

Definition:

Let $(G\ ,\mu,\nu)$ be an intuitionistic fuzzy group, i-e. $(G\ ,.)$ is a group, and

$\mu\colon\ G\times G\to[0,1]\ ;\ \begin{cases}\mu(xy)\geq\min(\mu(x).\mu(y))\\ \mu(x^{-1})=\mu(x)\end{cases}$, $\nu\colon\ G\times G\to[0,1]\ ;\ \begin{cases}\nu(xy)\leq\max(\nu(x),\nu(y))\\ \nu(x^{-1})=\nu(x)\end{cases}$

We define the binary two-fold algebra of the intuitionistic fuzzy group $(G\ ,\mu,\nu)$ as follows:

$\Delta_G=\{(x_{\mu(y)},z_{\nu(t)})\ ;\ x,y,z,t\ \in G\}$. We define the following binary two-fold operation:

$*\colon\Delta_G\times\Delta_G\to\Delta_G$ such that:

$$(x_{\mu(y)},a_{\nu(b)})*\left(z_{\mu(t)},c_{\nu(d)}\right)=((x\cdot z)_{\max(\mu(y),\mu(t))},(a.c)_{\min(\nu(d),\nu(b))})$$

Definition:

Let $(x_{\mu(y)},a_{\nu(b)}),\left(z_{\mu(t)},c_{\nu(d)}\right)\in\Delta_G$, we define the relation:

$$(x_{\mu(y)},a_{\nu(b)})\equiv\left(z_{\mu(t)},c_{\nu(d)}\right)\Leftrightarrow\begin{cases}x=z,a=b\\ \mu(y)=\mu(t),\nu(b)=\nu(d)\end{cases};x,y,a,b,d,z,t\in G.$$

Theorem (1):

$\equiv$ is an equivalence relation on Δ_G.

Remark:

We denote to the equivalence classes of $(\equiv)$ by $\overline{\Delta_G}=\{[(x_{\mu(y)},a_{v(b)})] \quad ;x,a,b,y\in G\}$, where:

$[(x_{\mu(y)},a_{v(b)})]=\{(z_{\mu(t)},c_{v(d)})\in\Delta_G \quad ;x=z,a=b,\mu(y)=\mu(t),v(b)=v(d) \ \}$.

Theorem (2):

1] $(*)$ is associative.

2] $(*)$ has an identity $(e_{\mu(a),}e_{v(b)})$.

3] Every $(x_{\mu(y)},a_{v(b)})$ has an inverse.

Example:

Consider $(z_3^*=\{1,2\}.\cdot)$ the group of integers modulo 3 under multiplication, take $\mu: z_3^*\times z_3^*\to z_3^* \quad ;$

$$\mu(x)=\begin{cases}1;x=1\\ \frac{1}{2};x=2\end{cases}.$$

$v: z_3^*\times z_3^*\to z_3^* \ ;$

$$v(x)=\begin{cases}\frac{1}{3};x=1\\ 1;x=2\end{cases}.$$

Δ_G

$=\{\left(1_1,1_{\frac{1}{3}}\right),(1_1,2_1),\left(2_{\frac{1}{2}},1_{\frac{1}{3}}\right),\left(2_{\frac{1}{2}},2_1\right),\left(1_{\frac{1}{2}},1_{\frac{1}{3}}\right),\left(1_{\frac{1}{2}},2_1\right),\left(2_1,1_{\frac{1}{3}}\right),(2_1,2_1),\left(1_{\frac{1}{2}},1_1\right),\left(1_{\frac{1}{2}},2_{\frac{1}{3}}\right),(2_1,1_1),\left(2_1,2_{\frac{1}{3}}\right)$

$,(1_1,1_1),\left(1_1,2_{\frac{1}{3}}\right),\left(2_{\frac{1}{2}},1_1\right),\left(2_{\frac{1}{2}},2_{\frac{1}{3}}\right)\}$.

Take: $X=\left(1_{\frac{1}{2}},2_1\right),Y=(2_1,2_{\frac{1}{3}})$, then:

$X*Y=(2_1,2_{\frac{1}{3}})$.

Definition:

Let $(x_{\mu(y)},a_{v(b)})\in\Delta_G$, we define:

$\overline{(x_{\mu(y)},a_{v(b)})}=(x_{\mu(y)}^{-1},a_{v(b)}^{-1})$.

Theorem (3):

Let $(x_{\mu(y)},a_{v(b)})\in\Delta_G$, then:

$(x_{\mu(y)},a_{v(b)})*\overline{(x_{\mu(y)},a_{v(b)})}=(e_{\mu(a),}e_{v(b)})$.

Definition:

Let S be a non-empty subset of Δ_G, we say that it is a binary twofold sub-algebra if and only if:

$(x_{\mu(y)}, a_{v(b)}) * \overline{(z_{\mu(t)}, c_{v(d)})} \in S$ for all$(x_{\mu(y)}, a_{v(b)}), (z_{\mu(t)}, c_{v(d)}) \in S$.

Theorem (4):

Let S be a non-empty subset of Δ_G , then S is a binary two-fold subalgebra if and only if:

$S = \{(x_{\mu(y)}, a_{v(b)}) \ ; x \in H, , a \in K; \ H, K$ are subgroup$s$ of $G\}$.

Definition:

The twofold sub-algebra $S = \{(x_{\mu(y)}, a_{v(b)}) \ ; x \in H, , a \in K; \ H, K$ are subgroup$s$ of $G\}$ is denoted by $\Delta_G^{H,K}$.

Definition:

The binary twofold subalgebra $\Delta_G^{H,K}$ is called normal if and only

if $H, K \ are$ normal subgroup$s$ of G.

Theorem (6):

Let $\Delta_G^{H,K}$ be a binary twofold subalgebra of Δ_G , then:

1] $\Delta_G^{H,K}$is abelian if and only if H,K are abelian.

2] $\Delta_G^{H,K}$is normal if and only if: $(x_{\mu(y)}, a_{v(b)}) * (z_{\mu(t)}, c_{v(d)}) * \overline{(x_{\mu(y)}, a_{v(b)})} \in \Delta_G^{H,K}$ for all $(x_{\mu(y)}, a_{v(b)}) \in \Delta_G$, $(z_{\mu(t)}, c_{v(d)}) \in \Delta_G^{H,K}$.

Definition:

We define the center of Δ_G as follows:

$Z(\Delta_G) = \{(x_{\mu(y)}, a_{v(b)}) \in \Delta_G \ ; \ (x_{\mu(y)}, a_{v(b)}) * (z_{\mu(t)}, c_{v(d)}) = (z_{\mu(t)}, c_{v(d)}) *$

$(x_{\mu(y)}, a_{v(b)}) \ ; \ \forall (z_{\mu(t)}, c_{v(d)}) \in \Delta_G\}$.

Theorem (7):

1] $Z(\Delta_G)$ is an abelian binary twofold subalgebra of Δ_G.

2] $Z(\Delta_G) = \Delta_G^{Z(G),Z(G)}$.

Theorem (8):

Let $\Delta_G^{H,L}$, $\Delta_G^{K,S}$ be binary twofold subalgebras of Δ_G,then:

1] $\Delta_G^{H,L} \cap \Delta_G^{K,S} = \Delta_G^{H \cap K, L \cap S}$

2] $\Delta_G^{H,L} * \Delta_G^{K,S} = \Delta_G^{HK,LS}$

3] if H,L are normal, then $\Delta_G^{H,L} * \Delta_G^{K,S}$ is binary twofold subalgebra of Δ_G.

Definition:

1] The binary twofold algebra of the intuitionistic fuzzy group $(G\ ,\mu,v)$, is called n-abelian if

$$(x_{\mu(y)}, a_{v(b)})^n * \left(z_{\mu(t)}, c_{v(d)}\right)^n = ((xz)^n_{\max(\mu(y),\mu(t))}, (ac)^n_{\min(v(d),v(b))}.$$

2] it is called n-power closed if: $(x_{\mu(y)}, a_{v(b)})^n * \left(z_{\mu(t)}, c_{v(d)}\right)^n = \left((J)^n_{\mu(s)}, (I)^n_{v(k)}\right)$ $; I, J, x, y, z, a, b, c, s, k \in G.$

Theorem (9):

Let Δ_G be the binary twofold algebra of the intuitionistic fuzzy group $(G\ ,\mu,v)$, then:

1] Δ_G is n-abelian if and only if G is n-abelian group.

2] Δ_G is n-power closed if and only if G is n-power closed group.

Proof of theorem (1):

$(x_{\mu(y)}, a_{v(b)}) \equiv (x_{\mu(y)}, a_{v(b)})$, that is because $\begin{cases} x = x, a = a \\ \mu(y) = \mu(y), v(b) = v(b) \end{cases}$.

If $(x_{\mu(y)}, a_{v(b)}) \equiv \left(z_{\mu(t)}, c_{v(d)}\right)$, then $\begin{cases} x = z, a = c \\ \mu(y) = \mu(t), v(d) = v(d) \end{cases}$, so that $\left(z_{\mu(t)}, c_{v(d)}\right) \equiv (x_{\mu(y)}, a_{v(b)})$.

If $(x_{\mu(y)}, a_{v(b)}) \equiv \left(z_{\mu(t)}, c_{v(d)}\right)$, and $\left(z_{\mu(t)}, c_{v(d)}\right) \equiv (l_{\mu(k)}, s_{v(n)})$, then $\begin{cases} x = l = z, a = c = s \\ \mu(y) = \mu(t) = \mu(k), v(a) = v(d) = v(n) \end{cases}$ and $(x_{\mu(y)}, a_{v(b)}) \equiv (l_{\mu(k)}, s_{v(n)})$.

Proof of theorem (2):

1] For $x, y, z, a, b, c, d, n, k \in G$, we have:

$$(x_{\mu(y)}, a_{v(b)}) * \left(\left(z_{\mu(t)}, c_{v(d)}\right) * \left(l_{\mu(k)}, s_{v(n)}\right)\right) = (x_{\mu(y)}, a_{v(b)}) *$$

$$((zl)_{\max(\mu(t).\mu(k))}, (cs)_{\min(v(d),v(n))}) = ((xzl)_{\max(\mu(y),\mu(t),\mu(k))}, (acs)_{min(v(b),v(d),v(n))}) =$$

$$((x_{\mu(y)}, a_{v(b)}) * \left(\left(z_{\mu(t)}, c_{v(d)}\right)) * ((l_{\mu(k)}, s_{v(n)})\right).$$

2] $(x_{\mu(y)}, a_{v(b)}) * (e_{\mu(a)}, e_{v(b)}) = (x_{\mu(y)}, a_{v(b)})$.

3] $(x_{\mu(y)}, a_{v(b)}) * (x^{-1}_{\mu(y)}, a^{-1}_{v(b)}) = (e_{\mu(a)}, e_{v(b)})$.

Proof of theorem (3):

It is easy and clear.

Proof of theorem (4):

Let $(x_{\mu(y)}, a_{v(b)}), (z_{\mu(t)}, c_{v(d)}) \in S$, then: $(x_{\mu(y)}, a_{v(b)}) * \overline{(z_{\mu(t)}, c_{v(d)})} \in S$, so that $xz^{-1}, ac^{-1} \in K$ and H, K are subgroups of G, where:

$\Delta_G^{H,K} = S = \{(x_{\mu(y)}, a_{v(b)}) \ ; x \in H \ ; a \in K\}$.

Proof of theorem (5):

1] If H is abelian, then $x \cdot y = y \cdot x$ for all $x, y \in H, a \cdot c = c \cdot a$ for all $x, y \in H, a, c \in K$, thus:

$(x_{\mu(y)}, a_{v(b)}) * (z_{\mu(t)}, c_{v(d)}) = (z_{\mu(t)}, c_{v(d)}) * (x_{\mu(y)}, a_{v(b)})$, thus $\Delta_G^{H,K}$ is abelian.

2] Δ_G^{H}, K is normal if and only if H,K are normal, thus $\Delta_G^{H,K}$ is normal subalgebra if and only if:

$(x_{\mu(y)}, a_{v(b)}) * (z_{\mu(t)}, c_{v(d)}) * \overline{(x_{\mu(y)}, a_{v(b)})} \in \Delta_G^{H,K}$, that is because $xyx^{-1} \in H, aca^{-1} \in K$.

Proof of theorem (6):

1] For all $(x_{\mu(y)}, a_{v(b)}), (z_{\mu(t)}, c_{v(d)}) \in Z(\Delta_G)$, we have:

$(x_{\mu(y)}, a_{v(b)}) * \overline{(z_{\mu(t)}, c_{v(d)})} \in Z(\Delta_G)$, that is because for $z_{\mu(t)}, c_{v(d)} \in G$.

2] $(x_{\mu(y)}, a_{v(b)}) \in Z(\Delta_G)$, then $b, y \in G$, and $x, a \in Z(G)$, so that $Z(\Delta_G) = \Delta_G^{Z(G),Z(G)}$.

Proof of theorem (7):

1] Let $(x_{\mu(y)}, a_{v(b)}) \in \Delta_G^{H\cap K, L\cap S}$, then $\begin{cases} x \in H \cap K \\ y \in G \end{cases}, \begin{cases} a \in L \cap S \\ b \in G \end{cases}$ and $\begin{cases} (x_{\mu(y)}, a_{v(b)}) \in \Delta_G^{H,L} \\ (x_{\mu(y)}, a_{v(b)}) \in \Delta_G^{K,S} \end{cases}$ so that:

$(x_{\mu(y)}, a_{v(b)}) \in \Delta_G^{H,L} \cap \Delta_G^{K,S}$.

Conversely, if $(x_{\mu(y)}, a_{v(b)}) \in \Delta_G^{H,L} \cap \Delta_G^{K,S}$, then $\begin{cases} (x_{\mu(y)}, a_{v(b)} \in \Delta_G^{H,L} \\ (x_{\mu(y)}, a_{v(b)} \in \Delta_G^{K,S} \end{cases}$ so that: $\begin{cases} a \in L \cap S \\ x \in H \cap K \end{cases}$

, hence

$(x_{\mu(y)}, a_{v(b)}) \in \Delta_G^{H\cap K, L\cap S}$ and $\Delta_G^{H\cap K, L\cap S} = \Delta_G^{H,L} \cap \Delta_G^{K,S}$.

2] It can be proved by a similar argument.

Proof of theorem (8):

1] Δ_G is n-abelian if and only if $(x_{\mu(y)}, a_{v(b)})^n * (z_{\mu(t)}, c_{v(d)})^n = ((xz)^n_{\max(\mu(y),\mu(t))}, (ac)^n_{min(v(b),v(d))})$, which is equivalent to: $x^n y^n = (xy)^n$, and G is n-abelian.

2] Δ_G is n-power closed if and only if: $(x_{\mu(y)}, a_{v(b)})^n * \left(z_{\mu(t)}, c_{v(d)}\right)^n = \left(\left(\left(l_{\mu(k)}, s_{v(n)}\right)\right)^n\right)$ $; z, c, a, bd, n, k \in G.$

This is equivalent to: $x^n y^n = l^n$, hence G is n-power closed group.

Conclusion

In this paper, we studied the binary two-fold algebra built over intuitionistic fuzzy groups, where the two-fold binary operations on these algebras are defined and studied with some related substructures such as two-fold sub-algebras of intuitionistic fuzzy groups two-fold algebras, binary two-fold centers, and binary normality.

References

[1] Florentine Smarandache. "Neutrosophic Two-Fold Algebra", Plithogenic Logic and Computation, Vol.1, No.1 2024. PP.11-15.

[2] Mohammad Abobala. "On The Foundations of Fuzzy Number Theory and Fuzzy Diophantine Equations." Galoitica: Journal of Mathematical Structures and Applications, Vol. 10, No. 1, 2023 ,PP. 17-25 (**Doi :** https://doi.org/10.54216/GJMSA.0100102).

[3] Mohammad Abobala. (2023). On a Two-Fold Algebra Based on the Standard Fuzzy Number Theoretical System. Journal of Neutrosophic and Fuzzy Systems, 7 (2), 24-29 (**Doi :** https://doi.org/10.54216/JNFS.070202).

[4] Ahmed Hatip, Necati Olgun. (2023). On the Concepts of Two- Fold Fuzzy Vector Spaces and Algebraic Modules. Journal of Neutrosophic and Fuzzy Systems, 7 (2), 46-52 (**Doi :** https://doi.org/10.54216/JNFS.070205).

[5] Abdallah Shihadeh, Khaled Ahmad Mohammad Matarneh, Raed Hatamleh, Randa Bashir Yousef Hijazeen, Mowafaq Omar Al-Qadri, Abdallah Al-Husban. (2024). An Example of Two-Fold Fuzzy Algebras Based On Neutrosophic Real Numbers, Neutrosophic Sets and Systems, Vol. 67.

[6] Mohammad Abobala. (2020). n-Cyclic Refined Neutrosophic Algebraic Systems of Sub-Indeterminacies, An Application to Rings and Modules. International Journal of Neutrosophic Science, 12 (2), 81-95 (**Doi :** https://doi.org/10.54216/IJNS.120203)

[7] Malath Fared Alaswad, Rasha Dallah. (2023). Neutrosophic Divisor Point of A Straight Line Segment With A Given Ratio. Pure Mathematics for Theoretical Computer Science, 2 (1), 18-23 (**Doi :** https://doi.org/10.54216/PMTCS.020102)

[8] Rashel Abu Hakmeh, Murhaf Obaidi. (2024). On Some Novel Results About Fuzzy n-Standard Number Theoretical Systems and Fuzzy Pythagoras Triples. Journal of Neutrosophic and Fuzzy Systems, 8 (1), 18-22

(**Doi :** https://doi.org/10.54216/JNFS.080102)

[9] T. M. Anthony, H. Sherwood, A characterization of fuzzy subgroups, Fuzzy Sets and Systems 7 (1982), 297-305.

[10] Palaniappan, N, Naganathan,S and Arjunan, K " A study on Intuitionistic L-Fuzzy Subgroups", Applied Mathematical Sciences, vol. 3 , 2009, no. 53 , 2619-2624.

[11] P.K. Sharma , "(α , β) – Cut of Intuitionistic fuzzy Groups" International Mathematical Forum,Vol. 6, 2011 , no. 53 , 2605-2614.

Received: April 23, 2024. Accepted: Aug 222, 2024

NSS
Neutrosophic Sets and Systems, Vol. 72, 2024
University of New Mexico

The extended study of 2-refined neutrosophic numbers

Yaser Ahmad Alhasan[1,*], Florentin Smarandache[2], Abuobida Alfahal[3] and Raja Abdullah Abdulfatah[4]

[1]Deanship of the Preparatory Year, Prince Sattam bin Abdulaziz University, Alkharj, Saudi Arabia.;y.alhasan@psau.edu.sa
[2]University of New Mexico, Mathematics Department, Gallup, NM 87301, USA; smarand@unm.edu
[3]Deanship the Preparatory Year, Prince Sattam bin Abdulaziz University, Alkharj Saudi Arabia.; a.alfahal@psau.edu.sa
[4]Deanship the Preparatory Year, Prince Sattam bin Abdulaziz University, Alkharj, Saudi Arabia.; ra.raj.1960@hotmail.coma

[*]Corresponding author: y.alhasan@psau.edu.sa

Abstract: Numerical roots play a crucial role in real or complex equations, as well as in various mathematical models involving differentiation, integration, and other mathematical relationships. In the realm of mathematics, there is a growing trend of utilizing new formulas that incorporate non-classical numbers, such as neutrosophic and refined neutrosophic numbers. The objective of this research is to establish precise and comprehensive mathematical procedures for dealing with refined neutrosophic roots within mathematical formulas, be it equations or other mathematical constructs. This paper presents an extensive study on 2-refined neutrosophic numbers, focusing on the square root of a 2-refined neutrosophic real or complex number. Additionally, this work introduces the concept of 2-refined neutrosophic real or complex polynomials and explores the process of finding the refined neutrosophic roots to solve 2-refined neutrosophic equations. To illustrate these concepts, several examples have been provided.

Keywords: refined neutrosophic; square root; complex polynomial; real polynomial.

1. Introduction and Preliminaries

To describe a mathematical model of uncertainty, vagueness, ambiguity, imprecision, undefined, unknown, incompleteness, inconsistency, redundancy, and contradiction, Smarandache suggested the neutrosophic Logic as an alternative to the current logics. Smarandache made refined neutrosophic numbers available in the following form: $(a, b_1I_1, b_2I_2, \dots, b_nI_n)$ where $a, b_1, b_2, \dots, b_n \in R \text{ or } C$ [1]

Agboola introduced the concept of refined neutrosophic algebraic structures [2]. Also, the refined neutrosophic rings I was studied in paper [3], where it assumed that I splits into two indeterminacies I_1 [contradiction (true (T) and false (F))] and I_2 [ignorance (true (T) or false (F))]. It then follows logically that: [3]

$$I_1I_1 = {I_1}^2 = I_1 \quad (1)$$
$$I_2I_2 = {I_2}^2 = I_2 \quad (2)$$
$$I_1I_2 = I_2I_1 = I_1 \quad (3)$$

In addition, there are many papers presenting studies on refined neutrosophic numbers [4-5-6-7-8-12-13-14-15] and Mehmet Celik and Ahmed Hatip presented a study on the refined ah-isometry

and its applications in refined neutrosophic surfaces. Smarandache discussed neutrosophic indefinite integral (Refined Indeterminacy) [11]

Alhasan also presented several papers on calculus, in which he discussed neutrosophic definite and indefinite integrals. He also presented the most important applications of definite integrals in neutrosophic logic [9-10].

This paper dealt with several topics, in the first part of which introduction and preliminaries were presented, and in the main discussion part the 2-refined neutrosophic numbers that contain two part of indeterminacy (I_1, I_2). In the last part, a conclusion to the paper is given.

2. Main Discussion

2.1 The square root of a 2-refined neutrosophic real number

First, let's compute the square root: $\sqrt{a+bI_1+cI_2}$ whereas $a \geq 0, a+c \geq 0, a+b+c \geq 0$, while $I_1, I_2 =$ indeterminacy

$$\sqrt{a+bI_1+cI_2} = x+yI_1+zI_2$$

Where x, y and z are real unknowns.

By raise both sides to the second power, we get:

$$a+bI_1+cI_2 = (x+yI_1+zI_2)^2$$

$$a+bI_1+cI_2 = (x+yI_1)^2 + 2(x+yI_1)(zI_2) + (zI_2)^2$$

$$a+bI_1+cI_2 = x^2 + 2xyI_1 + (yI_1)^2 + 2(x+yI_1)(zI_2) + (zI_2)^2$$

$$a+bI_1+cI_2 = x^2 + 2xyI_1 + y^2I_1 + 2xzI_2 + 2yzI_1 + z^2I_2$$

$$a+bI_1+cI_2 = x^2 + (y^2+2xy+2yz)I_1 + (z^2+2xz)I_2$$

Whence:

$$\begin{cases} x^2 = a \\ y^2+2xy+2yz = b \\ z^2+2xz = c \end{cases}$$

$$\Longrightarrow \begin{cases} x = \pm\sqrt{a} \\ y^2+2xy+2yz = b \quad (1) \\ z^2+2xz = c \quad (2) \end{cases}$$

Case1: $x = \sqrt{a}$ by substitution in (2)

$$z^2 + 2\sqrt{a}\ z - c = 0$$
$$\Delta = 4a + 4c$$

Then:

$$\begin{cases} z = \dfrac{-2\sqrt{a}+2\sqrt{a+c}}{2} = -\sqrt{a}+\sqrt{a+c} \\ z = \dfrac{-2\sqrt{a}-2\sqrt{a+c}}{2} = -\sqrt{a}-\sqrt{a+c} \end{cases}$$

- For $z = -\sqrt{a}+\sqrt{a+c}$ we substitute in (1)

$$y^2 + 2\sqrt{a}y + 2\left(-\sqrt{a}+\sqrt{a+c}\right)y - b = 0$$

$$y^2 + 2\sqrt{a+c}\ y - b = 0$$

$$\Delta= 4(a+c)+4b$$

Then:

$$\begin{cases} y=\dfrac{-2\sqrt{a+c}+2\sqrt{a+c+b}}{2}=-\sqrt{a+c}+\sqrt{a+c+b} \\ y=\dfrac{-2\sqrt{a+c}-2\sqrt{a+c+b}}{2}=-\sqrt{a+c}-\sqrt{a+c+b} \end{cases}$$

Hence:

$$\sqrt{a+bI_1+cI_2}=\sqrt{a}+\left(-\sqrt{a+c}+\sqrt{a+c+b}\right)I_1+\left(-\sqrt{a}+\sqrt{a+c}\right)I_2$$

Or:

$$=\sqrt{a}+\left(-\sqrt{a+c}-\sqrt{a+c+b}\right)I_1+\left(-\sqrt{a}+\sqrt{a+c}\right)I_2$$

- For $z=-\sqrt{a}-\sqrt{a+c}$ we substitute in (1)

$$y^2+2\sqrt{a}y+2\left(-\sqrt{a}-\sqrt{a+c}\right)y-b=0$$

$$y^2-2\sqrt{a+c}\ \ y-b=0$$

$$\Delta= 4(a+c)+4b$$

Then:

$$\begin{cases} y=\dfrac{2\sqrt{a+c}+2\sqrt{a+c+b}}{2}=\sqrt{a+c}+\sqrt{a+c+b} \\ y=\dfrac{2\sqrt{a+c}-2\sqrt{a+c+b}}{2}=\sqrt{a+c}-\sqrt{a+c+b} \end{cases}$$

Hence:

$$\sqrt{a+bI_1+cI_2}=\sqrt{a}+\left(\sqrt{a+c}+\sqrt{a+c+b}\right)I_1+\left(-\sqrt{a}-\sqrt{a+c}\right)I_2$$

Or:

$$=\sqrt{a}+\left(\sqrt{a+c}-\sqrt{a+c+b}\right)I_1+\left(-\sqrt{a}-\sqrt{a+c}\right)I_2$$

Case2: $x=-\sqrt{a}$ by substitution in (2)

$$z^2-2\sqrt{a}\ \ z-c=0$$

$$\Delta= 4a+4c$$

Then:

$$\begin{cases} z=\dfrac{2\sqrt{a}+2\sqrt{a+c}}{2}=\sqrt{a}+\sqrt{a+c} \\ z=\dfrac{2\sqrt{a}-2\sqrt{a+c}}{2}=\sqrt{a}-\sqrt{a+c} \end{cases}$$

- For $z=\sqrt{a}+\sqrt{a+c}$ we substitute in (1)

$$y^2-2\sqrt{a}y+2\left(\sqrt{a}+\sqrt{a+c}\right)y-b=0$$

$$y^2+2\sqrt{a+c}\ \ y-b=0$$

$$\Delta= 4(a+c)+4b$$

Then:

$$\begin{cases} y = \dfrac{-2\sqrt{a+c} + 2\sqrt{a+c+b}}{2} = -\sqrt{a+c} + \sqrt{a+c+b} \\ y = \dfrac{-2\sqrt{a+c} - 2\sqrt{a+c+b}}{2} = -\sqrt{a+c} - \sqrt{a+c+b} \end{cases}$$

Hence:

$$\sqrt{a + bI_1 + cI_2} = -\sqrt{a} + \left(-\sqrt{a+c} + \sqrt{a+c+b}\right)I_1 + \left(\sqrt{a} + \sqrt{a+c}\right)I_2$$

Or:

$$= -\sqrt{a} + \left(-\sqrt{a+c} - \sqrt{a+c+b}\right)I_1 + \left(\sqrt{a} + \sqrt{a+c}\right)I_2$$

- For $z = \sqrt{a} - \sqrt{a+c}$ we substitute in (1)

$$y^2 - 2\sqrt{a}y + 2\left(\sqrt{a} - \sqrt{a+c}\right)y - b = 0$$

$$y^2 - 2\sqrt{a+c}\ \ y - b = 0$$

$$\Delta = 4(a+c) + 4b$$

Then:

$$\begin{cases} y = \dfrac{2\sqrt{a+c} + 2\sqrt{a+c+b}}{2} = \sqrt{a+c} + \sqrt{a+c+b} \\ y = \dfrac{2\sqrt{a+c} - 2\sqrt{a+c+b}}{2} = \sqrt{a+c} - \sqrt{a+c+b} \end{cases}$$

Hence:

$$\sqrt{a + bI_1 + cI_2} = -\sqrt{a} + \left(\sqrt{a+c} + \sqrt{a+c+b}\right)I_1 + \left(\sqrt{a} - \sqrt{a+c}\right)I_2$$

Or:

$$= -\sqrt{a} + \left(\sqrt{a+c} - \sqrt{a+c+b}\right)I_1 + \left(\sqrt{a} - \sqrt{a+c}\right)I_2$$

The eight results are:

$(x, y, z) = \left(\sqrt{a}\ , -\sqrt{a+c} + \sqrt{a+c+b}\ , -\sqrt{a} + \sqrt{a+c}\right), \left(\sqrt{a}\ , -\sqrt{a+c} - \sqrt{a+c+b}\ , -\sqrt{a} + \sqrt{a+c}\right)$

$\left(\sqrt{a}\ , \sqrt{a+c} + \sqrt{a+c+b}\ , -\sqrt{a} - \sqrt{a+c}\right), \left(\sqrt{a}\ , \sqrt{a+c} - \sqrt{a+c+b}\ , -\sqrt{a} - \sqrt{a+c}\right)$

$\left(-\sqrt{a}\ , -\sqrt{a+c} + \sqrt{a+c+b}\ , \sqrt{a} + \sqrt{a+c}\right), \left(-\sqrt{a}\ , -\sqrt{a+c} - \sqrt{a+c+b}\ , \sqrt{a} + \sqrt{a+c}\right)$

$\left(-\sqrt{a}\ , \sqrt{a+c} + \sqrt{a+c+b}\ , \sqrt{a} - \sqrt{a+c}\right), \left(-\sqrt{a}\ , \sqrt{a+c} - \sqrt{a+c+b}\ , \sqrt{a} - \sqrt{a+c}\right)$

Because we are now calculating the square root of a 2-refined neutrosophic number (according to classical analysis), we only take the result with a positive value, hence:

$$\sqrt{a + bI_1 + cI_2} = \sqrt{a} + \left(-\sqrt{a+c} + \sqrt{a+c+b}\right)I_1 + \left(-\sqrt{a} + \sqrt{a+c}\right)I_2$$

Clearly: $\sqrt{a} \geq 0\ , -\sqrt{a+c} + \sqrt{a+c+b} \geq 0\ \ and\ \ -\sqrt{a} + \sqrt{a+c} \geq 0$

However, when we solve the 2-refined neutrosophic equation, we take all eight results.

Example 1

Let's find: $\sqrt{9 + 9I_1 + 7I_2}$

$$\sqrt{9+9I_1+7I_2} = x + yI_1 + zI_2$$

By raise both sides to the second power, we get:

$$9+9I_1+7I_2 = (x+yI_1+zI_2)^2$$

$$9+9I_1+7I_2 = (x+yI_1)^2 + 2(x+yI_1)(zI_2) + (zI_2)^2$$

$$9+9I_1+7I_2 = x^2 + 2xyI_1 + (yI_1)^2 + 2(x+yI_1)(zI_2) + (zI_2)^2$$

$$9+9I_1+7I_2 = x^2 + 2xyI_1 + y^2I_1 + 2xzI_2 + 2yzI_1 + z^2I_2$$

$$9+9I_1+7I_2 = x^2 + (y^2+2xy+2yz)I_1 + (z^2+2xz)I_2$$

Whence:

$$\begin{cases} x^2 = 9 \\ y^2+2xy+2yz = 9 \\ z^2+2xz = 7 \end{cases}$$

$$\Longrightarrow \begin{cases} x = \pm 3 \\ y^2+2xy+2yz = 9 \quad (1) \\ z^2+2xz = 7 \quad (2) \end{cases}$$

Case1: $x = 3$ by substitution in (2)

$$z^2+6z-7 = 0$$
$$(z-1)(z+7) = 0$$

Then:

$$\begin{cases} z = 1 \\ z = -7 \end{cases}$$

- For $z = 1$ we substitute in (1)

$$y^2+8y-9 = 0$$
$$(y+9)(y-1) = 0$$

Then:

$$\begin{cases} y = 1 \\ y = -9 \end{cases}$$

Hence:

$$\sqrt{9+9I_1+7I_2} = 3 + I_1 + I_2 \quad \text{(Accepted)}$$

Or:

$$= 3 - 9I_1 + I_2 \quad \text{(Rejected)}$$

- For $z = -7$ we substitute in (1)

$$y^2-8y-9 = 0$$
$$(y-9)(y+1) = 0$$

Then:

$$\begin{cases} y = 9 \\ y = -1 \end{cases}$$

Hence:

$$\sqrt{9+9I_1+7I_2} = -3 + 9I_1 - 7I_2 \text{ (Rejected)}$$

Or:

$$= -3 - I_1 - 7I_2 \quad \text{(Rejected)}$$

Case2: $x=-3$ by substitution in (2)

$$z^2-6z-7=0$$
$$(z-7)(z+1)=0$$

Then:

$$\begin{cases} z=7 \\ z=-1 \end{cases}$$

- For $z=7$ we substitute in (1)

$$y^2+8y-9=0$$

$$(y-1)(y+9)=0$$

Then:

$$\begin{cases} y=1 \\ y=-9 \end{cases}$$

Hence:

$$\sqrt{9+9I_1+7I_2}=-3+I_1+7I_2 \text{ (Rejected)}$$

Or:

$$=-3-9I_1+7I_2 \text{ (Rejected)}$$

- For $z=-1$ we substitute in (1)

$$y^2-8y-9=0$$
$$(y-9)(y+1)=0$$

$$\begin{cases} y=9 \\ y=-1 \end{cases}$$

Hence:

$$\sqrt{9+9I_1+7I_2}=-3+9I_1-I_2 \text{ (Rejected)}$$

Or:

$$=-3-I_1-I_2 \text{ (Rejected)}$$

Remarks

As a particular case we can compute $\sqrt{I_1+I_2}$

$$\sqrt{I_1+I_2}=x+yI_1+zI_2$$

By raise both sides to the second power, we get:

$$I_1+I_2=(x+yI_1+zI_2)^2$$

$$I_1+I_2=(x+yI_1)^2+2(x+yI_1)(zI_2)+(zI_2)^2$$

$$I_1+I_2=x^2+2xyI_1+(yI_1)^2+2(x+yI_1)(zI_2)+(zI_2)^2$$

$$I_1+I_2=x^2+2xyI_1+y^2I_1+2xzI_2+2yzI_1+z^2I_2$$

$$I_1+I_2=x^2+(y^2+2xy+2yz)I_1+(z^2+2xz)I_2$$

Whence:

$$\begin{cases} x^2=0 \\ y^2+2xy+2yz=1 \\ z^2+2xz=1 \end{cases}$$

$$\Rightarrow \begin{cases} x = 0 \\ y^2 + 2yz = 1 \\ z^2 = 1 \end{cases}$$

$$\Rightarrow \begin{cases} x = 0 \\ y^2 + 2yz = 1 \quad (1) \\ z = \pm 1 \end{cases}$$

- For $z = 1$ we substitute in (1)

$$y^2 + 2y - 1 = 0$$
$$\Delta = 8$$

Then:

$$\begin{cases} y = \dfrac{-2 + 2\sqrt{2}}{2} = -1 + \sqrt{2} \\ y = \dfrac{-2 - 2\sqrt{2}}{2} = -1 - \sqrt{2} \end{cases}$$

Hence:

$$\sqrt{I_1 + I_2} = \left(-1 + \sqrt{2}\right) I_1 + I_2$$

Or:

$$= \left(-1 - \sqrt{2}\right) I_1 + I_2$$

- For $z = -1$ we substitute in (1)

$$y^2 - 2y - 1 = 0$$
$$\Delta = 8$$

Then:

$$\begin{cases} y = \dfrac{2 + 2\sqrt{2}}{2} = 1 + \sqrt{2} \\ y = \dfrac{2 - 2\sqrt{2}}{2} = 1 - \sqrt{2} \end{cases}$$

Hence:

$$\sqrt{I_1 + I_2} = \left(1 + \sqrt{2}\right) I_1 - I_2$$

Or:

$$= \left(1 - \sqrt{2}\right) I_1 - I_2$$

The four results are:

$$(x, y, z) = \left(0 \ , -1 + \sqrt{2} \ , 1\right), \left(0 \ , -1 - \sqrt{2} \ , 1\right)$$

$$\left(0 \ , 1 + \sqrt{2} \ , -1\right), \left(0 \ , 1 - \sqrt{2} \ , -1\right)$$

Because we are now calculating the square root of a 2-refined neutrosophic number (according to classical analysis), we only take the result with a positive value, hence:

$$\sqrt{I_1 + I_2} = \left(-1 + \sqrt{2}\right) I_1 + I_2$$

However, when we solve the 2-refined neutrosophic equation, we take all four results.

2.3 2-Refined neutrosophic real or complex polynomial

Definition:

A polynomial whose coefficients (at least one of them containing I_1 or I_2 or both I_1, I_2) are 2-refined neutrosophic numbers is called 2-Refined Neutrosophic Polynomials.

Similarly, we may have 2-Refined Neutrosophic Real Polynomials if its coefficients are refined neutrosophic real numbers and 2-Refined Neutrosophic Complex Polynomials if its coefficients are 2-refined neutrosophic complex numbers.

Example 2

- $P(x) = 10x^2 + (5 - 7I_1 + 3I_2)x - 4 + 2I_2$
  Is a 2-refined refined neutrosophic real polynomial
- $Q(x) = x^4 + (2 + 3I_2 - 4i + 3I_1 i)x^3 + 6I_2 x^2 + (9 - 8I_1 + 3I_2 i)x - 4 + 2I_2 + 4I_1 i$
  Is a 2-refined refined neutrosophic complex polynomial.

Example 3

Solve the equation: $x^2 - 1 - 5I_1 - 3I_2 = 0$

Solution:

$$x^2 - 1 - 5I_1 - 3I_2 = 0$$

$$x^2 = 1 + 5I_1 + 3I_2$$

Let's find: $\sqrt{1 + 5I_1 + 3I_2}$

$$\sqrt{1 + 5I_1 + 3I_2} = x + yI_1 + zI_2$$

By raise both sides to the second power, we get:

$$1 + 5I_1 + 3I_2 = (x + yI_1 + zI_2)^2$$

$$1 + 5I_1 + 3I_2 = (x + yI_1)^2 + 2(x + yI_1)(zI_2) + (zI_2)^2$$

$$1 + 5I_1 + 3I_2 = x^2 + 2xyI_1 + (yI_1)^2 + 2(x + yI_1)(zI_2) + (zI_2)^2$$

$$1 + 5I_1 + 3I_2 = x^2 + 2xyI_1 + y^2 I_1 + 2xzI_2 + 2yzI_1 + z^2 I_2$$

$$1 + 5I_1 + 3I_2 = x^2 + (y^2 + 2xy + 2yz)I_1 + (z^2 + 2xz)I_2$$

Whence:

$$\begin{cases} x^2 = 1 \\ y^2 + 2xy + 2yz = 5 \\ z^2 + 2xz = 3 \end{cases}$$

$$\Rightarrow \begin{cases} x = \pm 1 \\ y^2 + 2xy + 2yz = 5 \quad (1) \\ z^2 + 2xz = 3 \quad (2) \end{cases}$$

Case1: $x = 1$ by substitution in (2)

$$z^2 + 2z - 3 = 0$$
$$(z - 1)(z + 3) = 0$$

Then:

$$\begin{cases} z = 1 \\ z = -3 \end{cases}$$

- For $z = 1$ we substitute in (1)

$$y^2 + 4y - 5 = 0$$
$$(y + 5)(y - 1) = 0$$

Then:

$$\begin{cases} y = 1 \\ y = -5 \end{cases}$$

Hence:

$$\sqrt{1 + 5I_1 + 3I_2} = 1 + I_1 + I_2$$

Or:

$$= 1 - 5I_1 + I_2$$

- For $z = -3$ we substitute in (1)

$$y^2 - 4y - 5 = 0$$
$$(y - 5)(y + 1) = 0$$

Then:

$$\begin{cases} y = 5 \\ y = -1 \end{cases}$$

Hence:

$$\sqrt{1 + 5I_1 + 3I_2} = 1 + 5I_1 - 3I_2$$

Or:

$$= 1 - I_1 - 3I_2$$

Case2: $x = -1$ by substitution in (2)

$$z^2 - 2z - 3 = 0$$
$$(z - 3)(z + 1) = 0$$

Then:

$$\begin{cases} z = 3 \\ z = -1 \end{cases}$$

- For $z = 3$ we substitute in (1)

$$y^2 + 4y - 5 = 0$$

$$(y - 1)(y + 5) = 0$$

Then:

$$\begin{cases} y = 1 \\ y = -5 \end{cases}$$

Hence:

$$\sqrt{1 + 5I_1 + 3I_2} = -1 + I_1 + 3I_2$$

Or:

$$= -1 - 5I_1 + 3I_2$$

- For $z = -1$ we substitute in (1)

$$y^2 - 4y - 5 = 0$$
$$(y - 5)(y + 1) = 0$$

$$\begin{cases} y = 5 \\ y = -1 \end{cases}$$

Hence:

$$\sqrt{1 + 5I_1 + 3I_2} = -1 + 5I_1 - I_2$$

Or:

$$= -1 - I_1 - I_2$$

Hence, we got eight 2-refined neutrosophic solutions:

$$x = \sqrt{1 + 5I_1 + 3I_2} = 1 + I_1 + I_2$$

Or:

$$= 1 - 5I_1 + I_2$$

Or:

$$= 1 + 5I_1 - 3I_2$$

Or:

$$= 1 - I_1 - 3I_2$$

Or:

$$= -1 + I_1 + 3I_2$$

Or:

$$= -1 - 5I_1 + 3I_2$$

Or:

$$= -1 + 5I_1 - I_2$$

Or:

$$= -1 - I_1 - I_2$$

First 2-refined neutrosophic factoring:

$$P(x) = x^2 - 1 - 5I_1 - 3I_2 = (x - 1 - I_1 - I_2)(x + 1 + I_1 + I_2)$$

Second 2-refined neutrosophic factoring:

$$P(x) = x^2 - 1 - 5I_1 - 3I_2 = (x - 1 + 5I_1 - I_2)(x + 1 - 5I_1 + I_2)$$

Third 2-refined neutrosophic factoring:

$$P(x) = x^2 - 1 - 5I_1 - 3I_2 = (x - 1 - 5I_1 + 3I_2)(x + 1 + 5I_1 - 3I_2)$$

Fourth 2-refined neutrosophic factoring:

$$P(x) = x^2 - 1 - 5I_1 - 3I_2 = (x - 1 + I_1 + 3I_2)(x + 1 - I_1 - 3I_2)$$

Differently from the classical polynomial with real or complex coefficients, the 2-refined neutrosophic polynomials do not have a unique factoring! If we check each solution, we get:

$$P(x_1) = P(x_2) = P(x_3) = P(x_4) = P(x_5) = P(x_6) = P(x_7) = P(x_8) = 0$$

Let's compute:

$$P(x_5) = P(-1 + I_1 + 3I_2) = (-1 + I_1 + 3I_2)^2 - 1 - 5I_1 - 3I_2$$

$$= 1 - 2I_1 + I_1 - 6I_2 + 6I_1 + 9I_2 - 1 - 5I_1 - 3I_2 = 0 \text{ (True)}$$

$$P(x_8) = P(-1 - I_1 - I_2) = (-1 - I_1 - I_2)^2 - 1 - 5I_1 - 3I_2$$

$$= 1 + 2I_1 + I_1 + 2I_2 + 2I_1 + I_2 - 1 - 5I_1 - 3I_2 = 0 \text{ (True)}$$

And so on for the rest of the results.

2.3 The square root of a 2-refined neutrosophic complex number

Let $a + bi + (c + di)I_1 + (e + fi)I_2$ be a neutrosophic complex number, where a, b, c, d, e, f are reals. Let's compute square root of it:

$$\sqrt{a + bi + (c + di)I_1 + (s + ti)I_2} = x + yi + (z + wi)I_1 + (e + fi)I_2$$

$$a + bi + (c + di)I_1 + (s + ti)I_2 = (x + yi + (z + wi)I_1 + (e + fi)I_2)^2$$

$$= (x + yi + (z + wi)I_1)^2 + 2(x + yi + (z + wi)I_1)(e + fi)I_2 + ((e + fi)I_2)^2$$

$$= (x + yi)^2 + 2(x + yi)(z + wi)I_1 + ((z + wi)I_1)^2 + 2(x + yi + (z + wi)I_1)(e + fi)I_2 + ((e + fi)I_2)^2$$

$$= x^2 + 2xyi - y^2 + 2xzI_1 + 2xwiI_1 + 2yziI_1 - 2ywI_1 + z^2I_1 + 2zwiI_1 - w^2I_1 + 2xeI_2 + 2xfiI_2 + 2yeiI_2 - 2yfI_2 + 2zeI_1 + 2zfiI_1 + 2weiI_1 - 2wfI_1 + e^2I_2 + 2efiI_2 - f^2I_2$$

$$= x^2 - y^2 + 2xyi + (2xz - 2yw + z^2 + 2ze - 2wf - w^2)I_1 + (2xw + 2yz + 2zw + 2zf + 2we)iI_1 + (2xeI_2 - 2yf + e^2)I_2 + (2xf + 2ye + 2ef - f^2)iI_2$$

Then we get a non-linear algebraic system in six variables (x, y, z, w, e, f) and six equations:

$$\begin{cases} x^2 - y^2 = a \\ 2xy = b \\ 2xz - 2yw + z^2 + 2ze - 2wf - w^2 = c \\ 2xw + 2yz + 2zw + 2zf + 2we = d \\ 2xeI_2 - 2yf + e^2 = s \\ 2xf + 2ye + 2ef - f^2 = t \end{cases}$$

That we need to solve.

5. Conclusions

This paper presents an extensive study on 2-refined neutrosophic numbers. The research explores the process of finding the square root of a 2-refined neutrosophic real or complex number. One of the key contributions of this study is that it provides all possible solutions when solving the 2-refined neutrosophic equation, rather than just one solution as in the case of finding the square root of a 2-refined neutrosophic number. Additionally, the obtained results were tested by substitution into the basic equation presented. We highly recommend that researchers take advantage of this study, as it greatly simplifies calculations in various mathematical formulas for future applications.

Acknowledgments "This study is supported via funding from Prince sattam bin Abdulaziz University project number (PSAU/2024/R/1445)".

References

[1] Smarandache, F; "(T,I,F)- Neutrosophic Structures", Neutrosophic Sets and Systems, Volume8, PP:3-10, 2015.

[2] Agboola,A.A.A; On Refined Neutrosophic Algebraic Structures. Neutrosophic Sets and Systems, Volume10, PP: 99-101, 2015.

[3] Adeleke, E.O., Agboola, A.A.A.,and Smarandache, F; Refined Neutrosophic Rings I. International Journal of Neutrosophic Science, Volume 2, Issue 2, PP:77-81, 2020.

[4] Smarandache, F; n-Valued Refined Neutrosophic Logic and Its Applications in Physics. Progress in Physics, USA, Volume 4, PP: 143-146, 2013.

[5] Vasantha Kandasamy,W.B; Smarandache,F; Neutrosophic Rings" Hexis, Phoenix, Arizona, http://fs.gallup.unm.edu/NeutrosophicRings.pdf, 2006.

[6] Zeina, M., Abobala, M; On The Refined Neutrosophic Real Analysis Based on Refined Neutrosophic Algebraic AH-Isometry", Neutrosophic Sets and Systems, Volume 54, PP: 158-168, 2023.

[7] Agboola, A.A.A.; Akinola, A.D; Oyebola, O.Y; Neutrosophic Rings I. Int. J. of Math. Comb, Volume 4, PP:1-14, 2011.

[8] Celik, M., and Hatip, A; On the Refined AH-Isometry and Its Applications in Refined Neutrosophic Surfaces. Galoitica Journal of Mathematical Structures and Applications, 2022.

[9] Alhasan, Y; The neutrosophic integrals and integration methods. Neutrosophic Sets and Systems, Volume 43, PP: 290-301, 2021.

[10] Alhasan, Y; The definite neutrosophic integrals and its applications. Neutrosophic Sets and Systems, Volume 49, PP: 277-293, 2022.

[11] Smarandache, F; Neutrosophic Precalculus and Neutrosophic Calculus. Book, 2015.

[12] Celik, M., and Hatip, A; On the Refined AH-Isometry and Its Applications in Refined Neutrosophic Surfaces. International Journal of Neutrosophic Science, Volume 2, Issue 1, PP: 21-28, 2022.

[13] Alhasan, Y; Ahmed, M; Abdulfatah, R; Sheen, S; The refined indefinite neutrosophic integral, Neutrosophic Sets and Systems, Vol. 67, 127- 134, 2024.

[14] Alhasan, Y; Mohamed, M; Abdulfatah, R; The limits of 2- refined neutrosophic, Neutrosophic Sets and Systems, Vol. 68, 39-49, 2024.

[15] Smarandache, F; Abobala, M; Operations with n-Refined Literal Neutrosophic Numbers using the Identification Method and the n-Refined AH-Isometry, Neutrosophic Sets and Systems, Vol. 70, 350-358, 2024.

Received: April 17, 2024. Accepted: Aug 21, 2024

NSS
Neutrosophic Sets and Systems, Vol. 72, 2024
University of New Mexico

Unveiling Big Data Insights: A Neutrosophic Classification Approach for Enhanced Prediction with Machine Learning

Ahmed Z.M. Elsherif [1], A. A. Salama, [1]O. M. Khaled [1], Mostafa Herajy [1], E. I. Elsedimy[2], Huda E. Khalid[3], Ahmed K. Essa[3]

[1]Department of Mathematics and Computer Science, Faculty of Science, Port Said University, Port Said, Egypt.

ahmad.elsherif@sci.psu.edu.eg, *drsalama44@gmail.com*, *ahmed_salama_2000@sci.psu.edu.eg*

[2] Department of Information Technology Management, Faculty of Management Technology and Information Systems, Port Said University, Port Said, Egypt

[3] University of Telafer, The Administration Assistant for the President of the Telafer University, Telafer, Iraq; https://orcid.org/0000-0002-0968-5611 , dr.huda-ismael@uotelafer.edu.iq, ahmed.k.essa@uotelafer.edu.iq

*Correspondence: dr.huda-ismael@uotelafer.edu.iq

Abstract: The ever-growing volume and complexity of Big Data pose challenges for traditional classification tasks. This paper explores the potential of Neutrosophic Sets (NS), a powerful framework for handling uncertainty, in building robust classification models for Big Data prediction using Machine Learning (ML) techniques. We provide a detailed background on NS and discuss its advantages over Fuzzy Sets. We then propose a methodology that integrates NS with relevant ML algorithms for classification. We evaluate the performance of our Neutrosophic-based model on a Big Data source. The results are analyzed to assess the effectiveness of the Neutrosophic approach for Big Data prediction. This research contributes to the advancement of uncertainty management in Big Data classification and paves the way for further exploration of Neutrosophic-based ML models for various prediction tasks. Results show that the Neutrosophic Neural Networks (NNs) model achieved commendable performance across various metrics, with an accuracy of 79.08%, precision of 74.58%, recall of 77.64%, and an F1-score of 75.63%. These metrics indicate that the Neutrosophic NNs model effectively balances the trade-offs between precision and recall, providing a robust classification performance in the context of the evaluated dataset.

Keywords: Big Data, Neutrosophic Sets, Machine Learning, Classification, Prediction, Uncertainty Management, Fuzzy Sets

1. Introduction

The exponential growth of data, often referred to as Big Data, presents both tremendous opportunities and significant challenges [1, 2]. While vast data volumes hold the key to uncovering

valuable insights, extracting meaningful patterns for classification tasks can be a complex endeavor [1]. Traditional classification algorithms often struggle with inherent uncertainties and inconsistencies within Big Data [3]. This paper explores the potential of Neutrosophic Sets (NS) as a novel approach to address these challenges in Big Data classification. NS offers a powerful mathematical framework for handling uncertainty by incorporating three distinct truth membership functions: truth (T), indeterminacy (I), and falsity (F) [4]. This stands in contrast to traditional Fuzzy Sets (FS), which only utilize truth membership degrees [5]. By introducing indeterminacy, NS allows for a more nuanced representation of data points that may exhibit ambiguity or partial truth [6].

Machine Learning (ML) has emerged as a powerful tool for building predictive models that can learn from data and make accurate classifications. However, conventional ML techniques often rely on crisp data with well-defined categories [7]. Here, we propose to leverage the capabilities of NS within the realm of ML.

The primary objective of this research is to investigate the effectiveness of Neutrosophic-based classification models for Big Data prediction using Machine Learning techniques. We aim to explore how NS can be integrated with existing ML algorithms to improve classification accuracy and handle the inherent uncertainties present within Big Data. Through this research, we contribute to the advancement of uncertainty management in Big Data classification and pave the way for further exploration of Neutrosophic-based ML models for various prediction tasks.

In this study, we leveraged advanced machine learning models to significantly enhance liver disease prediction, a critical step towards improving patient care and saving lives. Utilizing models such as Neutrosophic NNs, we navigated the complexities of big data through rigorous preprocessing, feature extraction, and predictive analysis. The Neutrosophic NNs model demonstrated commendable performance with an accuracy of 79.08%, precision of 74.58%, recall of 77.64%, and an F1-Score of 75.63%. These results underscore the potential of Neutrosophic NNs in effectively predicting liver disease, highlighting the importance of robust data processing and analysis in healthcare applications.

This paper is structured as follows: Section 2 outlines the methods and stages employed to using Neutrosophic NNs to convert traditional data into Neutrosophic data set, then analyzing and predicting using the NNS model and its enormous capabilities in classification. Section 3 details the experimental results obtained using the Python environment. Finally, Section 4 concludes with a summary of the main findings and provides useful suggestions for future research directions.

2. Background:

This section delves into the theoretical foundations of our research, exploring Neutrosophic Sets (NS) and their potential integration with Machine Learning (ML) for Big Data classification.

2.1 Neutrosophic Sets

Neutrosophic Sets Introduced by Florentin Smarandache [4], Neutrosophic Sets (NS) offer a powerful framework for representing and managing uncertainty. NS generalizes the concept of Fuzzy Sets (FS) by incorporating three distinct truth membership functions [5]:

- Truth (T): Denotes the degree to which an element belongs to a set. Values range from 0 (completely false) to 1 (completely true).

- Indeterminacy (I): Represents the degree of uncertainty or lack of knowledge about an element's membership. Values range from 0 (completely determinate) to 1 (completely indeterminate) [4].
- Falsity (F): Denotes the degree to which an element does not belong to a set. Values range from 0 (completely true) to 1 (completely false) [1]. For any element x in a neutrosophic set A, these memberships are denoted as T(x), I(x), and F(x), satisfying the condition: $0 \leq T(x) + I(x) + F(x) \leq 3$ [6]. NS operations like union, intersection, complement, etc., are defined using various operators on the truth, indeterminacy, and falsity membership functions. These operations allow for more nuanced representation of complex data points compared to traditional sets.

2.2 Neutrosophic Sets vs. Fuzzy Sets

While Fuzzy Sets (FS) have been instrumental in handling data with varying degrees of truth membership, they are limited in their ability to represent situations with inherent ambiguity or partial truth [5]. NS addresses this limitation by introducing the concept of indeterminacy [6]. This allows data points to belong to a set, be indeterminate about their membership, and not belong to the set, all to varying degrees. This richer representation of uncertainty is particularly valuable for Big Data, where data quality and inherent inconsistencies are often prevalent [3].

2.3 Machine Learning for Classification

Machine Learning (ML) offers a suite of algorithms that can learn from data and make accurate predictions. In the context of classification, these algorithms learn to identify patterns within labeled data and then use those patterns to classify new, unseen data points [7-11,25-30]. Several well-established ML algorithms are suitable for classification tasks, including:

Neural Networks (NNs): Neural networks consist of interconnected nodes organized in layers, allowing for complex pattern recognition and decision-making tasks. They can accommodate neutrosophic data by incorporating activation functions that account for truth, indeterminacy, and falsity membership values within the network architecture [7].

3. Literature Review

The application of Neutrosophic Sets (NS) for classification tasks has gained increasing attention in recent years. This section reviews existing research to understand the current state of the art, focusing on its potential for Big Data classification. Several studies have explored the use of NS for classification in various domains, including image processing, medical diagnosis, and pattern recognition [12- 15]. These studies highlight several advantages of NS:

Improved Uncertainty Handling: Compared to Fuzzy Sets, NS allows for a more nuanced representation of uncertainty by incorporating the concept of indeterminacy [4]. This is particularly beneficial for real-world data, where ambiguity and partial truth are often present [3].

Enhanced Classification Accuracy: Studies have shown that Neutrosophic-based classification models can achieve higher accuracy compared to traditional methods, especially when dealing with noisy or incomplete data [13, 16].

Flexibility: NS can be integrated with various Machine Learning (ML) algorithms for classification tasks [7]. This allows researchers to leverage the strengths of existing ML techniques while incorporating uncertainty management through NS.

However, limitations and open challenges also need to be addressed:

Limited Applications with Big Data: While research on Neutrosophic classification is growing, there are relatively few studies focusing specifically on Big Data applications [3, 17-21]. Further research is needed to explore the scalability and efficiency of NS-based models when dealing with large and complex datasets [23-28].

Computational Complexity: Neutrosophic operations and computations can be more complex compared to Fuzzy Sets [4]. This can pose challenges when dealing with Big Data, where processing speed and resource efficiency are crucial [16].

Standardization and Optimization: Further research is needed to develop standardized methods for neutrosophication (conversion of traditional data into NS) and optimization of NS-based classification algorithms for Big Data settings [17].

Despite these limitations, the existing research demonstrates the potential of NS for Big Data classification. By addressing the identified challenges and exploring new applications, NS can be a valuable tool in unlocking valuable insights from vast and complex datasets. While there is a limited pool of research focusing specifically on Big Data applications of Neutrosophic Sets for classification, some studies explore the potential benefits and challenges in this context. For instance, Amin et al. [16] discuss the applicability of NS in Big Data healthcare analytics, highlighting its ability to handle inherent uncertainties in medical data. Similarly, Yasser et al. [15] propose a Neutrosophic classifier framework for COVID-19 classification using chest X-ray images, demonstrating its potential for handling noisy or incomplete medical imagery data, often encountered in Big Data settings. These initial explorations pave the way for further research on integrating NS with scalable Big Data processing techniques and resource-efficient ML algorithms.

4. Proposed Methodology:

This section outlines the methodology for exploring Neutrosophic-based classification models for Big Data prediction using Machine Learning techniques.

4.1 Machine Learning Algorithm Selection

We propose utilizing NNs as the primary Machine Learning algorithm for our Neutrosophic classification model. NNs excel at learning intricate patterns and relationships within data, making them well suited for handling the inherent uncertainties represented by the truth, indeterminacy, and falsity membership functions in Neutrosophic Sets. Through their adaptive learning capabilities, NNs can effectively discern optimal decision boundaries, facilitating the segregation of data points belonging to different classes. This inherent flexibility and adaptability make neural networks a suitable choice for Neutrosophic classification tasks.

4.2 Handling Missing Data:

Given the presence of missing values within our dataset, we employed median imputation to address this issue. The choice of median imputation was due to its robustness against outliers, which

is particularly important in clinical datasets where outliers can represent significant anomalies. The mathematical formulation for median imputation is straightforward but effective [21-27]:

$$m = median(D_i) \quad (1)$$

Where $D_i$represents the set of non-missing values for biomarker i. Each missing value in biomarker i was replaced with mm, ensuring a complete dataset for further processing.

4.3 Data Normalization:

To prepare the data for Neutrosophic transformation and neural network modeling, we applied data normalization. This process adjusted the scale of the data features, enabling more effective learning by the neural network models. The normalization was conducted using the Min-Max scaling technique [22], defined by:

$$x' = \frac{x - \min(x)}{\max(x) - \min(x)} \quad (2)$$

Where x is the original value, and x' is the normalized value. This scaling ensured that all input features contributed equally to the analysis, preventing features with larger scales from dominating the learning process.

4.4 Outlier Detection and Treatment:

We also implemented a method to detect and treat outliers, which could skew the results of our analysis. Using the Interquartile Range (IQR) method, outliers were identified and treated. The IQR is calculated as [23]:

$$IQR = Q3 - Q1 \quad (3)$$

Where Q1 and Q3 are the 25th and 75th percentiles, respectively. Values falling below $Q1 - 1.5 \times IQR$ or above $Q3 + 1.5 \times IQR$ were considered outliers and were capped or floored accordingly to reduce their impact.

These preprocessing steps ensured that the data was clean, normalized, and ready for the subsequent transformation into Neutrosophic sets and analysis via neural network modeling.

4.5 Big Data Representation with Neutrosophic Sets

To leverage NS for Big Data classification, we will employ a neutrosophication technique to convert traditional data points into neutrosophic values. Here is a possible approach:

1. **Feature Scaling:** Standardize all data features within a specific range (e.g., 0-1) to ensure consistent membership function application.
2. **Membership Function Definition**: Define appropriate membership functions for truth (T), indeterminacy (I), and falsity (F) based on the characteristics of the data and the classification task. These functions can be designed using various mathematical expressions or through expert knowledge.
3. **Neutrosophic Data Generation**: Apply the defined membership functions to each data point, resulting in truth, indeterminacy, and falsity membership values for each feature. This transforms the traditional data into a neutrosophic representation suitable for the NNs algorithm. To

enrich the analytical depth, the dataset underwent a transformation into Neutrosophic sets. This process involved converting each biomarker's value into three components based on Neutrosophic logic [24]:

- Truth (T): Represents how true the proposition of normalcy is.
- Falsehood (F): Represents how false this proposition is.
- Indeterminacy (I): Captures the indeterminacy or uncertainty.

These components were calculated using the equations:

$$T(X) = \max(0, \min(1, \frac{x-l}{u-l})) \quad (4)$$

$$F(X) = \max(0, \min(1, \frac{u-x}{u-l})) \quad (5)$$

$$I(X) = I - T(x) - F(x) \quad (6)$$

Where x is the observed biomarker value, and L and U are the predefined lower and upper bounds of the normal clinical range, respectively.

4.6 Flowchart for Neutrosophic Data Transformation and Neural Network Classification

Below is the flowchart for the Neutrosophic Data Transformation and Neural Network Classification process:

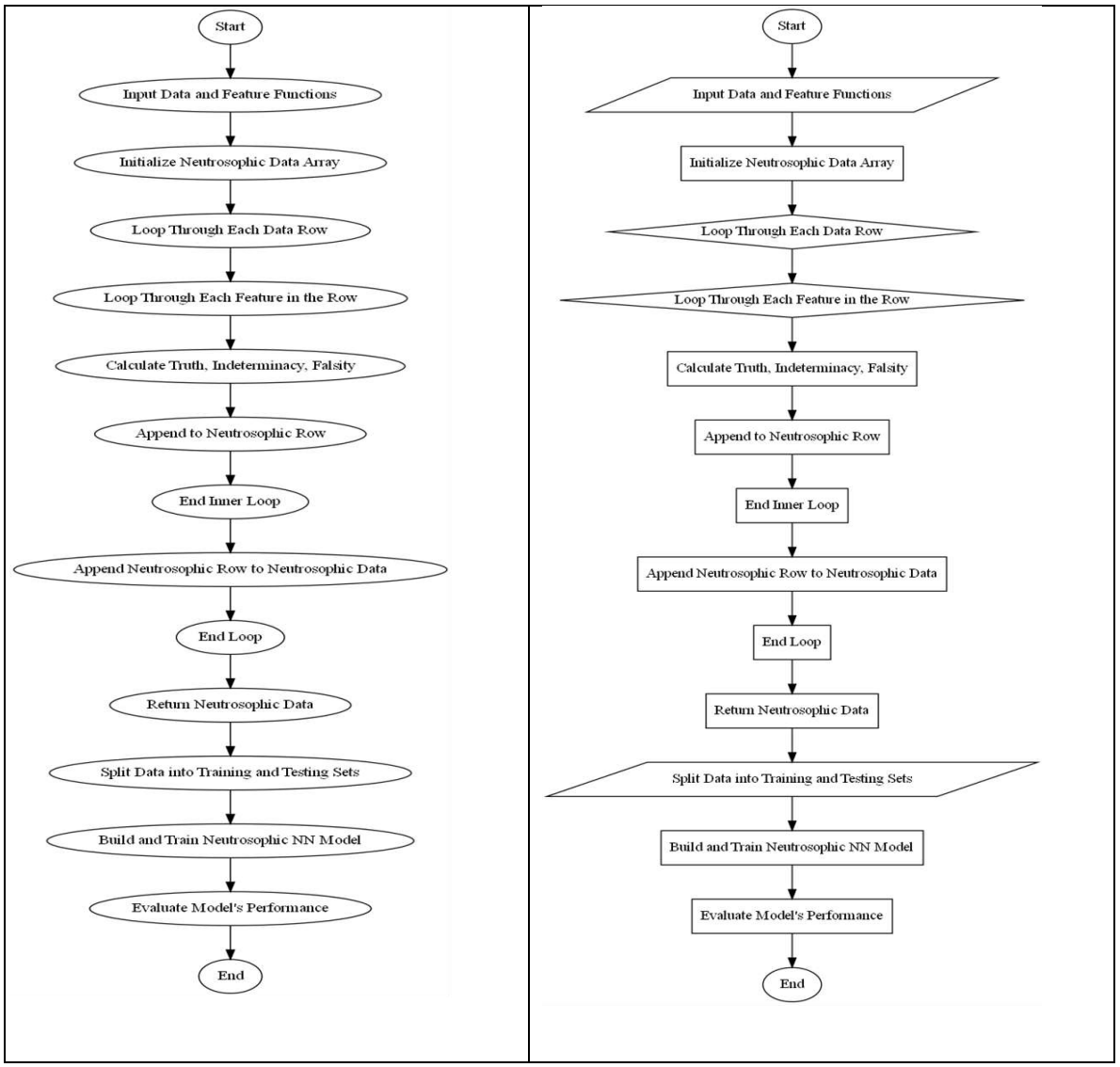

Input Data and Feature Functions: Load the liver disease patient data and the list of feature transformation functions.

Initialize Neutrosophic Data Array: Create an empty array to store Neutrosophic data.

Loop Through Each Data Row: Iterate over each record in the dataset.

Loop Through Each Feature in the Row: For each feature in the record, calculate Neutrosophic values.

Calculate Truth, Indeterminacy, Falsity: Apply transformation functions to obtain truth, indeterminacy, and falsity values for each feature.

Append to Neutrosophic Row: Store the calculated values in the Neutrosophic row.

End Inner Loop: Complete processing for all features in the current row.

Append Neutrosophic Row to Neutrosophic Data: Add the completed Neutrosophic row to the Neutrosophic data array.

End Loop: Complete processing for all records in the dataset.

Return Neutrosophic Data: The dataset is now transformed into its Neutrosophic representation.

Split Data into Training and Testing Sets: Divide the Neutrosophic data into training and testing subsets.

Build and Train Neutrosophic NN Model: Construct and train a neural network model using the training data.

Evaluate Model's Performance: Assess the trained model's performance using accuracy, precision, recall, and F1-score metrics on the testing data.

End

4.7 Python Code for Neutrosophication of Customer Purchase Features

Algorithm 1 Neutrosophic Data

```
function NEUTROSOPHIFY(data, feature_funcs)
    neutrosophic_data ← []
    for i = 1 to length(data) do
        row ← data.iloc[i]
        neutrosophic_row ← []
        for feature_idx, feature in enumerate(data.columns) do
            truth, indeterminacy, falsity ← feature_funcs[feature_idx](row[feature])
            neutrosophic_row.append((truth, indeterminacy, falsity))
        end for
        neutrosophic_data.append(neutrosophic_row)
    end for
    return neutrosophic_data
end function
```

Algorithm 1 outlines the NEUTROSOPHIFY function, which transforms traditional data into a Neutrosophic representation. It accepts a dataset (data) and a list of transformation functions (feature_funcs) for each feature. The algorithm initializes an empty list, neutrosophic_data, and iterates over each record, extracting rows and initializing neutrosophic_row for Neutrosophic values. For each feature, it applies the corresponding transformation function to compute truth, indeterminacy, and falsity values, which are appended to neutrosophic_row. After processing all features, the completed neutrosophic_row is appended to neutrosophic_data. The function returns neutrosophic_data, effectively converting the dataset into a form that better manages uncertainty and indeterminacy, thereby enhancing the robustness and accuracy of subsequent analyses or machine learning models.

4.8 Neutrosophic Data Transformation and Neutrosophic NNs Classification Framework

```
import numpy as np
```

```
from sklearn.model_selection import train_test_split
from sklearn.metrics import accuracy_score, precision_score, recall_score, f1_score
from keras.models import Sequential
from keras.layers import Dense
def neutrosophify(data, feature_funcs):
    """
    Transforms traditional data into Neutrosophic representation.
    Args:
        data (pandas.DataFrame): DataFrame containing liver disease patient data.
        feature_funcs (list): List of functions for calculating T, I, F values for each feature.
    Returns:
        numpy.ndarray: Neutrosophic dataset with T, I, F values for each feature and patient.
    """
    neutrosophic_data = []
    for i in range(len(data)):
        row = data.iloc[i]
        neutrosophic_row = []
        for feature_idx, feature in enumerate(data.columns):
            # Calculate T, I, F values using provided functions
            truth, indeterminacy, falsity = feature_funcs[feature_idx](row[feature])
            neutrosophic_row.extend([truth, indeterminacy, falsity])
        neutrosophic_data.append(neutrosophic_row)
    return np.array(neutrosophic_data)
def build_neutrosophic_nn(input_dim):
    Builds a Neutrosophic Neural Network model for classification.
    Args:
        input_dim (int): Dimension of the input features.
    Returns:
        Sequential: Compiled Neutrosophic NN model.
    model = Sequential()
    model.add(Dense(64, input_dim=input_dim, activation='relu'))
    model.add(Dense(32, activation='relu'))
    model.add(Dense(1, activation='sigmoid'))
    model.compile(loss='binary_crossentropy', optimizer='adam', metrics=['accuracy'])
    return model
def evaluate_model(model, X_test, y_test):
```

```
    Evaluates the performance of the trained model.
    Args:
        model (Sequential): Trained Neutrosophic NN model.
        X_test (numpy.ndarray): Testing data (Neutrosophic features).
        y_test (numpy.ndarray): Testing labels.
    Prints:
        Accuracy, Precision, Recall, F1-Score
    y_pred = (model.predict(X_test) > 0.5).astype("int32")
    accuracy = accuracy_score(y_test, y_pred)
    precision = precision_score(y_test, y_pred)
    recall = recall_score(y_test, y_pred)
    f1 = f1_score(y_test, y_pred)
    print("Accuracy:", accuracy)
    print("Precision:", precision)
    print("Recall:", recall)
    print("F1-Score:", f1)
# Example usage (replace with your actual data loading and feature functions)
# Assuming you have your liver disease patient data loaded into a pandas DataFrame 'data'
# and target labels for liver disease prediction ('y')
# Define membership function functions (replace placeholders with your logic)
def age_truth(age, max_age):
    return age / max_age
def bilirubin_truth(bilirubin, max_bilirubin):
    return bilirubin / max_bilirubin
def enzyme_indeterminacy(enzyme, max_enzyme):
    return enzyme / (max_enzyme + 1)  # Normalize between 0 and 1

def protein_falsity(protein, max_protein):
    return protein / max_protein
# Feature function list (order should match data columns)
feature_funcs = [age_truth, bilirubin_truth, enzyme_indeterminacy, protein_falsity]
# Neutrosophify the data
neutrosophic_data = neutrosophify(data, feature_funcs)
# Split data into training and testing sets
X_train, X_test, y_train, y_test = train_test_split(neutrosophic_data, y, test_size=0.2,
random_state=42)
```

```
# Build and train the Neutrosophic NN model
model = build_neutrosophic_nn(X_train.shape[1])
model.fit(X_train, y_train, epochs=50, batch_size=32, validation_data=(X_test, y_test))
# Evaluate the model's performance
evaluate_model(model, X_test, y_test)
```

The implementation of the proposed Neutrosophic Neural Network (NN) model for liver disease classification involves several crucial steps, starting with the transformation of traditional data into a Neutrosophic representation. The neutrosophify function processes the dataset by applying feature-specific transformation functions to calculate the truth, indeterminacy, and falsity values for each feature, resulting in a comprehensive Neutrosophic dataset. This transformed data is then split into training and testing sets. The build_neutrosophic_nn function constructs a neural network model with an input layer matching the dimensionality of the transformed features, followed by two hidden layers and an output layer configured for binary classification. The model is compiled with the Adam optimizer and binary cross-entropy loss function. After training the model with the training dataset for 50 epochs, the evaluate_model function assesses its performance using accuracy, precision, recall, and F1-score metrics on the testing set. This methodology effectively leverages Neutrosophic logic to handle uncertainty and imprecision in the data, enhancing the robustness and accuracy of the liver disease classification.

5. Discussion of Results

To assess the efficacy of our model, we conducted comprehensive testing and evaluation using the Liver Disease Patient Dataset transformed into Neutrosophic data. The following section provides a detailed overview of the developed framework, its components, and the implementation tools used. It then presents a thorough description of the dataset employed in the experiment, highlighting its transformation from traditional big data to Neutrosophic data to better manage uncertainty and imprecision. This transformation is followed by a discussion of the experimental setup and operational procedures. Additionally, this section outlines the evaluation criteria and benchmarks used in our experiment, providing a general overview before delving into a detailed analysis of the data.

5.1 Implementation Details

This subsection presents the implementation specifics of the proposed model, which is crucial to assess the feasibility, quality, and efficiency of our work. To achieve this objective, the proposed approach was executed on a laptop equipped with an Intel (R) CoreTM i7-9850H CPU operating at 2.6 GHz and 32 GB of RAM, running on the Windows 11 x64 operating system. For application development, the Python programming language was selected due to its extensive libraries and capabilities. The experiments were conducted using Jupyter Notebook within the Anaconda Navigator, involving creating, compiling, and building the code. The classification and assessment procedures were carried out using the sklearn package, while data processing tasks were handled using the Panda data frame. Data processing and visualization tasks were performed using the

Matplotlib and NumPy libraries. The transformation of traditional data into Neutrosophic data was also facilitated by these tools and the addition of the necessary Python codes and equations, enhancing the model's ability to manage uncertainty and improve predictive accuracy.

5.2 Dataset

The experiments were conducted using the Liver Disease Patient Dataset, which includes 30,000 training data records. This dataset comprises ten variables: Age of the patient, Gender of the patient, Total Bilirubin, Direct Bilirubin, Alkphos Alkaline Phosphatase, Sgpt Alamine Aminotransferase, Sgot Aspartate Aminotransferase, Total Proteins, Albumin, and Albumin and Globulin Ratio, along with a classification field where the labels (assigned by experts) are 1 for Liver Patient and 2 for Non-Liver Patient. Figure 2 shows a snapshot of the mentioned dataset.

The liver disease patient dataset is a representative example of big data, characterized by its volume, complexity, velocity, variety, veracity, and value. With 30,000 records, each containing ten attributes, the dataset's sheer size necessitates big data techniques for storage and analysis. The complex nature of the data, encompassing diverse factors like age, gender, bilirubin levels, and enzyme levels, demands sophisticated processing methods. While the dataset is static, its potential for rapid analysis to develop effective machine learning models highlights its velocity. The heterogeneity of data types, including text and numeric, contributes to its variety. The dataset's distribution across various healthcare sources, such as hospitals and clinics, exemplifies its veracity. Finally, the dataset's potential to aid in early liver disease detection, potentially saving lives, underscores its immense value.

Transforming traditional big data into Neutrosophic data further enhances its value by effectively managing the inherent uncertainty and imprecision in the dataset. Neutrosophic data allows for better modeling of complex and ambiguous information, leading to improved predictive accuracy and robustness of machine learning models. This transformation facilitates a more nuanced analysis, accommodating various degrees of truth, indeterminacy, and falsehood, which is particularly beneficial in medical paper where data often involves inherent uncertainties. An example of converting conventional data to neutrosophic data is shown in the following screenshot, illustrating the careful analysis of the augmentation that is verified through this conversion.

	Age of the patient	Gender of the patient	Total Bilirubin	Direct Bilirubin	Alkphos Alkaline Phosphotase	Sgpt Alamine Aminotransferase	Sgot Aspartate Aminotransferase	Total Protiens	ALB Albumin	A/G Ratio Albumin and Globulin Ratio	Result
0	65.0	Female	0.7	0.1	187.0	16.0	18.0	6.8	3.3	0.90	1
1	62.0	Male	10.9	5.5	699.0	64.0	100.0	7.5	3.2	0.74	1
2	62.0	Male	7.3	4.1	490.0	60.0	68.0	7.0	3.3	0.89	1
3	58.0	Male	1.0	0.4	182.0	14.0	20.0	6.8	3.4	1.00	1
4	72.0	Male	3.9	2.0	195.0	27.0	59.0	7.3	2.4	0.40	1

Screenshot (A) showing the traditional data.

Neutrosophic Total Bilirubin	Neutrosophic Direct Bilirubin	Neutrosophic Alkphos	Neutrosophic SGPT	Neutrosophic SGOT	Neutrosophic Proteins	Neutrosophic Albumin	Neutrosophic A/G Ratio
(0.9, 0.05, 0.05)	(0.9, 0.05, 0.05)	(0.4, 0.1, 0.5)	(0.9, 0.05, 0.05)	(0.9, 0.05, 0.05)	(0.4, 0.1, 0.5)	(0.9, 0.05, 0.05)	(0.9, 0.05, 0.05)
(0.1, 0.8, 0.1)	(0.1, 0.8, 0.1)	(0.1, 0.8, 0.1)	(0.4, 0.1, 0.5)	(0.1, 0.8, 0.1)	(0.4, 0.1, 0.5)	(0.9, 0.05, 0.05)	(0.9, 0.05, 0.05)
(0.1, 0.8, 0.1)	(0.1, 0.8, 0.1)	(0.1, 0.8, 0.1)	(0.4, 0.1, 0.5)	(0.4, 0.1, 0.5)	(0.4, 0.1, 0.5)	(0.9, 0.05, 0.05)	(0.9, 0.05, 0.05)
(0.9, 0.05, 0.05)	(0.4, 0.1, 0.5)	(0.4, 0.1, 0.5)	(0.9, 0.05, 0.05)	(0.9, 0.05, 0.05)	(0.4, 0.1, 0.5)	(0.9, 0.05, 0.05)	(0.4, 0.1, 0.5)
(0.1, 0.8, 0.1)	(0.1, 0.8, 0.1)	(0.4, 0.1, 0.5)	(0.9, 0.05, 0.05)	(0.4, 0.1, 0.5)	(0.4, 0.1, 0.5)	(0.9, 0.05, 0.05)	(0.9, 0.05, 0.05)

Screenshot (B) showing the data after it was converted (neutrosophic data).

5.3 Evaluation Metrics for Neutrosophic NNs Classification

To assess the performance of our Neutrosophic-based NNs model, we will employ several evaluation metrics commonly used in classification tasks:

Accuracy: Overall percentage of correctly classified data points.

$$Accuracy = \frac{TP+TN}{TP+TN+FP+FN} \quad (7)$$

Precision: Ratio of true positives (correctly classified positive cases) to all predicted positive cases.

$$Pr\,e\,cision = \frac{TP}{TP+FP} \quad (8)$$

Recall: Ratio of true positives to all actual positive cases in the data.

$$Re\,c\,all = \frac{TP}{TP+FN} \quad (10)$$

F1-Score: Harmonic mean of precision and recall, providing a balanced view of model performance.

$$F1Score = 2 \times \frac{Pr\,ecision \times Re\,call}{Pr\,ecision + Re\,call} \quad (11)$$

By evaluating these metrics, we can measurement the performance of our Neutrosophic-based model with a baseline NNs model. These metrics will help us assess the effectiveness of the Neutrosophic approach in handling uncertainty and improving classification accuracy for Big Data.

5.4 Result Analysis and Discussion

This section delves into the key findings from the experiment and explores the implications of incorporating Neutrosophic Sets for liver diseases. Where Neutrosophic NNs model demonstrates excellent performance in data classification, showcasing a high ability to accurately distinguish between different classes. The model effectively balances recognizing true positive cases while minimizing false positives, making it well suited for applications requiring high precision and reliable outcomes. It shows a strong capacity to detect most true positive instances, while maintaining a low rate of false positives; thereby enhancing its reliability in scenarios where failing to identify positive cases can be costly or dangerous. Overall, the model exhibits balanced and stable performance, establishing itself as an effective and dependable tool for complex classification tasks as shown as in Table 1

Model	**Accuracy**	**Precision**	**Recall**	**F1-Score**
Neutrosophic NNs	79.08 %	74.58 %	77.64%	75.63%

Table 1 shown as the Evaluation Matrix of Neutrosophic NNs model, achieved a noteworthy improvement in classification performance. With an accuracy of 79.08%, the model outperforms many traditional approaches, demonstrating its effectiveness in correctly classifying data points. Its precision of 74.58% indicates a strong ability to correctly identify positive cases, minimizing false positives. The recall of 77.64% reflects the model's proficiency in detecting most actual positive instances, reducing false negatives. Furthermore, the F1-score of 75.63% highlights a balanced performance between precision and recall, making the Neutrosophic NNs model a robust choice for applications that require reliable and accurate classification under conditions of uncertainty. This suggests that incorporating Neutrosophic Sets enhances the model's capability to handle ambiguous and indeterminate information effectively.

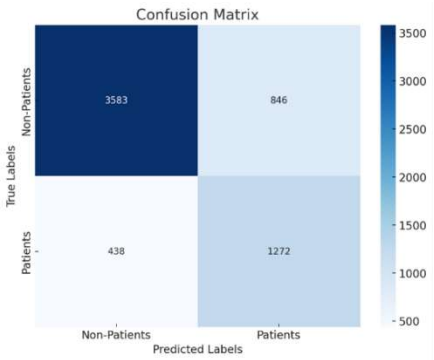

Figure.1. Confusion matrix for Neutrosophic NNs model. The model shows low rates of false positives and negatives, resulting in a higher number of true positives.

Figure 1 shows the Confusion matrix of Neutrosophic NNs model, That provides a detailed evaluation of the Neutrosophic NNs model used for predicting liver diseases. It displays the performance of the model by showing the actual versus predicted classifications across four quadrants: True Positives (Patiennon-patients identified as Patients), True Negatives (Non-Patients correctly identified as Non-Patients), False Positives (Non-Patients incorrectly identified as Patients), and False Negatives (Patients incorrectly identified as non-patients). Specifically, the matrix indicates that out of the total predictions, 3583 were correctly identified as non-patients, 1272 were correctly identified as Patients, 846 Non-Patients were misclassified as patients, and 438 Patients were misclassified as non-patients. This detailed breakdown allows for a comprehensive understanding of the model's accuracy, sensitivity, and specificity, demonstrating its effectiveness and areas for improvement in clinical settings for liver disease prediction.

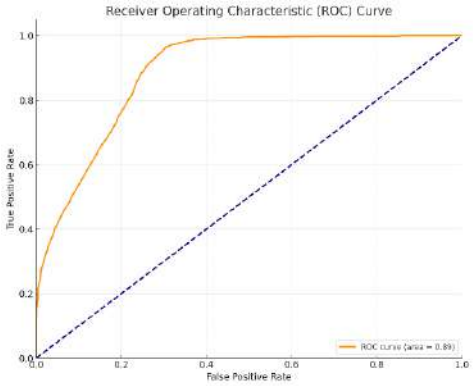

Figure.2. ROC curves for Neutrosophic NNs model The AUC values indicate the superior ability of Neutrosophic NNs model. These curves provide valuable insights into model performance, helping in making informed decisions for classification tasks.

Figure 2 presents the Operating Characteristic (ROC) curve for Neutrosophic NNs model, The Receiver of which is a crucial tool for evaluating the performance of a binary classification model by plotting the True Positive Rate (sensitivity) against the False Positive Rate (1-specificity) at various thresholds. The orange line represents the model's performance, while the diagonal dashed line signifies a random classifier with no discriminative power, having an Area under the Curve (AUC) of 0.5. Here, the AUC is 0.89, indicating a high discriminative ability, meaning there is an 89% chance that the model will correctly distinguish between positive and negative classes. The closer the ROC curve is to the top-left corner, the more accurate the model. This high AUC value underscores the model's effectiveness in differentiating between classes, making it a valuable tool for predictive analytics in medical research and practice, and essential for comparing and selecting the best-performing classification models.

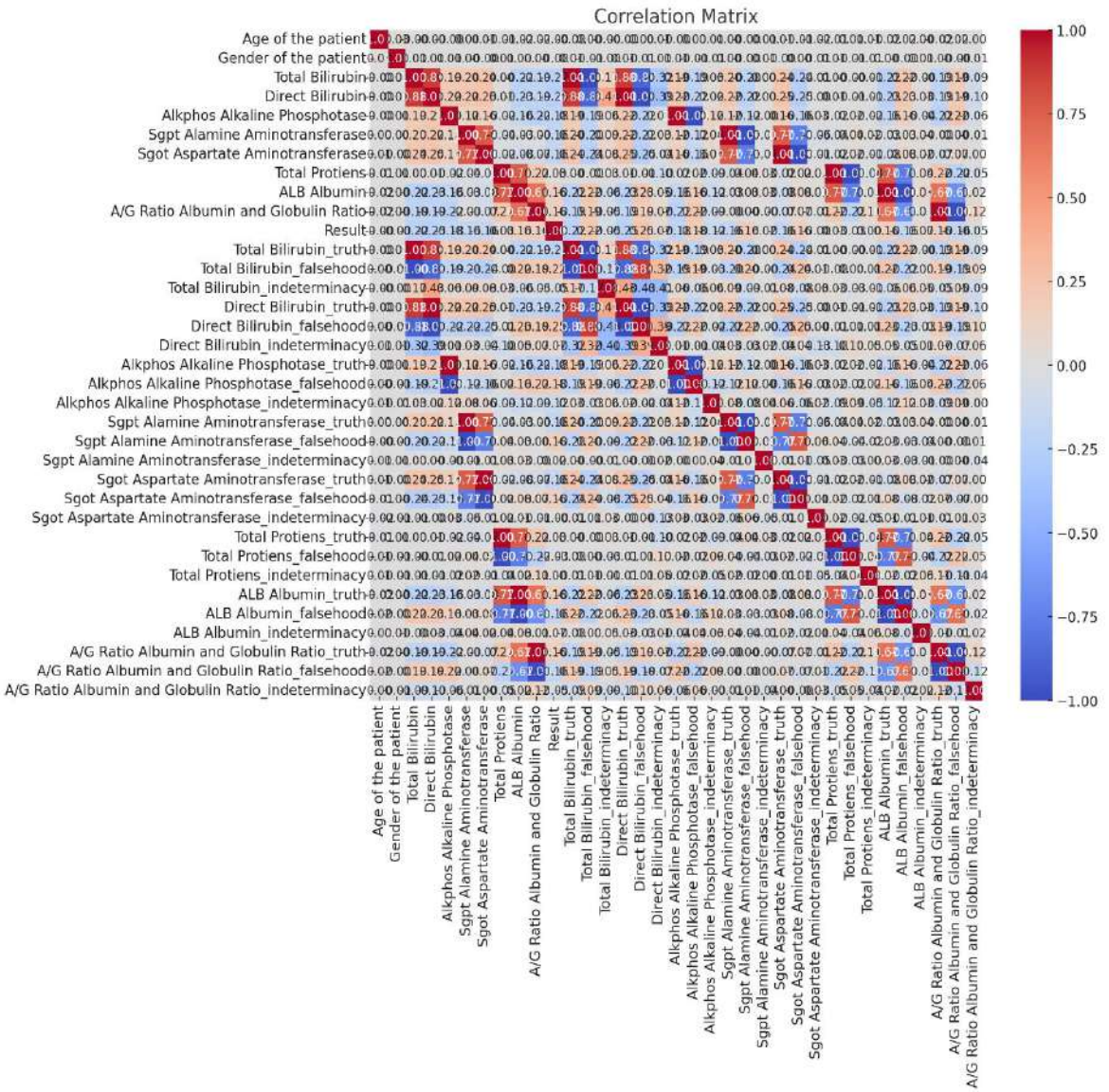

Figure 3 shows a correlation matrix revealing significant associations between liver enzymes and proteins, with gender showing a negative link, indicating crucial information for accurate liver function investigation.

Figure 3 presents the correlation matrix for Neutrosophic NNs model that represents the pairwise correlation coefficients between various clinical and biochemical parameters. The matrix includes a broad range of variables, such as age, gender, total and direct bilirubin levels, alkaline phosphatase, aspartate aminotransferase, albumin, and protein levels, among others. Each cell in the matrix indicates the correlation coefficient between the corresponding pair of variables, with values ranging from -1 to 1. A value close to 1 implies a strong positive correlation, meaning that as one variable increases, the other tends to increase as well. Conversely, a value close to -1 indicates a strong negative correlation, where an increase in one variable corresponds to a decrease in the other. A value around 0 suggests no linear correlation between the variables. The color gradient in the matrix helps in visualizing the strength and direction of the correlations, with red hues representing positive correlations, blue hues indicating negative correlations, and white or neutral colors denoting weak or no correlations. Notably, the matrix also distinguishes between 'truth', 'falsehood', and

'indeterminacy' for certain parameters, highlighting different states or categories within the dataset. This detailed correlation analysis is crucial for identifying potential relationships between clinical and biochemical markers, which can be instrumental in diagnostic and prognostic evaluations. Understanding these correlations helps in uncovering underlying patterns and associations, thereby contributing to more informed clinical decision-making and research insights in the medical field.

6. Conclusion:

This paper investigated the efficacy of neutrosophic neural networks (NNS) in predicting liver diseases. We employed a comprehensive dataset encompassing over 30,000 patient records and 10 different variables to train and evaluate the neutrosophic NNs model. Through this approach, we aim to contribute to the early and accurate detection of liver diseases. The neutrosophic NNs model's performance was assessed using critical metrics such as accuracy, precision, recall, F1-score, and AUC. Our analysis revealed that the neutrosophic NNs model achieved promising results, demonstrating its potential for liver disease prediction. While further research is warranted to explore more nuanced disease classification and individual risk assessment, this study establishes a foundation for utilizing neutrosophic NNs in the domain of liver disease diagnosis. By incorporating more interpretable data and refining the model's architecture, future work can enhance its effectiveness. Overall, this paper underscores the potential of neutrosophic NNs as a valuable tool for early liver disease detection, paving the way for improved healthcare interventions and patient care.

References:

1. Pramanik, P. K. D., Pal, S., Mukhopadhyay, M., & Singh, S. P. (2021). Big Data classification: techniques and tools. In Applications of Big Data in Healthcare (pp. 1-43). Academic Press.
2. Abdalla, H. B., & Abuhaija, B. (2023). Comprehensive analysis of various big data classification techniques: A challenging overview. Journal of Information & Knowledge Management, 22(01), 2250083.
3. Suthaharan, S. (2014). Big data classification: Problems and challenges in network intrusion prediction with machine learning. ACM SIGMETRICS Performance Evaluation Review, 41(4), 70-73.
4. Smarandache, F. (1999). A unifying field in Logics: Neutrosophic Logic. In Philosophy (pp. 1-141). American Research Press.
5. Smarandache, F. (2006, May). Neutrosophic set-a generalization of the intuitionistic fuzzy set. In 2006 IEEE international conference on granular computing (pp. 38-42). IEEE.
6. Smarandache, F. (2022). Operators on single-valued neutrosophic oversets, neutrosophic undersets, and neutrosophic offsets. Collected Papers, 9, 112.
7. Singh, S. K., Abolghasemi, V., & Anisi, M. H. (2022). Skin cancer diagnosis based on neutrosophic features with a deep neural network. Sensors, 22(16), 6261.
8. Rathore, M. M., Shah, S. A., Shukla, D., Bentafat, E., & Bakiras, S. (2021). The role of ai, machine learning, and big data in digital twinning: A systematic literature review, challenges, and opportunities. IEEE Access, 9, 32030-32052.

9. Ngiam, K. Y., & Khor, W. (2019). Big data and machine learning algorithms for health-care delivery. The Lancet Oncology, 20(5), e262-e273.
10. Stergiou, C. L., Plageras, A. P., Psannis, K. E., & Gupta, B. B. (2020). Secure machine-learning scenario from big data in cloud computing via internet of things network. Handbook of Computer Networks and Cyber Security: Principles and Paradigms, 525-554.
11. Rahman, M. S., & Reza, H. (2022). A systematic review towards big data analytics in social media. Big Data Mining and Analytics, 5(3), 228-244.
12. Salama, A. A., El-Ghareeb, H. A., Manie, A. M., & Smarandache, F. (2014). Introduction to develop some software programs for dealing with neutrosophic sets. Neutrosophic Sets and Systems, 3, 51-52.
13. Elwahsh, H., Gamal, M., Salama, A., & El-Henawy, I. (2018). A novel approach for classifying MANETs attacks with a neutrosophic intelligent system based on genetic algorithm. Security and Communication Networks, 2018, 1-7.
14. ElWahsh, H., Gamal, M., Salama, A., & El-Henawy, I. (2018). Intrusion detection system and neutrosophic theory for MANETs: A comparative study. Neutrosophic Sets and Systems, 23, 16-22.
15. Yasser, I., Twakol, A., Abd El-Khalek, A. A., Samrah, A., & Salama, A. A. (2020). COVID-X: novel health-fog framework based on neutrosophic classifier for confrontation covid-19. Neutrosophic Sets and Systems, 35, 1-21.
16. Amin, B., Salama, A. A., El-Henawy, I. M., Mahfouz, K., & Gafar, M. G. (2021). Intelligent neutrosophic diagnostic system for cardiotocography data. Computational Intelligence and Neuroscience, 2021, 1-12.
17. Pramanik, P. K. D., Pal, S., Mukhopadhyay, M., & Singh, S. P. (2021). Big Data classification: techniques and tools. In Applications of Big Data in Healthcare (pp. 1-43). Academic Press.
18. Abdalla, H. B., & Abuhaija, B. (2023). Comprehensive analysis of various big data classification techniques: A challenging overview. Journal of Information & Knowledge Management, 22(01), 2250083.
19. Oussous, A., Benjelloun, F. Z., Lahcen, A. A., & Belfkih, S. (2018). Big Data technologies: A survey. Journal of King Saud University-Computer and Information Sciences, 30(4), 431-448.
20. Provost, F., & Fawcett, T. (2013). Data science for business.
21. Lee, D. K., In, J., & Lee, S. (2015). Standard deviation and standard error of the mean. Korean journal of anesthesiology, 68(3), 220.
22. Huang, L., Qin, J., Zhou, Y., Zhu, F., Liu, L., & Shao, L. (2023). Normalization techniques in training dnns: Methodology, analysis and application. IEEE transactions on pattern analysis and machine intelligence, 45(8), 10173-10196.
23. Hu, K. (2020). Become competent within one day in generating boxplots and violin plots for a novice without prior R experience. Methods and protocols, 3(4), 64.
24. Abu Qamar, M., & Hassan, N. (2019). An approach toward a Q-neutrosophic soft set and its application in decision making. Symmetry, 11(2), 139.

25. Farag, R. M., Shams, M. Y., Aldawody, D. A., Khalid, H. E., El-Bakry, H. M., & Salama, A. A. (2024). Integration between Bioinformatics Algorithms and Neutrosophic Theory. Neutrosophic Sets and Systems, 66, 34-54.
26. Salama, A. A., Shams, M. Y., Khalid, H. E., & Mousa, D. E. (2024). Enhancing Medical Image Quality using Neutrosophic Fuzzy Domain and Multi-Level Enhancement Transforms: A Comparative Study for Leukemia Detection and Classification. Neutrosophic Sets and Systems, 65, 32-56.
27. Salama, A. A., Shams, M. Y., Elseuofi, S., & Khalid, H. E. (2024). Exploring Neutrosophic Numeral System Algorithms for Handling Uncertainty and Ambiguity in Numerical Data: An Overview and Future Directions. Neutrosophic Sets and Systems, 65, 253-295.
28. Alhabib, A., Alhabib, R., Khalid, H. E., & Salama, A. A. (2024). A Neutrosophic Study for the Transmission of Infection with Pathogenic Fungi from Males of Olive Fly Insects to Their Females. Neutrosophic Sets and Systems, 64, 38-45.
29. Salama, A. A., Tarek, Z., Darwish, E. Y., Elseuof, S., & Shams, M. Y. (2024). Neutrosophic Encoding and Decoding Algorithm for ASCII Code System. Neutrosophic Sets and Systems, 63, 105-129.
30. Essa, A. K., Sabbagh, R., Salama, A. A., Khalid, H. E., Aziz, A. A. A., & Mohammed, A. A. (2023). An Overview of Neutrosophic Theory in Medicine and Healthcare. Neutrosophic Sets and Systems, 61(1), 13.

Received: April 20, 2024. Accepted: Aug 22, 2024

NSS

Neutrosophic Sets and Systems, Vol. 72, 2024

University of New Mexico

Introduction to neutrosophic soft ideal topological spaces

Aysegül Çaksu Güler [1]

[1]Ege University, Faculty of Science, Department of Mathematics, 35100- İzmir, Turkey;
aysegul.caksu.guler@ege.edu.tr

*Correspondence: aysegul.caksu.guler@ege.edu.tr

Abstract. In this paper, we give the definition of neutrosophic soft Cl^*-closure, which is more general than neutrosophic soft closure of neutrosophic soft set, with the help of neutrosophic soft ideal and neutrosophic soft point. Then we investigate some basic properties of this new concept. Moreover, we define the notion of τ^* and give the concept of neutrosophic soft-$\mathfrak{I}-$compactness. Besides, we examine the relationship between these concepts and give the relations with previously given concepts.

Keywords: neutrosophic set; soft set; neutrosophic soft topology; neutrosophic soft ideal; neutrosophic soft-$\mathfrak{I}$-compact

1. Introduction

Due to the importance of mathematically expressing uncertain concepts, which can't be defined by classical logic, researchers offer new theories everyday. Some of the most important well known theories are of probability, statistic, fuzzy sets, soft sets and neutrosophic sets. Researchers in economics, medicine, engineering, business and etc are struggling with the complexity of undeterminate data modelling. Classical methods can't always be successful, because of the unambiguities that arise in these areas can take various forms. Probability theory, fuzzy sets, soft sets and neutrosophic sets are of famous and useful approaches in uncertainty identification.

In 1965, Zadeh [12] studied and improved fuzzy set theory, which plays a curcial role in covering the concept of uncertainty. Fuzzy set (briefly FS) is specified by membership function that defined on the closed interval $[0, 1]$. FS sets have been very popular in almost all branches of science. Later Atanassov [1] in 1986 defined intuitionistic fuzzy sets as a generalization of FS. Then Smarandache [11], defined neutrosophic sets in 2005 as a generalization of IFS (briefly, intuitionistic fuzzy set), where we have the degree of membership, the degree of indeterminacy

and the degree of non-membership of each element in X. In [7] Molodtsov initiated the concept of soft sets as a new mathematical tool for dealing with uncertainties. Hence, this theory has successful applications in various fields. Then P.K. Maji [6] gave the definition of neutrosophic soft set (briefly NSS) by using the NS set and SS sets. Bera [2] investigated the notion of neutrosophic soft topological spaces.(NSTS) T.Y. Öztürk et al. [8] redefined some operations on NSS and NSTS. They gave the definition of neutrosophic soft point (NSP).
In this study, we defined the concept of NS-ideal and the NS local function by using NSP which is given by Gündüz et al. [4]. Furthermore we investigate some basic properties of NS local function. Moreover we give the concept of NS $\star$-topology which is finer than NS topology. We also define and study the concept of nNS $\mathfrak{I}$-compactness via NSI. We present the relationship between the concepts of NS-compactness and NS-$\mathfrak{I}$-compactness.

2. **Preliminaries**

Definition 2.1. [11] A neutrosophic set N on the universe set W is described as

$$N = \{< \varpi, T_N(\varpi), I_N(\varpi), F_N(\varpi) >: \varpi \in W\}$$

where $T, I, F : W \rightarrow]^{-}0, 1^{+}[$ and $^{-}0 \leq T_N(\varpi) + I_N(\varpi) + F_N(\varpi) \leq 3^{+}$.

Maji [6] first defined the concept of the NSS, then Deli and Broumi [3] modified this definition as follow:

Definition 2.2. [3] A NSS $\widetilde{F}_P$ over W is a set defined by a set valued function $\widetilde{F} : P \rightarrow P(W)$, where $\widetilde{F}$ is called the approximate function of the NSS $\widetilde{F}_P$ and it can be written as a set of ordered pairs:

$$\widetilde{F}_P = \{(p, < \varpi, T_{\widetilde{F}(p)}(\varpi), I_{\widetilde{F}(p)}(\varpi), F_{\widetilde{F}(p)}(\varpi) >: \varpi \in W) : p \in P\}$$

where $T_{\widetilde{F}(p)}(\varpi), I_{\widetilde{F}(p)}(\varpi), F_{\widetilde{F}(p)}(w) \in [0, 1]$ called the truth-membership, indeterminancy-membership and falsity-membership function of $\widetilde{F}(p)$ respectively. Since the supremum of each T, F, I is 1, the equality $0 \leq T_{\widetilde{F}(p)}(\varpi) + I_{\widetilde{F}(p)}(\varpi) + F_{\widetilde{F}(p)}(\varpi) \leq 3$ is obtained. Let $NSS(W, P)$ be the family of all neutrosophic soft set over W.

Definition 2.3. [2] Let $\widetilde{F}_P \in NSS(W, P)$. The complement of $\widetilde{F}_P$ is denoted by $(\widetilde{F}_P)^c$ and is described as:

$$\widetilde{F}_P^c = (\widetilde{F}_p)^c = \{(p, < \varpi, F_{\widetilde{F}(p)}(\varpi), 1 - I_{\widetilde{F}(p)}(\varpi), T_{\widetilde{F}(p)}(\varpi) >: \varpi \in W) : p \in P\}.$$

It is obviuous that $((\widetilde{F}_P)^c)^c = (\widetilde{F}_P)$

Definition 2.4. [8] Let $\widetilde{F}_P \in NSS(W, P)$.

(a) $\widetilde{F}_P$ is said to be a null NSS if $T_{\widetilde{F}(p)}(\varpi) = 0$, $I_{\widetilde{F}(p)}(\varpi) = 0$, $F_{\widetilde{F}(p)}(\varpi) = 1$ $\forall \varpi \in W$, $\forall p \in P$. It is denoted by $0_{(W,P)}$.

(b) $\widetilde{F}_P$ is said to be an absolute NSS if $T_{\widetilde{F}(p)}(\varpi)= 1$, $I_{\widetilde{F}(p)}(\varpi)=1$, $F_{\widetilde{F}(p)}(\varpi)=0$ $\forall\varpi \in W$, $\forall p \in P$. It is denoted by $1_{(W,P)}$.
It is obviuous that $(1_{(W,P)})^c=0_{(W,P)}$.

Definition 2.5. [6] Let $\widetilde{F}_P, \widetilde{G}_P \in NSS(W,P)$. $\widetilde{F}_P$ is said to be NS subset of $\widetilde{G}_P$ if $T_{\widetilde{F}(p)}(\varpi) \leq T_{\widetilde{G}(p)}(\varpi)$, $I_{\widetilde{F}(p)}(\varpi)\leq I_{\widetilde{G}(\varpi)}(p)$ and $F_{\widetilde{F}(p)}(\varpi)\geq F_{\widetilde{G}_A}(\varpi)$, $\forall p \in P$, $\forall\varpi \in W$. It is denoted by $\widetilde{F}_P\sqsubseteq \widetilde{G}_P$. $\widetilde{F}_P$ is said to be neutrosophic soft equal to $\widetilde{G}_P$ if $\widetilde{F}_P$ is NS subset of $\widetilde{G}_P$ and $\widetilde{G}_P$ is NS subset of $\widetilde{F}_P$. It is denoted by $\widetilde{F}_P$=$\widetilde{G}_P$

Definition 2.6. [8] Let $\widetilde{F}_P, \widetilde{G}_P \in NSS(W,P)$. Then their union is denoted by $\widetilde{F}_P \sqcup \widetilde{G}_P = \widetilde{H}_P$ and is described as

$$\widetilde{H}_P = \{(p, <\varpi, T_{\widetilde{H}(p)}(\varpi), I_{\widetilde{H}(p)}(\varpi), F_{\widetilde{H}(p)}(\varpi) >: \varpi \in W) : p \in P\}$$

where $T_{\widetilde{H}(p)}(\varpi) = max\{T_{\widetilde{F}(p}(\varpi), T_{\widetilde{G}(p)}(\varpi)\}$, $I_{\widetilde{H}(p)}(\varpi) = max\{I_{\widetilde{F}(p)}(\varpi), I_{\widetilde{G}(p)}(\varpi)\}$ and $F_{\widetilde{H}(p)}(\varpi) =min\{F_{\widetilde{F}(p)}(\varpi), F_{\widetilde{G}(p)}(\varpi)\}$.

Definition 2.7. [8] Let $\widetilde{F}_P, \widetilde{G}_P \in NSS(W,P)$. Then their intersection is denoted by $\widetilde{F}_P \sqcap \widetilde{G}_P = \widetilde{H}_P$ and is described as

$$\widetilde{H}_P = \{(p, <\varpi, T_{\widetilde{H}(p)}(\varpi), I_{\widetilde{H}(p)}(\varpi), F_{\widetilde{H}(p)}(\varpi) >: \varpi \in W) : p \in P\}$$

where $T_{\widetilde{H}(p)}(\varpi) = min\{T_{\widetilde{F}(p)}(\varpi), T_{\widetilde{G}(p)}(\varpi)\}$, $I_{\widetilde{H}(p)}(\varpi) = min\{I_{\widetilde{F}(p)}(\varpi), I_{\widetilde{G}(p)}(\varpi)\}$ and $F_{\widetilde{H}(p)}(\varpi) = max\{F_{\widetilde{F}(p)}(\varpi), F_{\widetilde{G}(p)}(\varpi)\}$.

Definition 2.8. [4] The NSS $\varpi^a_{(\omega,u,\varrho)}$ is said to be neutrosophic soft point $(briefly, NSP(W,P))$ for every $\varpi \in W$, $0< \omega, u, \varrho< 1$, p $\in$ P, and is described as follows:

$$\varpi^p_{(\omega,u,\varrho)}(p')(v) = \begin{cases} (\omega,u,\varrho) & if\ p'=p\ and\ \varpi=v \\ (0,0,1), & if p'\neq p\ or\ \varpi\neq v. \end{cases} \quad (1)$$

A NSP $\varpi^a_{(\omega,u,\varrho)}$ belongs to NSS $\widetilde{F}_P$ over W if $\omega \leq T_{\widetilde{F}(p)}(\varpi)$, $u \leq I_{\widetilde{F}(p)}(\varpi)$, $\varrho \geq F_{\widetilde{F}(p)}(\varpi)$.

Definition 2.9. [8] Let $\tau \subset NSS(W,P)$. Then τ is said to be NS topology on W if :

(NST1) $0_{(W,P)}$, $1_{(W,P)}\in \tau$
(NST2) the intersection of any two NSS in τ belongs to τ;
(NST3) the union of any number of NSS in τ belongs to τ.
Then the triple (W,τ,P) is called a neutrosophic soft topological space (NSTS) over W. The members of τ are said to be $\tau-$ neutrosophic soft open set or simply, NS open (NSO) sets in X. A NSS over W is said to be neutrosophic soft closed (NSC) in W if its complement belongs to τ.

Theorem 2.10. *[10] Let (W,τ,P) be NSTS and $\beta \subset \tau$. Then the family β is NS basis of τ iff there exists a NSS $\widetilde{B}_P \in \beta$ such that $\varpi^p_{(\omega,u,\varrho)} \in \widetilde{B}_P \sqsubseteq \widetilde{F}_P$ for each $\widetilde{F}_P \in \tau$ and $\varpi^p_{(\omega,u,\varrho)} \in \widetilde{F}_P$.*

Definition 2.11. [5] Let (W,τ,P) and (V,τ',R) be two NSTS. $(f,\vartheta) : (W,\tau,P) \to (V,\tau,B)$ be a soft mapping and $\widetilde{F}_A$ be a NSS over W. Then the image of $\widetilde{F}_P$ under the mapping (f,ϑ) denoted by $(f,\vartheta)(\widetilde{F}_P)$ is NSS over V defined by for each p ∈ P,

$$(f,\vartheta)(\widetilde{F}_P) = ((f,\vartheta)(T),(f,\vartheta)(I),(f,\vartheta)(F)),$$

Definition 2.12. [5] Let (U,τ,P) and (V,τ',R) be two NSTS. $(f,\vartheta) : (W,\tau,P) \to (V,\tau',R)$ be a soft mapping and

$$\widetilde{H}_R = \{(r, < v, K_{\widetilde{H}(r)}(v), L_{\widetilde{H}(r)}(v), M_{\widetilde{H}(r)}(v) >: v \in V) : r \in R\}$$

be a NSS over V. Then the inverse image of $\widetilde{H}_R$ under the mapping (f,ϑ) denoted by $(f,\vartheta)^{-1}(\widetilde{H}_R)$ is NSS over W described as for each p ∈ P,

$$(f,\vartheta)^{-1}(\widetilde{H}_R) = ((f,\vartheta)^{-1}(K),(f,\vartheta)^{-1}(L),(f,\vartheta)^{-1}(M)),\ (f,\vartheta)^{-1}(K)(p)(\varpi) = K(\vartheta(p))(f(\varpi))$$
$$(f,\vartheta)^{-1}(L)(p)(\varpi) = L(\vartheta(p))(f(\varpi))$$
$$(f,\vartheta)^{-1}(P)(p)(\varpi) = M(\vartheta(p)(f(\varpi))$$

Definition 2.13. [5] Let (W,τ,P) and (V,τ',R) be two NSTS. $(f,\vartheta) : (W,\tau,P) \to (V,\tau',R)$ is a neutrosophic soft continuous function iff for each NSO $\widetilde{F}_R$ over V, $(f,\vartheta)^{-1}(\widetilde{F}_R)$ is NSO over W.

Definition 2.14. [5] Let (W,τ,P) and (V,τ',R) be two NSTS. $(f,\vartheta) : (W,\tau,P) \to (V,\tau',R)$ is NS open iff for each NSO $\widetilde{F}_P$ over W, $(f,\vartheta)(\widetilde{F}_P)$ is NSO over V.

Definition 2.15. [9] Let (W,τ,P) be a NSTS. If every NSO cover of $1_{(W,P)}$ has a finite subcover then (W,τ,P) is called NS-compact space. A space (W,τ,P) is said to be NS-compact if every NSO cover $\{(\widetilde{G_\lambda})_A : \lambda \in \Lambda\}$ of $\widetilde{1}_{(U,A)}$ there exists a finite subset Λ_0 of Λ such that $1_{(W,P)} = \bigsqcup\{(\widetilde{G_\lambda})_A : \lambda \in \Lambda_0\}$.

3. Neutrosophic Soft Ideal Topological Spaces

In this section, we define NS local function of a NSS with respect to $\mathfrak{I}$ and NST over W. By using this definition, we give the concept of NS Cl^*-closure which is a generalization of the concept of NS-closure of a NSS.

Definition 3.1. A neutrosophic soft ideal $\mathfrak{I}$ (NSI) is a non-empty collection of NSS over W which satisfies the following conditions :

(a) $\widetilde{F}_P \in \mathfrak{I}$ and $\widetilde{G}_P \sqsubseteq \widetilde{F}_P$ implies $\widetilde{G}_P \in \mathfrak{I}$

(b) $\widetilde{F}_P \in \mathfrak{I}$, $\widetilde{G}_P \in \mathfrak{I}$ implies $\widetilde{F}_P \sqcup \widetilde{G}_P \in \mathfrak{I}$

Example 3.2. Let $m^p_{(\omega,u,\varrho)} \in NSP(W,P)$. Then each of the following families are neutrosophic soft ideal over W.

(a) $\mathfrak{I}=\{0_{(W,P)}\}$
(b) $\mathfrak{I}$=NSS(W,P)
(c) $\mathfrak{I}=\{\widetilde{F}_P \in NSS(W,P) : m^p_{(\omega,u,\varrho)} \notin \widetilde{F}_P\}$

Theorem 3.3. *Let $\mathfrak{I}$ be a NSI over W and $\mathfrak{I} = \{(\widetilde{F_k})_P : (\widetilde{F_k})_P \in NSS(W,P),\ k \in K\}$ where $(\widetilde{F_k})_P = \{(p, < \varpi, T_{(\widetilde{F_k})(p)}(\varpi), I_{(\widetilde{F_k})(p)}(\varpi), F_{(\widetilde{F_k})(p)}(\varpi) >: \varpi \in W) : p \in P\}$ for each $k \in K$. Then*

$$\mathfrak{I}_1 = \{T_{(\widetilde{F_k})(p)} : (\widetilde{F_k})_P \in \mathfrak{I}\ \ p \in P\}$$
$$\mathfrak{I}_2 = \{I_{(\widetilde{F_k})(p)} : (\widetilde{F_k})_P \in \mathfrak{I}\ p \in P\}$$

are fuzzy soft ideals over W.

Proof. It is obvious. □

Remark 3.4. Let $\mathfrak{I}$ be a NSI over W and $\mathfrak{I} = \{(\widetilde{F_k})(p) : (\widetilde{F_k})_P \in NSS(W,P),\ k \in K\}$ where $(\widetilde{F_k})_P = \{(p, < \varpi, T_{(\widetilde{F_k})(p)}(\varpi), I_{(\widetilde{F_k})(p)}(\varpi), F_{(\widetilde{F_k})(p)}(\varpi) >: \varpi \in W) : p \in P\}$ for each k ∈ K. Then

$$\mathfrak{I}_3 = \{F_{(\widetilde{F_k})(p)} : (\widetilde{F_k})_P \in \mathfrak{I}, p \in P\}$$

couldn't be a fuzzy soft ideal over W.

Example 3.5. Let $W = \{\varpi_1, \varpi_2, \varpi_3\}$, $P = \{p_1, p_2, p_3\}$ and NSI
$\mathfrak{I}= \{\widetilde{G}_P \in NSS(W,P) : \widetilde{G}_P \sqsubseteq \widetilde{F}_P\}$, where NSS $\widetilde{F}_P$, over W defined as follows:

$$\widetilde{F}_A = \begin{array}{c} \\ \varpi_1 \\ \varpi_2 \\ \varpi_3 \end{array} \begin{array}{c} \begin{array}{ccc} p_1 & p_2 & p_3 \end{array} \\ \begin{pmatrix} (0.1,0.5,0.3) & (0.1,0.2,0.3) & (0.5,0.6,1) \\ (0.4,0.4,0.7) & (0.4,0.4,0.7) & (0.4,0.3,0.7) \\ (0.4,0.2,0.1) & (0.4,0.6,0.1) & (0.3,0.2,1) \end{pmatrix} \end{array}$$

Then $\mathfrak{I}_1 = \{T_{(\widetilde{H_k})(p)}(\varpi) : (\widetilde{H_k})_P \in \mathfrak{I}\} = \{T_{\widetilde{G}(p)} : T_{\widetilde{G}(p)} \leq T_{\widetilde{F}(p)}, p \in P\}$ where
$T_{\widetilde{F}(p_1)}=\{(\frac{\varpi_1}{0.1}, \frac{\varpi_2}{0.4}, \frac{\varpi_3}{0.4})\}$, $T_{\widetilde{F}(p_2)}=\{(\frac{\varpi_1}{0.1}, \frac{\varpi_2}{0.4}, \frac{\varpi_3}{0.4})\}$ and $T_{\widetilde{F}(p_3)}=\{(\frac{\varpi_1}{0.5}, \frac{\varpi_2}{0.4}, \frac{\varpi_3}{0.3})\}$.
Then $\mathfrak{I}_1$ is a fuzzy soft ideal over W.
But $\mathfrak{I}_3 = \{F_{(\widetilde{H_k})_P}(\varpi) : (\widetilde{H_k})_\varpi \in \mathfrak{I}, p \in P\} = \{F_{\widetilde{G}_P} : F_{\widetilde{F}_P} \leq F_{\widetilde{G}_P}\}$ where
$F_{\widetilde{F}(p_1)}=\{(\frac{\varpi_1}{0.3}, \frac{\varpi_2}{0.7}, \frac{\varpi_3}{0.1})\}$, $F_{\widetilde{F}(p_2)}=\{(\frac{\varpi_1}{0.3}, \frac{\varpi_2}{0.7}, \frac{\varpi_3}{0.1})\}$ and $F_{\widetilde{F}(\varpi_3)}=\{(\frac{\varpi_1}{1}, \frac{\varpi_2}{0.7}, \frac{\varpi_3}{1})\}$.
Then $\mathfrak{I}_3$ is not a fuzzy soft ideal over W since $0_W \notin \mathfrak{I}_3$

Definition 3.6. Let (W,τ,P) be a NST and $\mathfrak{I}$ be a NSI over W. Then

$$(\widetilde{F}_P)^*(\mathfrak{I},\tau)=\widetilde{F}_A^*=\bigsqcup\{\varpi^a_{(\omega,u,\varrho)}:\widetilde{O}_P\sqcap\widetilde{F}_P\notin\mathfrak{I}\ for\ every\ \widetilde{O}_P\in\mathcal{U}(\varpi^p_{(\omega,u,\varrho)})\}$$

is called the neutrosophic soft local function of $\widetilde{F}_A$ with respect to $\mathfrak{I}$ and τ, where $\mathcal{U}(\varpi^p_{(\omega,u,\varrho)})=\{\widetilde{O}_P\in\tau:\varpi^p_{(\omega,u,\varrho)}\in\widetilde{O}_P\}$.

Proposition 3.7. *Let (W,τ,P) be a NSTS, $\mathfrak{I}$ and $\mathfrak{I}_1$ be NSI over W with the same set of parameters A. For $\widetilde{F}_P,\widetilde{G}_P\in NSS(W,P)$,*

(a) $\widetilde{F}_P\sqsubseteq\widetilde{G}_P$ implies that $\widetilde{F}_P^*\sqsubseteq\widetilde{G}_P^*$.
(b) $\widetilde{F}_P^*\sqsubseteq Cl(\widetilde{F}_P)$.
(c) $\widetilde{F}_P^*$ is neutrosophic soft closed.
(d) $(\widetilde{F}_P^*)^*\sqsubseteq\widetilde{F}_P^*$.
(e) $(\widetilde{F}_P\sqcup\widetilde{G}_P)^*=\widetilde{F}_P^*\sqcup\widetilde{G}_P^*$
(f) $(\widetilde{F}_P\sqcup\widetilde{F}_P^*)=\widetilde{F}_P^*$.
(g) $\mathfrak{I}\subset\mathfrak{I}_1$ implies that $\widetilde{F}_P^*(\mathfrak{I}_1,\tau)\sqsubseteq\widetilde{F}_P^*(\mathfrak{I},\tau)$.

Proof.

(a) Let $\varpi^p_{(\omega,u,\varrho)}\notin\widetilde{G}_P^*$. Then there exists a subset $\widetilde{O}_P\in\tau$ containing $\varpi^p_{(\omega,u,\varrho)}$ such that $\widetilde{O}_P\sqcap\widetilde{G}_P\in\mathfrak{I}$. By hypothesis, $\widetilde{O}_P\sqcap\widetilde{F}_P\sqsubseteq\widetilde{O}_P\sqcap\widetilde{G}_P$ so that $\widetilde{O}_P\sqcap\widetilde{F}_P\in\mathfrak{I}$ and $\varpi^p_{(\omega,u,\varrho)}\notin\widetilde{F}_P^*$.
(b) Let $\varpi^p_{(\omega,u,\varrho)}\notin Cl(\widetilde{F}_P)$. Then there exists a subset $\widetilde{O}_P\in\tau$ containing $\varpi^p_{(\omega,u,\varrho)}$ such that $\widetilde{O}_P\sqcap\widetilde{F}_P=0_{(W,P)}\in\mathfrak{I}$. Then $\varpi^p_{(\omega,u,\varrho)}\notin\widetilde{F}_P^*$.
(c) Let $\varpi^p_{(\omega,u,\varrho)}\notin\widetilde{F}_P^*$. Then there exists a subset $\widetilde{O}_P\in\tau$ containing $\varpi^p_{(\omega,u,\varrho)}$ such that $\widetilde{O}_P\sqcap\widetilde{F}_P\in\mathfrak{I}$. By definition of $\widetilde{F}_P^*$, we obtain $\widetilde{O}_P\sqcap\widetilde{F}_P^*=0_{(W,P)}$ and $\varpi^a_{(\omega,u,\varrho)}\notin Cl(\widetilde{F}_P^*)$. So we get $\widetilde{F}_P^*=Cl(\widetilde{F}_P^*)$ i.e. $\widetilde{F}_P$ is NSC.
(d) It is obvious from (b) and (c).
(e) We obtain that $(\widetilde{F}_P\sqcup\widetilde{G}_P)^*\sqsupseteq\widetilde{F}_P^*\sqcup\widetilde{G}_P^*$ by (a). Let $\varpi^p_{(\omega,u,\varrho)}\notin\widetilde{F}_P^*\sqcup\widetilde{G}_P^*$. Then, there exist subsets $\widetilde{O_{1P}},\widetilde{O_{2P}}\in\tau$ containing $\varpi^p_{(\omega,u,\varrho)}$ such that $\widetilde{O_{1P}}\sqcap\widetilde{F}_P\in\mathfrak{I}$ and $\widetilde{O_{2P}}\sqcap\widetilde{G}_P\in\mathfrak{I}$. By definition of ideal, $\widetilde{O}_P\sqcap(\widetilde{F}_P\sqcup\widetilde{G}_P)\in\mathfrak{I}$ where $\widetilde{O}_P=\widetilde{O_{1P}}\sqcap\widetilde{O_{2P}}$ Then, we get $\varpi^p_{(\omega,u,\varrho)}\notin(\widetilde{F}_P\sqcup\widetilde{G}_P)^*$ Hence $(\widetilde{F}_P\sqcup\widetilde{G}_P)^*\sqsubseteq\widetilde{F}_P^*\sqcup\widetilde{G}_P^*$
(f) It is obvious from (d) and (e).
(g) Let $\mathfrak{I}\subset\mathfrak{I}_1$ and $\varpi^p_{(\omega,u,\varrho)}\notin\widetilde{F}_P^*(\mathfrak{I},\tau)$. Then there exists a subset $\widetilde{O}_P\in\tau$ containing $\varpi^p_{(\omega,u,\varrho)}$ such that $\widetilde{O}_P\sqcap\widetilde{F}_P\in\mathfrak{I}$. So $\widetilde{O}_P\sqcap\widetilde{F}_P\in\mathfrak{I}_1$ and we obtain $\varpi^p_{(\omega,u,\varrho)}\notin\widetilde{F}_P^*(\mathfrak{I}_1,\tau)$. Hence $\widetilde{F}_P^*(\mathfrak{I}_1,\tau)\sqsubset\widetilde{F}_P^*(\mathfrak{I},\tau)$. □

Example 3.8. Let $W = \{\varpi_1, \varpi_2, \varpi_3\}$, $P = \{p_1, p_2\}$ and $\tau = \{1_{(\varpi,P)}, 0_{(\varpi,P)}, \widetilde{F}_P, \widetilde{G}_P, \widetilde{H}_P, \widetilde{Z}_P\}$, $\mathfrak{I} = \{\widetilde{K}_P : \widetilde{K}_P \sqsubseteq \widetilde{L}_P\}$, where NSS $\widetilde{F}_P$, $\widetilde{G}_P$, $\widetilde{H}_P$, $\widetilde{Z}_P$ and $\widetilde{L}_P$ over W defined as follows:

$$\widetilde{F}_P = \begin{array}{c} \\ \varpi_1 \\ \varpi_2 \\ \varpi_3 \end{array} \begin{array}{c} \begin{array}{cc} p_1 & p_2 \end{array} \\ \begin{pmatrix} (0.6, 0.5, 0.3) & (0.5, 0.6, 1) \\ (0.4, 0.3, 0.7) & (0.4, 0.3, 0.7) \\ (0.9, 0.2, 0.1) & (0.3, 0.2, 1) \end{pmatrix} \end{array}$$

$$\widetilde{G}_P = \begin{array}{c} \\ \varpi_1 \\ \varpi_2 \\ \varpi_3 \end{array} \begin{array}{c} \begin{array}{cc} p_1 & p_2 \end{array} \\ \begin{pmatrix} (0.4, 0.7, 0.2) & (0.5, 0.3, 0.9) \\ (0.5, 0.3, 0.2) & (0.4, 0.3, 0.6) \\ (0.4, 0.2, 0.1) & (0.3, 0.2, 0.1) \end{pmatrix} \end{array}$$

$$\widetilde{H}_P = \begin{array}{c} \\ \varpi_1 \\ \varpi_2 \\ \varpi_3 \end{array} \begin{array}{c} \begin{array}{cc} p_1 & p_2 \end{array} \\ \begin{pmatrix} (0.6, 0.7, 0.2) & (0.5, 0.6, 0.9) \\ (0.5, 0.3, 0.2) & (0.4, 0.3, 0.6) \\ (0.9, 0.2, 0.1) & (0.3, 0.2, 0.1) \end{pmatrix} \end{array}$$

$$\widetilde{Z}_P = \begin{array}{c} \\ \varpi_1 \\ \varpi_2 \\ \varpi_3 \end{array} \begin{array}{c} \begin{array}{cc} p_1 & p_2 \end{array} \\ \begin{pmatrix} (0.4, 0.5, 0.3) & (0.5, 0.3, 1) \\ (0.4, 0.3, 0.7) & (0.4, 0.3, 0.7) \\ (0.4, 0.2, 0.1) & (0.3, 0.2, 1) \end{pmatrix} \end{array}$$

$$\widetilde{L}_P = \begin{array}{c} \\ \varpi_1 \\ \varpi_2 \\ \varpi_3 \end{array} \begin{array}{c} \begin{array}{cc} p_1 & p_2 \end{array} \\ \begin{pmatrix} (0.4, 0.3, 0.7) & (0.5, 0.4, 0.8) \\ (0.6, 0.3, 0.5) & (0.7, 0.4, 0.3) \\ (0.5, 0.4, 0.4) & (0.5, 0.4, 0.1) \end{pmatrix} \end{array}$$

Then $\widetilde{L}^*_P \neq Cl(\widetilde{L}_P)$.

Example 3.9. Let us consider Example 3.8. and take $\widetilde{M}_P$ as follows

$$\widetilde{M}_P = \begin{array}{c} \\ \varpi_1 \\ \varpi_2 \\ \varpi_3 \end{array} \begin{array}{c} \begin{array}{cc} p_1 & p_2 \end{array} \\ \begin{pmatrix} (0.6, 0.4, 0.1) & (0.4, 1, 0) \\ (0.7, 0.3, 0.4) & (0.6, 0.4, 0.2) \\ (0.6, 0.7, 0.1) & (0.7, 0.4, 0.1) \end{pmatrix} \end{array}$$

Then $\widetilde{L}_P \not\sqsubset \widetilde{M}_P$ but $\widetilde{L}^*_P \sqsubset \widetilde{M}^*_P$

Let (W, τ, P) be a NSTS and $\mathfrak{I}$ be a NSI over W.If $\widetilde{F}_A$ is NSS in W, then $Cl^*(\widetilde{F}_P) = \widetilde{F}_P \sqcup \widetilde{F}^*_P$.

Proposition 3.10. *Let (W, τ, P) be a NSTS and $\mathfrak{I}$ be a NSI over W with the same set of parameters P. Let $\widetilde{F}_P$, $\widetilde{G}_P$ are neutrosophic soft sets in (W, τ, P), then*

(a) $Cl^*(\widetilde{1}_{(W,P)}) = \widetilde{1}_{(W,P)}$, $Cl^*(\widetilde{0}_{(W,P)}) = \widetilde{0}_{(W,P)}$
(b) $\widetilde{F}_P \sqsubseteq \widetilde{G}_P$ *implies that* $Cl^*(\widetilde{F}_P) \sqsubseteq Cl^*(\widetilde{G}_P)$.
(c) $\widetilde{F}_P \sqsubseteq Cl^*(\widetilde{F}_P)$.
(d) $Cl^*(Cl^*(\widetilde{F}_P)) = Cl^*(\widetilde{F}_P)$.
(e) $Cl^*(\widetilde{F}_P \sqcup \widetilde{G}_P) = Cl^*(\widetilde{F}_P) \sqcup Cl^*(\widetilde{G}_P)$

Proof.

(a) It is obvious.
(b) By Proposition 3.7 (a), we get $\widetilde{F}_P^* \sqsubseteq \widetilde{G}_P^*$. Then $Cl^*(\widetilde{F}_P) = \widetilde{F}_P \sqcup \widetilde{F}_P^* \sqsubseteq \widetilde{G}_P \sqcup \widetilde{G}_P^* = Cl^*(\widetilde{G}_P)$. Then we have $Cl^*(\widetilde{F}_P) \sqsubseteq Cl^*(\widetilde{G}_P)$.
(c) By Proposition 3.7 (f), we get $Cl^*(Cl^*(\widetilde{F}_P)) = Cl^*(\widetilde{F}_P \cup \widetilde{F}_P^*) = (\widetilde{F}_P \sqcup \widetilde{F}_P^*) \sqcup \widetilde{F}_P^* = Cl^*(\widetilde{F}_P)$. Then we get $Cl^*(Cl^*(\widetilde{F}_P)) = Cl^*(\widetilde{F}_P)$.
(d) $Cl^*(\widetilde{F}_P \sqcup \widetilde{G}_P) = (\widetilde{F}_P \sqcup \widetilde{G}_P) \sqcup (\widetilde{F}_P \sqcup \widetilde{G}_P)^* = (\widetilde{F}_P \sqcup \widetilde{G}_P) \sqcup (\widetilde{F}_P^* \sqcup \widetilde{G}_P^*)$ from Proposition 3.7 (e). Then we get $Cl^*(\widetilde{F}_P \sqcup \widetilde{G}_P) = Cl^*(\widetilde{F}_P) \sqcup Cl^*(\widetilde{G}_P)$. □

Theorem 3.11. *Let (W, τ, P) be a NSTS and $\mathfrak{I}$ be a NSI over W. Then*

$$\tau^*(\mathfrak{I}, \tau) = \tau^* = \{\widetilde{F}_P \in NSS(W,P) : Cl^*((\widetilde{F}_P)^c) = \widetilde{F}_p^c\}$$

is a NS topology over W. Each member of $\tau^*(\mathfrak{I}, \tau)$ is said to be NS-$*$-open.

Proof. It is obvious from Proposition 3.10. □

Theorem 3.12. *Let (W, τ, P) be a NSTS and $\mathfrak{I}$ be a NSI over W. Then, $\tau \subset \tau^*(\mathfrak{I}, \tau)$*

Proof. Let $\widetilde{O}_P \in \tau$. Then $\widetilde{O}_P^c$ is neutrosophic soft $*$-closed iff $\widetilde{O}_P^c = Cl^*(\widetilde{O}_P^c)$. Then by Proposition 3.7. (c), we obtain $(\widetilde{O}_P^c)^* \sqsubseteq \widetilde{O}_P^c$ and we get $\widetilde{O}_P^c = \widetilde{O}_P^c \sqcup (\widetilde{O}_P^c)^* = Cl^*(\widetilde{O}_P^c)$. So $\widetilde{O}_P^c$ is neutrosophic soft $*$-closed i.e $\widetilde{O}_P \in \tau^\star$. □

Corollary 3.13. *Let (W, τ, P) be a NSTS and $\mathfrak{I}$ be a NSI. If $\widetilde{F}_P$ is a NSS, then $\widetilde{F}_P$ is neutrosophic soft -$*$-closed iff $\widetilde{F}_P^* \sqsubset \widetilde{F}_P$.*

Theorem 3.14. *Let (W, τ, P) be a NSTS and $\mathfrak{I}$ be NSI over W. Then*

$$\beta^*(\mathfrak{I}, \tau) = \beta^* = \{\widetilde{F}_P - \widetilde{G}_P : \widetilde{F}_P \in \tau \text{ and } \widetilde{G}_P \in \mathfrak{I}\}$$

is a neutrosophic soft basis of neutrosophic soft topology τ^*.

Proof. Let $\varpi^p_{(\omega,u,\varrho)} \in \widetilde{O}_P$ and $\widetilde{O}_P \in \tau^*$. Then $Cl^*(\widetilde{O}_P^c) = \widetilde{O}_P^c$ and $\varpi^p_{(\omega,u,\varrho)} \notin Cl^*(\widetilde{O}_P^c)$. By definition of $Cl^*((\widetilde{O}_P)^c)$, $\varpi^p_{(\omega,u,\varrho)} \notin ((\widetilde{O}_P)^c)^*$. Then there exists a subset $\widetilde{F}_P \in \tau$ containing

$\varpi^{p}_{(\omega,u,\varrho)}$ such that $\widetilde{I}_P = \widetilde{F}_P \sqcap (\widetilde{O}_P)^c \in \mathfrak{I}$. Hence we obtain $\widetilde{F}_P$ - $\widetilde{I}_P \sqsubset \widetilde{O}_P$. By Theorem 2.10, $\beta^*(\mathfrak{I},\tau)$ is a NS basis of NSTS τ^* . □

Example 3.15. Let us consider Example 3.8 and take $\widetilde{O}_P$ as follows:

$$\widetilde{O}_A = \begin{array}{c} \\ \varpi_1 \\ \varpi_2 \\ \varpi_3 \end{array} \begin{array}{c} \begin{array}{cc} p_1 & p_2 \end{array} \\ \begin{pmatrix} (0.6,0.5,0.4) & (0.5,0.6,1) \\ (0.4,0.3,0.7) & (0.3,0.3,0.7) \\ (0.4,0.2,0.5) & (0.1,0.2,1) \end{pmatrix} \end{array}$$

Then $\widetilde{O}_P \in \tau^*$ but it is not NSO in (W,τ,P)

Proposition 3.16. *Let (W,τ,P) be a NSTS and $\mathfrak{I}$ be a NSI over W. Then, the followings are equivalent:*

(a) $Cl(\widetilde{F}_P) \sqsubseteq Cl^*(\widetilde{F}_P)$ for each $\widetilde{F}_P \in NSS(W,P)$.
(b) Every NS $*$-closed set in U is NSC.
(c) $\tau = \tau^*$.

Proof. $(a) \Rightarrow (b)$: It is obvious. $(b) \Rightarrow (a)$: Let $\widetilde{F}_P \in NSS(W,P)$. Since $Cl^*(\widetilde{F}_P)$ is neutrosophic soft $*$-closed and by condition (b), we get $Cl^*(\widetilde{F}_P)$ is NSC. Then we obtain $Cl(\widetilde{F}_P) \sqsubseteq Cl^*(\widetilde{F}_P)$ by Proposition 3.7 (d).
$(b) \Rightarrow (c)$: Let $\widetilde{F}_P \in \tau^*$. Then $\widetilde{F}^c_P = Cl^*(\widetilde{F}^c_P)$ and so $\widetilde{F}^c_P$ is NS $*$-closed. By condition (b), we get $\widetilde{F}^c_P$ is NSC. Then, we obtain $\tau = \tau^*$ by Theorem 3.12.
$(c) \Rightarrow (b)$: It is obvious. □

Proposition 3.17. *Let (W,τ,P) be a NSTS and $\mathfrak{I}$ be a NSI over W. Then, the followings are equivalent:*

(a) $Cl^*(\widetilde{F}_P) \sqsubseteq Cl(\widetilde{F}_P)$ for each $\widetilde{F}_P \in NSS(W,P)$.
(b) Every NSC set in U is NS $*$-closed.
(c) $\tau \subset \tau^\star$.

Proof. It is obvious. □

4. Neutrosophic Soft $\mathfrak{I}$-Compact Spaces

In this section, we introduce the concept of NS-$\mathfrak{I}$-compactness on a set W and investigate some basic properties.

Definition 4.1. A space $(W, \tau, \mathfrak{I}, P)$ is said to be neutrosophic soft-$\mathfrak{I}$-compact (NSIC) if for every NSO-cover $\{(\widetilde{G_\lambda})_P : \lambda \in \Lambda\}$ of $\widetilde{1}_{(W,P)}$ there exists a finite subset Λ_0 of Λ such that $1_{(W,P)} - \bigsqcup\{(\widetilde{G_\lambda})_P : \lambda \in \Lambda_0\} \in \mathfrak{I}$.

A NSS $\widetilde{F}_P$ of a space $(X, \tau, \mathfrak{I}, P)$ is called NS- $\mathfrak{I}$-compact set in $(W, \tau, \mathfrak{I}, P)$ if for every NSO-cover $\{(\widetilde{G_\lambda})_P : \lambda \in \Lambda\}$ of $\widetilde{F}_P$ there exists a finite subset Λ_0 of Λ such that $\widetilde{F}_P - \bigsqcup\{(\widetilde{G_\lambda})_P : \lambda \in \Lambda_0\} \in \mathfrak{I}$.

Example 4.2. Let $W = IN$ be a universe, $P = \{p_1, p_2\}$ a parametric set and N_G be a neutrosophic set on W defined as follows:

$$N_G = \begin{cases} < \varpi, (1,1,0) > & if\ \varpi \in G \\ < \varpi, (0,0,1), > & if\ \varpi \notin G. \end{cases} \tag{2}$$

Let β=$\{(\widetilde{F_G})_A : 1 \in G, G \subset W\}$ be a NS base for τ where $(\widetilde{F_G})_P$ be a NSS defined as $\widetilde{F_G}(p_1)$ =$\widetilde{F_G}(p_2)$= $\{N_G : 1 \in G, G \subset W\}$. Let $\mathfrak{I}$=$\{(\widetilde{I_G})_P : 1 \notin G, G \subset W\} \cup \{0_{(W,P)}\}$ be a NSI where $(\widetilde{I_G})_P$ is a NSS defined as $\widetilde{I_G}(p_1)$ =$\widetilde{I_G}(p_2)$= $\{N_G : 1 \notin G, G \subset W\}$. Then $(W, \tau, \mathfrak{I}, P)$ is NSIC.

Proposition 4.3. *If (W, τ, P) is neutrosophic soft-compact, then $(U, \tau, A, \mathfrak{I})$ is NSIC.*

Proof. It is obvious since $0_{(W,P)} \in \mathfrak{I}$. □

Example 4.4. Let us consider Example 4.2. Then $(W, \tau, \mathfrak{I}, P)$ is neutrosophic soft-$\mathfrak{I}$-compact but it is not neutrosophic soft-compact.

Theorem 4.5. *Let (W, τ, P) be a NSTS and $\mathfrak{I}$ be a NSI over W. $(W, \tau, P, \mathfrak{I})$ is NSIC if and only if for every family $\{(\widetilde{F_\lambda})_P : \lambda \in \Lambda\}$ of NSC over W for which $\sqcap\{(\widetilde{F_\lambda})_P : \lambda \in \Lambda\} = 0_{(W,P)}$, there exists a finite subset Λ_0 of Λ such that $\sqcap\{(\widetilde{F_\lambda})_P : \lambda \in \Lambda_0\} \in \mathfrak{I}$.*

Proof. Let $(W, \tau^*(\mathfrak{I}, \tau), P)$ be NSIC and let $\{(\widetilde{F_\lambda})_P : \lambda \in \Lambda\}$ be NSC over W for which $\sqcap$ $\{(\widetilde{F_\lambda})_P : \lambda \in \Lambda\}$ =$0_{(W,P)}$. Then $\{1_{(W,P)} - (\widetilde{F_\lambda})_P : \lambda \in \Lambda\}$ is the NSO over W such that $\sqcup$ $\{1_{(W,P)} - (\widetilde{F_\lambda})_P : \lambda \in \Lambda\}$ =$1_{(W,P)}$. By hypothesis and Theorem 3.12, there exists a finite subset Λ_0 of Λ such that $1_{(W,P)} - \sqcup \{1_{(W,P)} - (\widetilde{F_\lambda})_P : \lambda \in \Lambda_0\}$= $(\sqcup\{1_{(W,P)} - (\widetilde{F_\lambda})_P : \lambda \in \Lambda_0\})^c$=$\sqcap\{(\widetilde{F_\lambda})_P : \lambda \in \Lambda_0\} \in \mathfrak{I}$. Thus, $(W, \tau, P, \mathfrak{I})$ is NSIC. □

Corollary 4.6. *[9] (W, τ, P) is NSC iff for every family of NSC sets with empty intersection in (W, τ, P) has a finite subfamily with empty intersection.*

Proof. It is obvious by previous theorem taking $\mathfrak{I} = \{0_{(W,P)}\}$. □

Theorem 4.7. *Let (W,τ,P) be a NSTS and $\mathfrak{I}$ be NSI over W.If $(W,\tau^*(\mathfrak{I},\tau),P)$ is NSC, then $(W,\tau,P,\mathfrak{I})$ is NSIC.*

Proof. Let $(W,\tau^*(\mathfrak{I},\tau),P)$ be NSC and $\{(\widetilde{G_\lambda})_P : \lambda\in\Lambda\}$ be a NSO-cover of W. By Theorem 3.12, $\{(\widetilde{G_\lambda})_P : \lambda\in\Lambda\}$ is a NS-$*$-open cover of W. Assuming that $(W,\tau^*(\mathfrak{I},\tau),P)$ be NSC, there exists a finite subset Λ_0 of Λ such that $1_{(W,P)}=\bigsqcup\{(\widetilde{G_\lambda})_P : \lambda\in\Lambda_0\}$. Then $1_{(W,P)}-\bigsqcup\{(\widetilde{G_\lambda})_P : \lambda\in\Lambda_0\}\in\mathfrak{I}$. Thus, $(W,\tau,P,\mathfrak{I})$ is NSIC. □

Theorem 4.8. *If $(W,\tau,P,\mathfrak{I})$ is NSIC and $\mathfrak{I}$ is a NSI on W with $\mathfrak{I}\subset\mathfrak{J}$, then $(W,\tau,P,\mathfrak{J})$ is NSIC.*

Proof. Let $(W,\tau,P,\mathfrak{I})$ is NSIC, $\mathfrak{I}$ is a NSI on W with $\mathfrak{I}\subset\mathfrak{J}$. Let $\{(\widetilde{G_\lambda})_P : \lambda\in\Lambda\}$ be a NSO-cover of U. Since $(W,\tau,\mathfrak{J},P)$ is NSIC, there exists a finite subset Λ_0 of Λ such that $1_{(W,P)}$-$\bigsqcup\{(\widetilde{G_\lambda})_P : \lambda\in\Lambda_0\}\in\mathfrak{I}$. Since $\mathfrak{I}\subset\mathfrak{J}$, $1_{(W,P)}-\bigsqcup\{(\widetilde{G_\lambda})_P : \lambda\in\Lambda_0\}\in\mathfrak{J}$. Thus, $(W,\tau,P,\mathfrak{J})$ is NSIC. □

Proposition 4.9. *Let (W,τ,P) and (V,τ',R) be two NST, $(f,\vartheta) : (W,\tau,P)\to(V,\tau',R)$ be a soft mapping and $\mathfrak{I}$ a NSI on W. Then, $(f,\vartheta)(\mathfrak{I})=\{(f,\vartheta)(\widetilde{F}_P):\widetilde{F}_P\in\mathfrak{I}\}$ is a NSI on V.*

Theorem 4.10. *Let $f:(W,\tau,P,\mathfrak{I})\to(V,\tau',R,\mathfrak{J})$ be a neutrosophic soft continuous surjection and $(f,\vartheta)(\mathfrak{I})\subseteq\mathfrak{J}$. If $(W,\tau,P,\mathfrak{I})$ is neutrosophic soft- $\mathfrak{I}$-compact, then $(V,\tau',R,\mathfrak{J})$ is NSIC.*

Proof. Let $\{(\widetilde{G_\lambda})_R : \lambda\in\Lambda\}$ be a NSO-cover of V. Since f is neutrosophic soft continuous , $\{(f,\vartheta)^{-1}((\widetilde{G_\lambda})_R) : \lambda\in\Lambda\}$ is a neutrosophic soft open cover of W. Assuming that $(W,\tau,P,\mathfrak{I})$ is NSIC, there exists a finite subset Λ_0 of Λ such that $1_{(W,P)}-\bigsqcup\{(f,\vartheta)^{-1}((\widetilde{G_\lambda})_R) : \lambda\in\Lambda_0\}\in\mathfrak{I}$. This implies that, $(f,\vartheta)(1_{(W,P)}-\bigsqcup\{f^{-1}((\widetilde{G_\lambda})_R) : \lambda\in\Lambda_0\})\in(f,\vartheta)(\mathfrak{I})$. Then $1_{(V,R)}-\bigsqcup\{(\widetilde{G_\lambda})_R : \lambda\in\Lambda_0\}\in\mathfrak{J}$. So, $(V,\tau',R,\mathfrak{J})$ is NSIC. □

Proposition 4.11. *Let (W,τ,P) and (V,τ,R) be two NST. $(f,\vartheta) : (W,\tau,P)\to(V,\tau,R)$ be an injective soft mapping and $\mathfrak{J}$ a NSI on V. Then, $(f,\vartheta)^{-1}(\mathfrak{J})$ is a NSI on W.*

Proof. It is obvious. □

Theorem 4.12. *Let $f:(W,\tau,P)\to(V,\tau',R,\mathfrak{J})$ be a neutrosophic soft open bijection. If $(V,\tau',R,\mathfrak{J})$ is neutrosophic soft-$\mathfrak{I}$-compact, then $(W,\tau,P,(f,\vartheta)^{-1}(\mathfrak{J}))$ is neutrosophic soft-$(f,\vartheta)^{-1}(\mathfrak{J})$-compact.*

Proof. Let $\{(\widetilde{G_\lambda})_P : \lambda \in \Lambda\}$ be a NSO-cover of U. Since f is neutrosophic soft open bijection, $\{(f,\vartheta)((\widetilde{G_\lambda})_P) : \lambda \in \Lambda\}$ is a neutrosophic soft τ'-open cover of V. Assuming that $(V,\tau',R,\mathfrak{J})$ is NSIC, there exists a finite subset Λ_0 of Λ such that $1_{(V,R)} - \bigsqcup\{(f,\vartheta)((\widetilde{G_\lambda})_P) : \lambda \in \Lambda_0\} \in \mathfrak{J}$. This implies that, $(f,\vartheta)^{-1}(1_{(V,R)} - \bigsqcup\{(f,\vartheta)((\widetilde{G_\lambda})_P) : \lambda \in \Lambda_0\}) \in (f,\vartheta)^{-1}(\mathfrak{J})$. Then $1_{(W,P)} - \bigsqcup\{(\widetilde{G_\lambda})_R : \lambda \in \Lambda_0\} \in (f,\vartheta)^{-1}(\mathfrak{J})$. So, $(W,\tau,P,(f,\vartheta)^{-1}(\mathfrak{J}))$ is neutrosophic soft-$(f,\vartheta)^{-1}(\mathfrak{J})$-compact. □

5. **Conclusions**

Smarandance introduced neutrosophic set as an extension of intuitionistic fuzzy set. Maji gave the concept of neutrosophic soft set and neutrosophic soft set theory has a lot of applications in different areas. Then Gündüz et all redefined basic notions of neutrosophic soft set and soft point. In this paper, we gave the definition of NS-Cl^*-closure, which is more general than neutrosophic soft closure of NSS, with the help of NSI and NSTS. Also we examined basic properties of this new concept. Moreover, we define the concept of NS-$*$-topology and NSIC. Besides, we studied the relationship between these concepts and investigate relations with those concepts. We plan to study the concept of connected in neutrosophic soft ideal topological space.

Funding: This research received no external funding

Acknowledgments: I wish to thank Prof. Dr. Saeid Jafari for suggestions. Also, I would like to thank the referees and the editor for their helpful suggestions.

Conflicts of Interest: The authors declare no conflict of interest.

Abbreviations:

FS fuzzy set
IFS intuitionistic fuzzy set
NS neutrosophic set
SS soft set
NSS neutrosophic soft set
NSP neutrosophic soft point
NSTS neutrosophic soft topological space
NSO neutrosophic soft open
NSC neutrosophic soft closed
NSI neutrosophic soft ideal
NSC neutrosophic soft compact
NSIC neutrosophic soft I-compact

References

1. K. Atanassov, Intuitionistic fuzzy sets, Fuzzy Set and Systems, (1986), 20, 87-96.
2. T. Bera and N. K. Mahapatra, Introduction to neutrosophic soft topological space, Opsearch, (2017), 54, 841-867.
3. I. Deli and S. Broumi, Neutrosophic soft relations and some properties, Ann. Fuzzy Math. Inform.,(2015), 9, 169-182.
4. C. Gündüz Aras, T. Y. Öztürk and S. Bayramov, Seperation axioms on neutrosophic soft topological spaces, Turk. J. Math., (2019), 43, 498-510.
5. C. Gündüz Aras, T. Y. Öztürk and S. Bayramov, Neutrosophic soft continuity in neutrosophic soft topological spaces, Filomat, (2020), 34, 3495-3506.
6. P. K. Maji, Neutrosophic soft set, Ann. Fuzzy Math. Inform., (2013), 5, 157-168.
7. D. Molodtsov, Soft Set Theory-First Results, Comput. Math. Appl., (1999), 37, 19-31.
8. T. Y. Öztürk, C. Gündüz Aras and S. Bayramov, A new approach to operations on neutrosophic soft sets and to neutrosophic soft topological spaces, Communication in Mathematics and Applications, (2019), 10, 481-493.
9. T. Y. Öztürk, A. Benek, and A. Özkan, Neutrosophic soft compact spaces, Afrika Matematika, (2021), 32, 301-316.
10. T. Y. Öztürk, Some structures on neutrosophic topological spaces, Applied Mathematics and Nonlinear Sciences, (2021), 6, 467-478.
11. F. Smarandache, Neutrosophic set, a generalisation of the intuitionistic fuzzy sets, Int. J. Pure Appl. Math., (2005), 24, 287-297.
12. LA. Zadeh, Fuzzy sets Information and Control, (1965), 8, 338-353.

Received: April 7, 2024. Accepted: Aug 25, 2024

NSS
Neutrosophic Sets and Systems, Vol. 72, 2024
University of New Mexico

Circular Economy Strategies to Promote Sustainable Development using t-Neutrosophic Fuzzy graph

M. Kaviyarasu [1]*, Hossein Rashmanlou [2], Saeed Kosari [3] Said Broumi [4], R. Venitha [5], M. Rajeshwari[6]* and and Farshid Mofidnakhaei[7]

[1,5] Department of Mathematics, Vel Tech Rangarajan Dr. Sagunthala R&D Institute of Science and Technology, Chennai, Avadi, india-600 062. email: kavitamilm@gmail.com
[2] School of Physics, Damghan University, Damghan, Iran. email: Rashmanlou.1987@gmail.com
[3] Institute of Computing Science and Technology, Guangzhou University, Guangzhou, China. email id: Saeedkosari38@gzhu.edu.cn
[4] Laboratory of Information Processing, Faculty of Science Ben M'Sik, University of Hassan II, Casablanca, Morocco & Regional Center for the Professions of Education and Training(C.R.M.E.F), Casablanca, Morocco. broumisaid78@gmail.com
[6] Department of Mathematics, Presidency University, Bangalore,India. Email: rajeakila@gmail.com
[7] Department of Physics, Sari Branch, Islamic Azad University, Sari, Iran. email:Farshid.mofidnakhaei@gmail.com

* Correspondence: kavitamilm@gmail.com and rajeakila@gmail.com

Abstract: This study discusses the use of t-neutrosophic graphs to express and understand complex interactions. It also shows how these graphs might manage intricate relationships with a wide range of variables or scenario elements. Additionally, it offers fundamental t-neutrosophic graph operations and talks about concepts in these graphs such as homomorphism and isomorphism. Additionally, the study addresses how this approach may be applied in practical contexts to address circular economies and sustainability growth. Through the use of t-neutrosophic graphs, various components, and their connections, the research demonstrates that managing the several circular dimensions is feasible. financial system. This example shows how adaptable and practical t-neutrosophic graphs are as a tool for developing policies and making decisions about complicated social issues that involve some numbers principles.

Keywords: Graph Theory, t- Neutrosophic Fuzzy Graph, Decision Making, and Sustainability.

1. Introduction

One of the pioneering works that popularized fuzzy sets was Lotfi A. Zadeh [1]. Unlike typical sets with distinct membership criteria, fuzzy sets assign degrees of membership to items, allowing for the depiction of ambiguity and uncertainty in the data. The book by Abraham Kandel [2] offers a thorough overview of fuzzy mathematical methods and their real-world applications. It is an invaluable resource for comprehending the use of fuzzy sets in a variety of fields and covers a broad range of topics. Fuzzy sets were extended to intuitionistic fuzzy sets by Krassimir T. Atanassov [3]. More details about the extent of non-membership are incorporated into intuitionistic fuzzy sets, which offer a more complex depiction of uncertainty. The book by Lotfi A. Zimmermann [4] offers a thorough introduction to fuzzy set theory and all of its various uses. It examines the applications of fuzzy sets in decision-making, control systems, and other domains, providing a fundamental resource for scholars and professionals. The book by George J. Klir and Bo Yuan [5] provides a thorough introduction to fuzzy logic and fuzzy sets. In addition to covering the theoretical underpinnings of fuzzy sets and logic, it offers real-world applications in domains including pattern recognition, decision analysis, and control systems. Jerry M. Mendel [6] paper provides an overview of fuzzy logic systems, with a focus on engineering applications. It goes over the fundamentals of fuzzy logic and offers some ideas about

how engineering systems might use it to handle imprecision and uncertainty. In [28-30] applied fuzzy set and their logic to find better decision making.

Mapari, and Naidu [7], Examines fuzzy set theory and its uses, offering a basic comprehension of fuzzy sets and their useful applications in various domains. Akrama M [8] focuses on neutrosophic graphs in the field of graph theory by concentrating on single-valued neutrosophic planar graphs. Nasir M. and Akram M. [9] examine certain bipolar neutrosophic competition graphs, probably with a focus on mathematical competition applications. Siddique S. and Akram M. [10] investigate applications of neutrosophic competition graphs and show how useful they are for fuzzy and intelligent systems. Waseem, Dudek, and Akram [11] explain specific kinds of edge m-polar fuzzy graphs, adding to our knowledge of fuzzy graphs with an emphasis on edge relativity. In 2020, Ajay, and Chellamani, [12] presented Pythagorean neutrosophic fuzzy graphs, presumably investigating the combination of neutrosophic sets and Pythagorean fuzzy sets in the context of graph theory. Dey, Pal, Long, Mohanta, and Son [13] carries out research on m-polar neutrosophic graphs with applications, perhaps looking at real-world uses for these graphs in intelligent systems. Mateen, Kausar, Gulzar, and Alghazzawi, [14] study a particular class of fuzzy subgroups that are t-intuitionistic, contributing to the study of subgroup theory and fuzzy algebra. P. Chellamani and D. Ajay [15] examine Pythagorean neutrosophic Dombi fuzzy graphs and apply them to multicriteria decision-making (MCDM), presumably demonstrating their usefulness in this context. Reviews the literature on intelligent traffic control systems using a variety of theoretical frameworks, such as fuzzy sets, rough sets, graph theory, and neutrosophic sets [16]. In 2016 [20-23] money researcher devolved fuzzy concept in graph theory.

In 2022, Broumi, Bakali, Shanmugapriya, Sundareswaran, and Talea [17] examine Fermatean neutrosophic graph theory and applications, possibly advancing knowledge of Fermatean neutrosophic structures in graph theory. Mohanta, Dey, Mondal, Pal, and Lakhwani [18] contribute to the study of operations and transformations in the field of Dombi neutrosophic graphs by looking into a few operations on them. Razaq, Alhamzi, Shuaib, Razzaque, Masmali, Latif, and Noor [19] offer a thorough examination of t-intuitionistic fuzzy graphs and investigates how to use them to combat poverty; this certainly contributes to both the theoretical and practical sides of fuzzy graph theory.

In [25] Victor Christianto and Florentin Smarandache discussed The Paradoxist Movement, Precursor of Neutrosophy, in the Shadow of a Totalitarian Regime. [26] Minxia Luo et al, Fuzzy Inference Quintuple Implication Method Based on introduced the Single Valued Neutrosophic t-representable t-norm. [27] Vázquez and Smarandache examines how postcolonial modernist ideas and indigenous philosophies may be integrated within the MultiAlism framework, showing how these disparate philosophical traditions in Latin America can interact and come together. Using areas of neutrality like cultural variety and criticisms of power structures, Florentin Smarandache's notion of MultiAlism is used to fill in the gaps and reconcile these systems. [31] Elsayed employ the Approach for Preference, Performance and Ranking Evaluation with SAtisfaction Level (APPRESAL) method to analyze the BRT system's features in accordance with user satisfaction. This will help address the shortcomings of multi-criteria decision-making (MCDM) methods, which are unable to adequately address user satisfaction or the impact of various factors on the analysis conducted in a type-2 neutrosophic numbers (T2NN) environment. Lastly, the method will help resolve any ambiguity or uncertainty that may arise from the data that has been gathered.

In [33] Ahmed El-Douh et al, presenting the technique of Multi-Attributive Border Approximation Area Comparisons. In order to manage untrue data, this MCDM approach is combined with a neutrosophic set and used to evaluate the sustainability of soil activities. [34] Zenat Mohamed

et al. provides a comprehensive review of sustainable supplier selection and looks at the key parameters and elements that should be considered when evaluating suppliers' sustainability performance. From the above

It has been demonstrated that using t-neutrosophic fuzzy graphs can assist manage ambiguity and uncertainty by providing a flexible approach to decision-making. These models act as a bridge between traditional numerical engineering models and symbolic expert systems. The t-neutrosophic fuzzy theory manages complex and uncertain circumstances well, communicating imprecision and unpredictability. We introduced the concept of a t-neutrosophic fuzzy graph that uses linear operators to solve practical problems. The parameter "t" reduces ambiguity in the decision-making process and enables precise control and customized solutions. This parameter offers a personalized uncertainty management plan while enhancing flexibility. t-neutrosophic fuzzy graphs provide a powerful tool for interpreting complex decision-making situations, allowing for a holistic approach to handling decision-making challenges. This strategy reduces the limitations of binary logic and significantly increases the precision of decision-making.

After a brief introduction to t-neutrosophic fuzzy graphs, the work is organized as follows: To help readers understand the originality of the work being presented, some basic terminology is provided in the "Preliminaries" section. "t-Neutrosophic Fuzzy Graph" discusses the concept of t-neutrosophic fuzzy graphs and highlights some of its salient characteristics. The set-theoretical operations of t-neutrosophic fuzzy graphs are examined and graphical representations of these operations are provided in the section "Operations on the t-neutrosophic fuzzy graph". The section "Isomorphism of t-neutrosophic fuzzy graphs" establishes the concepts of homomorphism and isomorphism specific to t-neutrosophic fuzzy graphs. In the section "Complement of t-neutrosophic fuzzy graph", the notion of the complement of t-neutrosophic fuzzy graphs is established and its key characteristics are analyzed. In the "Application of t-neutrosophic fuzzy graph" section, a mechanism for Sustainable Development through a Circular Economy is created using the recently developed technology. Finally, the "Comparative Analysis" and "Conclusion" sections provide a comparison of the article's many components and particular results.

1.1 Motivation

1. The main motivation behind the selection of t-neutrosophic graphs is their capacity to manage intricate scenarios including ambiguous information and hesitant, fluctuating elemental interactions.
2. These graphs offer a mechanism to assess and model various degrees of uncertainty and confidence in connections with the addition of the "t" parameter.
3. The integration and separation of uncertain information are managed by introducing a strategy that incorporates t-norms and t-conorms. This approach is especially meant to be used for making decisions in practical scenarios with a variety of inputs and results.
4. Applications for this method can be found in many different domains, including systems optimization, risk assessment, and decision analysis. Its objective is to strike a balance between usefulness in many contexts and undiscovered connections.

1.2 Novelty

1. To help establish an orderly and understandable depiction of unclear connections, the "t" parameter serves as a threshold reflecting reluctance.
2. The relationship visualization is enhanced by the addition of the "t" option, which determines which edges and nodes to display based on a predetermined confidence level.

3. It is possible to distinguish between strong and delicate associations with more accuracy using this strategy, which facilitates the methodical handling of ambiguity.
4. A t-neutrosophic approach connects various parameter values "t" to different graph layers, enabling multi-layered analysis. This makes it possible to analyze the relationships within the graph in detail while accounting for different levels of confidence, which leads to a deeper understanding of the underlying framework.

1.3 Goal

1. Explain the t-neutrosophic framework concept. The flexibility with which this framework may be used to communicate the ambiguity and uncertainty inherent in decision-making processes makes it valuable. Numerous academic fields, including as economics, chemistry, computer science, medicine, and engineering, depend on it.

2. Examine a number of set-theoretical operations within the framework of t-neutrosophic theory and identify the salient features of these freshly developed operations. These features support the development of informed decision-making across a range of domains, the integration of data, and the exploration of linkages.
3. Discuss homomorphism and isomorphism to t-neutrosophic theory and provide recently defined characteristics. These ideas facilitate data transmission and comparison analysis, particularly when hesitant and unclear graph topologies are involved.
4. Introduce the notion of a t-neutrosophic complement and verify its essential characteristics. This idea of ambiguity has applications in mistake detection, system verification, and decision analysis by revealing inverse linkages that were not immediately obvious in the original graph.
5. Utilize the recently established t-neutrosophic approach to pinpoint critical elements for reducing poverty in a certain community. This methodology facilitates improved representation, discerns vulnerable groups, distributes resources, tracks and assesses advancements, and develops educated policies.
6. Examine the complexities and uncertainties surrounding poverty to evaluate its causes, evolution, and effects using the t-neutrosophic framework.

Symbols	**Meaning**
NS	Neutrosophic Set
NG	Neutrosophic Graph
t-NS	t- Neutrosophic Set
t-NG	t- Neutrosophic Graph
$\mathbf{T}_{\mathcal{G}_t}$	Truth Membership Function
$\mathbf{I}_{\mathcal{G}_t}$	Indeterminacy Membership Function
$\mathbf{F}_{\mathcal{G}_t}$	Falsity Membership Function

Table 1 List of symbols used

2. t-Neutrosophic Graph

*2.1. Definition***.** Let G be the NS of a universal set U with t ∈ [0,1]. The $NS_{\mathcal{G}_t}$ of U, also known as a t-NS, is defined as $T_{\mathcal{G}_t}(u_1) = \min\{T_{\mathcal{G}}(u_1), t\}$, $I_{\mathcal{G}_t}(u_1) = \max\{I_{\mathcal{G}}(u_1), 1-t\}$ and $F_{\mathcal{G}_t}(u_1) = \max\{F_{\mathcal{G}}(u_1), 1-t\}$,$\forall\, u_1 \in U$. The form of t-NS is $\mathcal{G}_t = \{u_1, T_{\mathcal{G}}(u_1), I_{\mathcal{G}}(u_1), F_{\mathcal{G}}(u_1) : u_1 \in U\}$ where $T_{\mathcal{G}_t}, I_{\mathcal{G}_t}$ and $F_{\mathcal{G}_t}$ are

functions that assign to each degree. Moreover, the function $T_{\mathcal{G}_t}, I_{\mathcal{G}_t}$ *and* $F_{\mathcal{G}_t}$ satisfy the condition $0 \leq T_{\mathcal{G}}(u_1) + I_{\mathcal{G}}(u_1)+F_{\mathcal{G}}(u_1) \leq 1$.

2.2. Definition. Let $\mathcal{G} = (A, B)$ be a NG for a given simple graph G= (V,E). A t-NG is represented by the notation $\mathcal{G}_t = (A_t, B_t)$, where

$A_t = \{(u_i, T_{\mathcal{G}}(u_i), I_{\mathcal{G}}(u_i), F_{\mathcal{G}}(u_i)) : u_i \in V\}$ is a t-NS on V and
$B_t = \{((u_i, u_j), T_{\mathcal{G}}(u_i, u_j), I_{\mathcal{G}}(u_i, u_j), F_{\mathcal{G}}(u_i, u_j)) : (u_i, u_j) \in E\}$ is a t-NS on E$\subseteq V \times V$, such that $\forall (u_i, u_j) \in E$

$T_{B_t}(u_i, u_j) \leq \min\{T_{A_t}(u_i), T_{A_t}(u_j)\}$
$I_{B_t}(u_i, u_j) \leq \max\{I_{A_t}(u_i), I_{A_t}(u_j)\}$
$F_{B_t}(u_i, u_j) \leq \max\{F_{A_t}(u_i), F_{A_t}(u_j)\}$,

Satisfy the condition: $0 \leq T_{A_t}(u_i) + I_{A_t}(u_i)+F_{A_t}(u_i) \leq 1$ and $0 \leq T_{B_t}(u_i, u_j) + I_{B_t}(u_i, u_j) + F_{B_t}(u_i, u_j) \leq 1$.

2.3 Example Examine the $G' = (V, E)$ in which $V = \{a, b, c, d\}$ and $E = \{ab, ac, ad, bc, cd\}$. Given V, the node strengths of A *is* $\{(a, 0.2,0.4,0.6), (b, 0.5,0.4,0.7), (c, 0.3,0.6,0.9), (d, 0.8,0.7,0.1)\}$**.** The Edge strength of B *is* $\{(ab, 0.2,0.4,0.7), (ac, 0.2,0.6,0.9), (ad, 0.2,0.7,0.6), (bc, 0.3,0.6,0.9), (cd, 0.3,0.7,0.9)\}$**.** Applying the concept of t-NS to the two NS A and B that are provided, which correspond to the value t = 0.40, reveals that,

$A_{0.40} = \{(a, 0.2,0.6,0.6), (b, 0.4,0.6,0.7), (c, 0.3,0.6,0.9), (d, 0.4,0.7,0.6)\}$ and

$B_{0.40} = \{(ab, 0.2,0.6,0.7), (ac, 0.2,0.6,0.9), (ad, 0.2,0.6,0.7), (bc, 0.3,0.6,0.9), (cd, 0.3,0.7,0.9)\}$.

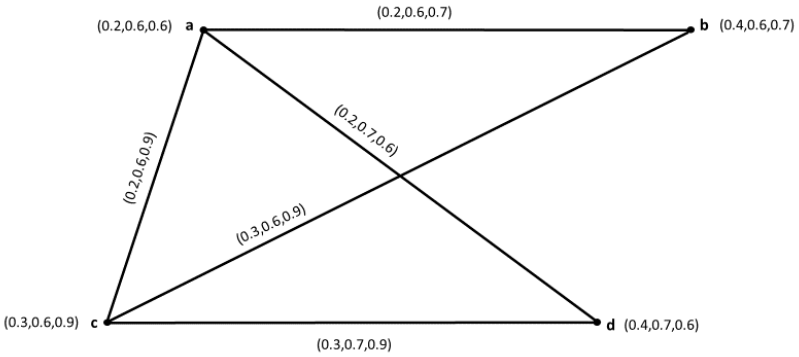

Figure 1. 0.4-NG $\mathcal{G}_{0.4}$

The graphical representation of t-NG, where t=0.4; $\mathcal{G}_{0.4} = (A_{0.40}, B_{0.40})$

*2.4. Definition***.** Let $\mathcal{G}_t = (A_t, B_t)$ be an t-NG then $\mathcal{H}_t = (A'_t, B'_t)$ is considered a t-neutrosophic subgraph if $A'_t \subseteq A_t$ and $B'_t \subseteq B_t$.

*2.5.Definition***.** A t-NG $\mathcal{G}_t$ is said to be a complete t-NG if it meets the requirements listed below:

$$T_{B_t}(u_1, u_2) = \min\{T_{A_t}(u_1), T_{A_t}(u_2)\}$$
$$I_{B_t}(u_1, u_2) = \max\{I_{A_t}(u_1), I_{A_t}(u_2)\}$$
$$F_{B_t}(u_1, u_2) = \max\{F_{A_t}(u_1), F_{A_t}(u_2)\} \ , \forall \ (u_1, u_2) \in E$$

2.6 Example. Figure 2 illustrates the entire 0.5-NG $\mathcal{G}_t$.

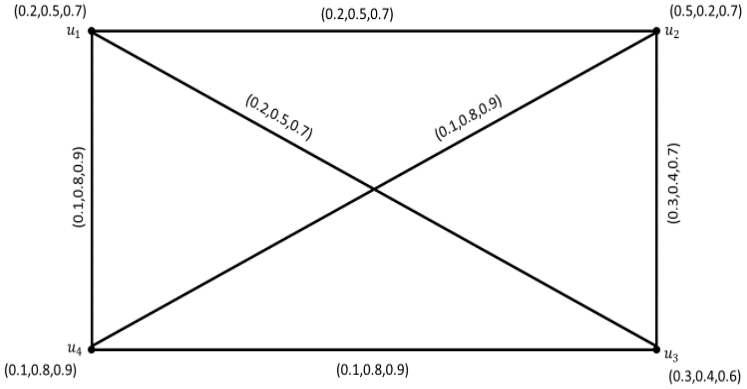

Figure 2. Complete 0.5-NG $\mathcal{G}_{0.5}$

2.7. Definition. In t-NG, the order is defined as follows

$$O(\mathcal{G}_t) = \left(\sum_{u_1 \in V} T_{A_t}(u_1), \sum_{u_1 \in V} I_{A_t}(u_1), \sum_{u_1 \in V} F_{A_t}(u_1) \right)$$

2.8. Example. The order of t-NG $\mathcal{G}_t$ is (1.3, 2.5, 2.8) from example 1.

2.9 Definition. The t-NG has a size defined by

$$S(\mathcal{G}_t) = \left(\sum_{(u_1,u_2) \in E} T_{B_t}(u_1,u_2), \sum_{(u_1,u_2) \in E} I_{B_t}(u_1,u_2), \sum_{(u_1,u_2) \in E} F_{B_t}(u_1,u_2) \right)$$

2.10. Definition. t-NG defines the degree of vertex u_1 in $\mathcal{G}_t$ *as follows:*

$$deg_{\mathcal{G}_t}(u_1) = \left(deg_{T_{B_t}}(u_1), deg_{I_{B_t}}(u_1), deg_{F_{B_t}}(u_1) \right)$$

$$deg_{\mathcal{G}_t}(u_1) = \left(\sum_{(u_1,u_2) \in E} T_{B_t}(u_1,u_2), \sum_{(u_1,u_2) \in E} I_{B_t}(u_1,u_2), \sum_{(u_1,u_2) \in E} F_{B_t}(u_1,u_2) \right)$$

2.11. Example. Referring to Example 1,

1. The degree of vertex in $\mathcal{G}_t$ are, $deg_{\mathcal{G}_t}(a) = (0.6,1.9,2.2)$; $deg_{\mathcal{G}_t}(b) = (0.5,1.2,1.6)$; $deg_{\mathcal{G}_t}(c) = (0.8,1.9,2.7)$; $deg_{\mathcal{G}_t}(d) = (0.5,1.4,1.5)$.

2. The minimum degree $\delta(\mathcal{G}_t)$of t-NG is given by $\delta(\mathcal{G}_t) = (\delta_{T_{B_t}}(\mathcal{G}_t), \delta_{I_{B_t}}(\mathcal{G}_t). \delta_{F_{B_t}}(\mathcal{G}_t))$

$$\delta(\mathcal{G}_t) = \left(\min\left\{ deg_{T_{B_t}}(u_1) : u_1 \in V \right\}, \min\left\{ deg_{I_{B_t}}(u_1) : u_1 \in V \right\}, \min\left\{ deg_{F_{B_t}}(u_1) : u_1 \in V \right\} \right)$$

3. The maximum degree $\Delta(\mathcal{G}_t)$ of t-NG is given by $\Delta(\mathcal{G}_t) = (\Delta_{T_{B_t}}(\mathcal{G}_t), \Delta_{I_{B_t}}(\mathcal{G}_t). \Delta_{F_{B_t}}(\mathcal{G}_t))$

$$\Delta(\mathcal{G}_t) = \left(\max\left\{ deg_{T_{B_t}}(u_1) : u_1 \in V \right\}, \max\left\{ deg_{I_{B_t}}(u_1) : u_1 \in V \right\}, \max\left\{ deg_{F_{B_t}}(u_1) : u_1 \in V \right\} \right)$$

From Example 1: $\delta(\mathcal{G}_t)$ = (0.5, 1.2, 1.5); $\Delta(\mathcal{G}_t) = (0.8, 1.9, 2.7)$. In t-NG the following inequality holds, $\delta(\mathcal{G}_t) \leq \Delta(\mathcal{G}_t) \leq S(\mathcal{G}_t) \leq O(\mathcal{G}_t)$

3.2 Theorem. An t-NG is represented as G_t=(A_t,B_t), then

$$\sum deg_{\mathcal{G}_t}(u_i) = \left(2\sum T_{\mathcal{G}_t}(u_i,w), 2\sum I_{\mathcal{G}_t}(u_i,w), 2\sum F_{\mathcal{G}_t}(u_i,w)\right)$$

Proof. Considering t-NG represented by G_t=(A_t,B_t), let's investigate,

$$\sum deg_{\mathcal{G}_t}(u_i) = \left(\sum deg_{T_{B_t}}(u_i), \sum deg_{I_{B_t}}(u_i), \sum deg_{F_{B_t}}(u_i)\right)$$

$$= \left(deg_{T_{B_t}}(u_1), deg_{I_{B_t}}(u_1), deg_{F_{B_t}}(u_1)\right) + \left(deg_{T_{B_t}}(u_2), deg_{I_{B_t}}(u_2), deg_{F_{B_t}}(u_2)\right) \dots +$$

$$\left(deg_{T_{B_t}}(u_n), deg_{I_{B_t}}(u_n), deg_{F_{B_t}}(u_n)\right)$$

$$= \left(T_{B_t}(u_1,u_2), I_{B_t}(u_1,u_2), F_{B_t}(u_1,u_2)\right) + \left(T_{B_t}(u_1,u_3), I_{B_t}(u_1,u_3), F_{B_t}(u_1,u_3)\right) + \dots +$$
$$\left(T_{B_t}(u_1,u_n), I_{B_t}(u_1,u_n), F_{B_t}(u_1,u_n)\right) + \dots + \left(T_{B_t}(u_n,u_1), I_{B_t}(u_n,u_1), F_{B_t}(u_n,u_1)\right) +$$
$$\left(T_{B_t}(u_n,u_2), I_{B_t}(u_n,u_2), F_{B_t}(u_n,u_2)\right) + \dots + \left(T_{B_t}(u_n,u_{n-1}), I_{B_t}(u_n,u_{n-1}), F_{B_t}(u_n,u_{n-1})\right)$$
$$= \left(2(T_{B_t}(u_1,u_2), I_{B_t}(u_1,u_2), F_{B_t}(u_1,u_2)) + 2(T_{B_t}(u_1,u_3), I_{B_t}(u_1,u_3), F_{B_t}(u_1,u_3)) + \dots +\right.$$
$$\left. 2(T_{B_t}(u_1,u_n), I_{B_t}(u_1,u_n), F_{B_t}(u_1,u_n))\right)$$

$$= \left(2\sum T_{\mathcal{G}_t}(u_i,w), 2\sum I_{\mathcal{G}_t}(u_i,w), 2\sum F_{\mathcal{G}_t}(u_i,w)\right).$$

Hence proved.

3. Operation on t-Neutrosophic Graph

*3.1. Definition***.** Consider any two t-NG of G = (V,E) and G′=(V′,E′) correspond to $\mathcal{G}_t = (A_t, B_t)$ and $\mathcal{G}'_t = (A'_t, B'_t)$, respectively. $(A_t \times A'_t, B_t \times B'_t)$ defines the Cartesian product $\mathcal{G}_t \times \mathcal{G}'_t$ of two t-NG. Where $A_t \times A'_t$ and $B_t \times B'_t$ are t-NS on $V \times V' = \{(\varphi_1, \varpi_1), (\varphi_2, \varpi_2): \varphi_1 \& \varphi_2 \in V; \varpi_1 \& \varpi_2 \in V'\}$ and $E \times E' = \{(\varphi_1, \varpi_1), (\varphi_2, \varpi_2): \varphi_1 = \varphi_2, \varphi_1 \& \varphi_2 \in V, (\varpi_1, \varpi_2) \in E'\}\ U\ \{(\varphi_1, \varpi_1), (\varphi_2, \varpi_2): \varpi_1 = \varpi_2, \varpi_1 \& \varpi_2 \in V', (\varphi_1, \varphi_2) \in E\}\ U\ \{(\varphi_1, \varpi_1), (\varphi_2, \varpi_2): \varpi_1 \neq \varpi_2, \varphi_1 \neq \varphi_2, (\varpi_1, \varpi_2) \in E', (\varphi_1, \varphi_2) \in E\}$ respectively, which fulfills the given requirement.

1. $\forall((\varphi_1, \varpi_1) \in V \times V'$
   a) $T_{A_t \times A'_t}(\varphi_1, \varpi_1) = \min\left\{T_{A_t}(\varphi_1), T_{A_{t'}}(\varpi_1)\right\}$
   b) $I_{A_t \times A'_t}(\varphi_1, \varpi_1) = \max\left\{I_{A_t}(\varphi_1), I_{A_{t'}}(\varpi_1)\right\}$
   c) $F_{A_t \times A'_t}(\varphi_1, \varpi_1) = \max\left\{F_{A_t}(\varphi_1), F_{A_{t'}}(\varpi_1)\right\}$

2. If $\varphi_1 = \varphi_2$ and $\forall\ (\varpi_1, \varpi_2) \in E'$
   a) $T_{B_t \times B'_t}((\varphi_1, \varpi_1), (\varphi_2, \varpi_2)) = \min\left\{T_{A_t}(\varphi_1), T_{B_{t'}}(\varpi_1, \varpi_2)\right\}$
   b) $I_{B_t \times B'_t}((\varphi_1, \varpi_1), (\varphi_2, \varpi_2)) = \max\left\{I_{A_t}(\varphi_1), I_{B_{t'}}(\varpi_1, \varpi_2)\right\}$
   c) $F_{B_t \times B'_t}\left((\varphi_1, \varpi_1), (\varphi_2, \varpi_2)\right) = \max\left\{F_{A_t}(\varphi_1), F_{B_{t'}}(\varpi_1, \varpi_2)\right\}$
3. If $\varpi_1 = \varpi_2$ and $\forall\ (\varphi_1, \varphi_2) \in E$
   a) $T_{B_t \times B'_t}((\varphi_1, \varpi_1), (\varphi_2, \varpi_2)) = \min\left\{T_{B_t}(\varphi_1, \varphi_2), T_{A_{t'}}(\varpi_1)\right\}$
   b) $I_{B_t \times B'_t}((\varphi_1, \varpi_1), (\varphi_2, \varpi_2)) = \max\left\{I_{B_t}(\varphi_1, \varphi_2), I_{A_{t'}}(\varpi_1)\right\}$
   c) $F_{B_t \times B'_t}\left((\varphi_1, \varpi_1), (\varphi_2, \varpi_2)\right) = \max\left\{F_{B_t}(\varphi_1, \varphi_2), F_{A_{t'}}(\varpi_1)\right\}$
4. If $\varpi_1 \neq \varpi_2\ and \varphi_1 \neq \varphi_2,\ \forall\ (\varpi_1, \varpi_2) \in E', (\varphi_1, \varphi_2) \in E$
   a) $T_{B_t \times B'_t}((\varphi_1, \varpi_1), (\varphi_2, \varpi_2)) = \min\left\{T_{B_t}(\varphi_1, \varphi_2), T_{B_{t'}}(\varpi_1, \varpi_2)\right\}$

b) $I_{B_t\times B_t'}((\varphi_1,\varpi_1),(\varphi_2,\varpi_2)) = \max\left\{I_{B_t}(\varphi_1,\varphi_2), I_{B_{t'}}(\varpi_1,\varpi_2)\right\}$

c) $F_{B_t\times B_t'}\left((\varphi_1,\varpi_1),(\varphi_2,\varpi_2)\right) = \max\left\{F_{B_t}(\varphi_1,\varphi_2), F_{B_{t'}}(\varpi_1,\varpi_2)\right\}$

3.2 Example. The two 0.5-NG $\mathcal{G}_t$and$\mathcal{G}_t'$, which are the elements to be taken into consideration, are shown in Figures 3 and 4. Figure 5 displays the corresponding Cartesian product $\mathcal{G}_{0.5}\times\mathcal{G}_{0.5}'$.

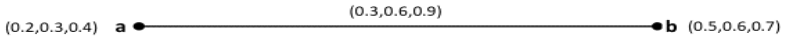

Figure 3. 0.5-NG $\mathcal{G}_{0.5}$

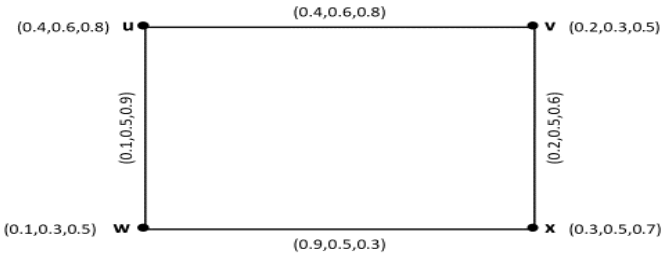

Figure 4. 0.5-NG $\mathcal{G}_{0.5}'$

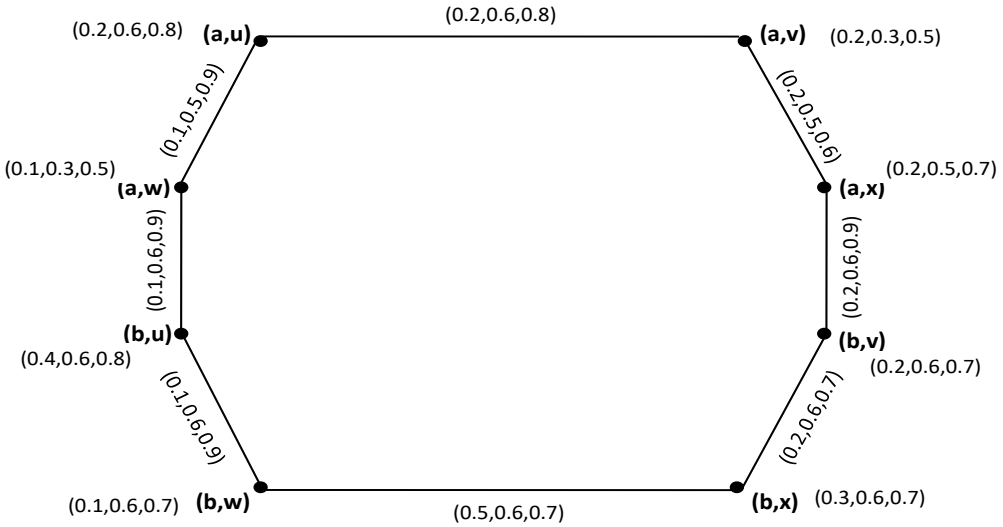

Figure 5. 0.5-NG $\mathcal{G}_{0.5}\times\mathcal{G}_{0.5}'$

3.3 Definition $deg_{\mathcal{G}_t\times\mathcal{G}_t'}(\varphi_1,\varpi_1) =$
$\left(\deg\left\{T_{B_t\times B_t'}\left((\varphi_1,\varpi_1),(\varphi_2,\varpi_2)\right)\right\}, \deg\left\{I_{B_t\times B_t'}\left((\varphi_1,\varpi_1),(\varphi_2,\varpi_2)\right)\right\}, \deg\left\{F_{B_t\times B_t'}\left((\varphi_1,\varpi_1),(\varphi_2,\varpi_2)\right)\right\}\right)$

Where,

$$\deg\left\{T_{B_t\times B_t'}((\varphi_1,\varpi_1),(\varphi_2,\varpi_2))\right\} = \sum_{\varphi_1=\varphi_2,(\varpi_1,\varpi_2)\in E'} \min\left\{T_{A_t}(\varphi_1), T_{B_t'}(\varpi_1,\varpi_2)\right\}$$
$$+\sum_{\varpi_1=\varpi_2,(\varphi_1,\varphi_2)\in E} \min\left\{T_{B_t}(\varphi_1,\varphi_2), T_{A_t'}(\varpi_1)\right\}$$
$$+\sum_{\varpi_1\neq\varpi_2,\varphi_1\neq\varphi_2} \min\left\{T_{B_t}(\varphi_1,\varphi_2), T_{B_t'}(\varpi_1,\varpi_2)\right\}$$
$$\deg\left\{I_{B_t\times B_t'}((\varphi_1,\varpi_1),(\varphi_2,\varpi_2))\right\} = \varphi_1=\varphi_2,(\varpi_1,\varpi_2)\in E'$$
$$+\sum_{\varpi_1=\varpi_2,(\varphi_1,\varphi_2)\in E} \max\left\{I_{B_t}(\varphi_1,\varphi_2), I_{A_t'}(\varpi_1)\right\}$$
$$+\sum_{\varpi_1\neq\varpi_2,\varphi_1\neq\varphi_2} \max\left\{T_{B_t}(\varphi_1,\varphi_2), I_{B_t'}(\varpi_1,\varpi_2)\right\}$$
$$\deg\left\{F_{B_t\times B_t'}((\varphi_1,\varpi_1),(\varphi_2,\varpi_2))\right\} = \sum_{\varphi_1=\varphi_2,(\varpi_1,\varpi_2)\in E'} \max\left\{F_{A_t}(\varphi_1), F_{B_t'}(\varpi_1,\varpi_2)\right\}$$
$$+\sum_{\varpi_1=\varpi_2,(\varphi_1,\varphi_2)\in E} \max\left\{F_{B_t}(\varphi_1,\varphi_2), F_{A_t'}(\varpi_1)\right\}$$
$$+\sum_{\varpi_1\neq\varpi_2,\varphi_1\neq\varphi_2} \max\left\{F_{B_t}(\varphi_1,\varphi_2), F_{B_t'}(\varpi_1,\varpi_2)\right\}$$

3.4 Example. Every vertex in $\mathcal{G}_t \times \mathcal{G}_t'$ has the following degree, per example 5.
$deg_{\mathcal{G}_t\times\mathcal{G}_t'}(a,u)$ = (0.3,1.1,1.7), $deg_{\mathcal{G}_t\times\mathcal{G}_t'}(a,v)$ = (0.4,1.1,1.4), $deg_{\mathcal{G}_t\times\mathcal{G}_t'}(a,w)$ = (0.2,1.1,1.8), $deg_{\mathcal{G}_t\times\mathcal{G}_t'}(a,x)$ = (0.4,1.1,1.5), $deg_{\mathcal{G}_t\times\mathcal{G}_t'}(b,u)$ = (0.2,1.2,1.8), $deg_{\mathcal{G}_t\times\mathcal{G}_t'}(b,v)$ = (0.4,1.2,1.6), $deg_{\mathcal{G}_t\times\mathcal{G}_t'}(b,w)$ = (0.6,1.2,1.6), $deg_{\mathcal{G}_t\times\mathcal{G}_t'}(b,x)$ = (0.7,1.2,1.4)

3.5. Theorem. The Cartesian products of two t-NGs, result is a new t-NG

Proof: The requirement is clear for $A_t \times A_t'$. Considering that $(\varpi_1,\varpi_2)\in E'$ and $\varphi_1 \in V$,

$$T_{B_t\times B_t'}((\varphi_1,\varpi_1),(\varphi_2,\varpi_2)) = \min\left\{T_{A_t}(\varphi_1), T_{B_t'}(\varpi_1,\varpi_2)\right\}$$

$$T_{B_t\times B_t'}((\varphi_1,\varpi_1),(\varphi_2,\varpi_2)) \leq \min\left\{T_{A_t}(\varphi_1), \min\{T_{A_t'}(\varpi_1), T_{A_t'}(\varpi_2)\}\right\}$$

$$T_{B_t\times B_t'}((\varphi_1,\varpi_1),(\varphi_2,\varpi_2)) \leq \min\left\{\min\{T_{A_t}(\varphi_1), T_{A_t'}(\varpi_1)\}, \min\{T_{A_t}(\varphi_1), T_{A_t'}(\varpi_2)\}\right\}$$

$$T_{B_t\times B_t'}((\varphi_1,\varpi_1),(\varphi_2,\varpi_2)) = \min\left\{T_{A_t\times A_t'}(\varphi_1,\varpi_1), T_{A_t\times A_t'}(\varpi_1,\varpi_2)\right\}$$

Consequently,

$T_{B_t\times B_t'}((\varphi_1,\varpi_1),(\varphi_2,\varpi_2)) \leq \min\left\{T_{A_t\times A_t'}(\varphi_1,\varpi_1), T_{A_t\times A_t'}(\varpi_1,\varpi_2)\right\}$ if $u_1 \in V$,

$(\varpi_1,\varpi_2)\in E'$. Similarly for,

$I_{B_t\times B_t'}((\varphi_1,\varpi_1),(\varphi_2,\varpi_2)) \leq \max\left\{I_{A_t\times A_t'}(\varphi_1,\varpi_1), I_{A_t\times A_t'}(\varpi_1,\varpi_2)\right\}$ if $u_1 \in V$,

$(\varpi_1,\varpi_2)\in E'$ and

$F_{B_t\times B_t'}((\varphi_1,\varpi_1),(\varphi_2,\varpi_2)) \leq \max\left\{F_{A_t\times A_t'}(\varphi_1,\varpi_1), F_{A_t\times A_t'}(\varpi_1,\varpi_2)\right\}$ if $u_1 \in V$,

$(\varpi_1,\varpi_2)\in E'$. Likewise we can demonstrate it for$\varpi_1 \in V'$,$(\varphi_1,\varphi_2)\in E$.

3.7. Definition. Consider any two t-NG of G = (V,E) and G′=(V′,E′) correspond to $\mathcal{G}_t = (A_t, B_t)$ and $\mathcal{G}'_t = (A'_t, B'_t)$, respectively. $(A_t \circ A'_t, B_t \circ B'_t)$ defines the composition $\mathcal{G}_t \circ \mathcal{G}'_t$ of two t-NG. Where $A_t \circ A'_t$ and $B_t \circ B'_t$ are t-NS on $V \times V' = \{(\varphi_1, \varpi_1), (\varphi_2, \varpi_2): \varphi_1 \& \varphi_2 \in V; \varpi_1 \& \varpi_2 \in V'\}$ and $E \times E' = \{(\varphi_1, \varpi_1), (\varphi_2, \varpi_2): \varphi_1 = \varphi_2, \varphi_1 \& \varphi_2 \in V, (\varpi_1, \varpi_2) \in E'\}\ U\ \{(\varphi_1, \varpi_1), (\varphi_2, \varpi_2): \varpi_1 = \varpi_2, \varpi_1 \& \varpi_2 \in V', (\varphi_1, \varphi_2) \in E\}\ U\ \{(\varphi_1, \varpi_1), (\varphi_2, \varpi_2): \varpi_1 \neq \varpi_2, \varphi_1 \neq \varphi_2, (\varpi_1, \varpi_2) \in E', (\varphi_1, \varphi_2) \in E\}$ respectively, which fulfills the given requirement.

1. $\forall((\varphi_1, \varpi_1) \in V \circ V'$

a) $T_{A_t \circ A'_t}(\varphi_1, \varpi_1) = \min\left\{T_{A_t}(\varphi_1), T_{A_{t'}}(\varpi_1)\right\}$

b) $I_{A_t \circ A'_t}(\varphi_1, \varpi_1) = \max\left\{I_{A_t}(\varphi_1), I_{A_{t'}}(\varpi_1)\right\}$

c) $F_{A_t \circ A'_t}(\varphi_1, \varpi_1) = \max\left\{F_{A_t}(\varphi_1), F_{A_{t'}}(\varpi_1)\right\}$

2. If $\varphi_1 = \varphi_2$ and $\forall\ (\varpi_1, \varpi_2) \in E'$

a) $T_{B_t \circ B'_t}((\varphi_1, \varpi_1), (\varphi_2, \varpi_2)) = \min\left\{T_{A_t}(\varphi_1), T_{B_{t'}}(\varpi_1, \varpi_2)\right\}$

b) $I_{B_t \circ B'_t}((\varphi_1, \varpi_1), (\varphi_2, \varpi_2)) = \max\left\{I_{A_t}(\varphi_1), I_{B_{t'}}(\varpi_1, \varpi_2)\right\}$

c) $F_{B_t \circ B'_t}\big((\varphi_1, \varpi_1), (\varphi_2, \varpi_2)\big) = \max\left\{F_{A_t}(\varphi_1), F_{B_{t'}}(\varpi_1, \varpi_2)\right\}$

3. If $\varpi_1 = \varpi_2$ and $\forall\ (\varphi_1, \varphi_2) \in E$

a) $T_{B_t \circ B'_t}((\varphi_1, \varpi_1), (\varphi_2, \varpi_2)) = \min\left\{T_{B_t}(\varphi_1, \varphi_2), T_{A_{t'}}(\varpi_1)\right\}$

b) $I_{B_t \circ B'_t}((\varphi_1, \varpi_1), (\varphi_2, \varpi_2)) = \max\left\{I_{B_t}(\varphi_1, \varphi_2), I_{A_{t'}}(\varpi_1)\right\}$

c) $F_{B_t \circ B'_t}\big((\varphi_1, \varpi_1), (\varphi_2, \varpi_2)\big) = \max\left\{F_{B_t}(\varphi_1, \varphi_2), F_{A_{t'}}(\varpi_1)\right\}$

4. If $\varpi_1 \neq \varpi_2$ and $\forall\ (\varphi_1, \varphi_2) \in E$

a) $T_{B_t \circ B'_t}((\varphi_1, \varpi_1), (\varphi_2, \varpi_2)) = \min\left\{T_{B_t}(\varphi_1, \varphi_2), T_{A_{t'}}(\varpi_1), T_{A_{t'}}(\varpi_2)\right\}$

b) $I_{B_t \circ B'_t}((\varphi_1, \varpi_1), (\varphi_2, \varpi_2)) = \max\left\{I_{B_t}(\varphi_1, \varphi_2), I_{A_{t'}}(\varpi_1), I_{A_{t'}}(\varpi_2)\right\}$

c) $F_{B_t \circ B'_t}\big((\varphi_1, \varpi_1), (\varphi_2, \varpi_2)\big) = \max\left\{F_{B_t}(\varphi_1, \varphi_2), F_{A_{t'}}(\varpi_1), F_{A_{t'}}(\varpi_2)\right\}$

5. If $\varphi_1 \neq \varphi_2$ and $\forall\ (\varpi_1, \varpi_2) \in E'$

a) $T_{B_t \circ B'_t}((\varphi_1, \varpi_1), (\varphi_2, \varpi_2)) = \min\left\{T_{A_t}(\varphi_1), T_{A_t}(\varphi_2), T_{B_{t'}}(\varpi_1, \varpi_2)\right\}$

b) $I_{B_t \circ B'_t}((\varphi_1, \varpi_1), (\varphi_2, \varpi_2)) = \max\left\{I_{A_t}(\varphi_1), I_{A_t}(\varphi_2), I_{B_{t'}}(\varpi_1, \varpi_2)\right\}$

c)$F_{B_t \circ B'_t}\big((\varphi_1, \varpi_1), (\varphi_2, \varpi_2)\big) = \max\left\{F_{A_t}(\varphi_1), F_{A_t}(\varphi_2), F_{B_{t'}}(\varpi_1, \varpi_2)\right\}$

3.8. Example. Consider the two 0.6-NG $\mathcal{G}_t$ and $\mathcal{G}'_t$ illustrated in figure 6 and 7.

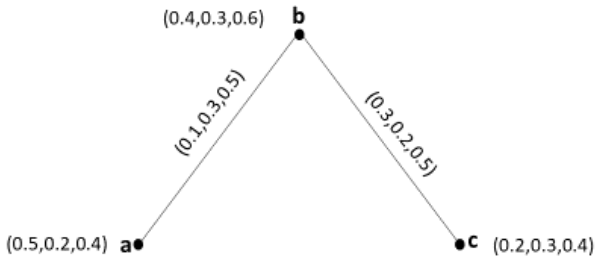

Figure 6. 0.6-NG $\mathcal{G}_{0.6}$

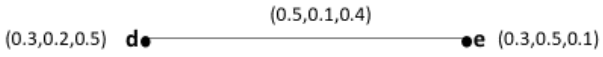

Figure 7. 0.6-NG $\mathcal{G}'_{0.6}$

Figure 8. Shows their corresponding Cartesian product $\mathcal{G}_{0.6} \circ \mathcal{G}'_{0.6}$

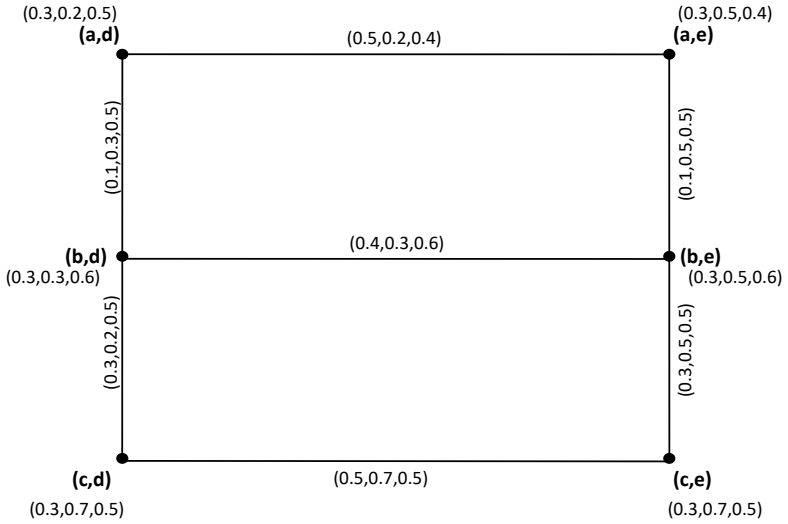

Figure 8. 0.6-NG $\mathcal{G}_{0.6} \circ \mathcal{G}'_{0.6}$

3.9. Definition. The degree of a vertex in $\mathcal{G}_t \circ \mathcal{G}'_t$ is defined as follows for any

$$(\varphi_1, \varpi_1) \in V \times V'; deg_{\mathcal{G}_t \circ \mathcal{G}'_t}(\varphi_1, \varpi_1)$$
$$= (\deg\left\{T_{B_t \circ B'_t}((\varphi_1, \varpi_1), (\varphi_2, \varpi_2))\right\}, \deg\left\{I_{B_t \circ B'_t}((\varphi_1, \varpi_1), (\varphi_2, \varpi_2))\right\}, \deg\{F_{B_t \circ B'_t}((\varphi_1, \varpi_1), (\varphi_2, \varpi_2))\})$$

Where, $\deg\left\{T_{B_t\circ B_t'}((\varphi_1,\varpi_1),(\varphi_2,\varpi_2))\right\} = \sum_{\varphi_1=\varphi_2,(\varpi_1,\varpi_2)\in E'} \min\left\{T_{A_t}(\varphi_1), T_{B_{t'}}(\varpi_1,\varpi_2)\right\}$

$$+\sum_{\varpi_1=\varpi_2,(\varphi_1,\varphi_2)\in E} \min\left\{T_{B_t}(\varphi_1,\varphi_2), T_{A_{t'}}(\varpi_1)\right\}$$

$$+\sum_{\varpi_1\neq\varpi_2,(\varphi_1,\varphi_2)\in E} \min\left\{T_{B_t}(\varphi_1,\varphi_2), T_{A_{t'}}(\varpi_1), T_{A_{t'}}(\varpi_2)\right\}$$

$$+\sum_{\varphi_1\neq\varphi_2,(\varpi_1,\varpi_2)\in E'} \min\left\{T_{A_t}(\varphi_1), T_{A_t}(\varphi_2), T_{B_{t'}}(\varpi_1,\varpi_2)\right\}$$

$$\deg\left\{I_{B_t\circ B_t'}((\varphi_1,\varpi_1),(\varphi_2,\varpi_2))\right\} = \sum_{\varphi_1=\varphi_2,(\varpi_1,\varpi_2)\in E'} \max\left\{I_{A_t}(\varphi_1), I_{B_{t'}}(\varpi_1,\varpi_2)\right\}$$

$$+\sum_{\varpi_1=\varpi_2,(\varphi_1,\varphi_2)\in E} \max\left\{I(\varphi_1,\varphi_2), I_{A_{t'}}(\varpi_1)\right\}$$

$$+\sum_{\varpi_1\neq\varpi_2,(\varphi_1,\varphi_2)\in E} \max\left\{I_{B_t}(\varphi_1,\varphi_2), I_{A_{t'}}(\varpi_1), I_{A_{t'}}(\varpi_2)\right\}$$

$$+\sum_{\varphi_1\neq\varphi_2,(\varpi_1,\varpi_2)\in E'} \max\left\{I_{A_t}(\varphi_1), I_{A_t}(\varphi_2), I_{A_{t'}}(\varpi_1,\varpi_2)\right\}$$

$$\deg\left\{F_{B_t\circ B_t'}((\varphi_1,\varpi_1),(\varphi_2,\varpi_2))\right\} = \sum_{\varphi_1=\varphi_2,(\varpi_1,\varpi_2)\in E'} \max\left\{F_{A_t}(\varphi_1), F_{B_{t'}}(\varpi_1,\varpi_2)\right\}$$

$$+\sum_{\varpi_1=\varpi_2,(\varphi_1,\varphi_2)\in E} \max\left\{F(\varphi_1,\varphi_2), F_{A_{t'}}(\varpi_1)\right\}$$

$$+\sum_{\varpi_1\neq\varpi_2,(\varphi_1,\varphi_2)\in E} \max\left\{F_{B_t}(\varphi_1,\varphi_2), F_{A_{t'}}(\varpi_1), F_{A_{t'}}(\varpi_2)\right\}$$

$$+\sum_{\varphi_1\neq\varphi_2,(\varpi_1,\varpi_2)\in E'} \max\left\{F_{A_t}(\varphi_1), F_{A_t}(\varphi_2), F_{A_{t'}}(\varpi_1,\varpi_2)\right\}$$

3.10. Example. In Example 7 shows that each vertex in $\mathcal{G}_t \circ \mathcal{G}_t'$ has the following degree $deg_{\mathcal{G}_t\times\mathcal{G}_t'}(a,d) = (0.6,0.5,0.9)$, $deg_{\mathcal{G}_t\times\mathcal{G}_t'}(a,e) = (0.6,0.7,0.9)$, $deg_{\mathcal{G}_t\times\mathcal{G}_t'}(b,d) = (0.4,0.5,1.0)$, $deg_{\mathcal{G}_t\times\mathcal{G}_t'}(b,e) = (0.4,1.0,1.0)$, $deg_{\mathcal{G}_t\times\mathcal{G}_t'}(c,d) = (0.8,0.9,1.0)$, $deg_{\mathcal{G}_t\times\mathcal{G}_t'}(c,e) = (0.8,1.2,1.0)$

3.11. Definition. Consider any two t-NG of G = (V,E) and G′=(V′,E′) correspond to $\mathcal{G}_t = (A_t, B_t)$ and $\mathcal{G}_t' = (A_t', B_t')$, respectively. $(A_t \cup A_t', B_t \cup B_t')$ defines the union $\mathcal{G}_t \cup \mathcal{G}_t'$ of two t-NG, where $A_t \cup A_t'$ and $B_t \cup B_t'$ respectively, represent t-NS on $V \cup V'$ and $E \cup E'$, which fulfills the given requirement,

1) If $\varphi_1 \in V$ and $\varphi_1 \notin V'$
   a) $T_{A_t\cup A_t'}(\varphi_1)=T_{A_t}(\varphi_1)$
   b) $I_{A_t\cup A_t'}(\varphi_1)=I_{A_t}(\varphi_1)$
   c) $F_{A_t\cup A_t'}(\varphi_1)=F_{A_t}(\varphi_1)$
2) If $\varphi_1 \notin V$ and $\varphi_1 \in V'$
   a) $T_{A_t\cup A_t'}(\varphi_1)=T_{A_t'}(\varphi_1)$
   b) $I_{A_t\cup A_t'}(\varphi_1)=I_{A_t'}(\varphi_1)$
   c) $F_{A_t\cup A_t'}(\varphi_1)=F_{A_t'}(\varphi_1)$
3) If $\varphi_1 \in V \cap V'$
   a) $T_{A_t\cup A_t'}(\varphi_1)= max\{T_{A_t}(\varphi_1), T_{A_t'}(\varphi_1)\}$
   b) $I_{A_t\cup A_t'}(\varphi_1)= min\{I_{A_t}(\varphi_1), I_{A_t'}(\varphi_1)\}$
   c) $F_{A_t\cup A_t'}(\varphi_1)= min\{F_{A_t}(\varphi_1), F_{A_t'}(\varphi_1)\}$
4) If $(\varphi_1,\varpi_1) \in E$ and $(\varphi_1,\varpi_1) \notin E'$
   a) $T_{B_t\cup B_t'}(\varphi_1,\varpi_1)=T_{B_t}(\varphi_1,\varpi_1)$
   b) $I_{B_t\cup B_t'}(\varphi_1,\varpi_1)=I_{B_t}(\varphi_1,\varpi_1)$

c) $F_{B_t \cup B_t'}(\varphi_1, \varpi_1)$=$F_{B_t}(\varphi_1, \varpi_1)$

5) If $(\varphi_1, \varpi_1) \notin E$ and $(\varphi_1, \varpi_1) \in E'$

a) $T_{B_t \cup B_t'}(\varphi_1, \varpi_1)$= $T_{B_t'}(\varphi_1, \varpi_1)$

b) $I_{B_t \cup B_t'}(\varphi_1, \varpi_1)$=$I_{B_t'}(\varphi_1, \varpi_1)$

c) $F_{B_t \cup B_t'}(\varphi_1, \varpi_1)$=$F_{B_t'}(\varphi_1, \varpi_1)$

6) If $(\varphi_1, \varpi_1) \in E \cap E'$

a) $T_{B_t \cup B_t'}(\varphi_1, \varpi_1) = max\{T_{B_t}(\varphi_1, \varpi_1), T_{B_t'}(\varphi_1, \varpi_1)\}$

b) $I_{B_t \cup B_t'}(\varphi_1, \varpi_1)= min\{I_{B_t}(\varphi_1, \varpi_1), I_{B_t'}(\varphi_1, \varpi_1)\}$

c) $F_{B_t \cup B_t'}(\varphi_1, \varpi_1)= min\{F_{B_t}(\varphi_1, \varpi_1), F_{B_t'}(\varphi_1, \varpi_1)\}$

3.12. Example. Figures 9 and 10 show 0.7-NG $\mathcal{G}_t$ and $\mathcal{G}_t'$.

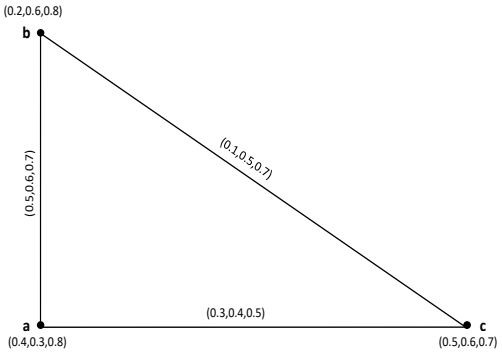

Figure 9. $0.7 - NG\mathcal{G}_{0.7}$

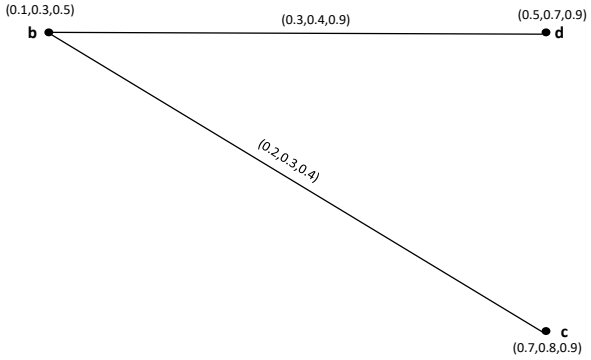

Figure 10. $0.7 - NG\mathcal{G}_{0.7}'$

Figure 11 shows their corresponding Cartesian product $\mathcal{G}_{0.5} \cup \mathcal{G}_{0.5}'$

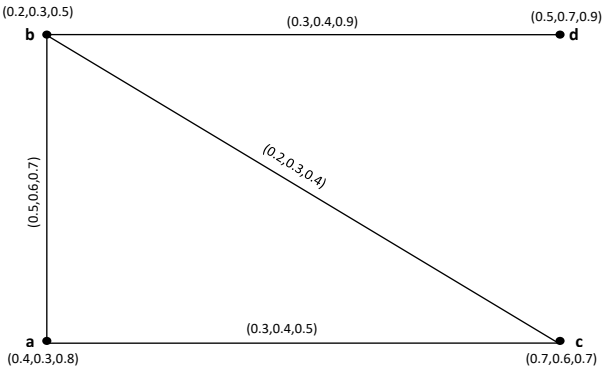

Figure 11. $\mathcal{G}_{0.7} \cup \mathcal{G}'_{0.7}$

3.13. Definition. The degree of vertex (φ_1, ϖ_1) at a t-NG for any $(\varphi_1, \varpi_1) \in V \cup V'$

$$deg_{\mathcal{G}_t \cup \mathcal{G}'_t}(\varphi_1, \varpi_1) = \left(\deg\left\{T_{B_t \cup B'_t}(\varphi_1, \varpi_1)\right\}, \deg\left\{I_{B_t \cup B'_t}(\varphi_1, \varpi_1)\right\}, \deg\left\{F_{B_t \cup B'_t}(\varphi_1, \varpi_1)\right\}\right)$$

Where

$$deg\left\{T_{B_t \cup B'_t}(\varphi_1, \varpi_1)\right\} = \sum_{(\varphi_1,\varpi_1)\in E, (\varphi_1,\varpi_1)\notin E'} T_{B_t}(\varphi_1, \varpi_1) + \sum_{(\varphi_1,\varpi_1)\notin E, (\varphi_1,\varpi_1)\in E'} T_{B'_t}(\varphi_1, \varpi_1) + \sum_{(\varphi_1,\varpi_1)\in E\cap E'} max\{T_{B_t}(\varphi_1, \varpi_1), T_{B'_t}(\varphi_1, \varpi_1)\}$$

$$deg\left\{I_{B_t \cup B'_t}(\varphi_1, \varpi_1)\right\} = \sum_{(\varphi_1,\varpi_1)\in E, (\varphi_1,\varpi_1)\notin E'} I_{B_t}(\varphi_1, \varpi_1) + \sum_{(\varphi_1,\varpi_1)\notin E, (\varphi_1,\varpi_1)\in E'} I_{B'_t}(\varphi_1, \varpi_1) + \sum_{(\varphi_1,\varpi_1)\in E\cap E'} min\{I_{B_t}(\varphi_1, \varpi_1), I_{B'_t}(\varphi_1, \varpi_1)\}$$

$$deg\left\{F_{B_t \cup B'_t}(\varphi_1, \varpi_1)\right\} = \sum_{(\varphi_1,\varpi_1)\in E, (\varphi_1,\varpi_1)\notin E'} F_{B_t}(\varphi_1, \varpi_1) + \sum_{(\varphi_1,\varpi_1)\notin E, (\varphi_1,\varpi_1)\in E'} F_{B'_t}(\varphi_1, \varpi_1) + \sum_{(\varphi_1,\varpi_1)\in E\cap E'} min\{F_{B_t}(\varphi_1, \varpi_1), F_{B'_t}(\varphi_1, \varpi_1)\}$$

3.14. Definition. . Consider two t-NGs $\mathcal{G}_t = (A_t, B_t)$ and $\mathcal{G}'_t = (A'_t, B'_t)$. These t-NGs join operation $\mathcal{G}_t + \mathcal{G}'_t$ is described as $(A_t + A'_t, B_t + B'_t)$, where $A_t + A'_t$ produces a t-NG on $V \cup V'$ and $B_t + B'_t$ forms a t-NG on $E \cup E' \cup E''$, subject to certain requirements.

1) If$\varphi_1 \in V$ and $\varphi_1 \notin V'$

a) $T_{A_t+A'_t}(\varphi_1)$=$T_{A_t}(\varphi_1)$

b) $I_{A_t+A'_t}(\varphi_1)$=$I_{A_t}(\varphi_1)$

c) $F_{A_t+A'_t}(\varphi_1)$=$F_{A_t}(\varphi_1)$

2) If $\varphi_1 \notin V$ and $\varphi_1 \in V'$

a) $T_{A_t+A'_t}(\varphi_1)=T_{A'_t}(\varphi_1)$

b) $I_{A_t+A'_t}(\varphi_1)=I_{A'_t}(\varphi_1)$

c)$F_{A_t+A'_t}(\varphi_1)=F_{A'_t}(\varphi_1)$

3) If $\varphi_1 \in V \cap V'$

a) $T_{A_t+A'_t}(\varphi_1)= max\{T_{A_t}(\varphi_1), T_{A'_t}(\varphi_1)\}$

b) $I_{A_t+A'_t}(\varphi_1)= min\{I_{A_t}(\varphi_1), I_{A'_t}(\varphi_1)\}$

c) $F_{A_t+A'_t}(\varphi_1)= min\{F_{A_t}(\varphi_1), F_{A'_t}(\varphi_1)\}$

4) If $(\varphi_1, \varpi_1) \in E$ and $(\varphi_1, \varpi_1) \notin E'$

a) $T_{B_t+B'_t}(\varphi_1, \varpi_1)=T_{B_t}(\varphi_1, \varpi_1)$

b) $I_{B_t+B'_t}(\varphi_1, \varpi_1)=I_{B_t}(\varphi_1, \varpi_1)$

c) $F_{B_t+B'_t}(\varphi_1, \varpi_1)=F_{B_t}(\varphi_1, \varpi_1)$

5) If $(\varphi_1, \varpi_1) \notin E$ and $(\varphi_1, \varpi_1) \in E'$

a) $T_{B_t+B'_t}(\varphi_1, \varpi_1)= T_{B'_t}(\varphi_1, \varpi_1)$

b) $I_{B_t+B'_t}(\varphi_1, \varpi_1)=I_{B'_t}(\varphi_1, \varpi_1)$

c) $F_{B_t+B'_t}(\varphi_1, \varpi_1)=F_{B'_t}(\varphi_1, \varpi_1)$

6) If $(\varphi_1, \varpi_1) \in E \cap E'$

a) $T_{B_t+B'_t}(\varphi_1, \varpi_1) = max\{T_{B_t}(\varphi_1, \varpi_1), T_{B'_t}(u_1, w_1)\}$

b) $I_{B_t+B'_t}(\varphi_1, \varpi_1)= min\{I_{B_t}(\varphi_1, \varpi_1), I_{B'_t}(\varphi_1, \varpi_1)\}$

c) $F_{B_t+B'_t}(\varphi_1, \varpi_1)= min\{F_{B_t}(\varphi_1, \varpi_1), F_{B'_t}(\varphi_1, \varpi_1)\}$

7) If $(\varphi_1, \varpi_1) \in E''$

a) $T_{B_t+B'_t}(\varphi_1, \varpi_1) = max\{T_{B_t}(\varphi_1), T_{B'_t}(\varpi_1)\}$

b) $I_{B_t+B'_t}(\varphi_1, \varpi_1)= min\{I_{B_t}(\varphi_1), I_{B'_t}(\varpi_1)\}$

c) $F_{B_t+B'_t}(\varphi_1, \varpi_1)= min\{F_{B_t}(\varphi_1), F_{B'_t}(\varpi_1)\}$

*3.15. Example***.** From example 9, the graphical representation of 0.9-NG$\mathcal{G}_t + \mathcal{G}'_t$ is displayed in the image below.

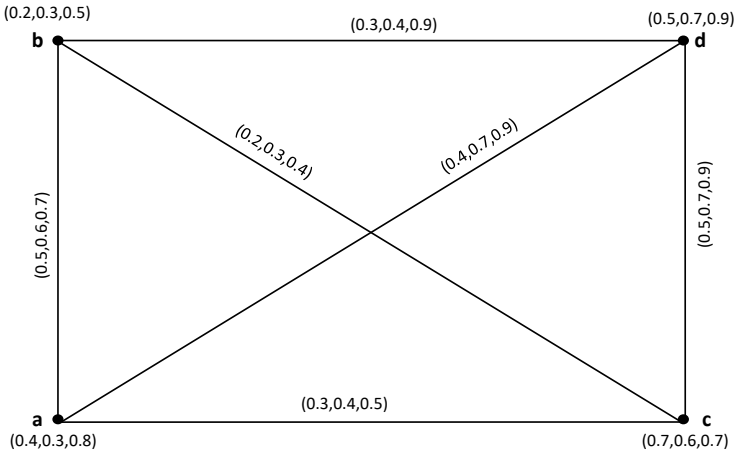

Figure 12. $\mathcal{G}_{0.7} + \mathcal{G}'_{0.7}$

*3.16. Definition***.** Examine the subsequent pair of t-NGs, $\mathcal{G}_t$ and $\mathcal{G}_t'$. The following describes the vertex degree in the t-NG $\mathcal{G}_t + \mathcal{G}_t'$. If $(\varphi_1, \varpi_1) \in V + V'$, then

$$deg_{\mathcal{G}_t+\mathcal{G}_t'}(\varphi_1, \varpi_1) = \left(deg\left\{T_{B_t+B_t'}(\varphi_1, \varpi_1)\right\}, deg\left\{I_{B_t+B_t'}(\varphi_1, \varpi_1)\right\}, deg\left\{F_{B_t+B_t'}(\varphi_1, \varpi_1)\right\}\right)$$

Where

$$deg\left\{T_{B_t\cup B_t'}(\varphi_1, \varpi_1)\right\} = \left(\sum_{(\varphi_1,\varpi_1)\in E,(\varphi_1,\varpi_1)\notin E'} T_{B_t}(\varphi_1, \varpi_1) + \sum_{(\varphi_1,\varpi_1)\notin E,(\varphi_1,\varpi_1)\in E'} T_{B_t'}(\varphi_1, \varpi_1) + \sum_{(\varphi_1,\varpi_1)\in E\cap E'} max\{T_{B_t}(\varphi_1, \varpi_1), T_{B_t'}(\varphi_1, \varpi_1)\} + \sum_{(\varphi_1,\varpi_1)\in E''} max\{T_{B_t}(\varphi_1), T_{B_t'}(\varpi_1)\}\right)$$

$$deg\left\{I_{B_t\cup B_t'}(\varphi_1, \varpi_1)\right\} = \left(\sum_{(\varphi_1,\varpi_1)\in E,(\varphi_1,\varpi_1)\notin E'} I_{B_t}(\varphi_1, \varpi_1) + \sum_{(\varphi_1,\varpi_1)\notin E,(\varphi_1,\varpi_1)\in E'} I_{B_t'}(\varphi_1, \varpi_1) + \sum_{(\varphi_1,\varpi_1)\in E\cap E'} min\{I_{B_t}(\varphi_1, \varpi_1), I_{B_t'}(\varphi_1, \varpi_1)\} + \sum_{(\varphi_1,\varpi_1)\in E''} min\{I_{B_t}(\varphi_1), I_{B_t'}(\varpi_1)\}\right)$$

$$deg\left\{F_{B_t\cup B_t'}(\varphi_1, \varpi_1)\right\} = \left(\sum_{(\varphi_1,\varpi_1)\in E,(\varphi_1,\varpi_1)\notin E'} F_{B_t}(\varphi_1, \varpi_1) + \sum_{(\varphi_1,\varpi_1)\notin E,(\varphi_1,\varpi_1)\in E'} F_{B_t'}(\varphi_1, \varpi_1) + \sum_{(\varphi_1,\varpi_1)\in E\cap E'} min\{F_{B_t}(\varphi_1, \varpi_1), F_{B_t'}(\varphi_1, \varpi_1)\} + \sum_{(\varphi_1,\varpi_1)\in E''} min\{F_{B_t}(\varphi_1), F_{B_t'}(\varpi_1)\}\right)$$

3.17. Theorem. For any two t-NGs, their union is a t-NG.

Proof. Let us assume a t-NG, $\mathcal{G}_t \cup \mathcal{G}_t'$. Let $(\varphi_1, \varpi_1) \in E$, $(\varphi_1, \varpi_1) \notin E'$, and $(\varphi_1, \varpi_1) \in V - V'$

Consider

$$T_{B_t}(\varphi_1, \varpi_1) = T_{B_t\cap B_t'}(\varphi_1, \varpi_1)$$

$$T_{B_t}(\varphi_1, \varpi_1) \leq \min\{T_{A_t\cup A_t'}(\varphi_1), T_{A_t\cup A_t'}(\varpi_1)\}$$

$$T_{B_t}(\varphi_1, \varpi_1) = \min\{T_{A_t}(\varphi_1), T_{A_t}(\varpi_1)\}$$

Consequently $T_{B_t}(\varphi_1, \varpi_1) \leq \min\{T_{A_t}(\varphi_1), T_{A_t}(\varpi_1)\}$.

Also

$$I_{B_t}(\varphi_1, \varpi_1) = I_{B_t\cap B_t'}(\varphi_1\varpi_1)$$

$$I_{B_t}(\varphi_1, \varpi_1) \leq \max\{I_{A_t\cup A_t'}(\varphi_1), I_{A_t\cup A_t'}(\varpi_1)\}$$

$$I_{B_t}(\varphi_1, \varpi_1) = \max\{I_{A_t}(\varphi_1), I_{A_t}(\varpi_1)\}$$

$$F_{B_t}(\varphi_1, \varpi_1) = F_{B_t \cap B_t'}(\varphi_1, \varpi_1)$$

$$F_{B_t}(\varphi_1, \varpi_1) \leq \max\{F_{A_t \cup A_t'}(\varphi_1), F_{A_t \cup A_t'}(\varpi_1)\}$$

$$F_{B_t}(\varphi_1, \varpi_1) = \max\{F_{A_t}(\varphi_1), F_{A_t}(\varpi_1)\}$$

Consequently$I_{B_t}(\varphi_1, \varpi_1) \leq \max\{I_{A_t}(\varphi_1), I_{A_t}(\varpi_1)\}$,$F_{B_t}(\varphi_1, \varpi_1) \leq \max\{F_{A_t}(\varphi_1), F_{A_t}(\varpi_1)\}$.

Hence, $\mathcal{G}_t = (A_t, B_t)$ is established as a t-NG. Likewise, we deduce that $\mathcal{G}_t' = (A_t', B_t')$ is a t-NG of G''. Given that $\mathcal{G}_t$ and $\mathcal{G}_t'$ are assumed, and since two t-NGs together produce a t-NG, we may deduce that $\mathcal{G}_t \cup \mathcal{G}_t'$.

4. Isomorphism of t-Neutrosophic Graph

4.1. Definition. Let $\mathcal{G}_t$ and $\mathcal{G}_t'$ be any two t-NG. A homomorphism θ from $\mathcal{G}_t$ and $\mathcal{G}_t'$ is a mapping $V to V'$, satisfies the following requirements:

1. $T_{A_t}(\varphi_1) \leq T_{A_t'}(\theta(\varphi_1))$,
   $I_{A_t}(\varphi_1) \leq I_{A_t'}(\theta(\varphi_1))$ and
   $F_{A_t}(\varphi_1) \leq F_{A_t'}(\theta(\varphi_1))$; $\forall \varphi_1 \in V$.
2. $T_{B_t}(\varphi_1, \varpi_1) \leq T_{B_t'}(\theta(\varphi_1), \theta(\varpi_1))$,
   $I_{B_t}(\varphi_1, \varpi_1) \leq I_{B_t'}(\theta(\varphi_1), \theta(\varpi_1))$ and
   $F_{B_t}(\varphi_1, \varpi_1) \leq F_{B_t'}(\theta(\varphi_1), \theta(\varpi_1))$; $\forall (\varphi_1, \varpi_1) \in E$.

4.2. Definition. A weak isomorphism $\theta: V \to V'$, from t-NG $\mathcal{G}_t$ to $\mathcal{G}_t'$ must meet the following conditions. the following condition: $T_{A_t}(\varphi_1) = T_{A_t'}(\theta(\varphi_1))$, $I_{A_t}(\varphi_1) \leq I_{A_t'}(\theta(\varphi_1))$ and $F_{A_t}(\varphi_1) \leq F_{A_t'}(\theta(\varphi_1))$; $\forall \varphi_1 \in V$.

4.3. Definition. A bijective mapping $\theta: V \to V'$ between any two t-NGs, $\mathcal{G}_t = (A_t, B_t)$ and $\mathcal{G}_t' = (A_t', B_t')$ of G=(V,E) and G′=(V′,E′) respectively, that satisfies the following criteria is called a strong co-isomorphism.

$T_{A_t}(\varphi_1) \leq T_{A_t'}(\theta(\varphi_1))$, $I_{A_t}(\varphi_1) \leq I_{A_t'}(\theta(\varphi_1))$ and $F_{A_t}(\varphi_1) \leq F_{A_t'}(\theta(\varphi_1))$; $\forall \varphi_1 \in V$.

1. $T_{B_t}(\varphi_1, \varpi_1) \leq T_{B_t'}(\theta(\varphi_1), \theta(\varpi_1))$, $I_{B_t}(\varphi_1, \varpi_1) \leq I_{B_t'}(\theta(\varphi_1), \theta(\varpi_1))$ and
   $F_{B_t}(\varphi_1, \varpi_1) \leq F_{B_t'}(\theta(\varphi_1), \theta(\varpi_1))$; $\forall (\varphi_1, \varpi_1) \in E$.
2. $T_{B_t}(\varphi_1, \varpi_1) = T_{B_t'}(\theta(\varphi_1), \theta(\varpi_1))$, $I_{B_t}(\varphi_1, \varpi_1) = I_{B_t'}(\theta(\varphi_1), \theta(\varpi_1))$ and
   $F_{B_t}(\varphi_1, \varpi_1) = F_{B_t'}(\theta(\varphi_1), \theta(\varpi_1))$; $\forall (\varphi_1, \varpi_1) \in E$.

4.4. Definition. An isomorphism between t-NGs $\mathcal{G}_t = (A_t, B_t)$ and $\mathcal{G}_t' = (A_t', B_t')$ is a bijective homomorphism mapping $\theta: V \to V'$ (written as $\mathcal{G}_t \approx \mathcal{G}_t'$) which satisfies the following condition:

1. $T_{A_t}(\varphi_1) = T_{A_t'}(\theta(\varphi_1))$, $I_{A_t}(\varphi_1) \leq I_{A_t'}(\theta(\varphi_1))$ and $F_{A_t}(\varphi_1) \leq F_{A_t'}(\theta(\varphi_1))$; $\forall \varphi_1 \in V$.
2. $T_{B_t}(\varphi_1, \varpi_1) = T_{B_t'}(\theta(\varphi_1), \theta(\varpi_1))$, $I_{B_t}(\varphi_1, \varpi_1) = I_{B_t'}(\theta(\varphi_1), \theta(\varpi_1))$ and
   $F_{B_t}(\varphi_1, \varpi_1) = F_{B_t'}(\theta(\varphi_1), \theta(\varpi_1))$; $\forall (\varphi_1, \varpi_1) \in E$.

4.5. Example. According to the following figures, take the two 0.7-$\mathcal{G}_t$ and $\mathcal{G}_t'$;

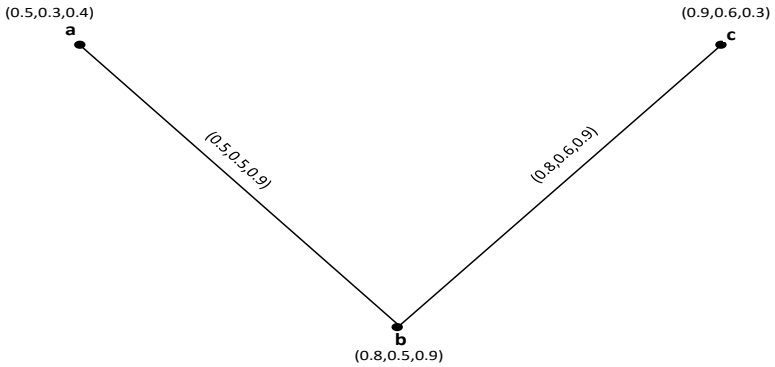

Figure 13. $0.7-NG\ \mathcal{G}_{0.7}$

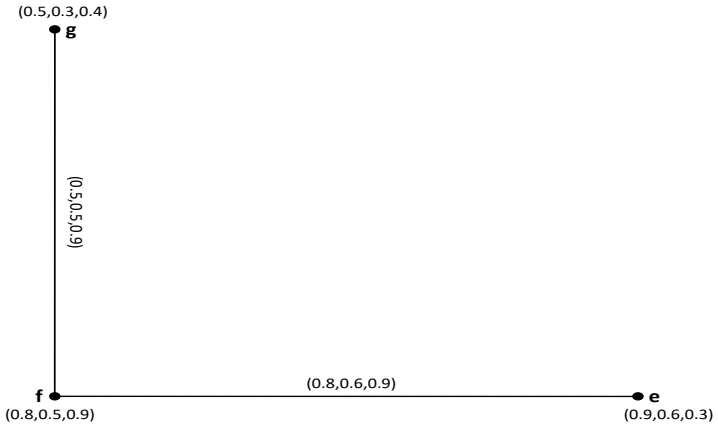

Figure 14. $0.7-NG\ \mathcal{G}'_{0.7}$

According to definition (22), the mapping ζ(a)=g, ζ(b)=f, and ζ(c)=e gives us $\mathcal{G}_{0.7} \approx \mathcal{G}'_{0.7}$

4.6. Theorem. The isomorphism between t-NGs satisfies the properties of an equivalence relation.

Proof: It is evident that there is symmetry and reflexivity. $\varphi: V \to V'$ and $\theta: V' \to V''$ indicate the isomorphisms of $\mathcal{G}_t$ onto $\mathcal{G}'_t$ and $\mathcal{G}'_t$ onto $\mathcal{G}''_t$, respectively. A bijective map fromV' to V'' is therefore $\theta \circ \varphi: V \to V''$, and it is defined as follows:

$$(\theta \circ \varphi)(\varphi_1) = \theta\big(\varphi(\varphi_1)\big), \forall \varphi_1 \in V$$

For a map $\varphi: V \to V'$defined by $\varphi(\varphi_1) = \varpi_1, \forall \varphi_1 \in V$, it is an isomorphism. Considering definition (22) we have

$$T_{A_t}(\varphi_1) = T_{A'_t}\big(\varphi(\varphi_1)\big) = T_{A'_t}(\varpi_1), \forall \varphi_1 \in V$$
$$I_{A_t}(\varphi_1) = I_{A'_t}\big(\varphi(\varphi_1)\big) = I_{A'_t}(\varpi_1), \forall \varphi_1 \in V$$
$$F_{A_t}(\varphi_1) = F_{A'_t}\big(\varphi(\varphi_1)\big) = F_{A'_t}(\varpi_1), \forall \varphi_1 \in V$$

and

$$T_{B_t}(\varphi_1, \varphi_2) = T_{B'_t}\big(\varphi(\varphi_1), \varphi(\varphi_2)\big) = T_{B'_t}(\varpi_1, \varpi_2), \forall (\varphi_1, \varphi_2) \in E$$
$$I_{B_t}(\varphi_1, \varphi_2) = I_{B'_t}\big(\varphi(\varphi_1), \varphi(\varphi_2)\big) = I_{B'_t}(\varpi_1, \varpi_2), \forall (\varphi_1, \varphi_2) \in E$$
$$F_{B_t}(\varphi_1, \varphi_2) = F_{B'_t}\big(\varphi(\varphi_1), \varphi(\varphi_2)\big) = F_{B'_t}(\varpi_1, \varpi_2), \forall (\varphi_1, \varphi_2) \in E$$

In the same way, we obtained that

$$T_{A'_t}(\varpi_1) = T_{A''_t}(v_1), \forall \varpi_1 \in V'$$
$$I_{A'_t}(\varpi_1) = I_{A''_t}(v_1), \forall \varpi_1 \in V'$$

$$F_{A_t'}(\varpi_1) = F_{A_t''}(v_1), \forall \varpi_1 \in V'$$

and

$$T_{B_t'}(\varpi_1, \varpi_2) = T_{B_t''}(v_1, v_2), \forall (\varpi_1, \varpi_2) \in E'$$
$$I_{B_t'}(\varpi_1, \varpi_2) = I_{B_t''}(v_1, v_2), \forall (\varpi_1, \varpi_2) \in E'$$
$$F_{B_t'}(\varpi_1, \varpi_2) = F_{B_t''}(v_1, v_2), \forall (\varpi_1, \varpi_2) \in E'$$

By using the relations above and $\varphi(\varphi_1) = \varpi_1$, $\forall \varphi_1 \in V$, we have

$$T_{A_t}(\varphi_1) = T_{A_t'}\big(\varphi(\varphi_1)\big) = T_{A_t'}(\varpi_1) = T_{A_t''}\big(\theta(\varpi_1)\big) = T_{A_t''}\Big(\theta\big(\varphi(\varphi_1)\big)\Big)$$
$$I_{A_t}(\varphi_1) = I_{A_t'}\big(\varphi(\varphi_1)\big) = I_{A_t'}(\varpi_1) = I_{A_t''}\big(\theta(\varpi_1)\big) = I_{A_t''}\Big(\theta\big(\varphi(\varphi_1)\big)\Big)$$
$$F_{A_t}(\varphi_1) = F_{A_t'}\big(\varphi(\varphi_1)\big) = F_{A_t'}(\varpi_1) = F_{A_t''}\big(\theta(\varpi_1)\big) = F_{A_t''}\Big(\theta\big(\varphi(\varphi_1)\big)\Big)$$

and

$$T_{B_t}(\varphi_1, \varphi_2) = T_{B_t'}(\varpi_1, \varpi_2) = T_{B_t''}\big(\theta(\varpi_1), \theta(\varpi_2)\big) = T_{B_t''}\Big(\theta\big(\varphi(\varphi_1)\big), \theta\big(\varphi(\varphi_2)\big)\Big)$$
$$I_{B_t}(\varphi_1, \varphi_2) = I_{B_t'}(\varpi_1, \varpi_2) = I_{B_t''}\big(\theta(\varpi_1), \theta(\varpi_2)\big) = I_{B_t''}\Big(\theta\big(\varphi(\varphi_1)\big), \theta\big(\varphi(\varphi_2)\big)\Big)$$
$$F_{B_t}(\varphi_1, \varphi_2) = F_{B_t'}(\varpi_1, \varpi_2) = F_{B_t''}\big(\theta(\varpi_1), \theta(\varpi_2)\big) = F_{B_t''}\Big(\theta\big(\varphi(\varphi_1)\big), \theta\big(\varphi(\varphi_2)\big)\Big)$$

Thus, $\mathcal{G}_t$ and $\mathcal{G}_t''$ are isomorphic using $\theta \circ \varphi$. As a consequence, the proof was completed.

5. Complement of t-Neutrosophic Graph

5.1. Definition. The t-NG of G=(V,E) is $\mathcal{G}_t = (A_t, B_t)$ .A t-NG $\overline{\mathcal{G}_t}$ on $\overline{G} = (\overline{V}, \overline{E})$ is the complement of a t-NG $\mathcal{G}_t$ and is defined as follows.

1. $\overline{V} = V$
2. If $u_1 \in V$ then $T_{\overline{A_t}}(\varphi_1) = T_{A_t}(\varphi_1), I_{\overline{A_t}}(\varphi_1) = I_{A_t}(\varphi_1)$ *and* $F_{\overline{A_t}}(\varphi_1) = F_{A_t}(\varphi_1)$
3. If $T_{B_t}(\varphi_1, \varphi_2) \neq 0, I_{B_t}(\varphi_1, \varphi_2) \neq 0$ *and* $F_{B_t}(\varphi_1, \varphi_2) \neq 0$ then $T_{\overline{B_t}}(\varphi_1, \varphi_2) \neq 0, I_{\overline{B_t}}(\varphi_1, \varphi_2) \neq 0$ *and* $F_{\overline{B_t}}(\varphi_1, \varphi_2) \neq 0$
4. If $T_{B_t}(\varphi_1, \varphi_2) = 0, I_{B_t}(\varphi_1, \varphi_2) = 0$ *and* $F_{B_t}(\varphi_1, \varphi_2) = 0$ then $T_{\overline{B_t}}(\varphi_1, \varphi_2) = \min\{T_{A_t}(\varphi_1), T_{A_t}(\varphi_2)\}, I_{\overline{B_t}}(\varphi_1, \varphi_2) = \max\{I_{A_t}(\varphi_1), I_{A_t}(\varphi_2)\}$ *and* $F_{\overline{B_t}}(\varphi_1, \varphi_2) = \max\{F_{A_t}(\varphi_1), F_{A_t}(\varphi_2)\}$.

5.2. Example. Consider a 0.7-NG$\mathcal{G}_t$ as shown in the below figure 15. Then the complement $\overline{\mathcal{G}_t}$ of 0.7-NG$\overline{\mathcal{G}_t}$ is shown in figure 16

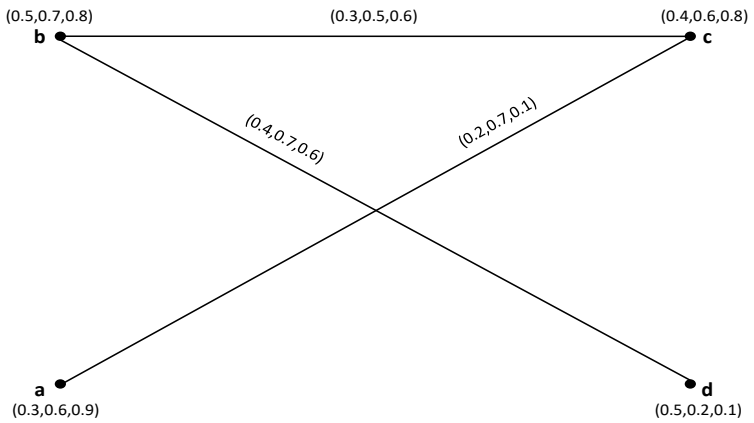

Figure 15. 0.7-NG$\mathcal{G}_{0.7}$

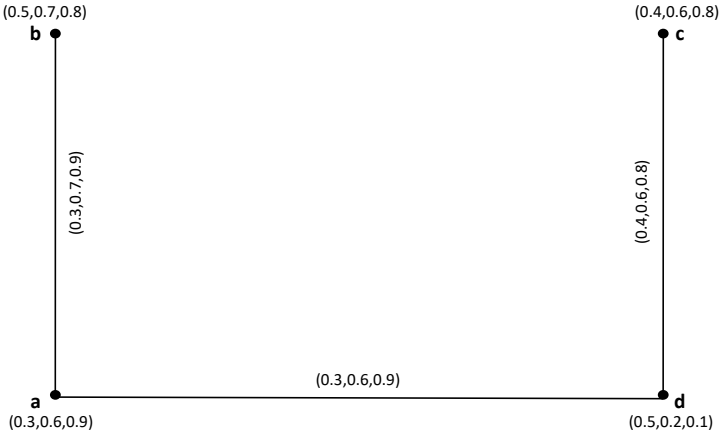

Figure 16. 0.7-NG$\overline{\mathcal{G}_{0.7}}$

5.3. Definition. A t-NG$\mathcal{G}_t$ is called self-complementary t-NG if $\overline{\mathcal{G}_t} \approx \mathcal{G}_t$.

5.4. Preposition. Let $\mathcal{G}_t = (A_t, B_t)$ be a self-complementary t-NG. Then

$$\sum_{\varphi_1 \neq \varphi_2} T_{B_t}(\varphi_1, \varphi_2) = \sum_{\varphi_1 \neq \varphi_2} min\{T_{A_t}(\varphi_1), T_{A_t}(\varphi_2)\}$$
$$\sum_{\varphi_1 \neq \varphi_2} I_{B_t}(\varphi_1, \varphi_2) = \sum_{\varphi_1 \neq \varphi_2} max\{I_{A_t}(\varphi_1), I_{A_t}(\varphi_2)\}$$
$$\sum_{\varphi_1 \neq \varphi_2} F_{B_t}(\varphi_1, \varphi_2) = \sum_{\varphi_1 \neq \varphi_2} max\{F_{A_t}(\varphi_1), F_{A_t}(\varphi_2)\}$$

5.5. Preposition. Let $\mathcal{G}_t = (A_t, B_t)$ t-NG. If

$$\sum_{\varphi_1 \neq \varphi_2} T_{B_t}(\varphi_1, \varphi_2) = \sum_{\varphi_1 \neq \varphi_2} min\{T_{A_t}(\varphi_1), T_{A_t}(\varphi_2)\}$$
$$\sum_{\varphi_1 \neq \varphi_2} I_{B_t}(\varphi_1, \varphi_2) = \sum_{\varphi_1 \neq \varphi_2} max\{I_{A_t}(\varphi_1), I_{A_t}(\varphi_2)\}$$
$$\sum_{\varphi_1 \neq \varphi_2} F_{B_t}(\varphi_1, \varphi_2) = \sum_{\varphi_1 \neq \varphi_2} max\{F_{A_t}(\varphi_1), F_{A_t}(\varphi_2)\} \; \forall \; \varphi_1, \varphi_2 \in V$$

Then $\mathcal{G}_t$ is a self-complementary t-NG

5.6. Preposition. For any two t-NG $\mathcal{G}_t$ and $\mathcal{G}_t'$. If $\mathcal{G}_t$ and $\mathcal{G}_t'$ have a strong homomorphism, then $\overline{\mathcal{G}_t}$ and $\overline{\mathcal{G}_t'}$ also have a strong isomorphism.

Proof. Let $\mathcal{G}_t$ and $\mathcal{G}_t'$ have a strong isomorphism, denoted by φ. Given that φ is a bijective map, φ^{-1} is thus a bijective map, with $\varphi^{-1}(\varpi_1) = \varphi_1, \forall \varpi_1 \in V'$. Thus

$$T_{A_t}\left(\varphi^{-1}(\varpi_1)\right) = T_{A_t'}(\varphi_1), I_{A_t}\left(\varphi^{-1}(\varpi_1)\right) = I_{A_t'}(\varphi_1) \; and \; F_{A_t}\left(\varphi^{-1}(\varpi_1)\right) = F_{A_t'}(\varphi_1), \forall \varpi_1 \in V'$$

Applying definition 23 makes it clear that:

$$T_{\overline{B_t}}(\varphi_1, \varpi_1) = \min\left\{T_{A_t}(\varphi_1), T_{A_t}(\varpi_1)\right\}$$
$$T_{\overline{B_t}}(\varphi_1, \varpi_1) \leq \min\left\{T_{A_t'}(\varphi(\varphi_2)), T_{A_t'}(\varphi(\varpi_2))\right\}$$
$$T_{\overline{B_t}}(\varphi_1, \varpi_1) \leq \min\left\{T_{A_t'}(\varphi_2), T_{A_t'}(\varpi_2)\right\}$$
$$T_{\overline{B_t}}(\varphi_1, \varpi_1) = T_{\overline{B_t}}(\varphi_2, \varpi_2)$$

Thus $T_{\overline{B_t}}(\varphi_1, \varpi_1) \leq T_{\overline{B_t}}(\varphi_2, \varpi_2)$

Also

$$I_{\overline{B_t}}(\varphi_1, \varpi_1) = \max\{I_{A_t}(\varphi_1), I_{A_t}(\varpi_1)\}$$
$$I_{\overline{B_t}}(\varphi_1, \varpi_1) \leq \max\left\{I_{A'_t}(\varphi(\varphi_2)), I_{A'_t}(\varphi(\varpi_2))\right\}$$
$$I_{\overline{B_t}}(\varphi_1, \varpi_1) \leq \max\left\{I_{A'_t}(\varphi_2), I_{A'_t}(\varpi_2)\right\}$$
$$I_{\overline{B_t}}(\varphi_1, \varpi_1) = I_{\overline{B_t}}(\varphi_2, \varpi_2)$$

And

$$F_{\overline{B_t}}(\varphi_1, \varpi_1) = \max\{F_{A_t}(\varphi_1), F_{A_t}(\varpi_1)\}$$
$$F_{\overline{B_t}}(\varphi_1, \varpi_1) \leq \max\left\{F_{A'_t}(\varphi(\varphi_2)), F_{A'_t}(\varphi(\varpi_2))\right\}$$
$$F_{\overline{B_t}}(\varphi_1, \varpi_1) \leq \max\left\{F_{A'_t}(\varphi_2), F_{A'_t}(\varpi_2)\right\}$$
$$F_{\overline{B_t}}(\varphi_1, \varpi_1) = F_{\overline{B_t}}(\varphi_2, \varpi_2)$$

Consequently $I_{\overline{B_t}}(\varphi_1, \varpi_1) \leq I_{\overline{B_t}}(\varphi_2, \varpi_2), F_{\overline{B_t}}(\varphi_1, \varpi_1) \leq F_{\overline{B_t}}(\varphi_2, \varpi_2)$

It follows from this that $\overline{\mathcal{G}_t}$ and $\overline{\mathcal{G}'_t}$ are strongly isomorphic.

6. Application: Sustainable Development through a Circular Economy:

The idea of a circular economy has gained popularity in the fight against poverty and for sustainable development. Regenerative systems, reduced waste, and increased resource efficiency are the goals of a circular economy. Let's examine a case where the seven vertices stand for important elements in the shift to a circular economy. Resource Efficiency (f_1) is the term used to describe how best to use resources while reducing waste production. Waste Management (f_2) this field focuses on effective methods for disposing of waste and recycling it. Green innovation (f_3) Promotes the creation and uptake of eco-friendly activities and technologies. The concept of Sustainable Consumption (f_4) involves encouraging conscientious and responsible consumption habits in both individuals and industries. Renewable Energy Adoption (f_5) Signifies the transition towards sustainable and renewable energy sources. Eco-friendly Production (f_6) Promotes the use of sustainable and environmentally friendly production techniques in industry.

Let $V = \{f_1, f_2, f_3, f_4, f_5, f_6\}$ be the vertex of set of factors that are Sustainable Development through a Circular Economy. The edges are the level of connections between two factors. The graphical representation of the factor of poverty reduction is given below;

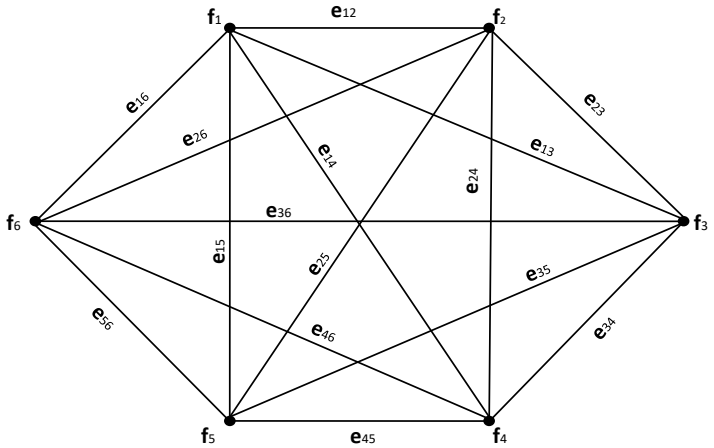

Figure 17.Neutrosophic Graph

Using the t-neutrosophic fuzzy model, decision-makers can examine the degree of correlation between these components. To illustrate how encouraging responsible consumer has a major impact on eco-friendly production practices, consider a high membership degree from Sustainable consumer (f_4) to Eco-friendly Production (f_6). This might indicate a substantial positive influence. Conversely, the degree of non-membership may suggest any felt disconnection or lack of significance. This illustration shows how a circular economy might function as a comprehensive plan that addresses a number of issues, including waste management, resource efficiency, green innovation, and community involvement. In order to negotiate the uncertainties associated with moving to a circular economy, decision-makers can utilize the t-neutrosophic fuzzy model to customize their strategy. They can do this by modifying the parameter't' based on their domain expertise and priorities. The edges of truth membership, indeterminacy membership and falsity membership degrees of factors as t-neutrosophic values, the truth membership value represents the possible way of two factors, the indeterminacy membership represents either connected or disconnected of two factors both can occur and the falsity membership values represents the disconnections of two factors. For example, the edge e_{12} represents the connection of 'Resource Efficiency' and 'Waste Management' indicates that the industrial properties creating the job opportunities. ie, $e_{12} = (0.7,0.3,0.3)$, the truth membership value 0.7 indicates the strong connection, the indeterminacy membership value 0.3 indicates the connection is either strong or weak or else average strength and the falsity membership value 0.3 indicates the weak connection between the two factors. The decision-makers can customize the t-NG according to their background and situation by using the stated values of't'. Furthermore, various't' values correspond to varied attitudes toward risk and uncertainty. Table 1 displays the NS and 0.7-NS highlighted for the edges.

Edges	**NS**	**0.7-NS**	**Edges**	**NS**	**0.7-NS**
$e_{12}=(f_1,f_2)$	(0.8,0.2,0.1)	(0.7,0.3,0.3)	$e_{26}=(f_2,f_6)$	(0.8,0.4,0.4)	(0.7,0.4,0.4)
$e_{13}=(f_1,f_3)$	(0.6,0.4,0.3)	(0.6,0.4,0.3)	$e_{34}=(f_3,f_4)$	(0.6,0.3,0.1)	(0.6,0.3,0.3)
$e_{14}=(f_1,f_4)$	(0.7,0.3,0.2)	(0.7,0.3,0.3)	$e_{35}=(f_3,f_5)$	(0.3,0.1,0.3)	(0.3,0.3,0.3)
$e_{15}=(f_1,f_5)$	(0.6,0.2,0.3)	(0.6,0.3,0.3)	$e_{36}=(f_3,f_6)$	(0.5,0.3,0.6)	(0.5,0.3,0.6)
$e_{16}=(f_1,f_6)$	(0.8,0.1,0.2)	(0.7,0.3,0.3)	$e_{45}=(f_4,f_5)$	(0.8,0.2,0.7)	(0.7,0.3,0.7)
$e_{23}=(f_2,f_3)$	(0.9,0.4,0.5)	(0.7,0.4,0.5)	$e_{46}=(f_4,f_6)$	(0.9,0.6,0.5)	(0.7,0.6,0.5)
$e_{24}=(f_2,f_4)$	(0.5,0.2,0.3)	(0.5,0.3,0.3)	$e_{56}=(f_5,f_6)$	(0.8,0.7,0.4)	(0.7,0.7,0.4)
$e_{25}=(f_2,f_5)$	(0.4,0.1,0.2)	(0.4,0.3,0.3)			

Table 2: Edges of NS and 0.7-NS

The table of truth membership, indeterminacy membership and falsity membership degree of each factor is given below;

factors	**Degree of each factor**
f_1	$\deg(f_1) = (3.3,1.6,1.5)$
f_2	$\deg(f_2) = (3.0,1.7,1.8)$
f_3	$\deg(f_3) = (2.7,1.7,2.0)$
f_4	$\deg(f_4) = (3.2,1.8,2.1)$
f_5	$\deg(f_5) = (2.7,1.9,2.0)$

f_6	$\deg(f_6) = (3.3, 2.3, 2.2)$

Table 3: Degree of each Factor

The score function of edges are defined as:

$$\mathfrak{T} = \sqrt{T_j^2 + (1 - I_j)^2 + (1 - F_j)^2}\,, 1 \leq j \leq 6$$

By using this definition in the above table in order to find the optimal factor for reducing the poverty is given below;

factors	Score function $\mathfrak{T}(f_j)$
f_1	3.38673
f_2	3.18276
f_3	2.96310
f_4	3.47706
f_5	3.01662
f_6	3.97663

Table 4: Score function

Comparatively, $\mathfrak{T}(f_6)$ =3.97663 is the greatest value. So, by our assumption f_6 factor has the high potential to Sustainable Development through a Circular Economy.

6.1 Comparative Analysis

The specific requirements of the decision-making issue dictate the form of fuzzy graph to use: t-neutrosophic or t-intuitionistic. Both approaches employ the 't' parameter to fine-tune uncertainty, but when a more extensive, exact, and detailed representation of uncertainty is necessary, t-neutrosophic fuzzy graphs excel. t-neutrosophic fuzzy graphs are particularly beneficial in complicated choice situations such as pattern recognition, medical diagnosis, and sophisticated decision support systems due to their ability to independently judge truth, indeterminacy, and falsehood. Because of their exceptional flexibility and meticulous treatment of uncertainty factors, t-neutrosophic fuzzy graphs are the preferred choice for high levels of precision and granularity in uncertainty modeling.

7. Conclusion

This study concludes by introducing and examining the use of t-neutrosophic graphs as an effective tool for comprehending and visualizing elaborate scenarios and complex interactions. The study provides a strong theoretical framework for t-neutrosophic graphs by introducing ideas like homomorphism and isomorphism. These graphs can be used to effectively describe relationships involving multiple variables thanks to the suggested core procedures. The ability of t-neutrosophic graphs to handle various aspects of complex systems is demonstrated by their practical application in addressing sustainable development through a circular economy. Through the consideration of several components and their interdependencies, t-neutrosophic graphs are an adaptable and useful tool for policy formulation and well-informed decision making about complex social issues.

This study demonstrates how flexible and helpful t-neutrosophic graphs are when handling complex situations in the real world. Their proven ability to tackle the circular economy demonstrates how they can support the objectives of sustainable development. t-neutrosophic graphs are a visual and analytical tool that shed light on complex linkages and serve as a foundation for well-informed policy formation and decision-making. All things considered, this study advances our knowledge of t-neutrosophic graphs and their useful applications, opening us new avenues for investigation in a variety of contexts and challenging problem-solving situations.

Future work: We planned to extend this work in following

1. Super hyper t-neutrsophic graphs
2. Maximum product of t- Super hyper t-neutrsophic graphs
3. Complements of t- Super hyper t-neutrsophic graphs

Funding: The authors received no specific funding for this study.

Acknowledgments: M. Kaviyarasu: Conceptualization, Hossein Rashmanlou: Methodology, Saeed kosari: Supervision, Said Broumi: Investigation, R. Venitha: Data curation, M Rajeshwari: Writing review & editing, Farshid Mofidnakhaei Project administration.

Conflicts of Interest: The authors declare no conflict of interest.

Reference

1. Zadeh, L. A. Fuzzy sets. Inf. Control 8, 338–353 (1965).
2. Kandel, A. Fuzzy Mathematical Techniques with Applications 325 (Addison-Wesley Educational Publishers Inc, Boston, 1986).
3. Atanassov, K. T. Intuitionistic fuzzy sets. Fuzzy Set Syst. 20, 87–96 (1986).
4. Zimmermann, L. A. Fuzzy Set Theory and Its Applications 2nd edn. (Kluwer, 1991).
5. Klir, G. J. & Yuan, B. Fuzzy Sets and Fuzzy Logic: Theory and Applications 1–12 (Prentice-Hall, 1995).
6. Mendel, J. M. Fuzzy logic systems for engineering: A tutorial. Proc. IEEE 83, 345–377 (1995).
7. Mapari, B. G. & Naidu, A. Study of fuzzy set theory and its applications. IOSR-JM 12, 148–154 (2016).
8. Akrama M (2016) Single-valued neutrosophic planar graphs. Infinite Study
9. Akram M, Nasir M (2017) Certain bipolar neutrosophic competition graphs. J Indonesian Math Soc 23(2):1–23
10. Akram M, Siddique S (2017) Neutrosophic competition graphs with applications. J Intell Fuzzy Syst 33(2):921–935
11. Akram M, Waseem N, Dudek WA (2017) Certain types of edge m-polar fuzzy graphs. Iran J Fuzzy Syst 14(4):27–50
12. Ajay, D. and Chellamani, P., 2020. Pythagorean neutrosophic fuzzy graphs. *International Journal of Neutrosophic Science*, *11*(2), pp.108-114.
13. Mohanta, K., Dey, A., Pal, A., Long, H.V. and Son, L.H., 2020. A study of m-polar neutrosophic graph with applications. *Journal of Intelligent & Fuzzy Systems*, *38*(4), pp.4809-4828.
14. Gulzar, M., Alghazzawi, D., Mateen, M.H. and Kausar, N., 2020. A certain class of t-intuitionistic fuzzy subgroups. *IEEE access*, *8*, pp.163260-163268.
15. Chellamani, P. and Ajay, D., 2021. Pythagorean neutrosophic Dombi fuzzy graphs with an application to MCDM. *Neutrosophic Sets and Systems*, *47*, pp.411-431.
16. Said, B., Lathamaheswari, M., Singh, P.K., Ouallane, A.A., Bakhouyi, A., Bakali, A., Talea, M., Dhital, A. and Deivanayagampillai, N., 2022. An Intelligent Traffic Control System Using Neutrosophic Sets, Rough sets, Graph Theory, Fuzzy sets and its Extended Approach: A Literature Review. *Neutrosophic Sets Syst*, *50*, pp.10-26.
17. Broumi, S., Sundareswaran, R., Shanmugapriya, M., Bakali, A. and Talea, M., 2022. Theory and Applications of Fermatean Neutrosophic Graphs. *Neutrosophic Sets and Systems*, *50*, pp.248-286.
18. Lakhwani, T.S., Mohanta, K., Dey, A., Mondal, S.P. and Pal, A., 2022. Some operations on Dombi neutrosophic graph. *Journal of Ambient Intelligence and Humanized Computing*, pp.1-19.
19. Razzaque, A., Masmali, I., Latif, L., Shuaib, U., Razaq, A., Alhamzi, G. and Noor, S., 2023. On t-intuitionistic fuzzy graphs: A comprehensive analysis and application in poverty reduction. *Scientific Reports*, *13*(1), p.17027.

20. Rashmanlou, Hossein, and Rajab Ali Borzooei. New concepts of interval-valued intuitionistic (S, T)-fuzzy graphs. Journal of Intelligent & Fuzzy Systems 30.4 (2016): 1893-1901.
21. Borzooei, R. A., and Hossein Rashmanlou. Cayley interval-valued fuzzy graphs. UPB Scientific Bulletin, Series A: Applied Mathematics and Physics 78.3 (2016): 83-94.
22. Saha, Abhijit, et al. Neutrosophic Sets and Systems (2016).
23. Rashmanlou, Hossein, et al. A study on vague graphs. SpringerPlus 5.1 (2016): 1-12.
24. Lakdashti, Abolfazl, et al. New Concepts of Bipolar Fuzzy Graphs. Journal of Multiple-Valued Logic & Soft Computing 33 (2019).
25. Christianto, V., & Smarandache, F. (2024). The Paradoxist Movement, Precursor of Neutrosophy, in the Shadow of a Totalitarian Regime. Neutrosophic Optimization and Intelligent Systems, 2, 1-6. https://doi.org/10.61356/j.nois.2024.29989.
26. Luo, M., Sun, Z., & Wu, L. (2024). Fuzzy Inference Quintuple Implication Method Based on Single Valued Neutrosophic t-representable t-norm. Neutrosophic Optimization and Intelligent Systems, 3, 8-22. https://doi.org/10.61356/j.nois.2024.3233.
27. Vázquez, M. L., & Smarandache, F. (2024). Integrating Contradictory Perspectives in Latin American Philosophy: A Multi-Alism Approach. Neutrosophic Optimization and Intelligent Systems, 3, 1-7. https://doi.org/10.61356/j.nois.2024.3226
28. Saila, S. B. Application of Fuzzy Graph Theory to Successional Analysis of a Multispecies Trawl Fishery. Transactions of the American Fisheries Society, 121(2), (1992), 211–233.
29. Klir, George, and Bo Yuan. Fuzzy sets and fuzzy logic. Vol. 4. New Jersey: Prentice hall, (1995).
30. Lotfi A. Zadeh, Toward a theory of fuzzy information granulation and its centrality in human reasoning and fuzzy logic, Fuzzy Sets and Systems, 90(2),(1997),111-127.
31. Elsayed, A. (2024). Evaluating Performance and Satisfaction of Bus Raid Transit Using the Hybrid T2NN-APPRESAL Method. Neutrosophic Optimization and Intelligent Systems, 1, 14-30. https://doi.org/10.61356/j.nois.2024.15989
32. Mohamed, M., Salam, A., Ye, J., & Yong, R. (2024). Single-Valued Neutrosophic MCDM Approaches Integrated with MEREC and RAM for the Selection of UAVs in Forest Fire Detection and Management. Neutrosophic Systems with Applications, 19, 1-14.
33. El-Douh A, Lu S, Abdelhafeez A, Aziz A. A Neutrosophic Multi-Criteria Model for Evaluating Sustainable Soil Enhancement Methods and their Cost 2 Implications in Construction. SMIJ. 2023 Oct 25;5(2):11. doi:10.61185/SMIJ.2023.55101.
34. Mohamed Z, Ismail MM, Abd El-Gawad A. Sustainable supplier selection using neutrosophic multi-criteria decision making methodology. Sustainable Machine Intelligence Journal. 2023 Jun 10;3:2-1. doi:10.61185/SMIJ.2023.33102.

Received: April 7, 2024. Accepted: Aug 22, 2024

NSS

Neutrosophic Sets and Systems, Vol. 72, 2024

University of New Mexico

On Extension of Metricspace to Neutro Hypermetricspace

Kianoosh Polvan*

Department of Mathematics, University of Payame Noor, Tehran, Iran.

K.kianoosh@pnu.ac.ir

*Correspondence: K.kianoosh@pnu.ac.ir, P.O. Box 19395-4697

Abstract. Polvan introduced the impression of strong neutro metricspaces. He demonstrtated this impression depending on the neutro precepts from the neutro function one of the impressions of Smarandache. In this study, we introduce an extension of neutro metricspaces as neutro hypermetricspaces and investigated their qualities. We show that neutro hypermetricspaces are an extension of metricspaces and analyzed the relations between metricspaces and neutro hypermetricspaces. The basic impressions such as open positive-ball subsets and open negative-ball subsets are defined and are presented by some finite and finite neutro hypermetricspaces. Based on the open positive-ball subsets and open negative-ball subsets, we demonstrate the impressions of neutro negative-open sets and neutro positive-open sets, respectively.

Keywords: (Neutro) hypermetricspace, neutro-negative-open set, neutro-positive-open set, unified set.

1. Introduction

M. K. EL Gayyar, introduced the notion of neutrosophic topological structures. He presented it in two different types of impressions of neutrosophic topological space, closure interior [6]. Florentin Smarandache [8] et al. introduced an impression of generalized neutrosophic bipolar vague sets (N.B.V.S) and vague topology in topological spaces. Neutrosophic vague theory is a pragmatic manner to practice fragmentary and erratic information. Indeed, they interpolated the perception of an N.B.V.S as a combination of N. S, B. S, and V. S. Some researchers have presented the N. S in neutro metricspace and other neutro algebras such as [1–5, 7–12]. We interpolate the new thought of hypermetricspace as a generalization of metricspaces and present their qualities. In the real world, there is no exact size and most sizes are approximate. For example, we say the length of a wall that has a fracture and is somewhat angled is between 100 and 102 meters, or we say the weight of a package is between 200 and 201 kg. These approximations indicate that the sizes are not exact and fall within

a range. These real issues motivate us to interpolate supermeters. In addition, sometimes we can't measure some objects and we say that this size is not known to us. Sometimes we cannot take the distance of an object from itself to zero, because an object fills a volume in three-dimensional space and we have a distance on this object itself. These issues make us interpolate the cloud meter to have a more realistic model of the world around us. In this study, we extended the metricspace to neutro hypermetricspace and considered the relations between of their precepts. We have shown that the open sets in neutro hypermetricspaces are different, for instance, we show that there exist two types of neutro-open sets negative-open set and positive-open set. In a final show, the union of neutro-open sets is not a neutro set necessarily.

2. Preliminaries

Here we address the needs of our work.

Definition 2.1. [9] Assume $\nu : \mathcal{Q}^2 \to \mathbb{R}$, with $\mathcal{Q} \neq \emptyset$. Then, $(\mathcal{Q}, \nu)$ is called a *neutro metricspace*, if obtain

$(NM\text{-}1)$ $(o, o' \in \mathcal{Q}$ so $o\nu o' \geq 0)$, $\big(o_1, o_2 \in \mathcal{Q}$ so $o_1\nu o_2 < 0$ or inconclusive $\big)$;

$(NM\text{-}2)$ $(o \in \mathcal{Q}$ so $o\nu o = 0)$, $\big(o' \in \mathcal{Q}$ such that, $o'\nu o' \neq 0$ or inconclusive $\big)$;

$(NM\text{-}3)$ $(o, o', o'' \in \mathcal{Q}$, such that $o\nu o'' \leq o\nu o' + o'\nu o'')$, $\big(o_1, o_2, o_3 \in \mathcal{Q}$, such that $o_1\nu o_3 > o_1\nu o_2 + o_2\nu o_3$ or inconclusive $\big)$;

$(NM\text{-}4)$ $(o, o' \in \mathcal{Q}$, such that $o\nu o' = o'\nu o)$, $\big(o_1, o_2 \in \mathcal{Q}$, such that $o_1\nu o_2 \neq o_2\nu o_1$ or inconclusive $\big)$.

Definition 2.2. [7] Assume $\nu : \mathcal{Q}^2 \to \mathbb{R}^{\geq 0}$, with $\mathcal{Q} \neq \emptyset$. Then, $(\mathcal{Q}, \nu)$ is called a *strong neutro*, if

$(NM\text{-}1)$ $\big(o \in \mathcal{Q}$ so $o\nu o = 0\big)$ and $\big(o' \in \mathcal{Q}$ so $o'\nu o' \neq 0$ or inconclusive $\big)$;

$(NM\text{-}2)$ $\big(o, o', o'' \in \mathcal{Q}$, such that $o\nu o'' \leq o\nu o' + o'\nu o''$ and $\big(o_1, o_2, o_3 \in \mathcal{Q}$, such that $0_1\nu o_3 > o_1\nu o_2 + o_2\nu o_3$ or inconclusive $\big)$;

$(NM\text{-}3)$ $\big(o, o' \in \mathcal{Q}$, such that $o\nu o' = o'\nu o$ and $\big(o_1, o_2 \in \mathcal{Q}$, such that $o_1\nu o_2 \neq o_2\nu o_1$ or inconclusive $\big)$.

3. Hypermetricspace

In this section, we interpolate the notation of hypermetricspace as an extension of metricspaces and present their qualities.

Definition 3.1. Presume $\vartheta : M \times M \to P^*(\mathbb{R})$ be a map and $M \neq \emptyset$. Then (M, ϑ) is a *hypermetricspace*, if

$(Hm\text{-}1)$ obtain $r \geq 0$, s.t $[0, r] \Subset \vartheta(x, y)$;

$(Hm\text{-}2)$ $\vartheta(x,x)=\{0\}$;
$(Hm\text{-}3)$ $\vartheta(x,z)\Subset\vartheta(x,y)+\vartheta(y,z)$;
$(Hm\text{-}4)$ $\vartheta(x,y)=\vartheta(y,x)$;

which for any $\mathcal{A},\mathcal{B}\in P^*(\mathbb{R}),\mathcal{A}\Subset\mathcal{B}$ iff for any $a\in\mathcal{B}$ obtain $b\in\mathcal{B}$ so $b-a\geq 0(a\leq b)$ and ϑ is called a *hypermeter* on M.

For each set $\{A_i\}_{i=1}^n$ of subset of $\mathbb{R}$, recall, $\sum_{i=1}^{n}A_i=\{a_1+a_2+a_3+\ldots+a_n \mid a_i\in A_i\}$. Then get the following results.

Theorem 3.2. *Presume $(\mathcal{Q},\vartheta)$ be a hypermetricspace. Then for each $x,y\in\mathcal{Q},A,B\in P^*(\mathbb{R})$;*

(i) $\{0\}\Subset\vartheta(x,y)$,
(ii) $\vartheta(x,y)\Subset\vartheta(x,y)$,
(iii) *if $A\subseteq B$, then $A\Subset B$,*
(iv) $A\Subset A+B$.

Proof. (i) For each $x,y\in\mathcal{Q},[0,0]\subseteq\vartheta(x,y)$, $\{0\}\subseteq\vartheta(x,y)$. Hence $0\in\vartheta(x,y)$ and so $\{0\}\Subset\vartheta(x,y)$.

(ii) Presume $x,y\in\mathcal{Q}$, since for each $a\in\vartheta(x,y),a\leq a$, we get that $\vartheta(x,y)\Subset\vartheta(x,y)$.

(iii) For each $x\in A,x\in B$ and $x\leq x$, we get that $A\Subset B$.

(iv) Since $A\subseteq A+B$, by item (iii), $A\Subset A+B$. □

Corollary 3.3. *Presume $(\mathcal{Q},\vartheta)$ be a hypermetricspace. Then for each $x,y,z\in\mathcal{Q},A_i\in P^*(\mathbb{R}),1\leq i\leq n$;*

(i) $A_i\Subset A_i$,
(ii) $A_i\Subset\sum_{i=1}^{n}A_i$,
(iii) $\vartheta(x,y)\Subset\vartheta(x,y)+\vartheta(y,z)$.

Example 3.4. (i) Any metricspace $(\mathcal{Q},\vartheta)$ is a hypermetricspace.

$(Hm\text{-}1)$ For each $x,y\in\mathcal{Q}$, since $0\leq\vartheta(x,y)$, for $r=0$, we get that $[0,r]\Subset\vartheta(x,y)$. Clearly $(Hm\text{-}2)$ and $(Hm\text{-}4)$ are valid.

$(Hm\text{-}3)$ For each $x,y,z\in\mathcal{Q}$, since $\vartheta(x,z)\leq\vartheta(x,y)+\vartheta(y,z)$, based Theorem 3.2, $\vartheta(x,z)\Subset\vartheta(x,y)+\vartheta(y,z)$.

(ii) Presume $\mathcal{Q}=\{a,b,c,d\}$. Then $(\mathcal{Q},d)$ is a hypermetricspace as Table 2.

ϑ	a	b	c	d
a	$\{0\}$	$[0,1]$	$[0,2]$	$[0,3]$
b	$[0,1]$	$\{0\}$	$[0,2]$	$[0,3]$
c	$[0,2]$	$[0,2]$	$\{0\}$	$[0,3]$
d	$[0,3]$	$[0,3]$	$[0,3]$	$\{0\}$

TABLE 1. Hypermetricspace$(\mathcal{Q},\vartheta)$.

For each intervals $In(a,b), In(c,d)$, recall that $In(a,b)+In(c,d)=In(a+c,b+d)$, which $In(w,y)=[w,y]$ and get the following results.

Theorem 3.5. *Any non–avoid subset of* $\mathbb{R}$ *can be a hypermetricspace.*

Proof. Presume $\emptyset \neq A \subseteq \mathbb{R}$ be arbitrary. For each $x,y \in A$, define $\vartheta : \mathbb{R}\times\mathbb{R} \to P^*(\mathbb{R})$ by $\vartheta(x,y)=[0,|\max\{x,y\}-\min\{x,y\}|]$. For each $(x_1,y_1),(x_2,y_2)\in A^2$, since $(x_1,y_1)=(x_2,y_2)$ implies that $(0,|\max\{x_1,y_1\}-\min\{x_1,y_1\}|)=(0,|\max\{x_2,y_2\}-\min\{x_2,y_2\}|)$, we get that $\vartheta(x_1,y_1)=\vartheta(x_2,y_2)$ and so ϑ is well-defined. Moreover,

$(Hm\text{-}1)$ Presume $x,y\in A$. Then for $r=\dfrac{|\max\{x,y\}-\min\{x,y\}|}{2}$, we get that $[0,r]\Subset[|x|,|y|]$.

$(Hm\text{-}2)$ Presume $x\in A$. Computations show that $\vartheta(x,x)=[0,|\max\{x,x\}-\min\{x,x\}|]=[0,0]=\{0\}$.

$(Hm\text{-}3)$ Presume $x,y,z\in A$. Then

$$\begin{aligned}\vartheta(x,z)&=[0,|\max\{x,z\}-\min\{x,z\}|]\\&\Subset[0,|\max\{x,y\}-\min\{x,y\}|+|\max\{y,z\}-\min\{y,z\}|]\\&\Subset[0,|\max\{x,y\}-\min\{x,y\}|]+[0,|\max\{y,z\}-\min\{y,z\}|]=\vartheta(x,y)+\vartheta(y,z).\end{aligned}$$

$(Hm\text{-}4)$ Presume $x,y\in A$. Then

$$\vartheta(x,y)=[0,|\max\{x,y\}-\min\{x,y\}|]=[0,|\max\{y,x\}-\min\{y,x\}|]=\vartheta(y,x).$$

It follows that (A,ϑ) is a hypermetricspace. □

Presume $\mathcal{Q}$ be a non-avoid set. We say that $\mathcal{Q}$ is a reproduced hypermetricspace, if obtain a hypermeter ϑ on $\mathcal{Q}$, such that $(\mathcal{Q},\vartheta)$ is a hypermetricspace. In addition, we denote $\mathcal{H}m(\mathcal{Q})=\{\vartheta \mid \vartheta \text{ is a hypertmeter on } \mathcal{Q}\}$, as the set of all hypermeters on $\mathcal{Q}$ and will get the following result.

Theorem 3.6. *For each non-avoid set* $\mathcal{Q}$*,*

(i) $\mathcal{Q}$ *is a reproduced hypermetricspace.*

(ii) $|\mathcal{H}m(\mathcal{Q})|=2^{\aleph}(\aleph=card(\mathbb{R}))$.

Proof. Presume $\mathcal{Q}$ be a non-avoid set.

$(i),(ii)$ For each $x,y\in\mathcal{Q}$, and for each $r\in\mathbb{R}$, define $\vartheta_r(x,y)=\begin{cases}\{0\} & if x=y,\\ [0,r] & if x\neq y,\end{cases}$. It is clear that $(\mathcal{Q},\vartheta_r)$ is a hypermetricspace. Hence $|\mathcal{H}m(\mathcal{Q})|=2^{\aleph}(\aleph=card(\mathbb{R}))$. □

Presume $(\mathcal{Q},\vartheta)$ be a hypermetricspace and $\epsilon\in\mathbb{R}^{>0}$. So $B_\epsilon(x)=\{y\in\mathcal{Q}\mid Sup(\vartheta(x,y))<\epsilon\}$, is called an open ball of radius ϵ and center $x\in\mathcal{Q}$.

Example 3.7. Consider the hypermetricspace $(\mathcal{Q},\vartheta)$ in Example 3.4. For each $0<\epsilon<1$, and each $x\in\mathcal{Q}, B_\epsilon(x)=\{x\}, B_1(a)=\{a\}, B_2(a)=\{a,b\}, B_3(a)=\{a,b,c\}, B_4(\epsilon)=\{a,b,c,d\}$ and for each $\epsilon\geq 4, B_\epsilon(a)=\mathcal{Q}$.

Theorem 3.8. *Presume $(\mathcal{Q},\vartheta)$ be a hypermetricspace and $\epsilon\in\mathbb{R}^{>0}$.*

(i) $Inf\{\vartheta(x,y)\mid x,y\in\mathcal{Q}\}=0$.
(ii) $x\in B_\epsilon(x)$.
(iii) $\mathcal{Q}=\bigcup_{x\in\mathcal{Q}} B_\epsilon(x)$.
(iv) *If* $Sup\{\vartheta(x,y)\mid x,y\in\mathcal{Q}\}=\epsilon$, *then for each* $\epsilon'>\epsilon, B_\epsilon(x)=B_{\epsilon'}(x)$.
(v) *There exists* $\epsilon\in\mathbb{R}^{>0}$ *so* $B_\epsilon(x)=\mathcal{Q}$.

Proof. (i) For each $x,y\in\mathcal{Q}$ and each $r\in\mathbb{R}^{\geq 0}, [0,r]\subseteq\vartheta(x,y)$, implies that $[0,r]\Subset\vartheta(x,y)$. It follows that obtain $z\in\vartheta(x,y)$ so $z\leq 0$. It follows that $(-\infty,0]$ is the set of all lower bounds of $\vartheta(x,y)$ and so $Inf\{\vartheta(x,y)\mid x,y\in\mathcal{Q}\}=0$.

(ii) Since $\epsilon>0$ and obtain $r\in\mathbb{R}^{\geq 0}, [0,r]\Subset\vartheta(x,y)$, for each $x\in\mathcal{Q}, B_\epsilon(x)=\{y\in\mathcal{Q}\mid Sup(\vartheta(x,y))<\epsilon\}\neq\emptyset$. In addition, by Theorem 3.2, $\{0\}\Subset\vartheta(x,x)\leq Sup(\vartheta(x,y))<\epsilon$, includes that $x\in B_\epsilon(x)$.

(iii) For each $x\in\mathcal{Q}$, by item $(i), \{x\}\subseteq B_\epsilon(x)$ and so $\mathcal{Q}=\bigcup_{x\in\mathcal{Q}}\{x\}\subseteq B_\epsilon(x)$. Hence $\mathcal{Q}=\bigcup_{x\in\mathcal{Q}} B_\epsilon(x)$.

(iv) Presume $Sup\{\vartheta(x,y)\mid x,y\in\mathcal{Q}\}=\epsilon$. Then for each $x,y\in\mathcal{Q}, \vartheta(x,y)\leq Sup(\vartheta(x,y))<\epsilon$ and so $B_\epsilon(x)=\{y\in\mathcal{Q}\mid Sup(\vartheta(x,y))<\epsilon\}=\mathcal{Q}$. So for each $\epsilon'>\epsilon, B_\epsilon(x)=\{y\in\mathcal{Q}\mid Sup(\vartheta(x,y))<\epsilon'\}=\mathcal{Q}$.

(v) By item (iv), consider $\epsilon=Sup\{\vartheta(x,y)\mid x,y\in\mathcal{Q}\}$, then $B_\epsilon(x)=\{y\in\mathcal{Q}\mid Sup(\vartheta(x,y))<\epsilon\}=\mathcal{Q}$. □

3.1. **On neutro hypermetricspace**

In this subsection, we interpolate the new impression of neutro hypermetricspace as an extension of neutro metricspaces and in general as an extension of metricspaces. We analyze the qualities of neutro hypermetricspaces with respect to joint of sumsets and presented the relation of neutro hypermetricspaces and neutro metricspaces.

Definition 3.9. Presume $\vartheta : M \times M \to P^*(\mathbb{R})$ be a map and $M \neq \emptyset$.The structure (M, ϑ) is called a *neutro hypermetricspace*, if

$(Hm\text{-}1)$ $(\exists\ r \geq 0, x, y \in M,$ so $[0, r] \Subset \vartheta(x, y))$ and $(\exists\ s \leq 0, z, w \in M$ so $[s, 0] \Subset \vartheta(z, w)$ or inconclusive);

$(Hm\text{-}2)$ $(\exists\ x \in \mathcal{Q}, such\ that\ \vartheta(x, x) = \{0\})$ and $(\exists\ y \in \mathcal{Q}, such\ that\ \vartheta(y, y) \neq \{0\}$ or inconclusive);

$(Hm\text{-}3)$ $(\exists\, x, y \in \mathcal{Q} such\ that\ \vartheta(x, z) \Subset \vartheta(x, y) + \vartheta(y, z))$ and $(\exists\, z, w, u \in \mathcal{Q}, such\ that\ \vartheta(z, w) \succ \vartheta(z, u) + \vartheta(u, w)$ or inconclusive);

$(Hm\text{-}4)$ $(\exists\ x, y \in \mathcal{Q}, such\ that\ \vartheta(x, y) = \vartheta(y, x))$ and $(\exists\ w, z \in \mathcal{Q}, such\ that\ \vartheta(z, w) \neq \vartheta(w, z)$ or inconclusive);

which for each $A, B \subseteq \mathbb{R}, A \Subset B$ iff for each $a \in A$ obtain $b \in B$ so$b - a \geq 0 (a \leq b)$ and $A \succ B$ obtain $a \in A$ so for each $b \in B$ $a > b$. We will call ϑ as a *neutro hypermeter* on $\mathcal{Q}$.

Example 3.10. Presume $\mathcal{Q} = \{a, b, c, d, e\}$. Then $(\mathcal{Q}, \vartheta)$ is a neutro hypermetricspace as Table 2.

ϑ	a	b	c	d	e
a	$\{0\}$	$[0, 1]$	$[-2, 0]$	$[0, 3]$	$[-3, 0]$
b	$[0, 1]$	$\{0\}$	$[0, 2]$	$[0, 3]$	$[0, 3]$
c	$[0, 2]$	$[0, 2]$	$\{0\}$	$[0, 3]$	$[0, 3]$
d	$[0, 3]$	$[0, 3]$	$[0, 3]$	$\{-2, -3\}$	$[0, 3]$
e	$[0, 3]$	$[0, 3]$	$[0, 3]$	$[0, 3]$	$\{4, 5\}$

TABLE 2. Neutro hypermetricspace $(\mathcal{Q}, \vartheta)$.

We see that $\vartheta(a, a) = \{0\}, \vartheta(d, d) \neq \{0\}, \vartheta(a, d) = \vartheta(d, a), \vartheta(a, b) \Subset \vartheta(a, d) + \vartheta(d, b)$ and $\vartheta(e, e) \succ \vartheta(e, a) + \vartheta(a, e)$. Hence $(\mathcal{Q}, \vartheta)$ is a neutro hypermetricspace.

Presume $n \in \mathbb{N}$ and $f : \mathbb{R}^n \to \mathbb{R}$ be odd bounded continuous map. Then define $\vartheta : \mathbb{R}^n \times \mathbb{R}^n \to P^*(\mathbb{R}^n)$ by $\vartheta((\overline{r_1}, \overline{r_2}, \ldots, \overline{r_n}), (\overline{s_1}, \overline{s_2}, \ldots, \overline{s_n})) = Range(f(\overline{r_1}, \overline{r_2}, \ldots, \overline{r_n}) + f(\overline{s_1}, \overline{s_2}, \ldots, \overline{s_n}))$ and $\vartheta((\pi, \pi, \ldots, \pi), (2\pi, 2\pi, \ldots, 2\pi)) \neq \vartheta((2\pi, 2\pi, \ldots, 2\pi), (\pi, \pi, \ldots, \pi))$.

Theorem 3.11. *Presume $n \in \mathbb{N}$. Then $(\mathbb{R}^n, \vartheta)$ is a hypermetricspace.*

Proof. Since f is bounded, obtain $m \in \mathbb{R}$, so for each $(\overline{r_1}, \overline{r_2}, \ldots, \overline{r_n}) \in \mathbb{R}^n, m \leq f(\overline{r_1}, \overline{r_2}, \ldots, \overline{r_n}) \leq M$. Presume $(\overline{r_1}, \overline{r_2}, \ldots, \overline{r_n}), (\overline{s_1}, \overline{s_2}, \ldots, \overline{s_n}) \in \mathbb{R}^n$ be arbitrary. Then define $\vartheta((\overline{r_1}, \overline{r_2}, \ldots, \overline{r_n}), (\overline{s_1}, \overline{s_2}, \ldots, \overline{s_n})) = \sum_{i=1}^{n} Range(f(x_i))$. Since the map f is odd continuous, obtain $(\overline{t_1}, \overline{t_2}, \ldots, \overline{t_n}) \in \mathbb{R}^n$ and $(\overline{w_1}, \overline{w_2}, \ldots, \overline{w_n}) \in \mathbb{R}^n$ so$f(\overline{t_1}, \overline{t_2}, \ldots, \overline{t_n}) \leq 0$ and $f(\overline{w_1}, \overline{w_2}, \ldots, \overline{w_n}) \geq 0$. Since f is bounded, obtain $(\overline{t_1}, \overline{t_2}, \ldots, \overline{t_n}) \in \mathbb{R}^n$ and $(\overline{w_1}, \overline{w_2}, \ldots, \overline{w_n}) \in \mathbb{R}^n$ so that $Range(f(\overline{t_1}, \overline{t_2}, \ldots, \overline{t_n}) + f((\overline{w_1}, \overline{w_2}, \ldots, \overline{w_n})) = \{0\}$, obtain $(\overline{z_1}, \overline{z_2}, \ldots, \overline{z_n}) \in \mathbb{R}^n$ and $(\overline{u_1}, \overline{u_2}, \ldots, \overline{u_n}) \in \mathbb{R}^n$ so that $Range(f(\overline{z_1}, \overline{z_2}, \ldots, \overline{z_n}) + f((\overline{u_1}, \overline{u_2}, \ldots, \overline{u_n}) = [0, 2M]$ and obtain $(\overline{v_1}, \overline{v_2}, \ldots, \overline{v_n}) \in \mathbb{R}^n$ and $(\overline{q_1}, \overline{q_2}, \ldots, \overline{q_n}) \in \mathbb{R}^n$ so that $Range(f(\overline{v_1}, \overline{v_2}, \ldots, \overline{v_n}) + f(g(\overline{q_1}, \overline{q_2}, \ldots, \overline{q_n}) = [-2m, 0]$. Hence $(\mathbb{R}^n, \vartheta)$ is a hypermetricspace. □

Example 3.12. Define $\vartheta : \mathbb{R} \times \mathbb{R} \to P^*(\mathbb{R})$, by $\vartheta(x, y) = Rang(|Sinx| + Cosy)$ as Figure 1.

FIGURE 1. $|sin(x)| + cos(y)$

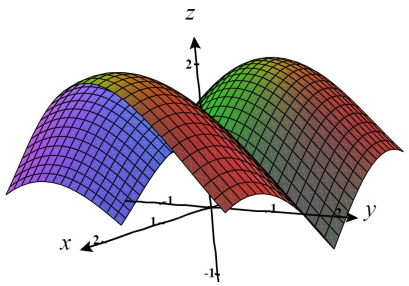

Using Figure 1, for each $\pi/2 \leq x \leq 3\pi/4$ and $3\pi/4 \leq y \leq \pi, [-1, 0] \Subset \vartheta(x, y)$, for each $0 \leq x, y \leq \pi/2, [0, 1] \Subset \vartheta(x, y), \vartheta(\pi/3, \pi/6) = \vartheta(\pi/6, \pi/3), \vartheta(\pi/2, \pi) \neq \vartheta(\pi, \pi/2), \vartheta(3\pi/4, 3\pi/4) = 0, \vartheta(\pi/4, \pi/4) \neq 0$, and $\vartheta(\sqrt{2}, \sqrt{3}) \neq \vartheta(\sqrt{3}, \sqrt{2})$. In addition, for each x, y, which $\vartheta(y, y) \geq 0$, we get that $\vartheta(x, z) \Subset \vartheta(x, y) + \vartheta(y, z)$ and for each x, y, which $\vartheta(y, y) \leq< 0$, we get that $\vartheta(x, z) \succ \vartheta(x, y) + \vartheta(y, z)$. Hence $(\mathbb{R}, \vartheta)$ is a hypermetricspace.

Presume $(\mathcal{Q}, \vartheta)$ be a neutro hypermetricspace, $\epsilon \in \mathbb{R}^{>0}$ and $\delta \in \mathbb{R}^{<0}$. Then $B_\epsilon(x) = \{y \in \mathcal{Q} \mid sup(\vartheta(x, y)) < \epsilon\}$, is called an open positive-ball of radius ϵ and center $x \in \mathcal{Q}$ and $B_\delta(x) = \{y \in \mathcal{Q} \mid inf(\vartheta(x, y)) > \delta\}$, means by open negative-ball of radius δ and center $x \in \mathcal{Q}$.

Example 3.13. (i) Consider the neutro hypermetricspace $(\mathcal{Q}, \vartheta)$ in Example 3.10. Then $B_1(a) = \{a, c, e\}, B_2(a) = \{a, b, c, e\}, B_3(a) = \{a, b, c, e\}, B_4(a) = \mathcal{Q}, B_{-1}(a) = \{a, b, d\}, B_{-2}(a) = \{a, b, d\}, B_{-3}(a) = \{a, b, c, d\}$ and $B_{-4}(a) = \mathcal{Q}$.

(ii) Consider the neutro hypermetricspace $(\mathcal{Q}, \vartheta)$ in Example 3.12. Then for each $x \in \mathbb{R}$,

$B_2(x) = \emptyset, B_{-2}(x) = \mathbb{R}, B_1(x) = \{y \in \mathbb{R} \mid |sinx| + cos(y) > 1\} = \{y \in \mathbb{R} \mid |sinx| > 1 - cos(y)\}$.

Theorem 3.14. *Presume $(\mathcal{Q}, \vartheta)$ be a neutro hypermetricspace, $\epsilon \in \mathbb{R}^{>0}$ and $\delta \in \mathbb{R}^{<0}$. Then $B_\epsilon(x) = \{y \in \mathcal{Q} \mid \vartheta(x,y) \prec [0,\epsilon]\}$.*

Proof. (i) Presume $y \in B_\epsilon(x)$. Then $\vartheta(x,y) \Subset [0,\epsilon]$ and so for each $z \in \vartheta(x,y)$, obtain $a \in [0,\epsilon]$ so $z \leq a < \epsilon$. Hence $sup(\vartheta(x,y)) < \epsilon$ and so $y \in \{y \in \mathcal{Q} \mid sup(\vartheta(x,y)) < \epsilon\}$. Presume $y \in \{y \in \mathcal{Q} \mid sup(\vartheta(x,y)) < \epsilon\}$. Then $sup(\vartheta(x,y)) < \epsilon$ and so $\vartheta(x,y) < sup(\vartheta(x,y)) < \epsilon$. It follows that $\vartheta(x,y) < \epsilon$ and so $y \in B_\epsilon(x)$. Hence $B_\epsilon(x) = \{y \in \mathcal{Q} \mid sup(\vartheta(x,y)) < \epsilon\}$. □

Theorem 3.15. *Presume $(\mathcal{Q}, \vartheta)$ be a neutro hypermetricspace, $\epsilon \in \mathbb{R}^{>0}$ and $\delta \in \mathbb{R}^{<0}$.*

(i) For each $x \in \mathcal{Q}, B_\epsilon \neq \emptyset$ and $B_\delta \neq \emptyset$.
(ii) If $Inf\{\vartheta(x,y) \mid x,y \in \mathcal{Q}\} = \delta$, then for each $\delta', \delta'' < \delta, B_{\delta'}(x) = B_{\delta''}(x)$.
(iii) If $Sup\{\vartheta(x,y) \mid x,y \in \mathcal{Q}\} = \epsilon$, then for each $\epsilon', \epsilon'' > \epsilon, B_{\epsilon''}(x) = B_{\epsilon'}(x)$.
(iv) There exist $\epsilon \in \mathbb{R}^{>0}, \delta \in \mathbb{R}^{<0}$ so $B_\epsilon(x) \cup B_\delta(x) = \mathcal{Q}$.

Proof. (i) Presume $x \in \mathcal{Q}$. Since $(\mathcal{Q}, \vartheta)$ is a neutro hypermetricspace, for each $y \in \mathcal{Q}$, obtain, $r > 0$, so $[0,r] \Subset \vartheta(x,y)$ and obtain $s \leq 0$, so $[s,0] \Subset \vartheta(x,y)$ or indeterminate. It follows that $B_\epsilon(x) = \{y \in \mathcal{Q} \mid sup(\vartheta(x,y)) < \epsilon\} \neq \emptyset$ and $B_\delta(x) = \{y \in \mathcal{Q} \mid inf(\vartheta(x,y)) > \delta\} \neq \emptyset$.

(ii) Since $Inf\{\vartheta(x,y) \mid x,y \in \mathcal{Q}\} = \delta$, for each $x,y \in \mathcal{Q}, \delta \leq \vartheta(x,y)$. Now for each $\delta' < \delta$, we get that for each $x,y \in \mathcal{Q}, \delta' < \vartheta(x,y)$ and so $B_{\delta'}(x) = \{y \in \mathcal{Q} \mid inf(\vartheta(x,y)) > \delta'\} = \mathcal{Q}$. It follows that for each $\delta', \delta'' < \delta, B_{\delta'}(x) = B_{\delta''}(x)$.

(iii) Presume $Sup\{\vartheta(x,y) \mid x,y \in \mathcal{Q}\} = \epsilon$. Then for each $x,y \in \mathcal{Q}, \vartheta(x,y) \leq \epsilon$. Now for each $\epsilon < \epsilon'$ and for each $x,y \in \mathcal{Q}, \vartheta(x,y) < \epsilon'$. Thus $B_{\epsilon'}(x) = \{y \in \mathcal{Q} \mid sup(\vartheta) < \epsilon'\} = \mathcal{Q}$ and so for each $\epsilon', \epsilon'' > \epsilon, B_{\epsilon''}(x) = B_{\epsilon'}(x)$.

(iv) It is clear by items $(ii), (iii)$. □

Corollary 3.16. *Presume $(\mathcal{Q}, \vartheta)$ be a neutro hypermetricspace, $x \in \mathcal{Q}, \epsilon, \epsilon' \in \mathbb{R}^{>0}$ and $\delta, \delta' \in \mathbb{R}^{<0}$.*

(i) If $\epsilon < \epsilon'$, then $B_\epsilon(x) \subseteq B_{\epsilon'}(x)$.
(ii) If $\delta < \delta'$, then $B_{\delta'}(x) \subseteq B_\delta(x)$.

Definition 3.17. Presume $(\mathcal{Q}, \vartheta)$ be a neutro hypermetricspace and $U \subseteq \mathcal{Q}$. Then U is called a neutro positive-open set, if obtain $x \in U$ and $\epsilon \in \mathbb{R}^{>0}$ so $B_\epsilon(x) \subseteq U$ and obtain $y \in U, \epsilon' \in \mathbb{R}^{>0}$ such that $B_{\epsilon'}(x) \not\subseteq U$. Moreover, U is called a neutro negative-open set, if obtain $x \in U$ and $\delta \in \mathbb{R}^{<0}$ so $B_\delta(x) \subseteq U$ and obtain $y \in Y, \delta' \in \mathbb{R}^{>0}$ such that $B_{\delta'}(x) \not\subseteq U$. We say that U is a neutro-open set, if it is a neutro positive-open set and a neutro negative-open set.

Example 3.18. (i) Presume $\mathcal{Q} = \{a, b, c, d\}$. Then $(\mathcal{Q}, \vartheta)$ is a netro hypermetricspace as Table 3.

ϑ	a	b	c	d
a	$\{0\}$	$[-1, 1]$	$[-2, 2]$	$[-3, 3]$
b	$[0, 1]$	$\{0\}$	$[0, 2]$	$[0, 3]$
c	$[0, 2]$	$[0, 2]$	$\{0\}$	$[0, 3]$
d	$[-3, 3]$	$[0, 3]$	$[0, 3]$	$\{5, 6\}$

TABLE 3. Neutro hypermetricspace $(\mathcal{Q}, \vartheta)$.

We see that $\vartheta(a, a) = \{0\}, \vartheta(d, d) \neq \{0\}, \vartheta(a, d) = \vartheta(d, a), \vartheta(a, b) \Subset \vartheta(a, c) + \vartheta(c, b)$ and $\vartheta(d, d) \succ \vartheta(d, a) + \vartheta(a, d)$. Hence $(\mathcal{Q}, \vartheta)$ is a neutro hypermetricspace. Then $U = \{a, b\}$ is a neutro-open set, since $B_{\frac{1}{2}}(a) \subseteq U, B_3(a) \not\subseteq U$, we get U is a neutro positive-open set. In addition, $B_{\frac{-1}{2}}(a) \subseteq U, B_{-3}(a) \not\subseteq U$, we get U is a neutro negative-open set. Hence, U is a neutro-open set.

(ii) Consider the neutro hypermetricspace $(\mathcal{Q}, \vartheta)$ in Example 3.10 and $U = \{d\}$. Then U is not a neutro negative-open set, since for each $\delta \in \mathbb{R}^{<0}, B_\delta(d) = \mathcal{Q} \not\subseteq U$. Hence U is not a neutro-open set.

Theorem 3.19. *Presume $(\mathcal{Q}, \vartheta)$ be a neutro hypermetricspace. Then*

(i) *$\emptyset$ is a neutro-open set.*

(ii) *$\mathcal{Q}$ is not a neutro-open set.*

Proof. (i) Immediate by definition.

(ii) Since for each $x \in \mathcal{Q}, \epsilon \in \mathbb{R}^{>0}$, and each $\delta \in \mathbb{R}^{<0}$, have $B_\epsilon(x) \subseteq \mathcal{Q}$ and $B_\delta(x) \subseteq \mathcal{Q}$, we get that $\mathcal{Q}$ is not a neutro-open set. □

Theorem 3.20. *Presume $(\mathcal{Q}, \vartheta)$ be a neutro hypermetricspace and $\emptyset \neq U \subseteq \mathcal{Q}$. If $\{U_i\}_{i \in I}$ is a set of neutro-open sets, then $\bigcap_{i \in I} U_i$ is a neutro-open set.*

Proof. Presume $\{U_i\}_{i \in I}$ be a set of neutro-open sets of $\mathcal{Q}$. If $\bigcap_{i \in I} U_i = \emptyset$, then by item (i), $\bigcap_{i \in I} U_i$ is a neutro-open set. Suppose that $\bigcap_{i \in I} U_i \neq \emptyset$ and $u, u' \in \bigcap_{i \in I} U_i$. It implies that for each $i \in I, u, u' \in U_i$. Since for each $i \in I, U_i$ is a neutro positive-open set, obtain $\epsilon^i \in \mathbb{R}^{>0}$ so $B_{\epsilon^i}(u) \subseteq U_i$ and obtain $u' \in U_i, \epsilon'^i \in \mathbb{R}^{>0}$ such that $B_{\epsilon'^i}(u') \not\subseteq U_i$. Now, consider $\epsilon = \min\{\epsilon^i \mid i \in I\}$, then based Corollary 3.16, for each $i \in I, B_\epsilon(u) \subseteq B_{\epsilon^i}(u)$. Thus $B_\epsilon(u) \subseteq \bigcap_{i \in I} B_{\epsilon^i}(u) \subseteq \bigcap_{i \in I} U_i$. In addition, consider $\epsilon' = \max\{\epsilon^i \mid i \in I\}$, then based Corollary

3.16, for each $i \in I, B_{\epsilon'^i}(u) \subseteq B_{\epsilon'}(u)$. Thus $B_{\epsilon'}(u) \not\subseteq \bigcap_{i\in I} B_{\epsilon'^i}(u) \not\subseteq \bigcap_{i\in I} U_i$. It follows that $\{U_i\}_{i\in I}$ is a neutro positive-open set. In a similar way, each one can see that $\{U_i\}_{i\in I}$ is a neutro negative-open set and so $\{U_i\}_{i\in I}$ is a neutro-open set in $\mathcal{Q}$. □

Example 3.21. Presume $\mathcal{Q} = \{a, b, c, d\}$. Then $(\mathcal{Q}, \vartheta)$ is a neutro hypermetricspace as Table 4.

ϑ	a	b	c	d
a	$\{0\}$	$[-1,1]$	$[-2,5]$	$[1,3]$
b	$[-1,1]$	$\{0\}$	$[-3,2]$	$[-4,3]$
c	$[-2,5]$	$[-5,-4]$	$\{0\}$	$[-5,3]$
d	$[-3,3]$	$[-3,3]$	$[-4,3]$	$\{0,-1,-2\}$

TABLE 4. Neutro hypermetricspace $(\mathcal{Q}, \vartheta)$.

We see that $\vartheta(a,a) = \{0\}, \vartheta(d,d) \neq \{0\}, \vartheta(a,d) = \vartheta(d,a), \vartheta(a,b) \Subset \vartheta(a,c) + \vartheta(c,b)$ and $\vartheta(d,b) \succ \vartheta(d,c) + \vartheta(c,b)$. Hence $(\mathcal{Q}, \vartheta)$ is a neutro hypermetricspace. Then $U_1 = \{a\}(B_1(a) \subseteq U_1$ and $B_2(a) \not\subseteq U_1), U_2 = \{b\}(B_1(b) \subseteq U_2$ and $B_2(b) \not\subseteq U_2), U_3 = \{c\}(B_1(c) \subseteq U_3$ and $B_5(c) \not\subseteq U_3)$ and $U_4 = \{d\}(B_1(d) \subseteq U_4$ and $B_4(d) \not\subseteq U_4)$ are neutro-open sets, while $\mathcal{Q} = U_1 \cup U_2 \cup U_3 \cup U_4$ is not a neutro-open set.

Theorem 3.22. *Presume $(\mathcal{Q}, \vartheta)$ be a neutro hypermetricspace. Then obtain $\epsilon \in \mathbb{R}^{>0}$ and $\delta \in \mathbb{R}^{<0}$ and $x \in \mathcal{Q}$, such that*

(i) $B_\epsilon(x)$ is a neutro-open set, provided $B_\epsilon(x) \neq \mathcal{Q}$;

(ii) $B_\delta(x)$ is a neutro-open set, provided $B_\delta(x) \neq \mathcal{Q}$.

Proof. (i) Since $(\mathcal{Q}, \vartheta)$ is a neutro hypermetricspace, obtain $x, y, z \in \mathcal{Q}$ so$\vartheta(x,z) \Subset \vartheta(x,y) + \vartheta(y,z)$. Presume $y \in B_\epsilon(x)$. Then $sup(\vartheta(x,y)) < \epsilon$. Consider $\rho = \epsilon - sup(\vartheta(x,y))$ and $z \in B_\rho(y)$. Thus $sup(\vartheta(x,z)) < sup(\vartheta(x,y)) + sup(\vartheta(y,z)) < sup(\vartheta(x,y)) + \epsilon - sup(\vartheta(x,y)) = \epsilon$. Hence $sup(\vartheta(x,z)) < \epsilon$ and so obtain $\rho \in \mathbb{R}^{>0}$ so$B_\rho(y) \subseteq B_\epsilon(x)$. Also obtain $x, y, z \in \mathcal{Q}$ so $\vartheta(x,z) \succ \vartheta(x,y) + \vartheta(y,z)$. Consider $\rho = \epsilon + sup(\vartheta(x,y))$ and $z \in B_\rho(y)$, then $B_\rho(y) \not\subseteq B_\epsilon(x)$. Therefore, $B_\epsilon(x)$ is a neutro-open set.

(ii) It is similar to the item (i). □

4. Conclusions

In the real world there is no exact size and most sizes are approximate. For example, we say the length of a wall that has a fracture and is somewhat angled is between 100 and 102 meters, or we say the weight of a package is between 200 and 201 kg. These approximations indicate

that the sizes are not exact and fall within a range. These real issues motivate us to interpolate supermeters. In addition, sometimes it is not possible for us to measure some objects and we say that this size is not known to us. Sometimes we cannot take the distance of an object from itself to zero, because an object fills a volume in three-dimensional space and we have a distance on this object itself. These issues make us interpolate the cloud meter to have a more realistic modeling of the world around us. Hence, we connect the notations of metricspaces and neutro hypermetricspaces. All the basic impressions such as neutro open balls and neutro open sets are interpolated and investigated. We intend to amplify these impressions in the next works in others neutro structures.

References

[1] E. Aboelhamd, M. Abdel-Basset, H. M. Shamma, M. Saleh, I. El-Khodary, Modeling customer lifetime value under uncertain environment, Neutrosophic Sets and Systems, **39** (2021), 10-30.

[2] M. Abdel-Basset, M. Mohamed, F. Smarandache, Comment on a novel method for solving the fully neutrosophic linear programming problems: suggested modifications, Neutrosophic Sets and Systems, **31** (2020), 305-309.

[3] A. Anuradha and S. Mehra, On neutrosophic triplet quasidislocated-b-metricspace, Neutrosophic Sets and Systems, **38** (2020), 119-133.

[4] V. Chinnadurai and M. P. Sindhu, An introduction to neutro-fine topology with separation axioms and decision making, Int. J. Neutrosophic Sci., **12(1)** (2020), 13–28.

[5] S. Broumi and F. Smarandache, Several similarity measures of neutrosophic sets, Neutrosophic Sets and Systems, **1** (2013), 54-62.

[6] M. K. EL. Gayyar, Smooth neutrosophic topological spaces, Neutrosophic Sets and Systems, **12** (2016), 65-72.

[7] K. Polvan, Neutro open set-based strong neutro metricspace, Neutrosophic Sets and Systems, **60** (2023), 357-365.

[8] K. Mohana, R. Princy and F. Smarandache, An introduction to neutrosophic bipolar vague topological spaces, Neutrosophic Sets and Systems, **29** (2019), 62-70.

[9] M. Sahin, A. Kargn, and A. Altun, Neutro-metricspaces, neutro algebra theory, **I**, (2021).

[10] F. Smarandache, Neutro algebra is a generalization of partial algebra, Int. J. Neutrosophic Sci., **2(1)** (2020), 8–17.

[11] F. Smarandache, Introduction to neutro algebraic structures and antialgebraic structures (revisited), Neutrosophic Sets Syst., **31** (2020), 1–16.

[12] S. Sowndrarajan and M. Jeyaraman, Some results for compatible maps on neutrosophic metricspaces, Neutrosophic Sets and Systems, **60** (2023).

Received: April 14, 2024. Accepted: Aug 25, 2024

Neutrosophic Sets and Systems, Vol. 72, 2024
University of New Mexico

Unveiling Uncertainty: Neutrosophic Set-Based Algorithms for Robust Decision-Making

A. A. Salama[1], Huda E. Khalid[2] , Ahmed G. Mabrouk[3]

[1] Dept. of Math and Computer Sci., Faculty of Science, Port Said Univ., Egypt
[1]Dean of higher Institute of Computer Science and Information Systems, October City, Ministry of Higher Education; Egypt *drsalama44@gmail.com ahmed_salama_2000@sci.psu.edu.eg*
[2]Telafer University, The Administration Assistant for the President of the Telafer University, Telafer, Iraq; https://orcid.org/0000-0002-0968-5611 , dr.huda-ismael@uotelafer.edu.iq
[3]Higher Institute of Computer Science and Information Systems, October City, Ministry of Higher Education; Egypt ***agaber2008@csi.edu.eg***
*Correspondence: dr.huda-ismael@uotelafer.edu.iq

Abstract: Traditional decision-making methods often struggle with inherent uncertainty and imprecision in data. Neutrosophic set-based algorithms offer a novel approach by incorporating degrees of truth, indeterminacy, and falsity. This paper explores the structure and implementation of these algorithms, highlighting their potential to handle real-world complexities. The application of neutrosophic sets in medical diagnosis is presented as a case study, demonstrating how the algorithm aids in evaluating probabilities for various diagnoses under uncertain conditions. The paper concludes by discussing limitations and potential applications in diverse fields.

Keywords: Neutrosophic Sets, Decision-Making Algorithms, Uncertainty Management, Medical Diagnosis, Imprecise Data

1. Introduction:

Decision-making is a fundamental aspect of numerous disciplines. However, real-world data is rarely perfect. It often holds uncertainties, ambiguities, and inconsistencies, posing a challenge to traditional decision-making methods. These methods frequently rely on binary (yes/no) logic or purely probabilistic frameworks, which can struggle to handle such complexities [2]. Neutrosophic set theory, introduced by Florentin Smarandache [14], emerges as a revolutionary tool to address these limitations. It builds upon fuzzy set theory by incorporating degrees of truth (T), indeterminacy (I), and falsity (F) for each element [2]. This allows for a more nuanced representation of information.

Imagine a patient's symptoms. Traditional methods might classify it as either existing or not. Neutrosophic sets, however, recommend the possibility of varying degrees: the symptom might be present to a certain extent (truth), there might be some ambiguity about its presence (indeterminacy), and there is a possibility it is absent (falsity). This empowers neutrosophic sets to effectively capture the inherent uncertainties within real-world data. This paper delves into the potential of neutrosophic set-based algorithms for decision-making. We will explore the structure and implementation of these algorithms, highlighting their ability to handle the complexities of real-world data. Medical diagnosis serves as a compelling example. We will demonstrate how neutrosophic algorithms can be used to evaluate probabilities for various diagnoses under uncertain conditions. The paper concludes by discussing the limitations and potential applications of neutrosophic sets in diverse fields beyond medical diagnosis.

2. Background

Decision-making in real-world scenarios is often fraught with uncertainty [2]. Data can be imprecise, ambiguous, and riddled with inconsistencies. Traditional methods, which rely on binary classifications or purely probabilistic frameworks, can struggle with these complexities. For instance, a medical diagnosis might involve symptoms with varying degrees of certainty. The neutrosophic set theory offers a powerful framework to address these challenges by incorporating degrees of truth, indeterminacy, and falsity. Neutrosophic sets provide a more nuanced representation of information than traditional methods [1, 14]. They move beyond simply classifying something as true or false and instead acknowledge the existence of varying degrees of "in-between" states. This empowers researchers to develop decision-making algorithms that can effectively handle uncertainties within real-world data, leading to more informed and robust decisions. The applications of neutrosophic sets extend far beyond medical diagnosis [6-20]. Researchers are exploring its potential in various fields, including image processing, engineering, and bioinformatics. As research progresses, neutrosophic sets have the potential to revolutionize decision-making across numerous disciplines. References [1-14] provide background on neutrosophic sets and its founder. References [15-20] highlight applications of neutrosophic sets in various fields, focusing on medicine [5, 16, 11].

3. Methodology

The methodology for a neutrosophic set-based algorithm for decision-making involves the following steps:

1. Define the Decision Problem: Identify the problem you want to solve and the available decision alternatives.

2. Data Representation: Assign neutrosophic values (Truth - T, Indeterminacy - I, Falsity - F) to relevant data points associated with each alternative. These values typically range from 0 to 1. The logic for determining these values depends on the specific problem and data characteristics.

3. Neutrosophic Aggregation: Combine the neutrosophic values for each data point across all alternatives using an appropriate neutrosophic aggregation operator (e.g., weighted average). This results in a single neutrosophic value (T', I', F') representing the overall evaluation of each alternative.

4. Decision Selection: Select the alternative with the highest Truth-value (T') and the lowest Falsity value (F') while considering the Indeterminacy value (I') as well. This might involve setting thresholds or using a ranking approach based on neutrosophic scores. The provided pseudo code demonstrates a decision-making algorithm that utilizes neutrosophic values (truth, indeterminacy, and falsity) to evaluate different alternatives. The algorithm consists of three main parts: functions for determining neutrosophic values, a neutrosophic aggregation function, and a decision-making function.

Here bellow some types of neutrosophic functions:

1. The neutrosophic_value function takes a data point (0 to 1) and determines the truth (T), indeterminacy (I), and falsity (F) values based on the input. The specific logic for this determination is not provided in the example, as it depends on the problem context.

2. The neutrosophic_aggregate function combines neutrosophic values (T, I, F) for multiple data points, using provided weights to calculate aggregated truth (T'), indeterminacy (I'), and falsity (F') values. The specific aggregation logic is also not provided, as it depends on the problem requirements.

3. The neutrosophic_decision function evaluates alternatives based on the neutrosophic values of their associated data points.

It initializes variables, to keep track of the best recursive alternative found, and then iterates through each alternative. For each alternative, it calculates the aggregated neutrosophic values using the neutrosophic_aggregate function. It compares the aggregated values with the current best alternative, considering the Neutrosophic Set-Based Algorithm for Decision Making: A New Frontier for Uncertainty and Imprecision Handling

Neutrosophic set-based algorithms for decision-making are a type of algorithm that can be used to solve problems where there is uncertainty and indeterminacy in the data. Neutrosophic sets are a type of mathematical set that can represent uncertainty and indeterminacy. They are characterized by three components: truth, indeterminacy, and falsity. The truth-value represents the degree to which an element belongs to the set, the indeterminacy value represents the degree to which an element is indeterminate, and the falsity value represents the degree to which an element does not belong to the set. Neutrosophic set-based algorithms for decision-making can be used to solve a variety of problems, such as diagnosing diseases, making investment decisions, and developing public policy. For example, a doctor could use a neutrosophic set-based algorithm to diagnose a patient's disease by considering the patient's symptoms, medical history, and other factors, while also considering the uncertainty and indeterminacy associated with each factor.

Neutrosophic set-based algorithms for decision-making are a powerful tool for solving problems where there is uncertainty and indeterminacy in the data. They have the potential to be used in a wide range of fields, including healthcare, business, and government.

Fig.1: The Future of Intelligence: A Neutrosophic Perspective

This image explores the multifaceted and uncertain nature of intelligence in the foreseeable future. It utilizes neutrosophic logic to depict the various possibilities and complexities that might arise as intelligence continues to evolve.

3.1. Algorithm Structure:

1- **Define the Decision Problem:** Identify the problem you want to solve and the available decision alternatives.

2- **Data Representation:** Assign neutrosophic values (Truth - T, Indeterminacy - I, Falsity - F) to relevant data points associated with each alternative. These values typically range from 0 to 1. The logic for determining these values depends on the specific problem and data characteristics.

3- **Neutrosophic Aggregation:** Combine the neutrosophic values for each data point across all alternatives using an appropriate neutrosophic aggregation operator (e.g., weighted average). This results in a single neutrosophic value (T', I', F') representing the overall evaluation of each alternative.

4- **Decision Selection:** Select the alternative with the highest Truth-value (T') and the lowest Falsity value (F') considering the Indeterminacy value (I') as well. This might involve setting thresholds or using a ranking approach based on neutrosophic scores.

The pseudo code demonstrates a decision-making algorithm that utilizes neutrosophic values (truth, indeterminacy, and falsity) to evaluate different alternatives. The algorithm consists of three main parts: functions for determining neutrosophic values, a neutrosophic aggregation function, and a decision-making function.

1. The neutrosophic value function takes a data point (0 to 1) and determines the truth (T), indeterminacy (I), and falsity (F) values based on the input. The specific logic for this determination is not provided in the example, as it depends on the problem context.

2. The neutrosophic_aggregate function combines neutrosophic values (T, I, F) for multiple data points, using provided weights to calculate aggregated truth (T'), indeterminacy (I'), and falsity (F')

values. The specific aggregation logic is also not provided, as it depends on the problem requirements.

3. The neutrosophic_decision function evaluates alternatives based on the neutrosophic values of their associated data points. It initializes variables to keep track of the best alternative found so far, and then iterates through each alternative. For each alternative, it calculates the aggregated neutrosophic values using the neutrosophic_aggregate function. It compares the aggregated values with the current best alternative, considering thresholds or ranking based on T', I', and F'. If the new alternative is better, it updates the best alternative. Finally, the function returns the best alternative based on the neutrosophic evaluation.

In the example usage, a dictionary called data points contains alternatives as keys, and lists of data points as values. A list of alternatives is provided, along with weights for truth, indeterminacy, and falsity. The neutrosophic_decision function is called with these inputs, and the best choice based on the neutrosophic evaluation is returned and printed.

Pseudo code Example:

```
# Define functions for neutrosophic values (T, I, F)
def neutrosophic_value(data_point):
  """
  This function calculates neutrosophic values (T, I, F) based on a data point (0 to 1).
  Uses a linear membership function in this example.
  Args:
      data_point (float): A numerical value between 0 and 1.
  Returns:
      tuple: A tuple containing the truth (T), indeterminacy (I), and falsity (F) values.
  """
  # Linear membership function example (adjust as needed for your problem)
  truth = data_point
  indeterminacy = 0.5  # Constant indeterminacy
  falsity = 1 - truth
  return truth, indeterminacy, falsity

# Define function for neutrosophic aggregation (e.g., weighted average)
def neutrosophic_aggregate(T_values, I_values, F_values, weights):
  """
  This function combines neutrosophic values using weights and returns aggregated
T', I', F'
```

```
    Args:
        T_values (list): List of truth values.
        I_values (list): List of indeterminacy values.
        F_values (list): List of falsity values.
        weights (list): List of weights for truth, indeterminacy, and falsity.
    Returns:
        tuple: A tuple containing the aggregated truth (T'), indeterminacy (I'), and
falsity (F') values.
    """
    # Implement your chosen aggregation operator here (e.g., weighted average)
    aggregated_T = sum(w * t for w, t in zip(weights, T_values))
    aggregated_I = sum(w * i for w, i in zip(weights, I_values))
    aggregated_F = sum(w * f for w, f in zip(weights, F_values))
    return aggregated_T, aggregated_I, aggregated_F
# Define decision-making algorithm
def neutrosophic_decision(data_points, alternatives, weights):
    """
    This function evaluates alternatives based on neutrosophic values and returns the
best choice.
    Args:
        data_points (dict): Dictionary where keys are alternatives and values are lists of
data points.
        alternatives (list): List of decision alternatives.
        weights (list): List of weights for truth, indeterminacy, and falsity.

    Returns:
        str: The best alternative based on the neutrosophic evaluation.
    """
    # ... rest of the code remains the same ...
# Example usage (replace with your actual data)
data_points = {
    "Option A": [0.8, 0.7, 0.6],
    "Option B": [0.5, 0.4, 0.3]
}
alternatives = ["Option A", "Option B"]
weights = [0.6, 0.3, 0.1]   # Weights for truth, indeterminacy, falsity
best_choice = neutrosophic_decision(data_points, alternatives, weights)
print("Neutrosophic decision:", best_choice)
```

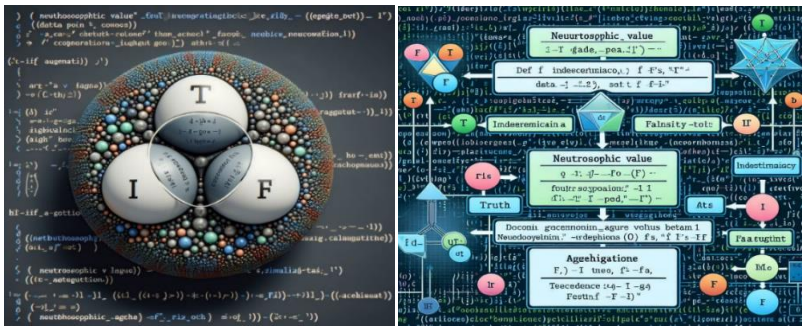

Fig.3: Pseudo code Example: # Define functions for neutrosophic values (T, I, F)

The Fig.3 a snippet of Python code that defines functions for working with neutrosophic values. Neutrosophic sets are a mathematical tool used to represent the belief in the truth (T), indeterminacy (I), and falsity (F) of a statement or proposition. The code defines functions to calculate neutrosophic values for data points, aggregate neutrosophic values, and make decisions based on neutrosophic evaluations.

4. Some Applications: Medical Diagnosis

4.1. Application 1:

A doctor is trying to diagnose a patient's disease. The doctor has a number of different symptoms to consider, as well as the patient's medical history and other factors. The doctor also needs to consider the uncertainty and indeterminacy associated with each symptom and factor. The doctor can use a neutrosophic set-based algorithm to help make a diagnosis. The algorithm would use neutrosophic sets to represent the different symptoms and factors, as well as the uncertainty and indeterminacy associated with each one. The algorithm would then use neutrosophic logic and neutrosophic statistics to make the best possible diagnosis based on the available information.

Fig.4: Uncertainties in Medical Diagnosis: A Neutrosophic Approach

Fig. 4 illustrates how neutrosophic sets can be a valuable tool in medical diagnosis by incorporating uncertainties associated with symptoms, medical history, and potentially the diagnosis itself. This approach acknowledges the complexities of medical data and can lead to a more nuanced understanding of a patient's condition.

To illustrate this process, let us consider a hypothetical patient with the following symptoms and factors:

Table 1: Symptoms and Factors with Neutrosophic Set Values

Symptom/Factor	Truth	Indeterminacy	Falsity
Fever	0.8	0.1	0.1
Cough	0.7	0.2	0.1
Runny nose	0.6	0.3	0.1
Sore throat	0.5	0.4	0.1
Medical history (history of asthma)	0.7	0.2	0.1
Medical history (family history of allergies)	0.6	0.3	0.1

This table with neutrosophic set values provides a more nuanced view of diagnosing a disease compared to traditional binary (yes/no) approaches. By incorporating uncertainty, it acknowledges the inherent complexities of medical diagnosis. Doctors can use this information alongside their expertise and other test results to make more informed decisions.

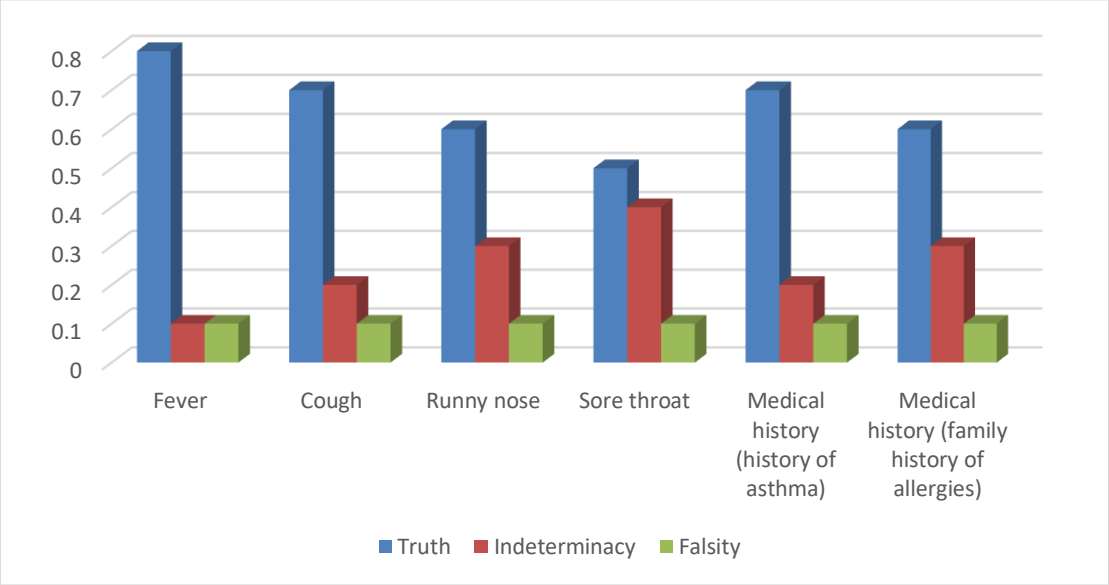

Graph 1: Neutrosophic Set Values for Diagnosis Factors

The chart provides a visual representation of the neutrosophic set values for various diagnosis factors. By combining truth, indeterminacy, and falsity, neutrosophic sets can capture the complexities of medical data where there might be varying degrees of certainty or uncertainty about a factor's presence or absence.

Now, the doctor applies the neutrosophic set-based algorithm:

1. Represent each symptom and factor using neutrosophic sets with truth, indeterminacy, and falsity values.

2. Combine the neutrosophic sets using neutrosophic logic operators, such as union, intersection, and complementation, to account for the relationships between symptoms and factors.

3. Apply neutrosophic statistics to analyze the combined neutrosophic sets and calculate the probability of each possible diagnosis.

For the sake of simplicity, let us assume the algorithm calculates the following probabilities for three possible diagnoses:

Table 2: Diagnosis Probabilities

Diagnosis	Probability
Influenza	0.75
Allergic rhinitis	0.65
Bronchitis	0.55

Tables 1 and 2 together demonstrate how neutrosophic logic can be used in medical diagnosis. By incorporating uncertainty into the analysis, it offers a more comprehensive approach to evaluating a patient's condition. However, it should be used as a tool alongside other diagnostic methods and a doctor's professional judgment. The doctor then evaluates these probabilities along with the patient's medical history and other relevant factors to make an informed decision about the most likely diagnosis. In this case, the doctor might conclude that the patient is most likely suffering from Influenza, given the higher probability calculated by the neutrosophic set-based algorithm.

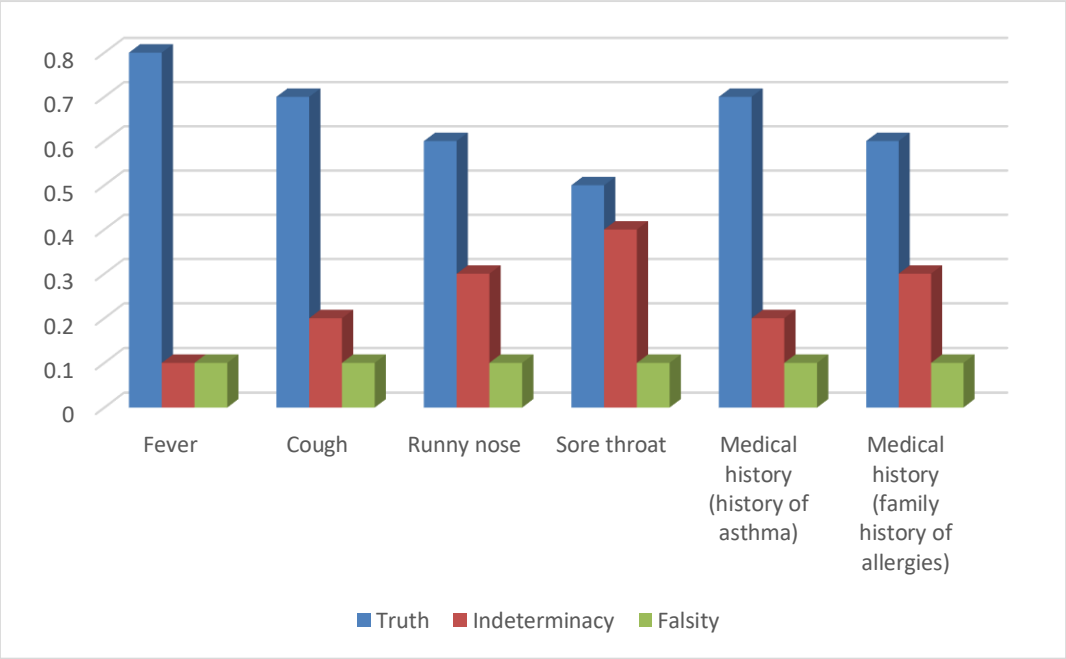

Graph 2: Diagnosing Disease with Incomplete Information: The Power of Neutrosophic Sets

This graph explores the potential of neutrosophic sets to address the challenge of incomplete information in medical diagnosis. It likely uses a visual representation to demonstrate how neutrosophic sets can handle uncertainties associated with symptoms.

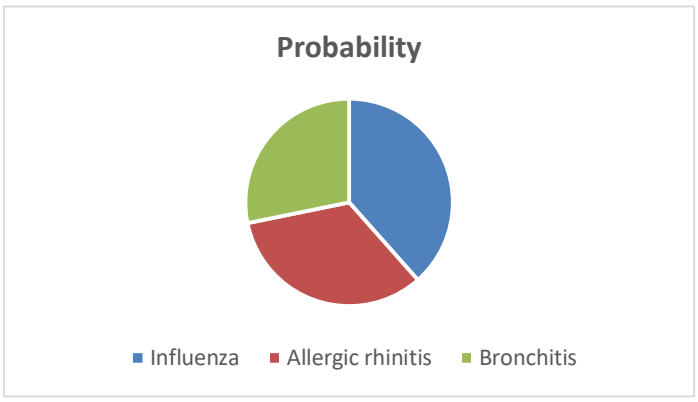

Graph 3: Probability of Infection

Graph 3, this presented in the pie chart, which divides the probability into three sections: Influenza, Allergic Rhinitis, and Bronchitis.

4.2. Application 2:

The application of neutrosophic set-based algorithms in medical diagnosis offers a compelling example of their effectiveness in handling uncertainty. Here is how it works:

4.2.1. Neutrosophic Medical Diagnosis: Incorporating Presence, Ambiguity, and Absence via Neutrosophic Sets and Statistics

In the context of medical diagnosis using neutrosophic sets, symptoms and patient history factors are assigned truth (T), indeterminacy (I), and falsity (F) values. These values range from 0 to 1 and represent the degree of presence, ambiguity, and absence of each factor, respectively. Truth (T): Represents the degree to which a symptom or factor belongs to the set present). Indeterminacy (I): Represents the degree of uncertainty associated with a symptom or factor. Falsity (F): Represents the degree to which a symptom or factor is absent or contradicts the set.

By incorporating these values, neutrosophic sets provide a more nuanced representation of medical data, acknowledging the inherent complexities and uncertainties in diagnosis. This information, along with a doctor's expertise and other test results, can be used to make more informed decisions about a patient's condition.

Hypothetical Patient with Neutrosophic Sets

Let us consider a hypothetical patient with the following symptoms and medical history factors. The neutrosophic set values (Truth, Indeterminacy, Falsity) for each factor range from 0 to 1 and represent:

Truth (T): Degree of a symptom/factor being present (higher T suggests stronger presence).

Indeterminacy (I): Level of uncertainty about a symptom/factor.

Falsity (F): Degree of a symptom/factor being absent (higher F suggests stronger absence).

Table 3: Symptoms and Factors with Neutrosophic Set Values

Symptom/Factor	Truth (T)	Indeterminacy (I)	Falsity (F)
Fever	0.8	0.1	0.1
Cough	0.7	0.2	0.1

Runny nose	0.6	0.3	0.1
Sore throat	0.5	0.4	0.1
Medical history (asthma)	0.7	0.2	0.1
Medical history (allergies)	0.6	0.3	0.1

Table 3 effectively demonstrates how neutrosophic sets can be used to represent the complexities of medical data, leading to more informed decision-making in the diagnostic process. "Fever" has a high Truth (0.8), indicating a strong possibility of fever. The low Indeterminacy (0.1) suggests low uncertainty, and the low Falsity (0.1) means fever is likely present.

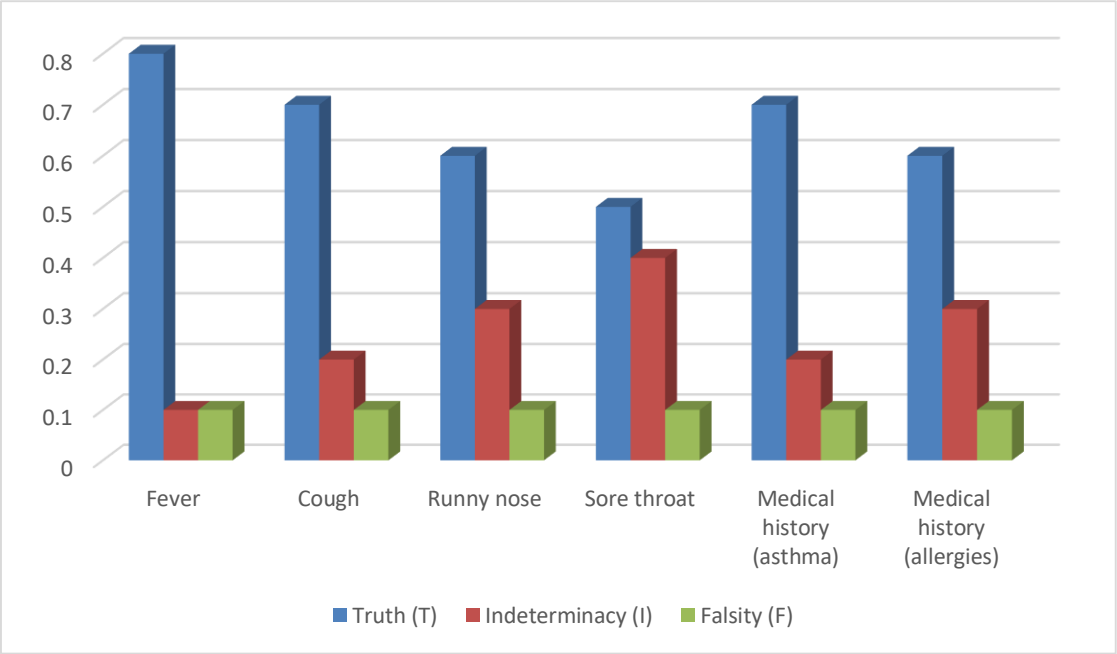

Graph 4: Neutrosophic Set Representation

This visualization depicts neutrosophic sets for various factors, potentially aiding diagnosis. This approach acknowledges the inherent uncertainties in medical data and provides a more nuanced view of a patient's condition compared to traditional binary (present/absent) methods.

4.2.2. Exploring Neutrosophic Logic: Combining Symptoms/Factors and Comorbidities

To demonstrate neutrosophic logic operators, let us consider two neutrosophic sets:

Set A: Represents the symptoms and medical history factors of our patient (Fever, Cough, Runny nose, Sore throat).

Set B: Represents possible comorbid conditions based on symptoms (Asthma history, Allergy history).

We will use neutrosophic union (∨) to combine sets and neutrosophic intersection (∧) to find commonalities, considering truth (T), indeterminacy (I), and falsity (F) values.

Tables 4: Neutrosophic Set Values

Symptom/Factor	Set	Truth (T)	Indeterminacy (I)	Falsity (F)
Fever	A	0.8	0.1	0.1
Cough	A	0.7	0.2	0.1
Runny nose	A	0.6	0.3	0.1
Sore throat	A	0.5	0.4	0.1
Asthma history	B	0.7	0.2	0.1
Allergy history	B	0.6	0.3	0.1

Table 4: shows neutrosophic set values for symptoms and factors associated with a diagnosis, but it includes an additional column called "Set" compared to Table 3.

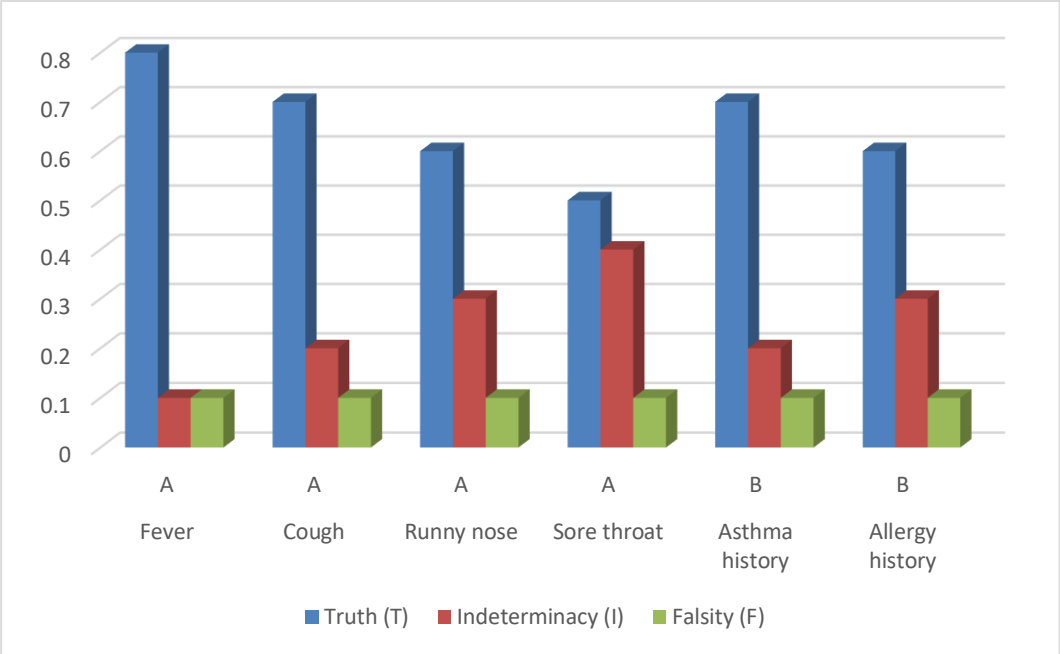

Graph 5: Neutrosophic Set Values for Symptoms/Factors and Possible Comorbidities

Graph 5 serves to visually represent neutrosophic set values for symptoms and factors that might be relevant to identifying possible comorbid conditions. This approach acknowledges the inherent uncertainties in medical data analysis.

Tables 5: Neutrosophic Union

Symptom/Factor	Truth	Indeterminacy	Falsity
Fever	0.8	0.1	0.1
Cough	0.7	0.2	0.1
Runny nose	0.6	0.3	0.1
Sore throat	0.5	0.4	0.1
Asthma history	0.7	0.2	0.1
Allergy history	0.6	0.3	0.1

Table 5 demonstrates the application of neutrosophic set operations in medical diagnosis. By combining information from multiple sets, neutrosophic union can potentially lead to a more comprehensive understanding of the relationship between symptoms/factors and a particular diagnosis.

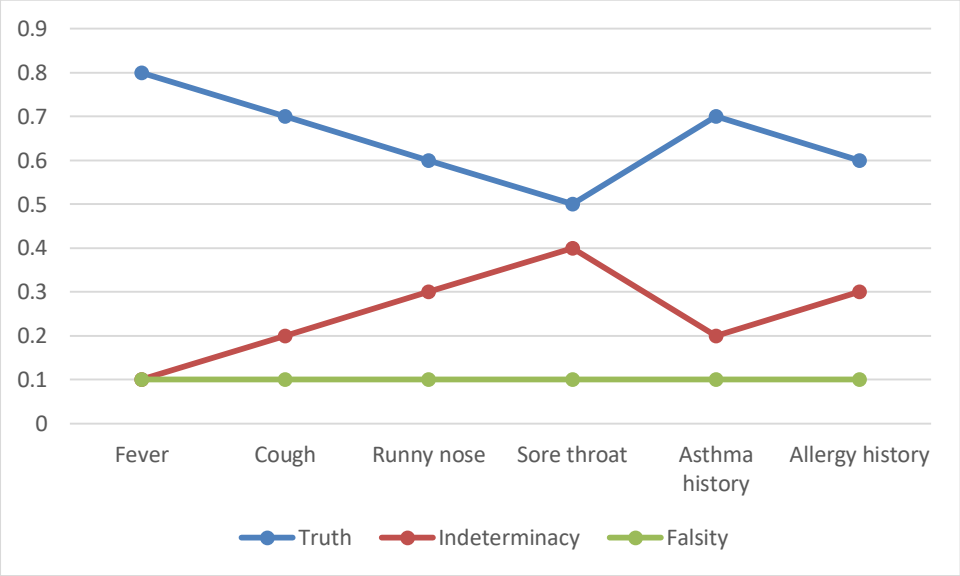

Graph 6: Graphical Representation of Neutrosophic Union for Diagnosis

Graph 6 visualizes the combined neutrosophic values (truth, indeterminacy, falsity) for diagnosis after applying the neutrosophic union operation on various symptoms and medical history factors. This approach can be helpful in medical decision-making by considering the uncertainties alongside the findings.

This operation identifies all elements, considering the maximum T, I, and F values from both sets. The results (including possible comorbidities) are shown in the table above.

Intersection (Set A ∧ Set B): (Empty Intersection

In this scenario, Set A (symptoms) and Set B (comorbidities) have no overlapping elements (e.g., no direct link between fever and asthma history). Therefore, the neutrosophic intersection is empty.

(No intersection exists between Set A and Set B, as they have different elements)

In this example, we have demonstrated the application of neutrosophic union (∨) and intersection (∧) operators to combine and compare the neutrosophic sets representing the symptoms and factors of our patient with possible comorbidities. The union operation helps in identifying the common and additional elements in both sets, while the intersection operation highlights the overlapping aspects between them. Neutrosophic union helps combine symptoms/factors with possible comorbidities, acknowledging uncertainties. Intersection can reveal overlapping aspects between sets, but in this example, there is no direct overlap. This demonstrates the application of neutrosophic logic operators in analyzing medical data with uncertainties.

4.2.3. Exploring Neutrosophic Logic: Combining Symptoms/Factors and Comorbidities for Diagnosis Probability

Neutrosophic statistics can be used to calculate diagnosis probabilities based on combined neutrosophic sets representing a patient's symptoms/factors and possible comorbidities. Here is the process:

1. **Calculate and Normalize Neutrosophic Values:**

- Combine neutrosophic sets using union (Set A ∨ Set B) to get total truth (T), indeterminacy (I), and falsity (F) values for each symptom/factor. (Table 6).
- Normalize the total values by dividing each (T, I, F) by the sum of all T values across symptoms/factors. This ensures values range from 0 to 1.

Table 6: Combined Neutrosophic Values for Symptoms/Factors and Comorbidities

Symptom/Factor	Set	Truth (T)	Indeterminacy (I)	Falsity (F)	Normalized Truth
Fever	A	0.8	0.1	0.1	0.2222
Cough	A	0.7	0.2	0.1	0.1944
Runny nose	A	0.6	0.3	0.1	0.1667
Sore throat	A	0.5	0.4	0.1	0.1389
Asthma history	B	0.7	0.2	0.1	0.1944
Allergy history	B	0.6	0.3	0.1	0.1667

Table 6 showcases neutrosophic sets used to analyze symptoms/factors and comorbidities while incorporating their relative importance through a normalized truth-value.

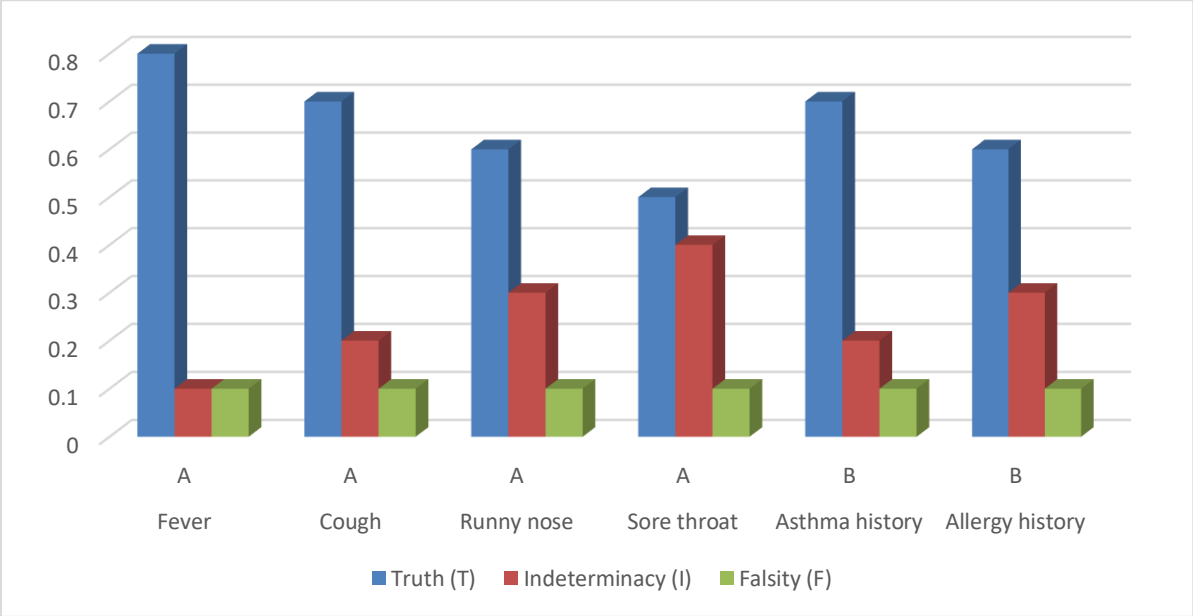

Graph 7: Distribution of Neutrosophic Truth Values for Symptoms/Factors and Comorbidities

Graph 7 Represent different symptoms, factors, and comorbidities (underlying medical conditions) relevant to a particular diagnosis.

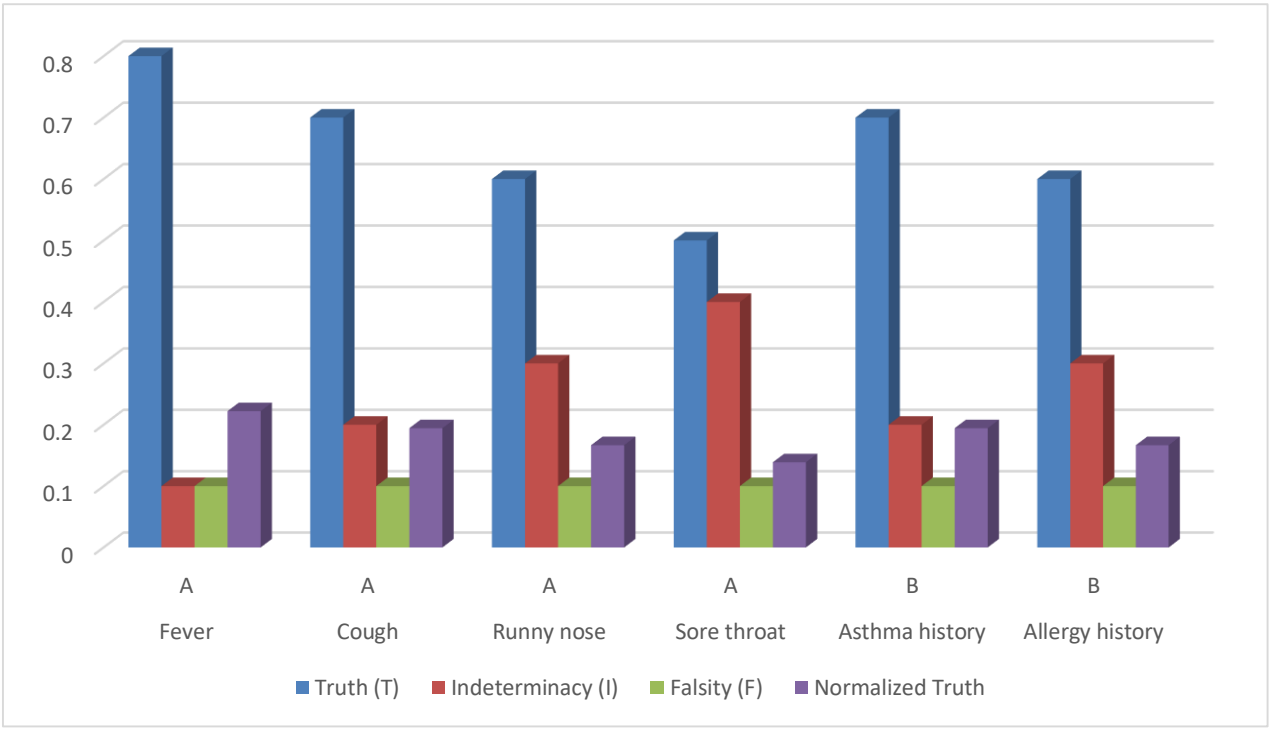

Graph 8: Normalized Truth Values of Symptoms/Factors for Diagnosis

Graph 8 focuses on the core relationship between symptoms/factors and a specific diagnosis using neutrosophic set theory. "Normalized" the truth-values.

Probability of Each Diagnosis (Di):

We can now use the normalized truth values from the combined neutrosophic sets (refer to the revised table) to calculate the probability of each potential diagnosis (Di). The formula is:

P (Di) = (Sum of normalized truth values for symptoms/factors related to Di) / (Sum of all normalized truth values)

This considers the contribution of each symptom/factor to a specific diagnosis.

Example with Three Diagnoses (D1, D2, D3):

- We will assume specific normalized truth-values are assigned to each diagnosis based on symptom/factor analysis (details on this assignment are not required here).
- Calculate the sum of all normalized truth-values (mentioned previously in the text).
- Calculate the probability of each diagnosis (Di) using the formula.

Interpretation and Conclusion:

- The calculated probabilities (P (D1), P (D2), P (D3)) indicate the likelihood of each diagnosis based on the neutrosophic analysis.
- This approach incorporates uncertainty and provides a more nuanced view compared to traditional methods that might only give yes/no answers.
- It is crucial to remember that neutrosophic statistics serve as a decision-making aid for doctors. A doctor's expertise and other diagnostic tests remain essential for informed conclusions about a patient's condition.

5. Discussing Neutrosophic Logic for Diagnosis

Neutrosophic logic offers a promising approach to medical diagnosis by handling inherent uncertainties. It allows us to represent symptoms and patient history factors using neutrosophic sets. These sets assign values for truth (degree of presence), indeterminacy (ambiguity), and falsity (degree of absence) for each factor.

*** Demonstrating Neutrosophic Operators:**

- Neutrosophic Union (∨): This operator combines sets, considering the maximum truth, indeterminacy, and falsity values. It represents the most optimistic scenario where all possibilities are considered.

- Neutrosophic Intersection (∧): This operator reflects the common ground between sets, using the minimum values for truth, indeterminacy, and falsity. It signifies the most conservative scenario with only overlapping elements considered.

In **Example:** We used two neutrosophic sets:

- Set A (Symptoms and Factors) representing symptoms a patient experiences.

- Set B (Possible Comorbidities) representing potential underlying conditions.

Important Note:

In this example, Set A and Set B have no overlapping elements (e.g., fever is not the same as asthma history). Therefore, the neutrosophic intersection results in an empty set. However, the neutrosophic union (Set A ∨ Set B) combines both sets, providing a comprehensive view of symptoms and potential comorbidities.

Next Steps: Calculating Diagnosis Probabilities

To calculate probabilities for various diagnoses based on the combined neutrosophic sets, we follow these steps:

1. Calculate Total Neutrosophic Values: Sum the truth, indeterminacy, and falsity values for each symptom/factor in the combined set (using union).

2. Normalize Values: Divide the values obtained in step 1 by the sum of all truth-values across symptoms/factors. This ensures values range from 0 to 1.

3. Calculate Diagnosis Probabilities: Use a formula involving normalized truth-values for symptoms/factors related to each potential diagnosis.

This approach provides a more nuanced view compared to traditional methods that might give binary (yes/no) answers. However, it's crucial to remember that neutrosophic statistics serve as a decision-making aid for doctors. A doctor's expertise and other diagnostic tests remain essential for reaching informed conclusions.

6. Conclusion

In conclusion, neutrosophic set-based algorithms hold great potential in addressing the challenges posed by uncertainty and imprecision in decision-making processes. By incorporating degrees of truth, indeterminacy, and falsity, these algorithms can effectively tackle complex real-world scenarios. The application of neutrosophic sets in medical diagnosis serves as a compelling example of their usefulness, particularly when dealing with uncertain data. However, it is essential to recognize the limitations of these algorithms and continue exploring ways to enhance their performance and applicability. The field of neutrosophic set-based decision-making algorithms has a promising future, with potential applications in various domains that involve imprecise data. As researchers and practitioners delve deeper into this area, the goal should be to refine the algorithms, expand their scope, and promote their adoption in diverse industries for more robust and accurate decision-making.

Acknowledgement

This research is supported by the Neutrosophic Science International Association (NSIA) in both of its headquarters at New Mexico University and its Iraqi branch at Telafer University, for more details about (NSIA) see the URL http://neutrosophicassociation.org/.

Conflicts of Interest: The authors declare no conflict of interest.

References

1. El-Hefenawy, N., Metwally, M. A., Ahmed, Z. M., & El-Henawy, I. M. (2016). A review on the applications of neutrosophic sets. Journal of Computational and Theoretical Nanoscience, 13(1), 936-944.
2. Tian, Z. P., Zhang, H. Y., Wang, J., Wang, J. Q., & Chen, X. H. (2016). Multi-criteria decision-making method based on a cross-entropy with interval neutrosophic sets. International Journal of Systems Science, 47(15), 3598-3608.
3. Radwan, N., Senousy, M. B., & Alaa El Din, M. (2016). Neutrosophic logic approach for evaluating learning management systems. Neutrosophic Sets and Systems, 3, 3-7.
4. Garg, H. (2016). An improved score function for ranking neutrosophic sets and its application to decision-making process. International Journal for Uncertainty Quantification, 6(5).
5. Hassan, M. H., Darwish, S. M., & Elkaffas, S. M. (2023). Type-2 Neutrosophic Set and Their Applications in Medical Databases Deadlock Resolution. Computers, Materials & Continua, 74(2).
6. Kavitha, B., Karthikeyan, S., & Maybell, P. S. (2012). An ensemble design of intrusion detection system for handling uncertainty using Neutrosophic Logic Classifier. Knowledge-Based Systems, 28, 88-96.

7. Premalatha, R., & Dhanalakshmi, P. (2023). Robust neutrosophic fusion design for magnetic resonance (MR) brain images. Biomedical Signal Processing and Control, 84, 104824.
8. Hawas, A. R., Ashour, A. S., & Guo, Y. (2019). Neutrosophic set in medical image clustering. In Neutrosophic Set in Medical Image Analysis (pp. 167-187). Academic Press.
9. Jayaraman, M., Vellingiri, K., & Guo, Y. (2019). Neutrosophic set in medical image denoising. In Neutrosophic Set in Medical Image Analysis (pp. 77-100). Academic Press.
10. Kaur, L., & Lal, M. (2020). Neutrosophic Sets and its Applications in Biomedical Image Processing: A Review. NeuroQuantology, 18(12), 85.
11. Yasser, I., Twakol, A., Abd El-Khalek, A. A., Samrah, A., & Salama, A. A. (2020). COVID-X: novel health-fog framework based on neutrosophic classifier for confrontation covid-19. Neutrosophic Sets and Systems, 35, 1-21.
12. Siri, S. K., & Latte, M. V. (2019). A novel approach to extract exact liver image boundary from abdominal CT scan using neutrosophic set and fast marching method. Journal of Intelligent Systems, 28(4), 517-532.
13. Shi, G. (2023). Diagnosis results of athletes with ankle joint pain based on the neutrosophic ensemble image. International Journal of Biomedical Engineering and Technology, 42(1), 78-95.
14. Smarandache, F. (2005) Neutrosophic Set, a Generalization of the Intuitionistic Fuzzy Sets. International Journal of Pure and Applied Mathematics, 24, 287-297.
15. Farag, R. M., Shams, M. Y., Aldawody, D. A., Khalid, H. E., El-Bakry, H. M., & Salama, A. A. (2024). Integration between Bioinformatics Algorithms and Neutrosophic Theory. Neutrosophic Sets and Systems, 66, 34-54.
16. Salama, A. A., Shams, M. Y., Khalid, H. E., & Mousa, D. E. (2024). Enhancing Medical Image Quality using Neutrosophic Fuzzy Domain and Multi-Level Enhancement Transforms: A Comparative Study for Leukemia Detection and Classification. Neutrosophic Sets and Systems, 65, 32-56.
17. Salama, A. A., Shams, M. Y., Elseuofi, S., & Khalid, H. E. (2024). Exploring Neutrosophic Numeral System Algorithms for Handling Uncertainty and Ambiguity in Numerical Data: An Overview and Future Directions. Neutrosophic Sets and Systems, 65, 253-295.
18. Alhabib, A., Alhabib, R., Khalid, H. E., & Salama, A. A. (2024). A Neutrosophic Study for the Transmission of Infection with Pathogenic Fungi from Males of Olive Fly Insects to Their Females. Neutrosophic Sets and Systems, 64, 38-45.
19. Salama, A. A., Tarek, Z., Darwish, E. Y., Elseuof, S., & Shams, M. Y. (2024). Neutrosophic Encoding and Decoding Algorithm for ASCII Code System. Neutrosophic Sets and Systems, 63, 105-129.
20. Essa, A. K., Sabbagh, R., Salama, A. A., Khalid, H. E., Aziz, A. A. A., & Mohammed, A. A. (2023). An Overview of Neutrosophic Theory in Medicine and Healthcare. Neutrosophic Sets and Systems, 61(1), 13.

Received: April 27, 2024. Accepted: Aug 24, 2024

NSS
Neutrosophic Sets and Systems, Vol. 72, 2024
University of New Mexico

The Principles of (Partial Locality, Partial Indeterminacy, Partial NonLocality) and (Multi Locality, Multi Indeterminacy, Multi NonLocality)

Florentin Smarandache[1,*]

[1] University of New Mexico; Mathematics, Physics, and Natural Science Division, Gallup, NM 87301, USA
* Correspondence: smarand@unm.edu

Abstract: This article introduces new neutrosophic principles aiming to extend and generalize the concepts of locality and nonlocality by addressing scenarios involving indeterminacy, together with partiality and multitude, in physics, mechanics, cosmology, biology, medicine, chemistry, economics, ecology, sociology. Locality refers to interactions or processes confined within a limited region of space or time. But there may be a Total (100%) Locality, or a Partial Locality (less than 100% and greater than 0%). The effects are constrained to the immediate environment. Contrariwise, NonLocality refers to interactions or connections between entities separated by space or time. The changes in one location have instantaneous effects on another. Similarly, there may be a Total (100%) NonLocality, or a Partial NonLocality (less than 100% and greater than 0%). Total (100%) or Partial (less than 100% and greater than 0%) Indeterminacy may arise from hidden variables and from environment. For instance, it may involve nonlocal connections between objects that are only partially entangled or influence each other in limited ways, rather than exhibiting complete freedom. The Principle of Partial Locality, Partial Indeterminacy, and Partial NonLocality implies an interplay of locality, indeterminacy, and nonlocality acting in a dynamic neutrosophic system. A generalization of (Locality, Indeterminacy, NonLocality) is the (MultiLocality, MultiIndeterminacy, MultiNonLocality). Practical examples from different fields are provided.

Keywords: locality, indeterminacy, nonlocality, multilocality, multiindeterminacy, multinonlocality, multiaction at a distance, universal gravitation, superposition, superluminal, quantum physics, quantum computing, quantum field theory, quantum information, quantum entanglement, Bell Inequality, hidden variables, dark energy, dark matter, electromagnetic forces, Bohmian mechanics, Copenhagen interpretation, cell (in biology), paracrine, CPU caches, Latent Dirichlet Allocation, curling, pollination, trophic cascade.

1. Introduction

Let's start by briefly discuss —with simple, quasi-random examples— the concepts of locality and non-locality, and then explain and illustrate some theoretical hidden variables parameters in scientific models.

In ecosystems, the interactions within and between ecosystems can show both local and nonlocal characteristics. Migratory species travel sometimes vast distances[1] between different ecosystems, yet their migration patterns connect those distant ecosystems, meaning their presence and behaviors have nonlocal effects and exert widespread consequences on food webs, predator-prey relationships, or nutrient cycling across regions, whilst daily interactions within a specific local habitat, such as

[1] In Tanzania's Serengeti region, plains animals, especially wildebeests (*Connochaetes taurinus*) and zebras, migrate over 1,600 kilometers (1,000 miles) seasonally [Dorst 2024].

feeding, mating, and nesting behaviors, are local.[2] Keystone species[3] have disproportionate effects on their ecosystems relative to their abundance.[4] This type of nonlocal effects (known as the 'trophic cascade'[5]) illustrate how changes in one species can ripple throughout the ecosystem, shaping environmental conditions and affecting other species that are far removed from the original source of change.

The effects of a collision between two objects are local to the region of contact. When two curling[6] stones[7] collide, the forces exerted and the resulting changes in motion are confined to the immediate area where they touch. Velocity and direction, as any other interactions and resulting effects, are purely local to the point of impact.[8]

The production of car parts in a local factory involves local labor, resources, and economic interactions. The final assembly of a car often involves sourcing parts from various countries. Disruptions in one part of the supply chain (e.g., a factory shutdown in one country) can have significant nonlocal effects, impacting production schedules and economic conditions in other parts of the world.[9]

Hidden variables are theoretical parameters or entities in scientific models that are not directly observable but are postulated to exist in order to explain certain phenomena [Kochen et al. 1975].

[2] Such as the herds of caribou (*Rangifer tarandus*) that settle during the summer in the barrens, which are relatively flat wastelands with sparse vegetation, while, in July, they begin an irregular southward migration, and they spend the winter in the taiga, where each herd moves according to local conditions, lacking a well-defined pattern [Dorst 2024].

[3] Elephants (*genus Loxodonta*), for example, are considered as "ecosystem engineers" because they modify their environment by dispersing seeds, uprooting trees, or creating water holes, stimulating "plant richness to peak (…), setting up a creative browsing-grazing tension and a patchwork of habitats" [Western et al. 2021].

[4] The reintroduction of gray wolves (*Canis lupus*) in Yellowstone National Park in 1995/1996 after a 70-year absence has led to cascading effects on the entire ecosystem, including the recovery of aspen trees, which provide habitats for birds and other species. Wolves are apex predators that hunt large herbivores like elk. By reducing elk populations, overgrazing is prevented, and vegetation is allowed to recover [Ripple et al. 2012; Farquhar 2023].

[5] American zoologist Robert Paine coined the term in 1980's to describe changes in food webs caused by manipulations of predators. Others employed the term to describe changes in aquatic ecosystems arising from factors such as sudden increases or dramatic declines in predatory fishes, caused, e.g., by overfishing [Carpenter 2023].

[6] Curling is an ice-played game akin to lawn bowls, where two teams – each consisting of four players – compete, sliding round stones across the ice toward a target (button). The stones are concave at the bottom and have a handle on top. The button is located at the center of a circle marked with concentric rings (house). The aim of the game is for each team to position their stones as close to the center as possible. For more info on this game, see Britannica – The Editors of Encyclopedia. "curling". Encyclopedia Britannica, 11 Apr. 2024, https://www.britannica.com/sports/curling. Accessed 26 June 2024.

[7] Curling regulations specify that a curling stone can weigh up to 20 kilograms, with most stones typically weighing between 17 and 20 kg. Additionally, the maximum permissible circumference of a stone is 36 inches (910 mm), while the minimum height is 4.5 inches (110 mm). The substantial weight allows the stone to glide the length of the rink without slowing down too soon.

[8] The curl distance for a curling stone, given a typical angular velocity (four rotations over 28.35 meters in 23 seconds, equivalent to 1.09 rad/s or 62.6°/s), ranges from approximately 0.5 to 1.5 meters when aimed at a circular target 28.35 meters away on ice. Various factors influence these curl distances, including the ice surface conditions (such as temperature, pebble density, and the size and shape of the pebbles) and the characteristics of the curling stones themselves. [Kameda et al. 2020]

[9] In recent decades, economic globalization has led to a substantial shift of manufacturing to regions with lower perceived costs, notably moving production to China and other Asian countries. Although this approach initially seemed economically sensible, its significant downsides have become apparent in the past three years. Consequently, many industries, especially the automotive sector, are now embracing a "local for local" production strategy, particularly with the shift towards electric vehicles. [Abuelsamid 2022]

Bohmian mechanics[10] offers an interpretation of quantum mechanics by introducing hidden variables to translate quantum phenomena "in an objective way using deterministic dynamics" [Dabin 2009, 40], unlike the standard inherently probabilistic Copenhagen interpretation. According to this theory, particles possess definite positions at all times even when unobserved. These positions are hidden variables guided by a "pilot wave" [Goldstein 2024]. Valentini has expanded this theory to incorporate signal nonlocality, enabling entanglement to function as an independent communication channel, and thus eliminating the need for a secondary classical "key" signal to "unlock" the message encoded in the entanglement [Valentini 1991, 2009].

Two concepts proposed in cosmology to explain observable phenomena such as galaxies' rotation curves and the universe's rapid expansion, and deduced from gravitational effects on visible stuff and the universe's large-scale structure, are *dark matter* and *dark energy*.[11] They are also hidden variables. The observable universe consists of *matter*, which occupies only 5% of the cosmos. The remaining 95% is made up of *dark matter* (27%) and *dark energy* (68%), mysterious substances still under investigation by scientists.[12] Normal matter, composed of protons, neutrons, and electrons, can be seen directly or through telescopes. Dark matter, however, does not interact with light, making it invisible.

Latent variables are employed to model topics in machine learning. Latent Dirichlet Allocation (LDA) is a three-level hierarchical Bayesian model that identifies hidden subjects in a set of documents. It depicts each item in a collection as a finite mixture over a set of topics, and each topic as an infinite mixture over a set of topic probabilities [Blei et al. 2003].

In the construction of measurement models for psychological data (psychometrics), *latent traits* —describing veiled psychological abilities or skills like motivation, or anxiety, so on— are hidden variables, being not immediately quantifiable, but only inferred from outcomes of genetic profiles and psychological tests. [Hambleton&Cook 1977, 75].

Certain *genetic mutations* (alterations) —that are are not readily visible, but can be found by genetic testing— raise the risk of an individual of developing cancer or other serious health issues.[13]

In the study of *infectious diseases*, *asymptomatic carriers* are individuals who harbor a pathogen without showing symptoms and can transmit the disease to others. The presence of these carriers is a hidden variable in epidemiological models, complicating efforts to track and control the spread of infections.[14]

2. The Principles of Locality, NonLocality, and Neutrosophic Locality

2.1. ***The Principle of Locality***

The Principle of Locality means that an object is influenced directly only by its immediate surroundings.

Let's briefly review a few cases from various fields.

[10] Also known as the de Broglie-Bohm theory, proposed by Louis de Broglie in 1927 and reshaped by David Bohm in 1952.

[11] The concepts were proposed in the 20th century by Fritz Zwicky, and confirmed by Vera Rubin in the 1970s.

[12] Percentages estimated by the European Space Agency (ESA), https://www.esa.int/Science_Exploration/Space_Science/What_are_dark_matter_and_dark_energy. Dark matter and dark energy stories are updated continuously on United States National Aeronautics and Space Administration (NASA) website, https://science.nasa.gov/universe/dark-matter-dark-energy/.

[13] See, for example, a case study about risks and mechanisms of cancer in women with inherited susceptibility to epithelial ovarian cancer [Shulman 2011].

[14] See, for example, a case study about Coronaviruses SARS-CoV, MERS-CoV, and SARS-CoV-2 in asymptomatic pediatric population [Aleebrahim-Dehkordi et al. 2021].

2.1.1. *Computer Science*: CPU Cache

In computer architecture, locality is a key principle in the design of memory hierarchies. For example, if a particular memory location is accessed, it is likely to be accessed again in the near future (this is called *temporal locality*). Also, if a particular memory location is accessed, nearby memory locations are likely to be accessed soon (and this is called *spatial locality*). CPU caches[15] exploit these principles by locally storing frequently accessed data, close to the processor, to minimize access time and improve performance.

2.1.2. *Biology: Cellular Processes*

Cell signaling often operates on a local level. For example, paracrine[16] signaling involves the release of signaling molecules[17] from one cell that affect nearby target cells. These molecules typically do not travel far from their point of release. Their effects are localized to the immediate cellular environment.

2.1.3. *Ecology: Habitat Interactions*

In many ecosystems, pollination[18] is a local process. Bees, butterflies, and other pollinators typically collect and transfer pollen within a specific area. The interactions between plants and their pollinators occur in close proximity, and the effects[19] are localized to that region [Kevan 2001; 2020].

2.1.4. *Medicine: Local Anesthesia*

Local anesthetics are used to numb a part of the body during minor surgical procedures. When a local anesthetic is administered, its effects are confined to the targeted area, blocking nerve signals and preventing pain in that specific region while the patient remains unaffected elsewhere.

2.1.5. *Chemistry: Chemical Reactions*

In a simple acid-base neutralization reaction,[20] the interactions and resultant effects (like the formation of water and salt) occur at the molecular level in the immediate vicinity where the reactants come into contact. The reaction is localized to the solution where the chemicals are mixed.

2.1.6. *Sociology: Community Dynamics*

Neighborhood Watch Programs[21] are examples of local initiatives where community members collaborate to monitor and improve safety within their immediate area. The actions and effects[22] of these programs are confined to the neighborhood level.

---

[15] A short but comprehensive introduction in CPU Cache offers *Britannica* – The Editors of Encyclopaedia. "cache memory". Encyclopedia Britannica, 20 May. 2021, https://www.britannica.com/technology/cache-memory. Accessed 23 June 2024.

[16] More on the paracrine control can be read on *Britannica* – Utiger, Robert D. "human endocrine system". Encyclopedia Britannica, 17 Apr. 2019, https://www.britannica.com/science/human-endocrine-system. Accessed 24 June 2024.

[17] Like growth factors.

[18] A basic but extended entry about pollination can be read here: The Editors of Scholarly Community Encyclopedia "Efficient Pollination Technology of Crops", https://encyclopedia.pub/entry/40852. Accessed 20 June 2024.

[19] Successful pollination and subsequent seed production.

[20] Such as mixing hydrochloric acid (HCl) with sodium hydroxide (NaOH).

[21] Read more about the US program and statistics of crime prevention through neighborhood collaboration on the National Neighborhood Watch (a Division of the National Sheriffs' Association) website: https://www.nnw.org.

[22] These would be reducing crime rates and increasing community cohesion.

2.1.7. *Economics: Local Markets*

Farmers' markets operate on a local scale, involving transactions between local farmers and consumers. The economic activities are confined to a specific geographic area, and the effects (exchange of goods, pricing, and consumer satisfaction) are localized to the community where the market takes place.

*2.2. **The Principle of Non-Locality***

The Principle of Non-Locality (Instantaneity), or Action at a Distance, means that an object is influenced by another object without being in physical contact (e.g., gravity, Colomb's Law, Electric Forces, and so on).

2.2.1. *Physics: Quantum Entanglement*

In quantum mechanics, entangled particles exhibit nonlocal behavior. When two particles become entangled, the state of one particle is directly related to the state of the other, regardless of the distance separating them. If you measure the spin of one entangled particle, the spin of the other particle is instantly known, even if they are light-years apart. This phenomenon has been experimentally confirmed and is a cornerstone of quantum mechanics, defying classical intuition.[23]

2.2.2. *Classical Physics: Gravitational and Electromagnetic Forces (pre-relativity)*

Gravitational and electromagnetic forces were thought to operate at a distance instantaneously prior to the postulation of relativity. Two masses exert an attractive force on one other regardless of distance, with no apparent intermediate impact, according to Newton's law of universal gravitation.[24] Equally, Coulomb's inverse-square law[25] is an experimental physical law that determines the amount of force between two electrically charged particles at rest.

2.2.3. *Computer Science: Blockchain Technology*

The verification and recording of transactions in blockchain systems demonstrates nonlocal interactions. Many nodes must validate a transaction that is broadcasted to the network. The consensus process[26] ensures that all nodes agree on the blockchain's current state. Proving nonlocality, the addition of a new block or other changes to the blockchain are immediately returned throughout the network.

2.2.5. *Genetics: Epigenetic Modifications*

Epigenetic changes[27] can have nonlocal effects across generations. Environmental factors like diet, stress, and exposure to toxins can cause epigenetic modifications that do not change the DNA sequence but affect gene expression. These changes can be passed down to offspring, influencing their development and health.

2.2.6. Ecology: Ecosystem Dynamics

Migrations of a vast numbers of individuals from diverse taxa occur worldwide. It plays a crucial role in transporting nutrients, and other organisms, as they forage and are preyed upon. The

[23] See, for example, a paper on the exploration of the relationship between quantum nonlocality and entanglement [Cao et al. 2023], or on quantum entanglement without nonlocal causation [Pettini 2023].

[24] Britannica, The Editors of Encyclopaedia. "Newton's law of gravitation". Encyclopedia Britannica, 12 Apr. 2024, https://www.britannica.com/science/Newtons-law-of-gravitation. Accessed 2 August 2024.

[25] Britannica, The Editors of Encyclopaedia. "Coulomb's law". Encyclopedia Britannica, 25 Jul. 2024, https://www.britannica.com/science/Coulombs-law. Accessed 2 August 2024.

[26] Such as *Proof of Work* or *Proof of Stake*, used to verify new cryptocurrency transactions [Napoletano 2023].

[27] Such as DNA methylation [Moore 2013].

movement of migrating species across extensive spatial scales influences the ecosystems through which these animals travel. Hidden variables include the genetic traits or physiological states of migratory species that determine their migration patterns and behavior. [Cohen et al. 2020], [Bauer et al. 2014], [Garcia et al. 2024]

2.3. Principle of Partial Locality, Partial Indeterminacy (because of the hidden variables that may influence the object), and Partial Non-Locality

We propose for the first time the Principle of Partial Locality, Partial Indeterminacy (because of the hidden variables that may influence the object), and Partial Non-Locality, which we call the Principle of Neutrosophic Locality.

The Aharonov-Bohm effect, which is a quantum mechanic phenomen, proved that: an electrically charged particle is affected by an electromagnetic potential that is totally outside of the particle (the particle being situated in a region where the intensity of the magnetic field is zero).

This Non-Locality event, first observed by the Soviets, was later on investigated by other secret services in order to control the Human Psyche from a distance.

The Action at a Distance may be:

i. Continuous action;
ii. Quantized action, or action by quantas, which are small subdivisions of physical processes and phenomena of a particular system.

We may call it infinitdecimally discrete action.

3. Degree of Locality, Degree of NonLocality, and Degree of Indeterminacy (neither Locality, nor NonLocality)

3.1. Degree of Locality

Locality means that an object is directly influenced only by its immediate surroundings. The Degree of Locality measures the degree to which a system or interaction follows this principle. A high degree of locality indicates that there is little to no effect from far-off particles or events, meaning that the interactions are very limited.

3.2. Degree of NonLocality

The phenomenon known as NonLocality describes the ability of particles that are distant in space to instantly display linked actions by a Degree of NonLocality in the system. Strong correlations between far-off particles or systems indicate a high degree of nonlocality.

3.3. Degree of Indeterminacy (neither Locality nor NonLocality)

There are situations when uncertainty or lack of definitive behavior falter in terms of locality and nonlocality, therefore the system does not exhibit clear characteristics of either local or nonlocal interactions. The Degree of Indeterminacy quantifies the degree to which the behavior of a system defies simple classification as exclusively local or completely nonlocal. When a system displays behaviors that are unclear, inconsistent, or that don't easily fit into the categories of locality or nonlocality, it is said to have a high degree of indeterminacy.

3.4. Measuring These Degrees

To quantify these degrees in practice, one typically relies on experimental setups that test the correlations between particles or systems, such as:

- **Bell Inequality Test** is a "real-world physics experiment designed to test the theory of quantum mechanics" against the concept of local realism[28]
- Theories of Local Hidden Variables aim "to attribute 'hidden' definite outcomes to any potential measurement on a quantum system" [Bertlman 2023]
- **Neutrosophic Statistical Analysis** [Smarandache 2013] evaluates indeterminacy by analyzing the variance and distribution of measurement outcomes to see if they defy categorization into local or nonlocal.

4. Recapitulation, generalization, and applications

Quantum Non-Locality states that a quantum particle instantaneously knows the state of – and correlates the behavior with – other quantum particle.

Quantum Entanglement asserts that two entangled particles correlate their behaviors simultaneously (therefore faster than light), as such our faster-than-light speed hypothesis has been confirmed.

John Clauser, an American physicist, in 1970's, and Alain Aspect, a French physicist, in 1980's, has proved that the entanglement is real, and, as a consequence, the superluminal speed is real.

Faraday said that some medium transmits the electrical force (not action at a distance).

Quantum Teleportation is the transfer from sender to receiver of quantum information, whose basic unit is the qubit.

The Copenhagen Interpretation of "wave-particle duality" that "the electron travels as a wave and is detected as a particle", and "an electron is in more places at the same time" are popular (mis)interpretations.

The behavior of a particle is described by a wave fluctuation (ψ) that has the shape of an equation.

The wave-particle duality is actually the indeterminate part of the neutrosophic form of the electron, because it fluctuates between – or is a superposition of – the opposites (wave vs. particle).

Locality (or Local Causality) was named by Bell; others called it later local realism.

Bell's Inequality: In Quantum Mechanics, when electrons are sent across the magnetic field, half of the electrons get deflected towards to the right, and the other held to the left.

Violation of Bell's Inequality: In Experiments the predictions of local realistic models disagree with those of quantum mechanics.

Realism means the assumption that measurement outcomes are well-defined prior to and independent of the measurements.

We now introduce for the first time Partial Locality Causality, Partial NonLocal Causality, and Partial Indeterminate Causality.

*

Partial Locality means that an object is influenced only partially by its immediate surroundings.

Similarly, Partial NonLocality means that an object is only partially influenced by another object without being in physical contact.

Partial Indeterminacy means that it is not clear that an object is influenced either by its immediate surroundings, or by another object without being in physical contact, or by both.

Such behavior is exhibited by an ambiguous, vague, incomplete, or inconsistent system.

*

Quantum Physics defy the Classical Physics, because the behavior of erattic atomic and subatomic particle.

The degrees of locality, nonlocality, and indeterminacy may be measured for each system, upon the interactions between touching objects (Locality), non-touching objects (NonLocality), and the influence of hidden variables (Indeterminacy) on these interferences.

[28] See *Scholarly Community Encyclopedia*, "Bell Test Experiments.". Available online: https://encyclopedia.pub/entry/36569 (accessed on 02 August 2024).

Quantum Physics: The correlation between particles can be tested by experiments. At the quantum level, the degree of NonLocality may be measured by checking in what degree the test results violate the Bell Inequalities.

Degree of Indeterminacy by using statistical analysis: comparing the means, mediums, standard deviations, variance, distributions of the outcomes.

Degree of Locality: Predictions versus real measurement outcomes. That may be compared to the models of hidden variables.

Entangled Particles: In quantum physics, the state of one particle has an instantaneous effect on the state of its entangled particle, no matter how far away they are of each other. This is NonLocality.

By measuring the spin of one particle, the spin of its entangled particle is immediately known, defying the classical physical intuition.

Epigenetics study the heritable traits, that do not change the DNA sequence, and may result from normal development or from environmental conditions, such as stress, tocins, diet, etc. DNA methylation, as a strong epigenetic change, has nonlocal effects across generations, therefore passed down to offsprings.

Ecosystems: The presence or absence of a species in an ecosystem has cascading effects on the whole chain of species in that ecosystem. These are NonLocal effects. Local effects: feeding, mating, nesting together, or predatory-prey relationships, or plants that are pollinated by insects. NonLocal and Local Effects occur by the interaction between the ecosystems. For examples, the whales travel long distances from a sea (or ocean) zone to another water zone, connecting various ecosystems (NonLocality). Similarly the migratory birds.

Blockchain Systems: Social Networks, Brain Networks (neuronal interactions), Financial/Economic/Commercial/Cultural/Political etc. Networks function as blockchain systems, where the NonLocal interactions facilitate the transactions between multiple nodes.

If two nodes are adjacent, the communication between them is Local, but for non-adjacent nodes it is a NonLocal interaction.

Each node has two types of functionalities: Local and NonLocal simultaneously.

In general, in an open system, its elements has practically local interactions, partially nonlocal interactions, partially indeterminate interaction when the hidden variables of the environment influence the decoherence process.

5. MultiAction at a Distance and (MultiLocality, MultiIndeterminacy, MultiNonLocality)

5.1. MultiNonLocality caused by MultiAction at a Distance in Newton's Law of Universal Gravitation and in Superposition

Electromagnetic and gravitational forces instantaneously act at a distance. Newton's Law of Universal Gravitation states that, in the universe, a particle attracts another particle with a force that is direct proportional with the product of their masses, and inversely proportional with the square of the distance between them.

For objects, their masses are considered concentrated at their centers of gravity.

$F = G \cdot \frac{m_1 m_2}{r^2}$,

where F = attraction force; G = the universal gravitational constant; m_1, m_2 = the masses of the two particles (or objects); r = the distance between the two particles (or objects).

Herein too, we have a MultiAction at a Distance, for example many objects at various altitudes starting to fall on the Eart at the same time. SO, the Earth has an action (attraction) at a distance on each object separately, or MultiNonLocality.

5.2. MultiNonLocality caused by MultiAction at a Distance in Superposition

The Superposition Principle enables us to calculate the force exerted on a charge by considering the effects of multiple other charges. To illustrate, let's consider three charged particles. Using Coulomb's Law, we can determine the force between any pair of these particles. According to the

Superposition Principle, the total force acting on any single charge is the vector sum of the individual forces exerted by each of the other charges, as if each of these charges were the only one present. This means that we add up the forces from each charge independently to find the overall force on the target charge.

5.3. Coulomb's Law in scalar form

The Coulomb's Law in scalar form is the following:

$$|F_{12}| = k_e \cdot \frac{|q_1| \cdot |q_2|}{r_{12}^2} = \frac{|q_1| \cdot |q_2|}{4\pi\varepsilon_0 \cdot r_{12}^2}$$

where F_{12} = the electrostatic (attractive or repulsive) force between point charges q_1 and q_2

q_1, q_2 = point charges

r_{12} = distance between charges q_1 and q_2

k_e = Coulomb's constant

$k_e = \frac{1}{4\pi\varepsilon_0}$, where ε_0 is the electric constant

$|\ |$ means absolute value.

Coulomb's Law states that the absolute value of electrostatic force between two charged particles (points) is directly proportional to the product of the magnitudes square of the distance between them (similar to the Newton's Law of Universal Gravitation).

Opposite charges attract each other, while the like charges repel each other.

5.4. Superposition Formula

For multiple charges, the total force on a particular charge is the vector sum of the forces exerted by all other charges.

$$F_i = k_e \sum j \neq i \frac{q_i q_j}{r_{ij}^2} \widehat{r_{ij}}$$

where r_{ij} is the unit vector from q_i and q_j.

The Law of Superposition is an extension of Coulomb's Law from two to three or more point charges, for linear bilateral networks.

On a single point charge many forces act from the other point charges:

Therefore, one has some multi-action at a distance, and correspondingly MultiNonLocality.

5.5. *MultiLocality* results from a group of things that touch and influence together two by two.

5.6. While *MultiIndeterminacy* is produced by hidden variables, unclear environments, uncertainty between many Local and NonLocal interactions, as a result of MultiActions locally and MultiActions at a Distance.

Conclusion

In this article, we introduced a new neutrosophic principle (The Principle of Partial Locality, Partial Indeterminacy, and Partial Non-Locality) that extends and generalizes the concepts of locality and nonlocality by addressing scenarios involving indeterminacy. Locality pertains to interactions confined within a limited space or time, with effects restricted to the immediate environment. In contrast, nonlocality refers to interactions between entities separated by space or time, where changes in one location instantly affect another without intermediaries. Indeterminacy involves hidden variables, such as nonlocal connections between partially entangled objects. This principle works within a dynamic neutrosophic system.

The Principle of Partial Locality, Partial Indeterminacy, and Partial NonLocality implies an interplay of locality, indeterminacy, and nonlocality acting in a dynamic neutrosophic system. A

generalization of (Locality, Indeterminacy, NonLocality) is the (MultiLocality, MultiIndeterminacy, MultiNonLocality).

MultiLocality results from a group of things that touch and influence together two by two. *MultiIndeterminacy* is produced by hidden variables, unclear environments, uncertainty between many Local and NonLocal interactions, because of MultiActions locally and MultiActions at a Distance. While *MultiNonLocality* is caused by a MultiAction at a Distance. Practical examples from different fields were provided.

References

[1] Abuelsamid, Sam (2022). "Local for Local Is the New Automotive Manufacturing Paradigm." *Guidehouse Insights*, Dec. 12, 2022. Retrieved from: https://guidehouseinsights.com/news-and-views/local-for-local-is-the-new-automotive-manufacturing-paradigm

[2] Aleebrahim-Dehkordi, Elahe; Soveyzi, Faezeh; Deravi, Niloofar; Rabbani, Zahra; Saghazadeh, Amene; Rezaei, Nima (2021). "Human Coronaviruses SARS-CoV, MERS-CoV, and SARS-CoV-2 in Children." *Journal of Pediatric Nursing* 56: 70-79, https://doi.org/10.1016/j.pedn.2020.10.020; Retrieved from: https://www.sciencedirect.com/science/article/pii/S088259632030631X

[3] Bauer, Silke; Hoye, Bethany J (2014). "Migratory Animals Couple Biodiversity and Ecosystem Functioning Worldwide." *Science* 344, 1242552. https://www.science.org/doi/10.1126/science.1242552

[4] Bertlmann, Reinhold A.; Friis, Nicolai (20230. 'Hidden-Variable Theories', *Modern Quantum Theory: From Quantum Mechanics to Entanglement and Quantum Information* (Oxford, 2023; online edn, Oxford Academic, 23 Nov. 2023), https://doi.org/10.1093/oso/9780199683338.003.0012. Accessed 1 Aug. 2024.

[5] Blei, David M.; Ng, Andrew Y.; Jordan, Michael I. (2003). "Latent Dirichlet Allocation." *Journal of Machine Learning Research 3:993-1022.* Retrieved from: https://www.jmlr.org/papers/volume3/blei03a/blei03a.pdf

[6] Cao, Hai-Qing; Zuo, Hui-Juan (2023). "Locally distinguishing nonlocal sets with entanglement resource." *Physica A: Statistical Mechanics and its Applications* 623, 128852; https://doi.org/10.1016/j.physa.2023.128852; Retrieved from: https://www.sciencedirect.com/science/article/pii/S0378437123004077

[7] Carpenter, Stephen (2023). "Trophic cascade." *Encyclopedia Britannica*, https://www.britannica.com/science/trophic-cascade

[8] Çevik, Ahmet; Topal, Selçuk; Smarandache, Florentin (2018). "Neutrosophic Logic Based Quantum Computing." *Symmetry* 10(11): 656; https://doi.org/10.3390/sym10110656

[9] Christianto, Victor; Florentin Smarandache, Florentin (2020). "A Review on Superluminal Physics and Superluminal Communication in light of the Neutrosophic Logic perspective." *International Journal of Neutrosophic Science* 6(2), 87-96; DOI: 10.5281/zenodo.3841630. Online at: https://fs.unm.edu/AReviewOnSuperluminal.pdf

[10] Cohen, E.B.; Satterfield, D.A. (2020). "'Chancing on a spectacle:' co-occurring animal migrations and interspecific interactions." *Ecography* 43: 1657-1671. https://doi.org/10.1111/ecog.04958

[11] Dabin, Robert (2009). "De Broglie-Bohm Theory: A Hidden Variables Approach to Quantum Mechanics." A thesis supervised by Dr. A. Valentini and submitted in part fulfilment of the requirements for the degree of Doctor of Philosophy in Physics of Imperial College London. Online at: https://www.imperial.ac.uk/media/imperial-college/research-centres-and-groups/theoretical-physics/msc/dissertations/2009/Robert-Dabin-Dissertation.pdf

[12] Dorst, Jean P. (2024). "Migration." *Encyclopedia Britannica*, https://www.britannica.com/science/migration-animal

[13] Farquhar, Brodie (2023). "Wolf Reintroduction Changes Ecosystem in Yellowstone: Wolves are causing a trophic cascade of ecological change, including helping to increase beaver populations and bring back aspen, and vegetation." Yellowstone National Park's website: https://www.yellowstonepark.com/things-to-do/wildlife/wolf-reintroduction-changes-ecosystem/?scope=anon

[14] Garcia Lorenzana, Giulia; Altieri, Ada; Biroli, Giulio (2024). "Interactions and migration rescuing ecological diversity." *PRX Life*, In press. hal-04444066, https://hal.science/hal-04444066/document

[15] Goldstein, Sheldon (2024). "Bohmian Mechanics." In Edward N. Zalta & Uri Nodelman (eds.): *The Stanford Encyclopedia of Philosophy*, https://plato.stanford.edu/archives/sum2024/entries/qm-bohm

[16] Hambleton, R. K.; Cook, L. L. (1977). "Latent Trait Models and Their Use in the Analysis of Educational Test Data." *Journal of Educational Measurement* 14(2):75–96. http://www.jstor.org/stable/1434009

[17] Kameda, T., Shikano, D., Harada, Y. et al. (2020) "The importance of the surface roughness and running band area on the bottom of a stone for the curling phenomenon." *Sci Rep* 10, 20637. https://www.nature.com/articles/s41598-020-76660-8

[18] Kevan, P. G. (2001). "Pollination: Plinth, pedestal, and pillar for terrestrial productivity. The why, how, and where of pollination protection, conservation, and promotion." In C. S. Stubbs & F. A. Drummond (Eds.), "Bees and crop pollination – Crisis, crossroads, conservation", pp. 7–68. Lanham: Entomological Society of America.

[19] Kevan, P., Silva, P.N. (2020). "Pollination and Agriculture." In: Starr, C. (eds) "Encyclopedia of Social Insects." Springer, Cham. https://doi.org/10.1007/978-3-319-90306-4_176-1

[20] Kochen, S., Specker, E.P. (1975). "The Problem of Hidden Variables in Quantum Mechanics." In: Hooker, C.A. (eds): *The Logico-Algebraic Approach to Quantum Mechanics*. The University of Western Ontario Series in Philosophy of Science, vol 5a. Springer, Dordrecht. https://doi.org/10.1007/978-94-010-1795-4_17

[21] Moore, L., Le, T. & Fan, G. (2013). "DNA Methylation and Its Basic Function." *Neuropsychopharmacol* 38, 23–38. https://doi.org/10.1038/npp.2012.112

[22] Napoletano, E. (2023) "Proof Of Stake Explained." In *Forbes Advisor*, Aug 25, 2023, https://www.forbes.com/advisor/investing/cryptocurrency/proof-of-stake/

[23] Pettini, M. (2023). "Quantum Entanglement without nonlocal causation in (3,2)-dimensional spacetime." https://arxiv.org/abs/2311.17070

[24] Ripple, William J.; Beschta, Robert L. (2012). "Trophic cascades in Yellowstone: The first 15years after wolf reintroduction." *Biological Conservation* 145(1): 205-213. https://doi.org/10.1016/j.biocon.2011.11.005

[25] Shulman, L.P.; Dungan J.S. (2010). "Cancer genetics: risks and mechanisms of cancer in women with inherited susceptibility to epithelial ovarian cancer." *Cancer Treat Res.* 156:69-85. DOI: 10.1007/978-1-4419-6518-9_6. PMID: 20811826; PMCID: PMC3086477. Online at: https://www.ncbi.nlm.nih.gov/pmc/articles/PMC3086477/

[26] Smarandache, Florentin (2004). "Quantum Causality Threshold and Paradoxes." *Draft work.* Online at: https://fs.unm.edu/ScArt/QuantumCausalityThreshold-PhysicalEssays.pdf

[27] Smarandache, Florentin (2004). "An Introduction to The Neutrosophic Probability Applied in Quantum Physics ." *Draft work.* Online at: https://fs.unm.edu/ScArt/Neutr-Prob-QuantumPhysics-new.pdf

[28] Smarandache, Florentin (2005). "Quantum Quasi-Paradoxes and Quantum Sorites Paradoxes." *Progress in Physics* 1, 7-8. Online at: https://fs.unm.edu/PP-01-02.pdf

[29] Smarandache, Florentin (2006). "Verifying Unmatter by Experiments, More Types of Unmatter, and a Quantum Chromodynamics Formula." *Infinite Energy* 67, 1-4. Online at: https://fs.unm.edu/PP-02-11.pdf

[30] Smarandache, Florentin (2013). "Introduction to Neutrosophic Measure, Neutrosophic Integral, and Neutrosophic Probability." Sitech - Education Publisher, Craiova - Columbus, 2013.

[31] Smarandache, Florentin (2014). "Introduction to Neutrosophic Statistics." https://digitalrepository.unm.edu/math_fsp/33

[32] Smarandache, Florentin (2015). "Superluminal Physics & Instantaneous Physics as New Trends in Research." *Bulletin of Pure and Applied Science*, Physics 34D(2), 81-84; DOI: 10.5958/2320-3218.2015.00009.3. Online at: https://fs.unm.edu/SuperluminalPhysics.pdf

[33] Smarandache, Florentin (2016). "Neutrosophic Quantum Computer." *International Journal of Fuzzy Mathematical Archive* 10(2), 139-145. Online at: https://archive.org/details/neutrosophic-quantum-computer

[34] Utiger, Robert D. (2019). "human endocrine system". *Encyclopedia Britannica*, https://www.britannica.com/science/human-endocrine-system.

[35] Valentini, Antony (1991). "Signal-Locality, Uncertainty and the Subquantum H-Theorem. II." *Physics Letters* A. 158 (1–2): 1-8. https://doi.org/10.1016/0375-9601(91)90330-B

[36] Valentini, Antony (2009). "Beyond the quantum." *Physics World* 22 (11): 32–37. https://arxiv.org/abs/1001.2758

[37] Western, David; N. Mose, N. Victor (2021). "Cascading effects of elephant-human interactions in a savanna ecosystem and the implications for ecology and conservation". A preprint in *bioRxiv* 2021.08.18.456886; DOI: https://doi.org/10.1101/2021.08.18.456886

[38] Wright, Jason (2001). "Superluminals and The Speed of Light." *Bulletin of Pure and Applied Science*, Physics 20D(2), 107-110. Online at: https://fs.unm.edu/Jason-Wright-superluminal.pdf

Received: April 29, 2024. Accepted: Aug 24, 2024

Neutrosophic Sets and Systems, Vol. 72, 2024
University of New Mexico

Implementation of Circle-Breaking Algorithm on Fermatean Neutrosophic Graph to discover Shortest Path

S. krishna Prabha [1], Said Broumi [2,3,*], Souhail Dhouib [4], Mohamed Talea[2]

[1] Department of Mathematics, PSNA college of Engineering and Technology, Dindigul, Tamil Nadu, India. krishna_praba@psnacet.edu.in
[2] Laboratory of Information Processing, Faculty of Science Ben M'Sik, University of Hassan II, Casablanca, Morocco. broumisaid78@gmail.com
[3] STIE team, Regional Center for the Professions of Education and Training (C.R.M.E.F), Casablanca- Settat, Morocco.
[4] Higher Institute of Industrial Management, University of Sfax, Tunisia. souh.dhou@gmail.com
* broumisaid78@gmail.com

Abstract: In many scientific domains, there is a growing interest in the shortest path problem. Traffic routes that can be precisely defined become arbitrary due to the damage that natural catastrophes inflict on roads and bridges. The truth membership, indeterminacy membership, and falsity membership of the component elements make up a neutrosophic set. Their axis of symmetry is indeterminacy membership, and it has a symmetric form. The neutrosophic number is a better way to express the edge distance in uncertain circumstances. With an edge distance stated using Fermatean neutrosophic numbers (**FrNN**), the study aims to solve the shortest path problem of the Fermatean neutrosophic graph. Additionally, the edge distance will be resolved based on the score and precise functions derived from the FrNN. In order to solve the shortest path problem and determine the shortest distance, the application of a circle-breaking algorithm is suggested.

Keywords: circle-breaking algorithm**;** neutrosophic graph**;** shortest path problem; Fermatean neutrosophic numbers**.**

1. Introduction

In many sectors, the Shortest Path Problem (SPP) is one of the most important and well-known problems, and it is the heart of network instabilities. Fuzzy numbers are useful in conventional problems where the node distance is supposed to be known. In these situations, the optimal solution can be obtained in an unknown setting. Calculating the minimum cost of a path for each vertex is known as single source SPP. Especially when trying to find the shortest way, finding the path with the fewest bends is crucial and will yield the greatest

outcomes.

Senapati et al. came up with the novel concept of the Fermatean fuzzy set [21, 22]. One of its constraints is that the total of the membership and non-membership grades' third powers cannot be equal to one. More spatial severity in the membership and non-membership grades allows Fermatean Fuzzy Sets (FFSs) to assist with unpredictability of data more successfully. Later on, they use FFSs to figure out a few techniques. A thorough examination of FFSs and its uses is given in reference. Thamizhendhi et al. [25] defined Fermatean Fuzzy Hyper-Graphs (FFHGs) and gave them many interpretations and characteristics. Operators on single-valued Neutrosophic graphs are investigated in the source material [6] by Talea et al. Furthermore, activities on Neutrosophic ambiguous graphs are clarified in [7].

The Bellman algorithm was suggested by Tan et al. [7]. Broumi used the original Bellman algorithm to find the shortest path from the start point to the end point. Broumi et al. [5] found the solution for an Isolated single valued neutrosophic graph. Tan [24] applied an improved dynamic programming algorithm to the SPP of a trapezoidal fuzzy medium intelligence graph, beginning the search from the end point, and the NN was not accurate during the operation process. Scoring function and accuracy function for the pentagonal NN's were applied to the SPP by Chakraborty [9].

The circle-breaking algorithm functions more effortlessly than the Dijkstra approach in order to tackle the least spanning tree problem of undirected graphs, Guan [15] invented the circle-breaking technique in 1975. Beginning with the original graph, the circle-breaking technique iteratively removes the longest edge within the closed circle until it yields a minimal spanning tree. Consequently, one edge of the longer of the two paths that create the closed circle can be constantly eliminated when this technique is applied to the directed neutrosophic graph, allowing any two points to be connected while disconnecting the considerably longer path. Numerous clarifications of neutroshopic sets and graphs are provided in [18,19,20] by various researchers. Ultimately, the algorithm resolves the neutrosophic graph's SPP. Lehua et al [17] explored the Shortest Path Trapezoidal Fuzzy Neutrosophic Graph with Circle-Breaking Algorithm. Amala et al [1], presented Modified Circle Breaking Algorithm to solve a Shortest Path Problem. Very recently, an innovative optimal technique entitled Dhouib-Matrix-SPP (DM-SPP) is invented by Dhouib in [11]. In addition, the DM-SPP is enhanced for cognitive mobile robot (using four and eight movement directions) by Dhouib in [12, 13, 14]. Zeng et al proposed an Islanding Algorithm of Distribution System with Distributed Generations based on Circle-breaking Algorithm [28].

In unidentified scenarios, it is customary to determine the edge distance utilizing the neutrosophic number. The investigation seeks to solve the shortest path difficulties of the Fermatean neutrosophic graph with an edge distance provided by Fermatean neutrosophic numbers (FrNN). For weighted, connected, and undirected graphs, the lowest cost spanning tree problem can be solved with the help of the circle-breaking algorithm. The edge distance will be resolved based on the score and precise functions derived from the FrNN. Furthermore, the SPP for directed graphs will be expanded, and the graphs will be examined in search of a closed circle

that connects the beginning and ending vertices. Until there are no more circles in the picture, the previous procedures are repeated after removing the final edge of the longer path. The ability to handle issues occurring in Fermatean neutrosophic graphs is what makes the proposed method new. The results of this study will be used to develop new frameworks and algorithms that will determine the optimal path for a given network in a variety of fixed contexts and neutrosophic environments in the future. The aforementioned method has relevance to all kinds of neutrosophic structures. This algorithmic rule can be implemented to machine learning, shipping, computerized systems, research facilities, manufacturing facilities, and other locales where shortest path explanations are crucial. The datasets evolved and/or scrutinized during this study are not exposed to the community at large.

The layout of this article is arranged systematically as follows: Introduction about the research work is given in section1.Section 2 provides some basic concepts of Fermatean neutrosophic numbers and graphs. In section 3, Circle-Breaking Algorithm is provided. In Section 4, a numerical example is deliberated. The conclusion of this research work is summarized in the last Section 5.

2. Preliminaries:

Definition: 2.1 [18]

Let X be a non-empty set (universe). The concept of Fermatean neutrosophic sets (FN sets) $\mathcal{N}$ on $\mathfrak{U}$ is an object that can be represented mathematically by A on x is of the following format: $A = \{(x, \acute{o}_P(x), \acute{\upsilon}_P(x), \acute{\omega}_P(x))/x \in X\}$, Where $\acute{o}_P(x), \acute{\upsilon}_P(x), \acute{\omega}_P(x) \in [0,1]$, $0 \le (\acute{o}_P(x))^3 + (\acute{\upsilon}_P(x))^3 \le 1$ and $0 \le (\acute{\omega}_P(x))^3 \le 1$.

Then $0 \le (\acute{o}_P(x))^3 + (\acute{\upsilon}_P(x))^3 + (\acute{\omega}_P(x))^3 \le 2$, $for\ all\ x\ in\ X$ $\acute{o}_P(x)$ is the degree of membership, $\acute{\upsilon}_P(x)$ is the degree of indeterminacy and $\acute{\omega}_P(x)$ is the degree of non-membership. Here $\acute{o}_P(x) and\ \acute{\upsilon}_P(x)$ are dependent components and $\acute{\omega}_P(x)$ is an independent component.

Definition: 2.2 [18]

Let X be a nonempty set and I the unit interval [0, 1]. A Fermatean neutrosophic sets K and L of the form $K = \{(x, \acute{o}_P(x), \acute{\upsilon}_P(x), \acute{\omega}_P(x))/x \in X\}$and $L = \{(x, \acute{o}_Q(x), \acute{\upsilon}_Q(x), \acute{\omega}_Q(x))/x \in X\}$. Then

1) $K^c = \{(x, \acute{o}_P(x), 1 - \acute{\upsilon}_P(x), \acute{\omega}_P(x)): x \in X\}$

2) $K \cup L = \{(x, \max(\acute{o}_P(x), \acute{o}_Q(x)), \min(\acute{\upsilon}_P(x), \acute{\upsilon}_Q(x)), \min(\acute{\omega}_P(x), \acute{\omega}_Q(x)): x \in X\}$

3) $K \cap L = \{(x, \min(\acute{o}_P(x), \acute{o}_Q(x)), \max(\acute{\upsilon}_P(x), \acute{\upsilon}_Q(x)), \max(\acute{\omega}_P(x), \acute{\omega}_Q(x)): x \in X\}$

Definition: 2.3 [18]

Let $P = (\acute{o}_P, \acute{\upsilon}_P, \acute{\omega}_P)$ and $Q = (\acute{o}_Q, \acute{\upsilon}_Q, \acute{\omega}_Q)$ be any two Fermatean neutrosophic numbers on a vertices on any graph G then the edge length from Q to P is defined as

$$\acute{O}_Q(u, v) = \min\{\acute{o}_P(u), \acute{o}_P(v)\}$$

$$\acute{\upsilon}_Q(u, v) = \min\{\acute{\upsilon}_P(u), \acute{\upsilon}_P(v)\}$$

$$\acute{\omega}_Q(u, v) = \min\{\acute{\omega}_P(u), \acute{\omega}_P(v)\}, \text{ if } \acute{o}_Q(u, v), \acute{\upsilon}_Q(u, v), \acute{\omega}_Q(u, v) \in [0,1]$$

Definition: 2.4 [18]

Let the vertices $\acute{o}_s(u,v)$, $\acute{\upsilon}_s(u,v)$, $\acute{\omega}_s(u,v)$ be Fermatean neutrosophic number then the score function is defined as

$$S = \frac{\acute{o}s(u,v)+\acute{\upsilon}s(u,v),+1-\acute{\omega}s(u,v)}{3} \quad (1)$$

Definition: 2.5 [20]

Let G = (V, E) be a graph which is an ordered pair a set of vertices (nodes or points) and a set of edges (links or lines), which an edge is associated with two distinct vertices.

Definition: 2.6 [20]

Any fuzzy relation μ: $S \times S \rightarrow [0,1]$ can be regarded as defining a weighted graph, or fuzzy graph, where the arc $(x, y) \in S \times S$, for all x, y in S has weight $\mu(X, Y) \in [0,1]$.

Definition: 2.7 [20]

A Neutrosophic graph is of the form $G^* = (V, \sigma, \mu)$ where $\sigma = (T_1, I_1, F_1)$ & $\mu = (T_2, I_2, F_2)$

(i) $V = \{v_1, v_2, v_3, \ldots v_n\}$ such that $T_1 : V \longrightarrow [0,1]$, $I_1 : V \longrightarrow [0,1]$ and $F_1 : V \rightarrow [0,1]$ denote the degree of truth-membership function, indeterminacy–membership function and falsity membership function of the vertex $v_1 \in V$ respectively and $0 \leq T_i(v) + I_i(v) + (v) \leq 3$, $\forall\, vi \in V$ (i = 1,2 , 3, … n).

(ii) $T_2 : V \times V \longrightarrow [0,1]$, $I_2 : V \times V \longrightarrow [0,1]$ and $F_2 : V \times V \rightarrow [0,1]$ where $T_2(v_i, v_j)$, $I_2(v_i, v_j)$ and $F_2(v_i, v_j)$ denote the degree of truth-membership function , indeterminacy –membership function and falsity-membership function of the edge (v_i, v_j) respectively such that for every edge (vi, vj),

$$T_2(, vj) \leq \min\{T_1(v_i), T_1(v_j)\},$$
$$I_2(, vj) \leq \min\{I_1(v_i), I_1(v_j)\},$$
$$F_2(, vj) \leq \max\{F_1(v_i), F_1(v_j)\},$$
$$\text{and } T_2(v_i, v_j) + I_2(v_i, v_j) + F_2(v_i, v_j) \leq 3$$

Definition: 2.8 [20]

A Fermatean fuzzy Graph (FFG) on a universal set X is a pair $\mathbb{G} = (\mathcal{P}, \mathcal{Q})$ where $\mathcal{P}$ is Fermatean fuzzy set on X and $\mathcal{Q}$ is a Fermatean fuzzy relation on X such that :

$\{_q(u, v) \leq \min\{T_{\mathcal{P}}(u), T_{\mathcal{P}}(v)\}$

$\{_q(u, v) \geq \max\{F_{\mathcal{P}}(u), F_{\mathcal{P}}(v)\}$ and

$0 \leq T_Q^3(u, v) + F_Q^3(u, v) \leq 1\ for\ all\ u, v \in X$, where , T_Q: $X \times X \rightarrow [0,1]$, F_Q: $X \times X \rightarrow [0,1]$ indicates degree of membership and degree of non-membership of $\mathcal{Q}$, correspondingly. Here $\mathcal{P}$ is the Fermatean fuzzy vertex set of $\mathbb{G}$ and $\mathcal{Q}$ is the Fermatean fuzzy edge set of $\mathbb{G}$.

Definition: 2.9 [20]

Let X be a universal set. A mapping $\mathcal{P} = (T_{\mathcal{P}},, F_{\mathcal{P}}) : X \times X \rightarrow [0,1]$ is called a Fermatean Neutrosophic relation on X such that $T_{\mathcal{P}}(u, v)$, $I_{\mathcal{P}}(u,v)$, $F_{\mathcal{P}}(u,v) \in [0,1]$ for all $u, v \in X$.

Definition: 2.10 [20]

Let $\mathcal{P} = (T_{\mathcal{P}}, I_{\mathcal{P}}, F_{\mathcal{P}})$ and $\mathcal{Q} = (T_{\mathcal{Q}}, I_{\mathcal{Q}}, F_{\mathcal{Q}})$ be Fermatean Neutrosophic sets on X if $\mathcal{Q}$ is Fermatean Neutrosophic relation on X, then $\mathcal{Q}$ is called a Fermatean Neutrosophic relation on $\mathcal{P}$ if $\{ T_{\mathcal{Q}}(u,v) \leq$

$\min\{T_{\mathcal{P}}(u), T_{\mathcal{P}}(v)\}$ $I_{\mathcal{Q}}(u,v) \geq \max\{I_{\mathcal{P}}(u), I_{\mathcal{P}}(v)\}$ $F_{\mathcal{Q}}(u,v) \geq \max\{F_{\mathcal{P}}(u), F_{\mathcal{P}}(v)\}$ if $T_{\mathcal{P}}(u, v)$, $I_{\mathcal{P}}(u, v)$, $F_{\mathcal{P}}(u,v) \in [0,1]$ for all $u, v \in X$.

Definition: 2.11 [20]

A Fermatean neutrosophic graph on a universal set X is a pair $\mathbb{G} = (\mathcal{P}, \mathcal{Q})$ where $\mathcal{P}$ is Fermatean Neutrosophic set on X and $\mathcal{Q}$ is a Fermatean Neutrosophic relation on X such that:

$$\begin{cases} T_Q(u,v) \leq \min\{T_p(u), T_p(v)\} \\ I_Q(u,v) \geq \max\{I_p(u), I_p(v)\} \\ F_Q(u,v) \geq \max\{F_p(u), F_p(v)\} \end{cases}$$

and $0 \leq T_Q^3(u, v) + T_Q^3(u, v) + T_Q^3(u, v) \leq 2$, for all $u, v \in X$

where , T_Q: x × x → [0,1], I_Q: x × x → [0,1] and F_Q:x × x → [0,1] indicates degree of membership, degree of indeterminacy-membership and degree of non-membership of Q, correspondingly. Here, P is the Fermatean Neutrosophic vertex set of G and Q is the Fermatean Neutrosophic edge set of G.

Definition: 2.12 [19]

Let $(\eta, \xi) \in N$, $L = \langle (\eta, \xi);\ T^\tau, I^\tau, F^\tau \rangle$, is a Fermatean neutrosophic normal number (FNNN), where its degree of truth, indeterminacy and falsity membership are defined, $T_L^T = T_L^T e^{-\left(\frac{x-\eta}{\xi}\right)^3}$, $T_L^I = T_L^I e^{-\left(\frac{x-\eta}{\xi}\right)^3}$, $T_L^F = 1 - (1 - T_L^F) e^{-\left(\frac{x-\eta}{\xi}\right)^3}$, $x \in X$ respectively, where x is a non empty set and $T^\tau, I^\tau, F^\tau \in [0,1]$ and $0 \leq T_L^T(x)^3 + T_L^I(x)^3 + T_L^F(x)^3 \leq 2$.

If $L_1 = \langle (\eta_1, \xi_1);\ T_1^T, T_1^I, T_1^F \rangle$, $L_2 = \langle (\eta_2, \xi_2);\ T_2^T, T_2^I, T_2^F \rangle$ be any two FNNNs and $\wedge$ be a positive integer, then

1. $L_1 \oplus L_2 = \left((\eta_1 + \eta_2, \xi_1 + \xi_2);\ \sqrt[3\wedge]{(T_1^T)^{3\wedge} + (T_2^T)^{3\wedge} - (T_1^T)^{3\wedge}(T_2^T)^{3\wedge}}, \right.$

$$\left. \sqrt[\wedge]{(T_1^I)^\wedge + (T_2^I)^\wedge - (T_1^I)^\wedge (T_2^I)^\wedge}, (T_1^F . T_2^F) \right) \quad (2)$$

2. $L_1 \otimes L_2 = (((\eta_1 . \eta_2, \xi_1 . \xi_2); (T_1^T, T_2^T), \sqrt[\wedge]{(T_1^I)^\wedge + (T_2^I)^\wedge - (T_1^I)^\wedge (T_2^I)^\wedge},$

$$\sqrt[3\wedge]{(T_1^F)^{3\wedge} + (T_2^F)^{3\wedge} - (T_1^F)^{3\wedge}(T_2^F)^{3\wedge}}) \quad (3)$$

3. $\wedge . L_1 = ((\wedge.\eta_1, \wedge.\xi_1);\ \sqrt[3\wedge]{1 - (1 - (T_1^T)^{3\wedge})^\wedge}, (T_1^I)^\wedge, (T_1^F)^\wedge) \quad (4)$

4. $L_1^\wedge = ((\eta_1^\wedge . \xi_1^\wedge); (T_1^T)^\wedge (T_2^T)^\wedge, \sqrt[3\wedge]{1 - (1 - (T_1^F)^{3\wedge})^\wedge}) \quad (5)$

Definition: 2.13 [19]

Let $L_1 = \langle (\eta_1, \xi_1);\ T_1^T, T_1^I, T_1^F \rangle$, $L_2 = \langle (\eta_2, \xi_2);\ T_2^T, T_2^I, T_2^F \rangle$ be any two FNNNs be the any two FrNN s. Then,

(i) The Euclidean distance between L_1 and L_2 is defined as $D_E(L_1, L_2)$, where

$$D_E(L_1, L_2) = \frac{1}{3}\sqrt[3]{\left(\frac{1+(T_1^T)^3+(T_1^I)^3-(T_1^F)^3}{3}\eta_1 - \frac{1+(T_2^T)^3+(T_2^I)^3-(T_2^F)^3}{3}\eta_2\right)^3 + \frac{1}{3}\left(\frac{1+(T_1^T)^3+(T_1^I)^3-(T_1^F)^3}{3}\xi_1 - \frac{1+(T_2^T)^3+(T_2^I)^3-(T_2^F)^3}{3}\xi_2\right)^3} \quad (6)$$

(ii) The Hamming distance between L_1 and L_2 is defined as $D_E(L_1, L_2)$, where

$$D_H(L_1, L_2) = \frac{1}{3}\sqrt[3]{\left|\frac{1+(T_1^T)^3+(T_1^I)^3-(T_1^F)^3}{3}\eta_1 - \frac{1+(T_2^T)^3+(T_2^I)^3-(T_2^F)^3}{3}\eta_2\right| + \frac{1}{3}\left|\frac{1+(T_1^T)^3+(T_1^I)^3-(T_1^F)^3}{3}\xi_1 - \frac{1+(T_2^T)^3+(T_2^I)^3-(T_2^F)^3}{3}\xi_2\right|} \quad (7)$$

3. Procedure for Solving SPP with Circle-Breaking Algorithm on Fermatean Neutrosophic Graph.

With the circle-breaking algorithm, the lowest cost spanning tree issue for weighted, linked, and undirected graphs can be tackled (see Figure 1). In addition, it will extend the SPP for directed graphs and explore the graphs for a closed circle that binds the starting and terminating vertices. After eliminating the last edge of the longer path, the preceding steps are repeated until there are no more circles in the figure.

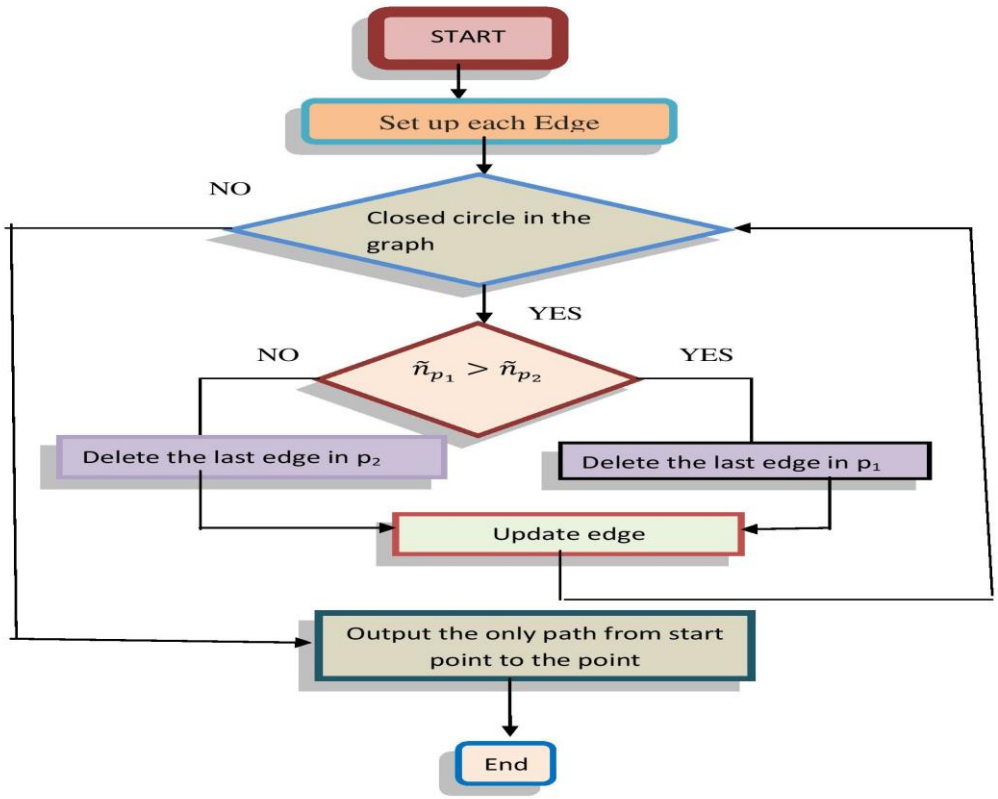

Figure 1: Procedure for Circle-Breaking Algorithm

The particular steps are outlined below,

Step 1: In the Fermatean neutrosophic graph, define a closed circle at random.

Then, determine the two pathways, p_1 and p_2, that encircle the closed circle.

These paths have a common starting node, N_0, and a common ending node, N_1.

Step 2: E v ery path's edges add up. The two pathways are then

represented by the trapezoidal fuzzy numbers $\tilde{n}_{p_1}$ and $\tilde{n}_{p_2}$.

Step 3: Determine the value of the scoring function.

Step 4: Employing the ranking function, correlate the sizes of S($\tilde{n}_{p_1}$)1 and S($\tilde{n}_{p_2}$), then

locate and eliminate.

4. Numerical Example:

Consider the Fermatean neutrosophic shortest path problem, with six nodes (see Figure 2).

Table 1. Details of edge information in terms of Fermatean neutrosophic numbers (FrNN).

Vertices	Fermatean neutrosophic number
(1,2)	<(0.2,0.4);0.3,0.7,0.5 >
(1,3)	<(0.1,0.3);0.5,0.3.0.8>
(2,4)	<(0.2,0.3);0.4,0.8,0.6>
(2,5)	<(0.3,0.4);0.6,0.5,0.7>
(3,4)	<(0.1,0.4);0.7,0.6,0.8>
(3,5)	<(0.2,0.3);0.9,0.6,0.5>
(4,6)	<(0.3,0.5);0.8,0.4,0.6>
(5,6)	<(0.1,0.2); 0.4,0.3,0.5>

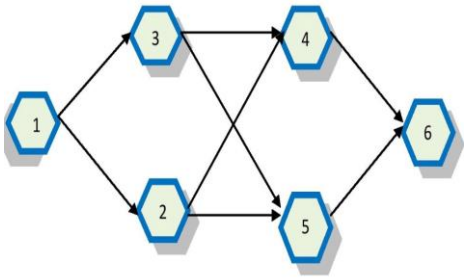

Figure 2: Fermatean neutrosophic graph.

The shortest path from ① to ⑥ is solved based on the circle-breaking algorithm. A circle is

randomly selected in the figure, the larger of the two paths surrounding the circle is determined, and the last edge of the circle is deleted. This process is repeated until no other circle can be found. Finally, the only path remaining from ① to ⑥ is the shortest path.

Step 1: Circle ①②④③① in Figure and paths

P_1= {(1,3),(3,4)} and P_2= {(1,2),(2,4)} that make up the closed circle, as indicated by the thick lines in Figure 3, are found.

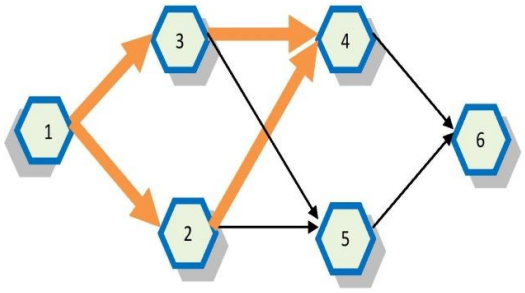

Figure 3: Closed circle ①②④③①

Step 2: According to Equation (2), all Fermatean neutrosophic edges of each path are summed, and the TrFNN of the two paths are obtained by determining and $\tilde{n}_{p_1}$and $\tilde{n}_{p_2}$.

$$\tilde{n}_{p_1} = \tilde{n}_{(1,2)} \oplus \tilde{n}_{(2,4)}$$

= <(0.2,0.4);0.3,0.7,0.5 > $\oplus$ <(0.2,0.3);0.4,0.8,0.6>

$=((0.2 + 0.2,0.4 + 0.3);\ \sqrt[3\wedge]{(0.3)^{3\wedge} + (0.4)^{3\wedge} - (0.3)^{3\wedge}(0.4)^{3\wedge}}$,

$$\sqrt[\wedge]{(0.7)^{\wedge} + (0.8)^{\wedge} - (0.7)^{\wedge}(0.8)^{\wedge}}, (0.5.0.6))$$

= ((0.4,0.7): $\sqrt[3]{(0.3)^3 + (0.4)^3 - (0.3)^3(0.4)^3}$,

$$\sqrt[\wedge]{(0.7)^1 + (0.8)^1 - (0.7)^1(0.8)^1}, (0.5.0.6))$$

= ((0.4, 0.7): $\sqrt[3]{0.027 + 0.064 - 0.027 * 0.064}$, $\sqrt[1]{0.7 + 0.8 - 0.7 * 0.8}, (0.5.0.6))$

= ((0.4, 0.7): $\sqrt[3]{0.027 + 0.064 - 0.001728}$, $\sqrt[1]{0.7 + 0.8 - 0.56}, (0.5.0.6))$

= ((0.4, 0.7) : $\sqrt[3]{0.089272}$, $\sqrt[1]{0.94}, (0.5.0.6))$

= ((0.4, 0.7) :0.45,0.97,0.3)

$\tilde{n}_{p_2} = \tilde{n}_{(1,3)} \oplus \tilde{n}_{(3,4)}$

= <(0.1,0.3);0.5,0.3.0.8> ⊕<(0.1,0.4);0.7,0.6,0.8>

$((0.1 + 0.1, 0.3 + 0.4);\ \sqrt[3\wedge]{(0.5)^{3\wedge} + (0.7)^{3\wedge} - (0.5)^{3\wedge}(0.7)^{3\wedge}}$,

$\sqrt[\wedge]{(0.3)^{\wedge} + (0.6)^{\wedge} - (0.3)^{\wedge}(0.6)^{\wedge}}, (0.8.0.8))$

= ((0.2,0.7): $\sqrt[3]{(0.5)^3 + (0.7)^3 - (0.5)^3(0.7)^3}$,

$\sqrt[\wedge]{(0.3)^1 + (0.6)^1 - (0.3)^1(0.6)^1}, (0.8.0.8))$

= ((0.2,0.7): $\sqrt[3]{0.125 + 0.343 - 0.125 * 0.343}$, $\sqrt[1]{0.3 + 0.6 - 0.3 * 0.6}, (0.8.0.8))$

= ((0.2, 0.7): $\sqrt[3]{0.125 + 0.343 - 0.042875}$. $\sqrt[1]{0.3 + 0.6 - 0.18}, (0.8.0.8))$

= ((0.2, 0.7) : $\sqrt[3]{0.425125}$, $\sqrt[1]{0.72}, (0.8.0.8))$

= ((0.2, 0.7) : 0.75 , $0.85, 0.64)$

Step 3: The Score function of is given by S = $\frac{T+I+1-F}{3}$

$\tilde{n}_{p_1}$= ((0.4, 0.7) : 0.45,0.97,0.3)

S_{p_1} = $\frac{0.45+0.97+1-0.3}{3}$ =$\frac{2.12}{3}$ = 0.71

$\tilde{n}_{p_2}$= ((0.2, 0.7) : 0.75 , $0.85, 0.64)$

S_{p_2} = $\frac{0.75+0.85+1-0.64}{3}$ =$\frac{1.96}{3}$ = 0.653

Step 4: Because S_{p_1}>S_{p_2} , $\tilde{n}_{p_1} > \tilde{n}_{p_2}$according to Definition 7. Thus, by deleting the last edge, (3, 4), in p1, the Fermatean neutrosophic graph in Figure. 4 can be obtained.

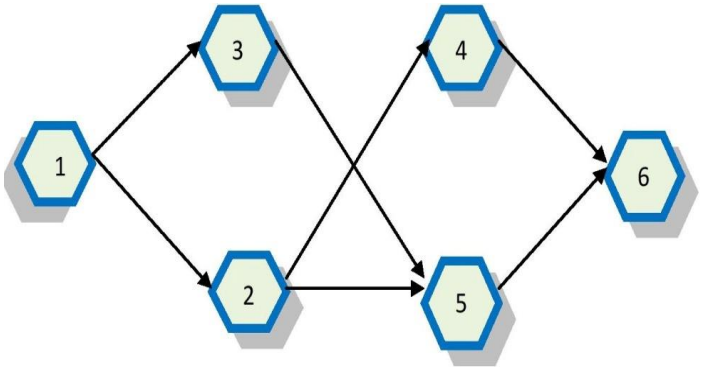

Figure 4: Removal of edge (3, 4).

Step 5: Closed circle ①②⑤③① in Figure 4 is selected, and paths P_3 = {(1,3),(3,5)} and P_4 ={(1,2),(2,5)} that make up the closed circle, as indicated by the thick lines in Figure 5, are obtained. Once this task is completed, we return to Step 2.

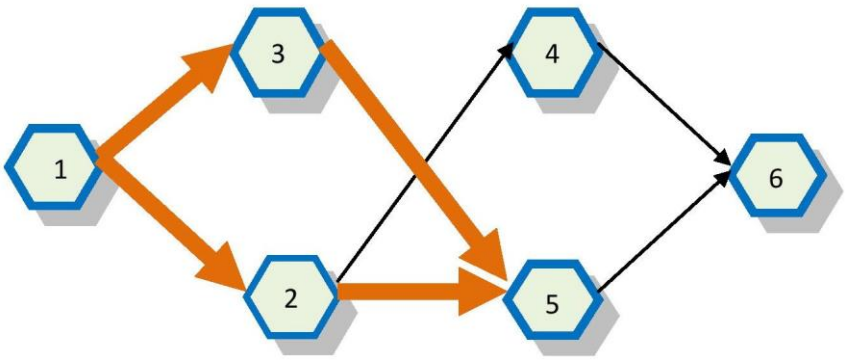

Figure 5: Closed circle ①②⑤③①

Step 6: According to Equation (2), all neutrosophic edges of each path are summed, and the FrNN of the two paths are obtained by determining $\tilde{n}_{p_3}$ and $\tilde{n}_{p_4}$.

$\tilde{n}_{p_3} = \tilde{n}_{(1,3)} \oplus \tilde{n}_{(3,5)}$

= <(0.1,0.3);0.5,0.3.0.8> $\oplus$ <(0.2,0.3);0.9,0.6,0.5>

= $((0.1 + 0.2, 0.3 + 0.3);\ \sqrt[3\wedge]{(0.5)^{3\wedge} + (0.9)^{3\wedge} - (0.5)^{3\wedge}(0.9)^{3\wedge}}$,

$\sqrt[\wedge]{(0.3)^{\wedge} + (0.6)^{\wedge} - (0.3)^{\wedge}(0.6)^{\wedge}}, (0.8.0.5))$

=$((0.3,0.6):\ \sqrt[3]{(0.5)^3 + (0.9)^3 - (0.5)^3(0.9)^3}$,

$\sqrt[\wedge]{(0.3)^1 + (0.6)^1 - (0.3)^1(0.6)^1}, (0.8.0.5))$

= ((0.3,0.6): $\sqrt[3]{0.125 + 0.729 - 0.125 * 0.729}$, $\sqrt[1]{0.3 + 0.6 - 0.3 * 0.6}, (0.8.0.5))$

= ((0.3,0.6): $\sqrt[3]{0.125 + 0.729 - 0.091125}$, $\sqrt[1]{0.3 + 0.6 - 0.18}, (0.8.0.5))$

= ((0.3,0.6) : $\sqrt[3]{0.7629}$, $\sqrt[1]{0.72}, (0.8.0.5))$ = $((0.3,0.6): 0.914 , 0.85, 0.40)$

$\tilde{\eta}_{p_4} = \tilde{\eta}_{(1,2)} \oplus \tilde{\eta}_{(2.5)}$

= <(0.2,0.4);0.3,0.7,0.5 >$\oplus$ <(0.3,0.4);0.6,0.5,0.7>

$((0.2 + 0.3,0.4 + 0.4);\ \sqrt[3\wedge]{(0.3)^{3\wedge} + (0.6)^{3\wedge} - (0.3)^{3\wedge}(0.6)^{3\wedge}}$,

$\sqrt[\wedge]{(0.7)^{\wedge} + (0.5)^{\wedge} - (0.7)^{\wedge}(0.5)^{\wedge}}, (0.5.0.7))$

= ((0.5,0.8): $\sqrt[3]{(0.3)^3 + (0.6)^3 - (0.3)^3(0.6)^3}$,

$\sqrt[\wedge]{(0.7)^1 + (0.5)^1 - (0.7)^1(0.5)^1}, (0.5.0.7))$

= ((0.5,0.8): $\sqrt[3]{0.027 + 0.216 - 0.027 * 0.216}$, $\sqrt[1]{0.7 + 0.5 - 0.7 * 0.5}, (0.5.0.7))$

= ((0.5,0.8): $\sqrt[3]{0.027 + 0.216 - 0.027 * 0.216}$, $\sqrt[1]{0.7 + 0.5 - 0.7 * 0.5}, (0.5.0.7))$

= ((0.5,0.8) : $\sqrt[3]{0.237}$, $\sqrt[1]{0.85}, (0.5.0.7))$ = $((0.5, 0.8) : 0.62, 0.92, 0.35)$

Step 7: The Score function of is given by S = $\frac{T+I+1-F}{3}$

$\tilde{\eta}_{p_3}$= $((0.3,0.6): 0.91 , 0.85, 0.40)$, $S_{p_3} = \frac{0.91+0.85+1-0.40}{3} = \frac{2.36}{3} = 0.79$

$\tilde{\eta}_{p_4}$= $((0.5, 0.8) : 0.62, 0.92, 0.35)$. $S_{p_4} = \frac{0.62+0.92+1-0.35}{3} = \frac{2.19}{3} = 0.73$

Step 8: Because $\tilde{\eta}_{p_3} > \tilde{\eta}_{p_4}$, $S_{p_3} > S_{p_4}$can be obtained according to Definition 7. Thus, by deleting the last edge, (3, 5), in p3, the Fermatean neutrosophic graph depicted in Figure 6 can be obtained.

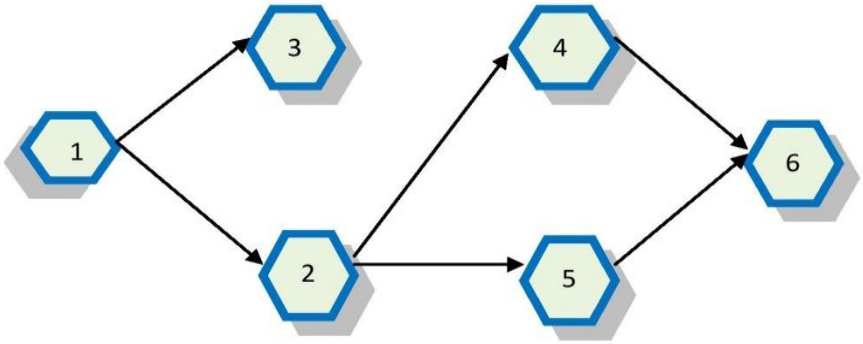

Figure 6: Removal of edge (3, 5)

Step 9: Another closed circle ②④⑥⑤② in Figure 6 is identified, such that paths P_5 ={(2,4),(4,6)} and P_6={(2,5),(5,6)} make up a closed circle, as indicated by the thick lines in Figure 7. Once this task is completed, we return to Step 2.

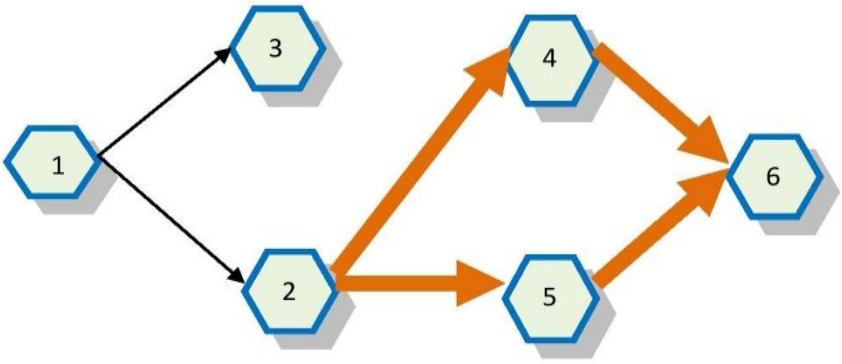

Figure 7: Closed circle ②④⑥⑤②.

Step 10: According to Equation (5), all Fermatean neutrosophic edges of each path are summed, and the FrNN of the two paths are obtained by computing $\tilde{\eta}_{P_5}$ and $\tilde{\eta}_{P_6}$.

$\tilde{\eta}_{P_5} = \tilde{\eta}_{(2,4)} \oplus \tilde{\eta}_{(4,6)}$

<(0.2,0.3);0.4,0.8,0.6>$\oplus$ <(0.3,0.5);0.8,0.4,0.6>

$= \left(\left(0.2+0.3, 0.3+0.5\right); \sqrt[3\wedge]{(0.4)^{3\wedge}+(0.8)^{3\wedge}-(0.4)^{3\wedge}(0.8)^{3\wedge}}\right.,$

$\left.\sqrt[\wedge]{(0.8)^{\wedge}+(0.4)^{\wedge}-(0.8)^{\wedge}(0.4)^{\wedge}}, (0.6.0.6)\right)$

$= ((0.5,0.8): \sqrt[3]{(0.4)^3+(0.8)^3-(0.4)^3(0.8)^3}\ ,$

$\sqrt[\wedge]{(0.8)^1+(0.4)^1-(0.8)^1(0.4)^1}, (0.6.0.6))$

$= ((0.5,0.8): \sqrt[3]{0.064+0.512-0.064*0.512}\ ,\ \sqrt[1]{0.8+0.4-0.8*0.4}, (0.6.0.6)$

$= ((0.5, 0.8): \sqrt[3]{0.064+0.512-0.0328}\ ,\ \sqrt[1]{0.8+0.4-0.32}, (0.6.0.6))$

= ((0.5, 0.8) : $\sqrt[3]{0.543}$, $\sqrt[1]{0.88}$, (0.6.0.6)) = ((0.5, 0.8) : 0.82,0.94, 0.36)

$\tilde{\eta}_{P_6} = \tilde{\eta}_{(2.5)} \oplus \tilde{\eta}_{(5.6)}$

= <(0.3,0.4);0.6,0.5,0.7>$\oplus$ <(0.1,0.2); 0.4,0.3,0.5>

$((0.3 + 0.1, 0.4 + 0.2);\ \sqrt[3\wedge]{(0.6)^{3\wedge} + (0.4)^{3\wedge} - (0.6)^{3\wedge}(0.4)^{3\wedge}}$,

$\sqrt[\wedge]{(0.5)^{\wedge} + (0.3)^{\wedge} - (0.5)^{\wedge}(0.3)^{\wedge}}, (0.7.0.5))$

=((0.4,0.6): $\sqrt[3]{(0.6)^3 + (0.4)^3 - (0.6)^3(0.4)^3}$,

$\sqrt[\wedge]{(0.5)^1 + (0.3)^1 - (0.5)^1(0.3)^1}, (0.7.0.5))$

= ((0.4,0.6): $\sqrt[3]{0.216 + 0.064 - 0.216 * 0.064}$,

$\sqrt[1]{0.5 + 0.3 - 0.5 * 0.3}, (0.7.0.5))$

= ((0.4, 0.6): $\sqrt[3]{0.216 + 0.064 - 0.014}$,$\sqrt[1]{0.5 + 0.3 - 0.15}, (0.7.0.5))$

= ((0.4, 0.6) : $\sqrt[3]{0.266}$, $\sqrt[1]{0.65}$, (0.7.0.5)),

= ((0.4, 0.6) : 0.64 , 0.81, 0.35)

The Score function of is given by S = $\frac{T+I+1-F}{3}$

$\tilde{\eta}_{P_5}$= ((0.5, 0.8) : 0.82,0.94, 0.36)

$S_{P_5} = \frac{0.82+0.94+1-0.36}{3} = \frac{2.4}{3} = 0.8$

$\tilde{\eta}_{P_6}$= ((0.4, 0.6) : 0.64 , 0.81, 0.35)

$S_{P_6} = \frac{0.64+0.81+1-0.35}{3} = \frac{2.1}{3} = 0.7$

Step 11: Because $S(\tilde{\eta}_{P_5}) > S(\tilde{\eta}_{P_6})$, according to Definition 7, we can obtain $\tilde{\eta}_{P_5} > \tilde{\eta}_{P_6}$. The last edge, (4, 6), in P_5 is deleted, and the Fermatean neutrosophic graph is obtained, as depicted in Figure 8.

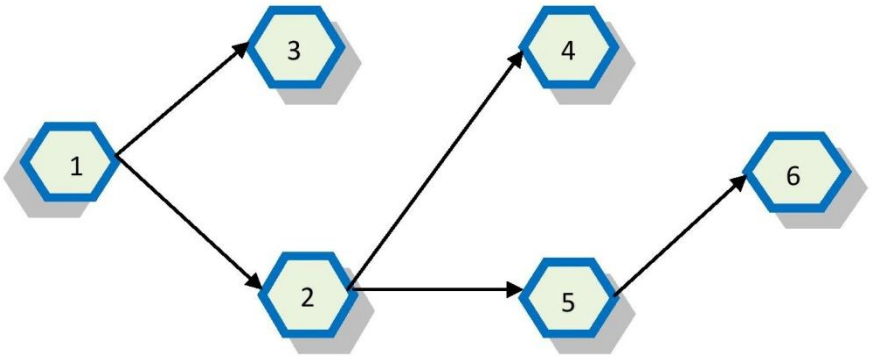

Figure 8: Removal of edge (4, 6)

Step 12: In the Fermatean neutrosophic graph illustrated in Figure 8, it is no longer possible to find a closed circle and the circle-breaking algorithm ends. As indicated by the dotted line in Figure 9, only one path exists from starting node 1 to ending node 6, which is the shortest path sought.

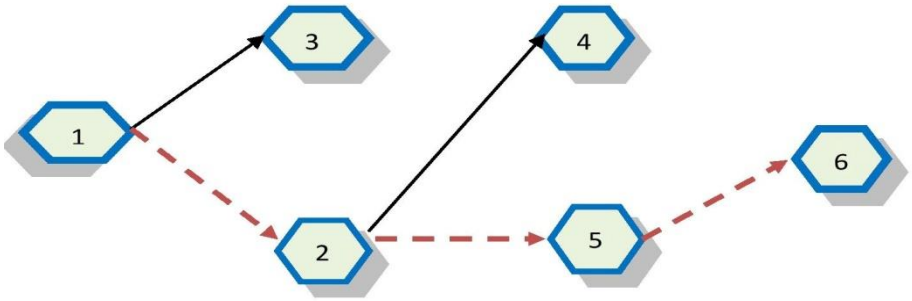

Figure 9: Shortest Path

5. Conclusion:

Circle-breaking algorithm is applied in this paper to fix the SPP of a Fermatean neutrosophic graph, and we utilized an example to confirm the algorithm's viability. The suggested framework may be expanded upon and enhanced in the future to enable it to figure out the distance or shortest path between two locations on a map that depicts various kinds of networks. This paper concludes that it has painstakingly developed a sound theoretical framework, pointing out the shortcomings of the existing methods and emphasizing the need for Fermatean neutrosophic numbers. Trigonometric similarities and more distance measurements can be presented in the future, and many real-world decision-making issues can be resolved.

Funding: This research received no external funding.

Acknowledgments: The author is grateful to the editorial and reviewers, as well as the correspondent author, who offered assistance in the form of advice, assessment, and checking during the study period.

Conflicts of Interest: The authors declare no conflict of interest.

References

1. Amala S., Richard, A.Rajkumar, D.Nagarajan, Broumi Said, Shortest Path Problem on

Neutrosophic Environment using Modified Circle Breaking Algorithm, *International Journal of Neutrosophic Science (IJNS) ,Vol. 18, No. 04, PP. 385-394, 2022*.

2. Atanassov K., Intuitionistic fuzzy sets, *Fuzzy Sets and Systems 20: 87-96, 1986*.
3. Aydın, S., A Fuzzy MCDM Method Based on New Fermatean Fuzzy Theories. In *International Journal of Information Technology & Decision Making (pp. 1–22). World Scientific Pub Co Pte Lt. https://doi.org/10.1142/s021962202150019x .2021.*
4. Barraza, R., Sepúlveda, J. M., & Derpich, I., Application of Fermatean fuzzy matrix in codesign of urban projects, *Procedia Computer Science, Vol. 199, pp. 463–47.2022.*
5. Broumi S., Bakali A., Talea M., Smarandache F., Isolated single valued neutrosophic graphs. *Neutrosophic Sets Systems, 11, pp.74–78, 2016b.*
6. Broumi S., Talea M., Bakali A., Smarandache F, Single valued neutrosophic graphs. *J New Theory, 10, pp.86–101, (2016a).*
7. Broumi, S., Dey, A., Talea, M., Bakali, A., Smarandache, F.Nagarajan, D. Lathamaheswari, M.Kumar, R., Shortest path problem using Bellman algorithm under neutrosophic environment. *Complex Intell. Syst. 5*, 409–416, 2019.
8. Broumi, S., krishna P., Fermatean Neutrosophic Matrices and Their Basic Operations. *Neutrosophic Sets and Systems 58, 1,35, 2023. https://digitalrepository.unm.edu*
9. Chakraborty, A., Application of Pentagonal Neutrosophic Number in Shortest Path Problem. *Int. J. Neutrosophic Sci*, *3*, 21–28, 2020.
10. Deng, Z., Wang, J., Evidential Fermatean fuzzy multicriteria decision-making based on Fermatean fuzzy entropy. *In International Journal of Intelligent Systems, Vol. 36, Issue 10, pp. 5866–5886, 2021.Wiley.* https://doi.org/10.1002/int.22534.
11. Dhouib, S., An optimal method for the Shortest Path Problem: The Dhouib-Matrix-SPP (DM-SPP*), Results in Control and Optimization, Vol. 12, ID: 100269,* 2023, *DOI: 10.1016/j.rico.2023.100269.*
12. Dhouib, S., Shortest Path Planning via the Rapid Dhouib-Matrix-SPP (DM-SPP) Method for the Autonomous Mobile Robot. *Results in Control and Optimization, Vol. 13*, ID: 100299, 2023, DOI: 10.1016/j.rico.2023.100299.
13. Dhouib, S., Faster than Dijkstra and A* Methods for the Mobile Robot Path Planning Problem Using Four Movement Directions: The Dhouib-Matrix-SPP-4. *Advances in Transdisciplinary Engineering, Mechatronics and Automation Technology*, Vol. 46, pp. 284-290, 2024, DOI: 10.3233/ATDE231116.
14. Dhouib, S., Intelligent Path Planning for Cognitive Mobile Robot Based on Dhouib-Matrix-SPP Method. *Cognitive Robotics, Vol. 4:62-73, 2024 DOI: 10.1016/j.cogr.2024.02.001.*
15. Guan, M.G., Algorithm of breaking circle for minimum tree. *J. Math. Pract. Theory*, *4*, 40–43, 1975.
16. Gul, M., Lo, H.-W., & Yucesan, M., Fermatean fuzzy TOPSIS-based approach for occupational risk assessment in manufacturing. *In Complex & Intelligent Systems ,Vol. 7, Issue 5, pp. 2635–2653,2021.*
17. Lehua, Y., Dongmei, L., Ruipu, T., Shortest Path Solution of Trapezoidal Fuzzy

Neutrosophic Graph Based on Circle-Breaking Algorithm,*Symmetry*, 12,1-20, doi:10.3390/sym12081360, 2020.

18. Raut P.K., Behera. S.P, Broumi. S., Mishra, D., Calculation of shortest path on Fermatean Neutrosophic Networks, *Neutrosophic Sets and Systems*, Vol. 57, 2023.
19. Palanikumar, M., Arulmozhi, K., Santanu, A., MADM Approach For Fermatean Neutrosophic Normal Aggregation Operator Framework, arXiv:2206.03700v1 [math.GM] 8 Jun 2022.
20. Broumi, S., Sundareswaran, R., Shanmugapriya, M., Bakali, A., Talea, M., Theory and Applications of Fermatean Neutrosophic Graphs, *Neutrosophic Sets and Systems, Vol. 50, 2022*
21. Senapati, T., Yager, R., Fermatean Fuzzy Sets, *Journal of Ambient Intelligence and Humanized Computing , 11, pp. 663-674, 2019.*
22. Senapati, T., Yager, R., Some New Operations Over Fermatean Fuzzy Numbers and Application of Fermatean Fuzzy WPM in Multiple Criteria Decision Making. *In Informatica , Vol. 30, Issue 2, pp. 391–412, 2019.*
23. Smarandache, F., A unifying field in logics neutrosophy: neutrosophic probability, set and logic, *American Research Press, Rehoboth 1998.*
24. Tan, R.P., Zhang, W.D., Broumi, S., Solving methods for the shortest path problem based on trapezoidal fuzzy neutrosophic numbers. *Control Decis.*, *34*, 851–860,2019.
25. Thamizhendhi, G., Kiruthica, C., Suresh, S., Fermatean fuzzy hypergraph,*Journal of Hunan University Natural Sciences, Vol. 48. No. 12, pp.2333-2340, 2011.*
26. Yang, Z., Garg, H., Li, X., Differential Calculus of Fermatean Fuzzy Functions: Continuities, Derivatives, and Differentials. *In International Journal of Computational Intelligence Systems ,Vol. 14, Issue 1, p. 282, 2020. Springer Science and Business Media LLC. https://doi.org/10.2991/ijcis.d.201215.001*.
27. Zadeh, L.A, Fuzzy sets, *Information and Control*, 8(5): 338- 353; 1965.
28. Zeng, J.B., Zhang, W., Li, X.Y., Islanding Algorithm of Distribution System with Distributed Generations based on Circle-breaking Algorithm. *Power Sys. Eng*, *35*, 15–19, 2019.

Received: April 26, 2024. Accepted: Aug 25, 2024

NSS
Neutrosophic Sets and Systems, Vol. 72, 2024
University of New Mexico

Exploring Neutrosophic Over Supra Exterior Modal Topological Structure: Theory and Application in Healthcare Decision-Making

R.Narmada Devi[1,*] and Yamini Parthiban [2]
[1,2]Department of Mathematics,Vel Tech Rangarajan Dr.Sagunthala R&D Institute of Science and Technology,Avadi,Chennai,Tamil Nadu,India.
[1]narmadadevi23@gmail.com and [2]yaminiparthiban.msc@gmail.com
*Correspondence: narmadadevi23@gmail.com.

Abstract. Neutrosophic environments have gained significant relevance across diverse disciplines. Neutrosophic Over Supra Exterior Modal Topological Structure is introduced, demonstrating the generation of two distinct structures through traditional Neutrosophic Over supra topological operations, denoted as $\boxplus$ (closure) and $\boxdot$ (interior), along with novel Neutrosophic Over Supra Exterior Modal Operations, expressed as $\circledast$ (modal closure) and $\odot$ (modal interior). This exploration delves into the essential properties and characteristics of these structures, illuminating their behavior and implications. To illustrate the practical relevance, a numerical example is presented, demonstrating the identification of disease types using a score function. The study conclusively shows that the Neutrosophic Over Supra Exterior Modal Topological Structure effectively classifies diseases such as tuberculosis (bacterial), malaria (parasitic), swine flu (viral), and ringworm (fungal). This dual approach ensures a holistic understanding of the topic, appealing to both theoretical and practitioners seeking practical solutions in the neutrosophic over environment.

1. Introduction

In the tapestry of everyday life, uncertainty emerges prominently in various scenarios, such as rolling a die or tossing a coin onto an uneven surface. These moments underscore the prevalence of uncertainty. Zadeh, [25] credited in 1965 for the origination of fuzzy sets, introduced the concept of membership degrees, laying the foundation not only for a theory of possibility [26] but also inspiring Bellman and colleagues to explore decision-making in contexts influenced by fuzziness [4]. Atanassov later extended Zadeh's work by introducing intuitionist fuzzy sets, emphasizing both degrees of membership non-membership [3].

Smaracheand [21] is credited with the discovery exploration of novel trends applications within neutrosophic theory in 1999. Bustince Burillo, in 1995 [5] investigated the correlation of intuitionist fuzzy sets, particularly in scenarios involving interval values. Christianto postulated three potential utilities of neutrosophic sets [7]. Molodtsov [17], in 1999, brought attention to primary results concerning soft sets.Maji in 2003 develped soft set theory [15]. Neutrosophic sets have found practical utility in medical contexts, with correlation measures employed to discern intricate connections between variables.

In 2021, Radha et al. [19] introduced the concept of neutrosophic Pythagorean sets and their heightened correlation. Ye, in 2013 [24] presented an alternative facet of correlation. Wang et al. delved into single-valued neutrosophic sets [23], while Mallick Pramanik, in 2020 [16] discussed pentapartitioned neutrosophic sets. Jansi et al., [13] in 2019, explored neutrosophic Pythagorean sets, featuring both dependent and independent components. Smaracheand introduced the innovative notion of neutrosophic sets with over, under, and off limits in 2016 [22]. Many researchers like Chinnadurai,Al-Hamido etc are intruducing different ways of neutrosophic logic [1, 2, 6, 8, 12, 18, 20]. Additionally, RN Devi and Yamini Parthiban introduced a decision-making process using neutrosophic Pythagorean soft sets, utilizing a measure of correlation [9] in 2023.

Neutrosophic sets play a crucial role in addressing uncertainties that classical sets and fuzzy sets may struggle to manage. Unlike classical sets, which define membership in a binary manner, and fuzzy sets, which introduce partial membership degrees, neutrosophic sets accommodate indeterminacy where elements can simultaneously belong, partially belong, and not belong to a set due to incomplete or conflicting information (Smarandache, 1999). This capability to represent indeterminate and conflicting information makes neutrosophic sets particularly powerful in modeling and analyzing complex systems where precise boundaries and membership degrees are ambiguous or evolving.

Existing methods like fuzzy logic and traditional neutrosophic sets inadequately handle complex uncertainties and struggle to integrate with topological structures. The Neutrosophic Over Supra Exterior Modal Topological Structure addresses these gaps by incorporating modal operations, enhancing uncertainty management, and bridging the integration gap with operations respecting topological properties and neutrosophic elements. This framework extends applicability to fields such as IT and healthcare, accommodating complex real-world data and decision-making scenarios. Additionally, it includes practical demonstrations, validating its effectiveness in real-world applications.

The Neutrosophic Over Supra Exterior Modal Topological Structure addresses limitations in current neutrosophic frameworks by integrating modal operations with topological structures, effectively handling over and under limits. This integration enhances the modeling of complex

relationships and spatial dependencies, crucial for applications in healthcare decision-making, information systems, and multi-criteria decision analysis.

In this manuscript an introduction to the Neutrosophic Over Supra Exterior Modal Topological Structure is given. It is not only introduces the theoretical underpinnings of this innovative framework but also provides a tangible demonstration of its effectiveness in healthcare decision-making. This dual approach ensures a holistic understanding of the topic, appealing to both theoretical and practitioners seeking practical solutions in the neutrosophic over environment using a score function.

2. **Preliminary**

Definition 2.1. Let $\mathcal{H}$ be an non empty set $\mathcal{J}$ is said to be an NS.Then

$$\mathcal{J} = \{\langle \mathsf{h}, \aleph(\mathsf{h}), \eth(\mathsf{h}), \Upsilon(\mathsf{h})\rangle : \mathsf{h} \in \mathcal{H}\}$$

where $\aleph, \eth, \Upsilon : \mathcal{H} \to [0,1]$ $0 \leq \aleph(\mathsf{h}) + \eth(\mathsf{h}) + \Upsilon(\mathsf{h}) \leq 3$. Here $\aleph(\mathsf{h}), \eth(\mathsf{h})$ and $\Upsilon(\mathsf{h})$ are degree of true membership,degree of indeterminacy and degree of falsity.

Definition 2.2. Let $\mathcal{J}$ be an NS in $\mathcal{H}$.If $\mathcal{J}$ is said to be an $\mathcal{N}^{\mathfrak{o}}$ in an non-empty set $\mathcal{H}$ then it has at-least one neutrosophic component is > 1 and no other component are < 0 is defined as,

$$\mathcal{J} = \{\langle \mathsf{h}, \aleph(\mathsf{h}), \eth(\mathsf{h}), \Upsilon(\mathsf{h})\rangle : \mathsf{h} \in \mathcal{H}\}$$

Where $\aleph, \eth, \Upsilon : \mathcal{H} \to [0, \Omega]$, $0 \leq \aleph(\mathsf{h}) + \eth(\mathsf{h}) + \Upsilon(\mathsf{h}) \leq 3$ and Ω is said to be over-limit of $\mathcal{N}^{\mathfrak{o}}$.

Note: $\rho(\mathcal{H}^{\mathfrak{h}})$ is a set of all Neutrosophic Over Set($\mathcal{N}^{\mathfrak{o}}$) in $\mathcal{H}$

Definition 2.3. The $\mathcal{N}^{\mathfrak{o}}$ $\rhd = \{\langle \mathsf{h}, 0, 0, \Omega\rangle : \mathsf{h} \in \mathcal{H}\}$ is said to be a Null $\mathcal{N}^{\mathfrak{o}}$ and $\blacktriangleright = \{e, \{\langle \mathsf{h}, \Omega, \Omega, 0\rangle : \mathsf{h} \in \mathcal{H}\} : e \in \mathcal{E}\}$ is said to be an universal $\mathcal{N}^{\mathfrak{o}}$.

Definition 2.4. Let τ_{NT} is a collection of subsets of $\mathcal{H}$.Then τ_{NT} is known as neutrosophic topology if it is satisfies the conditions

(i) $\rhd$,$\blacktriangleright \in \tau_{NT}$.

(ii) The union of an arbitrary collection τ_{NT} is in τ_{NT}.

(iii) The finite intersection of subsets τ_{NT} is in τ_{NT}.

Then $(\mathcal{H}, \tau_{NT})$ is called neutrosophic topological structure(NTS).An element of τ_{NT} is called an neutrosophic open set and the complement of τ_{NT} is called an neutrosophic closed set.

Definition 2.5. Let $\tau_{\mathcal{N}^{\mathfrak{o}}}$ is a collection of subsets of $\mathcal{H}$.Then $\tau_{\mathcal{N}^{\mathfrak{o}}}$ is known as neutrosophic over topology if it is satisfies the conditions (i) $\rhd$,$\blacktriangleright \in \tau_{\mathcal{N}^{\mathfrak{o}}}$.

(ii) The union of an arbitrary collection $\tau_{\mathcal{N}^{\mathfrak{o}}}$ is in $\tau_{\mathcal{N}^{\mathfrak{o}}}$.

(iii) The finite intersection of subsets $\tau_{\mathcal{N}^{\mathfrak{o}}}$ is in $\tau_{\mathcal{N}^{\mathfrak{o}}}$.

Then $(\mathcal{H}, \tau_{\mathcal{N}^o})$ is called neutrosophic over topological structure($\mathcal{N}^o$-topological structure).An element of $\tau_{\mathcal{N}^o}$ is called an neutrosophic over open set and the complement of $\tau_{\mathcal{N}^o}$ is called an neutrosophic over closed set.

Definition 2.6. Let $\mathcal{J}$ and $\mathcal{W}$ be two $\mathcal{N}^o$, Then the union,intersection, compliment and subset are defined by

(i)$\mathcal{J} \tilde{\cup} \mathcal{W} = \{\langle \mathsf{h}, \max(\aleph_{\mathcal{J}}(\mathsf{h}), \aleph_{\mathcal{W}}(\mathsf{h})), \max(\eth_{\mathcal{J}}(\mathsf{h}), \eth_{\mathcal{W}}(\mathsf{h})), \min(\Upsilon_{\mathcal{J}}(\mathsf{h}), \Upsilon_{\mathcal{W}}(\mathsf{h}))\rangle : \mathsf{h} \in \mathcal{H}\}$

(ii)$\mathcal{J} \tilde{\cap} \mathcal{W} = \{\langle \mathsf{h}, min(\aleph_{\mathcal{J}}(\mathsf{h}), \aleph_{\mathcal{W}}(\mathsf{h})), min(\eth_{\mathcal{J}}(\mathsf{h}), \eth_{\mathcal{W}}(\mathsf{h})), max(\Upsilon_{\mathcal{J}}(\mathsf{h}), \Upsilon_{\mathcal{W}}(\mathsf{h}))\rangle : \mathsf{h} \in \mathcal{H}\}$

(iii)$\mathcal{J}^{\complement} = \{\langle \mathsf{h}, \Upsilon_{\mathcal{J}}(\mathsf{h}), \Omega - \eth_{\mathcal{J}}(\mathsf{h}), \aleph_{\mathcal{J}}(\mathsf{h})\rangle : \mathsf{h} \in \mathcal{H}\}$

(iv)$\mathcal{J} \subset \mathcal{W}$, then $\aleph_{\mathcal{J}}(\mathsf{h}) \leq \aleph_{\mathcal{W}}(\mathsf{h}), \eth_{\mathcal{J}}(\mathsf{h}) \leq \eth_{\mathcal{W}}(\mathsf{h}), \Upsilon_{\mathcal{J}}(\mathsf{h}) \geq \Upsilon_{\mathcal{W}}(\mathsf{h})$
In other words, $\mathcal{W}$ is an super set of $\mathcal{J}$

(v) Let $\mathcal{J} \subset \mathcal{W}$ and $\mathcal{W} \subset \mathcal{J}$ then $\mathcal{J} = \mathcal{W}$

Proposition 2.7. *Let $\mathcal{J}$ be an $\mathcal{N}^o$ on $\mathcal{H}$. Then*

(i). $\triangleright^{\complement} = \blacktriangleright$

(ii). $\blacktriangleright^{\complement} = \triangleright$

(iii). $(\mathcal{J}^{\complement})^{\complement} = \mathcal{J}$

Proof. 1. $\triangleright^{\complement} = \blacktriangleright$

$$\triangleright = \{\langle \mathsf{h}, 0, 0, \Omega\rangle : \mathsf{h} \in \mathcal{H}\}$$

$$\triangleright^{\complement} = \{\langle \mathsf{h}, \Omega, \Omega, 0\rangle : \mathsf{h} \in \mathcal{H}\} = \blacktriangleright$$

$$\Longrightarrow \triangleright^{\complement} = \blacktriangleright$$

2. $\blacktriangleright^{\complement} = \triangleright$

$$\blacktriangleright = \{\langle \mathsf{h}, \Omega, \Omega, 0\rangle : \mathsf{h} \in \mathcal{H}\}$$

$$\blacktriangleright^{\complement} = \{\langle \mathsf{h}, \Omega, \Omega, 0\rangle : \mathsf{h} \in \mathcal{H}\} = \triangleright$$

$$\Longrightarrow \blacktriangleright^{\complement} = \triangleright$$

3. $(\mathcal{J}^{\complement})^{\complement} = \mathcal{J}$

$$\mathcal{J}^{\complement} = \{\langle \mathsf{h}, \Upsilon_{\mathcal{J}}(\mathsf{h}), \Omega - \eth_{\mathcal{J}}(\mathsf{h}), \aleph_{\mathcal{J}}(\mathsf{h})\rangle : \mathsf{h} \in \mathcal{H}\}$$

$$(\mathcal{J}^{\complement})^{\complement} = \{\langle \mathsf{h}, \aleph_{\mathcal{J}}(\mathsf{h}), \Omega - \eth_{\mathcal{J}}(\mathsf{h}), \Upsilon_{\mathcal{J}}(\mathsf{h})\rangle : \mathsf{h} \in \mathcal{H}\} = \mathcal{J}$$

$$\Longrightarrow (\mathcal{J}^{\complement})^{\complement} = \mathcal{J}$$

□

Proposition 2.8. *Let $\mathcal{J}$ and $\mathcal{W}$ be an $\mathcal{N}^{o}$ on $\mathcal{H}$. Then*

(i). $\mathcal{J}\wp\mathcal{J} = \mathcal{J}\wp\mathcal{J} = \mathcal{J}$

(ii). $\mathcal{J}\wp\mathcal{W} = \mathcal{W}\wp\mathcal{J}$

(iii). $\mathcal{J}\wp\mathcal{W} = \mathcal{W}\wp\mathcal{J}$

(iv). $\mathcal{J}\wp \rhd = \mathcal{J}$ $\mathcal{J}\wp \blacktriangleright = \blacktriangleright$

(v). $\mathcal{J}\wp \rhd = \rhd$ $\mathcal{J}\wp \blacktriangleright = \mathcal{J}$

Proof. The proof is obvious from the definition. □

Theorem 2.9. *Let $\mathcal{J}$ and $\mathcal{W} \in \mathcal{N}^{o}$. Then*

(i). $(\mathcal{J}\wp\mathcal{W})^{\complement} = \mathcal{J}^{\complement}\wp\mathcal{W}^{\complement}$

(ii). $(\mathcal{J}\wp\mathcal{W})^{\complement} = \mathcal{J}^{\complement}\wp\mathcal{W}^{\complement}$

Proof. (i).By the union definition,

$$\mathcal{J}\wp\mathcal{W} = \{\langle \mathsf{h}, max(\aleph_{\mathcal{J}}(\mathsf{h}), \aleph_{\mathcal{W}}(\mathsf{h})), max(\eth_{\mathcal{J}}(\mathsf{h}), \eth_{\mathcal{W}}(\mathsf{h})), min(\Upsilon_{\mathcal{J}}(\mathsf{h}), \Upsilon_{\mathcal{W}}(\mathsf{h}))\rangle : \mathsf{h} \in \mathcal{H}\}$$

$$(\mathcal{J}\wp\mathcal{W})^{\complement} = \{\langle \mathsf{h}, min(\Upsilon_{\mathcal{J}}(\mathsf{h}), \Upsilon_{\mathcal{W}}(\mathsf{h})), max(\Omega - \eth_{\mathcal{J}}(\mathsf{h}), \Omega - \eth_{\mathcal{W}}(\mathsf{h})), max(\aleph_{\mathcal{J}}(\mathsf{h}), \aleph_{\mathcal{W}}(\mathsf{h}))\rangle : \mathsf{h} \in \mathcal{H}\} \tag{1}$$

By the definition of compliment

$$\mathcal{J}^{\complement} = \{\langle \mathsf{h}, \Upsilon_{\mathcal{J}}(\mathsf{h}), \Omega - \eth_{\mathcal{J}}(\mathsf{h}), \aleph_{\mathcal{J}}(\mathsf{h})\rangle : \mathsf{h} \in \mathcal{H}\}$$

$$\mathcal{W}^{\complement} = \{\langle \mathsf{h}, \Upsilon_{\mathcal{W}}(\mathsf{h}), \Omega - \eth_{\mathcal{W}}(\mathsf{h}), \aleph_{\mathcal{W}}(\mathsf{h})\rangle : \mathsf{h} \in \mathcal{H}\}$$

$$\mathcal{J}^{\complement}\wp\mathcal{W}^{\complement} = \{\langle \mathsf{h}, min(\Upsilon_{\mathcal{J}}(\mathsf{h}), \Upsilon_{\mathcal{W}}(\mathsf{h})), max(\Omega - \eth_{\mathcal{J}}(\mathsf{h}), \Omega - \eth_{\mathcal{W}}(\mathsf{h})), max(\aleph_{\mathcal{J}}(\mathsf{h}), \aleph_{\mathcal{W}}(\mathsf{h}))\rangle : \mathsf{h} \in \mathcal{H}\} \tag{2}$$

From (1) and (2) we get,

$$(\mathcal{J}\wp\mathcal{W})^{\complement} = \mathcal{J}^{\complement}\wp\mathcal{W}^{\complement}$$

(ii). By the union definition we know that,

$$\mathcal{J}\wp\mathcal{W} = \{\langle \mathsf{h}, min(\aleph_{\mathcal{J}}(\mathsf{h}), \aleph_{\mathcal{W}}(\mathsf{h})), min(\eth_{\mathcal{J}}(\mathsf{h}), \eth_{\mathcal{W}}(\mathsf{h})), max(\Upsilon_{\mathcal{J}}(\mathsf{h}), \Upsilon_{\mathcal{W}}(\mathsf{h}))\rangle : \mathsf{h} \in \mathcal{H}\}$$

$$(\mathcal{J}\wp\mathcal{W})^{\complement} = \{\langle \mathsf{h}, max(\Upsilon_{\mathcal{J}}(\mathsf{h}), \Upsilon_{\mathcal{W}}(\mathsf{h})), min(\Omega - \eth_{\mathcal{J}}(\mathsf{h}), \Omega - \eth_{\mathcal{W}}(\mathsf{h})), min(\aleph_{\mathcal{J}}(\mathsf{h}), \aleph_{\mathcal{W}}(\mathsf{h}))\rangle : \mathsf{h} \in \mathcal{H}\} \tag{3}$$

By the definition of compliment

$$\mathcal{J}^{\complement} = \{\langle \mathsf{h}, \Upsilon_{\mathcal{J}}(\mathsf{h}), \Omega - \eth_{\mathcal{J}}(\mathsf{h}), \aleph_{\mathcal{J}}(\mathsf{h})\rangle : \mathsf{h} \in \mathcal{H}\}$$

$$\mathcal{W}^{\complement} = \{\langle \mathsf{h}, \Upsilon_{\mathcal{W}}(\mathsf{h}), \Omega - \eth_{\mathcal{W}}(\mathsf{h}), \aleph_{\mathcal{W}}(\mathsf{h})\rangle : \mathsf{h} \in \mathcal{H}\}$$

$$\mathcal{J}^{\complement}\wp\mathcal{W}^{\complement} = \{\langle \mathsf{h}, max(\Upsilon_{\mathcal{J}}(\mathsf{h}), \Upsilon_{\mathcal{W}}(\mathsf{h})), min(\Omega - \eth_{\mathcal{J}}(\mathsf{h}), \Omega - \eth_{\mathcal{W}}(\mathsf{h})), min(\aleph_{\mathcal{J}}(\mathsf{h}), \aleph_{\mathcal{W}}(\mathsf{h}))\rangle : \mathsf{h} \in \mathcal{H}\} \tag{4}$$

From (3) and (4) we get,

$(\mathcal{J} \wr \mathcal{W})^{\complement} = \mathcal{J}^{\complement} \wr \mathcal{W}^{\complement}$ □

3. Neutrosophic Over Supra Exterior Modal Topological Structure

Definition 3.1. Let $\tau_{\mathcal{N}^{o}}$ is a collection of subsets of $\mathcal{H}$.Then $\tau_{\mathcal{N}^{o}}$ is known as neutrosophic over supra topology if it is satisfies the conditions

(i) $\triangleright, \blacktriangleright \in \tau_{\mathcal{N}^{o}}$.

(ii) The union of an arbitrary collection $\tau_{\mathcal{N}^{o}}$ is in $\tau_{\mathcal{N}^{o}}$.

Then $(\mathcal{H}, \tau_{\mathcal{N}^{o}})$ is called neutrosophic over supra topological structure($\mathcal{N}^{o}$-supra topological structure). An element of $\tau_{\mathcal{N}^{o}}$ is called an neutrosophic over supra open set and the complement of $\tau_{\mathcal{N}^{o}}$ is called an neutrosophic over supra closed set.

Definition 3.2. An $\mathcal{N}^{o}$ $\mathcal{T} \in \mathcal{H}$, then neutrosophic over supra topological interior and closure are $\boxdot(\mathcal{T})$ and $\boxplus(\mathcal{T})$ is defined as:

$\boxdot(\mathcal{T}) = \curlyvee\{\mathfrak{N} : \mathfrak{N} \subseteq \mathcal{H} \quad \text{and} \quad \mathfrak{N} \in \tau_{\mathcal{N}^{o}}\}$

$\boxplus(\mathcal{T}) = \wr\{\mathcal{O} : \mathcal{H} \subseteq \mathcal{O} \quad \text{and} \quad \mathcal{O}^{\complement} \in \tau_{\mathcal{N}^{o}}\}$.

Proposition 3.3. *Let $(\mathcal{H}, \tau_{\mathcal{N}^{o}})$ be a $\mathcal{N}^{o}$-supra topological structure $\mathcal{R}$ is a subset of $\mathcal{H}$, then*

(i) $\boxdot(\mathcal{R})$ is the largest $\mathcal{N}^{o}$-supra open set contained in $\mathcal{R}$.

(ii) $\boxplus(\mathcal{R})$ is the smallest $\mathcal{N}^{o}$-supra closed set containing $\mathcal{R}$.

Proof. (i) By the definition of interior, $\boxdot(\mathcal{R})$.Let $\mathcal{N}$ be an open set such that $\mathfrak{N} \subset \mathcal{R}$. $\because \mathfrak{N}$ is open and $\mathcal{N} \subset \mathcal{R}$,then

$\mathfrak{N} \subset \boxdot(\mathcal{R}) \implies \boxdot(\mathcal{R})$ is the largest open set contained in $\mathcal{R}$.

(ii) By the closure definition,

$\boxplus(\mathcal{R}) = \wr\{\mathcal{O} : \mathcal{H} \subseteq \mathcal{O} \qquad \mathcal{O}^{\complement} \in \tau_{\mathcal{N}^{o}}\}$

$\boxplus(\mathcal{R})$ is the smallest closed set containing $\mathcal{R}$. □

Definition 3.4. Let $\mathcal{T}$ be a $\mathcal{N}^{o}$ over $\mathcal{H}$.Then two stard Neutrosophic Over Supra Modal Operations are expressed as $\circledast$ and $\odot$ is defined as

$\circledast\, \mathcal{T} = \{\langle \mathsf{h}, min(\aleph_{\mathcal{T}}(\mathsf{h}), \Omega), \eth_{\mathcal{T}}(\mathsf{h}), \Omega - \sqrt{|\aleph_{\mathcal{T}}(\mathsf{h}) - \eth_{\mathcal{T}}(\mathsf{h})|}\rangle : \mathsf{h} \in \mathcal{H}\}$

$\odot \mathcal{T} = \{\langle \mathsf{h}, max(\aleph_{\mathcal{T}}(\mathsf{h}), \Omega), \sqrt{(\aleph_{\mathcal{T}}(\mathsf{h}))(\Upsilon_{\mathcal{T}}(\mathsf{h}))}, |\sqrt{\Omega} - \Upsilon_{\mathcal{T}}(\mathsf{h})|\rangle : \mathsf{h} \in \mathcal{H}\}$

Example 3.5. Let $\mathcal{T} = \{\langle \mathsf{h}, 1.3, 0.8, 0.7\rangle : \mathsf{h} \in \mathcal{H}\}$ and $\Omega = 1.5$ be a $\mathcal{N}_{o}$. Then,

$\circledast\, \mathcal{T} = \{\langle \mathsf{h}, 1.3, 0.8, 0.5\rangle : \mathsf{h} \in \mathcal{H}\}$

$\odot \mathcal{T} = \{\langle \mathsf{h}, 1.3, 0.9, 0.4\rangle : \mathsf{h} \in \mathcal{H}\}$

Note: For any $\mathcal{N}_{o}$ $\mathcal{T}$,$\circledast\, \mathcal{T} \subseteq \mathcal{T} \subseteq \odot \mathcal{T}$

Definition 3.6. Let neutrosophic over supra topological structure $(\mathcal{H}, \tau_{\mathcal{N}^{\mathfrak{o}}})$ then neutrosophic over supra exterior $\mathcal{N}^{\mathfrak{o}}$ $\mathcal{T}$ is denoted by $\mathfrak{ext}(\mathcal{T})$ $\mathfrak{ext}_{\circledast}(\mathcal{T}) = (\circledast\ (\mathcal{T}))^{\complement}$ or $\mathfrak{ext}_{\odot}(\mathcal{T}) = \odot(\mathcal{T}^{\complement})$

Definition 3.7. An $\mathcal{N}^{\mathfrak{o}}$ $\mathcal{T}$ $\mathcal{W} \in \mathfrak{P}(\mathcal{H}^{\mathfrak{h}})$. Then $\langle \mathfrak{P}(\mathcal{H}^{\mathfrak{h}}), \boxplus, \wr, \wr\!\!\wr, \mathfrak{ext}_{\circledast} \rangle$ is said to be an neutrosophic over supra exterior modal topological closure if it satisfies the following condition:

$(i)\ \boxplus\ (\mathcal{T} \wr \mathcal{W}) = \boxplus(\mathcal{T}) \wr \boxplus\ (\mathcal{W})$,

$(ii) \mathcal{T} \subseteq \boxplus(\mathcal{T})$

$(iii)\ \boxplus\ (\mathfrak{K}) = \mathfrak{K}$

$(iv)\ \boxplus\ (\boxplus(\mathcal{T})) = \boxplus(\mathfrak{T})$

$(v) \mathfrak{ext}_{\circledast}(\mathcal{T} \wr\!\!\wr \mathcal{W}) = \mathfrak{ext}_{\circledast}(\mathcal{T}) \wr\!\!\wr \mathfrak{ext}_{\circledast}(\mathcal{W})$

$(vi) \mathfrak{ext}_{\circledast}(\mathcal{T}) \subseteq \mathcal{T}$

$(vii) \mathfrak{ext}_{\circledast}(\mathfrak{K}) = \mathfrak{K}$

$(viii) \mathfrak{ext}_{\circledast}(\mathfrak{ext}_{\circledast}(\mathcal{T})) = \mathfrak{ext}_{\circledast}(\mathcal{T})$

$(ix) \mathfrak{ext}_{\circledast}(\boxplus(\mathcal{T})) = \boxplus(\mathfrak{ext}_{\circledast}(\mathcal{T}))$

Theorem 3.8. *If $\mathcal{T}$ $\mathcal{W}$ be two $\mathcal{N}^{\mathfrak{o}}$. Then $\langle \mathfrak{P}(\mathcal{H}^{\mathfrak{h}}), \boxplus, \wr, \wr\!\!\wr, \mathfrak{ext}_{\circledast} \rangle$ is a neutrosophic over supra modal topological closure.*

Proof. Let $\mathcal{T}$ $\mathcal{W}$ be two $\mathcal{N}_{\mathfrak{DG}}$

$\mathcal{T}, \mathcal{W} \in \mathcal{P}(\mathcal{H}^{\mathfrak{h}})$ then,

$(i) \boxplus(\mathcal{T} \wr \mathcal{W}) = \boxplus(\{\langle \mathsf{h}, \aleph_{\mathcal{T}}(\mathsf{h}), \eth_{\mathcal{T}}(\mathsf{h}), \Upsilon_{\mathcal{T}}(\mathsf{h})\rangle : \mathsf{h} \in \mathcal{H}\} \wr \{\langle \mathsf{h}, \aleph_{\mathcal{W}}(\mathsf{h}), \eth_{\mathcal{W}}(\mathsf{h}), \Upsilon_{\mathcal{W}}(\mathsf{h})\rangle : \mathsf{h} \in \mathcal{H}\})$

$= \boxplus(\{\langle \mathsf{h}, max(\aleph_{\mathcal{T}}(\mathsf{h}), \aleph_{\mathcal{W}}(\mathsf{h})), max(\eth_{\mathcal{T}}(\mathsf{h}), \eth_{\mathcal{W}}(\mathsf{h})), min(\Upsilon_{\mathcal{T}}(\mathsf{h}), \Upsilon_{\mathcal{W}}(\mathsf{h}))\rangle : \mathsf{h} \in \mathcal{H}\})$

$= \{\langle \mathsf{h}, \sup_{\mathsf{g}\in\mathcal{H}} max(\aleph_{\mathcal{T}}(\mathsf{g}), \aleph_{\mathcal{W}}(\mathsf{g})), \sup_{\mathsf{g}\in\mathcal{H}} max(\eth_{\mathcal{T}}(\mathsf{g}), \eth_{\mathcal{W}}(\mathsf{g})),$
$\inf_{\mathsf{g}\in\mathcal{H}} min(\Upsilon_{\mathcal{T}}(\mathsf{g}), \Upsilon_{\mathcal{W}}(\mathsf{g}))\rangle : \mathsf{h} \in \mathcal{H}\}$

$= \{\langle \mathsf{h}, max(\sup_{\mathsf{g}\in\mathcal{H}} \aleph_{\mathcal{T}}(\mathsf{g}), \sup_{\mathsf{g}\in\mathcal{H}} \aleph_{\mathcal{W}}(\mathsf{g})), max(\sup_{\mathsf{g}\in\mathcal{H}} \eth_{\mathcal{T}}(\mathsf{g}), \sup_{\mathsf{g}\in\mathcal{H}} \eth_{\mathcal{W}}(\mathsf{g})),$
$min(\inf_{\mathsf{g}\in\mathcal{H}} \Upsilon_{\mathcal{T}}(\mathsf{g}), \inf_{\mathsf{g}\in\mathcal{H}} \Upsilon_{\mathcal{W}}(\mathsf{g}))\rangle : \mathsf{h} \in \mathcal{H}\}$
$= \boxplus(\mathcal{T}) \wr \boxplus\ (\mathcal{W})$

$(ii) \mathcal{T} = \{\langle \mathsf{h}, \aleph_{\mathcal{T}}(\mathsf{h}), \eth_{\mathcal{T}}(\mathsf{h}), \Upsilon_{\mathcal{T}}(\mathsf{h})\rangle : \mathsf{h} \in \mathcal{H}\} \subseteq \{\langle \mathsf{h}, \sup_{\mathsf{g}\in\mathcal{H}} \aleph_{\mathcal{T}}(\mathsf{g}), \sup_{\mathsf{g}\in\mathcal{H}} \eth_{\mathcal{T}}(\mathsf{g}),$
$\inf_{\mathsf{g}\in\mathcal{H}} \Upsilon_{\mathcal{T}}(\mathsf{g})\rangle : \mathsf{h} \in \mathcal{H}\} = \boxplus(\mathcal{T})$

$(iii)\ \boxplus\ (\mathfrak{K}) = \boxplus(\{\langle \mathsf{h}, 0, 0, \Omega\rangle : \mathsf{h} \in \mathcal{H}\}) = \{\langle \mathsf{h}, \sup_{\mathsf{g}\in\mathcal{H}} 0, \sup_{\mathsf{g}\in\mathcal{H}} 0, \inf_{\mathsf{g}\in\mathcal{H}} \Omega\rangle : \mathsf{h} \in \mathcal{H}\}$
$= \{\mathsf{h}, 0, 0, \Omega : \mathsf{h} \in \mathcal{H}\} = \mathfrak{K}$

$(iv)\ \boxplus\ (\boxplus(\mathcal{T})) = \boxplus(\boxplus(\{\langle \mathsf{h}, \aleph_{\mathcal{T}}(\mathsf{h}), \eth_{\mathcal{T}}(\mathsf{h}), \Upsilon_{\mathcal{T}}(\mathsf{h})\rangle : \mathsf{h} \in \mathcal{H}\}))$
$= \boxplus(\{\langle \mathsf{h}, \sup_{\mathsf{g}\in\mathcal{H}} \aleph_{\mathcal{T}}(\mathsf{g}), \sup_{\mathsf{g}\in\mathcal{H}} \eth_{\mathcal{T}}(\mathsf{g}), \inf_{\mathsf{g}\in\mathcal{H}} \Upsilon_{\mathcal{T}}(\mathsf{g})\rangle : \mathsf{h} \in \mathcal{H}\})$

$$= \{\langle \mathsf{h}, \sup_{\mathsf{g}\in\mathcal{H}} \aleph_{\mathcal{T}}(\mathsf{g}), \sup_{\mathsf{g}\in\mathcal{H}} \eth_{\mathcal{T}}(\mathsf{g}), \inf_{\mathsf{g}\in\mathcal{H}} \Upsilon_{\mathcal{T}}(\mathsf{g})\rangle : \mathsf{h} \in \mathcal{H}\} = \boxplus(\mathcal{T})$$

$$\begin{aligned}(v)\mathfrak{ext}_{\otimes}(\mathcal{T}\wr\mathcal{W}) &= \mathfrak{ext}_{\otimes}(\{\mathsf{h}, \langle min(\aleph_{\mathcal{T}}(\mathsf{h}), \aleph_{\mathcal{W}}(\mathsf{h})), min(\eth_{\mathcal{T}}(\mathsf{h}), \eth_{\mathcal{W}}(\mathsf{h})), max(\Upsilon_{\mathcal{T}}(\mathsf{h}), \Upsilon_{\mathcal{W}}(\mathsf{h}))\rangle\}) \\ &= \{\mathsf{h}, \langle min(min(\aleph_{\mathcal{T}}(\mathsf{h}), \aleph_{\mathcal{W}}(\mathsf{h}), \Omega), min(\eth_{\mathcal{T}}(\mathsf{h}), \eth_{\mathcal{W}}(\mathsf{h})), \\ &\quad \Omega - \sqrt{min(\aleph_{\mathcal{T}}(\mathsf{h}), \aleph_{\mathcal{W}}(\mathsf{h})) - min(\eth_{\mathcal{T}}(\mathsf{h}), \eth_{\mathcal{W}}(\mathsf{h}))})\rangle\} \\ &= \{\mathsf{h}, \langle min(\aleph_{\mathcal{T}}(\mathsf{h}), \aleph_{\mathcal{W}}(\mathsf{h})), min(\eth_{\mathcal{T}}(\mathsf{h}), \eth_{\mathcal{W}}(\mathsf{h})), \\ &\quad \Omega - \sqrt{max(\aleph_{\mathcal{T}}(\mathsf{h}) - \eth_{\mathcal{T}}(\mathsf{h}), \aleph_{\mathcal{W}}(\mathsf{h}) - \eth_{\mathcal{W}}(\mathsf{h}))})\rangle\} \\ &= \mathfrak{ext}_{\otimes}(\mathcal{T})\wr\mathfrak{ext}_{\otimes}(\mathcal{W})\end{aligned}$$

The proof of $(vi) - (ix)$ is obvious from the Definition(3.10,3.11 and 3.12). □

Definition 3.9. An $\mathcal{N}^{\mathfrak{o}}$ $\mathcal{T}$ $\mathcal{W} \in \mathfrak{P}(\mathcal{H}^{\mathfrak{h}})$. Then $\langle \mathfrak{P}(\mathcal{H}^{\mathfrak{h}}), \boxdot, \wr, \curlyvee, \mathfrak{ext}_{\odot}\rangle$ is said to be an neutrosophic over supra exterior modal topological interior if it satisfies the following condition:

$(i)\ \boxdot(\mathcal{T}\wr\mathcal{W}) = \boxdot(\mathcal{T})\wr\boxdot(\mathcal{W})$,

$(ii)\ \boxdot(\mathcal{T}) \subseteq \mathcal{T}$

$(iii)\ \boxdot(\mathfrak{K}) = \mathfrak{K}$

$(iv)\ \boxdot(\boxdot(\mathcal{T})) = \boxdot(\mathfrak{T})$

$(v)\mathfrak{ext}_{\odot}(\mathcal{T}\curlyvee\mathcal{W}) = \mathfrak{ext}_{\odot}(\mathcal{T})\curlyvee\mathfrak{ext}_{\odot}(\mathcal{W})$

$(vi)\mathcal{T} \subseteq \mathfrak{ext}_{\odot}(\mathcal{T})$

$(vii)\mathfrak{ext}_{\odot}(\mathfrak{K}) = \mathfrak{K}$

$(viii)\mathfrak{ext}_{\odot}(\mathfrak{ext}_{\odot}(\mathcal{T})) = \mathfrak{ext}_{\odot}(\mathcal{T})$

$(ix)\mathfrak{ext}_{\odot}(\boxdot(\mathcal{T})) = \boxdot(\mathfrak{ext}_{\odot}(\mathcal{T}))$

Theorem 3.10. *If $\mathcal{T}$ $\mathcal{W}$ be two $\mathcal{N}^{\mathfrak{o}}$.Then $\langle \mathfrak{P}(\mathcal{H}^{\mathfrak{h}}), \boxdot, \wr, \curlyvee, \mathfrak{ext}_{\odot}\rangle$ is a neutrosophic over exterior modal topological interior.*

Proof. The proof is obvious. □

Definition 3.11. Let two $\mathcal{N}^{\mathfrak{o}}$ as $\mathcal{T} = \{\langle \mathsf{h}, \aleph_{\mathcal{T}}(\mathsf{h}), \eth_{\mathcal{T}}(\mathsf{h}), \Upsilon_{\mathcal{T}}(\mathsf{h})\rangle : \mathsf{h} \in \mathcal{H}\}$ $\mathcal{W} = \{\langle \mathsf{g}, \aleph_{\mathcal{W}}(\mathsf{g}), \eth_{\mathcal{W}}(\mathsf{g}), \Upsilon_{\mathcal{W}}(\mathsf{g})\rangle.\ \mathsf{g} \in \mathcal{H}\}$ $\mathfrak{f} : \mathcal{H} \to \mathcal{H}$ be a function,

(i)$\mathfrak{f}(\mathcal{T}) = \{\langle \mathsf{g}, \mathfrak{f}(\aleph_{\mathcal{T}})(\mathsf{g}), \mathfrak{f}(\eth_{\mathcal{T}})(\mathsf{g}), (1 - \mathfrak{f}(1 - \Upsilon_{\mathcal{T}}))(\mathsf{g})\rangle : \mathsf{g} \in \mathcal{H}\}$ is a $\mathcal{N}^{\mathfrak{o}}$ on $\mathcal{H}$ called the image of $\mathcal{T}$ under $\mathfrak{f}$

(ii) $.\mathfrak{f}^{-1}(\mathcal{W}) = \{\langle x, \mathfrak{f}^{-1}(\aleph_{\mathcal{W}})(\mathsf{h}), \mathfrak{f}^{-1}(\eth_{\mathcal{W}})(\mathsf{h}), \mathfrak{f}^{-1}(\Upsilon_{\mathcal{W}})(\mathsf{h})\rangle : \mathsf{h} \in \mathcal{H}\}$ is a $\mathcal{N}^{\mathfrak{o}}$ on $\mathcal{H}$ is called the pre-image of $\mathcal{W}$ under $\mathfrak{f}$, where

$$\mathfrak{f}(\aleph_{\mathcal{T}})(\mathsf{g}) = \begin{cases} \sup_{\mathsf{h}\in\mathfrak{f}^{-1}}(\mathsf{g})\aleph_{\mathcal{T}}(\mathsf{h}), & \text{if } \mathfrak{f}^{-1}(\mathsf{g}) \neq \emptyset \\ 0, & \text{otherwise} \end{cases}$$

$$\mathfrak{f}(\eth_{\mathcal{T}})(\mathsf{g}) = \begin{cases} \sup_{\mathsf{h}\in\mathfrak{f}^{-1}}(\mathsf{g})\eth_{\mathcal{T}}(\mathsf{h}), & \text{if } \mathfrak{f}^{-1}(\mathsf{g}) \neq \emptyset \\ 0, & \text{otherwise} \end{cases}$$

$$(1-\mathfrak{f}(1-\Upsilon_{\mathcal{T}}))(\mathsf{g}) = \begin{cases} \inf_{\mathsf{h}\in\mathfrak{f}^{-1}}(\mathsf{g})\Upsilon_{\mathcal{T}}(\mathsf{h}), & \text{if only if } \mathfrak{f}^{-1}(\mathsf{g}) \neq \emptyset \\ 1, & \text{otherwise} \end{cases}$$

Let us introduce the $\mathfrak{f}_{-}(\Upsilon_{\mathcal{T}})$ for $(1-\mathfrak{f}(1-\Upsilon_{\mathcal{T}}))$

Corollary 3.12. *Let $\{\mathcal{T}\}_{i\in\alpha}^{\infty}, \mathcal{T}$ $\mathcal{W}$ be $\mathcal{N}^{\mathfrak{o}}$ on $\mathcal{H}$, then the following are true*

(i) $(\wp_{i\in\alpha}\mathcal{T}_i)^{\complement} = \mho_{i\in\alpha}\mathcal{T}_i^{\complement}, (\mho_{i\in\alpha}\mathcal{T}_i)^{\complement} = \wp_{i\in\alpha}\mathcal{T}_i^{\complement}$

(ii) $(\mathcal{T}^{\complement})^{\complement} = \mathcal{T}\cdot\mathcal{W}^{\complement} \subseteq \mathcal{T}^{\complement}$, *if* $\mathcal{W}\subseteq\mathcal{T}$

Proof. (i) $(\wp_{i\in\alpha}\mathcal{T}_i)^{\complement} = \{\langle \mathsf{h}, |1-\inf_{i\in\alpha}\{\aleph_{\mathcal{T}}(\mathsf{h})\}|, |1-\inf_{i\in\alpha}\{\eth_{\mathcal{T}}(\mathsf{h})\}|, |\ 1-\sup_{i\in\alpha}\{\Upsilon_{\mathcal{T}}(\mathsf{h})\ |\}\rangle : \mathsf{h}\in\mathcal{H}\}$

$= \{\langle x, \sup_{i\in\alpha}(|1-\aleph_{\mathcal{T}i}(x)|), \sup_{i\in\alpha}(|1-\eth_{\mathcal{T}i}(x)|).., \inf\ ..\in\alpha(|1-\Upsilon_{\mathcal{T}i}(x)|)\rangle : x\in\mathcal{H}\}$

$= \mho_{i\in\alpha}\mathcal{T}_i^{\complement}$.

Similarly, $(\mho_{i\in\alpha}\mathcal{T}_i)^{\complement} = \wp_{i\in\alpha}\mathcal{T}_i^{\complement}$ is obvious

(ii) we can prove it from (i) □

Definition 3.13. Let single valued neutrosophic over score function is denoted by $\mathfrak{S}_{\mathfrak{F}}$ defined by $\mathfrak{S}_{\mathfrak{F}} = \frac{1}{3m}[\sum_{i=1}^{m}[|2+\aleph_i-\eth_i-\Upsilon_i|]]$

4. Algorithm

Step 1:Collection of data

Consider $\mathfrak{m}$ attributes $\mathcal{A}_1, \mathcal{A}_2, \mathcal{A}_3, \ldots, \mathcal{A}_{\mathfrak{m}}$,$\mathfrak{n}$ attributes $\mathfrak{E}_1, \mathfrak{E}_2, \mathfrak{E}_3, \ldots, \mathfrak{E}_{\mathfrak{n}}$ and $\mathfrak{p}$ attributes $\mathfrak{H}_1, \mathfrak{H}_2, \mathfrak{H}_3, \ldots, \mathfrak{H}_{\mathfrak{p}}$

$(\mathfrak{n}\leq\mathfrak{p})$ for multi-attributes decision making problem(MADMP).

$\mathcal{A}_{\mathfrak{i}}\backslash\mathfrak{E}_{\mathfrak{j}}$	$\mathfrak{E}_1$	$\mathfrak{E}_2$	.	.	.	$\mathfrak{E}_n$
$\mathcal{A}_1$	$\mathfrak{a}_{11}$	$\mathfrak{a}_{12}$	.	.	.	$\mathfrak{a}_{1n}$
$\mathcal{A}_2$	$\mathfrak{a}_{21}$	$\mathfrak{a}_{22}$	.	.	.	$\mathfrak{a}_{2n}$
$\mathcal{A}_3$	$\mathfrak{a}_{31}$	$\mathfrak{a}_{32}$	.	.	.	$\mathfrak{a}_{3n}$
.	.	.	.	.	.	.
.	.	.	.	.	.	.
$\mathcal{A}_m$	$\mathfrak{a}_{m1}$	$\mathfrak{a}_{m2}$	.	.	.	$\mathfrak{a}_{mn}$

$\mathfrak{H}_{\mathfrak{p}}\backslash\mathcal{A}_{\mathfrak{i}}$	$\mathcal{A}_1$	$\mathcal{A}_2$	.	.	.	$\mathcal{A}_m$
$\mathfrak{H}_1$	$\mathfrak{d}_{11}$	$\mathfrak{d}_{12}$	.	.	.	$\mathfrak{d}_{1m}$
$\mathfrak{H}_2$	$\mathfrak{d}_{21}$	$\mathfrak{d}_{22}$	.	.	.	$\mathfrak{d}_{2m}$
$\mathfrak{H}_3$	$\mathfrak{d}_{31}$	$\mathfrak{d}_{32}$	.	.	.	$\mathfrak{d}_{3m}$
.	.	.	.	.	.	.
.	.	.	.	.	.	.
$\mathfrak{H}_p$	$\mathfrak{d}_{p1}$	$\mathfrak{d}_{p2}$	.	.	.	$\mathfrak{d}_{pm}$

Step 2: Construction of neutrosophic over supra exterior topology for $(\mathfrak{E}_{\mathfrak{j}})$ $(\mathfrak{H}_{\mathfrak{k}})$:

(i)$\tau_{\mathfrak{j}}^{\mathcal{S}} = \mathcal{A}\wp\mathcal{B}$, Where $\mathcal{A} = \{\triangleright, \blacktriangleright, \mathfrak{a}_{1\mathfrak{j}}, \mathfrak{a}_{2\mathfrak{j}}, \mathfrak{a}_{3\mathfrak{j}}, \ldots, \mathfrak{a}_{\mathfrak{m}\mathfrak{j}}\}$ and $\mathcal{B} = \{\mathfrak{a}_{1\mathfrak{j}}\cup\mathfrak{a}_{2\mathfrak{j}}, \mathfrak{a}_{1\mathfrak{j}}\cup\mathfrak{a}_{3\mathfrak{j}}, \ldots, \mathfrak{a}_{\mathfrak{m}-1\mathfrak{j}}\cup\mathfrak{a}_{\mathfrak{m}\mathfrak{j}}\}$

(ii)$\nu_{\mathfrak{k}}^{\varsigma} = \mathcal{C}\wp\mathcal{D}$, Where $\mathcal{C} = \{\triangleright, \blacktriangleright, \mathfrak{d}_{\mathfrak{k}1}, \mathfrak{d}_{\mathfrak{k}2}, \mathfrak{d}_{\mathfrak{k}3}, \ldots, \mathfrak{d}_{\mathfrak{k}\mathfrak{m}}\}$ and $\mathcal{D} = \{\mathfrak{d}_{\mathfrak{k}1} \cup \mathfrak{d}_{\mathfrak{k}2}, \mathfrak{d}_{\mathfrak{k}1} \cup \mathfrak{d}_{\mathfrak{k}3}, \ldots, \mathfrak{d}_{\mathfrak{k}\mathfrak{m}-1} \cup \mathfrak{d}_{\mathfrak{k}\mathfrak{m}}\}$

Step 3:Find single valued neutrosophic over score function:

Single valued neutrosophic over score functions($\mathfrak{S}_{\mathfrak{F}}$) of $\mathcal{A}, \mathcal{B}, \mathcal{C}, \mathcal{D}, \mathfrak{E}_{\mathfrak{j}}$ $\mathfrak{H}_{\mathfrak{k}}$

(i)$\mathfrak{S}_{\mathfrak{F}}(\mathfrak{E}_{\mathfrak{j}}) = \begin{cases} \mathfrak{S}_{\mathfrak{F}}(\mathcal{A}) & if \mathfrak{S}_{\mathfrak{F}}(\mathcal{B}) = 0 \\ \frac{1}{2}[\mathfrak{S}_{\mathfrak{F}}(\mathcal{A}) + \mathfrak{S}_{\mathfrak{F}}(\mathcal{B})] & otherwise \end{cases}$

where, (1) $\mathfrak{S}_{\mathfrak{F}}(\mathcal{A}) = \frac{1}{3(\mathfrak{m}+2)}\left(\sum_{\mathfrak{i}=1}^{\mathfrak{m}+2}[2 + \aleph_i - \eth_i - \Upsilon_i]\right)$

(2) $\mathfrak{S}_{\mathfrak{F}}(\mathcal{B}) = \frac{1}{3\mathfrak{q}}\left(\sum_{\mathfrak{i}=1}^{\mathfrak{q}}[2 + \aleph_i - \eth_i - \Upsilon_i]\right)$

$\forall$ $\mathfrak{j}$ denotes the number of elements in $\mathcal{B}$ $\mathfrak{j} = 1, 2, \ldots, n$

(ii) $\mathfrak{S}_{\mathfrak{F}}(\mathfrak{H}_{\mathfrak{k}}) = \begin{cases} \mathfrak{S}_{\mathfrak{F}}(\mathcal{C}) & if \mathfrak{S}_{\mathfrak{F}}(\mathcal{D}) = 0 \\ \frac{1}{2}[\mathfrak{S}_{\mathfrak{F}}(\mathcal{C}) + \mathfrak{S}_{\mathfrak{F}}(\mathcal{D})] & otherwise \end{cases}$

where, (1) $\mathfrak{S}_{\mathfrak{F}}(\mathcal{C}) = \frac{1}{3(\mathfrak{m}+2)}\left(\sum_{\mathfrak{i}=1}^{\mathfrak{m}+2}[2 + \aleph_i - \eth_i - \Upsilon_i]\right)$

(2) $\mathfrak{S}_{\mathfrak{F}}(\mathcal{D}) = \frac{1}{3\mathfrak{r}}\left(\sum_{\mathfrak{i}=1}^{\mathfrak{r}}[2 + \aleph_i - \eth_i - \Upsilon_i]\right)$

$\forall$ $\mathfrak{r}$ denotes the number of elements in $\mathcal{D}$ $\mathfrak{k} = 1, 2, \ldots, \mathfrak{p}$

Step 4:Final decision

Establish the single-valued neutrosophic over score values for decisions $\mathfrak{E}_1 \leq \mathfrak{E}_2 \leq \cdots \leq \mathfrak{E}_{\mathfrak{n}}$ and also for the attributes $\mathfrak{H}_1 \leq \mathfrak{H}_2 \leq \cdots \leq \mathfrak{H}_{\mathfrak{p}}$ .Choose the attribute $\mathfrak{H}_{\mathfrak{p}}$ for $\mathfrak{E}_1$,$\mathfrak{H}_{\mathfrak{p}-1}$ for $\mathfrak{E}_2$ etc,. If $\mathfrak{p} > \mathfrak{n}$ then leave out $\mathfrak{H}_{\mathfrak{k}}$, where $\mathfrak{k} = 1, 2, \ldots, \mathfrak{n} - \mathfrak{p}$.

5. Numerical Illustration

In contemporary times, there is a discernible surge in the prevalence of infectious diseases, primarily attributed to the proliferation of viruses, bacteria, fungi, and other pathogens. The task of systematically categorizing diverse sets of symptoms under a singular disease classification presents a formidable challenge within the domain of medical diagnosis. Within this context, the previously mentioned strategy is employed to underscore its efficacy and pertinence.

As infectious diseases persist in their evolution diversification, healthcare professionals grapple with the intricate task of precisely diagnosing these conditions. This involves discerning the specific causative agents, considering the myriad symptoms exhibited by affected individuals, establishing a comprehensive understing of the disease's pathogenesis. The process of classifying a myriad of symptoms under a single disease umbrella necessitates a methodical well-considered approach.

In the context of our discussion, a disease identification problem serves as a practical demonstration of the aforementioned strategy's efficiency and relevance. This illustrative example highlights how a systematic and holistic approach to diagnosis can assist in tackling the burgeoning challenges posed by infectious diseases, ultimately leading to more efficacious treatments improved public health outcomes.

Step 1:Collection of data

The information acquired from consultations with medical professionals, covering four classifications of microorganisms viruses, bacteria, fungi, and parasites recognized for inducing infectious diseases, along with the corresponding symptoms such as rhinorrhea, decreased appetite, diarrhea, alopecia, and anemia, has been methodically structured into a tabular format. The aim is to ascertain the pathogens establish the diseases they induce, which include common cold, stomach flu, E.coli infection, ringworm, and hookworm infestation.

Table 1. Symptoms for microorganism

Symptoms\Microorganism	Parasite($\mathfrak{E}_1$)	Fungi($\mathfrak{E}_2$)	Bacteria($\mathfrak{E}_3$)	Virus($\mathfrak{E}_4$)
Runny nose($\mathcal{A}_1$)	(1.35,0.9,0.1)	(1.34,0.3,0.25)	(1.19,0.53,1.01)	(1.26,0.3,0.11)
Loss of appetite($\mathcal{A}_2$)	(1.22,0.3,0.6)	(1.21,0.2,0.3)	(1.07,0.53,1)	(1.2,0.14,0.22)
Diarrhea ($\mathcal{A}_3$)	(1.17,0.2,0.3)	(0.52,0.1,1.18)	(1.13,0.21,0.6)	(0.4,0.2,1.16)
Hair loss ($\mathcal{A}_4$)	(1.35,0.15,0.5)	(1.3,0.3,0.7)	(1.09,0.1,0.1)	(1.25,0.2,0.5)
Anemia ($\mathcal{A}_5$)	(0.6,0.3,1.14)	(1.34,0.2,0.6)	(1.02,0.17,0.8)	(1.21,0.3,0.6)

Table 2. Symptoms for the diseases

Diseases\Symptoms	Runnynose($\mathcal{A}_1$)	Loss of appetite($\mathcal{A}_2$)	Diarrhea ($\mathcal{A}_3$)	Hair loss ($\mathcal{A}_4$)	Anemia($\mathcal{A}_5$)
Tuberculosis($\mathfrak{H}_1$)	(1.31,0.53,0.04)	(1.32,0.61,0.3)	(1.24,0.73,0.1)	(1.2,0.4,0.1)	(1.32,0.4,0.1)
Common cold ($\mathfrak{H}_3$)	(1.1,0.1,0.9)	(1.22,0.3,0.8)	(1.12,0.3,0.8)	(1.13,0.4,0.6)	(1.09,0,0.1)
Ring worm ($\mathfrak{H}_5$)	(1.09,0,0.1)	(0,0.2,1.1)	(1.07,0.2,0.3)	(1.2,0.3,0.1)	(1.02,0,0.8)
Swin flu ($\mathfrak{H}_4$)	(1.12,0.5,0.8)	(1.1,0.4,0.9)	(1.22,0.5,0.8)	(1.2,0.3,0.8)	(1.32,0.4,0.8)
Malaria ($\mathfrak{H}_2$)	(1.29,0.1,0.1)	(1.23,0.6,0.7)	(1.23,0.6,0.7)	(1.13,0.1,0.7)	(1.15,0.3,0.5)

Step 2: Construction of neutrosophic over supra exterior topology for $(\mathfrak{E}_j)$ $(\mathfrak{H}_\ell)$:

Table 3. $\mathfrak{E}_j$

	$\mathcal{A}$ and $\mathcal{B}$
τ_1^ς	$\mathcal{A} = \{(1.5,1.5,0),(0,0,1.5),(1.35,0.9,0.1),(1.22,0.3,0.6),(1.17,0.2,0.3)(1.35,0.15,0.5),(0.6,0.3,1.14)\}$ and $\mathcal{B} = \{(1.35,0.9,0.1)\}$
τ_2^ς	$\mathcal{A} = \{(1.5,1.5,0),(0,0,1.5),(1.34,0.3,0.25),(1.21,0.2,0.3),(0.52,0.1,1.18),(1.3,0.3,0.7),(1.34,0.2,0.6)\}$ and $\mathcal{B} = \{(1.34,0.3,0.25)\}$
τ_3^ς	$\mathcal{A} = \{(1.5,1.5,0),(0,0,1.5),(1.19,0.53,1.01),(1.07,0.53,1),(1.13,0.21,0.6),(1.09,0.1,0.1),(1.02,0.17,0.8)\}$ and $\mathcal{B} = \{(1.19,0.53,1.01)\}$
τ_4^ς	$\mathcal{A} = \{(1.5,1.5,0),(0,0,1.5),(1.26,0.3,0.11),(1.2,0.14,0.22),(0.4,0.2,1.16),(1.25,0.2,0.5),(1.21,0.3,0.6)\}$ and $\mathcal{B} = \{(1.26,0.3,0.11)\}$

TABLE 4. $\mathfrak{H}_{\mathfrak{k}}$

	$\mathcal{C}$ and $\mathcal{D}$
ν_1^{ς}	$\mathcal{C} = \{(1.5, 1.5, 0), (0, 0, 1.5), (1.31, 0.53, 0.04), (1.1, 0.1, 0.9), (1.09, 0, 0.1), (1.12, 0.5, 0.8), (1.29, 0.1, 0.1)\}$ and $\mathcal{D} = \{(1.31, 0.53, 0.04)\}$
ν_2^{ς}	$\mathcal{C} = \{(1.5, 1.5, 0), (0, 0, 1.5), (1.32, 0.61, 0.3), (1.22, 0.3, 0.8), (0, 0.2, 1.1), (1.1, 0.4, 0.9), (1.23, 0.6, 0.7)\}$ and $\mathcal{D} = \{(1.32, 0.61, 0.3)\}$
ν_3^{ς}	$\mathcal{C} = \{(1.5, 1.5, 0), (0, 0, 1.5), (1.24, 0.73, 0.1), (1.12, 0.3, 0.8), (1.07, 0.2, 0.3), (1.22, 0.5, 0.8), (1.23, 0.6, 0.7)\}$ and $\mathcal{D} = \{(1.24, 0.73, 0.1)\}$
ν_4^{ς}	$\mathcal{C} = \{(1.5, 1.5, 0), (0, 0, 1.5), (1.2, 0.4, 0.1), (1.13, 0.4, 0.6), (1.2, 0.3, 0.1), (1.2, 0.3, 0.8), (1.13, 0.1, 0.7)\}$ and $\mathcal{D} = \{(1.2, 0.4, 0.1)\}$
ν_5^{ς}	$\mathcal{C} = \{(1.5, 1.5, 0), (0, 0, 1.5), (1.32, 0.4, 0.1), (1.09, 0, 0.1), (1.02, 0, 0.8), (1.32, 0.4, 0.8), (1.15, 0.3, 0.5)\}$ and $\mathcal{D} = \{(1.32, 0.4, 0.1)\}$

Step 3:Find single valued neutrosophic over score function:

TABLE 5. $\mathfrak{S}_{\mathfrak{F}}\mathfrak{E}_{\mathfrak{j}}$

$\mathcal{A}$	$\mathcal{B}$	$\mathfrak{E}_{\mathfrak{j}}$
0.6523	0.7833	$\mathfrak{E}_1 = 0.7178$
0.6647	0.9300	$\mathfrak{E}_2 = 0.7973$
0.6166	0.5500	$\mathfrak{E}_3 = 0.5833$
0.6309	0.9500	$\mathfrak{E}_4 = 0.7904$

TABLE 6. $\mathfrak{S}_{\mathfrak{F}}\mathfrak{H}_{\mathfrak{k}}$

$\mathcal{C}$	$\mathcal{D}$	$\mathfrak{H}_{\mathfrak{k}}$
0.7257	0.1826	$\mathfrak{H}_1 = 0.4541$
0.5457	0.1606	$\mathfrak{H}_2 = 0.3531$
0.6357	0.1606	$\mathfrak{H}_3 = 0.3981$
0.6933	0.1800	$\mathfrak{H}_4 = 0.4366$
0.7142	0.1880	$\mathfrak{H}_5 = 0.4511$

Step 4:Final decision

Arrange $\mathfrak{S}_{\mathfrak{F}}$ for the attributes $\mathfrak{H}_1, \mathfrak{H}_2, \mathfrak{H}_3, \mathfrak{H}_4, \mathfrak{H}_5$ and alternatives $\mathfrak{E}_1, \mathfrak{E}_2, \mathfrak{E}_3, \mathfrak{E}_4$ in progression is result to $\mathfrak{H}_2 < \mathfrak{H}_3 < \mathfrak{H}_4 < \mathfrak{H}_5 < \mathfrak{H}_1$ and $\mathfrak{E}_3 < \mathfrak{E}_1 < \mathfrak{E}_4 < \mathfrak{E}_2$.

6. Conclusion

This manuscript introduces the innovative concept of Neutrosophic Over Supra Exterior Modal Topological Structure and outlines its foundational properties. Where model closure ($\circledast$) and model interior ($\odot$) operations in the Neutrosophic Over Supra Exterior Modal Topological Structures framework provide tools for managing and analyzing sets with complex membership degrees and modalities. They ensure comprehensive coverage of set elements (closure) and extraction of core characteristics (interior), respectively, thereby enhancing the framework's capability to handle nuanced uncertainty and ambiguity in practical applications. It concludes by definitively classifying several diseases: tuberculosis as bacterial, malaria as parasitic, swine flu as viral, and ringworm as fungal. Moreover, $\mathcal{N}^{\mathfrak{o}}$ is shown to be indispensable across various domains such as information technology, decision-making support systems, electronic databases, disease detection, and multi-criteria cognitive problem-solving. Its versatility and applicability underscore its vital role in enhancing understanding and decision-making in complex systems and uncertain environments.

7. Future Research

For future research, expanding the Neutrosophic Over Supra Exterior Modal Topological Structure to incorporate additional modalities and refine existing operations could further enhance its robustness and applicability. Empirical validation across diverse domains and scenarios would provide concrete evidence of its effectiveness and reliability. Furthermore, developing computational tools and algorithms tailored to implement this framework in practical settings could facilitate its adoption and integration into decision support systems and real-time applications. Collaborative efforts across disciplines could explore new applications and synergies, unlocking novel insights and capabilities offered by neutrosophic theory and modal topological structures.

Funding: This research received no external funding.

Conflicts of Interest: The authors declare no conflict of interest.

References

[1] Al-Hamido, R.K., 2022. Separation axioms in neutrosophic supra topological structure neutrosophic supra bi-topological structure. *Neutrosophic Sets Systems*, 51(1), p.51.

[2] Al-Hamido, R.K., 2023. New Operators Using Neutrosophic Crisp Open Set. International Journal of Neutrosophic Science (IJNS), 20(1).

[3] Atanassov, K.T., 2012. On intuitionistic fuzzy sets theory (Vol. 283). *Springer*.

[4] Bellman, R.E. Zadeh, L.A., 1970. Decision-making in a fuzzy environment.*Management science*, 17(4), pp.B-141.

[5] Bustince, H. Burillo, P., 1995. Correlation of interval-valued intuitionistic fuzzy sets. *Fuzzy sets systems*, 74(2), pp.237-244.

[6] Chinnadurai, V., & Sindhu, M. P. 2020. A novel approach: neutro-spot topology its supra topology with separation axioms computing the impact on COVID-19 (Vol. 38). *Infinite Study*.

[7] Christianto, V., Boyd, R.N. Smaracheand, F., 2020. Three possible applications of neutrosophic logic in fundamental applied sciences. *Infinite Study*.

[8] Christianto, V., & Smarandache, F. 2024. Assuming Photon as Extended Point Particle in the HyperSoft Topological Space and other Hypotheses: Issues and Trend Analysis. *Infinite Study*.

[9] Devi, R. N., & Parthiban, Y. 2023. Decision making process over neutrosophic pythagorean soft sets using mesure of correlation. *Southeast Europe Journal of Soft Computing*, 12(2), 06-09.

[10] Devi, R.N. and Parthiban, Y., 2024.Decision Making By Neutrosophic Over Soft Topological Space.*Neutrosophic Sets and Systems*, vol 66.

[11] Devi, R.N. and Parthiban, Y., 2024.Enhancing Decision-Making for Parents: A Neutrosophic Pythagorean Plithogenic Hypersoft Set Approach to School Selection With TOPSIS Method, Multi-Criteria Decision Making Models and Techniques: Neutrosophic Approaches. IGI Global, 76-94.

[12] Dey, S., Paul, P., & Ray, G. C. 2024. On b-anti-Open Sets: A Formal Definition, Proofs, and Examples. *Neutrosophic Systems with Applications*, 13, 23-31.

[13] Jansi, R., Mohana, K. Smaracheand, F., 2019. Correlation measure for Pythagorean neutrosophic sets with T F as dependent neutrosophic components. *Infinite Study*.

[14] Kumaravel, S.K., Murugesan, R., Nagaram, N.B., Rasappan, S. and Yamini, G., (2023). Applications of fuzzy cognitive maps and neutrosophic cognitive maps on analysis of dengue fever. *Fuzzy Logic Applications in Computer Science and Mathematics*, pp.249-265.

[15] Maji, P.K., Biswas, R. Roy, A.R., 2003. Soft set theory. *Computers & mathematics with applications*, 45(4-5), pp.555-562.

[16] Mallick, R. Pramanik, S., 2020. Pentapartitioned neutrosophic set its properties (Vol. 36). *Infinite Study*.

[17] Molodtsov, D., 1999. Soft set theory?first results.*Computers & mathematics with applications*, 37(4-5), pp.19-31.

[18] Murugesan, R., Parthiban, Y., Devi, R., Mohan, K.R. Kumarave, S.K., 2023. A Comparative Study of Fuzzy Cognitive Maps Neutrosophic Cognitive Maps on Covid Variants. *Neutrosophic Sets Systems*, 55(1), p.20.

[19] Radha, R., Mary, A.S.A., Prema, R. Broumi, S., 2021. Neutrosophic pythagorean sets with dependent neutrosophic pythagorean components its improved correlation coefficients. *Neutrosophic Sets Systems*, 46, pp.77-86.

[20] Saeed, M., Saqlain, M., Mehmood, A. Yaqoob, S., 2020. Multi-polar neutrosophic soft sets with application in medical diagnosis Decision-making. *Neutrosophic Sets Systems*, 33, pp.183-207.

[21] Smarandache, F., 1999. A unifying field in Logics: Neutrosophic Logic. In Philosophy. *American Research Press*, pp. 1-141.

[22] Smarandache, F., 2016. Neutrosophic Overset, Neutrosophic Underset, and Neutrosophic Offset. Similarly for Neutrosophic Over-/Under-/Off-Logic, Probability, and Statistics. *Infinite Study*.

[23] Wang, H., Smarandache, F., Zhang, Y. and Sunderraman, R., 2010. Single valued neutrosophic sets. *Infinite study*, 12.

[24] Ye, J., 2013. Another form of correlation coefficient between single valued neutrosophic sets and its multiple attribute decision-making method. *Neutrosophic Sets and systems*, 1(1), pp.8-12.

[25] Zadeh, L.A., 1965. Fuzzy sets. *Information and control*, 8(3), pp.338-353.

[26] Zadeh, L.A., 1978. Fuzzy sets as a basis for a theory of possibility. *Fuzzy sets and systems*, 1(1), pp.3-28.

Received: March 15, 2024. **Accepted**: August 30, 2024.

NSS

Neutrosophic Sets and Systems, Vol. 72, 2024

University of New Mexico

Evaluating the nuclear power plant safety system under neutrosophic environment

Debapriya Mondal[1], Totan Garai[2], Gopal Chandra Roy [3] and Shariful Alam[1*]

[1] Department of Mathematics, IIEST, Shibpur, Howrah-711103, India.

[2]Department of Mathematics, Syamsundar College, Purba Bardhaman, WB, India.

[3]Department of Mining Engineering, IIEST, Shibpur, Howrah-711103, India.

[*]Correspondence: salam@math.iiests.ac.in; Tel.: +919874452995

Abstract. The safety system of nuclear power plants is very crucial for protecting the environment and the living world. In this article, we have addressed the nuclear power plant safety system in a neutrosophic environment. Here, we have mathematically presented a nuclear power plant safety system in terms of neutrosophic differential equations. We have thoroughly examined and discussed both analytically and numerically the solution of the nuclear power plant safety model considering the underlying model parameter as single-valued triangular neutrosophic number. We have focused to find out probability of the nuclear power plant's safety system working normally and shutdown in safe mode when the model parameters are imprecise in nature. It has been observed that the normal operation and shutdown probability of nuclear power plant safety systems under uncertain conditions are predicted with robust accuracy.

Keywords: Neutrosophic set; Single valued neutrosophic set; Triangular single valued neutrosophic number; Neutrosophic differential equation; Nuclear power plant safety model

1. Introduction

Safety measures in Nuclear Power Plants (NPP) have become essential for reducing risks to human health and the critical environmental hazards. Good precautionary safety strategies can help safeguard all the workers involved in NPPs from the incidence of catastrophic accidents and significantly protect the environment from the risks of unintentional radiation exposure. Recently, several research studies have been carried out on the safety issues of NPPs. Jyotish et. al. [1] used reachability graphs to analyse the failure mode of different components of the safety system involved in the NPPs and evaluated the system through mathematical modelling. Hyvärinen et. al. [2] argued that comprehensive understanding of the safety of nuclear reactors is very much essential and incorporated defense-in-depth knowledge to improve the

NPP safety systems. Bao et. al. [3] has suggested an improved framework to assess the risk of digital control systems of a nuclear power plant by integrating three typical risk stages, namely 'qualitative hazard analysis', 'quantitative reliability' and 'consequence analyses'. Zhang et. al. [4] recommended multi-criterion and multi-context evaluations to enhance the safety of nuclear power plants. So and Kim [5] shows that the 'Chernoff-bound' can be used to estimate the higher level of the failure probability in a NPP safety system incorporating the concept of passive safety system. Wu et. al. [6] developed safety archetype identification and used behaviour modelling to get ride off human dependability in NPP operations. Marton et. al. [7] pointed out that the ageing impact on the reliability of system equipment has to be appraised to guarantee the safety standards of an NPP. They presented a risk impact evaluation model incorporating several operation safety factors like ageing & obsolescence of system equipment, self-assessment of maintenance plans, surveillance requirements, wear-out phase of the equipment lifetime, etc., where the model parameters are estimated through long-term historical data. Ahn et. al. [8] have designed and improved operator support system used in NPPs through artificial intelligence algorithm that validates operational system activity and alert human errors to ward off the adverse effect of the integrity of power plant. Ayodeji et. al. [9] proposed deep learning for assessing the dependability, explainability, and research potential of nuclear power reactors. Singh and Singh [10] addressed on the dependability measurement of NPP control and instrumentation systems. Abdel-Basset et. al. [11] described an effective risk assessment and mitigation strategy for solar power plants based on real data. Abdel-Basset et. al. [12] investigated the assessment of sustainable flue gas treatment systems for the iron and steel industry using a novel multi-stage technique based on spherical fuzzy MCDM. Abdel-Basset et. al. [13] presented a conceptual framework for assessing the optimal sustainability of electric car charging stations for green energy in smart cities. Mondal et. al. [14] examined the design and assessment of a picture fuzzy mining safety system using picture fuzzy differential equations. Although a substantial number of research works have been carried out on the various aspects of safety issues of nuclear power plats, but the majority these studies was performed in the crisp environment.

The safety system of an NPP is a complex phenomenon [15] and many factors like human operations error, human-machine interaction, assessment of prospective risk, and evaluation of reliability & engineering-resilience are involved, which are inherently imprecise in nature. Thus, it is very much realistic to analyze the NPP model system in an imprecise environment. To handle various types of uncertainty and indistinctness, the theories of impreciseness have been geared up in which the structure of neutrosophic numbers is the latest addition. In the year 1998 Smarandache [16] first demonstrate the impression of the neutrosophic set

as a compatible mixture of three independent membership functions: truthness, falsity and doubtfulness. Indeed, neutrosophic set was a genuine and sensible extension of intuitionistic set introduced by Atanassov [17]. Purba et. al. [18] discussed about the fuzzy probability-based event tree analysis, which is used in the NPP probabilistic safety assessment. Moreover, Purba [19] incorporated fuzzy based probability to assess reliability of NPP safety model system. Sleem and Elhenawy [20] investigated the energy efficiency and material cost reductions realised by the evolution of solar panels used in photovoltaic systems using the neutrosophic model. Sallam and Mohamed [21] highlighted the neutrosophic MCDM approach for analysing onshore wind for power generation and ecological sustainability. Mondal et. al. [22] addressed safety measures of oil and gas sector by using an FDE system. On the other hand, Melliani and Chadli [23] introduced intuitionistic fuzzy differential equations (IFDE) by use of the derivatives of degrees of membership and non-membership functions. Amma et. al. [24] developed diagonally implicit block backward differential formulae to provide a numerical solution to the IFDE problem. Man et. al. [25] provided a clear procedure for resolving a fuzzy heat equation that is based on IFDE. Melliani et. al. [26] utilized the homotrophy analysis approach to provide an approximate solution to the IFDE using the linear differential operator. But all these work did not consider refusal terms which is common in real life problems. Smarandache use the word "indeterminacy" to capture the refusal terms in the concept neutrosophic numbers and subsequently, in order to simulate indeterminacy, NDE was created. Sumathi and Priya [27] presented a novel viewpoint on the NDE. Sumathi and Sweety [28] discussed a novel method for solving differential equations using the trapezoidal neutrosophic number. Son et. al. [29] discussed an equation with a linear quadratic regulator that is controlled by granular neutrosophic fractional differential equations. Alamin et. al. [30] discussed solution and interpretation of neutrosophic homogeneous difference equations. Parikh and Shani [31] researched on the Sumudu Transform in order to solve the NS initial conditions of the second ODE. Mondal et. al. [32] developed a model outlining the use of the NDE in mining safety. Parikh et. al. [33] investigated using an analytical and numerical approach in an NS context to solve a first-order initial value issue. Acharya et. al. [34] investigated an NDE method for simulating glucose transport in the circulation using neutrosophic sets. Garai et. al. [35] discussed softmax function based neutrosophic aggregation operators and application in multi-attribute decision making problem.

In reality, in many situations, it was observed that the collected data are insufficient and transmit some misinformation. In such situations, incorporating neutrosophic numbers offers better results. Although some studies have been done on NPP safety model system in fuzzy environments, but have not noticed any work in this regard in the neutrosophic environments. In this article, we have mathematically described the nuclear power plant safety model

system(NPPSMS) [36], in terms of neutrosophic differential equations (NDE). We have thoroughly examined and discussed both analytically and numerically the solution of the model system considering the underlying model parameter as single-valued triangular neutrosophic number and focused to find out probability shutting down the NPP in safe mode.

1.1. *Motivation*

The safety system of NPP is very much essential and crucial as it has a high risk impact both on the biotic and abiotic elements of environment. Many uncertain information & factors are involved in the NPP system. Naturally, several ambiguities and uncertainties are associated with the underlying parameters involved in the mathematical model of NPP safety system. Now with the introduction of the neutrosophic set by Smarandache [16], we have noticed that a neutrosophic data set can handle imprecise data more efficiently where doubtfulness is inherently and independently embedded into the data set. Moreover, as per our knowledge, no study of the NPP model system has been carried out in the NS environment. Thus, we mathematically formulate the NPP system in terms of neutrosophic differential equations and analyze it both analytically and numerically.

1.2. *Novelty*

Despite the fact that some patterns are followed, fresh attention and new efforts have been made by way of ourselves, which is stated as below:

• NPP safety issues has been first time addressed in the neutrosophic set environment. Here, we have mathematically presented NPP safety system in terms of neutrosophic differential equations.

• Both analytical and numerical solutions of the NPP safety model system have been obtained in crisp as well as neutrosophic environment using classical method, zadeh's extension principle, and generalised hukuhara differentiability(GH_{ii}) and results are compared.

1.3. *Structure of this paper*

The remaining portions of this article are ornamented as follows: Section-2 gives some preliminaries concept and definition. Section-3 contains first order linear homogeneous neutrosophic differential equation. Section-4 contains description of NPPSMS. Section-5 contains analytical solution of the NPPSMS model system. Section-6 contains numerical solution of the NPPSMS and consequently, conclusions are discussed in Section-7.

TABLE 1. List of abbreviation with description

Abbreviation	Description
CS	crisp set
FS	fuzzy set
IFS	intuitonistic fuzzy set
CSNs	crisp number
NS	neutrosophic set
SVNS	single valued neutrosophic set
TSVNNs	triangular single valued neutrosophic number
ODE	Ordinary differential equation
FDE	fuzzy differential equation
IFDE	intutionistic fuzzy differential equation
NDE	neutrosophic differential equation
IC	initial condition
NPPSMS	nuclear power plant safety model system

1.4. *List of abbreviation*

2. **Preliminaries**

2.1. ***Definition of NS*** *[32]*

Let $\mathfrak{V}$ represent an universal set. A NS $\tilde{\mathbb{A}}^{NS}$ of $\mathfrak{V}$ be defined by $\tilde{\mathbb{A}}^{NS}=\langle(\hat{\mathfrak{u}};\ \mu_T(\hat{\mathfrak{u}}),\ \nu_I(\hat{\mathfrak{u}}),\ \sigma_F(\hat{\mathfrak{u}})) :\ \hat{\mathfrak{u}} \in \mathfrak{V}\rangle$ where $\mu_T(\hat{\mathfrak{u}}),\ \nu_I(\hat{\mathfrak{u}}),\ \sigma_F(\hat{\mathfrak{u}})$ be outlined as the truth membership, indeterminacy membership, falsity membership grade of $\hat{\mathfrak{u}}$ in $\tilde{\mathbb{A}}^{NS}$ which are real standard or non-standard subsets of $^-]0,1[^+$ & $\mu_T(\hat{\mathfrak{u}})+\nu_I(\hat{\mathfrak{u}})+\sigma_F(\hat{\mathfrak{u}}) \leqslant 3^+$.

2.2. ***Definition of SVNS*** *[32]*

Let $\mathfrak{V}$ be a Universal set. A SVNS $\tilde{\mathbb{A}}^{NS}$ of $\mathfrak{V}$ be defined by $\tilde{\mathbb{A}}^{NS}=\langle(\hat{\mathfrak{u}};\ \mu_T(\hat{\mathfrak{u}}),\ \nu_I(\hat{\mathfrak{u}}),\ \sigma_F(\hat{\mathfrak{u}})) : \hat{\mathfrak{u}} \in \mathfrak{V}\rangle$ where $\mu_T(\hat{\mathfrak{u}}),\ \nu_I(\hat{\mathfrak{u}}),\ \sigma_F(\hat{\mathfrak{u}})$ be outlined as the truth membership, indeterminacy membership, falsity membership grade of $\hat{\mathfrak{u}}$ in $\tilde{\mathbb{A}}^{NS}$ which are subset of $[0,1]$ & $\mu_T(\hat{\mathfrak{u}})+\nu_I(\hat{\mathfrak{u}})+\sigma_F(\hat{\mathfrak{u}}) \leqslant 3$.

2.3. ***Definition of TSVNNs*** *[32]*

A TSVNNs is denoted by $\tilde{\mathbb{A}}^{NS}=\langle\hat{\mathfrak{a}}_1,\ \hat{\mathfrak{a}}_2,\ \hat{\mathfrak{a}}_3;\ f_\mu,\ f_\nu,\ f_\sigma\rangle$ whose truth, indeterminacy and falsity membership functions are defined by

$$\mu_T(\hat{\mathfrak{u}})=\begin{cases}(\frac{\hat{\mathfrak{u}}-\hat{\mathfrak{a}_1}}{\hat{\mathfrak{a}_2}-\hat{\mathfrak{a}_1}})f_\mu & \text{when } \hat{\mathfrak{a}_1}\leqslant\hat{\mathfrak{u}}\leqslant\hat{\mathfrak{a}_2}\\ f_\mu & \text{when } \hat{\mathfrak{u}}=\hat{\mathfrak{a}_2}\\ (\frac{\hat{\mathfrak{a}_3}-\hat{\mathfrak{u}}}{\hat{\mathfrak{a}_3}-\hat{\mathfrak{a}_2}})f_\mu & \text{when } \hat{\mathfrak{a}_2}\leqslant\hat{\mathfrak{u}}\leqslant\hat{\mathfrak{a}_3}\\ 0 & \text{when } \hat{\mathfrak{u}}\leqslant\hat{\mathfrak{a}_1} \text{ or } \hat{\mathfrak{u}}\geqslant\hat{\mathfrak{a}_3}\end{cases}$$

$$\nu_I(\hat{\mathfrak{u}})=\begin{cases}\frac{(\hat{\mathfrak{a}_2}-\hat{\mathfrak{u}})+(\hat{\mathfrak{u}}-\hat{\mathfrak{a}_1})f_\nu}{\hat{\mathfrak{a}_2}-\hat{\mathfrak{a}_1}} & \text{when } \hat{\mathfrak{a}_1}\leqslant\hat{\mathfrak{u}}\leqslant\hat{\mathfrak{a}_2}\\ f_\nu & \text{when } \hat{\mathfrak{u}}=\hat{\mathfrak{a}_2}\\ \frac{(\hat{\mathfrak{u}}-\hat{\mathfrak{a}_2})+(\hat{\mathfrak{a}_3}-\hat{\mathfrak{u}})f_\nu}{\hat{\mathfrak{a}_3}-\hat{\mathfrak{a}_2}} & \text{when } \hat{\mathfrak{a}_2}\leqslant\hat{\mathfrak{u}}\leqslant\hat{\mathfrak{a}_3}\\ 1 & \text{when } \hat{\mathfrak{u}}\leqslant\hat{\mathfrak{a}_1} \text{ or } \hat{\mathfrak{u}}\geqslant\hat{\mathfrak{a}_3}\end{cases}$$

$$\sigma_F(\hat{\mathfrak{u}})=\begin{cases}\frac{(\hat{\mathfrak{a}_2}-\hat{\mathfrak{u}})+(\hat{\mathfrak{u}}-\hat{\mathfrak{a}_1})f_\sigma}{\hat{\mathfrak{a}_2}-\hat{\mathfrak{a}_1}} & \text{when } \hat{\mathfrak{a}_1}\leqslant\hat{\mathfrak{u}}\leqslant\hat{\mathfrak{a}_2}\\ f_\sigma & \text{when } \hat{\mathfrak{u}}=\hat{\mathfrak{a}_2}\\ \frac{(\hat{\mathfrak{u}}-\hat{\mathfrak{a}_2})+(\hat{\mathfrak{a}_3}-\hat{\mathfrak{u}})f_\sigma}{\hat{\mathfrak{a}_3}-\hat{\mathfrak{a}_2}} & \text{when } \hat{\mathfrak{a}_2}\leqslant\hat{\mathfrak{u}}\leqslant\hat{\mathfrak{a}_3}\\ 1 & \text{when } \hat{\mathfrak{u}}\leqslant\hat{\mathfrak{a}_1} \text{ or } \hat{\mathfrak{u}}\geqslant\hat{\mathfrak{a}_3}\end{cases}$$

where $\mu_T(\hat{\mathfrak{u}})+\nu_I(\hat{\mathfrak{u}})+\sigma_F(\hat{\mathfrak{u}})\leqslant 3$ & $w_\mu\in(0,1]$, $w_\nu,\ w_\sigma\in[0,1)$.

2.4. *Cut Set* [32]

Let, $\tilde{\mathbb{A}}^{NS}$ be any SVNS, then $(r,\ \beta,\ \gamma)$-cut of SVNS is denoted by $\mathbb{A}(r,\ \beta,\ \gamma)$ and it is defined by $\mathbb{A}(r,\ \beta,\ \gamma)=\langle\hat{\mathfrak{u}}\in\mathfrak{V}:\ \mu_T(\mathfrak{u})\geqslant r,\ \nu_I(\mathfrak{u})\leqslant\beta,\ \sigma_F(\mathfrak{u})\leqslant\gamma;\ 0<r\leqslant 1, 0\leqslant\beta<1,\ 0\leqslant\gamma<1\rangle$.
Now the basic arithmetic operation on TSVNNs can be written as:
Consider two TSVNNs, $\tilde{\mathbb{A}}^{NS}=\langle\hat{\mathfrak{a}_1},\ \hat{\mathfrak{a}_2},\ \hat{\mathfrak{a}_3};\ f_\mu,\ f_\nu,\ f_\sigma\rangle$; $\tilde{\mathbb{B}}^{NS}=\langle\hat{\mathfrak{b}_1},\ \hat{\mathfrak{b}_2},\ \hat{\mathfrak{b}_3};\ g_\mu,\ g_\nu,\ g_\sigma\rangle$, the following operation are:

- **Addition:**

$\tilde{\mathbb{A}}^{NS}+\tilde{\mathbb{B}}^{NS}=\langle[(\hat{\mathfrak{a}_1}+\hat{\mathfrak{b}_1},\ \hat{\mathfrak{a}_2}+\hat{\mathfrak{b}_2},\ \hat{\mathfrak{a}_3}+\hat{\mathfrak{b}_3});\ f_\mu\wedge g_\mu,\ f_\nu\vee g_\nu,\ f_\sigma\vee g_\sigma]\rangle$

- **Substraction:**

$\tilde{\mathbb{A}}^{NS}\text{-}\tilde{\mathbb{B}}^{NS}=\langle[(\hat{\mathfrak{a}_1}-\hat{\mathfrak{b}_3},\ \hat{\mathfrak{a}_2}-\hat{\mathfrak{b}_2},\ \hat{\mathfrak{a}_3}-\hat{\mathfrak{b}_1});\ f_\mu\wedge g_\mu,\ f_\nu\vee g_\nu,\ f_\sigma\vee g_\sigma]\rangle$

- **Multiplication:**

$\tilde{\mathbb{A}}^{NS}.\tilde{\mathbb{B}}^{NS}=\langle[(\hat{\mathfrak{a}_1}\hat{\mathfrak{b}_1},\ \hat{\mathfrak{a}_2}\hat{\mathfrak{b}_2},\ \hat{\mathfrak{a}_3}\hat{\mathfrak{b}_3});\ f_\mu\wedge g_\mu,\ f_\nu\vee g_\nu,\ f_\sigma\vee g_\sigma]\rangle$

- **Division:**

$$\frac{\tilde{\mathbb{A}}^{NS}}{\tilde{\mathbb{B}}^{NS}}=\left\langle\left[\left(\frac{\hat{\mathfrak{a}_1}}{\hat{\mathfrak{b}_3}},\ \frac{\hat{\mathfrak{a}_2}}{\hat{\mathfrak{b}_2}},\ \frac{\hat{\mathfrak{a}_3}}{\hat{\mathfrak{b}_1}}\right);\ f_\mu\wedge g_\mu,\ f_\nu\vee g_\nu,\ f_\sigma\vee g_\sigma\right]\right\rangle$$

Where $\wedge=Min,\vee=Max$

3. First Order linear homogeneous neutrosophic differential equation: [32]

Let us consider an ODE

$$\frac{d\mathcal{Y}}{d\mathfrak{t}}=\mathcal{L}\mathcal{Y},\mathfrak{t}\in[0,\infty) \tag{1}$$

with IC $\mathcal{Y}(\mathfrak{t}_0)=\mathcal{Y}_0$. Now the above ODE will be treated as NDE when at-least one of the parameter $\mathcal{L}$ or initial condition $\mathcal{Y}_0$ are considered as SVNNs.

Now, the classical technique [37], Zadeh's extension principle [38], generalised Hukuhara differentiability(GH_{ii}) [39], and other approaches can each be used to solve the NDE mentioned above.

3.1. Definition of strong solution

Let $\tilde{\mathcal{Y}}^{NS}(\mathfrak{t})$ be the classical solution (as described in [37]) and its cut be $\mathcal{Y}(\mathfrak{t},\ r,\ \beta,\ \gamma)=\langle[\mathcal{Y}_1(\mathfrak{t},\ r),\mathcal{Y}_2(\mathfrak{t},\ r)],\ [\mathcal{Y}_1'(\mathfrak{t},\ \beta),\mathcal{Y}_2'(\mathfrak{t},\ \beta)],\ [\mathcal{Y}_1''(\mathfrak{t},\ \gamma),\ \mathcal{Y}_2''(\mathfrak{t},\ \gamma)]\rangle$.

The solution is strong if

(i) $\frac{d\mathcal{Y}_1(\mathfrak{t},\ r)}{dr}>0,\ \frac{d\mathcal{Y}_2(\mathfrak{t},\ r)}{dr}<0\ \forall\ r\in(0,\ 1],\ \mathcal{Y}_1(\mathfrak{t},\ 1)\leqslant\mathcal{Y}_2(\mathfrak{t},\ 1)$

(ii) $\frac{d\mathcal{Y}_1'(\mathfrak{t},\ \beta)}{d\beta}<0,\ \frac{d\mathcal{Y}_2'(\mathfrak{t},\ \beta)}{d\beta}>0\ \forall\ \beta\in[0,1),\ \mathcal{Y}_1'(\mathfrak{t},0)\leqslant\mathcal{Y}_2'(\mathfrak{t},\ 0)$

(iii) $\frac{d\mathcal{Y}_1''(\mathfrak{t},\ \gamma)}{d\gamma}<0,\ \frac{d\mathcal{Y}_2''(\mathfrak{t},\ \gamma)}{d\gamma}>0\ \forall\ \gamma\in[0,1),\ \mathcal{Y}_1''(\mathfrak{t},\ 0)\leqslant\mathcal{Y}_2''(\mathfrak{t},\ 0)$

A weak solution would result from anything less.

4. **Description of NPPSMS**

The design, production, operation, and maintenance of several types of nuclear power power-producing cost billions of dollars per year. Around 436 commercial nuclear reactors were operational in 2011 and produced 16% of the world's electricity. NPPSMS frequently have issues with dependability, safety, human factors, and human error. For instance, human error was responsible for almost 27% of commercial NPPSMS breakdowns in the US between 1990 and 1994.

Here, we proposed to study on NPPSMS. [36] in terms of a NDE. Following are our key areas of focus in this paper:

- Establish a model for NPPSMS.
- Determine the model's solution in a CS environment.
- Determine the model's solution in the NS environment.

4.1. ***Mathematical formulation of NPPSMS***

4.2. ***Acceptation***

(I) Every event exists independently of the others.

(II) In the finite time period δt, the probability of changing from one system state to another is given by the expression $\Psi\delta t$, where Ψ is the rate of change between system states.

(III) A single transition from one system state to another taking place more than once in the finite time interval δt is extremely unlikely, that is $(\Psi\delta t)(\Psi\delta t) \to 0$.

4.3. ***Notation***

t	time interval.
δt	finite time interval.
λ_s	is the continuous failure rate of the NPPSMS.
$\mathcal{P}_0(t)$	is the probability that the NPPSMS is working normally.
$\mathcal{P}_1(t)$	is the probability that the NPPSMS will collapse.
$\mathcal{P}_0(t+\delta t)$	is the probability that the NPPSMS will be in the off-state at time $t+\delta t$.
$\mathcal{P}_1(t+\delta t)$	is the probability that the NPPSMS will collapse at any given time $t+\delta t$.
$j=0$	represents the normal position.
$j=1$	is the collapse state.
$\mathcal{P}_j(t)$	denotes the probability of being in position j at time interval t.
$\lambda_s\delta t$	is the probability that NPPSMS will collapse within the time period δt.
(1 - $\lambda_s\delta t$)	is the probability that there won't be a collapse in the time frame δt.

Assume that a system utilised by the NPPSMS may either be in a functioning condition or a collapsing state. The system's constant failure rate is λ_s. The diagram of the system state space is shown in Fig-1. The statuses of the NPPSMS are indicated by the numbers 0 and 1 in the boxes. State 0 denotes the NPPSMS in normal operation, whereas State 1 denotes NPPSMS shutdown. Let λ_s indicate the constant failure rate from state 0 to state 1. The meaning of t, δt, $\mathcal{P}_0(t+\delta t)$, $\mathcal{P}_1(t+\delta t)$, $\mathcal{P}_0(t)$, $\mathcal{P}_1(t)$, $\lambda_s\delta t$ and (1 - $\lambda_s\delta t$) already discussed in section-4.3. Suppose that the NPPSMS is operated under the conditions of normal operation, independent occurrence of system failure, and constant rate of system failure.

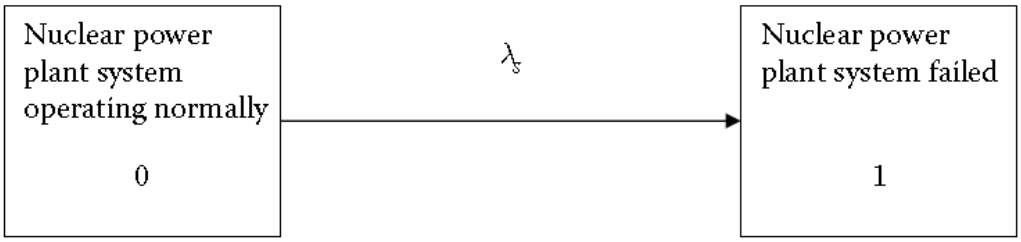

FIGURE 1. Nuclear power plant system state space diagram

Now using the notation of section-4.2, it is clear that at the initial time, $\mathcal{P}_0(0)$=1 and $\mathcal{P}_1(0)$=0. Now, the first two equations may be constructed using the fundamentals of probability theory:

$$\mathcal{P}_0(\mathfrak{t}+\delta\mathfrak{t}) = \mathcal{P}_0(\mathfrak{t})(1-\lambda_s\delta\mathfrak{t}) \tag{2}$$

$$\mathcal{P}_1(\mathfrak{t}+\delta\mathfrak{t}) = \mathcal{P}_0(\mathfrak{t})(\lambda_s\delta\mathfrak{t}) + \mathcal{P}_1(\mathfrak{t})(1-o\delta\mathfrak{t}) \tag{3}$$

Now, from equation (2) we get

$$\mathcal{P}_0(\mathfrak{t}+\delta\mathfrak{t}) - \mathcal{P}_0(\mathfrak{t}) = -\lambda_s\mathcal{P}_0(\mathfrak{t})\delta\mathfrak{t} \tag{4}$$

Now using definition of differentiability from equation (4), we get

$$\lim_{\delta\mathfrak{t}\to 0}\frac{\mathcal{P}_0(\mathfrak{t}+\delta\mathfrak{t}) - \mathcal{P}_0(\mathfrak{t})}{\delta\mathfrak{t}} = -\lambda_s\mathcal{P}_0(\mathfrak{t})$$

$$\therefore \frac{d\mathcal{P}_0(\mathfrak{t})}{d\mathfrak{t}} = -\lambda_s\mathcal{P}_0(\mathfrak{t}) \tag{5}$$

Similarly from equation (3), we get

$$\frac{d\mathcal{P}_1(\mathfrak{t})}{d\mathfrak{t}} = \lambda_s\mathcal{P}_0(\mathfrak{t}) \tag{6}$$

So, the required NPPSMS model system as follows

$$\therefore \frac{d\mathcal{P}_0(\mathfrak{t})}{d\mathfrak{t}} = -\lambda_s\mathcal{P}_0(\mathfrak{t}) \tag{7}$$

$$\frac{d\mathcal{P}_1(\mathfrak{t})}{d\mathfrak{t}} = \lambda_s\mathcal{P}_0(\mathfrak{t}) \tag{8}$$

with IC: $\mathcal{P}_0(0) = 1$ & $\mathcal{P}_1(0) = 0$.

5. Analytical solution of the NPPSMS model system

There are two approaches to solving equations (7) and (8): in a CS environment and in an imprecise one. To solve imprecise environments, NS environments are employed. The details of everything are provided below.

Crisp Solution of the NPPSMS model system: Taking the input value λ_s as crisp number, we get following solutions:

$$P_0(\mathrm{t}) = e^{-\lambda_s \mathrm{t}} \tag{9}$$

$$P_1(\mathrm{t}) = 1 - e^{-\lambda_s \mathrm{t}} \tag{10}$$

NS Solution of the NPPSMS model system:

Taking the input value $\tilde{\lambda_s}^{NS}$ as triangular neutrosophic number, let, $\tilde{\mathcal{P}_0(\mathrm{t})}^{NS}$, $\tilde{\mathcal{P}_1(\mathrm{t})}^{NS}$ be the NS solution of the model system whose $r,\ \beta,\ \gamma$-cut values are as follows:

$\mathcal{P}_0(\mathrm{t},\ r,\ \beta,\ \gamma)=\langle[\mathcal{P}_{01}(\mathrm{t},\ r), \mathcal{P}_{02}(\mathrm{t},\ r)],\ [\mathcal{P}'_{01}(\mathrm{t},\ \beta),\ \mathcal{P}'_{02}(\mathrm{t},\ \beta)],\ [\mathcal{P}''_{01}(\mathrm{t},\ \gamma),\ \mathcal{P}''_{02}(\mathrm{t},\ \gamma)]\rangle$

$\mathcal{P}_1(\mathrm{t},\ r,\ \beta,\ \gamma)=\langle[\mathcal{P}_{11}(\mathrm{t},\ r),\ \mathcal{P}_{12}(\mathrm{t},\ r)],\ [\mathcal{P}'_{11}(\mathrm{t},\ \beta),\ \mathcal{P}'_{12}(\mathrm{t},\ \beta)],\ [\mathcal{P}''_{11}(\mathrm{t},\ \gamma),\ \mathcal{P}''_{12}(\mathrm{t},\ \gamma)]\rangle$

Consequently, following significant computation, we may write,

$$\mathcal{P}_{01}(\mathrm{t},\ r) = \frac{e^{\mathrm{t}\sqrt{\mathbb{A}_1(r)\mathbb{A}_2(r)}}}{2}\left(1 - \sqrt{\frac{\mathbb{A}_2(r)}{\mathbb{A}_1(r)}}\right) + \frac{e^{-\mathrm{t}\sqrt{\mathbb{A}_1(r)\mathbb{A}_2(r)}}}{2}\left(1 + \sqrt{\frac{\mathbb{A}_2(r)}{\mathbb{A}_1(r)}}\right) \tag{11}$$

$$\mathcal{P}_{02}(\mathrm{t},\ r) = \frac{e^{-\mathrm{t}\sqrt{\mathbb{A}_1(r)\mathbb{A}_2(r)}}}{2}\left(\sqrt{\frac{\mathbb{A}_1(r)}{\mathbb{A}_2(r)}} + 1\right) + \frac{e^{\mathrm{t}\sqrt{\mathbb{A}_1(r)\mathbb{A}_2(r)}}}{2}\left(1 - \sqrt{\frac{\mathbb{A}_1(r)}{\mathbb{A}_2(r)}}\right) \tag{12}$$

$$\mathcal{P}'_{01}(\mathrm{t},\beta) = \frac{e^{-\mathrm{t}\sqrt{\mathbb{A}'_1(\beta)\mathbb{A}'_2(\beta)}}}{2}\left(\sqrt{\frac{\mathbb{A}'_2(\beta)}{\mathbb{A}'_1(\beta)}} + 1\right) - \frac{e^{\mathrm{t}\sqrt{\mathbb{A}'_1(\beta)\mathbb{A}'_2(\beta)}}}{2}\left(\sqrt{\frac{\mathbb{A}'_2(\beta)}{\mathbb{A}'_1(\beta)}} - 1\right) \tag{13}$$

$$\mathcal{P}'_{02}(\mathrm{t},\ \beta) = \frac{e^{-\mathrm{t}\sqrt{\mathbb{A}'_1(\beta)\mathbb{A}'_2(\beta)}}}{2}\left(\sqrt{\frac{\mathbb{A}'_1(\beta)}{\mathbb{A}'_2(\beta)}} + 1\right) + \frac{e^{\mathrm{t}\sqrt{\mathbb{A}'_1(\beta)\mathbb{A}'_2(\beta)}}}{2}\left(1 - \sqrt{\frac{\mathbb{A}'_1(\beta)}{\mathbb{A}'_2(\beta)}}\right) \tag{14}$$

$$\mathcal{P}''_{01}(\mathrm{t},\ \gamma) = \frac{e^{-\mathrm{t}\sqrt{\mathbb{A}''_1(\gamma)\mathbb{A}''_2(\gamma)}}}{2}\left(\sqrt{\frac{\mathbb{A}''_2(\gamma)}{\mathbb{A}''_1(\gamma)}} + 1\right) - \frac{e^{\mathrm{t}\sqrt{\mathbb{A}''_1(\gamma)\mathbb{A}''_2(\gamma)}}}{2}\left(\sqrt{\frac{\mathbb{A}''_2(\gamma)}{\mathbb{A}''_1(\gamma)}} - 1\right) \tag{15}$$

$$\mathcal{P}''_{02}(\mathrm{t},\ \gamma) = \frac{e^{-\mathrm{t}\sqrt{\mathbb{A}''_1(\gamma)\mathbb{A}''_2(\gamma)}}}{2}\left(\sqrt{\frac{\mathbb{A}''_1(\gamma)}{\mathbb{A}''_2(\gamma)}} + 1\right) + \frac{e^{\mathrm{t}\sqrt{\mathbb{A}''_1(\gamma)\mathbb{A}''_2(\gamma)}}}{2}\left(1 - \sqrt{\frac{\mathbb{A}''_1(\gamma)}{\mathbb{A}''_2(\gamma)}}\right) \tag{16}$$

$$\mathcal{P}_{11}(\mathrm{t},\ r) = 1 - \frac{e^{-\mathrm{t}\sqrt{\mathbb{A}_1(r)\mathbb{A}_2(r)}}}{2}\left(\sqrt{\frac{\mathbb{A}_1(r)}{\mathbb{A}_2(r)}} + 1\right) - \frac{e^{\mathrm{t}\sqrt{\mathbb{A}_1(r)\mathbb{A}_2(r)}}}{2}\left(1 - \sqrt{\frac{\mathbb{A}_1(r)}{\mathbb{A}_2(r)}}\right) \tag{17}$$

$$\mathcal{P}_{12}(\mathrm{t},\ r) = 1 - \frac{e^{-\mathrm{t}\sqrt{\mathbb{A}_1(r)\mathbb{A}_2(r)}}}{2}\left(\sqrt{\frac{\mathbb{A}_2(r)}{\mathbb{A}_1(r)}} + 1\right) + \frac{e^{\mathrm{t}\sqrt{\mathbb{A}_1(r)\mathbb{A}_2(r)}}}{2}\left(\sqrt{\frac{\mathbb{A}_2(r)}{\mathbb{A}_1(r)}} - 1\right) \tag{18}$$

$$\mathcal{P}'_{11}(\mathrm{t},\ \beta) = 1 - \frac{e^{-\mathrm{t}\sqrt{\mathbb{A}'_1(\beta)\mathbb{A}'_2(\beta)}}}{2}\left(\sqrt{\frac{\mathbb{A}'_1(\beta)}{\mathbb{A}'_2(\beta)}} + 1\right) - \frac{e^{\mathrm{t}\sqrt{\mathbb{A}'_1(\beta)\mathbb{A}'_2(\beta)}}}{2}\left(1 - \sqrt{\frac{\mathbb{A}'_1(\beta)}{\mathbb{A}'_2(\beta)}}\right) \tag{19}$$

$$\mathcal{P}'_{12}(\mathfrak{t},\ \beta) = 1 - \frac{e^{-\mathfrak{t}\sqrt{\mathbb{A}'_1(\beta)\mathbb{A}'_2(\beta)}}}{2}\left(\sqrt{\frac{\mathbb{A}'_2(\beta)}{\mathbb{A}'_1(\beta)}} + 1\right) + \frac{e^{\mathfrak{t}\sqrt{\mathbb{A}'_1(\beta)\mathbb{A}'_2(\beta)}}}{2}\left(\sqrt{\frac{\mathbb{A}'_2(\beta)}{\mathbb{A}'_1(\beta)}} - 1\right) \tag{20}$$

$$\mathcal{P}''_{11}(\mathfrak{t},\ \gamma) = 1 - \frac{e^{-\mathfrak{t}\sqrt{\mathbb{A}''_1(\gamma)\mathbb{A}''_2(\gamma)}}}{2}\left(\sqrt{\frac{\mathbb{A}''_1(\gamma)}{\mathbb{A}''_2(\gamma)}} + 1\right) - \frac{e^{\mathfrak{t}\sqrt{\mathbb{A}''_1(\gamma)\mathbb{A}''_2(\gamma)}}}{2}\left(1 - \sqrt{\frac{\mathbb{A}''_1(\gamma)}{\mathbb{A}''_2(\gamma)}}\right) \tag{21}$$

$$\mathcal{P}''_{12}(\mathfrak{t},\ \gamma) = 1 - \frac{e^{-\mathfrak{t}\sqrt{\mathbb{A}''_1(\gamma)\mathbb{A}''_2(\gamma)}}}{2}\left(\sqrt{\frac{\mathbb{A}''_2(\gamma)}{\mathbb{A}''_1(\gamma)}} + 1\right) + \frac{e^{\mathfrak{t}\sqrt{\mathbb{A}''_1(\gamma)\mathbb{A}''_2(\gamma)}}}{2}\left(\sqrt{\frac{\mathbb{A}''_2(\gamma)}{\mathbb{A}''_1(\gamma)}} - 1\right) \tag{22}$$

Where $\langle[\mathbb{A}_1(r),\ \mathbb{A}_2(r)],\ [\mathbb{A}'_1(\beta),\ \mathbb{A}'_2(\beta)],\ [\mathbb{A}''_1(\gamma),\ \mathbb{A}''_2(\gamma)]\rangle$ is the cut set of $\tilde{\lambda_S}^{NS}$. Solution is strong or weak if it satisfies the condition of NDE.

6. **Numerical solution of the NPPSMS**

Assume that 0.0002 failures occur per hour on a system that is utilised in an NPPSMS. Determine how likely it is that the NPPSMS will function correctly and fail throughout an 800-hour mission in (i) the CS environment and (ii) the NS environment.

6.1. ***Crisp Solution***

When we take respective input values λ_s=0.0002; $\mathfrak{t}$=800-h, we get the following output results $\mathcal{P}_0(800)$=0.852144 and $\mathcal{P}_1(800)$=0.147856.

6.2. ***NS Solution***

We numerically solve the model system in the NS environment. Here, we take, $\tilde{\lambda_s}^{NS}$= $\langle 0.0001,\ 0.0002,\ 0.0003;\ 0.9,\ 0.6,\ 0.5\rangle$, and $\mathfrak{t}$=800-h. We get the numerical values of $\langle r, \beta, \gamma\rangle$-cut of probability of NPPSMS working normally $[\ \mathcal{P}_0(\mathfrak{t},\ r,\ \beta,\ \gamma)]$ and probability of NPPSMS failed $[\mathcal{P}_1(\mathfrak{t},\ r,\ \beta,\ \gamma)]$ for $r \in (0,\ 1]$ and $\beta,\ \gamma \in [0,\ 1)$ that are shown in Table-2. From Table-2 it is observed that when r increases, the values of $\mathcal{P}_{01}(\mathfrak{t},\ r)$ and $\mathcal{P}_{11}(\mathfrak{t},\ r)$ are increasing but the values of $\mathcal{P}_{02}(\mathfrak{t},\ r)$ and $\mathcal{P}_{12}(\mathfrak{t},\ r)$ are decreasing. If both the values of β and γ increase then the values of $\mathcal{P}'_{02}(\mathfrak{t},\ \beta)$, $\mathcal{P}'_{12}(\mathfrak{t},\ \beta)$, $\mathcal{P}''_{02}(\mathfrak{t},\ \gamma)$, $\mathcal{P}''_{12}(\mathfrak{t},\ \gamma)$ increase whereas values of $\mathcal{P}'_{01}(\mathfrak{t},\ \beta)$ and $\mathcal{P}'_{11}(\mathfrak{t},\ \beta)$; $\mathcal{P}''_{01}(\mathfrak{t},\ \gamma)$ and $\mathcal{P}''_{11}(\mathfrak{t},\ \gamma)$ decrease. We developed the solution's graph, which is depicted in Figure-2. Figure-2(a) present the graph of truth, indeterminacy and falsity membership function of the nuclear power plant system when it is working normally mode and Figure-2(b) present the graph of truth, indeterminacy and falsity membership function of the nuclear power plant system when it is failed mode. So the triangular single valued neutrosophic value of the probability of NPPSMS working normally in 800 hours time interval is $\mathcal{P}_0(\tilde{800})^{NS}$=$\langle 0.768847,\ 0.852144,\ 0.929359;\ 0.9,\ 0.6,\ 0.5\rangle$, where truth $(\mu_{\mathcal{P}_0}(\mathfrak{u}))$, indeterminacy $(\eta_{\mathcal{P}_0}(\mathfrak{u}))$ and falsity $(\nu_{\mathcal{P}_0}(\mathfrak{u}))$ membership functions are respectively as follows:

$$\mu_{\mathcal{P}_0}(\mathfrak{u}) = \begin{cases} (\frac{\mathfrak{u}-0.768847}{0.083297}).0.9 & \text{when } 0.768847 \leqslant \mathfrak{u} \leqslant 0.852144 \\ 0.9 & \text{when } \mathfrak{u} = 0.852144 \\ (\frac{0.929359-\mathfrak{u}}{0.077215}).0.9 & \text{when } 0.852144 \leqslant \mathfrak{u} \leqslant 0.929359 \\ 0 & \text{when } \mathfrak{u} \leqslant 0.768847 \text{ or } \mathfrak{u} \geqslant 0.929359 \end{cases}$$

$$\eta_{\mathcal{P}_0}(\mathfrak{u}) = \begin{cases} \frac{0.390836-0.4.\mathfrak{u}}{0.083297} & \text{when } 0.768847 \leqslant \mathfrak{u} \leqslant 0.852144 \\ 0.6 & \text{when } \mathfrak{u} = 0.852144 \\ \frac{0.4\mathfrak{u}-0.294529}{0.077215} & \text{when } 0.852144 \leqslant \mathfrak{u} \leqslant 0.929359 \\ 1 & \text{when } \mathfrak{u} \leqslant 0.768847 \text{ or } \mathfrak{u} \geqslant 0.929359 \end{cases}$$

$$\nu_{\mathcal{P}_0}(\mathfrak{u}) = \begin{cases} \frac{0.467721-0.5.\mathfrak{u}}{0.083297} & \text{when } 0.768847 \leqslant \mathfrak{u} \leqslant 0.852144 \\ 0.5 & \text{when } \mathfrak{u} = 0.852144 \\ \frac{0.5\mathfrak{u}-0.387465}{0.077215} & \text{when } 0.852144 \leqslant \mathfrak{u} \leqslant 0.929359 \\ 1 & \text{when } \mathfrak{u} \leqslant 0.768847 \text{ or } \mathfrak{u} \geqslant 0.929359 \end{cases}$$

where $\mu_{\mathcal{P}_0}(\mathfrak{u}) + \eta_{\mathcal{P}_0}(\mathfrak{u}) + \nu_{\mathcal{P}_0}(\mathfrak{u}) \leqslant 3$

Also the triangular single valued neutrosophic value of the probability of nuclear power plant system failed in 800 hours time interval is $\mathcal{P}_1(\tilde{800})^{NS}$=$\langle 0.070641,\ 0.147856,\ 0.231153;\ 0.9,\ 0.6,\ 0.5\rangle$, where truth$(\mu_{\mathcal{P}_1}(\mathfrak{u}))$, indeterminacy$(\eta_{\mathcal{P}_1}(\mathfrak{u}))$ and falsity$(\nu_{\mathcal{P}_1}(\mathfrak{u}))$ membership functions are respectively as follows:

$$\mu_{\mathcal{P}_1}(\mathfrak{u}) = \begin{cases} (\frac{\mathfrak{u}-0.070641}{0.077215}).0.9 & \text{when } 0.070641 \leqslant \mathfrak{u} \leqslant 0.147856 \\ 0.9 & \text{when } \mathfrak{u} = 0.147856 \\ (\frac{0.231153-\mathfrak{u}}{0.083297}).0.9 & \text{when } 0.147856 \leqslant \mathfrak{u} \leqslant 0.231153 \\ 0 & \text{when } \mathfrak{u} \leqslant 0.070641 \text{ or } \mathfrak{u} \geqslant 0.231153 \end{cases}$$

$$\eta_{\mathcal{P}_1}(\mathfrak{u}) = \begin{cases} \frac{0.105471-0.4.\mathfrak{u}}{0.077215} & \text{when } 0.070641 \leqslant \mathfrak{u} \leqslant 0.147856 \\ 0.6 & \text{when } \mathfrak{u} = 0.147856 \\ \frac{0.4\mathfrak{u}-0.009164}{0.083297} & \text{when } 0.147856 \leqslant \mathfrak{u} \leqslant 0.231152 \\ 1 & \text{when } \mathfrak{u} \leqslant 0.0.070641 \text{ or } \mathfrak{u} \geqslant 0.231153 \end{cases}$$

$$\nu_{\mathcal{P}_1}(\mathfrak{u}) = \begin{cases} \frac{0.112536-0.5.\mathfrak{u}}{0.077215} & \text{when } 0.070641 \leqslant \mathfrak{u} \leqslant 0.147856 \\ 0.5 & \text{when } \mathfrak{u} = 0.147856 \\ \frac{0.5\mathfrak{u}-0.032280}{0.083297} & \text{when } 0.147856 \leqslant \mathfrak{u} \leqslant 0.231152 \\ 1 & \text{when } \mathfrak{u} \leqslant 0.0.070641 \text{ or } \mathfrak{u} \geqslant 0.231153 \end{cases}$$

where $\mu_{\mathcal{P}_1}(\mathfrak{u}) + \eta_{\mathcal{P}_1}(\mathfrak{u}) + \nu_{\mathcal{P}_1}(\mathfrak{u}) \leqslant 3$.

From the table values and graph, we see that $\mathcal{P}_{01}(\mathfrak{t},\ r)$, $\mathcal{P}_{11}(\mathfrak{t},\ r)$ are increasing function and

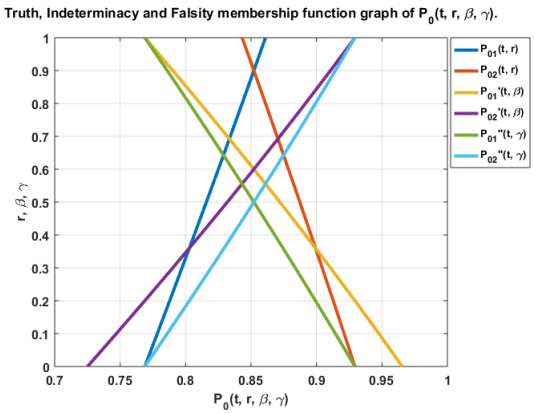

(a) Depicts the truth, indeterminacy and falsity membership function graph of the probability of nuclear power plant system working normally at time (t=800).

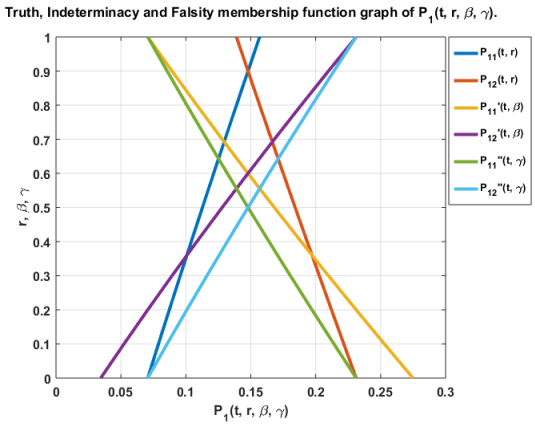

(b) Depicts the truth, indeterminacy and falsity membership function graph of the probability of nuclear power plant system failed at time (t=800).

FIGURE 2. Depicts the truth, indeterminacy and falsity membership function graph of the probability of nuclear power plant system at time t=800 when parameter λ_s is TSVNNs.

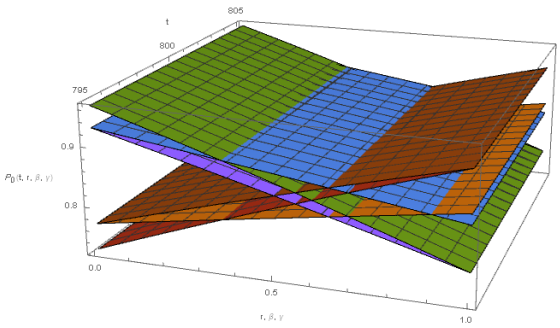

(a) Depicts the 3D plot of the the truth, indeterminacy and falsity membership function graph of the probability of nuclear power plant system working normally at time interval between 795 hrs to 805 hrs.

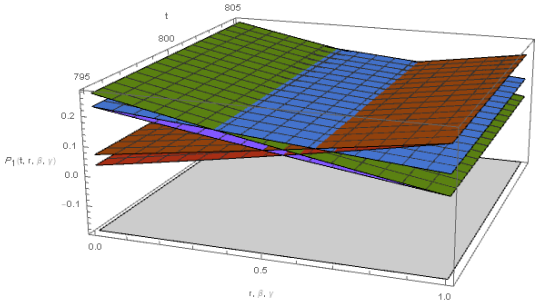

(b) Depicts 3D plot of the truth, indeterminacy and falsity membership function graph of the probability of nuclear power plant system failed at time interval between 795 hrs to 805 hrs.

FIGURE 3. Depicts the 3D plot of the truth, indeterminacy and falsity membership function graph of the probability of nuclear power plant system at time interval between 795 hrs to 805 hrs when parameter λ_s is TSVNNs.

$\mathcal{P}_{02}(\mathfrak{t},\ r)$, $\mathcal{P}_{12}(\mathfrak{t},\ r)$ are decreasing function, whereas $\mathcal{P}'_{01}(\mathfrak{t},\ \beta)$, $\mathcal{P}''_{01}(\mathfrak{t},\ \gamma)$, $\mathcal{P}'_{11}(\mathfrak{t},\ \beta)$, $\mathcal{P}''_{11}(\mathfrak{t},\ \gamma)$

TABLE 2. Values of $\mathcal{P}_0(\mathfrak{t},\ r,\ \beta,\ \gamma)$ and $\mathcal{P}_1(\mathfrak{t},\ r,\ \beta,\ \gamma)$ when $\tilde{\lambda}_s^{NS}$ is a TSVNNs.

$r,\ \beta,\ \gamma$	$\mathcal{P}_{01}(\mathfrak{t},\ r)$	$\mathcal{P}_{02}(\mathfrak{t},\ r)$	$\mathcal{P}'_{01}(\mathfrak{t},\ \beta)$	$\mathcal{P}'_{02}(\mathfrak{t},\ \beta)$	$\mathcal{P}''_{01}(\mathfrak{t},\ \gamma)$	$\mathcal{P}''_{02}(\mathfrak{t},\ \gamma)$	$\mathcal{P}_{11}(\mathfrak{t},\ r)$	$\mathcal{P}_{12}(\mathfrak{t},\ r)$	$\mathcal{P}'_{11}(\mathfrak{t},\ \beta)$	$\mathcal{P}'_{12}(\mathfrak{t},\ \beta)$	$\mathcal{P}''_{11}(\mathfrak{t},\ \gamma)$	$\mathcal{P}''_{12}(\mathfrak{t},\ \gamma)$
0	0.768847	0.929359	0.965531	0.725082	0.929359	0.768847	0.070641	0.231153	0.274918	0.034470	0.231153	0.070641
0.1	0.778386	0.921096	0.947654	0.747134	0.914427	0.785968	0.078904	0.221614	0.252866	0.052346	0.210432	0.085573
0.2	0.787856	0.912752	0.929359	0.768847	0.899235	0.802862	0.087248	0.212144	0.231153	0.070641	0.197138	0.100765
0.3	0.797256	0.904328	0.910653	0.790213	0.883788	0.819526	0.095672	0.202744	0.209787	0.089347	0.180474	0.116212
0.4	0.806585	0.895825	0.891543	0.811223	0.868090	0.835954	0.104175	0.193415	0.188777	0.018260	0.164046	0.131910
0.5	0.815843	0.887243	0.872038	0.831870	0.852144	0.852144	0.112757	0.184157	0.168130	0.108457	0.147856	0.147856
0.6	0.825028	0.878583	0.852144	0.852144	0.835954	0.868090	0.121417	0.174972	0.147856	0.147856	0.131910	0.164046
0.7	0.834141	0.869846	0.831870	0.872038	0.819526	0.883788	0.130154	0.165859	0.127962	0.168130	0.116212	0.180474
0.8	0.843179	0.861033	0.811223	0.891543	0.802862	0.899235	0.138967	0.156821	0.108457	0.188777	0.100765	0.197138
0.9	0.852144	0.852144	0.790213	0.910653	0.785968	0.914427	0.147856	0.147856	0.089347	0.209787	0.08573	0.214032
1.0	0.861033	0.843179	0.768847	0.929359	0.768847	0.929359	0.156821	0.138967	0.070641	0.231153	0.070641	0.231153

are decreasing functions and $\mathcal{P}'_{02}(\mathfrak{t},\ \beta)$, $\mathcal{P}''_{02}(\mathfrak{t},\ \gamma)$, $\mathcal{P}'_{12}(\mathfrak{t},\ \beta)$, $\mathcal{P}''_{12}(\mathfrak{t},\ \gamma)$ are increasing functions. Hence, the solutions are strong solution.

6.3. *Comparison study*

TABLE 3. Comparison analysis

Method	$\mathcal{P}_0(\mathfrak{t})$	$\mathcal{P}_1(\mathfrak{t})$
Zadeh's extension principle	Strong solution	Strong solution
Generalized Hukuhara differentiability(GH_{ii})	Weak solution	Weak solution
Classical method	Strong solution	Strong solution

After completing the lengthy calculation task and consulting Table-3, We found that the solutions will be of a strong variety of our NPPSMS is solved by employing Zadeh's extension principle approach. Once again, the result will be weak if the model is solved using the Generalized Hukuhara Differentiability(GH_{ii}) method. We used the classical technique to solve our problem, resulting in a strong solution. Now it turns out that we are getting robust solutions with both Zadeh's extension principle and classical methods. But, $\langle r,\ \beta,\ \gamma\rangle$-cut solution cannot be obtained directly while we are using Zadeh's extension principle; instead, we must depend on crisp solution. On the other hand, we may obtain the $\langle r,\ \beta,\ \gamma\rangle$-cut solution without depending on the crisp solution when we use the classical method. Thus, the solution produced using the classical approach appears to be quite good. Comparing the numerical results from these two procedures reveals that the classical method's approach is the most acceptable. Based on all these findings, the classical technique is the most acceptable and error-free.

We will now perform a comparative analysis between the results obtained in crisp and neutrosophic environments. In a crisp environment, for λ_s=0.0002; $\mathfrak{t}$=800-h, the probability value of

normal operation of a NPPSMS is 0.852144, and the probability value of failure is 0.147856. We take the value of parameter λ_s as a single-valued triangular neutrosophic number instead of a crisp number. So the maximum tolerance is assumed to be 50% on both sides while shifting the value of the parameter from a crisp environment to a neutrosophic environment. Here, the maximum truth membership value is assumed to be 0.9, with the minimum indeterminacy and falsity membership values being 0.6 and 0.5, respectively. Now in the neutrosophic environment, for the values of $\tilde{\lambda_s}^{NS}$=$\langle 0.0001,\ 0.0002,\ 0.0003;\ 0.9,\ 0.6,\ 0.5\rangle$, and t=800-h., the single valued triangular neutrosophic value of the probability of normal operation of the NPPSMS is $\mathcal{P}_0(\tilde{800})^{NS}$=$\langle 0.768847,\ 0.852144,\ 0.929359;\ 0.9,\ 0.6,\ 0.5\rangle$, and the single valued triangular neutrospheric value of the probability of failure is $\mathcal{P}_1(\tilde{800})^{NS}$=$\langle 0.070641,\ 0.147856,\ 0.231153;\ 0.9,\ 0.6,\ 0.5\rangle$. Here, the values in the neutrosophic environment are much more flexible compared to the crisp environment. Also, the value of the probability of normal operation of a NPPSMS in a neutrosophic environment indicates that the maximum permissible tolerances on its left and right sides are 9.77% and 9.06%, respectively; the maximum truth membership value is 0.9; and the minimum indeterminacy and falsity membership values are 0.6 and 0.5, respectively. Again, the failure probability value of the NPPSMS indicates that the maximum allowable tolerances on its left and right sides are 52.22% and 56.34%, the maximum truth membership value is 0.9, and the minimum indeterminacy and falsity membership values are 0.6 and 0.5, respectively. These conclusive findings show that the neutrosophic environment is more flexible, realistic, and acceptable than the crisp environment.

7. **Conclusion**

In this article we have discussed the definition of NS, SVNS, TSVNNs, and $\langle r, \beta, \gamma\rangle$-cut set of SVNS. We have also explored the idea of a first-order linear homogeneous neutrosophic differential equation and discussed its robustness in view of strong and weak nature of it's solutions. Then, we argued and pointed out the need of analyzing NPP safety system in NS-environment and mathematically formulate an NPPSMS model system in terms of a single-valued triangular neutrosophic differential equation. We have used TSVNNs to analyse and quantitatively discuss the solutions of the NPPSMS above model system with appropriate emphasis on the model parameter rates of failure λ_s. We have obtained the solutions of the model system both in crisp and NS environment. Robust solutions of the NPPSMS model system have been found in both crisp and NS environments. Moreover, solutions are compared by applying there distinct methods namely Zadeh's extension principle, Generalized Hukuhara differentiability (GH_{ii}) and Classical method. It is observed that solutions obtained by Classical method are reliable with less error. However, we have noticed one limitation in

our model system. The initial conditions of the model cannot be treated as single-valued triangular neutrosophic numbers. If the initial conditions are assumed to be single-valued triangular neutrosophic numbers, then it contradicts the theory of basic probability. A special advantage of our nuclear power plant safety model is that it can provide robust solutions in any imprecise environment as it is composed of only one parameter.

As an future extension of this work, neutrosophic differential equation can be utilized incorporating other powerful fuzzy environments like trapezoidal neutrosophic numbers or trapezoidal single-valued neutrosophic numbers to capture and handle many real-world problems where impreciseness are inherently involved. In the future, the outcomes of our research may be used to patient safety systems, medical safety systems, human error safety systems, power generation safety systems, compressor safety systems, engineering maintenance safety systems, and so on.

References

[1] Jyotish, N.K., Singh, L.K. and Kumar, C. Availability analysis of safety-critical systems of nuclear power plant using ordinary differential equations and reachability graph. Progress in Nuclear Energy, 159, 104624, 2023.

[2] Hyvärinen, J., Vihavainen, J., Ylönen, M. and Valkonen, J. An overall safety concept for nuclear power plants. Annals of Nuclear Energy, 178, 109353, 2022.

[3] Bao, H., Zhang, H., Shorthill, T., Chen, E. and Lawrence, S. Quantitative evaluation of common cause failures in high safety-significant safety-related digital instrumentation and control systems in nuclear power plants. Reliability Engineering & System Safety, 230, 108973, 2023.

[4] Zhang, S., Ma, Z., Zhang, H. and Smith, C.L. Multicriterion benefit evaluation methodology for safety enhancements in nuclear power plants and application for FLEX strategies. Nuclear Engineering and Design, 376, 111135, 2021.

[5] So, E. and Kim, M.C. Application of Chernoff bound to passive system reliability evaluation for probabilistic safety assessment of nuclear power plants. Nuclear Engineering and Technology, 54(8), 2915-2923, 2022.

[6] Wu, G., Mao, Y., He, Y., Lu, Y., Jia, M. and Fu, S. Safety archetypes identification and behavior simulation for nuclear power plant operation human reliability improvement. Annals of Nuclear Energy, 174, 109189, 2022.

[7] Martón, I., Sánchez, A.I., Carlos, S., Mullor, R. and Martorell, S. Prognosis of wear-out effect on of safety equipment reliability for nuclear power plants long-term safe operation. Reliability Engineering & System Safety, 233, 109121, 2023.

[8] Ahn, J., Bae, J., Min, B.J. and Lee, S.J. Operation validation system to prevent human errors in nuclear power plants. Nuclear Engineering and Design, 397, 111949, 2022.

[9] Ayodeji, A., Amidu, M.A., Olatubosun, S.A., Addad, Y. and Ahmed, H. Deep learning for safety assessment of nuclear power reactors: Reliability, explainability, and research opportunities. Progress in Nuclear Energy, 151, 104339, 2022.

[10] Singh, P. and Singh, L.K. Reliability measurement of control and instrumentation systems of nuclear power plants. IEEE Transactions on Reliability, 72(2), 727-736, 2023.

[11] Abdel-Basset, M., Gamal, A., Hezam, I.M. and Sallam, K.M. An Effective Analysis of Risk Assessment and Mitigation Strategies of Photovoltaic Power Plants Based on Real Data: Strategies, Challenges, Perspectives, and Sustainability. International Journal of Energy Research, 1-33, 2023.

[12] Abdel-Basset, M., Gamal, A., Sallam, K.M., Hezam, I.M. and Alshamrani, A.M. Sustainable Flue Gas Treatment System Assessment for Iron and Steel Sector: Spherical Fuzzy MCDM-Based Innovative Multistage Approach. International Journal of Energy Research, 1-25, 2023.

[13] Abdel-Basset, M., Gamal, A., Hezam, I.M. and Sallam, K.M. Sustainability assessment of optimal location of electric vehicle charge stations: a conceptual framework for green energy into smart cities. Environment, Development and Sustainability, 1-39, 2023.

[14] Mondal, D., Garai, T., Roy, G.C. and Alam, S. The design and evaluation of a picture fuzzy mining safety system with picture fuzzy differential equations. Decision Analytics Journal, 9, 100322, 2023.

[15] Hamer, R., Waterson, P. and Jun, G.T. Human factors and nuclear safety since 1970–A critical review of the past, present and future. Safety Science, 133, 105021, 2021.

[16] Smarandache, F. In: Neutrosophy. Neutrisophic Property, Sets, and Logic. American Research Press. Rehoboth. USA, 1998.

[17] Atanassov, K. T. Intuitionistic fuzzy sets. Fuzzy sets and system, 20, 87-96, 1986.

[18] Purba, J.H., Tjahyani, D.S., Widodo, S. and Ekariansyah, A.S. Fuzzy probability based event tree analysis for calculating core damage frequency in nuclear power plant probabilistic safety assessment. Progress in Nuclear Energy, 125, 103376, 2020.

[19] Purba, J.H. Fuzzy probability on reliability study of nuclear power plant probabilistic safety assessment: A review. Progress in Nuclear Energy, 76, 73-80, 2014.

[20] Sleem, A. and Elhenawy, I. Energy Efficiency and Material Cost Savings by Evolution of Solar Panels Used in Photovoltaic Systems under Neutrosophic Model. Neutrosophic Systems with Applications, 5, 36-43, 2023.

[21] Sallam, K.M. and Mohamed, A.W. Neutrosophic MCDM Methodology for Evaluation Onshore Wind for Electricity Generation and Sustainability Ecological. Neutrosophic Systems with Applications, 4, 53-61, 2023.

[22] Mondal, D., Garai, T., Roy, G.C. and Alam, S. Application of a fuzzy differential equation system to the oil and gas industry safety model. International Journal of Information Technology, 15(3), 1243-1253, 2023.

[23] Melliani, S. and Chadli, L.S. Intuitionistic fuzzy differential equation. Notes on Intuitionistic Fuzzy Sets, 6(2), 37-41, 2000.

[24] Amma, B.B., Melliani, S. and Chadli, L.S. Numerical solution of intuitionistic fuzzy differential equations by Diagonally implicit block backward differentiation formulas. International Journal On Optimization and Applications, 1(3), 17-22, 2021.

[25] Man, S., Saw, B.C. and Hazra, S.B. An Explicit Method for Solving Intuitionistic Fuzzy Heat Equation. Advances in Fuzzy Mathematics (AFM), 16(1), 27-39, 2021.

[26] Melliani, S., Belhallaj, Z., Elomari, M. and Chadli, L.S. Approximate Solution of Intuitionistic Fuzzy Differential Equations with the Linear Differential Operator by the Homotopy Analysis Method. Advances in Fuzzy Systems, 1-10, 2021.

[27] Sumathi, I.R. and Priya, V.M. A new perspective on neutrosophic differential equation. International Journal of Engineering & Technology, 7 (4.10), 422-425, 2018.

[28] Sumathi, I.R. and Antony Crispin Sweety, C. New approach on differential equation via trapezoidal neutrosophic number. Complex & Intelligent Systems, 5(4), 417-424, 2019.

[29] Son, N.T.K., Dong, N.P., Long, H.V. and Khastan, A. Linear quadratic regulator problem governed by granular neutrosophic fractional differential equations. ISA transactions, 97, 296-316, 2020.

[30] Alamin, A., Mondal, S.P., Alam, S., Ahmadian, A., Salahshour, S. and Salimi, M. Solution and interpretation of neutrosophic homogeneous difference equation. Symmetry, 12(7), 1091, 2020.

[31] Parikh, M. and Sahni, M. Sumudu Transform for Solving Second Order Ordinary Differential Equation under Neutrosophic Initial Conditions, Neutrosophic Sets and Systems, 38(18), 258-275, 2020.

[32] Mondal, D., Tudu, S., Roy, G.C. and Roy, T.K. A Model Describing the Neutrosophic Differential Equation and Its Application On Mine Safety. Neutrosophic Sets and Systems, 46, 386-401, 2021.

[33] Parikh, M., Sahni, M. and Sahni, R. Solution of First Order Initial Value Problem using Analytical and Numerical Method in Neutrosophic Environment. Neutrosophic Sets and Systems, An International Journal in Information Science and Engineering, 51(20), 311-329, 2022.

[34] Acharya, A., Mahata, A., Mukherjee, S., Biswas, M.A., Das, K.P., Mondal, S.P. and Roy, B. A Neutrosophic differential equation approach for modeling glucose distribution in the bloodstream using neutrosophic sets. Decision Analytics Journal, 8, 100264, 2023.

[35] Garai, T., Dalapati, S. and Smarandache, F. Softmax function based neutrosophic aggregation operators and application in multi-attribute decision making problem. Neutrosophic Sets and Systems, 56(1), 1-26, 2023.

[36] Dhillon, B.S. Safety, reliability, human factors, and human error in nuclear power plants. CRC Press Florida, 79-82, 2017.

[37] Buckley, J.J., Eslami, E. and Feuring, T. Fuzzy mathematics in economics and engineering, Physica Heidelberg, 91, 146, 2002.

[38] Mondal, S.P., Khan, N.A., Razzaq, O.A., Tudu, S. and Roy, T.K. Adaptive strategies for system of fuzzy differential equation: Application of arms race model. J. Math. Comput. Sci, 18(2), 192-205, 2018.

[39] Biswas, M.A. and Acharya, A., Numerical Solution of Fuzzy Delayed Prey-Predator Model: Hukuhara Derivative Approach, Gradiva Review Journal, 8(7), 1400-1411, 2022.

Received: March 25, 2024. **Accepted**: August 29, 2024.

NSS

Neutrosophic Sets and Systems, Vol. 72, 2024

University of New Mexico

Neutrosophic Quadruple H_v-modules and their fundamental module

Madeleine Al Tahan[1], Saba Al-Kaseasbeh [2,*], and Bijan Davvaz [3]

[1]College of Engineering, Abu Dhabi University, United Arab Emirates; altahan.madeleine@gmail.com

[2]Department of Mathematics, Tafila Technical University, Tafila, Jordan; saba.alkaseasbeh@gmail.com

[3] Department of Mathematical Sciences, Yazd University, Yazd, Iran; davvaz@yazd.ac.ir

*Correspondence:saba.alkaseasbeh@gmail.com

Abstract. This article aims to explore the deeper connections between neutrosophy and hyperstructures. Specifically, we introduce the concept of neutrosophic quadruple H_v-modules over neutrosophic quadruple H_v-rings, examine their properties, and identify their fundamental module.

Keywords: H_v-module; neutrosophic quadruple number; neutrosophic quadruple H_v-module; fundamental ring; fundamental module.

1. Introduction

In 1934, Marty [15] introduced the concept of hypergroups by generalizing the notion of a group. In a hypergroup, the binary operation is defined on a non-empty set and satisfies properties such as associativity, the existence of an identity element, and the presence of invertible elements. Hypergroups can be seen as a natural extension of groups and have applications in various fields, including physics, computer science, and combinatorics. Beyond hypergroups, other algebraic hyperstructures such as hyperrings and hyperfields also exist. These structures are utilized in algebraic geometry, number theory, and many areas of pure and applied mathematics (see [3–5, 9–12, 25]).

Vougiouklis introduced the notion of weak hyperstructures, also known as H_v-structures, at the Fourth Congress of the Algebraic Hyperstructures and its Applications (AHA) in 1990 [23, 24]. A weak hyperstructure is a generalization of a hyperstructure where the binary

operation is not necessarily defined for all pairs of elements in the set, but only for certain subsets of pairs. This weakening of the definition of a hyperstructure allows for a wider range of structures to be studied, and has applications in fields such as topology and fuzzy logic. Vougiouklis's work on weak hyperstructures has also led to the development of other related concepts, such as soft sets and rough sets, which are used in data analysis and decision making.

Fuzzy set theory, introduced by Lotfi A. Zadeh [26] in 1965, deals with the concept of partial truth, where an element can belong to a set to a certain degree, rather than being either completely in or completely out of the set. While fuzzy set theory has many real-life applications, it has limitations when it comes to dealing with situations of indeterminacy. This is where neutrosophy comes in. Neutrosophy, introduced by Florentin Smarandache in 1995, is a generalization of fuzzy set theory that deals with situations of indeterminacy, inconsistency, and incomplete knowledge. It extends the concept of partial truth by introducing the concept of "neutrosophic truth," where a statement can be simultaneously true, false, and indeterminate to different degrees. Neutrosophy allows for a more flexible and nuanced way of modeling real-world situations, and it has applications in a variety of fields, including philosophy, mathematics, and artificial intelligence. Symbolic neutrosophic theory refers to the use of abstract symbols, such as the letters T, I, and F, to represent the neutrosophic components of truth, indeterminacy, and falsehood. This notation allows for a more concise and precise way of expressing neutrosophic statements and computations, and it has been used in a variety of applications, such as decision-making, image processing, and expert systems. Fore more detail about neutrosophy, we refer to [16, 18–21].

In 2015, Florentin Smarandache [17] introduced the concept of neutrosophic quadruple numbers, which are a generalization of real and complex numbers that incorporate the neutrosophic concept of partial truth. Neutrosophic quadruple numbers consist of four components: a real component, an imaginary component, a neutrosophic truth component, and a neutrosophic falsity component. Smarandache presented the arithmetic operations of addition, subtraction, multiplication, and scalar multiplication on the set of neutrosophic quadruple numbers. Agboola et al. [1] subsequently established a connection between neutrosophy and algebraic structures by considering the set of neutrosophic quadruple numbers and using the defined operations to discuss neutrosophic quadruple algebraic structures, such as neutrosophic groups and neutrosophic rings. Akinleye et al. [2] further generalized this work in 2016 by considering the set of neutrosophic quadruple numbers and defining hyperoperations on it, leading to the study of neutrosophic quadruple hyperstructures, such as neutrosophic hypergroups and neutrosophic hyperrings. Overall, the introduction of neutrosophic quadruple numbers and the study of neutrosophic algebraic structures and hyperstructures have opened up new avenues

of research and applications in fields such as mathematics, computer science, and engineering. In neutrosophic mathematics, a neutrosophic quadruple H_v-group is a hypergroup with four binary operations, namely neutrosophic addition, neutrosophic multiplication, neutrosophic h-addition, and neutrosophic h-multiplication, which satisfy certain axioms. Similarly, a neutrosophic quadruple H_v-ring is a ring with four binary operations that satisfy additional axioms.

The study of neutrosophic quadruple H_v-groups and neutrosophic quadruple H_v-rings is a relatively new area of research in neutrosophic mathematics, and many of their properties and characteristics are still being explored. However, it is interesting to note that the concept of the fundamental group, which is a central concept in algebraic topology, has been extended to neutrosophic quadruple H_v-groups, and its properties have been studied.

In particular, it has been shown that the fundamental group of a neutrosophic quadruple H_v-group is also a neutrosophic quadruple group, which is a group-like structure with four components representing truth, falsehood, indeterminacy, and non-membership. This result provides a deeper understanding of the topological properties of neutrosophic quadruple H_v-groups and their relationship to algebraic structures.

The authors in [6, 7] discussed neutrosophic quadruple H_v-groups and neutrosophic quadruple H_v-rings and studied their properties. Then in [8], they found the fundamental group of neutrosophic quadruple H_v-groups and proved that it is a neutrosphic quadruple group. Our paper extends their results to H_v-modules and it is constructed as follows: after an Introduction, Section 2 presents the basic concepts that are used throughout our paper. Section 3 defines neutrosophic H_v-modules and studies their basic properties. Finally, Section 4 characterizes the fundamental module of neutrosophic H_v-modules up to isomorphism.

2. **Preliminaries**

This section provides some hyperstructure theory, definitions and theorems that are used throughout the paper. (See [10, 12, 25].)

A hyperoperation on a non-empty set H is a binary operation $\circ : H \times H \to \mathcal{P}^*(H)$, where $\mathcal{P}^*(H)$ is the set of all non-empty subsets of H. The operation $\circ$ is usually denoted by $\circ_n$ when it has arity n, that is, when it takes n arguments. For example, $\circ_2$ is the binary operation defined above.

A hyperoperation can be thought of as a generalization of a binary operation, which takes two elements of H and returns a single element of H. In contrast, a hyperoperation takes two elements of H and returns a non-empty subset of H.

Hyperoperations are used in the study of hypergroups, which are algebraic structures that generalize groups.

To clarify the definitions further, if we have given a hyperoperation $\circ$ on a non-empty set H and two non-empty subsets $A, B \subseteq H$, we define $A \circ B$ as the union of all elements of the form $a \circ b$ where $a \in A$ and $b \in B$. That is,

$$A \circ B = \bigcup_{a \in A, b \in B} a \circ b.$$

We also define $x \circ A$ as $\{x\} \circ A$ and $A \circ x$ as $A \circ \{x\}$.

Definition 2.1. Let $(H, \circ)$ be a hypergrupoid. Then:

- $(H, \circ)$ is a semihypergorup if $\circ$ is associative, meaning that for any $x, y, z \in H$, we have $(x \circ y) \circ z = x \circ (y \circ z)$.
- $(H, \circ)$ is a quasi-hypergroup if every element $x \in H$ reproduces the entire set H under the hyperoperation $\circ$, meaning that $x \circ H = H = H \circ x$.
- $(H, \circ)$ is a hypergroup if it is both a semihypergroup and a quasi-hypergroup.

Hypergroups generalize the notion of groups and provide a natural framework for studying non-associative algebraic structures.

The concept of H_v-structures were introduced by T. Vougiouklis [23, 24] is an important generalization of hyperstructures that allows for more flexible and weaker axioms, which can capture a wider range of algebraic systems. This makes H_v-structures a powerful tool for studying hyperstructures that arise in various areas of mathematics and science such as algebraic geometry, combinatorics, and physics, to model complex systems that cannot be described by traditional algebraic structures. However, Most of H_v-structures are used in representation theory.

Definition 2.2. A hypergroupoid $(H, \circ)$ is called an H_v-semigroup if it satisfies the following axiom:

$$(h_1 \circ (h_2 \circ h_3)) \cap ((h_1 \circ h_2) \circ h_3) \neq \emptyset \text{ for all } h_1, h_2, h_3 \in H.$$

This axiom is weaker than the associativity axiom of classical semigroups, which requires that $(h_1 \circ h_2) \circ h_3 = h_1 \circ (h_2 \circ h_3)$ for all $h_1, h_2, h_3 \in H$.

The H_v-semigroups are used to study non-associative algebraic structures that arise in representation theory.

An element $0 \in H$ is called an identity of $(H, \circ)$ if it satisfies the following axiom:

$$h \in 0 \circ h \cap h \circ 0 \text{ for all } h \in H.$$

Definition 2.3. A hypergroupoid $(H, \circ)$ is called an H_v-group if it is a quasi-hypergroup and an H_v-semigroup. A quasi-hypergroup is a hypergroupoid $(H, \circ)$ such that for every $h_1 \in H$, there exists $h_2 \in H$ such that $h_1 \in h_2 \circ h_1 \cap h_1 \circ h_2$.

An H_v-subgroup of an H_v-group $(H, \circ)$ is a non-empty subset $S \subseteq H$ such that $(S, \circ)$ is also an H_v-group.

Definition 2.4. A multivalued system $(R^{\sim}, +, \cdot)$ is a *hyperring* if (1) $(R^{\sim}, +)$ is a hypergroup; (2) $(R^{\sim}, \cdot)$ is a semihypergroup; (3) $\cdot$ is distributive with respect to $+$. And it is an H_v*-ring* if (1) $(R^{\sim}, +)$ is an H_v-group; (2) $(R^{\sim}, \cdot)$ is is an H_v-semigroup; (3) $\cdot$ is weak distributive with respect to $+$. $(R^{\sim}, +, \cdot)$ is said to be commutative if $\alpha + \beta = \beta + \alpha$ and $\alpha \cdot \beta = \beta \cdot \alpha$ for all $\alpha, \beta \in R^{\sim}$.

An element $1 \in R^{\sim}$ is called a *unit* if $\alpha \in 1 \cdot \alpha \cap \alpha \cdot 1$ for all $\alpha \in R^{\sim}$. A subset S of an H_v-ring $(R^{\sim}, +, \cdot)$ is called an H_v*-subring* of $R^{\sim}$ if $(S, +, \cdot)$ is an H_v-ring. To prove that $(S, +, \cdot)$ is an H_v-subring of $(R^{\sim}, +, \cdot)$, it suffices to show that $\alpha + S = S + \alpha = S$ and $\alpha \cdot \ \beta \subseteq S$ for all $\alpha, \beta \in R^{\sim}$.

Now, a homomorphism between two H_v-rings $(R^{\sim}, +, \star)$ and $(S, +', \star')$ is a function $f : R^{\sim} \to S$ that preserves the ring structure and the valuation function, meaning:

$f(\alpha + \beta) = f(\alpha) +' f(\beta)$ for all $\alpha, \beta \in R^{\sim}$. $f(\alpha \star \beta) = f(\alpha) \star' f(\beta)$ for all $\alpha, \beta \in R^{\sim}$. $v_S(f(\alpha)) = v_{R^{\sim}}(\alpha)$ for all $\alpha \in R^{\sim}$. Here, $v_R^{\sim}$ and v_S denote the valuation functions on $R^{\sim}$ and S, respectively.

Finally, two H_v-rings $R^{\sim}$ and S are isomorphic if there exists an H_v-ring homomorphism $f : R^{\sim} \to S$ that is bijective, and its inverse $f^{-1} : S \to R^{\sim}$ is also an H_v-ring homomorphism. In other words, $R^{\sim}$ and S are isomorphic if they have the same ring structure and the same valuation function, up to a bijective change of variables.

Definition 2.5. A non-empty set M is an H_v-module over an H_v-ring $R^{\sim}$, if $(M, +)$ is an H_v-group and there exists a map $\star : R \times M \longrightarrow \mathcal{P}^*(M)$, $(r, \alpha) \to r \star \alpha$, such that for all $\alpha, \beta \in M$, $r, s \in R$, the following conditions hold.

- $(r \star (\alpha + \beta)) \cap (r \star \alpha + r \star \beta) \neq \emptyset$;
- $((r + s) \star \alpha) \cap (r \star \alpha + s \star \alpha) \neq \emptyset$;
- $((rs) \star \alpha) \cap (r \star (s \star \alpha)) \neq \emptyset$.

Definition 2.6. A non-empty subset K of an H_v-module $(M, +, R, \cdot)$ over an H_v-ring R is called an H_v*-submodule* of M if $r \cdot x \subseteq K$ and $\alpha + K = K + \alpha = K$ for all $r \in R, \alpha, x \in K$.

These conditions ensure that K is a well-behaved subset of M that is stable under the action of R, and forms a group under addition that is closed under both vector addition and set addition. Note that if M is a finite-dimensional vector space over a field, then an H_v-submodule of M is simply a subspace of M.

Definition 2.7. An H_v-module homomorphism $f : M \to N$ is a structure-preserving map between H_v-modules $(M, +, R, \star)$ and $(N, +', S, \star')$ over H_v-rings R and S, respectively. It satisfies the following conditions:

- $f(x + y) = f(x) +' f(y)$ for all $x, y \in M$.
- There exists an H_v-ring homomorphism $g : R \to S$ such that $f(r \star x) = g(r) \star' f(x)$ for all $x \in M$ and $r \in R$. This means that f preserves the H_v-module structure of M and N, and also the ring structure of R and S.

Two H_v-modules $(M, +, R, \star)$ and $(N, +', S, \star')$ are isomorphic if there exists a bijective H_v-module homomorphism $f : M \to N$ and an H_v-ring isomorphism $g : R \to S$ such that $f(x + y) = f(x) +' f(y)$ and $f(r \star x) = g(r) \star' f(x)$ for all $x, y \in M$ and $r \in R$. This means that M and N have the same H_v-module structure and are related by an H_v-module homomorphism and an H_v-ring isomorphism.

Example 2.8. Let R be a ring, $(M, +, R, \star)$ be an R-module and N be a submodule of M. Then $(M, +, R, \cdot)$ is an R-H_v-module where "$\cdot$" is defined as follows: for all $(r, m) \in R \times M$, $r \cdot m = r \star m + N$.

For the special case $R = \mathbb{Z}$, $M = \mathbb{Z}_4$ (M is the $\mathbb{Z}$-module of integers under standard addition and multiplication modulo four.) and $N = 2\mathbb{Z}_4 = \{0, 2\}$. we get the following:

$$k \cdot 0 = k \cdot 2 = \{0, 2\},$$

$$k \cdot 1 = k \cdot 3 = \{k \mod 4, (k + 2) \mod 4\} = \begin{cases} \{0, 2\}, \text{if } k \text{ is an even integer;} \\ \{1, 3\}, \text{otherwise.} \end{cases}$$

Example 2.9. Let $F_2 = \{0, 1\}$ and define $(F_2, +)$ and $(F_2, \times)$ by the following tables:

$+$	0	1
0	0	1
1	1	F_2

$\times$	0	1
0	0	0
1	0	1

Define the map $\cdot : F_2^2 \times F_2 \to \mathcal{P}^*(F_2^2)$ as:

$$a \cdot (x, y) = (a \times x, a \times y)$$

for all $a, x, y, z \in F_2$.

It is clear that F_2^2 is an H_v-module over F_2. We present "$+_M$" by the following symmetric table after setting $m_0 = (0,0), m_1 = (1,0), m_2 = (0,1), m_3 = (1,1)$.

$+_M$	m_0	m_1	m_2	m_3
m_0	m_0	m_1	m_2	m_3
m_1		$\{m_0, m_1\}$	m_3	$\{m_2, m_3\}$
m_1			$\{m_0, m_2\}$	$\{m_1, m_3\}$
m_1				F_2^2

and "$\cdot$" as follows: $0 \cdot m_i = m_0$ and $1 \cdot m_i = m_i$ for $i = 0, 1, 2, 3$.

3. Neutrosophic quadruple H_v-modules and their properties

Neutrosophic quadruple algebraic structures are mathematical systems that generalize the concepts of groups, rings, and fields. They are defined based on the concept of a hyper-operation, which is a binary operation that can be extended to n-ary operations. In [1, 2], Agboola et al. and Akinleye et al. studied neutrosophic quadruple algebraic structures based on quadruple numbers over the set of real numbers. As an alternative to real or complex numbers, neutrosophic quadruple numbers are considered in this section, and they are used to define neutrosophic quadruple Hv-modules over neutrosophic quadruple numbers. Hv-rings.

Definition 3.1. [13] A neutrosophic quadruple X-number is an ordered quadruple (a_1, a_2T, a_3I, a_4F), where $a_1, a_2, a_3, a_4 \in X$ and a_2T, a_3I, a_4F are subsets of X such that $a_1 + a_2T + a_3I + a_4F = X$ and $a_2T \cap a_3I = a_3I \cap a_4F = a_4F \cap a_2T = \varnothing$.

Here, T, I, and F stand for the truth, indeterminacy, and falsity values, respectively. The neutrosophic quadruple X-number is used to represent the truth, indeterminacy, and falsity degrees of a statement with respect to a nonempty set X.

The element a_1 represents the true degree of the statement, while the sets a_2T, a_3I, and a_4F represent the indeterminate, uncertain, and false degrees of the statement, respectively. The sets a_2T, a_3I, and a_4F are mutually exclusive, meaning that a statement cannot have both a high degree of truth and a high degree of falsity. The set of all neutrosophic quadruple X-numbers is denoted by NQ(X), that is,

$$NQ(X) = \{(a_1, a_2T, a_3I, a_4F) : a_1, a_2, a_3, a_4 \in X\}.$$

The *Absorbance Law* for the multiplications of T, I, and F with respect to the preference law $T < I < F$ is defined as follows:

- $T \cdot T = T$
- $T \cdot I = I \times T = I$

- $T \cdot F = F \times T = F$
- $I \cdot I = I$
- $I \cdot F = F \times I = I$
- $F \cdot F = F$

This law governs how the neutrosophic values of truth, indeterminacy, and falsity interact with each other under multiplication. The law is called the Absorbance Law because it specifies that the values of indeterminacy and falsity are absorbed by the value of truth under multiplication.

For example, if a statement has a high degree of truth (T) and a moderate degree of indeterminacy (I), then the Absorbance Law implies that the overall degree of the statement should be closer to T than to I. Similarly, if a statement has a high degree of falsity (F) and a moderate degree of indeterminacy (I), then the overall degree of the statement should be closer to F than to I.

We recall some concepts and results related to neutrosophic quadruple H_v-groups and neutrosophic quadruple H_v-rings from [6, 7].
Let $(R, +, \times)$ be an H_v-ring with zero "0" and unit "1" and define "$\oplus$" and "$\otimes$" on $NQ(R)$ as follows:

$$\begin{aligned}&(x_1, x_2T, x_3I, x_4F) \oplus (y_1, y_2T, y_3I, y_4F)\\ &= \{(a, bT, cI, dF) : \ a \in x_1 + y_1, b \in x_2 + y_2, c \in x_3 + y_3, d \in x_4 + y_4\}.\end{aligned}$$

and

$$\begin{aligned}&(x_1, x_2T, x_3I, x_4F) \otimes (y_1, y_2T, y_3I, y_4F)\\ &= \{(a, bT, cI, dF) : \ a \in x_1 \times y_1, b \in x_1 \times y_2 \cup x_2 \times y_1 \cup x_2 \times y_2,\\ &jc \in x_1 \times y_3 \cup x_2 \times y_3 \cup x_3 \times y_1 \cup x_3 \times y_2 \cup x_3 \times y_3,\\ &d \in x_1 \times y_4 \cup x_2 \times y_4 \cup x_3 \times y_4 \cup x_4 \times y_1 \cup x_4 \times y_2 \cup x_4 \times y_3 \cup x_4 \times y_4\}.\end{aligned}$$

In the context of the paper, the symbols T, I, and F represent the truth, indeterminacy, and falsity values, respectively, with $T < I < F$ denoting the preference order of these values. Moreover, the mathematical structure under consideration is an H_v-ring denoted by $(R, +, \times)$, which satisfies the following conditions:

- R is a set equipped with two binary operations, $+$ (addition) and $\times$ (multiplication).
- $(R, +)$ is an abelian group with identity element 0.
- $(R, \times)$ is a monoid with identity element 1.
- The multiplication operation $\times$ distributes over the addition operation $+$, i.e., $a \times (b + c) = (a \times b) + (a \times c)$ and $(a + b) \times c = (a \times c) + (b \times c)$ for all $a, b, c \in R$.
- The element 0 is an absorbing element for the multiplication operation $\times$, i.e., $x \times 0 = 0 \times x = 0$ for all $x \in R$.

Theorem 3.2. *[6] Let H be a set with $0 \in H$. Then $(NQ(H), \oplus)$ is an H_v-group (called neutrosophic H_v-group) with identity $\overline{0} = (0, 0T, 0I, 0F)$ if and only if $(R, +)$ is an H_v-group with identity "0" and $0 + 0 = 0$.*

The following theorem characterizes the relationship between the hyperoperations on a set R and the hyperstructure of its neutrosophic quadruple numbers $NQ(R)$.

Theorem 3.3. *[7] $(NQ(R), \oplus, \otimes)$ is a neutrosophic H_v-ring with zero and unit as $\overline{0} = (0, 0T, 0I, 0F)$ and $\overline{1} = (1, 0T, 0I, 0F)$ respectively if and only if $(R, +, \times)$ is an H_v-ring with zero and unit as 0" and 1," respectively.*

The above theorem provides a useful criterion for determining whether a given hyperstructure of neutrosophic quadruple numbers is a neutrosophic H_v-ring. By checking whether the hyperoperations on R satisfy the conditions of an H_v-ring, we can determine whether the corresponding neutrosophic quadruple hyperstructure is also an H_v-ring.

Let $(M, \star, R, \cdot)$ be an R-H_v-module with $0_M \in M$, $0_M \star 0_M = 0_M$, $m \in 1 \cdot m$, $0_M \in 0_R \cdot m$, $0_M \in r \cdot 0_M$ for all $r \in R, m \in M$. We define the following hyperoperations on $NQ(M)$:

$$(m, nT, pI, qF) \boxplus (m', n\prime T, p\prime I, q\prime F) = (m \star m', (n \star n\prime)T, (p \star p\prime)I, (q \star q\prime)F)$$

and

$$(a, bT, cI, dF) \odot (m, nT, pI, qF) = (a \cdot m, (b \cdot n)T, (c \cdot p)I, (d \cdot q)F).$$

In what follows, $(M, \star, R, \cdot)$ is an R-H_v-module with identity $0_M \in M$, $0_M \star 0_M = 0_M$, $0_M \in 0_R \cdot m$ and $m \in 1 \cdot m$ for all $m \in M$ and $0_M \in r \cdot 0_M$ for all $r \in R$.

Theorem 3.4. *Let $(M, \star, R, \cdot)$ be an R-H_v-module. Then $(NQ(M), \boxplus, NQ(R), \odot)$ is an $NQ(R)$-H_v-module.*

Proof. Suppose that $(M, \star, R, \cdot)$ is an R-H_v-module. Then $(M, \star)$ is an H_v-group. Theorem 3.2 asserts that $(NQ(M), \boxplus)$ is an H_v-group. Since $R \cdot M \subseteq M$, it follows from the definition of "$\odot$" that $NQ(R) \odot NQ(M) \subseteq NQ(M)$. We prove now that the conditions of Definition 2.5 are satisfied. Let $\overline{r} = (r_1, r_2T, r_3I, r_4F), \overline{s} = (s_1, s_2T, s_3I, s_4F) \in NQ(R)$ and $\overline{m} = (m_1, m_2T, m_3I, m_4F), \overline{n} = (n_1, n_2T, n_3I, n_4F) \in NQ(M)$.

(1) We have: $(r_1, r_2T, r_3I, r_4F) \odot ((m_1, m_2T, m_3I, m_4F) \boxplus (n_1, n_2T, n_3I, n_4F)) = (r_1 \cdot (m_1 \star n_1), r_2 \cdot (m_2 \star n_2)T, r_3 \cdot (m_3 \star n_3)I, r_4 \cdot (m_4 \star n_4)F)$ and $((r_1, r_2T, r_3I, r_4F) \odot (m_1, m_2T, m_3I, m_4F)) \boxplus ((r_1, r_2T, r_3I, r_4F) \odot (n_1, n_2T, n_3I, n_4F))$
$= (r_1 \cdot m_1 \star r_1 \cdot n_1, (r_2 \cdot m_2 \star r_2 \cdot n_2)T, (r_3 \cdot m_3 \star r_3 \cdot n_3)I, (r_4 \cdot m_4 \star r_4 \cdot n_4)F)$. Having $(r_i \cdot (m_i \star n_i)) \cap (r_i \cdot m_i \star r_i \cdot n_i) \neq \emptyset$ for $i = 1, 2, 3, 4$ implies that $(r_1, r_2T, r_3I, r_4F) \odot ((m_1, m_2T, m_3I, m_4F) \boxplus)(n_1, n_2T, n_3I, n_4F)) \cap ((r_1, r_2T, r_3I, r_4F) \odot (m_1, m_2T, m_3I, m_4F)) \boxplus ((r_1, r_2T, r_3I, r_4F) \odot (n_1, n_2T, n_3I, n_4F)) \neq \emptyset$.

(2) We have: $((r_1, r_2T, r_3I, r_4F) \oplus (s_1, s_2T, s_3I, s_4F)) \odot (m_1, m_2T, m_3I, m_4F) = ((r_1 + s_1) \cdot m_1, ((r_2 + s_2) \cdot m_2)T, ((r_3 + s_3) \cdot m_3)I, ((r_4 + s_4) \cdot m_4)F)$ and $(r_1, r_2T, r_3I, r_4F) \odot (m_1, m_2T, m_3I, m_4F) \boxplus (s_1, s_2T, s_3I, s_4F)) \odot (m_1, m_2T, m_3I, m_4F) = ((r_1 \cdot m_1 \star s_1 \cdot m_1), (r_2 \cdot m_2 \star s_2 \cdot m_2)T, (r_3 \cdot m_3 \star s_3 \cdot m_3)I, (r_4 \cdot m_4 \star s_4 \cdot m_4)F)$. Having $((r_i + s_i) \cdot m_i) \cap (r_i \cdot m_i \star s_i \cdot m_i) \neq \emptyset$ for $i = 1, 2, 3, 4$ implies that $((r_1, r_2T, r_3I, r_4F) \oplus (s_1, s_2T, s_3I, s_4F)) \odot (m_1, m_2T, m_3I, m_4F) = ((r_1 + s_1) \cdot m_1, (r_2 + s_2) \cdot m_2T, (r_3 + s_3) \cdot m_3I, (r_4 + s_4) \cdot m_4F) \cap (r_1, r_2T, r_3I, r_4F) \odot (m_1, m_2T, m_3I, m_4F) \boxplus (s_1, s_2T, s_3I, s_4F)) \odot (m_1, m_2T, m_3I, m_4F) \neq \emptyset$.

(3) One can easily see that $(r_1 \star (s_1 \star m_1), (r_2 \star (s_2 \star m_2))T, (r_3 \star (s_3 \star m_3))I, (r_4 \star (s_4 \star m_4))F) \in \overline{r} \odot (\overline{s} \odot \overline{m})$ and that $((r_1 \times s_1) \star m_1, ((r_2 \times s_2) \star m_2)T, ((r_3 \times s_3) \star m_3)I, ((r_4 \times s_4) \star m_4)F) \in (\overline{r} \otimes \overline{s}) \odot \overline{m}$. Having $(r_i \star (s_i \star m_i)) \cap ((r_i \times s_i) \star m_i) \neq \emptyset$ for $i = 1, 2, 3, 4$ implies that $(\overline{r} \odot (\overline{s} \odot \overline{m})) \cap ((\overline{r} \otimes \overline{s}) \odot \overline{m})) \neq \emptyset$.

It is clear that $\overline{0_M} = (0_M, 0_MT, 0_MI, 0_MF)$ is an identity in $NQ(M)$ and that $\overline{0_M} \boxplus \overline{0_M} = \overline{0_M}$. Therefore, $NQ(M)$ is an H_v-module. □

Notation 1. *Let $(M, \star, R, \cdot)$ be an R-H_v-module. Then $(NQ(M), \boxplus, NQ(R), \odot)$ is called Neutrosophic quadruple H_v-module.*

Corollary 3.5. *Let $(M, \star, R, \cdot)$ be an R-H_v-module. Then we can construct infinite non-isomorphic Neutrosophic quadruple H_v-module.*

Proof. Suppose that $(M, \star, R, \cdot)$ is an R-H_v-module. Theorem 3.4 asserts that $(NQ(M), \boxplus, NQ(R), \odot)$ is a neutrosophic quadruple H_v-module over $NQ(R)$. Having $NQ(NQ(R))$ a neutrosophic quadruple H_v-ring and applying Theorem 3.4 on $(NQ(M), \boxplus, NQ(R), \odot)$, we get $(NQ(NQ(M)), \boxplus_1, NQ(NQ(R)), \odot_1)$ is a neutrosophic quadruple H_v-module over $NQ(NQ(R))$. Continuing on this pattern, we get $NQ(NQ(\dots NQ(\dots (M)) \dots)$ is a neutrosophic quadruple H_v-module over $NQ(NQ(\dots NQ(\dots (R)) \dots)$. □

Theorem 3.6. *Let M be a non-empty set with $0_M \in M$ and let $(NQ(M), \boxplus, NQ(R), \odot)$ be an R-H_v-module with identity $\overline{0_M}$ and $\overline{0_M} \boxplus \overline{0_M} = \overline{0_M}$. Then $(M, \star, R, \cdot)$ is an H_v-module.*

Proof. Theorems 3.2 and 3.3 assert that $(M, \star)$ is an H_v-group and $(R, +, \times)$ is an H_v-ring respectively. Let $r, s \in R$, $m, n \in M$. Then $\overline{r} = (r, 0T, 0I, 0F), \overline{s} = (s, 0T, 0I, 0F) \in NQ(R)$ and $\overline{m} = (m, 0_MT, 0_MI, 0_MF), \overline{n} = (n, 0_MT, 0_MI, 0_MF) \in NQ(M)$. Applying conditions of Definition 2.5 on $\overline{r}, \overline{s}, \overline{m}, \overline{n}$, we get the conditions of Definition 2.5 are satisfied for r, s, m, n. □

Using Theorem 3.4 and Theorem 3.6, we get the following Theorem.

Theorem 3.7. *Let M be a non-empty set with $0_M \in M$. Then $(NQ(M), \boxplus, NQ(R), \odot)$ is an $NQ(R)$-H_v-module if and only if $(M, \star, R, \cdot)$ is an R-H_v-module.*

Remark 3.8. Let $(M, \star, R, \cdot)$ be a finite R-H_v-module. Then $|NQ(M)| = |M|^4$.

Example 3.9. Let R be any ring with unit "1" and M be an R-module. Then $(NQ(M), \boxplus, NQ(R), \odot)$ is a neutrosophic quadruple H_v-module.

Example 3.10. Let $R = \mathbb{Z}$, $M = \mathbb{Z}_4$ be an R-module and $N = 2\mathbb{Z}_4 = \{0, 2\}$ in Example 2.8. Then $(NQ(\mathbb{Z}_4), \boxplus, NQ(\mathbb{Z}), \odot)$ is a neutrosophic quadruple H_v-module with 4^4 elements. We present how the hyperoperation "$\odot$" is defined: for all $m, n, p, q \in M$,
$(0, 0T, 0I, 0F) \odot (m, nT, pI, qF) = \{(a, bT, cI, dF) : a, b, c, d \in \{0, 2\}\}$, $(1, 1T, 0I, 0F) \odot (m, nT, pI, qF) = \{(a, bT, cI, dF) : a, b \in \{1, 3\}, c, d \in \{0, 2\}\}$.

Example 3.11. Let $(F_2^2, +_M, F_2, \cdot)$ be the H_v-module defined in Example 2.9 over F_2. Then $(NQ(F_2^2), \boxplus, NQ(F_2), \odot)$ is a neutrosophic quadruple H_v-module with 4^4 elements.

Definition 3.12. Let $(M, \star, R, \cdot)$ be an R-H_v-module. A subset X of $NQ(M)$ with $\overline{0_M} = (0_M, 0_M T, 0_M I, 0_M F) \in X$ is called a *Neutrosophic H_v-submodule of $NQ(M)$* if there exists $S \subseteq M$ such that $X = NQ(S)$ and $(X, \boxplus, NQ(R), \odot)$ is a neutrosophic quadruple H_v-module.

Proposition 3.13. *Let $(M, \star, R, \cdot)$ be an R-H_v-module and $S \subseteq M$. A subset $X = NQ(S) \subseteq NQ(M)$ is a Neutrosophic H_v-submodule of $NQ(M)$ if the following conditions are satisfied:*

(1) $\overline{0_M} = (0_M, 0_M T, 0_M I, 0_M F) \in X$;
(2) $(m, nT, pI, qF) \boxplus X = X \boxplus (m, nT, pI, qF) = X$ *for all* $(m, nT, pI, qF) \in X$;
(3) $NQ(R) \odot X \subseteq X$.

Proof. The proof is straightforward. □

Theorem 3.14. *Let $(M, \star, R, \cdot)$ be an R-H_v-module, N a non-empty subset of M and $X = NQ(N)$. Then $(X, \boxplus, NQ(R), \odot)$ is a neutrosophic H_v-submodule of $(NQ(M), \boxplus, NQ(R), \odot)$ if and only if N is an H_v-submodule of M with $0_M \in N$.*

Proof. Let $(M, \star, R, \cdot)$ be an R-H_v-module and X be a neutrosophic H_v-submodule of $NQ(M)$. Then there exist $N \subseteq M$ with $0_M \in N$ such that $X = NQ(N)$. We need to show that N is a submodule of M. For all $n \in N$ and $r \in R$, we have $(n, 0_M T, 0_M I, 0_M F) \in NQ(N)$ and $(r, 0T, 0I, 0F) \in NQ(R)$. Since $NQ(N)$ is a neutrosophic H_v-submodule of $NQ(M)$, it follows that $(n, 0_M T, 0_M I, 0_M F) \boxplus NQ(N) = NQ(N) \boxplus (n, 0_M T, 0_M I, 0_M F) = NQ(N)$ and that $(r \cdot n, 0_M T, 0_M I, 0_M F) = (r, 0T, 0I, 0F) \odot (n, 0_M T, 0_M I, 0_M F) \subseteq NQ(N)$. The latter implies that $n \star N = N \star n = N$ and that $r \cdot N \subseteq N$.

Conversely, let N be an H_v-submodule M with $0_M \in N$. It is clear that $\overline{0_M} = (0_M, 0_M T, 0_M I, 0_M F) \in X = NQ(N)$. Let $(m_1, m_2 T, m_3 I, m_4 F) \in NQ(N)$ and $(r_1, r_2 T, r_3 I, r_4 F) \in NQ(R)$. Having $m_i \in N, r_i \in R$ for $i = 1, 2, 3, 4$ and N an H_v-submodule

of M imply that $n_i \star N = N \star n_i = N$ and $r_i \cdot N \subseteq N$ for $i = 1, 2, 3, 4$. It is obvious now that $(m_1, m_2T, m_3I, m_4F) \boxplus NQ(N) = NQ(N) \boxplus (m_1, m_2T, m_3I, m_4F) = NQ(N)$ and that $(r_1, r_2T, r_3I, r_4F) \odot NQ(N) \subseteq NQ(N)$. □

Example 3.15. Let $(NQ(\mathbb{Z}_4), \boxplus, NQ(\mathbb{Z}), \odot)$ be the neutrosophic quadruple H_v-module defined in Example 3.11. Then $NQ(\mathbb{Z}_4), NQ(\{0\})$ and $NQ(\{0, 2\})$ are the only neutrosophic quadruple H_v-submodules of $NQ(\mathbb{Z}_4)$.

Example 3.16. Let $(NQ(F_2^2), \boxplus, NQ(F_2), \odot)$ be the neutrosophic quadruple H_v-module defined in Example 3.11. Then $NQ(F_2^2), NQ(\{m_0\}), NQ(\{m_0, m_1\}), NQ(\{m_0, m_2\})$ are the only neutrosophic quadruple H_v-submodules of $NQ(F_2^2)$.

Definition 3.17. Let $(NQ(M), \boxplus_1, NQ(R), \odot_1)$ and $(NQ(N), \boxplus_2, NQ(R), \odot_2)$ be neutrosophic quadruple H_v-modules. A function $\phi : NQ(M) \to NQ(N)$ is called *neutosophic homomorphism* if the following conditions are satisfied.

(1) $\phi(0_M, 0_MT, 0_MI, 0_MF) = (0_N, 0_NT, 0_NI, 0_NF)$;
(2) $\phi(x \boxplus_1 y) = \phi(x) \boxplus_2 \phi(y)$ for all $x, y \in NQ(M)$;
(3) $\phi(r \odot_1 x) = r \odot_2 \phi(x)$ for all $r \in NQ(R), x \in NQ(M)$.

If ϕ is a neutrosophic homomorphism and bijective then it is called *neutrosophic isomorphism* and we write $NQ(M) \cong NQ(N)$.

Proposition 3.18. *If $f : M \to N$ is an R-H_v-module homomorphism with $f(0_M) = 0_N$. Then there exist a neutrosophic homomorphism from $(NQ(M), \boxplus_1, NQ(R), \odot_1)$ to $(NQ(N), \boxplus_2, NQ(R), \odot_2)$.*

Proof. Let $\phi : NQ(M) \to NQ(N)$ be defined as follows:

$$\phi((m, nT, pI, qF)) = (f(m), f(n)T, f(p)I, f(q)F).$$

It is clear that ϕ is a neutrosophic homomorphism. □

Proposition 3.19. *Let $(M, +_1, R, \cdot_1)$ and $(N, +_2, R, \cdot_2)$ be isomorphic H_v-modules with our assumption on the conditions for $0_R, 1_R \in R$ and $0_M \in M, 0_N \in N$ and $f : (M, +_1, R, \cdot_1) \to (N, +_2, R, \cdot_2)$ be an isomorphism. Then $f(0_M) = 0_N$.*

Proof. Let $f(0_M) = a$. Since $a = f(0_M) = f(0_M +_1 0_M) = a +_2 a$ and $a +_2 y = f(0_M +_1 x) \ni f(x) = y$ for all $y \in N$, it follows that a is a zero of N satisfying $a +_2 a = a$. □

Corollary 3.20. *Let $(M, +_1, R, \cdot_1)$ and $(N, +_2, R, \cdot_2)$ be isomorphic H_v-modules. Then $(NQ(M), \boxplus_1, NQ(R), \odot_1)$ and $(NQ(N), \boxplus_2, NQ(R), \odot_2)$ are isomorphic neutrosophic quadruple H_v-modules.*

Proof. The proof is straightforward by using Proposition 3.18 and Proposition 3.19. □

Let $(M, \star, R, \cdot)$ be a commutative H_v-module, i.e. $(M, \star)$ is a commutative H_v-group, and S be an H_v-submodule of M containing 0_M. Then $(M/S, \star', R, \cdot')$ is an H_v-module under the following hyperoperations: For all $s, t \in S$, $r \in R$, we have:

$$(s \star S) \star' (t \star S) = (s \star t) \star S \text{ and } r \cdot' (s \star S) = (r \cdot s) \star S.$$

It is clear that S is a zero for M/S and that $S \star' S = S$.
We define "$\boxplus'$" and "$\odot'$" on $NQ(M/S)$ in the usual way as defining "$\boxplus$" and "$\odot$" on $NQ(M)$.

Proposition 3.21. *Let $(S, \star, R, \cdot)$ be an H_v-submodule of a commutative H_v-module $(M, \star, R, \cdot)$. Then $(NQ(M/S), \boxplus', NQ(R), \odot')$ is an H_v-module.*

Proof. The proof follows from having $(M/S, +', R, \cdot')$ an H_v-module with S as zero and from Theorem 3.7. □

Proposition 3.22. *[6] Let $(S, +)$ be an H_v-subgroup of a commutative H_v- group $(M, +)$. Then $(NQ(M/S), \oplus) \cong (NQ(M)/NQ(S), \oplus')$.*

The authors used in the proof of Proposition 3.22 a function $g : NQ(M)/NQ(S) \to NQ(M/S)$ and defined it as follows:

$$g((x_1, x_2T, x_3I, x_4F) \oplus NQ(S)) = (x_1 + S, (x_2 + S)T, (x_3 + S)I, (x_4 + S)F).$$

And they proved that it is an H_v-group isomorphism.

Proposition 3.23. *Let $(S, \star, R, \cdot)$ be an H_v-submodule of a commutative H_v-module $(M, \star, R, \cdot)$. Then $(NQ(M/S), \boxplus', NQ(R), \odot') \cong (NQ(M)/NQ(S), \boxplus'', NQ(R), \odot'')$.*

Proof. Let $g : NQ(M)/NQ(S) \to NQ(M/S)$ be defined as follows:

$$g((x_1, x_2T, x_3I, x_4F) \oplus NQ(S)) = (x_1 + S, (x_2 + S)T, (x_3 + S)I, (x_4 + S)F).$$

We claim that g is a neutrosophic isomorphism, that is, g is well defined, one-to-one, onto and neutrosophic homomorphism. The proof that g is well defined and one-to-one is the same as that in the proof of Proposition 3.22. (We refer to [6] for more details.) Moreover, it is clear that f is an onto function. We prove that g is neutrosophic homomorphism. Let $x_i \in M, r_i \in R$ for $i = 1, 2, 3, 4$.

- $g((0_M, 0_M T, 0_M I, 0_M F) \boxplus NQ(S)) = (S, ST, SI, SF)$,
- We have $g(((x_1, x_2T, x_3I, x_4F) \boxplus NQ(S)) \boxplus'' ((y_1, y_2T, y_3I, y_4F) \boxplus NQ(S))) = g((x_1 + y_1, (x_2 + y_2)T, (x_3 + y_3)I, (x_4 + y_4)F) \boxplus NQ(S)) = (x_1 + y_1 + S, (x_2 + y_2 + S)T, (x_3 + y_3 + S)I, (x_4 + y_4 + S)F)$.

  On the other hand, we have $g((x_1, x_2T, x_3I, x_4F) \boxplus NQ(S)) \boxplus' g((y_1, y_2T, y_3I, y_4F) \boxplus NQ(S)) = (x_1 + S, (x_2 + S)T, (x_3 + S)I, (x_4 + S)F) \boxplus (y_1 + S, (y_2 + S)T, (y_3 + S)I, (y_4 + S)F)$.
- We have:
  $(r_1, r_2T, r_3I, r_4F) \odot'' ((x_1, x_2T, x_3I, x_4F) \oplus NQ(S)) = (r_1 \cdot x_1, (r_2 \cdot x_2)T, (r_3 \cdot x_3)I, (r_4 \cdot x_4)F) \boxplus NQ(S)$ and $(r_1, r_2T, r_3I, r_4F) \odot' g((x_1, x_2T, x_3I, x_4F) \boxplus NQ(S)) = (r_1, r_2T, r_3I, r_4F) \odot' (x_1 + S, (x_2 + S)T, (x_3 + S)I, (x_4 + S)F) = (r_1 \cdot x_1 + S, (r_2 \cdot x_2 + S)T, (r_3 \cdot x_3 + S)I, (r_4 \cdot x_4 + S)F)$. It is clear that $g((r_1, r_2T, r_3I, r_4F) \odot'' ((x_1, x_2T, x_3I, x_4F) \oplus NQ(S))) = (r_1, r_2T, r_3I, r_4F) \odot' g((x_1, x_2T, x_3I, x_4F) \oplus NQ(S))$.

Therefore, $(NQ(M/S), \boxplus', NQ(R), \odot') \cong (NQ(M)/NQ(S), \boxplus'', NQ(R), \odot'')$. □

Example 3.24. Using Examples 3.10 and 3.15, we get $NQ(\mathbb{Z}_4/\{0, 2\}) \cong NQ(\mathbb{Z}_4)/NQ(\{0, 2\})$.

4. Fundamental module of neutrosophic H_v-module

In this section, we find the fundamental ring of neutrosophic quadruple H_v-rings and we use it to find the fundamental module of neutrosophic quadruple H_v-modules.

Fundamental relations are a key tool in connecting hyperstructures with classical algebraic structures. They are a generalization of the concept of subalgebra from classical algebra, and they allow us to define algebraic operations on subsets of a hyperstructure in a way that preserves the hyperstructure properties. In 1936, Marty in his seminal paper [15] introduced the concept of fundamental relations in hyperstructure theory, Then Koskas [14] later contributed to the study of fundamental relations and their applications in hyperstructure theory.

Definition 4.1. [11] For all $n \geq 2$, we define the relation γ on an H_v-ring $(R, +, \cdot)$ as follows:

$$a\gamma b \Leftrightarrow \{a, b\} \subseteq u \text{ where } u \text{ is finite sum of finite products of elements in } R.$$

Note that The relation γ is reflexive and symmetric. To see that it is reflexive, note that for any $a \in R$, we have $a \in a$, which is a finite sum of finite products of elements in R. Therefore, $a\gamma a$. To see that it is symmetric, suppose $a\gamma b$ for some $a, b \in R$. Then there exists a finite sum $s = \sum_{i=1}^{k} a_i$ of finite products of elements in R such that $a, b \in s$. But then we also have $b, a \in s$, so $b\gamma a$.

The fundamental equivalence relation $\gamma^\star$ is defined as the transitive closure of γ. This means that $a\gamma^\star b$ if and only if there exist elements $a_0, \ldots, a_n \in R$ such that $a = a_0\gamma a_1\gamma \cdots \gamma a_n = b$. In other words, $a\gamma^\star b$ if and only if a and b are connected by a chain of elements related by γ. It is easy to see that $\gamma^\star$ is an equivalence relation on R.

The fundamental ring $R/\gamma^\star$ is the quotient of R by the equivalence relation $\gamma^\star$. Elements of $R/\gamma^\star$ are equivalence classes $[a]$ of elements in R that are related by $\gamma^\star$. The addition and multiplication operations on $R/\gamma^\star$ are defined by $[a] + [b] = [a + b]$ and $[a] \times [b] = [a \times b]$. It can be shown that $R/\gamma^\star$ is a well-defined ring.

Similarly, we can define the relation γ_N on $NQ(R)$ and its fundamental equivalence relation $\gamma_N^\star$, which gives rise to the fundamental ring $NQ(R)/\gamma_N^\star$. This ring is obtained by quotienting the neutrosophic quadruple ring $NQ(R)$ by the equivalence relation $\gamma_N^\star$. The addition and multiplication operations on $NQ(R)/\gamma_N^\star$ are defined in a similar way to those on $R/\gamma^\star$.

Proposition 4.2. *Let $(R, +, \times)$ be an H_v-ring and $a, b, c, d \in R$. Then*

(1) $\gamma_N(a, 0T, 0I, 0F) = \gamma_N(a, bT, cI, dF)$;
(2) $\gamma_N^\star(a, 0T, 0I, 0F) = \gamma_N^\star(a, bT, cI, dF)$;
(3) $\gamma_N(0, 0T, 0I, 0F) = \gamma_N(0, bT, cI, dF)$;
(4) $\gamma_N^\star(0, 0T, 0I, 0F) = \gamma_N^\star(0, bT, cI, dF)$.

Proof. Let $a, b, c, d \in R$.

(1) Having $(1, 0T, 0I, 0F) \otimes (0, 1T, 0I, 0F) = \{(0, 0T, 0I, 0F), (0, 1T, 0I, 0F)\}$ implies that

$$\{(0, 0T, 0I, 0F), (0, bT, cI, dF)\} \subseteq (1, 0T, 0I, 0F) \otimes (0, 1T, 0I, 0F) \otimes (0, bT, cI, dF).$$

It is obvious that $(a, 0T, 0I, 0F), (0, bT, cI, dF) \in ((1, 0T, 0I, 0F) \otimes (a, 0T, 0I, 0F)) \oplus ((1, 0T, 0I, 0F) \otimes (0, 1T, 0I, 0F) \otimes (0, bT, cI, dF))$.

(2) It is straightforward by using 1.
(3) By setting $a = 0$ in 1., we get the required.
(4) It is straightforward by using 3.□

Proposition 4.3. *Let $(R, +, \times)$ be an H_v-ring and $a, a' \in R$. Then $a\gamma a'$ if and only if $\gamma_N(a, 0T, 0I, 0F) = \gamma_N(a', 0T, 0I, 0F)$.*

Proof. Let $a\gamma a'$. Then there exist $x_{ij} \in R$ and $n, k_i \in \mathbb{N}$ such that $a, a' \in \sum\limits_{1 \le i \le n} (\prod\limits_{1 \le j \le k_i} x_{ij})$. It is easy to see that

$$(a, 0T, 0I, 0F), (a', 0T, 0I, 0F) \in \sum_{1 \le i \le n} (\prod_{1 \le j \le k_i} \overline{x_{ij}}),$$

where $\overline{x_{ij}} = (x_{ij}, 0T, 0I, 0F)$.

Let $\gamma_N(a,0T,0I,0F)=\gamma_N(a',0T,0I,0F)$. Then there exist $(x_{ij},y_{ij}T,z_{ij}I,w_{ij}F)\in NQ(R)$, $n,k_i\in\mathbb{N}$ such that $(a,0T,0I,0F),(a',0T,0I,0F)\in\sum\limits_{1\leq i\leq n}(\prod\limits_{1\leq j\leq k_i}(x_{ij},y_{ij}T,z_{ij}I,w_{ij}F))$. Then it is clear that $a,a'\in\sum\limits_{1\leq i\leq n}(\prod\limits_{1\leq j\leq k_i}x_{ij})$. Thus, $a\gamma a'$. □

Proposition 4.4. *Let $(R,+,\times)$ be an H_v-ring and $a,a',b,b',c,c',d,d'\in R$.*
If $\gamma_N(a,bT,cI,dF)=\gamma_N(a',b'T,c'I,d'F)$ then $a\gamma a'$.

Proof. Let $(a,bT,cI,dF)\gamma_N(a',b'T,c'I,d'F)$. Then there exist $(x_{ij},y_{ij}T,z_{ij}I,w_{ij}F)\in NQ(R)$, $n,k_i\in\mathbb{N}$ such that

$$(a,bT,cI,dF),(a',b'T,c'I,d'F)\in\sum_{1\leq i\leq n}(\prod_{1\leq j\leq k_i}(x_{ij},y_{ij}T,z_{ij}I,w_{ij}F)).$$

Then it is clear that $a,a'\in\sum\limits_{1\leq i\leq n}(\prod\limits_{1\leq j\leq k_i}x_{ij})$. Thus, $a\gamma a'$. □

Proposition 4.5. *Let $(R,+,\times)$ be an H_v-ring and $a,a'\in R$. Then $a\gamma^\star a'$ if and only if $\gamma_N^\star(a,0T,0I,0F)=\gamma_N^\star(a',0T,0I,0F)$.*

Proof. Let $a\gamma^\star a'$. Then there exist $a_i\in R$ and $k\in\mathbb{N}$ with $i=1,2,\ldots,k$ such that $a\gamma a_1$, $a_1\gamma a_2,\ldots$, $a_k\gamma a'$. Using Proposition 4.3, we get $(a,0T,0I,0F)\gamma_N(a_1,0T,0I,0F)$, $(a_1,0T,0I,0F)\gamma_N(a_2,0T,0I,0F)$, …, $(a_k,0T,0I,0F)\gamma_N(a',0T,0I,0F)$. Thus, $(a,0T,0I,0F)\gamma_N^\star(a',0T,0I,0F)$.

Suppose that $(a,0T,0I,0F)\gamma_N^\star(a',0T,0I,0F)$. Then there exist $k\in\mathbb{N}$ and $\overline{x_i}=(x_i,y_iT,z_iI,w_iF)\in NQ(R)$, $i=1,2,3,4$ such that $(a,0T,0I,0F)\gamma_N\overline{x_1}$, $\overline{x_1}\gamma_N\overline{x_2}$, …, $\overline{x_k}\gamma_N(a',0T,0I,0F)$. Proposition 4.4 asserts that $a\gamma x_1$, $x_1\gamma x_2$, …$x_k\gamma a'$. Thus, $a\gamma^\star a'$. □

Proposition 4.6. *Let $(R,+,\times)$ be an H_v-ring and $a,b,c,d\in R$. Then $a\gamma^\star a'$ if and only if $\gamma_N^\star(a,bT,cI,dF)=\gamma_N^\star(a',b'T,c'I,d'F)$.*

Proof. Suppose that $a\gamma^\star a'$. Proposition 4.5 asserts that $(a,0T,0I,0F)\gamma_N^\star(a',0T,0I,0F)$. By using Proposition 4.2, we get

$$(a,0T,0I,0F)\gamma_N^\star(a,bT,cI,dF)\text{ and }(a',0T,0I,0F)\gamma_N^\star(a',b'T,c'I,d'F).$$

Having $\gamma_N^\star$ an equivalence relation on $NQ(R)$ implies that

$$(a,bT,cI,dF)\gamma_N^\star(a',b'T,c'I,d'F).$$

Conversely, let $(a,bT,cI,dF)\gamma_N^\star(a',b'T,c'I,d'F)$. By using Proposition 4.2, we get $(a,0T,0I,0F)\gamma_N^\star(a,bT,cI,dF)$ and $(a',0T,0I,0F)\gamma_N^\star(a',b'T,c'I,d'F)$. Having $\gamma_N^\star$ an equivalence relation on $NQ(R)$ implies that $(a,0T,0I,0F)\gamma_N^\star(a',0T,0I,0F)$. The latter and using Proposition 4.5 imply that $a\gamma^\star a'$. □

We define "$\oplus_\gamma$", "$\otimes_\gamma$" on $R/\gamma^\star$ and "$\oplus_{\gamma_N}$", "$\otimes_{\gamma_N}$" on $NQ(R)/\gamma_N^\star$ as follows: For all $r_i, s_i \in R$ with $i = 1, 2, 3, 4$, we have:

$$\gamma^\star(r_1) \oplus_\gamma \gamma^\star(r_2) = \gamma^\star(r), \text{ where } r \in r_1 + r_2,$$

$$\gamma^\star(r_1) \otimes_\gamma \gamma^\star(r_2) = \gamma^\star(r), \text{ where } r \in r_1 \times r_2,$$

$$\begin{aligned}&\gamma_N^\star(r_1, r_T, r_3 I, r_4 F) \oplus_{\gamma_N} \gamma_N^\star(s_1, s_2 T, s_3 I, s_4 F)\\ &= \gamma_N^\star(\overline{r}), \overline{r} \in (r_1, r_T, r_3 I, r_4 F) \oplus (s_1, s_2 T, s_3 I, s_4 F),\end{aligned}$$

$$\begin{aligned}&\gamma_N^\star(r_1, r_T, r_3 I, r_4 F) \otimes_{\gamma_N} \gamma_N^\star(s_1, s_2 T, s_3 I, s_4 F)\\ &= \gamma_N^\star(\overline{r}), \overline{r} \in (r_1, r_2 T, r_3 I, r_4 F) \otimes (s_1, s_2 T, s_3 I, s_4 F).\end{aligned}$$

Theorem 4.7. *Let $(R, +, \times)$ be an H_v-ring. Then $NQ(R)/\gamma_N^\star \cong R/\gamma^\star$.*

Proof. Suppose that $\psi : NQ(R)/\gamma_N^\star \to R/\gamma^\star$ be defined as follows:

$$\psi(\gamma_N^\star(a, bT, cI, dF)) = \gamma^\star(a).$$

Proposition 4.6 asserts that ψ is well defined and one-to-one. Moreover, it is clear that ψ is onto as $\psi(\gamma_N^\star(a, 0T, 0I, 0F)) = \gamma^\star(a)$ for all $a \in R$. We need to show that ψ is ring homomorphism. We have:

(1) $\psi(\gamma_N^\star(a, bT, cI, dF) \oplus_{\gamma_N} \gamma_N^\star(a', b'T, c'I, d'F)) = \psi(\gamma_N^\star(e, fT, gI, hF)) = \gamma^\star(e)$, where $(e, fT, gI, hF) \in (a, bT, cI, dF) \oplus (a', b'T, c'I, d'F) = (a+a', (b+b')T, (c+c')I, (d+d')F)$. On the other hand, we have

$$\psi(\gamma_N^\star(a, bT, cI, dF)) \oplus_\gamma \psi(\gamma_N^\star(a', b'T, c'I, d'F)) = \gamma^\star(a) \oplus_\gamma \gamma^\star(a') = \gamma^\star(e),$$

where $e \in a + a'$. Consequently, we obtain

$$\begin{aligned}&\psi(\gamma_N^\star(a, bT, cI, dF) \oplus_{\gamma_N} \gamma_N^\star(a', b'T, c'I, d'F))\\ &= \psi(\gamma_N^\star(a, bT, cI, dF)) \oplus_\gamma \psi(\gamma_N^\star(a', b'T, c'I, d'F)).\end{aligned}$$

(2) $\psi(\gamma_N^\star(a, bT, cI, dF) \otimes_{\gamma_N} \gamma_N^\star(a', b'T, c'I, d'F)) = \psi(\gamma_N^\star(e, fT, gI, hF)) = \gamma^\star(e)$ where $(e, fT, gI, hF) \in (a, bT, cI, dF) \otimes (a', b'T, c'I, d'F)$. It is clear that $e \in a \times a'$. On the other hand, we have $\psi(\gamma_N^\star(a, bT, cI, dF)) \otimes_\gamma \psi(\gamma_N^\star(a', b'T, c'I, d'F)) = \gamma^\star(a) \otimes_\gamma \gamma^\star(a') = \gamma^\star(e)$ where $e \in a \times a'$. Thus, $\psi(\gamma_N^\star(a, bT, cI, dF) \otimes_{\gamma_N} \gamma_N^\star(a', b'T, c'I, d'F)) = \psi(\gamma_N^\star(a, bT, cI, dF)) \otimes_\gamma \psi(\gamma_N^\star(a', b'T, c'I, d'F))$. □

Corollary 4.8. *Let $(R, +, \times)$ be an H_v-ring. Then $NQ(R)$ has a trivial fundamental ring if and only if R has a trivial fundamental ring.*

Proof. The proof follows from Theorem 4.7. □

The authors in [**?**,4] considered the set of arithmetic functions R and defined hyperoperations $+$ and $\times$ on it as follows:

$$\alpha + \beta(n) = \{\alpha(d) + \beta(\frac{n}{d}) : d|n\};$$

and

$$\alpha \times \beta(n) = \{\alpha(d)\beta(\frac{n}{d}) : d|n\}.$$

Let $0_\star(n) = 0$ for all $n \in \mathbb{N}$ and

$$\iota(n) = \begin{cases} 1 & \text{if } n = 1 \\ 0 & \text{otherwise.} \end{cases}$$

It is clear that $0_\star + 0_\star = 0_\star$ and that $\iota \times \iota = \iota$. The authors proved that $(R, +, \times)$ is an H_v-ring with $0_\star$ as zero and ι as unit and found its fundamental ring as the ring of complex numbers $\mathbb{C}$ under standard addition and multiplication.
It is obvious that $0_\star$ is an absorbing element.

Proposition 4.9. *Let $(R, +, \times)$ be the H_v-ring of arithmetic functions under the above hyperoperations. Then $(NQ(R), \oplus, \otimes)$ is a neutrosophic quadruple H_v-ring.*

Proof. The proof follows from Theorem 3.3. □

Example 4.10. Let $(R, +, \times)$ be the H_v-ring of arithmetic functions. Then the ring of complex numbers $\mathbb{C}$ under standard addition and multiplication is the fundamental ring of $(NQ(R), \oplus, \otimes)$.

Definition 4.11. For all $n > 1$, we define the relation ε on an H_v-module $(M, +, R, \star)$ over an H_v-ring R as follows: $x\varepsilon y$ if and only if there exist $n, n_i \in \mathbb{N}$, $(m_1, \cdots, m_n) \in M^n$, $(k_1, \cdots, k_n) \in \mathbb{N}^n$, $(x_{i1}, \cdots, x_{ik}) \in R^{k_i}$ such that

$$x, y \in \sum_{i=1}^{n} m'_i, m'_i = m_i \text{ or } m'_i = \sum_{j=1}^{n_i} (\prod_{k=1}^{k_i j} x_{ijk}) m_i.$$

Clearly, the relation ε is reflexive and symmetric. Denote by ε^* the transitive closure of ε. The $\varepsilon^\star$ is called the *fundamental equivalence relation* on M and M/ε^* is the *fundamental module*.

In what follows, $(M, \star, R, \cdot)$ is an R-H_v-module with identity $0_M \in M$, $0_M \star 0_M = 0_M$, $0_M \in 0_R \cdot m$ and $m \in 1 \cdot m$ for all $m \in M$ and $0_M \in r \cdot 0_M$ for all $r \in R$ and $\varepsilon, \varepsilon_N$ the relation on $R, NQ(R)$ and $\varepsilon^\star, \varepsilon_N^\star$ their fundamental relations respectively.

Proposition 4.12. *Let $(M, \star, R, \cdot)$ be an H_v-module and $m, n, p, q \in M$. Then*

(1) $\varepsilon_N(m, 0_M T, 0_M I, 0_M F) = \varepsilon_N(m, nT, pI, qF)$;
(2) $\varepsilon_N^\star(m, 0_M T, 0_M I, 0_M F) = \varepsilon_N^\star(m, nT, pI, qF)$;

(3) $\varepsilon_N(0_M, 0_M T, 0_M I, 0_M F) = \varepsilon_N(0_M, nT, pI, qF)$;

(4) $\varepsilon_N^\star(0_M, 0_M T, 0_M I, 0_M F) = \varepsilon_N^\star(0_M, nT, pI, qF)$.

Proof. We prove 1., the others are straightforward. One can easily see that

$$\begin{aligned}
&(m, 0_M T, 0_M I, 0_M F), (m, nT, pI, qF)\\
&\in ((1, 0T, 0I, 0F) \odot (m, 0_M T, 0_M I, 0_M F))\\
&\quad \boxplus(((1, 0T, 0I, 0F) \otimes (0, 1T, 0I, 0F)) \odot (0_M, nT, 0_M I, 0_M F))\\
&\quad \boxplus(((1, 0T, 0I, 0F) \otimes (0, 0T, 1I, 0F)) \odot (0_M, 0_M T, pI, 0_M F))\\
&\quad \boxplus(((1, 0T, 0I, 0F) \otimes (0, 0T, 0I, 1F)) \odot (0_M, 0_M T, 0_M I, qF)).
\end{aligned}$$

□

Proposition 4.13. *Let $(M, \star, R, \cdot)$ be an H_v-module and $m, m' \in M$. Then $m\varepsilon m'$ if and only if $\varepsilon_N(m, 0_M T, 0_M I, 0_M F) = \varepsilon_N(m', 0_M T, 0_M I, 0_M F)$.*

Proof. Let $m\varepsilon m'$. Then there exist $n, n_i \in \mathbb{N}$, $(m_1, \cdots, m_n) \in M^n$, $(k_1, \cdots, k_n) \in \mathbb{N}^n$, $(x_{i1}, \cdots, x_{ik}) \in R^{k_i}$ such that

$$m, m \in \sum_{i=1}^{n} m_i', m_i' = m_i \text{ or } m_i' = \sum_{j=1}^{n_i} (\prod_{k=1}^{k_i j} x_{ijk}) m_i.$$

It is easy to see that

$$(m, 0_M T, 0_M I, 0_M F), (m', 0_M T, 0_M I, 0_M F) \in \sum_{i=1}^{n} \overline{m_i'}, \overline{m_i'} = \overline{m_i} \text{ or } \overline{m_i'} = \sum_{j=1}^{n_i} (\prod_{k=1}^{k_i j} \overline{x_{ijk}}) \overline{m_i}.$$

where $\overline{x_{ij}} = (x_{ij}, 0T, 0I, 0F)$ and $\overline{m_i} = (m_i, 0_M T, 0_M I, 0_M F)$. In a similar way, we prove the backward direction. □

Proposition 4.14. *Let $(M, \star, R, \cdot)$ be an H_v-module and $m, m', n, n', p, p', q, q' \in M$. Then $m\varepsilon^\star m'$ if and only if $\varepsilon_N^\star(m, nT, pI, qF) = \varepsilon_N^\star(m', n'T, p'I, q'F)$;*

Proof. The proof is similar to that of Proposition 4.6. □

Let $(M, \star, R, \cdot)$ be an H_v-module. Then $NQ(M)/\varepsilon_N^\star$ is an $NQ(R)/\gamma_N^\star$-module and that $M/\varepsilon^\star$ is an $R\gamma^\star$-module.

We define "$\boxplus_\varepsilon$", "$\odot_\varepsilon$" on $M/\varepsilon^\star$ and "$\boxplus_{\varepsilon_N}$", "$\odot_{\varepsilon_N}$" on $NQ(M)/\varepsilon_N^\star$ as follows: For all $m_i, n_i \in M$, $r_i \in R$ with $i = 1, 2, 3, 4$, we have:

$$\varepsilon^\star(m_1) \boxplus_\varepsilon \varepsilon^\star(m_2) = \varepsilon^\star(m) \text{ where } m \in m_1 + m_2,$$

$$\gamma^\star(r_1) \odot_\varepsilon \varepsilon^\star(m_1) = \varepsilon^\star(m) \text{ where } m \in r_1 \cdot m_1,$$

$$\varepsilon_N^\star(m_1, m_2 T, m_3 I, m_4 F)) \boxplus_{\varepsilon_N} \varepsilon_N^\star(n_1, n_2 T, n_3 I, n_4 F) = \varepsilon_N^\star(\overline{m}),$$

$$\gamma_N^\star(r_1, r_T, r_3I, r_4F) \odot_{\varepsilon_N} \varepsilon_N^\star(m_1, m_2T, m_3I, m_4F) = \varepsilon_N^\star(\overline{n}),$$

where $\overline{m} \in (m_1, m_2T, m_3I, m_4F) \boxplus ((n_1, n_2T, n_3I, n_4F)$ and $\overline{n} \in (r_1, r_2T, r_3I, r_4F) \odot (m_1, m_2T, m_3I, m_4F)$,

Theorem 4.15. *Let $(M, \star, R, \cdot)$ be an H_v-module. Then $NQ(M)/\varepsilon_N^\star \cong M/\varepsilon^\star$.*

Proof. Let $\chi : NQ(M)/\varepsilon_N^\star \to M/\varepsilon^\star$ be defined as follows:

$$\chi(\varepsilon_N^\star(a, bT, cI, dF)) = \varepsilon^\star(a).$$

Proposition 4.14 asserts that χ is well defined and one-to-one. Moreover, it is clear that χ is onto as $\chi(\varepsilon_N^\star(a, 0_MT, 0_MI, 0_MF)) = \varepsilon^\star(a)$ for all $a \in M$. We need to show that χ is module homomorphism. We have:

(1) $\chi(\varepsilon_N^\star(a, bT, cI, dF) \boxplus_{\varepsilon_N} \varepsilon_N^\star(a', b'T, c'I, d'F)) = \chi(\varepsilon_N^\star(e, fT, gI, hF)) = \varepsilon^\star(e)$ where $(e, fT, gI, hF) \in (a, bT, cI, dF) \boxplus (a', b'T, c'I, d'F) = (a \star a', (b \star b')T, (c \star c')I, (d \star d')F)$. On the other hand, we have $\chi(\varepsilon_N^\star(a, bT, cI, dF)) \boxplus_\varepsilon \chi(\varepsilon_N^\star(a', b'T, c'I, d'F)) = \varepsilon^\star(a) \boxplus_\varepsilon \varepsilon^\star(a') = \varepsilon^\star(e)$ where $e \in a \star a'$. Thus, we obtain $\chi(\varepsilon_N^\star(a, bT, cI, dF) \boxplus_{\varepsilon_N} \varepsilon_N^\star(a', b'T, c'I, d'F)) = \chi(\varepsilon_N^\star(a, bT, cI, dF)) \boxplus_\varepsilon \chi(\varepsilon_N^\star(a', b'T, c'I, d'F))$.

(2) $\chi(\gamma_N^\star(r_1, r_2T, r_3I, r_4F) \odot_{\varepsilon_N} \varepsilon_N^\star(a, bT, cI, dF)) = \chi(\varepsilon_N^\star(e, fT, gI, hF)) = \varepsilon^\star(e)$ where $(e, fT, gI, hF) \in (r_1, r_2T, r_3I, r_4F) \odot (a, bT, cI, dF)$. It is clear that $e \in r_1 \cdot a$. On the other hand, we have $\gamma^\star(r_1) \odot_\varepsilon \chi(\varepsilon_N^\star(a, bT, cI, dF)) = \gamma^\star(r_1) \odot_\varepsilon \varepsilon^\star(a) = \varepsilon^\star(e)$ where $e \in r_1 \cdot a$. Thus, $\chi(\gamma_N^\star(r_1, r_2T, r_3I, r_4F) \odot_{\varepsilon_N} \varepsilon_N^\star(a, bT, cI, dF)) = \psi(r_1, r_2T, r_3I, r_4F) \odot_\varepsilon \chi(\varepsilon_N^\star(a, bT, cI, dF))$. Here "$\psi$ is the ring isomorphism defined in the proof of Theorem 4.7. □

Corollary 4.16. *Let $(M, \star, R, \cdot)$ be an H_v-module. Then $NQ(M)$ has a trivial fundamental module if and only if M has a trivial fundamental module.*

Proof. The proof follows from Theorem 4.15. □

Example 4.17. Let $R = \mathbb{Z}$, $M = \mathbb{Z}_4$ and $N = 2\mathbb{Z}_4 = \{0, 2\}$ in Example 2.8. One can easily see that $M/\varepsilon^\star \cong M/N \cong \mathbb{Z}_2$ where $(\mathbb{Z}_2, +, \mathbb{Z}, \cdot)$ is the $\mathbb{Z}$-module of integers under standard addition and multiplication modulo two. Using Theorem 4.15, we get $(NQ(\mathbb{Z}_4/\varepsilon_N^\star)) \cong \mathbb{Z}_2$.

5. Conclusion

The paper presented a detailed study on neutrosophic quadruple H_v-modules. It established that if M and N are isomorphic H_v-modules, then their corresponding neutrosophic quadruple H_v-modules are also isomorphic. Furthermore, the paper provided significant insights into the properties and characteristics of neutrosophic quadruple H_v-modules, thereby contributing to the understanding and application of neutrosophic logic in the field of mathematics.

References

1. A. A. A. Agboola, B. Davvaz and F. Smarandache, *Neutrosophic quadruple algebraic hyperstructures*, Ann. Fuzzy Math. Inform., 14 (2017) 29-42.
2. S. A. Akinleye, F. Smarandache and A. A. A. Agboola, *On neutrosophic quadruple algebraic structures*, Neutrosophic Sets and Systems, 12 (2016) 122-126.
3. M. Al-Tahan, B. Davvaz, *On the existence of hyperrings associated to arithmetic functions*, J. Number Theory, 174 (2017) 136-149.
4. M. Al-Tahan and B. Davvaz, *Strongly regular relations of arithmetic functions*, J. Number Theory, 187 (2018) 391-402.
5. M. Al-Tahan and B. Davvaz, *Chemical Hyperstructures for Elements with Four Oxidation States*, Iranian Journal of Mathematical Chemistry, 13(2) (2022), 85-97.
6. M. Al-Tahan and B. Davvaz, *On neutrosophic quadruple H_v-groups and their properties*, Southeast Asian Bulletin of Mathematics, 44 (2020) 13–625.
7. M. Al-Tahan and B. Davvaz, *On neutrosophic quadruple H_v-rings and their properties*,Neutrosophic Sets and Systems, 36 (2020) 256-270.
8. M. Al-Tahan, B. Davvaz, F. Smarandache, S. Al-Kaseasbeh, *Fundamental group and complete parts of Neutrosophic Quadruple Hv-groups*, Neutrosophic Sets and Systems, 53 (2023) 107-116.
9. M. Al-Tahan and B. Davvaz, *H_v-module of functions over H_v-ring of arithmetics and it's fundamental module*, Analele Stiintifice ale Universitatii Ovidius Constanta: Seria Matematica, 32(1) (2024), 5-18.
10. P. Corsini and V. Leoreanu, *Applications of Hyperstructures Theory*, Advances in Mathematics, Kluwer Academic Publisher, 2003.
11. B. Davvaz and V. Leoreanu-Fotea, *Hyperring Theory and Applications*, International Academic Press, USA, 2007.
12. B. Davvaz, *Polygroup Theory and Related Systems*, World Scientific Publishing Co. Pte. Ltd., Hackensack, NJ, 2013. viii+200 pp.
13. Y.B. Jun , S-Z. Song, F. Smarandache and H. Bordbar, *Neutrosophic quadruple BCK/BCI-algebras*, Axioms, 7(41) (2018) doi:10.3390/axioms7020041.
14. M. Koskas, *Groupoides, demi-hypergroupes et hypergroupes*, J. Math. Pure Appl., (9)49 (1970) 155-192.
15. F. Marty, *Sur une generalization de la notion de group*, In 8*th* Congress Math. Scandenaves, (1934), 45-49.
16. M. Muthuswamy, *Functions of Neu g ζ*H in NT Spaces*, Plithogenic Logic and Computation, 2 (2024), 10-19.
17. F. Smarandache, *Neutrosophic quadruple numbers, refined neutrosophic quadruple numbers, absorbance law, and the multiplication of neutrosophic quadruple numbers*, Neutrosophic Sets and Systems, 10 (2015) 96-98.
18. F. Smarandache, *Neutrosophy, neutrosophic probability, set, and logic*, American Research Press, USA, 1998.
19. F. Smarandache, *Neutrosophic set- A generalization of the intuitionistic fuzzy set*. Int. J. Pure Appl. Math., 24 (2005) 287-297.
20. F. Smarandache and M.Al-Tahan, Theory and Applications of NeutroAlgebras as Generalizations of Classical Algebras, IGI Global, 2022.
21. F. Smarandache and M.Al-Tahan, NeutroGeometry, NeutroAlgebra, and SuperHyperAlgebra in Today's World , IGI Global, 2023. DOI: 10.4018/978-1-6684-4740-6
22. T. Vougiouklis, *Cyclicity in a special class of hypergroups*, Acta Univ. Carolin. Math. Phys., 22(1) (1981) 3-6.
23. T. Vougiouklis, *Hyperstructures and their representations*, Hadronic Press Monographs in Mathematics, Hadronic Press, Inc., Palm Harbor, FL, 1994.

24. T. Vougiouklis, *The fundamental relation in hyperrings. The general hyperfield*, Algebraic hyperstructures and applications (Xnthi, 1990), 203-211, World Sci. Publ., Teaneck, NJ, 1991.
25. T. Vougiouklis, *From H_v-rings to H_v-fields*. Int. J. Algebraic Hyperstructures Appl., 1(1) (2014) 1-13.
26. L. A. Zadeh, *Fuzzy sets*, Inform and control, 8 (1965) 338-353.

Received: April 10, 2024. **Accepted**: August 29, 2024.

NSS
Neutrosophic Sets and Systems, Vol. 72, 2024
University of New Mexico

Evaluation of Distributed Leadership in Education Using Neutrosophic HyperSoft Set

Nouran Ajabnoor
Management Department, Applied College, Jazan University, Jazan, KSA
E-mail: nyusuf@jazanu.edu.sa

Abstract

Leadership in education needs to transcend, be responsive, and be adaptable to the boundaries of school leadership. Distributed leadership refers to various organizational stakeholders with a transformative framework and methodology. This paper proposed a decision-making methodology to evaluate distributed leadership in education based on multiple criteria and alternatives. The multi-criteria decision-making is used to deal with multiple criteria and alternatives. The Multi-Attributive Border Approximation Area Comparison (MABAC) approach ranks the alternatives. The neutrosophic set was used to deal with uncertainty and vague information in decision-making problems. This study used the neutrosophic HyperSoft Set. Neutrosophic HyperSoft Set is a new method for computational intelligence and decision-making to deal with vague information. This study used sixteen criteria and eight alternatives. The criteria weights show that Criterion Six has the highest weight, and Criterion Sixteen has the lowest. The results of the MABAC method show that alternative one is the best and alternative six is the worst.

Keywords: Leadership; Education; Decision-making; HyperSoft set; School leadership; Organizational stakeholders.

1. Introduction

Leadership plays a vital role in the education sector through organizational management and has undergone significant evolution. Distributed leadership has gained notable traction in recent studies. To obtain sustainable educational leadership, the educator must evolve and understand the intellectual structures of leadership. The role of leaders in schools has transcended their old boundaries in the education sector. The interconnected world offered a responsive, adaptable, and flexible leadership education. The set of stakeholders, decision-makers, and experts in the school framework, redefined leaders known as distributed leadership[1-2]. Distributed leadership refers to sharing various responsibilities instead of single in the organization by making effective leadership. Leadership is continuing to grow due to multiple factors, such as advanced technology, changes in curriculum, various study populations, and old models[3-4].

A fuzzy set (FS) is an extension of the crisp set. It is used to deal with fuzziness in different decision-making problems[5]. Various extensions of FS have been proposed in previous studies. FS was applied in multi-criteria decision-making (MCDM)[6]. The soft set (SS) was proposed in the literature. SS is very important in measuring problems to make different choices[7].

The neutrosophic set (NS) was proposed in the literature to solve problems of uncertain and vague information in the decision-making process[8]. NS has three functions: truth, indeterminacy, and falsity[9]. NS is essential for various decision-making applications due to its truth, indeterminacy, and falsity, which are independent[10-11]. HyperSoft set was proposed in the previous studies to handle more uncertainty applications by extending the hypersoft set to change functions into multiple functions[12]. The Multi-Attributive Border Approximation Area Comparison (MABAC) approach is an MCDM methodology[13]. This method builds the decision matrix between criteria and alternatives. It used the cost and positive criteria to normalize the decision matrix. It computes the border approximation area for each criterion. It defines the distance between alternatives from the border approximation area. Then, the alternatives are ranked according to the descending total distance for each alternative. This method has various options it is a compensatory approach, the criteria are independent of each other, and qualitative criteria are changed into quantitative criteria[14-15].

1.1 Leadership

Leadership is the ability of a single person or team to affect and guide a set of other persons and organizations or teams. Leadership refers to the criterion tied to the title of a person or organization in the hierarchy. Leadership criterion can anyone obtain or team. Leadership is a skill that can be obtained over time. Leaders are found and required in various firms, organizations, and businesses. Leaders can make complex decisions in firms and organizations to make the firms and organizations do better and attain their goals. Leaders can assign tasks to teams and people to achieve goals using information and knowledge from firms and organizations. Business leaders have various criteria and factors, such as robust communication with teams and users, management skills, best information and knowledge, innovation, awareness of risks and challenges, leadership skills, creativity, thinking, and confidence[1-4].

leadership is very important in various business firms, and organizations due to it has the success factors for business. Businesses and organizations depend on effective and successful methods to achieve their goals and missions by assigning tasks and activities to teams and other people. The criteria of a leader are important in crisis to make the best decisions [4].

Complex decision-making processes lead to the success of businesses and organizations. Business depends on leaders with high capabilities of success. These capabilities lead to improved productivity of businesses and organizations. Strong leadership is very important for businesses and organizations to compete with other originations due to innovation. Evaluating distributed leadership in education through the neutrosophic HyperSoft sets offers a modern method for understanding the complexities of leadership dynamics within schools. This approach integrates neutrosophic theory, which assists uncertainty with HyperSoft sets, which provide a flexible context for analyzing relationships and interactions.

By applying these concepts, educators can assess how effectively leadership responsibilities are shared among teachers, administrators, and other stakeholders. This evaluation allows for analysis of how distributed leadership impacts various aspects of the school environment, such as collaboration, decision-making, and overall effectiveness. It helps identify strengths and areas for

improvement in the distribution of leadership roles, ensuring that every participant's contributions are accurately recognized. Also, provides a comprehensive and adaptable tool for enhancing leadership practices and encouraging a more effective and comprehensive educational setting. The main contributions of this study are:

- This study proposed a decision-making methodology for evaluating distributed leadership in education.
- This study used the neutrosophic set to overcome uncertain information in the decision-making process.
- This study used a hypersoft set with a neutrosophic set for evaluation.
- This study used the MABAC method to rank the alternatives.
- Sixteen criteria and 8 alternatives are used in this study for evaluation in the decision-making process.

The rest of this study is organized as follows: Section two shows the education leadership. Section three shows the steps of the proposed methodology. Section four shows the results and discussions of the proposed method. Section five shows the conclusions of this study.

2. Leadership in Education

Education leadership plays a crucial role in today's schools, especially given the increasing responsibilities of school staff and the focus on accountability. Effective management and oversight are essential for improving administration within the education sector. Strong leadership is not just beneficial but necessary for advancing the quality of education, as it helps create supportive systems for both teachers and students. By enhancing learning environments and fostering positive change, leadership education contributes significantly to the development of educational systems [16].

Leadership education also impacts teacher practices and organizational policies, shaping how schools operate and adapt to new challenges. Various frameworks and methodologies have been explored in the literature to understand and improve education leadership. One such approach is distributed leadership, which builds upon existing theories and frameworks by emphasizing the sharing of leadership roles across various levels within a school. The characteristics of effective leadership and the key components necessary for its development are critical to advancing leadership education. These aspects help in identifying and nurturing the elements that contribute to successful school leadership. Understanding these properties not only supports the growth of individual leaders but also strengthens the overall educational environment, leading to more effective teaching and learning processes [16-17].

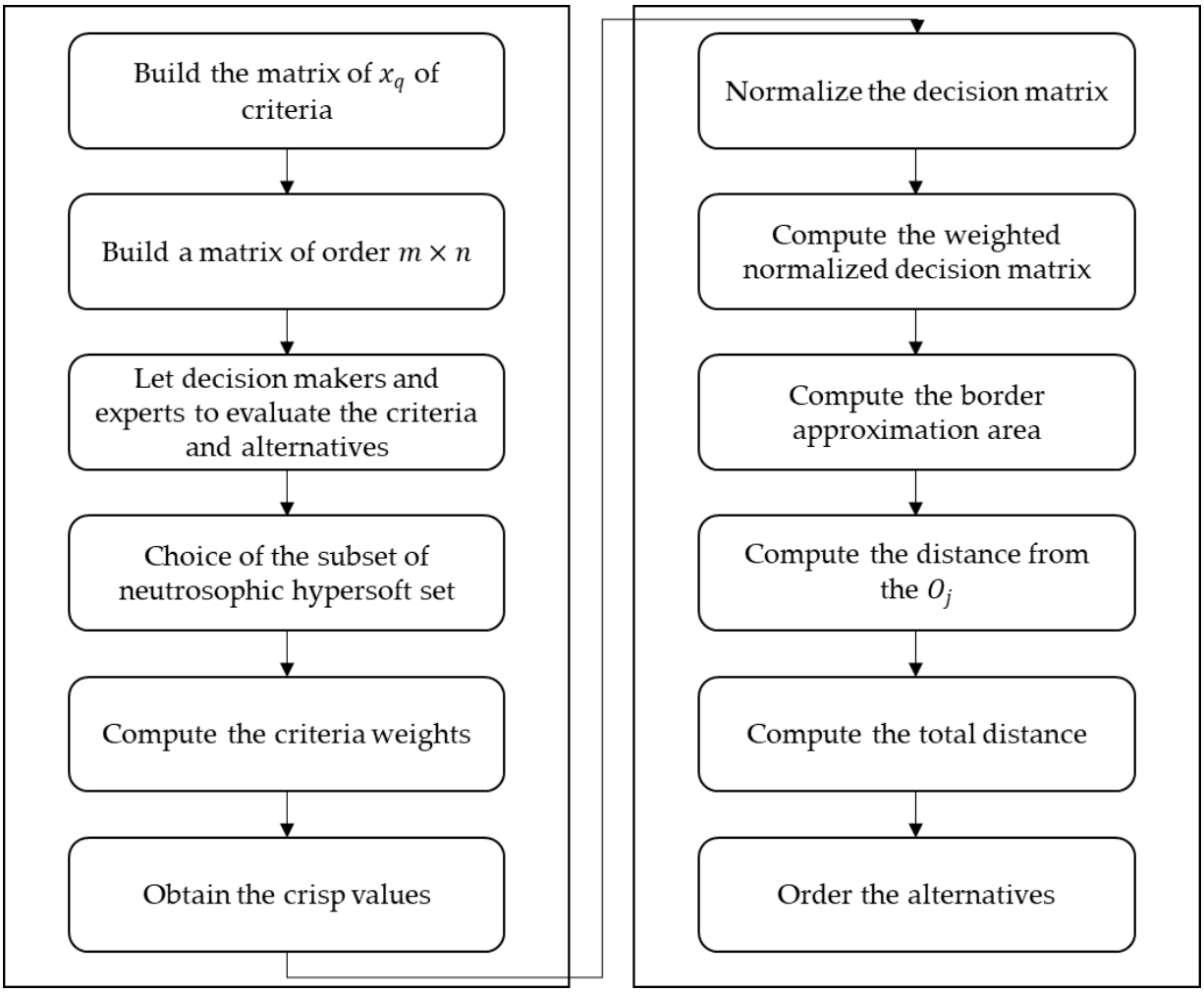

Figure 1. The steps of the methodology.

3. Methodology

This section introduces some operations of neutrosophic sets and steps of the MABAC methods with hypersoft set. Figure 1 shows the methodology steps. NS was used to deal with uncertainty in the decision-making process[18]. This paper used the single-valued neutrosophic set with three functions such as truth, indeterminacy, and falsity[19].

The operations of the single-valued neutrosophic set are shown as:

$0-\leq \sup T_A(x) + \sup I_A(x) + \sup F_A(x) \leq 3 +$

Let $A \text{ and } B \text{ are two single valued neutrosophic number as } A = (T_A, I_A, F_A) \text{ and } B = (T_B, I_B, F_B)$

$A^c = (F_B, 1 - I_B, T_B)$

$A \cup B = (\max\{T_A, T_B\}, \min\{I_A, I_B\}, \min\{F_A, F_B\})$

$A \cap B = (\min\{T_A, T_B\}, \max\{I_A, I_B\}, \max\{F_A, F_B\})$

$A \oplus B = (T_A + T_B - T_A T_B, I_A I_B, F_A F_B)$

$A \otimes B = (T_A T_B, I_A + I_B - I_A I_B, F_A + F_B - F_A F_B)$

$\lambda A = (1 - (1 - T_A)^{\lambda}, (I_A)^{\lambda}, (F_A)^{\lambda}, \lambda > 0)$

$A^{\lambda} = ((T_A)^{\lambda}, 1 - (1 - I_A)^{\lambda}, 1 - (1 - F_A)^{\lambda}), \lambda > 0$

Let the function be

$$Y: x_j \times x_k \times x_i \times \ldots \times x_m \to x(a), such\ that\ x_q = x_j, x_k, x_i, \ldots, x_m \quad (1)$$

Where

$$x_j = x_1, x_2, \ldots, x_n; \quad 1 \le j \le n \quad (2)$$

$$x_k = x_1, x_2, \ldots, x_n; \quad 1 \le k \le n \quad (3)$$

$$x_i = x_1, x_2, \ldots, x_n; \quad 1 \le i \le n \quad (4)$$

$\vdots$

$$x_m = x_1, x_2, \ldots, x_n; \quad 1 \le m \le n \quad (5)$$

refers to the neutrosophic criteria and is a universe of discourse.

Stage 1: Build the matrix of x_q of criteria of order $m \times n$.

$$T = \left[x_{qr}\right]_{m \times n}, 1 \le q \le m, 1 \le r \le n \quad (6)$$

Stage 2: Build a matrix of order $m \times n$.

To build the matrix, the columns are filled with zeros if multiple attributes are $\le n$.

Stage 3: Let decision-makers and experts evaluate the criteria and alternatives.

Stage 4: Choice of the subset of neutrosophic hypersoft set.

Stage 5: Compute the criteria weights.

The criteria weights are computed by using the average method.

Stage 6: Obtain the crisp values

The crisp values are obtained by using the score function.

Stage 7: Normalize the decision matrix

$$u_{ij} = \frac{x_{ij} - x_i^-}{x_i^+ - x_i^-}; i = 1, \ldots, m; j = 1, \ldots, n \quad (7)$$

$$u_{ij} = \frac{x_{ij} - x_i^+}{x_i^- - x_i^+}; i = 1, \ldots, m; j = 1, \ldots, n \quad (8)$$

Where $x_i^+ = \max(x_1, x_2, \ldots, x_m)$ and $x_i^- = \min(x_1, x_2, \ldots, x_m)$

Stage 8: Compute the weighted normalized decision matrix

$$Q_{ij} = w_j + u_{ij}w_j \tag{9}$$

Stage 9: Compute the border approximation area

$$O_j = \left(\prod_{i=1}^{m} Q_{ij}\right)^{\frac{1}{m}} \tag{10}$$

Stage 10: Compute the distance from the O_j

$$L_{ij} = Q_{ij} - O_j \tag{11}$$

Stage 11: Compute the total distance

$$D_i = \sum_{j=1}^{n} L_{ij} \tag{12}$$

Stage 12: Order the alternatives.

The alternatives are ordered based on the descending order of total distance.

4. Results and Discussions

This section shows the results of the proposed method. This study collects sixteen criteria and eight alternatives as shown in Figure 2.

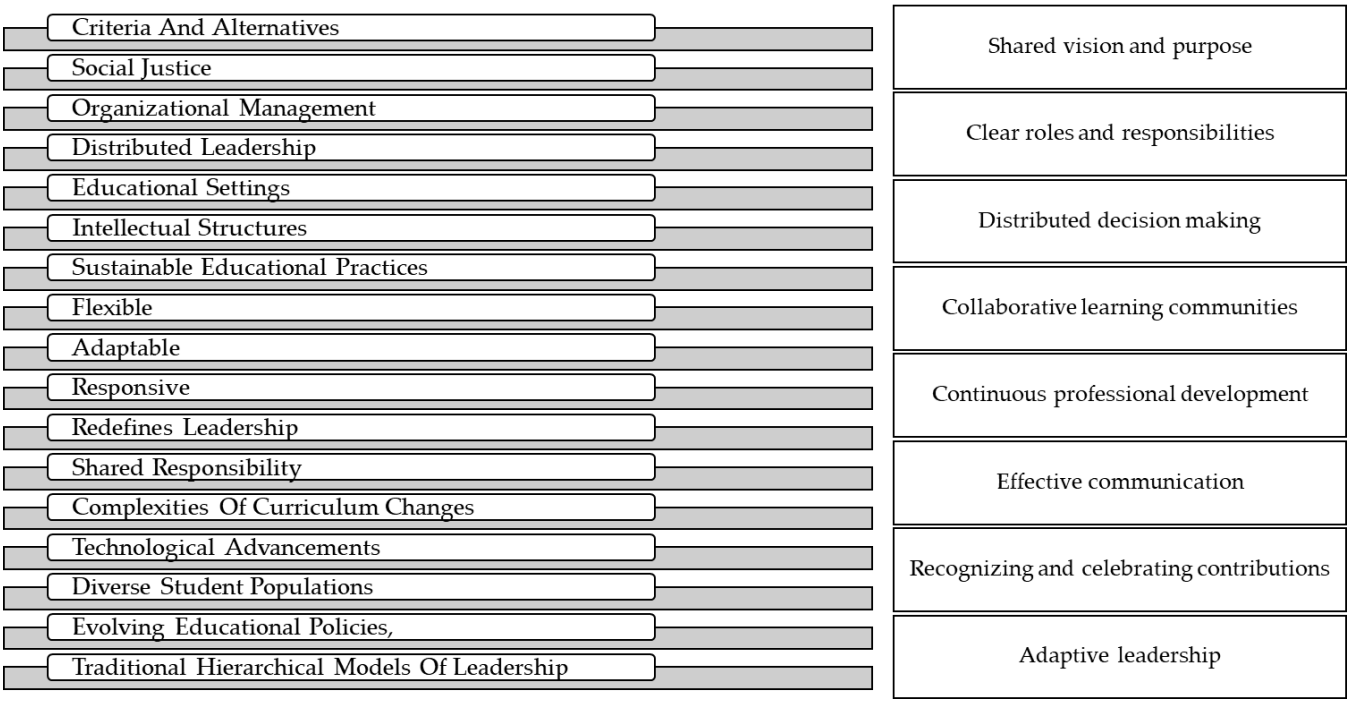

Figure 2. The criteria and alternatives.

Stage 1: Matrix of x_q of criteria of order $m \times n$ is built between criteria and alternatives.

Stage 2: Build a matrix of order $m \times n$.

Stage 3: Three experts who have expertise in leadership education evacuated the criteria and alternatives as shown in Table 1. Three experts used the linguistic terms of single-valued neutrosophic numbers.

Table 1. The opinions of three experts.

	LEA_1	LEA_2	LEA_3	LEA_4	LEA_5	LEA_6	LEA_7	LEA_8
LEC_1	(0.6,0.4,0.5)	(0.7,0.3,0.4)	(0.8,0.2,0.1)	(0.9,0.1,0.2)	(0.2,0.8,0.9)	(0.3,0.7,0.8)	(0.4,0.6,0.7)	(0.5,0.5,0.5)
LEC_2	(0.5,0.5,0.5)	(0.4,0.6,0.7)	(0.9,0.1,0.2)	(0.2,0.8,0.9)	(0.3,0.7,0.8)	(0.4,0.6,0.7)	(0.5,0.5,0.5)	(0.6,0.4,0.5)
LEC_3	(0.4,0.6,0.7)	(0.3,0.7,0.8)	(0.8,0.2,0.1)	(0.2,0.8,0.9)	(0.2,0.8,0.9)	(0.3,0.7,0.8)	(0.6,0.4,0.5)	(0.7,0.3,0.4)
LEC_4	(0.3,0.7,0.8)	(0.2,0.8,0.9)	(0.7,0.3,0.4)	(0.9,0.1,0.2)	(0.6,0.4,0.5)	(0.4,0.6,0.7)	(0.7,0.3,0.4)	(0.8,0.2,0.1)
LEC_5	(0.2,0.8,0.9)	(0.9,0.1,0.2)	(0.6,0.4,0.5)	(0.8,0.2,0.1)	(0.7,0.3,0.4)	(0.5,0.5,0.5)	(0.8,0.2,0.1)	(0.9,0.1,0.2)
LEC_6	(0.9,0.1,0.2)	(0.7,0.3,0.4)	(0.5,0.5,0.5)	(0.7,0.3,0.4)	(0.8,0.2,0.1)	(0.6,0.4,0.5)	(0.9,0.1,0.2)	(0.9,0.1,0.2)
LEC_7	(0.8,0.2,0.1)	(0.6,0.4,0.5)	(0.4,0.6,0.7)	(0.6,0.4,0.5)	(0.9,0.1,0.2)	(0.7,0.3,0.4)	(0.2,0.8,0.9)	(0.2,0.8,0.9)
LEC_8	(0.7,0.3,0.4)	(0.5,0.5,0.5)	(0.3,0.7,0.8)	(0.5,0.5,0.5)	(0.2,0.8,0.9)	(0.8,0.2,0.1)	(0.3,0.7,0.8)	(0.2,0.8,0.9)
LEC_9	(0.6,0.4,0.5)	(0.4,0.6,0.7)	(0.2,0.8,0.9)	(0.4,0.6,0.7)	(0.3,0.7,0.8)	(0.9,0.1,0.2)	(0.4,0.6,0.7)	(0.3,0.7,0.8)
LEC_{10}	(0.5,0.5,0.5)	(0.4,0.6,0.7)	(0.9,0.1,0.2)	(0.3,0.7,0.8)	(0.4,0.6,0.7)	(0.6,0.4,0.5)	(0.5,0.5,0.5)	(0.4,0.6,0.7)
LEC_{11}	(0.4,0.6,0.7)	(0.3,0.7,0.8)	(0.8,0.2,0.1)	(0.2,0.8,0.9)	(0.5,0.5,0.5)	(0.6,0.4,0.5)	(0.6,0.4,0.5)	(0.5,0.5,0.5)
LEC_{12}	(0.9,0.1,0.2)	(0.3,0.7,0.8)	(0.7,0.3,0.4)	(0.9,0.1,0.2)	(0.6,0.4,0.5)	(0.2,0.8,0.9)	(0.7,0.3,0.4)	(0.6,0.4,0.5)
LEC_{13}	(0.8,0.2,0.1)	(0.2,0.8,0.9)	(0.6,0.4,0.5)	(0.8,0.2,0.1)	(0.7,0.3,0.4)	(0.2,0.8,0.9)	(0.8,0.2,0.1)	(0.7,0.3,0.4)
LEC_{14}	(0.7,0.3,0.4)	(0.9,0.1,0.2)	(0.5,0.5,0.5)	(0.4,0.6,0.7)	(0.4,0.6,0.7)	(0.3,0.7,0.8)	(0.9,0.1,0.2)	(0.8,0.2,0.1)
LEC_{15}	(0.6,0.4,0.5)	(0.8,0.2,0.1)	(0.7,0.3,0.4)	(0.6,0.4,0.5)	(0.5,0.5,0.5)	(0.4,0.6,0.7)	(0.3,0.7,0.8)	(0.9,0.1,0.2)
LEC_{16}	(0.5,0.5,0.5)	(0.4,0.6,0.7)	(0.3,0.7,0.8)	(0.2,0.8,0.9)	(0.2,0.8,0.9)	(0.3,0.7,0.8)	(0.4,0.6,0.7)	(0.6,0.4,0.5)
	LEA_1	LEA_2	LEA_3	LEA_4	LEA_5	LEA_6	LEA_7	LEA_8
LEC_1	(0.6,0.4,0.5)	(0.6,0.4,0.5)	(0.5,0.5,0.5)	(0.4,0.6,0.7)	(0.3,0.7,0.8)	(0.2,0.8,0.9)	(0.4,0.6,0.7)	(0.5,0.5,0.5)
LEC_2	(0.6,0.4,0.5)	(0.5,0.5,0.5)	(0.4,0.6,0.7)	(0.3,0.7,0.8)	(0.2,0.8,0.9)	(0.4,0.6,0.7)	(0.5,0.5,0.5)	(0.6,0.4,0.5)
LEC_3	(0.4,0.6,0.7)	(0.3,0.7,0.8)	(0.6,0.4,0.5)	(0.5,0.5,0.5)	(0.4,0.6,0.7)	(0.3,0.7,0.8)	(0.2,0.8,0.9)	(0.7,0.3,0.4)
LEC_4	(0.3,0.7,0.8)	(0.2,0.8,0.9)	(0.7,0.3,0.4)	(0.6,0.4,0.5)	(0.5,0.5,0.5)	(0.4,0.6,0.7)	(0.3,0.7,0.8)	(0.2,0.8,0.9)
LEC_5	(0.2,0.8,0.9)	(0.9,0.1,0.2)	(0.6,0.4,0.5)	(0.5,0.5,0.5)	(0.4,0.6,0.7)	(0.3,0.7,0.8)	(0.2,0.8,0.9)	(0.9,0.1,0.2)
LEC_6	(0.9,0.1,0.2)	(0.6,0.4,0.5)	(0.5,0.5,0.5)	(0.4,0.6,0.7)	(0.3,0.7,0.8)	(0.2,0.8,0.9)	(0.9,0.1,0.2)	(0.9,0.1,0.2)
LEC_7	(0.6,0.4,0.5)	(0.5,0.5,0.5)	(0.4,0.6,0.7)	(0.3,0.7,0.8)	(0.2,0.8,0.9)	(0.7,0.3,0.4)	(0.2,0.8,0.9)	(0.2,0.8,0.9)
LEC_8	(0.7,0.3,0.4)	(0.6,0.4,0.5)	(0.5,0.5,0.5)	(0.4,0.6,0.7)	(0.3,0.7,0.8)	(0.2,0.8,0.9)	(0.2,0.8,0.9)	(0.2,0.8,0.9)
LEC_9	(0.6,0.4,0.5)	(0.6,0.4,0.5)	(0.5,0.5,0.5)	(0.4,0.6,0.7)	(0.3,0.7,0.8)	(0.2,0.8,0.9)	(0.4,0.6,0.7)	(0.3,0.7,0.8)
LEC_{10}	(0.5,0.5,0.5)	(0.4,0.6,0.7)	(0.6,0.4,0.5)	(0.5,0.5,0.5)	(0.4,0.6,0.7)	(0.3,0.7,0.8)	(0.2,0.8,0.9)	(0.4,0.6,0.7)
LEC_{11}	(0.6,0.4,0.5)	(0.5,0.5,0.5)	(0.4,0.6,0.7)	(0.3,0.7,0.8)	(0.2,0.8,0.9)	(0.3,0.7,0.8)	(0.2,0.8,0.9)	(0.5,0.5,0.5)
LEC_{12}	(0.6,0.4,0.5)	(0.6,0.4,0.5)	(0.5,0.5,0.5)	(0.4,0.6,0.7)	(0.3,0.7,0.8)	(0.2,0.8,0.9)	(0.3,0.7,0.8)	(0.2,0.8,0.9)
LEC_{13}	(0.8,0.2,0.1)	(0.6,0.4,0.5)	(0.6,0.4,0.5)	(0.5,0.5,0.5)	(0.4,0.6,0.7)	(0.3,0.7,0.8)	(0.2,0.8,0.9)	(0.7,0.3,0.4)
LEC_{14}	(0.6,0.4,0.5)	(0.5,0.5,0.5)	(0.4,0.6,0.7)	(0.6,0.4,0.5)	(0.5,0.5,0.5)	(0.4,0.6,0.7)	(0.3,0.7,0.8)	(0.2,0.8,0.9)
LEC_{15}	(0.6,0.4,0.5)	(0.6,0.4,0.5)	(0.5,0.5,0.5)	(0.4,0.6,0.7)	(0.3,0.7,0.8)	(0.2,0.8,0.9)	(0.3,0.7,0.8)	(0.9,0.1,0.2)
LEC_{16}	(0.6,0.4,0.5)	(0.5,0.5,0.5)	(0.4,0.6,0.7)	(0.3,0.7,0.8)	(0.2,0.8,0.9)	(0.3,0.7,0.8)	(0.4,0.6,0.7)	(0.6,0.4,0.5)
	LEA_1	LEA_2	LEA_3	LEA_4	LEA_5	LEA_6	LEA_7	LEA_8
LEC_1	(0.4,0.6,0.7)	(0.3,0.7,0.8)	(0.8,0.2,0.1)	(0.4,0.6,0.7)	(0.3,0.7,0.8)	(0.8,0.2,0.1)	(0.2,0.8,0.9)	(0.2,0.8,0.9)
LEC_2	(0.4,0.6,0.7)	(0.4,0.6,0.7)	(0.3,0.7,0.8)	(0.8,0.2,0.1)	(0.2,0.8,0.9)	(0.2,0.8,0.9)	(0.5,0.5,0.5)	(0.6,0.4,0.5)
LEC_3	(0.4,0.6,0.7)	(0.3,0.7,0.8)	(0.8,0.2,0.1)	(0.2,0.8,0.9)	(0.2,0.8,0.9)	(0.3,0.7,0.8)	(0.6,0.4,0.5)	(0.7,0.3,0.4)
LEC_4	(0.3,0.7,0.8)	(0.4,0.6,0.7)	(0.3,0.7,0.8)	(0.8,0.2,0.1)	(0.2,0.8,0.9)	(0.2,0.8,0.9)	(0.7,0.3,0.4)	(0.8,0.2,0.1)
LEC_5	(0.4,0.6,0.7)	(0.3,0.7,0.8)	(0.4,0.6,0.7)	(0.3,0.7,0.8)	(0.8,0.2,0.1)	(0.2,0.8,0.9)	(0.2,0.8,0.9)	(0.9,0.1,0.2)
LEC_6	(0.4,0.6,0.7)	(0.3,0.7,0.8)	(0.8,0.2,0.1)	(0.2,0.8,0.9)	(0.2,0.8,0.9)	(0.2,0.8,0.9)	(0.2,0.8,0.9)	(0.9,0.1,0.2)
LEC_7	(0.8,0.2,0.1)	(0.6,0.4,0.5)	(0.4,0.6,0.7)	(0.3,0.7,0.8)	(0.8,0.2,0.1)	(0.2,0.8,0.9)	(0.2,0.8,0.9)	(0.2,0.8,0.9)
LEC_8	(0.4,0.6,0.7)	(0.3,0.7,0.8)	(0.8,0.2,0.1)	(0.2,0.8,0.9)	(0.2,0.8,0.9)	(0.2,0.8,0.9)	(0.2,0.8,0.9)	(0.2,0.8,0.9)
LEC_9	(0.4,0.6,0.7)	(0.3,0.7,0.8)	(0.8,0.2,0.1)	(0.4,0.6,0.7)	(0.3,0.7,0.8)	(0.8,0.2,0.1)	(0.2,0.8,0.9)	(0.2,0.8,0.9)
LEC_{10}	(0.5,0.5,0.5)	(0.4,0.6,0.7)	(0.4,0.6,0.7)	(0.3,0.7,0.8)	(0.8,0.2,0.1)	(0.2,0.8,0.9)	(0.2,0.8,0.9)	(0.4,0.6,0.7)
LEC_{11}	(0.4,0.6,0.7)	(0.4,0.6,0.7)	(0.4,0.6,0.7)	(0.3,0.7,0.8)	(0.8,0.2,0.1)	(0.2,0.8,0.9)	(0.2,0.8,0.9)	(0.5,0.5,0.5)
LEC_{12}	(0.9,0.1,0.2)	(0.4,0.6,0.7)	(0.3,0.7,0.8)	(0.8,0.2,0.1)	(0.2,0.8,0.9)	(0.2,0.8,0.9)	(0.2,0.8,0.9)	(0.6,0.4,0.5)
LEC_{13}	(0.8,0.2,0.1)	(0.4,0.6,0.7)	(0.3,0.7,0.8)	(0.4,0.6,0.7)	(0.3,0.7,0.8)	(0.8,0.2,0.1)	(0.2,0.8,0.9)	(0.2,0.8,0.9)
LEC_{14}	(0.7,0.3,0.4)	(0.4,0.6,0.7)	(0.3,0.7,0.8)	(0.8,0.2,0.1)	(0.2,0.8,0.9)	(0.2,0.8,0.9)	(0.9,0.1,0.2)	(0.8,0.2,0.1)
LEC_{15}	(0.6,0.4,0.5)	(0.4,0.6,0.7)	(0.3,0.7,0.8)	(0.4,0.6,0.7)	(0.3,0.7,0.8)	(0.8,0.2,0.1)	(0.2,0.8,0.9)	(0.2,0.8,0.9)
LEC_{16}	(0.5,0.5,0.5)	(0.4,0.6,0.7)	(0.3,0.7,0.8)	(0.8,0.2,0.1)	(0.2,0.8,0.9)	(0.2,0.8,0.9)	(0.2,0.8,0.9)	(0.2,0.8,0.9)

Stage 4: Choice of the subset of neutrosophic hypersoft set.

$$LEC_1 = \{LEC_{11}, LEC_{12}, LEC_{13}\}$$

$$LEC_2 = \{LEC_{22}, LEC_{22}, LEC_{23}\}$$

$$LEC_3 = \{LEC_{31}, LEC_{32}, LEC_{33}\}$$

$$LEC_4 = \{LEC_{41}, LEC_{42}, LEC_{43}\}$$

$$LEC_5 = \{LEC_{51}, LEC_{52}, LEC_{53}\}$$

$$LEC_6 = \{LEC_{61}, LEC_{62}, LEC_{63}\}$$

$$LEC_7 = \{LEC_{71}, LEC_{72}, LEC_{73}\}$$

$$LEC_8 = \{LEC_{81}, LEC_{82}, LEC_{83}\}$$

$$LEC_9 = \{LEC_{91}, LEC_{92}, LEC_{93}\}$$

$$LEC_{10} = \{LEC_{101}, LEC_{102}, LEC_{103}\}$$

$$LEC_{11} = \{LEC_{111}, LEC_{112}, LEC_{113}\}$$

$$LEC_{12} = \{LEC_{121}, LEC_{122}, LEC_{123}\}$$

$$LEC_{13} = \{LEC_{131}, LEC_{132}, LEC_{133}\}$$

$$LEC_{14} = \{LEC_{141}, LEC_{142}, LEC_{143}\}$$

$$LEC_{15} = \{LEC_{151}, LEC_{152}, LEC_{153}\}$$

$$LEC_{16} = \{LEC_{161}, LEC_{162}, LEC_{163}\}$$

Stage 5: The criteria weights are computed as shown in Figure 3. We show that criterion six has the highest weight and criterion sixteen has the lowest weight.

Stage 6: Obtain the crisp values

Stage 7: Normalize the decision matrix as shown in Table 2.

Stage 8: Compute the weighted normalized decision matrix as shown in Table 3.

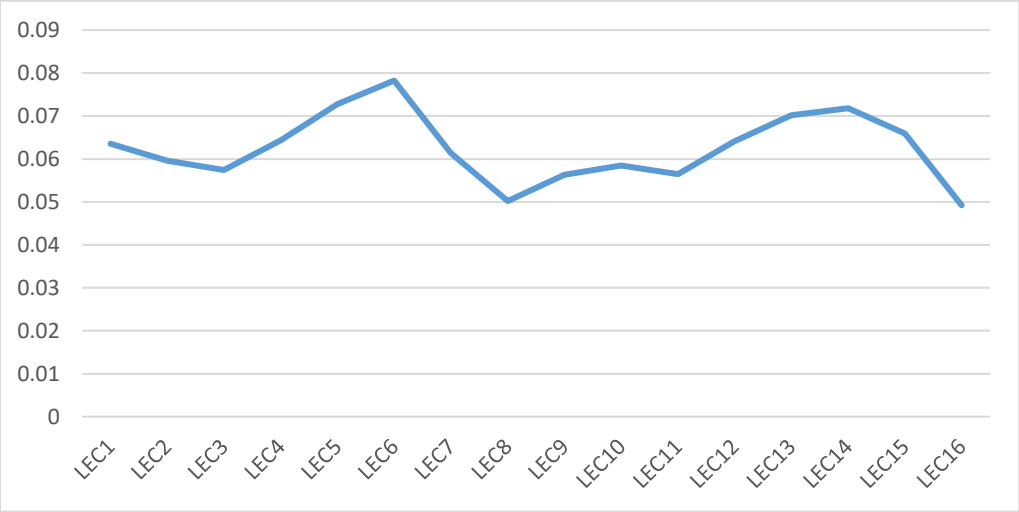

Figure 3. The criteria weights.

Table 2. The normalized decision matrix.

	LEA_1	LEA_2	LEA_3	LEA_4	LEA_5	LEA_6	LEA_7	LEA_8
LEC_1	0.545455	0.545455	1	0.613636	0	0.386364	0.136364	0.318182
LEC_2	0.757576	0.575758	0.818182	0.606061	0	0.272727	0.818182	1
LEC_3	0.26087	0.065217	1	0.086957	0	0.065217	0.391304	0.847826
LEC_4	0.06383	0	0.574468	1	0.340426	0.12766	0.574468	0.723404
LEC_5	0	0.684211	0.421053	0.473684	0.614035	0.122807	0.245614	1
LEC_6	0.705882	0.352941	0.54902	0.176471	0.215686	0	0.588235	1
LEC_7	1	0.653846	0.346154	0.346154	0.788462	0.576923	0	0
LEC_8	1	0.694444	0.916667	0.444444	0.083333	0.555556	0.083333	0
LEC_9	0.685714	0.428571	0.685714	0.342857	0.085714	1	0.171429	0
LEC_{10}	0.689655	0.275862	1	0.206897	0.758621	0.172414	0	0.275862
LEC_{11}	0.692308	0.5	1	0	0.923077	0.346154	0.230769	0.923077
LEC_{12}	1	0.388889	0.518519	0.87037	0.277778	0	0.333333	0.444444
LEC_{13}	1	0	0.214286	0.428571	0.142857	0.119048	0.047619	0.285714
LEC_{14}	0.916667	0.777778	0.277778	0.805556	0.194444	0	1	0.861111
LEC_{15}	0.833333	0.888889	0.611111	0.5	0.277778	0.555556	0	1
LEC_{16}	1	0.6875	0.375	0.71875	0	0.1875	0.375	0.75

Table 3. The weighted normalized decision matrix.

	LEA_1	LEA_2	LEA_3	LEA_4	LEA_5	LEA_6	LEA_7	LEA_8
LEC_1	0.098201	0.098201	0.127084	0.102533	0.063542	0.088092	0.072207	0.08376
LEC_2	0.104786	0.093946	0.108399	0.095753	0.05962	0.075879	0.108399	0.119239
LEC_3	0.072452	0.06121	0.114924	0.062459	0.057462	0.06121	0.079947	0.10618
LEC_4	0.068432	0.064326	0.10128	0.128653	0.086225	0.072538	0.10128	0.11086
LEC_5	0.072759	0.122542	0.103395	0.107224	0.117436	0.081695	0.09063	0.145519
LEC_6	0.133486	0.105869	0.121212	0.09206	0.095128	0.078251	0.12428	0.156501
LEC_7	0.122769	0.101521	0.082633	0.082633	0.109784	0.096799	0.061385	0.061385
LEC_8	0.100412	0.085071	0.096228	0.07252	0.05439	0.078098	0.05439	0.050206
LEC_9	0.094881	0.080408	0.094881	0.075583	0.06111	0.112571	0.065934	0.056286
LEC_{10}	0.098748	0.074565	0.116886	0.070534	0.102779	0.068519	0.058443	0.074565
LEC_{11}	0.095584	0.084722	0.112963	0.056482	0.108619	0.076033	0.069516	0.108619
LEC_{12}	0.12826	0.08907	0.097383	0.119947	0.081944	0.06413	0.085507	0.092633
LEC_{13}	0.14042	0.07021	0.085255	0.1003	0.08024	0.078568	0.073553	0.09027
LEC_{14}	0.137576	0.127607	0.091717	0.129601	0.085736	0.071779	0.143558	0.133588
LEC_{15}	0.120808	0.124469	0.106165	0.098843	0.0842	0.102504	0.065895	0.131791
LEC_{16}	0.098451	0.083068	0.067685	0.084606	0.049225	0.058455	0.067685	0.086144

Table 4. The distance matrix.

	LEA_1	LEA_2	LEA_3	LEA_4	LEA_5	LEA_6	LEA_7	LEA_8
LEC_1	0.008334	0.008334	0.037217	0.012667	-0.02633	-0.00177	-0.01766	-0.00611
LEC_2	0.011021	0.000181	0.014634	0.001988	-0.03415	-0.01789	0.014634	0.025474
LEC_3	-0.00206	-0.0133	0.04041	-0.01206	-0.01705	-0.0133	0.005433	0.031666
LEC_4	-0.02082	-0.02493	0.012024	0.039397	-0.00303	-0.01672	0.012024	0.021605
LEC_5	-0.03008	0.019706	0.000559	0.004389	0.0146	-0.02114	-0.01221	0.042683
LEC_6	0.022616	-0.005	0.010341	-0.01881	-0.01574	-0.03262	0.01341	0.045631
LEC_7	0.035359	0.014111	-0.00478	-0.00478	0.022374	0.009389	-0.02603	-0.02603
LEC_8	0.028803	0.013462	0.024619	0.00091	-0.01722	0.006489	-0.01722	-0.0214
LEC_9	0.016693	0.00222	0.016693	-0.0026	-0.01708	0.034383	-0.01225	-0.0219
LEC_{10}	0.017694	-0.00649	0.035831	-0.01052	0.021724	-0.01254	-0.02261	-0.00649
LEC_{11}	0.008785	-0.00208	0.026164	-0.03032	0.021819	-0.01077	-0.01728	0.021819
LEC_{12}	0.035347	-0.00384	0.004469	0.027033	-0.01097	-0.02878	-0.00741	-0.00028
LEC_{13}	0.052628	-0.01758	-0.00254	0.012508	-0.00755	-0.00922	-0.01424	0.002478
LEC_{14}	0.025651	0.015681	-0.02021	0.017675	-0.02619	-0.04015	0.031632	0.021663
LEC_{15}	0.018688	0.022349	0.004045	-0.00328	-0.01792	0.000384	-0.03622	0.029671
LEC_{16}	0.025688	0.010305	-0.00508	0.011843	-0.02354	-0.01431	-0.00508	0.013382

Stage 9: Compute the border approximation area

Stage 10: Compute the distance from the O_j as shown in Table 4.

Stage 11: Compute the total distance.

Stage 12: Order the alternatives as shown in Figure 4. We show that alternative one is the best and alternative six is the worst.

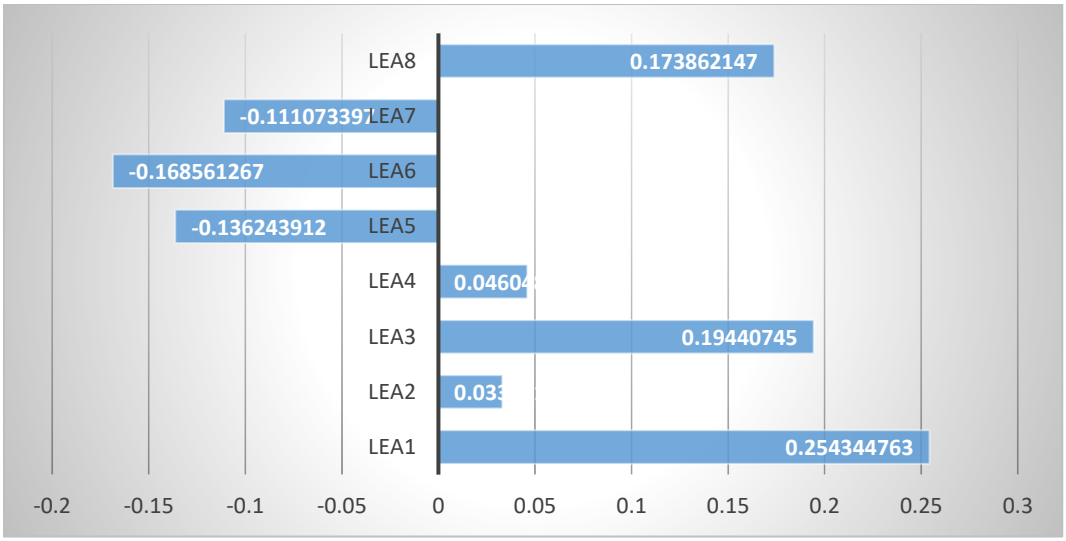

Figure 4. The total distances.

4.1 Findings

This part introduces the discussion of the results. This paper uses neutrosophic sets to overcome uncertainty in the evaluation process. The neutrosophic set is used with the hypersoft set. The MABAC method is used to rank the alternatives. This study uses sixteen criteria and eight alternatives. The criteria weights are computed using the average method.

Three decision-makers evaluated the criteria and alternatives. They used the linguistic terms of single-valued neutrosophic sets. Then, we replaced these terms by using the single-valued neutrosophic numbers. These numbers contain three values: truth, indeterminacy, and falsity. Then, we used the score function to convert these three values into one value. Then, we combine the tree matrices into a single matrix. Then, we obtained the criteria weights. The results show that criterion six has the highest weight with a value equal to 0.078, followed by criterion five with a weight equal to 0.072, criterion Fourteen with a weight equal to 0.071, criterion Thirteen with a weight equal to 0.070, and criterion Fifteen with a weight equal to 0.065. The results show that criterion Sixteen has the lowest importance with a weight equal to 0.049, followed by criterion eight with a weight equal to 0.050, criterion with a weight equal to 0.0562, and criterion Eleven with a weight equal to 0.0564. Then, we applied the MABAC method to show the rank of alternatives. We built the decision matrix between criteria and alternatives. Then, we normalize the decision matrix between criteria and alternatives. Then, we obtained a weighted normalized decision matrix. Then, we compute the border approximation area. Then, we compute the distance from the border approximation area. Then, we rank the alternatives based on the highest total distance. The results show that Alternative One has the highest rank with a total distance equal to 0.0254, followed by Alternative Three with a total distance equal to 0.194, and Alternative Eight with a total distance equal to 0.173. alternative six has the lowest total distance, and alternative Five.

4.2 Sensitivity Analysis

This part explains how we tested the results to see if they stayed consistent when we changed the weights of different criteria. We looked at seventeen different scenarios, as shown in Table 5.

In each scenario, we adjusted the weight of one criterion to 0.7 while keeping the weights of the other criteria the same. For example, in the first scenario, all criteria had equal weight. In the next scenarios, we changed the weight of one specific criterion to 0.7, such as the first criterion in the second case, the second criterion in the third case, and so on, up to the ninth criterion in the tenth case. Then, we applied the MABAC method to the criteria weights. Table 6 shows the total distance. Then, we rank the alternatives as shown in Figure 5. In the first case, we show the first alternative has the highest rank, followed by the third alternative. Alternative six has the lowest rank. In the second case, we show the first alternative has the highest rank, followed by the third alternative. Alternative six has the lowest rank. In the third case, we show the first alternative has the highest rank, followed by the third alternative. Alternative six has the lowest rank. In the fourth case, we show the first alternative has the highest rank, followed by the third alternative. Alternative six has the lowest rank. In the fifth case, we show the first alternative has the highest rank, followed by the third alternative. Alternative six has the lowest rank. In the sixth case, we show the first alternative has the highest rank, followed by the third alternative. Alternative six has the lowest rank. In the seventh case, we show the first alternative has the highest rank, followed by the third. Alternative six has the lowest rank. In the eighth case, we show the first alternative has the highest rank, followed by the third alternative. Alternative six has the lowest rank. In the ninth case, we show the first alternative has the highest rank, followed by the third alternative. Alternative six has the lowest rank. In the tenth case, we show the first alternative has the highest rank, followed by the third alternative. Alternative six has the lowest rank.

Table 4. The criteria weights under sensitivity analysis.

	S_1	S_2	S_3	S_4	S_5	S_6	S_7	S_8	S_9	S_{10}	S_{11}	S_{12}	S_{13}	S_{14}	S_{15}	S_{16}	S_{17}
LEC_1	0.0625	0.7	0.062	0.062	0.062	0.062	0.062	0.062	0.062	0.062	0.062	0.062	0.062	0.062	0.062	0.062	0.062
LEC_2	0.0625	0.062	0.7	0.062	0.062	0.062	0.062	0.062	0.062	0.062	0.062	0.062	0.062	0.062	0.062	0.062	0.062
LEC_3	0.0625	0.062	0.062	0.7	0.062	0.062	0.062	0.062	0.062	0.062	0.062	0.062	0.062	0.062	0.062	0.062	0.062
LEC_4	0.0625	0.062	0.062	0.062	0.7	0.062	0.062	0.062	0.062	0.062	0.062	0.062	0.062	0.062	0.062	0.062	0.062
LEC_5	0.0625	0.062	0.062	0.062	0.062	0.7	0.062	0.062	0.062	0.062	0.062	0.062	0.062	0.062	0.062	0.062	0.062
LEC_6	0.0625	0.062	0.062	0.062	0.062	0.062	0.7	0.062	0.062	0.062	0.062	0.062	0.062	0.062	0.062	0.062	0.062
LEC_7	0.0625	0.062	0.062	0.062	0.062	0.062	0.062	0.7	0.062	0.062	0.062	0.062	0.062	0.062	0.062	0.062	0.062
LEC_8	0.0625	0.062	0.062	0.062	0.062	0.062	0.062	0.062	0.7	0.062	0.062	0.062	0.062	0.062	0.062	0.062	0.062
LEC_9	0.0625	0.062	0.062	0.062	0.062	0.062	0.062	0.062	0.062	0.7	0.062	0.062	0.062	0.062	0.062	0.062	0.062
LEC_{10}	0.0625	0.062	0.062	0.062	0.062	0.062	0.062	0.062	0.062	0.062	0.7	0.062	0.062	0.062	0.062	0.062	0.062
LEC_{11}	0.0625	0.062	0.062	0.062	0.062	0.062	0.062	0.062	0.062	0.062	0.062	0.7	0.062	0.062	0.062	0.062	0.062
LEC_{12}	0.0625	0.062	0.062	0.062	0.062	0.062	0.062	0.062	0.062	0.062	0.062	0.062	0.7	0.062	0.062	0.062	0.062
LEC_{13}	0.0625	0.062	0.062	0.062	0.062	0.062	0.062	0.062	0.062	0.062	0.062	0.062	0.062	0.7	0.062	0.062	0.062
LEC_{14}	0.0625	0.062	0.062	0.062	0.062	0.062	0.062	0.062	0.062	0.062	0.062	0.062	0.062	0.062	0.7	0.062	0.062
LEC_{15}	0.0625	0.062	0.062	0.062	0.062	0.062	0.062	0.062	0.062	0.062	0.062	0.062	0.062	0.062	0.062	0.7	0.062
LEC_{16}	0.0625	0.062	0.062	0.062	0.062	0.062	0.062	0.062	0.062	0.062	0.062	0.062	0.062	0.062	0.062	0.062	0.7

Table 5. The total distances under sensitivity analysis.

	S_1	S_2	S_3	S_4	S_5	S_6	S_7	S_8	S_9	S_{10}	S_{11}	S_{12}	S_{13}	S_{14}	S_{15}	S_{16}	S_{17}
LEA_1	0.262514	0.316316	0.317702	0.316047	0.313888	0.313216	0.318484	0.320636	0.320619	0.31854	0.318587	0.317483	0.32045	0.321938	0.318996	0.318443	0.32023
LEA_2	0.035518	0.02732	0.027343	0.025584	0.024414	0.029352	0.026841	0.029045	0.029331	0.027616	0.026488	0.027045	0.026871	0.025442	0.028959	0.029864	0.028891
LEA_3	0.209805	0.173198	0.175039	0.178473	0.1746	0.173256	0.174189	0.172615	0.176876	0.175423	0.177796	0.176672	0.173721	0.172927	0.171087	0.173659	0.172425
LEA_4	0.041833	0.029375	0.029625	0.027801	0.033968	0.029827	0.027572	0.028791	0.029511	0.029027	0.028025	0.025349	0.032536	0.030711	0.031221	0.029002	0.031179
LEA_5	-0.14055	-0.11466	-0.11896	-0.11689	-0.11501	-0.11316	-0.11617	-0.11193	-0.11723	-0.11694	-0.11187	-0.11176	-0.11594	-0.11547	-0.1174	-0.1167	-0.11825
LEA_6	-0.15395	-0.1522	-0.15445	-0.15394	-0.15415	-0.15438	-0.15533	-0.15105	-0.15123	-0.14762	-0.15381	-0.15363	-0.15557	-0.15319	-0.1564	-0.15216	-0.15438
LEA_7	-0.12221	-0.10484	-0.103	-0.10413	-0.10344	-0.1061	-0.10356	-0.10802	-0.10742	-0.10648	-0.10774	-0.10714	-0.10571	-0.10636	-0.10154	-0.10897	-0.10562
LEA_8	0.154909	0.160916	0.164121	0.165049	0.163435	0.165316	0.16529	0.157737	0.157719	0.157998	0.160084	0.163814	0.160883	0.161181	0.16318	0.164293	0.162955

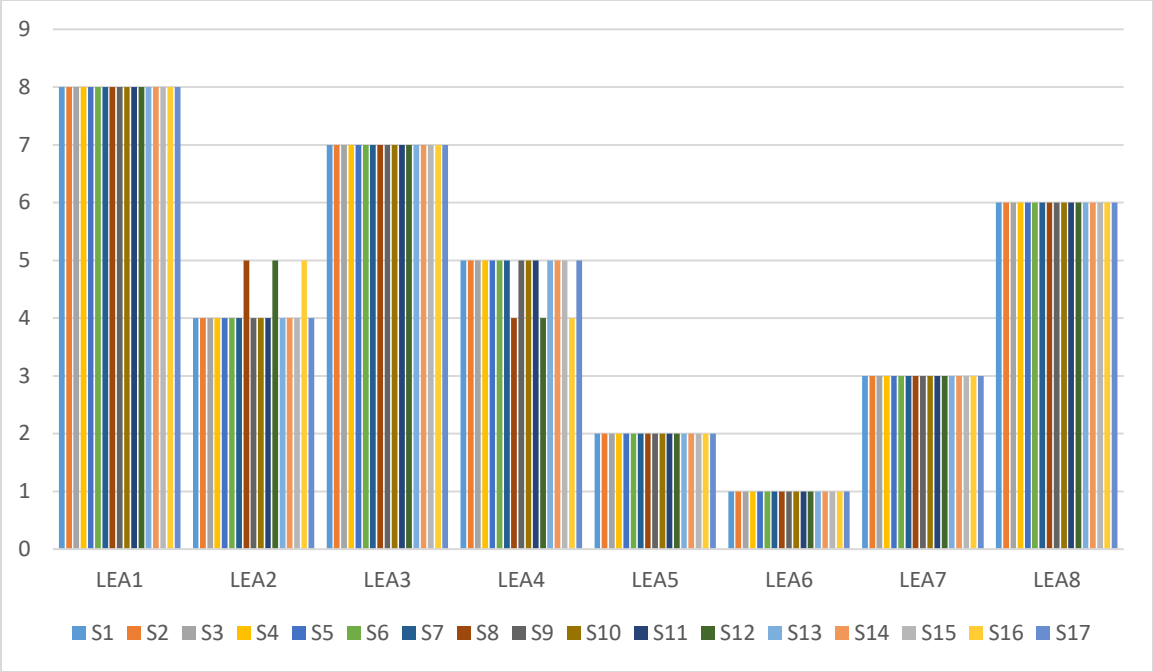

Figure 5. The rank of alternatives under different weights.

4.3 Comparative Analysis

This part shows the comparative study between our model and other models. We compared our model with TOPSIS, VIKOR, EDAS, WASPAS, and COPRAS methods. These methods are compared under the weights of this study. These methods are evaluated under single-valued neutrosophic sets. Figure 6 shows the comparative study. Figure 6 shows the comparative study. In our model, alternative one has the highest rank, followed by Alternative three, alternative eight, and alternative four. Alternative six has the lowest rank, followed by alternative five, and alternative seven. In the TOPSIS method, alternative 1 has the highest rank, followed by alternative eight, alternative three, and alternative four. Alternative six has the lowest rank, followed by Alternative four, and Alternative seven. In the VIKOR method, alternative one has the highest rank, followed by alternative three, alternative eight, and alternative four. Alternative six has the lowest rank, followed by Alternative seven, and Alternative five. In the WASPAS method, alternative one has the highest rank, followed by alternative four, alternative eight, and alternative three. Alternative six has the lowest rank, followed by Alternative five, and Alternative seven. In COPRAS, Alternative One has the highest rank, followed by Alternative Four, alternative 8, and Alternative Three. Alternative six has the lowest rank, followed by Alternative five, and Alternative seven. In the EDAS method, alternative one has the highest rank, followed by alternative two, alternative eight, and alternative four. Alternative six has the lowest rank, followed by Alternative seven, and Alternative five.

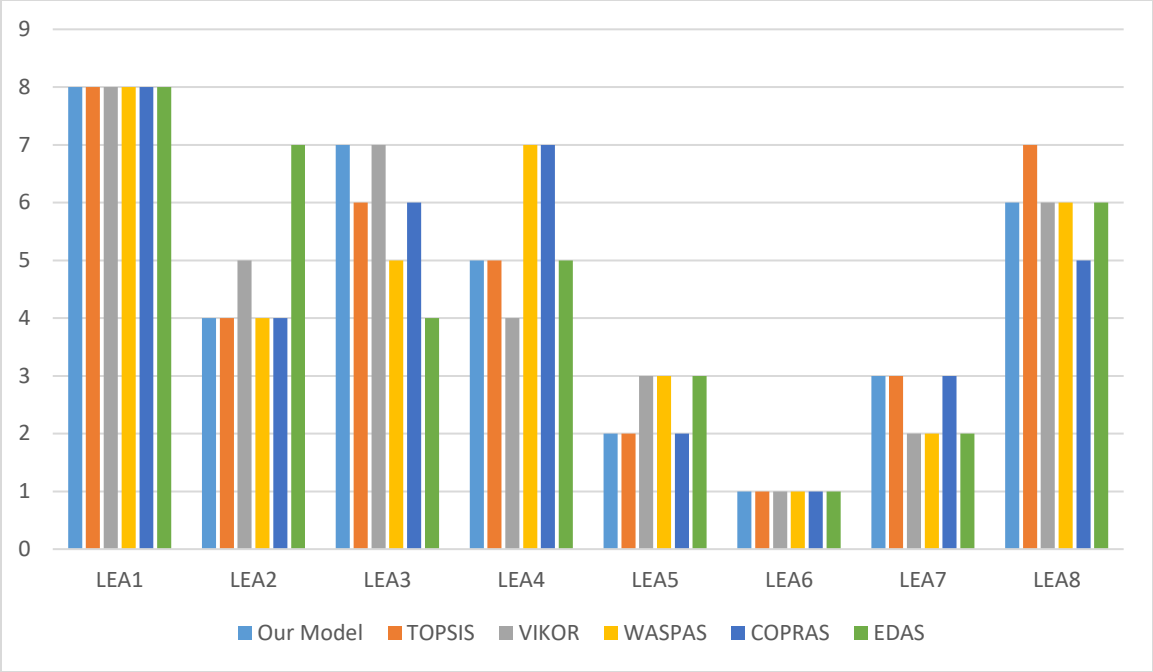

Figure 6. Comparative Study between other models.

5. Conclusions

This study introduced a new model for evaluating distributed leadership in education. To handle uncertainty in decision-making, we used a method called the neutrosophic hypersoft set. We applied a technique known as MCDM (Multi-Criteria Decision-Making) to manage different criteria and factors and used the MABAC method to rank the options. Three experts assessed sixteen criteria and eight options using descriptive terms. We then converted these assessments into single-valued neutrosophic numbers to get clear values. From this, we calculated the weights for each criterion. The results showed that criterion six was the most important, while criterion sixteen was the least important. Next, we used the MABAC method to rank the alternatives, finding that alternative one was the best and alternative six was the worst. For future research, other MCDM methods like AHP and DEMATEL could be used to determine criteria weights, and methods like VIKOR and TOPSIS could be used to rank the alternatives.

References

[1] C. A. Groenewald, E. Groenewald, F. Uy, J. M. Mugadza, A. N. Cuyos, and O. K. Kilag, "Exploring Multiculturalism and Educational Leadership: A Systematic Review of Global Perspectives," *International Multidisciplinary Journal of Research for Innovation, Sustainability, and Excellence (IMJRISE)*, vol. 1, no. 3, pp. 45–50, 2024.

[2] E. Groenewald, C. A. Groenewald, R. A. Dela Cruz, F. Uy, O. K. Kilag, and M. Villaver Jr, "Navigating Educational Leadership: Challenges, Styles, and Impacts–A Systematic Review," *International Multidisciplinary Journal of Research for Innovation, Sustainability, and Excellence (IMJRISE)*, vol. 1, no. 2, pp. 262–267, 2024.

[3] K. Leithwood, "Educational Leadership. A Review of the Research.," *Laboratory for*

Student Success (LSS), The Mid-Atlantic Regional Educational Laboratory, 2005.

[4] E. Daniëls, A. Hondeghem, and F. Dochy, "A review on leadership and leadership development in educational settings," *Educational research review*, vol. 27, pp. 110–125, 2019.

[5] A. M. Ali, A. Abdelhafeez, T. H. M. Soliman, and K. ELMenshawy, "A probabilistic hesitant fuzzy MCDM approach to selecting treatment policy for COVID-19," *Decision Making: Applications in Management and Engineering*, vol. 7, no. 1, pp. 131–144, 2024.

[6] M. M. Ismail, M. Ibrahim, A. Sleem, and M. Mohamed, "Blending Uncertainty Theory Innovative into Decision Support Framework for Selecting Agricultural Machinery Suppliers," *Optimization in Agriculture*, vol. 1, pp. 115–128, 2024.

[7] F. Smarandache, "New Types of Soft Sets" HyperSoft Set, IndetermSoft Set, IndetermHyperSoft Set, and TreeSoft Set": An Improved Version," *Neutrosophic Systems with Applications*, vol. 8, pp. 35–41, 2023.

[8] A. A. El-Douh, S. Lu, A. Abdelhafeez, and A. S. Aziz, "Assessment the Health Sustainability using Neutrosophic MCDM Methodology: Case Study COVID-19," *Sustainable Machine Intelligence Journal*, vol. 3, p. 1, 2023.

[9] A. Abdel-Monem and A. A. Gawad, "A hybrid Model Using MCDM Methods and Bipolar Neutrosophic Sets for Select Optimal Wind Turbine: Case Study in Egypt," *Neutrosophic Sets and Systems*, vol. 42, no. 1, p. 1, 2021.

[10] H. Wang, F. Smarandache, Y. Zhang, and R. Sunderraman, "Single valued neutrosophic sets," *Infinite study*, vol. 12, 2010.

[11] H.-L. Yang, C.-L. Zhang, Z.-L. Guo, Y.-L. Liu, and X. Liao, "A hybrid model of single valued neutrosophic sets and rough sets: single valued neutrosophic rough set model," *Soft Computing*, vol. 21, pp. 6253–6267, 2017.

[12] F. Smarandache, A. M. Ali, and A. Abdelhafeez, *Single Valued Neutrosophic HyperSoft Set based on VIKOR Method for 5G Architecture Selection*. Infinite Study, 2024.

[13] N. A. Nabeeh, A. Abdel-Monem, and A. Abdelmouty, "A novel methodology for assessment of hospital service according to BWM, MABAC, PROMETHEE II," *Neutrosophic Sets and Systems*, vol. 31, no. 1, pp. 63–79, 2020.

[14] D. Pamučar and G. Ćirović, "The selection of transport and handling resources in logistics centers using Multi-Attributive Border Approximation area Comparison (MABAC)," *Expert systems with applications*, vol. 42, no. 6, pp. 3016–3028, 2015.

[15] A. Alinezhad, J. Khalili, A. Alinezhad, and J. Khalili, "MABAC method," *New Methods and Applications in Multiple Attribute Decision Making (MADM)*, pp. 193–198, 2019.

[16] M. Prabhuswamy, R. Tripathi, M. Vijayakumar, T. Thulasimani, P. Sundharesalingam, and B. Sampath, "A Study on the Complex Nature of Higher Education Leadership: An Innovative Approach," in *Challenges of Globalization and Inclusivity in Academic Research*, IGI Global, 2024, pp. 202–223.

[17] A. McKay, K. MacDonald, and F. Longmuir, "The emotional intensity of educational leadership: A scoping review," *International Journal of Leadership in Education*, pp. 1–23, 2024.

[18] N. Nabeeh, "Assessment and Contrast the Sustainable Growth of Various 1 Road Transport Systems using Intelligent Neutrosophic 2 Multi-Criteria Decision-Making Model," *Sustainable Machine Intelligence Journal*, vol. 2, 2023.

[19] M. Luo, Z. Sun, and L. Wu, "Fuzzy Inference Quintuple Implication Method Based on Single Valued Neutrosophic t-representable t-norm," *Neutrosophic Optimization and Intelligent Systems*, vol. 3, pp. 8–22, 2024.

Received: January 03, 2024. **Accepted**: August 26, 2024.

Neutrosophic Sets and Systems, Vol. 72, 2024
University of New Mexico

Deneutrosophication of Neutrosophic Bézier Surface Approximation Model

Siti Nur Idara Rosli[1] and Mohammad Izat Emir Zulkifly[2,*]

[1] Faculty of Sciences, Department of Mathematics, Universiti Teknologi Malaysia (UTM), 81310 UTM Johor Bahru, Johor, Malaysia; sitinuridara99@gmail.com
[2] Faculty of Sciences, Department of Mathematics, Universiti Teknologi Malaysia (UTM), 81310 UTM Johor Bahru, Johor, Malaysia; izatemir@utm.my

* Correspondence: izatemir@utm.my

Abstract: The deneutrosophication process is a process transforming from neutrosophic values to crisp output values. It is the final step for the operations within a neutrosophic set and system. Neutrosophic set theories are a generalization of intuitionistic fuzzy and fuzzy set theories, focusing on truth, indeterminacy, and falsity memberships independently. However, it isn't easy to generate a geometrical model such as a Bézier surface by using neutrosophic set theory through the deneutrosophication process. Therefore, this paper used an average of triangular footprint method in the deneutrosophication process to construct the neutrosophic Bézier surface (NBS) models by using approximation methods. Before generating the model, the neutrosophic control net (NCN) must first be introduced using the deneutrosophication process. After that, the NCN will be blended with the Bernstein basis function to generate the NBS approximation model. Next, some numerical examples of NBS will be provided. Finally, the deneutrosophication of NBS approximation models will be visualized, and its algorithm will be shown.

Keywords: Deneutrosophication process; Bézier Surface; Approximation Method; Average of Triangular Footprints

1. Introduction

Numerous theories, such as probability theory, intuitionistic fuzzy set theory, fuzzy set theory, rough set theory, and many more, have been developed to address uncertainties. The notion of the neutrosophic set (NS), which involves an independent indeterminacy membership, was first suggested by Smarandache [1,2] in 1999. Various new set theories, such as fuzzy sets [3], intuitionistic fuzzy sets [4], and classic sets, are generalized by this function. Three different functions are utilized to quantify truth-membership (T), indeterminacy-membership (I), and false-membership (F) in an NS. These degrees operate independently of one another.

Deneutrosophication is determining actual output from neutrosophic data [5]. In 2005, Smarandache et al. [6] proposed a deneutrosophication approach utilizing synthesis and the center of gravity method. The synthesis technique described in [6] assigns an NS to FSs with different crisp values. Chakraborty et al. (2018) proposed deneutrosophication techniques for triangular neutrosophic numbers by using the removal area method and then applying it to imprecise project evaluation and route selection problems [10]. Meanwhile, in 2019, they also used the removal area method to study a deneutrosophication strategy for pentagonal neutrosophic numbers in the minimal spanning tree (MST) problem [7]. According to Azzah Awang et al. (2019), the

deneutrosophication equation used in [8] provides the neat truth grade rather than the actual event output. Said Broumi et al. (2019) discovered a deneutrosophicated value for a trapezoidal fuzzy number (TFN) utilizing a scoring function based on the TFN's center of gravity in the study [9]. However, there is another method for converting neutrosophic values to crisp output: an average of triangular footprint method introduced by Zakaria [15,16] for the fuzzification method and expanded for intuitionistic set by Zulkifly [29]. Therefore, as the targeted gap is based on the previous studies mentioned, this paper will contribute to introducing the deneutrosophication process based on neutrosophic geometric modeling and the average of the triangular footprint method.

Neutrosophic sets can be utilized to deal with challenges in curve and surface construction for computer-aided graphic designs (CAGD). This concept is required for building a smoother curve or surface model. NS and CAGD are two techniques that can be used to solve the ambiguity of control or data points. Wahab [11-13] developed a method for fuzzifying control points to create Bezier and B-spline curves. The study of fuzzy set theory with geometric modeling has been expanding in [14-19]. Besides that, some studies used the neutrosophic set theory with geometric modeling [20-25,28,30-32]. Additionally, some researchers use neutrosophic for other applications such as in decision-making for medical supplies, ranking cloud service, quantum communication, and virtual manufacturing environments by using type-2 neutrosophic set theory [33-36]. Nevertheless, no research has been done on how to visualize the modeling of neutrosophic geometry when presented with the deneutrosophication process.

The following is a summary of this work. Background information about the topic is given in the first part. A few neutrosophic set theories and their fundamental characteristics are covered in Section 2. The creation of a neutrosophic control net (NCN) via the deneutrosophication process will be covered in Section 3. The deneutrosophication process for the neutrosophic Bézier Surface (NBS) approximation is then seen and described in Section 4 using a numerical example of NCN. At the end of Section 4, an algorithm demonstrating the deneutrosophication procedure for NBS will be shown. Section 5 concludes with the discussion and conclusions.

2. Basic Properties

The fuzzy set only deals with membership, whereas the intuitionistic set deals with membership, non-membership, and uncertainty degrees and are dependent on each other. However, the NS treats the truth, indeterminacy, and falsity degrees independently [1]. An NS has three membership functions with the addition of the parameter "indeterminacy" to the NS specification [2]: a membership function, represented by the letter *T*; an indeterminacy membership function, denoted by the letter *I*; and a non-membership function, appointed by the letter *F*. This section will define neutrosophic set theory, neutrosophic relation notion, neutrosophic point, the (α,β,γ)-cut operations as the fundamentals and the triangular neutrosophic number. Therefore, the definitions are as follows.

Definition 1. [1] Let X be the universal set, with elements in X represented as x. The NS is an element in the structure as follows:

$$\hat{A} = \{\left\langle x : T_{\hat{A}(x)}, I_{\hat{A}(x)}, F_{\hat{A}(x)} \right\rangle | \ x \in X\} \tag{1}$$

where $T, I, F : X \to]^{-}0,1^{+}[$ represented as the degree of truth, indeterminacy, and falsity memberships respectively of the element $x \in X$ to the set $\hat{A}$ with the condition;

$$0^{-} \le T_{\hat{A}}(x) + I_{\hat{A}}(x) + F_{\hat{A}}(x) \le 3^{+} \tag{2}$$

There is no limit to the amount of $T_{\hat{A}}(x), I_{\hat{A}}(x)$ and $F_{\hat{A}}(x)$.

NS takes the value from real standard or non-standard subsets of $]^{-}0,1^{+}[$. But in technical applications the real value of the interval $[0,1]$ will be used since $]^{-}0,1^{+}[$ difficult to apply in real data such as scientific and engineering problems. Thus, the membership values used as follows:

$$\hat{A}=\{\left\langle x:T_{\hat{A}(x)},I_{\hat{A}(x)},F_{\hat{A}(x)}\right\rangle|\ x\in X\}\text{ and }T_{\hat{A}}(x),I_{\hat{A}}(x),F_{\hat{A}}(x)\in[0,1]$$

There is no limitation on the summation of $T_{\hat{A}}(x),I_{\hat{A}}(x)$ and $F_{\hat{A}}(x)$. But comply with the following conditions:

$$0\le T_{\hat{A}}(x)+I_{\hat{A}}(x)+F_{\hat{A}}(x)\le 3 \tag{3}$$

Definition 2. [20,21] Suppose $\hat{A}=\left\{\left\langle x:T_{\hat{A}(x)},I_{\hat{A}(x)},F_{\hat{A}(x)}\right\rangle|\ x\in\hat{A}\right\}$ and $\hat{B}=\left\{\left\langle y:T_{\hat{B}(y)},I_{\hat{B}(y)},F_{\hat{B}(y)}\right\rangle|\ y\in\hat{B}\right\}$ will be the neutrosophic elements. Thus, $R=\left\{\left\langle (x,y):T_{(x,y)},I_{(x,y)},F_{(x,y)}\right\rangle|\ x\in\hat{A},y\in\hat{B}\right\}$ is a neutrosophic relation (NR) on $\hat{A}$ and $\hat{B}$.

Definition 3 [20,21] Neutrosophic set of $\hat{A}$ in space X is neutrosophic point (NP) and $\hat{A}=\{\hat{A}_i\}$ where $i=0,...,n$ is a set of NPs where $T_{\hat{A}}:X\to[0,1]$ As a true degree, $I_{\hat{A}}:X\to[0,1]$ as indeterminacy membership and $F_{\hat{A}}:X\to[0,1]$ as false membership with

$$T_{\hat{A}}(\hat{A})=\begin{cases}0 & \text{if }\hat{A}_i\notin\hat{A}\\ a\in(0,1) & \text{if }\hat{A}_i\hat{\in}\hat{A}\\ 1 & \text{if }\hat{A}_i\in\hat{A}\end{cases}$$

$$I_{\hat{A}}(\hat{A})=\begin{cases}0 & \text{if }\hat{A}_i\notin\hat{A}\\ b\in(0,1) & \text{if }\hat{A}_i\hat{\in}\hat{A}\\ 1 & \text{if }\hat{A}_i\in\hat{A}\end{cases} \tag{4}$$

$$F_{\hat{A}}(\hat{A})=\begin{cases}0 & \text{if }\hat{A}_i\notin\hat{A}\\ c\in(0,1) & \text{if }\hat{A}_i\hat{\in}\hat{A}\\ 1 & \text{if }\hat{A}_i\in\hat{A}\end{cases}$$

Definition 4 [26] The $(\alpha,\beta,\gamma)-$cut of NS is denoted as $C_{(\alpha,\beta,\gamma)}$ where $\alpha,\beta,\gamma\in[0,1]$ and are fixed numbers, such that $0\le\alpha+\beta+\gamma\le 3$ is defined as $C_{(\alpha,\beta,\gamma)}=\begin{Bmatrix}\left\langle T_{\hat{A}}(x),I_{\hat{A}}(x),F_{\hat{A}}(x)\right\rangle:x\in X,\\ T_{\hat{A}}(x)\ge\alpha,I_{\hat{A}}(x)\le\beta,F_{\hat{A}}(x)\le\gamma\end{Bmatrix}$

Definition 5 [26] A NS $\hat{A}$ is mentioned in the whole conversation of real numbers $\square$ and it will be neutrosophic numbers if it follows the following properties:

i. $\hat{A}$ is normal if exist $x_0\in\square$ such that $T_{\hat{A}}(x_0)=1$ while $I_{\hat{A}}(x_0)=F_{\hat{A}}(x_0)=0$.

ii. $\hat{A}$ is convex set for truth function $T_{\hat{A}}(x)$ where $T_A(\mu x_1+(1-\mu)x_2)\ge\min(T_{\hat{A}}(x_1),T_{\hat{A}}(x_2))$, $\forall x_1,x_2\in\square,\mu\in[0,1]$.

iii. $\hat{A}$ is concave set for indeterminacy $I_{\hat{A}}(x)$ and false function $F_{\hat{A}}(x)$ where $I_{\hat{A}}(\mu x_1+(1-\mu)x_2)\ge\max(I_{\hat{A}}(x_1),I_{\hat{A}}(x_2))$, $\forall x_1,x_2\in\square,\mu\in[0,1]$ and $F_{\hat{A}}(\mu x_1+(1-\mu)x_2)\ge\max(F_{\hat{A}}(x_1),F_{\hat{A}}(x_2))$, $\forall x_1,x_2\in\square,\mu\in[0,1]$.

Definition 6 [10] Suppose $w_{\hat{A}}, u_{\hat{A}}, y_{\hat{A}} \in [0,1]$. A triangular neutrosophic number for $\hat{A} = \langle (a_1, b_1, c_1); w_{\hat{A}}, u_{\hat{A}}, y_{\hat{A}} \rangle$ is a special NS on the real number set, since there are three memberships which are truth, indeterminacy, and falsity membership functions, the following functions are defined:

$$T_{\hat{A}}(x) = \begin{cases} \dfrac{(x-a)w_{\hat{A}}}{(b-a)w_{\hat{A}}} & (a \le x \le b) \\ w_{\hat{A}} & (x = b_1) \\ \dfrac{(c-x)w_{\hat{A}}}{(c-b)} & (b \le x \le c) \\ 0 & \textit{otherwise} \end{cases}$$

$$I_{\hat{A}}(x) = \begin{cases} \dfrac{(b-x+u_{\hat{A}}(x-a))}{(b-a)} & (a \le x \le b) \\ \mathrm{u}_{\hat{A}} & (x = b) \\ \dfrac{(x-b+u_{\hat{A}}(c-x))}{(c-b)} & (b \le x \le c) \\ 1 & \textit{otherwise} \end{cases} \tag{5}$$

$$F_{\hat{A}}(x) = \begin{cases} \dfrac{(b-x+y_{\hat{A}}(x-a))}{(b-a)} & (a \le x \le b) \\ \mathrm{y}_{\hat{A}} & (x = b) \\ \dfrac{(x-b+y_{\hat{A}}(c-x))}{(c-b)} & (b \le x \le c) \\ 1 & \textit{otherwise} \end{cases}$$

Definition 6 can be visualized as in Figure 1. Figure 1 shows the triangular neutrosophic number for a set $\hat{A} = \langle (a_1, b_1, c_1); w_{\hat{A}}, u_{\hat{A}}, y_{\hat{A}} \rangle$ where $T_{\hat{A}}, I_{\hat{A}}, F_{\hat{A}} \in [0,1]$ represented as truth, indeterminacy, and falsity membership.

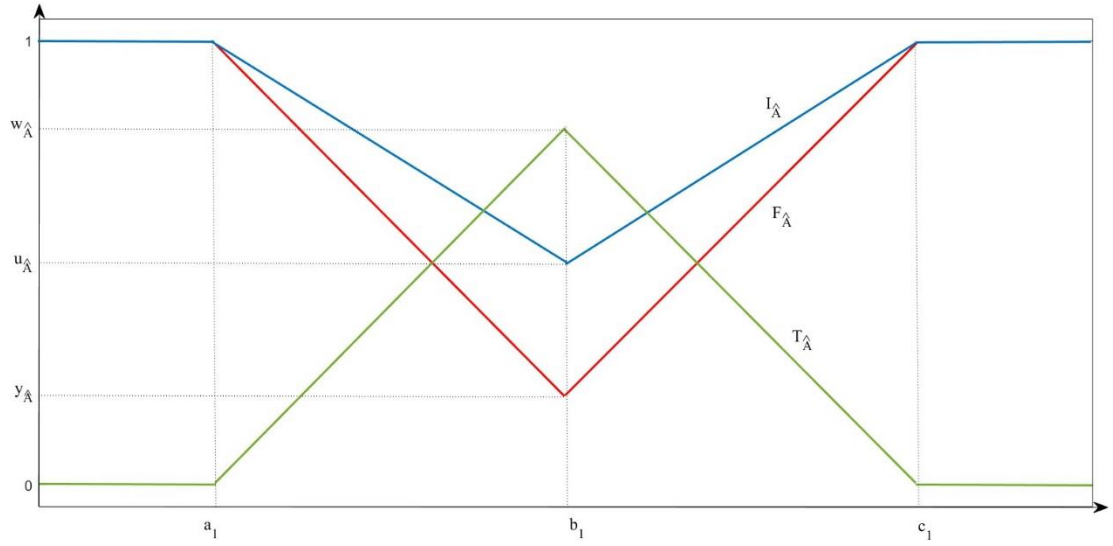

Figure 1 Triangular neutrosophic numbers for a set $\hat{A}=\langle(a,b,c);w_{\hat{A}},u_{\hat{A}},y_{\hat{A}}\rangle$

3. Deneutrosophication of Neutrosophic Control Net (NCN)

This section discussed the neutrosophic point relation (NPR), as well as the deneutrosophication of neutrosophic control net (NCN) for each $\langle\alpha,\beta,\gamma\rangle-$cut are introduced by using the average of triangular footprint method by [15,16,29]. NPR is built on the concept of NR as in Definition 2 and NP as in Definition 3, which was addressed in the previous section. If P,Q is a collection of Euclidean universal space points and $P,Q\in\mathbf{R}^2$ then NPR is defined as follows:

Definition 7 [22] Let X,Y collection of universal space points with a non-empty set and $P,Q,I\in\mathbf{R}\times\mathbf{R}\times\mathbf{R}$, then NPR is defined as

$$\hat{R}=\left\{\left\langle\left(p_i,q_j\right),T_R(p_i,q_j),I_R(p_i,q_j),F_R(p_i,q_j)\right\rangle\middle|T_R(p_i,q_j),I_R(p_i,q_j),F_R(p_i,q_j)\in I\right\} \tag{6}$$

where $\left(p_i,q_j\right)$ is an ordered pair of coordinates and $\left(p_i,q_j\right)\in P\times Q$ while $T_R(p_i,q_j),I_R(p_i,q_j),F_R(p_i,q_j)$ are the truth membership, indeterminacy membership, and false membership that follow the condition of the neutrosophic set which is $0\le T_{\hat{A}}(x)+I_{\hat{A}}(x)+F_{\hat{A}}(x)\le 3$.

The control point is crucial in the design, control, and manufacture of smooth curves [22]. The NCP is defined in this part by first applying the notion of fuzzy control point from Wahab et al. [12] in the following:

Definition 8 [22] Let $\hat{R}$ be an NPR, then $\hat{P}_i^T$, $\hat{P}_i^I$ and $\hat{P}_i^F$ denoted as NCPs for membership truth, indeterminacy where $i=1,...,n+1$ and the position vector of $n+1$ as control polygon vertices.

$$\begin{aligned}\hat{P}_i^T&=\left\{\hat{p}_1^T,\hat{p}_2^T,...,\hat{p}_{n+1}^T\right\}\\ \hat{P}_i^I&=\left\{\hat{p}_1^I,\hat{p}_2^I,...,\hat{p}_{n+1}^I\right\}\\ \hat{P}_i^F&=\left\{\hat{p}_1^F,\hat{p}_2^F,...,\hat{p}_{n+1}^F\right\}\end{aligned} \tag{7}$$

This study is primarily focused on surface modeling. Thus, it is crucial to introduce the concept of a neutrosophic control net. In surface modeling, the control net is obtained by combining the relations of each control point [27]. In contrast, the curve model only requires control points [27]. Thus, the neutrosophic control net (NCN) can be described as follows.

Definition 9 [25,23,28] Let $\hat{P}_i^T$, $\hat{P}_i^I$ and $\hat{P}_i^F$ as NCPs for each membership, and $\hat{P}_{i,j}^{T,I,F}$ represents as NCN for truth, indeterminacy, and falsity memberships where $i=1,...,n+1$ and $j=1,...,m+1$ and the position vector of $n+1$ and $m+1$ as control polygon vertices.

$$\hat{P}_{i,j}^{T}=\begin{bmatrix}\hat{P}_{1,1}^{T} & \hat{P}_{1,2}^{T} & \cdots & \hat{P}_{1,m+1}^{T}\\ \hat{P}_{2,1}^{T} & \hat{P}_{2,2}^{T} & \cdots & \hat{P}_{2,m+1}^{T}\\ \vdots & \vdots & \ddots & \vdots\\ \hat{P}_{n+1,1}^{T} & \hat{P}_{n+1,2}^{T} & \cdots & \hat{P}_{n+1,m+1}^{T}\end{bmatrix}$$

$$\hat{P}_{i,j}^{I}=\begin{bmatrix}\hat{P}_{1,1}^{I} & \hat{P}_{1,2}^{I} & \cdots & \hat{P}_{1,m+1}^{I}\\ \hat{P}_{2,1}^{I} & \hat{P}_{2,2}^{I} & \cdots & \hat{P}_{2,m+1}^{I}\\ \vdots & \vdots & \ddots & \vdots\\ \hat{P}_{n+1,1}^{I} & \hat{P}_{n+1,2}^{I} & \cdots & \hat{P}_{n+1,m+1}^{I}\end{bmatrix} \tag{8}$$

$$\hat{P}_{i,j}^{F}=\begin{bmatrix}\hat{P}_{1,1}^{F} & \hat{P}_{1,2}^{F} & \cdots & \hat{P}_{1,m+1}^{F}\\ \hat{P}_{2,1}^{F} & \hat{P}_{2,2}^{F} & \cdots & \hat{P}_{2,m+1}^{F}\\ \vdots & \vdots & \ddots & \vdots\\ \hat{P}_{n+1,1}^{F} & \hat{P}_{n+1,2}^{F} & \cdots & \hat{P}_{n+1,m+1}^{F}\end{bmatrix}$$

As mentioned in the introduction part, deneutrosophication is the process of determining actual output from neutrosophic data [5]. Therefore, $\hat{P}_{i,j}^{T,I,F}$ denoted as the neutrosophic value will transform to crisp output represented as $P_{i,j}^{T,I,F}$ for their respective memberships. Thus, Definition 10 describes the deneutrosophication process for each $\langle\alpha,\beta,\gamma\rangle-$cut in triangular forms. NCNs are deneutrosophicated based on $\langle\alpha,\beta,\gamma\rangle$ values when $\alpha,\beta,\gamma\in(0,1]$. Figure 2 and Definition 10 show the deneutrosophication of NCNs by using an average triangular footprint method. The average triangular footprint method is a division process that uses the footprint of left, mean, and right values of a triangular control point [29]. Therefore, the deneutrosophication of NCN is as follows:

Definition 10 Let $\hat{P}_{i,j}^{T,I,F}$ be the set of NCNs where $i=1,...,n+1$ and $j=1,...,m+1$. Then, ${}^{\alpha}P_{i,j}^{T}$ is $\alpha-$cut values for crisp truth membership, ${}^{\beta}P_{i,j}^{I}$ is $\beta-$cut values for crisp indeterminacy membership, and ${}^{\gamma}\hat{P}_{i,j}^{F}$ is the $\gamma-$cut values for crisp falsity membership, where $\alpha,\beta,\gamma\in(0,1]$ and the deneutrosophication of NCNs as follows:

$$\begin{aligned}{}^{\alpha}P_{i,j}^{T}&=\frac{1}{3}\sum_{i=1}^{n+1}\sum_{j=1}^{m+1}\left\langle {}^{\alpha}\hat{P}_{i,j}^{T(L)},{}^{\alpha}\hat{P}_{i,j}^{T(M)},{}^{\alpha}\hat{P}_{i,j}^{T(R)}\right\rangle\\ {}^{\beta}P_{i,j}^{I}&=\frac{1}{3}\sum_{i=1}^{n+1}\sum_{j=1}^{m+1}\left\langle {}^{\beta}\hat{P}_{i,j}^{I(L)},{}^{\beta}\hat{P}_{i,j}^{I(M)},{}^{\beta}\hat{P}_{i,j}^{I(R)}\right\rangle\\ {}^{\gamma}P_{i,j}^{F}&=\frac{1}{3}\sum_{i=1}^{n+1}\sum_{j=1}^{m+1}\left\langle {}^{\gamma}\hat{P}_{i,j}^{F(L)},{}^{\gamma}\hat{P}_{i,j}^{F(M)},{}^{\gamma}\hat{P}_{i,j}^{F(R)}\right\rangle\end{aligned} \tag{9}$$

where $\left\langle {}^{\alpha}\hat{P}_{i,j}^{T(L)}, {}^{\alpha}\hat{P}_{i,j}^{T(M)}, {}^{\alpha}\hat{P}_{i,j}^{T(R)} \right\rangle$ denoted as left, mean, and right NCN for truth membership at any α values, $\left\langle {}^{\beta}\hat{P}_{i,j}^{I(L)}, {}^{\beta}\hat{P}_{i,j}^{I(M)}, {}^{\beta}\hat{P}_{i,j}^{I(R)} \right\rangle$ denoted as left, mean, and right NCN for indeterminacy membership at any β values and $\left\langle {}^{\gamma}\hat{P}_{i,j}^{F(L)}, {}^{\gamma}\hat{P}_{i,j}^{F(M)}, {}^{\gamma}\hat{P}_{i,j}^{F(R)} \right\rangle$ denoted as left, mean, and right NCN for falsity membership at any γ values.

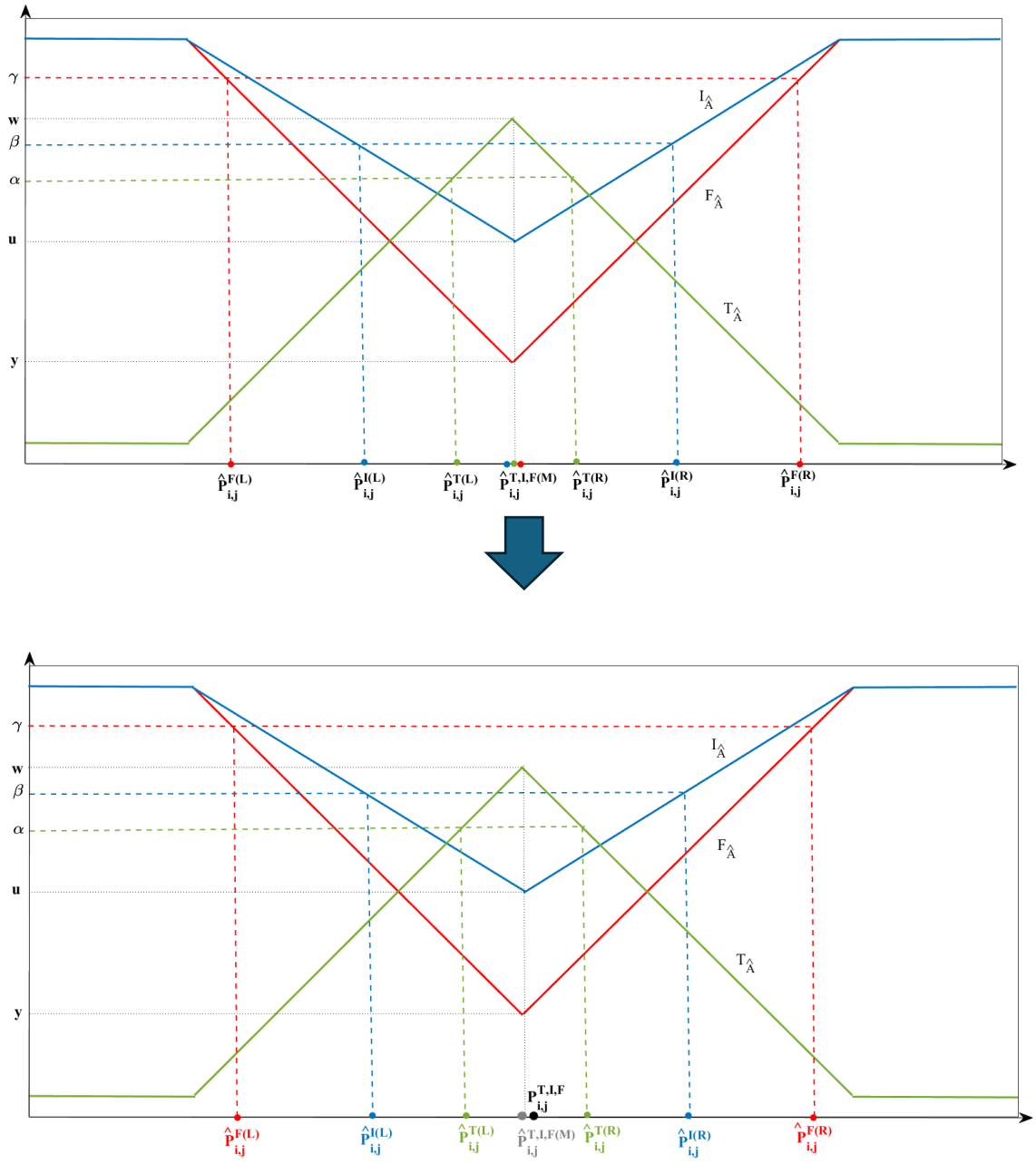

Figure 2. Deneutrosophication of neutrosophic control nets (NCNs)

4. Deneutrosophication of Neutrosophic Bézier Surface (NBS) Approximation Model

Before proceeding with the deneutrosophication of the neutrosophic Bézier surface (NBS) approximation model, the mathematical representation of the NBS approximation model was introduced in [25]. After that, the deneutrosophication process of NBS approximation for each

$\langle \alpha, \beta, \gamma \rangle -$ cut is discussed. By using the NCNs in Definition 9, the definition of NBS approximation is as follows:

Definition 11 [25] Let $\hat{P}_{i,j}^{T,I,F}$ be the set of NCNs where $i = 1,...,n+1$ and $j = 1,...,m+1$. Then, the NBS denoted as $BS(u,v)^T$ for truth membership, $BS(u,v)^I$ for indeterminacy membership and $BS(u,v)^F$ for falsity membership in the direction u and v. Cartesian Bézier surface is given by

$$\begin{aligned} BS(u,v)^T &= \sum_{i=1}^{n+1}\sum_{j=1}^{m+1} \hat{P}_{i,j}{}^T J_i^n(u) K_j^m(v) \\ BS(u,v)^I &= \sum_{i=1}^{n+1}\sum_{j=1}^{m+1} \hat{P}_{i,j}{}^I J_i^n(u) K_j^m(v) \\ BS(u,v)^F &= \sum_{i=1}^{n+1}\sum_{j=1}^{m+1} \hat{P}_{i,j}{}^F J_i^n(u) K_j^m(v) \end{aligned} \tag{10}$$

where $J_i^n(u)$ and $K_j^m(v)$ respectively are Bernstein basis functions that can be written as follows:

$$\begin{aligned} J_{(n,i)}(u) &= \binom{n}{i} u^i (1-u)^{n-i} \qquad (0)^0 \equiv 1 \\ K_{(m,j)}(v) &= \binom{m}{j} v^j (1-v)^{m-j} \qquad (0)^0 \equiv 1 \end{aligned} \tag{11}$$

$$\begin{aligned} \binom{n}{i} &= \frac{n!}{i!(n-1)!} \qquad (0)^0 \equiv 1 \\ \binom{m}{j} &= \frac{n!}{j!(m-1)!} \qquad (0)^0 \equiv 1 \end{aligned} \tag{12}$$

After that, the $\langle \alpha, \beta, \gamma \rangle -$ cut of NCNs from Definition, 10 was deneutrosophicated and blended with Equations 11 and 12 to form a deneutrosophication of the NBS approximation model. Therefore, the following is the mathematical representation of the NBS approximation model's deneutrosophication using the average of triangular footprint method:

Definition 12 Let $\hat{P}_{i,j}^{T,I,F}$ be the set of NCNs where $i = 1,...,n+1$ and $j = 1,...,m+1$. The deneutrosophication of NB-sS for truth, indeterminacy, and falsity denoted by $BS(u,v)^{T,I,F}$ and defined as follows:

$$BS(u,v)^{T,I,F} = \frac{1}{3}\sum_{i=1}^{n+1}\sum_{j=1}^{m+1} \hat{P}_{i,j}{}^{T,I,F} J_i^n(u) K_j^m(v) \tag{13}$$

For each $\langle \alpha, \beta, \gamma \rangle -$ cut can be written as:

$$\begin{aligned} {}^{\alpha}BS(u,v)^T &= \frac{1}{3}\sum_{i=1}^{n+1}\sum_{j=1}^{m+1} {}^{\alpha}P_{i,j}{}^T J_i^n(u) K_j^m(v) \\ {}^{\beta}BS(u,v)^I &= \frac{1}{3}\sum_{i=1}^{n+1}\sum_{j=1}^{m+1} {}^{\beta}P_{i,j}{}^I J_i^n(u) K_j^m(v) \\ {}^{\gamma}BS(u,v)^F &= \frac{1}{3}\sum_{i=1}^{n+1}\sum_{j=1}^{m+1} {}^{\gamma}P_{i,j}{}^F J_i^n(u) K_j^m(v) \end{aligned} \tag{14}$$

where ${}^{\alpha}P_{i,j}^{T}$ is $\alpha-\text{cut}$ values for crisp truth membership, ${}^{\beta}P_{i,j}^{I}$ is $\beta-\text{cut}$ values for crisp indeterminacy membership, and ${}^{\gamma}P_{i,j}^{F}$ is the $\gamma-\text{cut}$ values for crisp falsity membership with $\alpha,\beta,\gamma\in(0,1]$.

The deneutrosophication process of NBCs was constructed by $(\alpha,\beta,\gamma)-\text{cut}$ operations for left and right NCNs which the (α,β,γ) values are $\alpha=0.4,0.6,0.6,0.7,0.9,0.8,0.8,0.4,0.6,0.7,0.5,0.7$, $\beta=0.2,0.3,0.5,0.3,0.1,0.3,0.1,0.3,0.2,0.2,0.5,0.2$ and $\gamma=0.7,0.4,0.2,0.3,0.3,0.2,0.4,0.6,0.5,0.4,0.3,0.4$ where $\alpha_i,\beta_i,\gamma_i\in(0,1]$. The illustration for the selected (α,β,γ) values are presented in Figure 4-6 with their respective memberships. According to Definition 9, Table 2 displays the values of $\langle P_{i,j}^{T},P_{i,j}^{I},P_{i,j}^{F}\rangle$ after the deneutrosophication process. In this study, deneutrosophication for *x* and *y* data is considered.

Table 2. Left and right neutrosophic control points (NCPs) with their respective membership

Neutrosophic values, $\hat{P}_{i,j}$	**Triangular Neutrosophic Number,** $\langle\hat{P}_{i,j}^{(L)},\hat{P}_{i,j}^{(M)}\hat{P}_{i,j}^{(R)}\rangle$		**Deneutrosophication Process**				
	***x*- data**	***y*- data**	$\alpha-\text{cut}$	$\beta-\text{cut}$	$\gamma-\text{cut}$	$\langle P_{i,j}^{T},P_{i,j}^{I},P_{i,j}^{F}\rangle$	
						x	***y***
$\hat{P}_{1,1}=(-16,16)$	$\langle-12,-16,-20\rangle$	$\langle12,16,20\rangle$	$\alpha_1=0.4$	$\beta_1=0.2$	$\gamma_1=0.7$	-16	16
$\hat{P}_{1,2}=(-6,16)$	$\langle-2,-6,-10\rangle$	$\langle12,16,20\rangle$	$\alpha_2=0.6$	$\beta_3=0.3$	$\gamma_2=0.4$	-6	16
$\hat{P}_{1,3}=(6,16)$	$\langle2,6,10\rangle$	$\langle12,16,20\rangle$	$\alpha_3=0.6$	$\beta_3=0.5$	$\gamma_3=0.2$	6	16
$\hat{P}_{1,4}=(16,16)$	$\langle12,16,20\rangle$	$\langle12,16,20\rangle$	$\alpha_4=0.7$	$\beta_4=0.3$	$\gamma_4=0.3$	16	16
$\hat{P}_{2,1}=(-16,6)$	$\langle-12,-16,-20\rangle$	$\langle2,6,10\rangle$	$\alpha_5=0.9$	$\beta_5=0.1$	$\gamma_5=0.3$	-16	6
$\hat{P}_{2,2}=(-6,6)$	$\langle-2,-6,-10\rangle$	$\langle2,6,10\rangle$	$\alpha_6=0.8$	$\beta_6=0.3$	$\gamma_6=0.2$	-6	6
$\hat{P}_{2,3}=(6,6)$	$\langle2,6,10\rangle$	$\langle2,6,10\rangle$	$\alpha_7=0.8$	$\beta_7=0.1$	$\gamma_7=0.4$	6	6
$\hat{P}_{2,4}=(16,6)$	$\langle12,16,20\rangle$	$\langle2,6,10\rangle$	$\alpha_8=0.4$	$\beta_8=0.3$	$\gamma_8=0.6$	16	6
$\hat{P}_{3,1}=(-16,-16)$	$\langle-12,-16,-20\rangle$	$\langle-12,-16,-20\rangle$	$\alpha_9=0.6$	$\beta_9=0.2$	$\gamma_9=0.5$	-16	-16
$\hat{P}_{3,2}=(-6,-16)$	$\langle-2,-6,-10\rangle$	$\langle-12,-16,-20\rangle$	$\alpha_{10}=0.7$	$\beta_{10}=0.2$	$\gamma_{10}=0.4$	-6	-16
$\hat{P}_{3,3}=(6,-16)$	$\langle2,6,10\rangle$	$\langle-12,-16,-20\rangle$	$\alpha_{11}=0.5$	$\beta_{11}=0.5$	$\gamma_{11}=0.3$	6	-16
$\hat{P}_{3,4}=(16,-16)$	$\langle12,16,20\rangle$	$\langle-12,-16,-20\rangle$	$\alpha_{12}=0.7$	$\beta_{12}=0.2$	$\gamma_{12}=0.4$	16	-16

According to Definition 5, the numerical examples in Table 1 meet the neutrosophic number requirements. Next, using Definition 6, the triangular neutrosophic number, labeled as $\langle\hat{P}_{i}^{(L)},\hat{P}_{i}^{(M)}\hat{P}_{i}^{(R)}\rangle$, was shown in Table 2. For example, $\hat{P}_{1,1}^{T}=(-16,16)$ as an NCP after going through the triangular neutrosophic number will get $\langle-12,-16,-20\rangle$. Then, by using Definition 10 and Equation 9 which is the deneutrosophication process for $\alpha=0.4$, it will transform into a crisp value, $(-16,16)$.

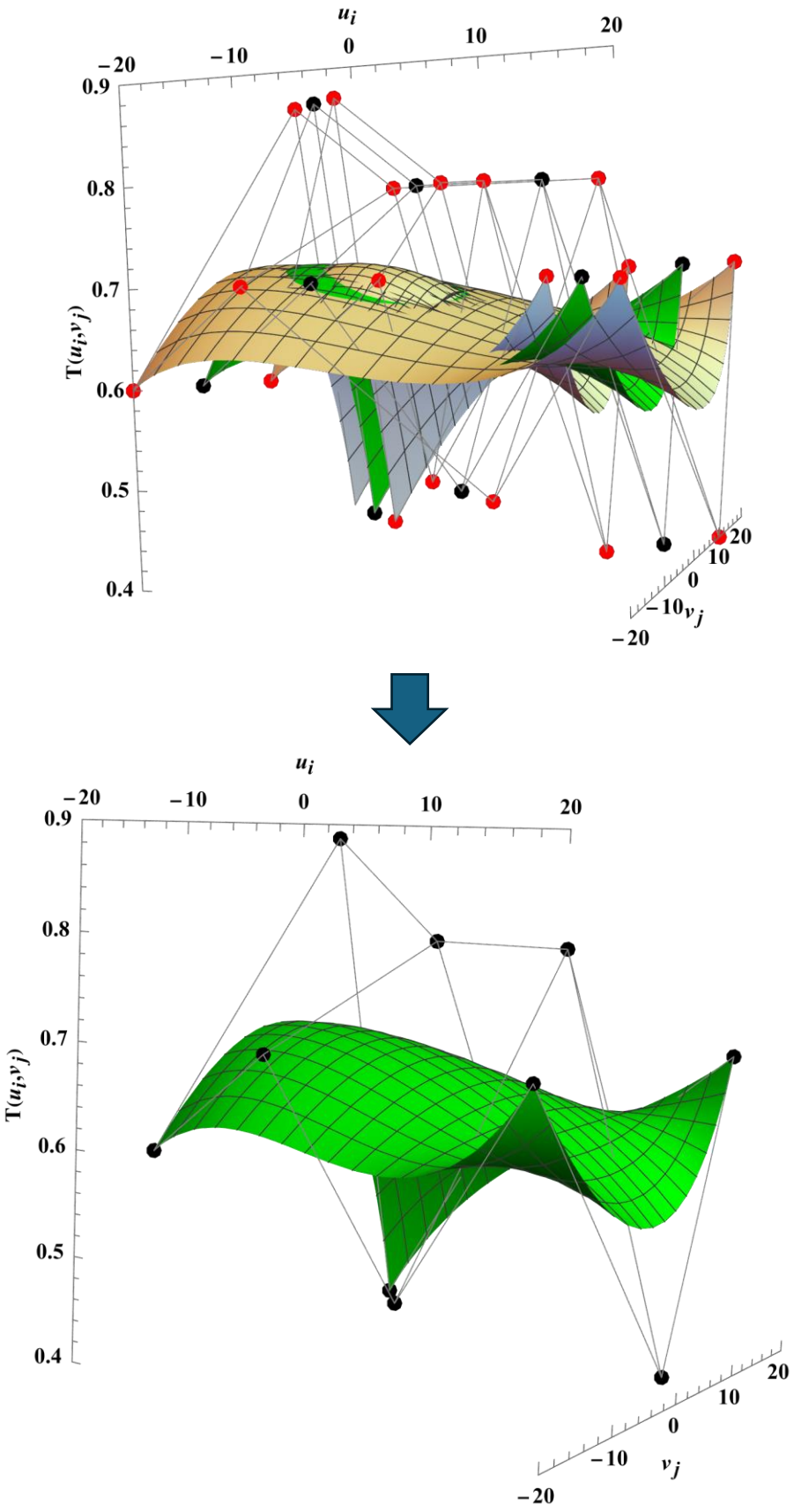

Figure 4. Deneutrosophication of NBSs approximation for truth membership with their respective alpha values

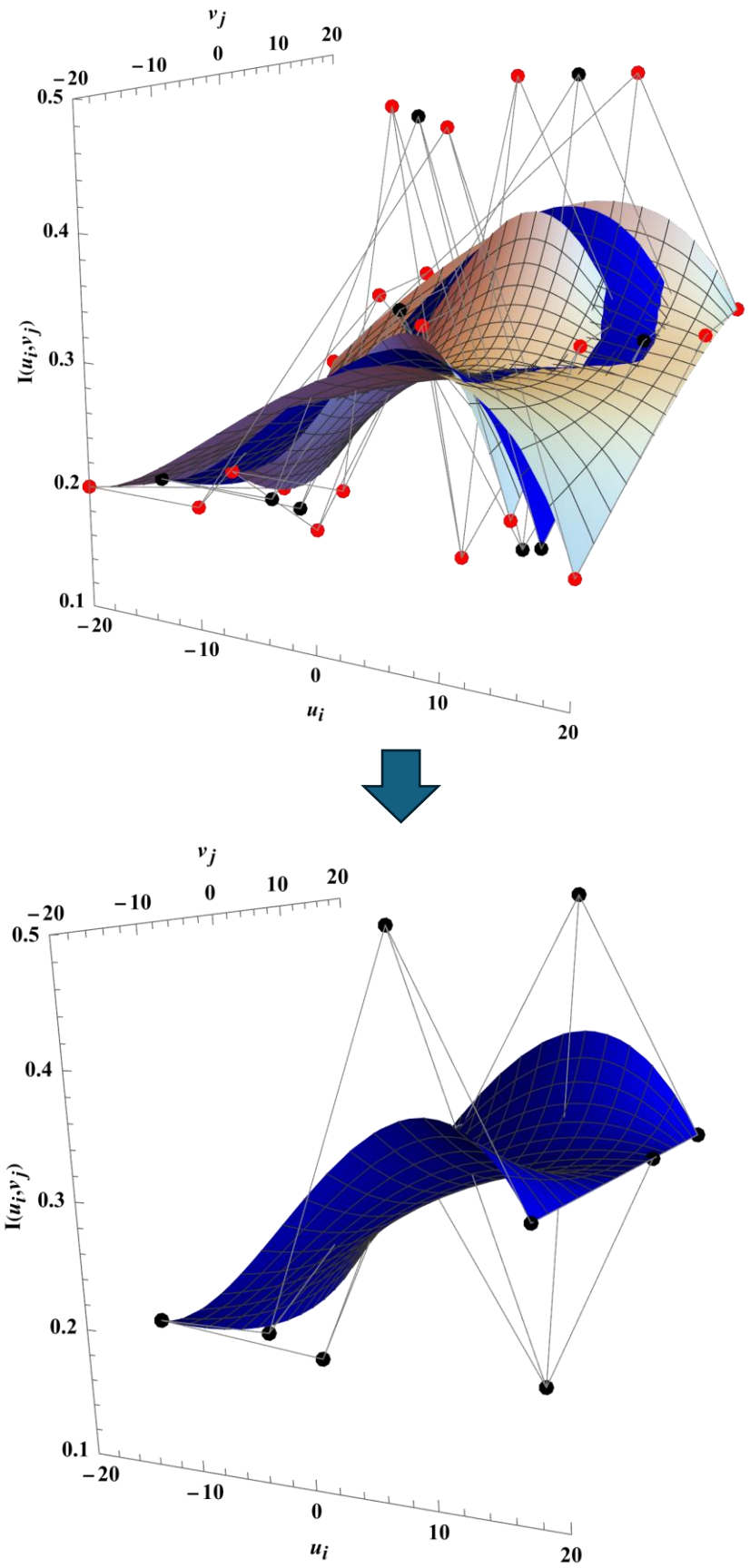

Figure 5. Deneutrosophication of NBSs approximation for indeterminacy membership with their respective betta values

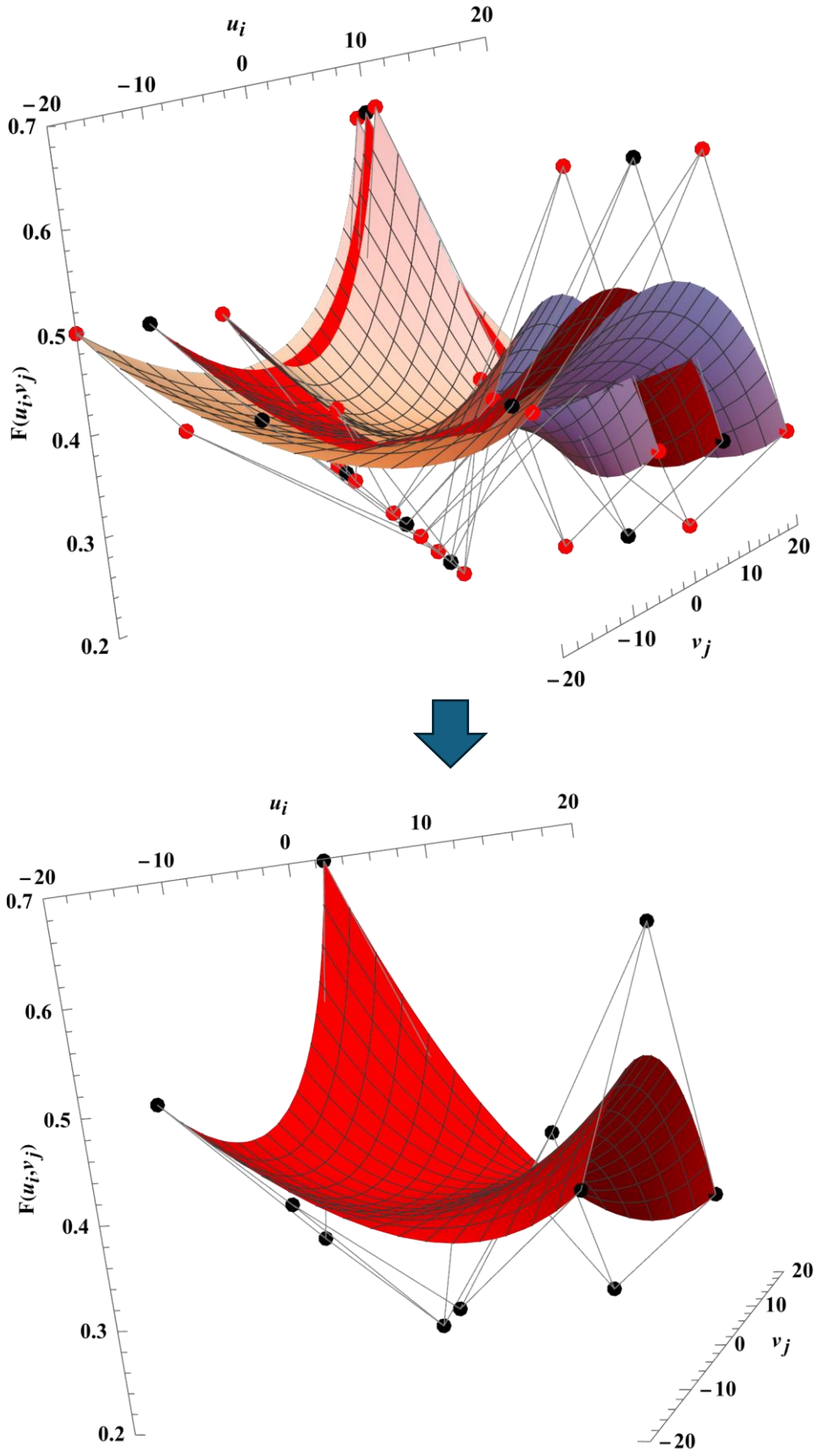

Figure 6. Deneutrosophication of NBSs approximation for falsity membership with their respective gamma values

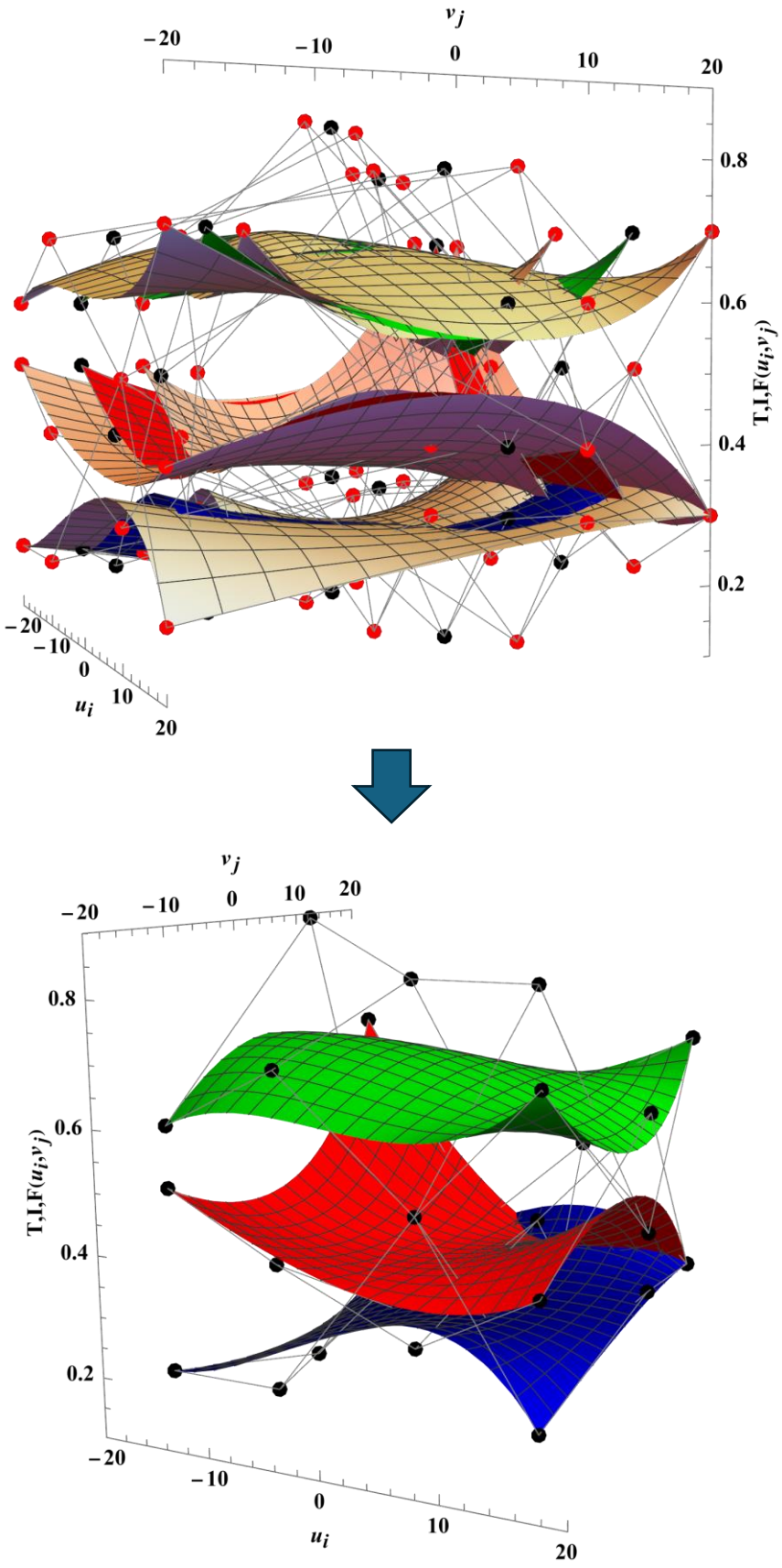

Figure 7. Deneutrosophication of NBSs approximation with their respective memberships and $\langle \alpha, \beta, \gamma \rangle$ values

Finally, Figure 7 shows the distinct surfaces between truth, indeterminacy, and falsity memberships for visualization of deneutrosophication of NBSs approximation for selected $\langle \alpha, \beta, \gamma \rangle$ values. In the figure, the green surface is denoted as NBSs for truth membership, the blue surface is denoted as NBSs for indeterminacy membership, and the red surface is denoted as NBSs for falsity membership. At the end of this section, an algorithm to generate the deneutrosophication of NBSs, the algorithm as shown in Figure 8 is demonstrated.

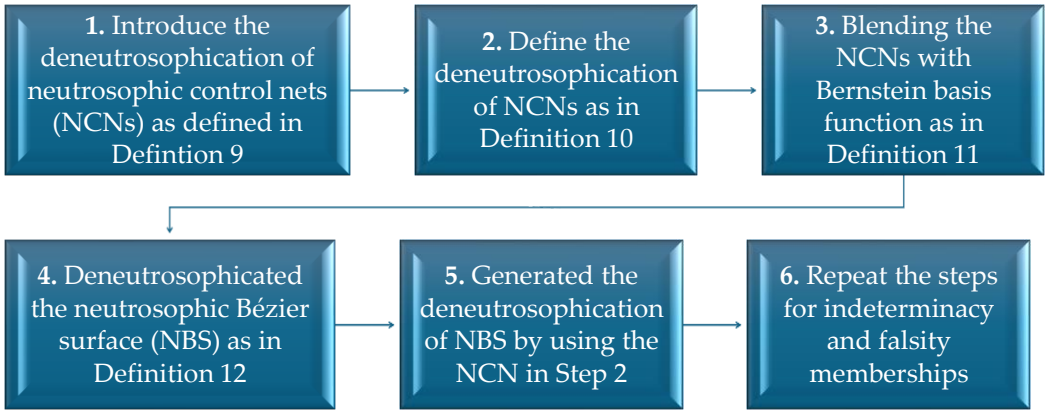

Figure 8. An algorithm to generate the deneutrosophication of neutrosophic Bézier surface approximation models.

6. Discussion and Conclusion

This work has introduced the deneutrosophication of neutrosophic Bézier surface (NBS) approximation model for truth, indeterminacy, and falsity memberships by using an average of triangular footprints. The operation of $\langle \alpha, \beta, \gamma \rangle$-cut can be utilized to describe the degree of truth membership, indeterminacy, and falsity based on the neutrosophic values. The advantages of utilizing this method include the ability to define the crisp values for each $\langle \alpha, \beta, \gamma \rangle$ values on the left and right NCNs of the NBS. As a proposition, this process will come out with a crisp output value from a range based on the neutrosophic feature numbers or the triangular neutrosophic values.

Future researchers can use other surface basis functions, such as the non-uniform rational B-splines (NURBS) geometric model, which could be used to simulate neutrosophic surfaces in the future. Furthermore, this research may be expanded to represent another model such as the B-spline model.

The deneutrosophication of NBS can be utilized in 3D surface modeling to build road surface boundaries, closed boundaries of map perimeter modeling, and calculate the area region based on $\langle \alpha, \beta, \gamma \rangle$ level values. This approach can also be used in engineering applications with uncertain collective data to remodel an entity based on its original uncertainty.

Acknowledgments: The first author would like to thank the University of Technology Malaysia (UTM), my supervisor for their assistance, and the MybrainSc 2023 scholarship and UTMFR 2024 grant for their funding in completing this research.

Conflicts of Interest: The authors declare no conflict of interest.

References

1. Smarandache, F. 1998. A Unifying Field in Logics. Neutrosophy: Neutrosophic Probability, Set and Logic, American Research Press, Rehoboth, United States.

2. Smarandache, F. 2005. Neutrosophic Set - A Generalization of the Intuitionistic Fuzzy Sets. International Journal of Pure and Applied Mathematics. 24(3): 287-297. DOI: https://dx.doi.org/10.2139/ssrn.2721587
3. Zadeh, L.A. 1965. Fuzzy Sets. Information and Control. 8(3): 338-353. DOI: doi:10.2307/2272014
4. Atanassov, K.T. 1986. Intuitionistic Fuzzy Sets. Fuzzy Sets Syst. 20(1): 87-96. DOI: https://doi.org/10.1016/S0165-0114(86)80034-3
5. Mandal, K. 2020. On Deneutrosophication. Neutrosophic Sets and Systems. 38: 409-422. DOI: 10.5281/zenodo.4300555.
6. Wang, Smarandache, Zhang, and Sunderraman. 2008. Interval neutrosophic sets and logic Interval Neutrosophic Set sand Logic: Theory and Applications in Computing. Phoenix, Arizona: Hexis.
7. Chakraborty, A., Mondal, S. and Broumi, S. 2019. De-Neutrosophication Technique of Pentagonal Neutrosophic Number and Application in Minimal Spanning Tree. Neutrosophic Sets and Systems. 29: 1-17.
8. Awang, A., Aizam, N.A.H and Abdullah, L. 2019. An Integrated Decision-Making Method Based on Neutrosophic Numbers for Investigating Factors of Coastal Erosion. Symmetry. 11: 328.
9. Broumi, S., Nagarajan, D., Bakali, A., Talea, M., Smarandache, F. and Lathamaheswari, M. 2019. The shortest path problem in the interval-valued trapezoidal and triangular neutrosophic environment. Complex and Intelligent Systems. 5: 391-402.
10. Chakraborty, A., Mondal, S., Ahmadian, A., Senu, N., Alam, S., & Salahshour, S. 2018. Different Forms of Triangular Neutrosophic Numbers, De-Neutrosophication Techniques, and their Applications. Symmetry. 10: 327. 10.3390/sym10080327.
11. Wahab, A. F., Ali, J. M., Majid, A. A. and M Tap, A. O. 2004. Fuzzy Set in Geometric Modeling, Proceedings International Conference on Computer Graphics, Imaging and Visualization, CGIV, Penang. 227–232.
12. Wahab, A. F., Ali, J. M. and Majid, A. A. 2009. Fuzzy geometric modeling. Sixth International Conference on Computer Graphics, Imaging and Visualization. 276-280.
13. Wahab, A. F., Ali, J. M., Majid, A. A. and Tap, A. O. M. 2010. Penyelesaian Masalah Data Ketakpastian Menggunakan Splin-B Kabur, Sains Malaysiana. 39(4): 661-670.
14. Zakaria, R., Wahab, A. F. and Jamaludin Md Ali, J. M. 2010. Offline handwritten signature verification using Alpha Cut of Triangular Fuzzy Number (TFN). Malaysian Journal of Fundamental and Applied Sciences. 6(2):148-153. DOI: http://dx.doi.org/10.11113/mjfas.v6n2.199
15. Zakaria, R., Wahab, A. F. and Gobithaasan. 2014. Normal Type-2 Fuzzy Interpolating B-Spline Curve. Proceedings of the 21st National Symposium on Mathematical Sciences (SKSM21), 1605: 476-481. DOI: 10.1063/1.4887635
16. Zakaria, Rozaimi & Wahab, Abd & Gobithaasan, R.U. (2013). Perfectly normal type-2 fuzzy interpolation B-spline curve. Applied Mathematical Sciences. 7. DOI: 10.12988/ams.2013.13095.
17. Blaga, P. and Bede, B. 2006. Approximation by fuzzy B-spline series, Journal of Applied Mathematics and Computing. 20(1–2): 157–169.
18. Saga, S. and Makino, H. 1993. Fuzzy spline interpolation and its application to on-line freehand curve identification, Proc. 2nd IEEE Internat. Conf. on Fuzzy Systems. 1183–1190.
19. Zakaria R, Wahab AF and Gobithaasan R, 2016. The Series of Fuzzified Fuzzy Bezier Curve, Jurnal Teknologi. 78: 103-107. DOI: https://doi.org/10.11113/jt.v78.6935
20. Tas, F. and Topal, S. 2017. Bezier Curve Modeling for Neutrosophic Data Problem. Neutrosophic set and system. University of New Mexico.
21. Topal, S. and Tas, F. 2018. Bézier Surface Modeling for Neutrosophic Data Problems. Neutrosophic set and system University of New Mexico. 19: 19-23.
22. Rosli, S. N. I., and Zulkifly, M. I. E. 2023. A Neutrosophic Approach for B-Spline Curve by Using Interpolation Method. Neutrosophic Systems with Applications. 9: 29–40. DOI: https://doi.org/10.61356/j.nswa.2023.43.
23. Rosli, S. N. I., and Zulkifly, M. I. E. 2023. Neutrosophic Bicubic B-spline Surface Interpolation Model for Uncertainty Data. Neutrosophic Systems with Applications. 10: 25–34. DOI: https://doi.org/10.61356/j.nswa.2023.69.
24. Rosli, S. N. I., and Zulkifly, M. I. E. 2023. 3-Dimensional Quartic Bézier Curve Approximation Model by Using Neutrosophic Approach. Neutrosophic Systems with Applications. 11: 11–21. DOI: https://doi.org/10.61356/j.nswa.2023.78.

25. Rosli, S. N. I., & Zulkifly, M. I. E. 2023. Neutrosophic Bicubic Bezier Surface Approximation Model for Uncertainty Data. MATEMATIKA, 39(3): 281–291. DOI: https://doi.org/10.11113/matematika.v39.n3.1502
26. Sumathi, I. R. and Antony C. 2019. New approach on differential equation via trapezoidal neutrosophic number. Complex & Intelligent Systems, 5: 417–424. DOI: https://doi.org/10.1007/s40747-019-00117-3
27. Piegl, L. and Tiller, W. The NURBS Book (Springer-Verlag Berlin Heidelberg, Germany), 1995.
28. Rosli, S. N. I., & Zulkifly, M. I. E. 2024. Neutrosophic B-spline Surface Approximation Model for 3-Dimensional Data Collection. Neutrosophic Sets and Systems, 63: 95-104. https://fs.unm.edu/nss8/index.php/111/article/view/3879
29. Zulkifly, M. I. E. (2018). Pemodelan Geometri Kabur Intusinistik Untuk Visualisasi Masalah Data Kompleks [Doctoral thesis, Universiti Malaysia Terengganu].
30. Rosli, S. N. I., & Zulkifly, M. I. E. 2024. Neutrosophic Bézier Curve Model for Uncertainty Problem Using Approximation Approach. ITM Web Conf., 67, https://doi.org/10.1051/itmconf/20246701029
31. Rosli, S. N. I., & Zulkifly, M. I. E. 2024. Bézier Curve Interpolation Model for Complex Data by Using Neutrosophic Approach. EDUCATUM Journal of Science, Mathematics, and Technology, 12(1), 1–9. https://doi.org/10.37134/ejsmt.vol12.1.1.2025
32. Rosli, S. N. I. & Zulkifly, M. I. E. 2024. Visualization of 3-dimensional Cubic B-spline Surface Approximation Model by using Interval Type-2 Neutrosophic Set Theory. 3rd International Conference on Frontiers in Academic Research. 372-380. https://drive.google.com/file/d/1TlxmdmI2ZXlvF-5NXEwomYFKl1UNgKEO/view
33. Salam, A., Mohamed, M., Yong, R., & Ye, J. 2024. A Robust Decision-Making Model for Medical Supplies via Selecting Appropriate Unmanned Aerial Vehicles. Neutrosophic Systems with Applications, 18, 14-30. https://doi.org/10.61356/j.nswa.2024.18263
34. Mohamed, M., Ayman, S., Yong, R., & Ye, J. 2024. Ranking Cloud Service Providers using SWARA-MARCOS in Type-2 Neutrosophic Number Set Environment. Neutrosophic Systems with Applications, 18, 46-59. https://doi.org/10.61356/j.nswa.2024.18284
35. Christianto, V. and Smarandache, F. 2024. Unveiling Quantum Communication: From Bell's Inequality to Neutrosophic Logic, Sustainable Machine Intelligence Journal, 6, pp. (6):1–6. doi:10.61356/SMIJ.2024.66106
36. Mohamed, M. 2024. Partnership of Lean Six Sigma and Digital Twin under Type 2 Neutrosophic Mystery Toward Virtual Manufacturing Environment: Real Scenario Application, Sustainable Machine Intelligence Journal, 8, pp. (6):99–109. doi:10.61356/SMIJ.2024.8302.

Received: April 20, 2024. Accepted: Aug 25, 2024

NSS

Neutrosophic Sets and Systems, Vol. 72, 2024

University of New Mexico

Product Operations on Pythagorean Co-Neutrosophic Graphs and its Application

G. Vetrivel[1], M. Mullai[2,3,*] and G. Rajchakit[4]

[1]Department of Mathematics, Alagappa University, Karaikudi, Tamilnadu, India;

Email: menakagovindan@gmail.com

[2]Department of Mathematics, Alagappa University, Karaikudi, Tamilnadu, India;

Email: mullaim@alagappauniversity.ac.in

[3]Research Fellow, INTI International University, Nilai Campus, Malaysia;

[4]Department of Mathematics, Faculty of Science, Maejo University, Chiang Mai 50290, Thailand;

Email: kreangkri@mju.ac.th

[*]Correspondence: mullaim@alagappauniversity.ac.in;

Abstract. Pythagorean Co-Neutrosophic Graphs (PyCNGs) have newly emerged after the foundation of Pythagorean fuzzy graph and Co-neutrosophic graphs, where the membership of indeterminacy(uncertain) is independent and membership of truth(existence) & false(non-existence) are dependent. This paper has a wide discussion of different product operations carried out in PyCNGs. Some properties like strong, complete with consideration of a vertex's degree in the graph are explored with examples. Also, an application related to the product on PyCNGs is demonstrated with brain network analysis and its function.

Keywords: Pythagorean co-neutrosophic graph; Modular product; Homomorphic product; Symmetric difference.

1. Introduction

Graph theory attains global importance in the kind of real-life related discussion based on the theoretical concepts that already exist. Though it gives a detailed graphical structure for many problems of the real world, but uncertainty and vagueness prevail in the final output. Zadeh [39] refined crisp set theory and laid a new foundation in name of fuzzy set theory. Then, Kaufmann [15] excavated ideas on fuzzy graphical system which shows high accuracy when compared to crisp graphs. Further innovations regarding fuzzy graph models and their

properties were discussed by Rosenfeld [29]. Bhattacharya [9], Bhuttani [10], and Nagoor Gani [18–22] laid an immense base by various discussions on structural representations of fuzzy graph and labelings. Other fuzzy field researchers followed up with more successful fuzzy graph-based works. With prior knowledge from Mordeson and Peng's [17] work, Nagoor Gani and Radha [20] applied conjunction over fuzzy graphs. Following that, various types of products on fuzzy graphs were developed and discussed briefly by Radha et al. [27, 28], and Shovan Dogra [32].

Krassimir Atannosov's [8] effort to reduce the inaccuracy occurs in fuzzy kind had succeeded by the introduction of intuitionistic fuzzy set(InFS), where explicit membership of non-existence becomes essential for coping with unforeseeable circumstances. R. Parvathi et al. [25, 26] extended the fuzzy graph concept to an intuitionistic fuzzy graph(InFG) with the help of InFS. M. Akram [5] and Nagoor Gani [23] elaborated on various properties of InFG which help to compare actual world components with InFG structure. Different types of products on InFG were demonstrated by Sankar Sahoo and Madhumangal Pal [30]. Yager [36–38] founded the Pythagorean fuzzy set(PyFS) to increase the flexibility of InFS, by adjusting the membership grades. M. Akram et al. [6] undertook research on Pythagorean fuzzy graphs (PyFG) and how they pertain to decision-making using PyFS.

F. Smarandache [33,34] successively enhanced the InFS by introducing a neutrosophic set(with explicit indeterminacy membership), which reduces the uncertain results of InFS in reality. The development of neutrosophic graphs, which include the expansion of neutrosophic sets, has been rendered viable thanks to the contributions of Smarandache. Wang et al. [35] devised a model for single-valued neutrosophic set (SVNS) via the neutrosophic set as its basis. Broumi and Smarandache [11] invented the notion of a single-valued neutrosophic graph (SVNG) and extensively investigated numerous features associated with its vertices and edges. Dhavaseelan et al. [12] analyzed the attributes of a single valued co-neutrosophic graph (SVCNG) by including anti-behavior aspects. They dealt with the degree and regularity of the reconstituted SVNG. With the Pythagorean neutrosophic set definition, Ajay et al. [1–4] innovated Pythagorean neutrosophic fuzzy graph (PyNFG). They exclusively dealt with labeling and regular property on PyNFG. Kartick Mohanta et al. [14] offered an in-depth investigation of a multitude of products derived from neutrosophic graphs. They particularly addressed the ideas of degree and total degree with these products. This work was extended to SVNG by Zeng [40] with some applications.

Pythagorean co-neutrosophic graphs(PyCNGs) are extensible when compared to neutrosophic graphs. Therefore, the results acquired through PyCNGs will be more accurate than neutrosophic graphs. In this paper, PyCNGs derived by using Pythagorean neutrosophic set(PyNS) have been taken and various types of products on PyCNGs were discussed and

verified briefly with some additional properties. Finally, the product of the PyCNGs concept has been related to brain network analysis and its applications have been found.

This paper comprises the subsequent sections: Section 2 includes a comprehensive overview of the fundamental terminology of the PyCNGs. In section 3, different kinds of products concerned to PyCNGs has been structured and some properties like strong, complete are investigated with theorems. Section 4 demonstrates the utilization of product on PyCNGs, by comparing the brain functions of two individuals.

2. **Preliminaries**

Definition 2.1. *([1])*

A neutrosophic set C is defined on Z (universal set) is given by $C = \{\langle a, \alpha_N(a), \beta_N(a), \gamma_N(a)\rangle / a \in Z\}$, *where* $\alpha_C : Z \to [0,1]$, $\beta_C : Z \to [0,1]$ *and* $\gamma_C : Z \to [0,1]$ *represent the membership degree of existence, uncertain and non-existence function of vertex a on C, respectively with the requirement* $0 \leq \alpha_C(a) + \beta_C(a) + \gamma_C(a) \leq 3$, $\forall\ a \in Z$.

Definition 2.2. *([1])*

A neutrosophic graph on Z is a graph$(Gr) = (C, D)$ with neutrosophic set C on Z and a neutrosophic relation D on Z, where $C = \{a_1, a_2, \cdots, a_n\}$ *such that*

(i) α_C, β_C and γ_C defined from Z to $[0,1]$ represent the membership degree of existence, uncertain and non-existence function of the vertex $a \in Z$ respectively with $0 \leq \alpha_C(a) + \beta_C(a) + \gamma_C(a) \leq 3$, *for all* $a \in Z$.

(ii) $D \subseteq Z \times Z$ *with α_D, β_D and γ_D defined from $Z \times Z$ to $[0,1]$ represent the membership degree of existence, uncertain and non-existence function of the edges $ab \in Z \times Z$ respectively such that*

$\alpha_D(ab) \leq min[\alpha_C(a), \alpha_C(b)]$,

$\beta_D(ab) \leq min[\beta_C(a), \beta_C(b)]$,

$\gamma_D(ab) \leq max[\gamma_C(a), \gamma_C(b)]$ *and*

$0 \leq \alpha_D(ab) + \beta_D(ab) + \gamma_D(ab) \leq 3$, *for every ab.*

Definition 2.3. *([1])*

A Pythagorean neutrosophic set (PyNS) on an universal set Z is an element of type $C = \{\langle a, \alpha_C(a), \beta_C(a), \gamma_C(a)\rangle / a \in Z\}$, *where* $\alpha_C : Z \to [0,1]$, $\beta_C : Z \to [0,1]$ *and* $\gamma_C : Z \to [0,1]$ *represent the membership degree of existence, uncertain and non-existence function of C respectively, with α_C, β_C and γ_C satisfy the requirement* $0 \leq \alpha_C^2(a) + \beta_C^2(a) + \gamma_C^2(a) \leq 2$, $\forall$ $a \in Z$.

Definition 2.4. *([1])*

A PyNS D on $Z \times Z$ is said to be a relation of Pythagorean neutrosophic type on Z, denoted

by $D = \{\langle ab, \alpha_D(ab), \beta_D(ab), \gamma_D(ab)\rangle / ab \in Z \times Z\}$, *where* $\alpha_D : Z \times Z \to [0,1]$, $\beta_D : Z \times Z \to [0,1]$ *and* $\gamma_D : Z \times Z \to [0,1]$ *represent the membership degree of existence, uncertain and non-existence function of D, with* α_D, β_D *and* γ_D *satisfy the requirement* $0 \leq \alpha_D^2(ab) + \beta_D^2(ab) + \gamma_D^2(ab) \leq 2$, $\forall\ ab \in Z \times Z$.

Definition 2.5. *([1])*

A Pythagorean neutrosophic graph (PyNG) on a non-empty set Z is a pair $Gr = (C, D)$ *with C, a PyNS on Z and D, a relation of Pythagorean neutrosophic type on Z such that*

$\alpha_D(ab) \leq \alpha_C(a) \wedge \alpha_C(b)$,

$\beta_D(ab) \leq \beta_C(a) \wedge \beta_C(b)$,

$\gamma_D(ab) \leq \gamma_C(a) \vee \gamma_C(b)$,

and $0 \leq \alpha_D^2(ab) + \beta_D^2(ab) + \gamma_D^2(ab) \leq 2$, $\forall\ a, b \in Z$, *where* $\alpha_D : Z \times Z \to [0,1]$, $\beta_D : Z \times Z \to [0,1]$ *and* $\gamma_D : Z \times Z \to [0,1]$ *represent the membership degree of existence, uncertain and non-existence function of D respectively.*

Definition 2.6. *([1])*

A Pythagorean neutrosophic preference relation on $Z = \{a_1, a_2, \cdots, a_n\}$ *is demonstrated by a matrix* $M_p = (m_{kl})$ *of order* $n \times n$, *where* $m_{kl} = (a_k a_l, \alpha(a_k a_l), \beta(a_k a_l), \gamma(a_k a_l))$, $\forall\ k, l = 1, 2, \cdots, n$. *Let* $m_{kl} = (\alpha_{kl}, \beta_{kl}, \gamma_{kl})$, *where* α_{kl} *indicates the degree to which the element* a_k *is preferred to the element* a_l, β_{kl} *indicates the uncertain degree to which the element* a_k *is preferred to the element* a_l, γ_{kl} *denotes the degree to which the element* a_k *is not preferred to the element* a_l, *and* $\pi_{kl} = 2 - \alpha_{kl}^2 - \beta_{kl}^2 - \gamma_{kl}^2$ *is implemented as a hesitancy degree, with the requirements:*

$\alpha_{kl}, \beta_{kl}, \gamma_{kl} \in [0,1]$, $\alpha_{kl}^2 + \beta_{kl}^2 + \gamma_{kl}^2 \leq 2$, $\alpha_{kl} = \beta_{lk}$, $\beta_{kl} = \gamma_{lk}$, $\gamma_{kl} = \alpha_{lk}$,

$\alpha_{kk} = \beta_{kk} = \gamma_{kk} = 1$, $\forall\ k, l = 1, 2, \cdots, n$.

Definition 2.7. *([30])*

The direct product of Pythagorean co-neutrosophic graphs $Gr_1 = (V^*, E^*, \kappa^*, \lambda^*)$ *and* $Gr_2 = (V^{**}, E^{**}, \kappa^{**}, \lambda^{**})$ *such that* $V^* \cap V^{**} = \phi$, *is defined to be the PyNG* $Gr_1 \sqcap Gr_2 = (V, E, \kappa^* \sqcap \kappa^{**}, \lambda^* \sqcap \lambda^{**})$ *where* $V = V^* \times V^{**}$, $E = \{((a_1, b_1), (a_2, b_2)) / (a_1, a_2) \in E^*, (b_1, b_2) \in E^{**}\}$. *The existence, uncertain and non-existence values of the vertex* (a, b) *in* $Gr_1 \sqcap Gr_2$ *are given by*

(i) $(\kappa_1^* \sqcap \kappa_1^{**})(a, b) = \kappa_1^*(a) \vee \kappa_1^{**}(b)$,

(ii) $(\kappa_2^* \sqcap \kappa_2^{**})(a, b) = \kappa_2^*(a) \vee \kappa_2^{**}(b)$ *and*

(iii) $(\kappa_3^* \sqcap \kappa_3^{**})(a, b) = \kappa_3^*(a) \wedge \kappa_3^{**}(b)$.

The existence, uncertain and non-existence values of the edge $((a_1, b_1), (a_2, b_2))$ *in* $Gr_1 \sqcap Gr_2$ *are given by*

$(\lambda_1^* \sqcap \lambda_1^{**})((a_1, b_1), (a_2, b_2)) = \lambda_1^*(a_1, a_2) \vee \lambda_1^{**}(b_1, b_2)$

$(\lambda_2^* \sqcap \lambda_2^{**})((a_1, b_1), (a_2, b_2)) = \lambda_2^*(a_1, a_2) \vee \lambda_2^{**}(b_1, b_2)$
$(\lambda_3^* \sqcap \lambda_3^{**})((a_1, b_1), (a_2, b_2)) = \lambda_3^*(a_1, a_2) \wedge \lambda_3^{**}(b_1, b_2)$.

Definition 2.8. *([13])*
The random walk graph kernel $k(Gr_1, Gr_2)$ of Gr_1 and Gr_2 is referred to be $k(Gr_1, Gr_2) := q^T(I - cW)^{-1}p$, where, W denotes the weight matrix, c refers to decay factor and p & q denote respectively the starting and stopping probabilities.

3. Products on Pythagorean Co-Neutrosophic Graphs

Definition 3.1.
A Pythagorean co-neutrosophic graph (PyCNG) on a non-empty set Z is a graph$(Gr) = (C, D)$ with C, a PyNS on Z and D, a relation of Pythagorean neutrosophic type on Z such that
$\alpha_D(ab) \geq \alpha_C(a) \vee \alpha_C(b)$,
$\beta_D(ab) \geq \beta_C(a) \vee \beta_C(b)$,
$\gamma_D(ab) \geq \gamma_C(a) \wedge \gamma_C(b)$,
and $0 \leq \alpha_D^2(ab) + \beta_D^2(ab) + \gamma_D^2(ab) \leq 2$, $\forall\ a, b \in Z$, where $\alpha_D : Z \times Z \to [0, 1]$, $\beta_D : Z \times Z \to [0, 1]$ and $\gamma_D : Z \times Z \to [0, 1]$ represent the membership degree of existence, uncertain and non-existence function of D respectively.

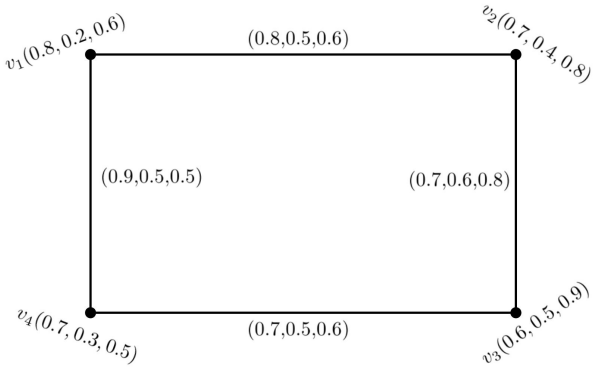

FIGURE 1. Pythagorean Co-Neutrosophic Graph

Definition 3.2. *(Modular product on Pythagorean co-neutrosophic graphs(PyCNGs))*
Consider $Gr_1 = (C_1, D_1)$ and $Gr_2 = (C_2, D_2)$ be PyCNGs of $\mathscr{G}_1 = (\mathscr{V}_1, \mathscr{E}_1)$ and $\mathscr{G}_2 = (\mathscr{V}_2, \mathscr{E}_2)$, respectively. The modular product $Gr_1 \odot Gr_2$ of Gr_1 and Gr_2 is denoted by $(C_1 \odot C_2, D_1 \odot D_2)$ with elemental vertex set $\mathscr{V}_1 \odot \mathscr{V}_2 = \{(a_1, b_1)/a_1 \in \mathscr{V}_1, b_1 \in \mathscr{V}_2\}$ and elemental edge set $\mathscr{E}_1 \odot \mathscr{E}_2 = \{(a_1, b_1)(a_2, b_2)/a_1a_2 \in \mathscr{E}_1, b_1b_2 \in \mathscr{E}_2$ or $a_1a_2 \notin \mathscr{E}_1, b_1b_2 \notin \mathscr{E}_2\}$ is defined as:
(i) $(\alpha_{C_1} \odot \alpha_{C_2})(a_1, b_1) = max(\alpha_{C_1}(a_1), \alpha_{C_2}(b_1))$
$(\beta_{C_1} \odot \beta_{C_2})(a_1, b_1) = max(\beta_{C_1}(a_1), \beta_{C_2}(b_1))$
$(\gamma_{C_1} \odot \gamma_{C_2})(a_1, b_1) = min(\gamma_{C_1}(a_1), \gamma_{C_2}(b_1))$,

where $a_1 \in \mathscr{V}_1$ *and* $b_1 \in \mathscr{V}_2$

(ii) $(\alpha_{D_1} \odot \alpha_{D_2})((a_1,b_1)(a_2,b_2)) =$

$$\begin{cases} max(\alpha_{D_1}(a_1a_2), \alpha_{D_2}(b_1b_2)) & \text{if } a_1a_2 \in \mathscr{E}_1, b_1b_2 \in \mathscr{E}_2 \\ max(\alpha_{C_1}(a_1), \alpha_{C_1}(a_2), \alpha_{C_2}(b_1), \alpha_{C_2}(b_2)) & \text{if } a_1a_2 \notin \mathscr{E}_1, b_1b_2 \notin \mathscr{E}_2 \end{cases}$$

$(\beta_{D_1} \odot \beta_{D_2})((a_1,b_1)(a_2,b_2)) =$

$$\begin{cases} max(\beta_{D_1}(a_1a_2), \beta_{D_2}(b_1b_2)) & \text{if } a_1a_2 \in \mathscr{E}_1, b_1b_2 \in \mathscr{E}_2 \\ max(\beta_{C_1}(a_1), \beta_{C_1}(a_2), \beta_{C_2}(b_1), \beta_{C_2}(b_2)) & \text{if } a_1a_2 \notin \mathscr{E}_1, b_1b_2 \notin \mathscr{E}_2 \end{cases}$$

$(\gamma_{D_1} \odot \gamma_{D_2})((a_1,b_1)(a_2,b_2)) =$

$$\begin{cases} min(\gamma_{D_1}(a_1a_2), \gamma_{D_2}(b_1b_2)) & \text{if } a_1a_2 \in \mathscr{E}_1, b_1b_2 \in \mathscr{E}_2 \\ min(\gamma_{C_1}(a_1), \gamma_{C_1}(a_2), \gamma_{C_2}(b_1), \gamma_{C_2}(b_2)) & \text{if } a_1a_2 \notin \mathscr{E}_1, b_1b_2 \notin \mathscr{E}_2 \end{cases}$$

Theorem 3.3. *Consider PyCNGs* $Gr_1 = (C_1, D_1)$ *and* $Gr_2 = (C_2, D_2)$*, then modular product* $Gr_1 \odot Gr_2$ *is also a PyCNG.*

Proof.

Let $Gr_1 = (C_1, D_1)$ and $Gr_2 = (C_2, D_2)$ be PyCNGs of the graph $\mathscr{G}_1 = (\mathscr{V}_1, \mathscr{E}_1)$ and $\mathscr{G}_2 = (\mathscr{V}_2, \mathscr{E}_2)$, respectively. Here, $C^{Gr_1 \odot Gr_2}$ denotes the Pythagorean co-neutrosophic set of $\mathscr{V}_1 \odot \mathscr{V}_2$ and $D^{Gr_1 \odot Gr_2}$ denotes the Pythagorean co-neutrosophic set of $\mathscr{E}_1 \odot \mathscr{E}_2$.

For all $(a_1,b_1)(a_2,b_2) \in \mathscr{E}_1 \odot \mathscr{E}_2$,

$$\begin{aligned} (\alpha_{D_1} \odot \alpha_{D_2})((a_1,b_1)(a_2,b_2)) &= max(\alpha_{D_1}(a_1a_2), \alpha_{D_2}(b_1b_2)) \ \ if\, a_1a_2 \in \mathscr{E}_1, b_1b_2 \in \mathscr{E}_2 \\ &\geq max(\alpha_{C_1}(a_1), \alpha_{C_1}(a_2), \alpha_{C_2}(b_1), \alpha_{C_2}(b_2)) \\ &\quad [since\ Gr_1\ \&\ Gr_2\ are\ PyCNGs] \end{aligned}$$

$$\begin{aligned} (\beta_{D_1} \odot \beta_{D_2})((a_1,b_1)(a_2,b_2)) &= max(\beta_{D_1}(a_1a_2), \beta_{D_2}(b_1b_2)) \ \ if\, a_1a_2 \in \mathscr{E}_1, b_1b_2 \in \mathscr{E}_2 \\ &\geq max(\beta_{C_1}(a_1), \beta_{C_1}(a_2), \beta_{C_2}(b_1), \beta_{C_2}(b_2)) \\ &\quad [since\ Gr_1\ \&\ Gr_2\ are\ PyCNGs] \end{aligned}$$

$$\begin{aligned} (\gamma_{D_1} \odot \gamma_{D_2})((a_1,b_1)(a_2,b_2)) &= min(\gamma_{D_1}(a_1a_2), \gamma_{D_2}(b_1b_2)) \ \ if\, a_1a_2 \in \mathscr{E}_1, b_1b_2 \in \mathscr{E}_2 \\ &\geq min(\gamma_{C_1}(a_1), \gamma_{C_1}(a_2), \gamma_{C_2}(b_1), \gamma_{C_2}(b_2)) \\ &\quad [since\ Gr_1\ \&\ Gr_2\ are\ PyCNGs] \end{aligned}$$

$$\begin{aligned} (\alpha_{D_1} \odot \alpha_{D_2})((a_1,b_1)(a_2,b_2)) &= max(\alpha_{C_1}(a_1), \alpha_{C_1}(a_2), \alpha_{C_2}(b_1), \alpha_{C_2}(b_2)), \ \ if\, a_1a_2 \notin \mathscr{E}_1, b_1b_2 \notin \mathscr{E}_2 \\ &= max((\alpha_{C_1} \odot \alpha_{C_2})(a_1,b_1), (\alpha_{C_1} \odot \alpha_{C_2})(a_2,b_2)) \end{aligned}$$

$$\begin{aligned} (\beta_{D_1} \odot \beta_{D_2})((a_1,b_1)(a_2,b_2)) &= max(\beta_{C_1}(a_1), \beta_{C_1}(a_2), \beta_{C_2}(b_1), \beta_{C_2}(b_2)), \ \ if\, a_1a_2 \notin \mathscr{E}_1, b_1b_2 \notin \mathscr{E}_2 \\ &= max((\beta_{C_1} \odot \beta_{C_2})(a_1,b_1), (\beta_{C_1} \odot \beta_{C_2})(a_2,b_2)) \end{aligned}$$

$$(\gamma_{D_1} \odot \gamma_{D_2})((a_1,b_1)(a_2,b_2)) = min(\gamma_{C_1}(a_1), \gamma_{C_1}(a_2), \gamma_{C_2}(b_1), \gamma_{C_2}(b_2)), \quad if\, a_1a_2 \notin \mathscr{E}_1, b_1b_2 \notin \mathscr{E}_2$$
$$= min((\gamma_{C_1} \odot \gamma_{C_2})(a_1,b_1), (\gamma_{C_1} \odot \gamma_{C_2})(a_2,b_2))$$

Therefore,

$$(\alpha_{D_1} \odot \alpha_{D_2})((a_1,b_1)(a_2,b_2)) \geq max((\alpha_{C_1} \odot \alpha_{C_2})(a_1,b_1), (\alpha_{C_1} \odot \alpha_{C_2})(a_2,b_2))$$
$$(\beta_{D_1} \odot \beta_{D_2})((a_1,b_1)(a_2,b_2)) \geq max((\beta_{C_1} \odot \beta_{C_2})(a_1,b_1), (\beta_{C_1} \odot \beta_{C_2})(a_2,b_2))$$
$$(\gamma_{D_1} \odot \gamma_{D_2})((a_1,b_1)(a_2,b_2)) \geq min((\gamma_{C_1} \odot \gamma_{C_2})(a_1,b_1), (\gamma_{C_1} \odot \gamma_{C_2})(a_2,b_2))$$

This proves that $Gr_1 \odot Gr_2$ is also a PyCNG.

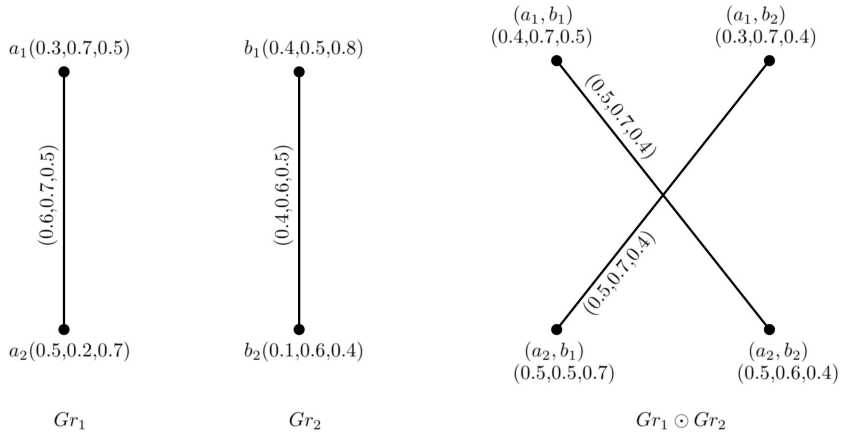

FIGURE 2. Modular product on PyCNGs

Theorem 3.4. *Consider strong PyCNGs $Gr_1 = (C_1, D_1)$ and $Gr_2 = (C_2, D_2)$. Then the modular product $Gr_1 \odot Gr_2$ is again a strong PyCNG.*

Proof.

Let us take $Gr_1 = (C_1, D_1)$ and $Gr_2 = (C_2, D_2)$ be strong PyCNGs of graphs $\mathscr{G}_1 = (\mathscr{V}_1, \mathscr{E}_1)$ and $\mathscr{G}_2 = (\mathscr{V}_2, \mathscr{E}_2)$, respectively. Here, $C^{Gr_1 \odot Gr_2}$ denotes the Pythagorean co-neutrosophic set of $\mathscr{V}_1 \odot \mathscr{V}_2$ and $D^{Gr_1 \odot Gr_2}$ denotes the Pythagorean co-neutrosophic set of $\mathscr{E}_1 \odot \mathscr{E}_2$.
$\forall (a_1,b_1)(a_2,b_2) \in \mathscr{E}_1 \odot \mathscr{E}_2$,

$$(\alpha_{D_1} \odot \alpha_{D_2})((a_1,b_1)(a_2,b_2)) = max(\alpha_{D_1}(a_1a_2), \alpha_{D_2}(b_1b_2)) \;\; if\, a_1a_2 \in \mathscr{E}_1, b_1b_2 \in \mathscr{E}_2$$
$$= max(\alpha_{C_1}(a_1), \alpha_{C_1}(a_2), \alpha_{C_2}(b_1), \alpha_{C_2}(b_2))$$
$$[since\ Gr_1\ \&\ Gr_2\ are\ strong\ PyCNGs]$$

$$\begin{aligned}(\beta_{D_1} \odot \beta_{D_2})((a_1,b_1)(a_2,b_2)) &= max(\beta_{D_1}(a_1a_2), \beta_{D_2}(b_1b_2)) \ \ if\, a_1a_2 \in \mathscr{E}_1, b_1b_2 \in \mathscr{E}_2 \\ &= max(\beta_{C_1}(a_1), \beta_{C_1}(a_2), \beta_{C_2}(b_1), \beta_{C_2}(b_2)) \\ &\quad [since\ Gr_1\ \&\ Gr_2\ are\ strong\ PyCNGs]\end{aligned}$$

$$\begin{aligned}(\gamma_{D_1} \odot \gamma_{D_2})((a_1,b_1)(a_2,b_2)) &= min(\gamma_{D_1}(a_1a_2), \gamma_{D_2}(b_1b_2)) \ \ if\, a_1a_2 \in \mathscr{E}_1, b_1b_2 \in \mathscr{E}_2 \\ &= min(\gamma_{C_1}(a_1), \gamma_{C_1}(a_2), \gamma_{C_2}(b_1), \gamma_{C_2}(b_2)) \\ &\quad [since\ Gr_1\ \&\ Gr_2\ are\ strong\ PyCNGs]\end{aligned}$$

$$\begin{aligned}(\alpha_{D_1} \odot \alpha_{D_2})((a_1,b_1)(a_2,b_2)) &= max(\alpha_{C_1}(a_1), \alpha_{C_1}(a_2), \alpha_{C_2}(b_1), \alpha_{C_2}(b_2)), \ \ if\, a_1a_2 \notin \mathscr{E}_1, b_1b_2 \notin \mathscr{E}_2 \\ &= max((\alpha_{C_1} \odot \alpha_{C_2})(a_1,b_1), (\alpha_{C_1} \odot \alpha_{C_2})(a_2,b_2))\end{aligned}$$

$$\begin{aligned}(\beta_{D_1} \odot \beta_{D_2})((a_1,b_1)(a_2,b_2)) &= max(\beta_{C_1}(a_1), \beta_{C_1}(a_2), \beta_{C_2}(b_1), \beta_{C_2}(b_2)), \ \ if\, a_1a_2 \notin \mathscr{E}_1, b_1b_2 \notin \mathscr{E}_2 \\ &= max((\beta_{C_1} \odot \beta_{C_2})(a_1,b_1), (\beta_{C_1} \odot \beta_{C_2})(a_2,b_2))\end{aligned}$$

$$\begin{aligned}(\gamma_{D_1} \odot \gamma_{D_2})((a_1,b_1)(a_2,b_2)) &= min(\gamma_{C_1}(a_1), \gamma_{C_1}(a_2), \gamma_{C_2}(b_1), \gamma_{C_2}(b_2)), \ \ if\, a_1a_2 \notin \mathscr{E}_1, b_1b_2 \notin \mathscr{E}_2 \\ &= min((\gamma_{C_1} \odot \gamma_{C_2})(a_1,b_1), (\gamma_{C_1} \odot \gamma_{C_2})(a_2,b_2))\end{aligned}$$

Therefore,

$$\begin{aligned}(\alpha_{D_1} \odot \alpha_{D_2})((a_1,b_1)(a_2,b_2)) &= max((\alpha_{C_1} \odot \alpha_{C_2})(a_1,b_1), (\alpha_{C_1} \odot \alpha_{C_2})(a_2,b_2)) \\ (\beta_{D_1} \odot \beta_{D_2})((a_1,b_1)(a_2,b_2)) &= max((\beta_{C_1} \odot \beta_{C_2})(a_1,b_1), (\beta_{C_1} \odot \beta_{C_2})(a_2,b_2)) \\ (\gamma_{D_1} \odot \gamma_{D_2})((a_1,b_1)(a_2,b_2)) &= min((\gamma_{C_1} \odot \gamma_{C_2})(a_1,b_1), (\gamma_{C_1} \odot \gamma_{C_2})(a_2,b_2))\end{aligned}$$

This proves that $Gr_1 \odot Gr_2$ is again a strong PyCNG.

Definition 3.5. *(Degree of modular product on PyCNGs)*
Let $Gr_1 = (C_1, D_1)$ and $Gr_2 = (C_2, D_2)$ be PyCNGs of the graph $\mathscr{G}_1 = (\mathscr{V}_1, \mathscr{E}_1)$ and $\mathscr{G}_2 = (\mathscr{V}_2, \mathscr{E}_2)$, respectively. At any vertex $(a_1, b_1) \in \mathscr{V}_1 \times \mathscr{V}_2$:

$$\begin{aligned}(d_\alpha)_{Gr_1 \odot Gr_2}(a_1,b_1) &= \sum_{((a_1,b_1),(a_2,b_2)) \in \mathscr{E}_1 \times \mathscr{E}_2} \alpha_{D_1} \odot \alpha_{D_2}((a_1,b_1),(a_2,b_2)) \\ &= \sum_{\substack{(a_1,a_2)\in\mathscr{E}_1, \\ (b_1,b_2)\in\mathscr{E}_2}} max(\alpha_{D_1}(a_1,a_2), \alpha_{D_2}(b_1,b_2)) \\ &\quad + \sum_{\substack{(a_1,a_2)\notin\mathscr{E}_1, \\ (b_1,b_2)\notin\mathscr{E}_2}} max(\alpha_{C_1}(a_1), \alpha_{C_1}(a_2), \alpha_{C_2}(b_1), \alpha_{C_2}(b_2)),\end{aligned}$$

$$
\begin{aligned}
(d_\beta)_{Gr_1 \odot Gr_2}(a_1, b_1) &= \sum_{((a_1,b_1),(a_2,b_2)) \in \mathscr{E}_1 \times \mathscr{E}_2} \beta_{D_1} \odot \beta_{D_2}((a_1, b_1), (a_2, b_2)) \\
&= \sum_{\substack{(a_1,a_2) \in \mathscr{E}_1, \\ (b_1,b_2) \in \mathscr{E}_2}} max(\beta_{D_1}(a_1, a_2), \beta_{D_2}(b_1, b_2)) \\
&\quad + \sum_{\substack{(a_1,a_2) \notin \mathscr{E}_1, \\ (b_1,b_2) \notin \mathscr{E}_2}} max(\beta_{C_1}(a_1), \beta_{C_1}(a_2), \beta_{C_2}(b_1), \beta_{C_2}(b_2)),
\end{aligned}
$$

$$
\begin{aligned}
(d_\gamma)_{Gr_1 \odot Gr_2}(a_1, b_1) &= \sum_{((a_1,b_1),(a_2,b_2)) \in \mathscr{E}_1 \times \mathscr{E}_2} \gamma_{D_1} \odot \gamma_{D_2}((a_1, b_1), (a_2, b_2)) \\
&= \sum_{\substack{(a_1,a_2) \in \mathscr{E}_1, \\ (b_1,b_2) \in \mathscr{E}_2}} min(\gamma_{D_1}(a_1, a_2), \gamma_{D_2}(b_1, b_2)) \\
&\quad + \sum_{\substack{(a_1,a_2) \notin \mathscr{E}_1, \\ (b_1,b_2) \notin \mathscr{E}_2}} min(\gamma_{C_1}(a_1), \gamma_{C_1}(a_2), \gamma_{C_2}(b_1), \gamma_{C_2}(b_2))
\end{aligned}
$$

Definition 3.6. *(Total degree of modular product on PyCNGs)*
Consider $Gr_1 = (C_1, D_1)$ and $Gr_2 = (C_2, D_2)$ to be PyCNGs of the graph $\mathscr{G}_1 = (\mathscr{V}_1, \mathscr{E}_1)$ and $\mathscr{G}_2 = (\mathscr{V}_2, \mathscr{E}_2)$, respectively. At any vertex $(a_1, b_1) \in \mathscr{V}_1 \times \mathscr{V}_2$:

$$
\begin{aligned}
(td_\alpha)_{Gr_1 \odot Gr_2}(a_1, b_1) &= \sum_{((a_1,b_1),(a_2,b_2)) \in \mathscr{E}_1 \times \mathscr{E}_2} \alpha_{D_1} \odot \alpha_{D_2}((a_1, b_1), (a_2, b_2)) + \alpha_{C_1} \odot \alpha_{C_2}(a_1, b_1) \\
&= \sum_{\substack{(a_1,a_2) \in \mathscr{E}_1, \\ (b_1,b_2) \in \mathscr{E}_2}} max(\alpha_{D_1}(a_1, a_2), \alpha_{D_2}(b_1, b_2)) \\
&\quad + \sum_{\substack{(a_1,a_2) \notin \mathscr{E}_1, \\ (b_1,b_2) \notin \mathscr{E}_2}} max(\alpha_{C_1}(a_1), \alpha_{C_1}(a_2), \alpha_{C_2}(b_1), \alpha_{C_2}(b_2)) \\
&\quad + max(\alpha_{C_1}(a_1), \alpha_{C_2}(b_1)),
\end{aligned}
$$

$$
\begin{aligned}
(td_\beta)_{Gr_1 \odot Gr_2}(a_1, b_1) &= \sum_{((a_1,b_1),(a_2,b_2)) \in \mathscr{E}_1 \times \mathscr{E}_2} \beta_{D_1} \odot \beta_{D_2}((a_1, b_1), (a_2, b_2)) + \beta_{C_1} \odot \beta_{C_2}(a_1, b_1) \\
&= \sum_{\substack{(a_1,a_2) \in \mathscr{E}_1, \\ (b_1,b_2) \in \mathscr{E}_2}} max(\beta_{D_1}(a_1, a_2), \beta_{D_2}(b_1, b_2)) \\
&\quad + \sum_{\substack{(a_1,a_2) \notin \mathscr{E}_1, \\ (b_1,b_2) \notin \mathscr{E}_2}} max(\beta_{C_1}(a_1), \beta_{C_1}(a_2), \beta_{C_2}(b_1), \beta_{C_2}(b_2)) \\
&\quad + max(\beta_{C_1}(a_1), \beta_{C_2}(b_1)),
\end{aligned}
$$

$$
\begin{aligned}
(td_\gamma)_{Gr_1\odot Gr_2}(a_1,b_1) &= \sum_{((a_1,b_1),(a_2,b_2))\in\mathscr{E}_1\times\mathscr{E}_2} \gamma_{D_1}\odot\gamma_{D_2}((a_1,b_1),(a_2,b_2))+\gamma_{C_1}\odot\gamma_{C_2}(a_1,b_1)\\
&= \sum_{\substack{(a_1,a_2)\in\mathscr{E}_1,\\(b_1,b_2)\in\mathscr{E}_2}} min(\gamma_{D_1}(a_1,a_2),\gamma_{D_2}(b_1,b_2))\\
&\quad+\sum_{\substack{(a_1,a_2)\notin\mathscr{E}_1,\\(b_1,b_2)\notin\mathscr{E}_2}} min(\gamma_{C_1}(a_1),\gamma_{C_1}(a_2),\gamma_{C_2}(b_1),\gamma_{C_2}(b_2))\\
&\quad+min(\gamma_{C_1}(a_1),\gamma_{C_2}(b_1)),
\end{aligned}
$$

Example 3.7.

Examine the modular product on PyCNGs, as shown in Figure 2. Then the degree of the vertex (a_1,b_1) *is* $d_{Gr_1\odot Gr_2}(a_1,b_1)=((d_\alpha)_{Gr_1\odot Gr_2}(a_1,b_1),(d_\beta)_{Gr_1\odot Gr_2}(a_1,b_1),(d_\gamma)_{Gr_1\odot Gr_2}(a_1,b_1))$ = *(0.5,0.7,0.4) and the total degree of the vertex* (a_1,b_1) *is* $td_{Gr_1\odot Gr_2}(a_1,b_1)=((td_\alpha)_{Gr_1\odot Gr_2}(a_1,b_1),(td_\beta)_{Gr_1\odot Gr_2}(a_1,b_1),(td_\gamma)_{Gr_1\odot Gr_2}(a_1,b_1))=$ *(0.9,1.4,0.9). In the same way, the remaining vertices degree and total degree are obtained by* $d_{Gr_1\odot Gr_2}(a_1,b_2)=$ *(0.5,0.7,0.4),* $td_{Gr_1\odot Gr_2}(a_1,b_2)=$ *(0.8,1.4,0.8),* $d_{Gr_1\odot Gr_2}(a_2,b_1)=$ *(0.5,0.7,0.4),* $td_{Gr_1\odot Gr_2}(a_2,b_1)=$ *(1.0,1.2,1.1),* $d_{Gr_1\odot Gr_2}(a_2,b_2)=$ *(0.5,0.7,0.4) and* $td_{Gr_1\odot Gr_2}(a_2,b_2)=$ *(1.0,1.3,0.8).*

Theorem 3.8. *Consider complete PyCNGs* $Gr_1=(C_1,D_1)$ *and* $Gr_2=(C_2,D_2)$.
(i) Let $\alpha_{D_1}\geq\alpha_{D_2}$, $\beta_{D_1}\geq\beta_{D_2}$, $\gamma_{D_1}\leq\gamma_{D_2}$ *then* $d_{Gr_1\odot Gr_2}(a_1,a_2)=d_{Gr_1}(a_1)$, *where* $d_{Gr_1\odot Gr_2}(a_1,a_2)=((d_\alpha)_{Gr_1}(a_1),(d_\beta)_{Gr_1}(a_1),(d_\gamma)_{Gr_1}(a_1))$
(ii) If $\alpha_{D_1}\leq\alpha_{D_2}$, $\beta_{D_1}\leq\beta_{D_2}$, $\gamma_{D_1}\geq\gamma_{D_2}$ *then* $d_{Gr_1\odot Gr_2}(a_1,a_2)=d_{Gr_2}(a_1)$, *where* $d_{Gr_1\odot Gr_2}(a_1,a_2)=((d_\alpha)_{Gr_1}(a_1),(d_\beta)_{Gr_1}(a_1),(d_\gamma)_{Gr_1}(a_1))$

Proof.

(i) We have, degree of each membership of a vertex in modular product as

$$
\begin{aligned}
(d_\alpha)_{Gr_1\odot Gr_2}(a_1,b_1) &= \sum_{((a_1,b_1),(a_2,b_2))\in\mathscr{E}_1\times\mathscr{E}_2} \alpha_{D_1}\odot\alpha_{D_2}((a_1,b_1),(a_2,b_2))\\
&= \sum_{\substack{(a_1,a_2)\in\mathscr{E}_1,\\(b_1,b_2)\in\mathscr{E}_2}} max(\alpha_{D_1}(a_1,a_2),\alpha_{D_2}(b_1,b_2))\\
&\quad+\sum_{\substack{(a_1,a_2)\notin\mathscr{E}_1,\\(b_1,b_2)\notin\mathscr{E}_2}} max(\alpha_{C_1}(a_1),\alpha_{C_1}(a_2),\alpha_{C_2}(b_1),\alpha_{C_2}(b_2))\\
&= \sum_{\substack{(a_1,a_2)\in\mathscr{E}_1,\\(b_1,b_2)\in\mathscr{E}_2}} max(\alpha_{D_1}(a_1,a_2),\alpha_{D_2}(b_1,b_2)) \quad [since\ both\ PyCNGs\ are\ complete]\\
&= \sum_{(a_1,a_2)\in\mathscr{E}_1} \alpha_{D_1}(a_1,a_2) \quad [since\ \alpha_{D_1}\geq\alpha_{D_2}]\\
&= (d_\alpha)_{Gr_1}(a_1),
\end{aligned}
$$

$$
\begin{aligned}
(d_\beta)_{Gr_1\odot Gr_2}(a_1,b_1) &= \sum_{((a_1,b_1),(a_2,b_2))\in\mathscr{E}_1\times\mathscr{E}_2} \beta_{D_1}\odot\beta_{D_2}((a_1,b_1),(a_2,b_2)) \\
&= \sum_{\substack{(a_1,a_2)\in\mathscr{E}_1,\\(b_1,b_2)\in\mathscr{E}_2}} max(\beta_{D_1}(a_1,a_2),\beta_{D_2}(b_1,b_2)) \\
&\quad + \sum_{\substack{(a_1,a_2)\notin\mathscr{E}_1,\\(b_1,b_2)\notin\mathscr{E}_2}} max(\beta_{C_1}(a_1),\beta_{C_1}(a_2),\beta_{C_2}(b_1),\beta_{C_2}(b_2)) \\
&= \sum_{\substack{(a_1,a_2)\in\mathscr{E}_1,\\(b_1,b_2)\in\mathscr{E}_2}} max(\beta_{D_1}(a_1,a_2),\beta_{D_2}(b_1,b_2)) \ \ [since\ both\ PyCNGs\ are\ complete] \\
&= \sum_{(a_1,a_2)\in\mathscr{E}_1} \beta_{D_1}(a_1,a_2) \ \ [since\ \beta_{D_1}\geq\beta_{D_2}] \\
&= (d_\beta)_{Gr_1}(a_1),
\end{aligned}
$$

$$
\begin{aligned}
(d_\gamma)_{Gr_1\odot Gr_2}(a_1,b_1) &= \sum_{((a_1,b_1),(a_2,b_2))\in\mathscr{E}_1\times\mathscr{E}_2} \gamma_{D_1}\odot\gamma_{D_2}((a_1,b_1),(a_2,b_2)) \\
&= \sum_{\substack{(a_1,a_2)\in\mathscr{E}_1,\\(b_1,b_2)\in\mathscr{E}_2}} min(\gamma_{D_1}(a_1,a_2),\gamma_{D_2}(b_1,b_2)) \\
&\quad + \sum_{\substack{(a_1,a_2)\notin\mathscr{E}_1,\\(b_1,b_2)\notin\mathscr{E}_2}} min(\gamma_{C_1}(a_1),\gamma_{C_1}(a_2),\gamma_{C_2}(b_1),\gamma_{C_2}(b_2)) \\
&= \sum_{\substack{(a_1,a_2)\in\mathscr{E}_1,\\(b_1,b_2)\in\mathscr{E}_2}} min(\gamma_{D_1}(a_1,a_2),\gamma_{D_2}(b_1,b_2)) \ \ [since\ both\ PyCNGs\ are\ complete] \\
&= \sum_{(a_1,a_2)\in\mathscr{E}_1} \gamma_{D_1}(a_1,a_2) \ \ [since\ \gamma_{D_1}\leq\gamma_{D_2}] \\
&= (d_\gamma)_{Gr_1}(a_1)
\end{aligned}
$$

Therefore, $d_{Gr_1\odot Gr_2}(a_1,a_2) = d_{Gr_1}(a_1)$.

(ii) Similar proof by reversing minimum and maximum conditions of (i).

Definition 3.9. *(Homomorphic product on Pythagorean co-neutrosophic graphs(PyCNGs)) Consider PyCNGs $Gr_1=(C_1,D_1)$ and $Gr_2=(C_2,D_2)$ of $\mathscr{G}_1=(\mathscr{V}_1,\mathscr{E}_1)$ and $\mathscr{G}_2=(\mathscr{V}_2,\mathscr{E}_2)$, respectively. Then homomorphic product $Gr_1\diamond Gr_2$ of Gr_1 and Gr_2 is denoted by $(C_1\diamond C_2, D_1\diamond D_2)$ with elemental vertex set $\mathscr{V}_1\diamond\mathscr{V}_2=\{(a_1,b_1)/a_1\in\mathscr{V}_1,b_1\in\mathscr{V}_2\}$ and elemental edge set $\mathscr{E}_1\diamond\mathscr{E}_2=\{(a_1,b_1)(a_2,b_2)/a_1=a_2,b_1b_2\in\mathscr{E}_2$ or $a_1a_2\in\mathscr{E}_1,b_1b_2\notin\mathscr{E}_2\}$ is defined as:*

(i) $(\alpha_{C_1}\diamond\alpha_{C_2})(a_1,b_1)=max(\alpha_{C_1}(a_1),\alpha_{C_2}(b_1))$

$(\beta_{C_1}\diamond\beta_{C_2})(a_1,b_1)=max(\beta_{C_1}(a_1),\beta_{C_2}(b_1))$

$(\gamma_{C_1}\diamond\gamma_{C_2})(a_1,b_1)=min(\gamma_{C_1}(a_1),\gamma_{C_2}(b_1))$,

$\forall (a_1, b_1) \in \mathscr{V}$ *and*

(ii)

$$(\alpha_{D_1} \diamond \alpha_{D_2})((a_1, b_1)(a_2, b_2)) = \begin{cases} max(\alpha_{C_1}(a_1), \alpha_{D_2}(b_1 b_2)) & \text{if } a_1 = a_2, b_1 b_2 \in \mathscr{E}_2 \\ max(\alpha_{D_1}(a_1, a_2), \alpha_{C_2}(b_1), \alpha_{C_2}(b_2)) & \text{if } a_1 a_2 \in \mathscr{E}_1, b_1 b_2 \notin \mathscr{E}_2 \end{cases}$$

$$(\beta_{D_1} \diamond \beta_{D_2})((a_1, b_1)(a_2, b_2)) = \begin{cases} max(\beta_{C_1}(a_1), \beta_{D_2}(b_1 b_2)) & \text{if } a_1 = a_2, b_1 b_2 \in \mathscr{E}_2 \\ max(\beta_{D_1}(a_1, a_2), \beta_{C_2}(b_1), \beta_{C_2}(b_2)) & \text{if } a_1 a_2 \in \mathscr{E}_1, b_1 b_2 \notin \mathscr{E}_2 \end{cases}$$

$$(\gamma_{D_1} \diamond \gamma_{D_2})((a_1, b_1)(a_2, b_2)) = \begin{cases} min(\gamma_{C_1}(a_1), \gamma_{D_2}(b_1 b_2)) & \text{if } a_1 = a_2, b_1 b_2 \in \mathscr{E}_2 \\ min(\gamma_{D_1}(a_1, a_2), \gamma_{C_2}(b_1), \gamma_{C_2}(b_2)) & \text{if } a_1 a_2 \in \mathscr{E}_1, b_1 b_2 \notin \mathscr{E}_2 \end{cases}$$

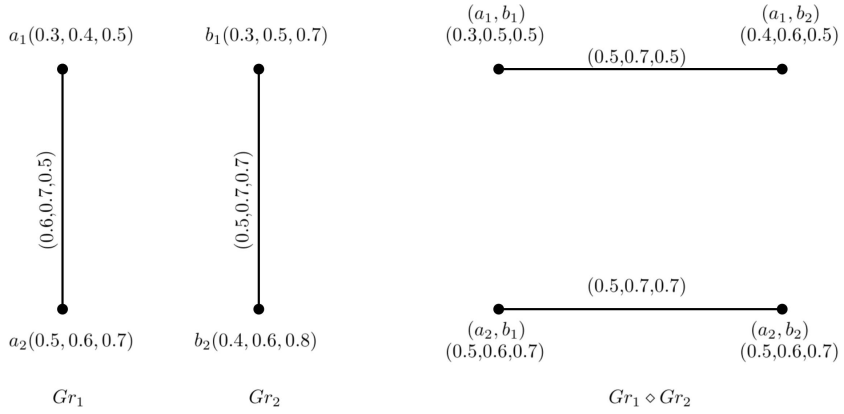

FIGURE 3. Homomorphic product on PyCNGs

Definition 3.10. *(Degree of homomorphic product on PyCNGs)*
Consider PyCNGs $Gr_1 = (C_1, D_1)$ *and* $Gr_2 = (C_2, D_2)$ *of the graph* $\mathscr{G}_1 = (\mathscr{V}_1, \mathscr{E}_1)$ *and* $\mathscr{G}_2 = (\mathscr{V}_2, \mathscr{E}_2)$*, respectively. At any vertex* $(a_1, a_2) \in \mathscr{V}_1 \times \mathscr{V}_2$*:*

$$\begin{aligned} (d_\alpha)_{Gr_1 \diamond Gr_2}(a_1, b_1) &= \sum_{((a_1,b_1),(a_2,b_2)) \in \mathscr{E}_1 \times \mathscr{E}_2} \alpha_{D_1} \diamond \alpha_{D_2}((a_1, b_1), (a_2, b_2)) \\ &= \sum_{\substack{a_1 = a_2, \\ (b_1, b_2) \in \mathscr{E}_2}} max(\alpha_{C_1}(a_1), \alpha_{D_2}(b_1, b_2)) \\ &\quad + \sum_{\substack{(a_1, a_2) \in \mathscr{E}_1, \\ (b_1, b_2) \notin \mathscr{E}_2}} max(\alpha_{D_1}(a_1, a_2), \alpha_{C_2}(b_1), \alpha_{C_2}(b_2)), \end{aligned}$$

$$\begin{aligned} (d_\beta)_{Gr_1 \diamond Gr_2}(a_1, b_1) &= \sum_{((a_1,b_1),(a_2,b_2)) \in \mathscr{E}_1 \times \mathscr{E}_2} \beta_{D_1} \diamond \beta_{D_2}((a_1, b_1), (a_2, b_2)) \\ &= \sum_{\substack{a_1 = a_2, \\ (b_1, b_2) \in \mathscr{E}_2}} max(\beta_{C_1}(a_1), \beta_{D_2}(b_1, b_2)) \\ &\quad + \sum_{\substack{(a_1, a_2) \in \mathscr{E}_1, \\ (b_1, b_2) \notin \mathscr{E}_2}} max(\beta_{D_1}(a_1, a_2), \beta_{C_2}(b_1), \beta_{C_2}(b_2)), \end{aligned}$$

$$
\begin{aligned}
(d_\gamma)_{Gr_1 \diamond Gr_2}(a_1, b_1) &= \sum_{((a_1,b_1),(a_2,b_2)) \in \mathscr{E}_1 \times \mathscr{E}_2} \gamma_{D_1} \diamond \gamma_{D_2}((a_1, b_1), (a_2, b_2)) \\
&= \sum_{\substack{a_1=a_2, \\ (b_1,b_2) \in \mathscr{E}_2}} min(\gamma_{C_1}(a_1), \gamma_{D_2}(b_1, b_2)) \\
&\quad + \sum_{\substack{(a_1,a_2) \in \mathscr{E}_1, \\ (b_1,b_2) \notin \mathscr{E}_2}} min(\gamma_{D_1}(a_1, a_2), \gamma_{C_2}(b_1), \gamma_{C_2}(b_2))
\end{aligned}
$$

Definition 3.11. *(Total degree of homomorphic product on PyCNGs)*
Consider PyCNGs $Gr_1 = (C_1, D_1)$ *and* $Gr_2 = (C_2, D_2)$ *of the graph* $\mathscr{G}_1 = (\mathscr{V}_1, \mathscr{E}_1)$ *and* $\mathscr{G}_2 = (\mathscr{V}_2, \mathscr{E}_2)$*, respectively. At any vertex* $(a_1, a_2) \in \mathscr{V}_1 \times \mathscr{V}_2$*:*

$$
\begin{aligned}
(td_\alpha)_{Gr_1 \diamond Gr_2}(a_1, b_1) &= \sum_{((a_1,b_1),(a_2,b_2)) \in \mathscr{E}_1 \times \mathscr{E}_2} \alpha_{D_1} \diamond \alpha_{D_2}((a_1, b_1), (a_2, b_2)) + \alpha_{C_1} \diamond \alpha_{C_2}(a_1, b_1) \\
&= \sum_{\substack{a_1=a_2, \\ (b_1,b_2) \in \mathscr{E}_2}} max(\alpha_{C_1}(a_1), \alpha_{D_2}(b_1, b_2)) \\
&\quad + \sum_{\substack{(a_1,a_2) \in \mathscr{E}_1, \\ (b_1,b_2) \notin \mathscr{E}_2}} max(\alpha_{D_1}(a_1, a_2), \alpha_{C_2}(b_1), \alpha_{C_2}(b_2)) \\
&\quad + max(\alpha_{C_1}(a_1), \alpha_{C_2}(b_1)),
\end{aligned}
$$

$$
\begin{aligned}
(td_\beta)_{Gr_1 \diamond Gr_2}(a_1, b_1) &= \sum_{((a_1,b_1),(a_2,b_2)) \in \mathscr{E}_1 \times \mathscr{E}_2} \beta_{D_1} \diamond \beta_{D_2}((a_1, b_1), (a_2, b_2)) + \beta_{C_1} \diamond \beta_{C_2}(a_1, b_1) \\
&= \sum_{\substack{a_1=a_2, \\ (b_1,b_2) \in \mathscr{E}_2}} max(\beta_{C_1}(a_1), \beta_{D_2}(b_1, b_2)) \\
&\quad + \sum_{\substack{(a_1,a_2) \in \mathscr{E}_1, \\ (b_1,b_2) \notin \mathscr{E}_2}} max(\beta_{D_1}(a_1, a_2), \beta_{C_2}(b_1), \beta_{C_2}(b_2)) \\
&\quad + min(\beta_{C_1}(a_1), \beta_{C_2}(b_1)),
\end{aligned}
$$

$$
\begin{aligned}
(td_\gamma)_{Gr_1 \diamond Gr_2}(a_1, b_1) &= \sum_{((a_1,b_1),(a_2,b_2)) \in \mathscr{E}_1 \times \mathscr{E}_2} \gamma_{D_1} \diamond \gamma_{D_2}((a_1, b_1), (a_2, b_2)) + \gamma_{C_1} \diamond \gamma_{C_2}(a_1, b_1) \\
&= \sum_{\substack{a_1=a_2, \\ (b_1,b_2) \in \mathscr{E}_2}} min(\gamma_{C_1}(a_1), \gamma_{D_2}(b_1, b_2)) \\
&\quad + \sum_{\substack{(a_1,a_2) \in \mathscr{E}_1, \\ (b_1,b_2) \notin \mathscr{E}_2}} min(\gamma_{D_1}(a_1, a_2), \gamma_{C_2}(b_1), \gamma_{C_2}(b_2)) \\
&\quad + max(\gamma_{C_1}(a_1), \gamma_{C_2}(b_1))
\end{aligned}
$$

Example 3.12.

Examine

the homomorphic product on PyCNGs, as shown in the Figure 3. Then the degree of the vertex (a_1, b_1) *is* $d_{Gr_1 \diamond Gr_2}(a_1, b_1) = ((d_\alpha)_{Gr_1 \diamond Gr_2}(a_1, b_1), (d_\beta)_{Gr_1 \diamond Gr_2}(a_1, b_1), (d_\gamma)_{Gr_1 \diamond Gr_2}(a_1, b_1))$

= (0.5,0.7,0.5) and the total degree of the vertex (a_1, b_1) *is* $td_{Gr_1 \diamond Gr_2}(a_1, b_1)$= $((td_\alpha)_{Gr_1 \diamond Gr_2}(a_1, b_1), (td_\beta)_{Gr_1 \diamond Gr_2}(a_1, b_1), (td_\gamma)_{Gr_1 \diamond Gr_2}(a_1, b_1))$= *(0.8,1.2,1.0). Likewise, the degree and total degree of remaining vertices are obtained by* $d_{Gr_1 \diamond Gr_2}(a_1, b_2)$= *(0.5,0.7,0.5),* $td_{Gr_1 \diamond Gr_2}(a_1, b_2)$= *(0.9,1.3,1.0),* $d_{Gr_1 \diamond Gr_2}(a_2, b_1)$= *(0.5,0.7,0.7),* $td_{Gr_1 \diamond Gr_2}(a_2, b_1)$= *(1.0,1.3,1.4),* $d_{Gr_1 \diamond Gr_2}(a_2, b_2)$= *(0.5,0.7,0.7) and* $td_{Gr_1 \diamond Gr_2}(a_2, b_2)$= *(1.0,,1.3,1.4).*

Theorem 3.13. *Consider PyCNGs* $Gr_1 = (C_1, D_1)$ *and* $Gr_2 = (C_2, D_2)$. *If* Gr_2 *is a Pythagorean co-neutrosophic complete graph and* $\alpha_{C_1} \geq \alpha_{D_2}$, $\beta_{C_1} \geq \beta_{D_2}$, $\gamma_{C_1} \leq \gamma_{D_2}$, *then* $d_{Gr_1 \diamond Gr_2}(a_1, b_1) = ((|\mathscr{V}_2| - 1)\alpha_{C_1}(a_1), |\mathscr{V}_2| - 1)\beta_{C_1}(a_1), |\mathscr{V}_2| - 1)\gamma_{C_1}(a_1))$.

Proof. We have, vertex degree of each membership in a homomorphic product as

$$
\begin{aligned}
(d_\alpha)_{Gr_1 \diamond Gr_2}(a_1, b_1) &= \sum_{((a_1,b_1),(a_2,b_2)) \in \mathscr{E}_1 \times \mathscr{E}_2} \alpha_{D_1} \diamond \alpha_{D_2}((a_1, b_1), (a_2, b_2)) \\
&= \sum_{\substack{a_1 = a_2, \\ (b_1,b_2) \in \mathscr{E}_2}} max(\alpha_{C_1}(a_1), \alpha_{D_2}(b_1, b_2)) \\
&\quad + \sum_{\substack{(a_1,a_2) \in \mathscr{E}_1, \\ (b_1,b_2) \notin \mathscr{E}_2}} max(\alpha_{D_1}(a_1, a_2), \alpha_{C_2}(b_1), \alpha_{C_2}(b_2)) \\
&= \sum_{\substack{a_1 = a_2, \\ (b_1,b_2) \in \mathscr{E}_2}} max(\alpha_{C_1}(a_1), \alpha_{D_2}(b_1, b_2)) \\
&\quad [since\ Gr_2\ is\ a\ pythagorean\ co-neutrosophic\ complete\ graph] \\
&= \sum_{a_1 = a_2} \alpha_{C_1}(a_1) \quad [since\ \alpha_{C_1} \geq \alpha_{D_2}] \\
&= (|\mathscr{V}_2| - 1)\alpha_{C_1}(a_1),
\end{aligned}
$$

$$
\begin{aligned}
(d_\beta)_{Gr_1 \diamond Gr_2}(a_1, b_1) &= \sum_{((a_1,b_1),(a_2,b_2)) \in \mathscr{E}_1 \times \mathscr{E}_2} \beta_{D_1} \diamond \beta_{D_2}((a_1, b_1), (a_2, b_2)) \\
&= \sum_{\substack{a_1 = a_2, \\ (b_1,b_2) \in \mathscr{E}_2}} max(\beta_{C_1}(a_1), \beta_{D_2}(b_1, b_2)) \\
&\quad + \sum_{\substack{(a_1,a_2) \in \mathscr{E}_1, \\ (b_1,b_2) \notin \mathscr{E}_2}} max(\beta_{D_1}(a_1, a_2), \beta_{C_2}(b_1), \beta_{C_2}(b_2)) \\
&= \sum_{\substack{a_1 = a_2, \\ (b_1,b_2) \in \mathscr{E}_2}} max(\beta_{C_1}(a_1), \beta_{D_2}(b_1, b_2)) \\
&\quad [since\ Gr_2\ is\ a\ pythagorean\ co-neutrosophic\ complete\ graph] \\
&= \sum_{a_1 = a_2} \beta_{C_1}(a_1) \quad [since\ \beta_{C_1} \geq \beta_{D_2}] \\
&= (|\mathscr{V}_2| - 1)\beta_{C_1}(a_1),
\end{aligned}
$$

$$
\begin{aligned}
(d_\gamma)_{Gr_1 \diamond Gr_2}(a_1, b_1) &= \sum_{((a_1,b_1),(a_2,b_2)) \in \mathscr{E}_1 \times \mathscr{E}_2} \gamma_{D_1} \diamond \gamma_{D_2}((a_1, b_1), (a_2, b_2)) \\
&= \sum_{\substack{u_1 = u_2, \\ (v_1, v_2) \in \mathscr{E}_2}} min(\gamma_{C_1}(a_1), \gamma_{D_2}(b_1, b_2)) \\
&\quad + \sum_{\substack{(a_1, a_2) \in \mathscr{E}_1, \\ (b_1, b_2) \notin \mathscr{E}_2}} min(\gamma_{D_1}(a_1, a_2), \gamma_{C_2}(b_1), \gamma_{C_2}(b_2)) \\
&= \sum_{\substack{a_1 = a_2, \\ (b_1, b_2) \in \mathscr{E}_2}} min(\gamma_{C_1}(a_1), \gamma_{D_2}(b_1, b_2)) \\
&\quad [since\ Gr_2\ is\ a\ pythagorean\ co-neutrosophic\ complete\ graph] \\
&= \sum_{a_1 = a_2} \gamma_{C_1}(a_1) \ \ [since\ \gamma_{C_1} \leq \gamma_{D_2}] \\
&= (|\mathscr{V}_2| - 1)\gamma_{C_1}(a_1)
\end{aligned}
$$

Therefore, we conclude that $d_{Gr_1 \diamond Gr_2}(a_1, b_1) = ((|\mathscr{V}_2| - 1)\alpha_{C_1}(a_1), |\mathscr{V}_2| - 1)\beta_{C_1}(a_1), |\mathscr{V}_2| - 1)\gamma_{C_1}(a_1))$.

Definition 3.14. *(Symmetric difference on PyCNGs)*
Consider PyCNGs $Gr_1 = (C_1, D_1)$ and $Gr_2 = (C_2, D_2)$ of the graphs $\mathscr{G}_1 = (\mathscr{V}_1, \mathscr{E}_1)$ and $\mathscr{G}_2 = (\mathscr{V}_2, \mathscr{E}_2)$, respectively. Then, the symmetric difference of Gr_1 and Gr_2 is denoted by $Gr_1 \oplus Gr_2 = (C_1 \oplus C_2, D_1 \oplus D_2)$ and defined as:

(a) $\forall (f, g) \in \mathscr{V}_1 \times \mathscr{V}_2$,
  (i) $\alpha_{C_1} \oplus \alpha_{C_2}(f, g) = max(\alpha_{C_1}(f), \alpha_{C_2}(g))$,
  (ii) $\beta_{C_1} \oplus \beta_{C_2}(f, g) = max(\beta_{C_1}(f), \beta_{C_2}(g))$ *and*
  (iii) $\gamma_{C_1} \oplus \gamma_{C_2}(f, g) = min(\gamma_{C_1}(f), \gamma_{C_2}(g))$;

(b) $\forall f \in \mathscr{V}_1$ *and* $(g, h) \in \mathscr{E}_2$,
  (i) $(\alpha_{D_1} \oplus \alpha_{D_2}((f, g), (f, h)) = max(\alpha_{C_1}(f), \alpha_{D_2}(g, h))$;
  (ii) $(\beta_{D_1} \oplus \beta_{D_2}((f, g), (f, h)) = max(\beta_{C_1}(f), \beta_{D_2}(g, h))$;
  (iii) $(\gamma_{D_1} \oplus \gamma_{D_2}((f, g), (f, h)) = min(\gamma_{C_1}(f), \gamma_{D_2}(g, h))$;

(c) $\forall f \in \mathscr{V}_2$ *and* $(g, h) \in \mathscr{E}_1$,
  (i) $(\alpha_{D_1} \oplus \alpha_{D_2}((g, f), (h, f)) = max(\alpha_{D_1}(g, h), \alpha_{C_2}(f))$;
  (ii) $(\beta_{D_1} \oplus \beta_{D_2}((g, f), (h, f)) = max(\beta_{D_1}(g, h), \beta_{C_2}(f))$;
  (iii) $(\gamma_{D_1} \oplus \gamma_{D_2}((g, f), (h, f)) = min(\gamma_{D_1}(g, h), \gamma_{C_2}(f))$;

(d) $\forall (f, g) \notin \mathscr{E}_1$ *and* $(h, e) \in \mathscr{E}_2$,
  (i) $(\alpha_{D_1} \oplus \alpha_{D_2}((f, h), (g, e)) = max(\alpha_{C_1}(f), \alpha_{C_1}(g), \alpha_{D_2}(h, e))$;
  (ii) $(\beta_{D_1} \oplus \beta_{D_2}((f, h), (g, e)) = max(\beta_{C_1}(f), \beta_{C_1}(g), \beta_{D_2}(h, e))$;

(iii) $(\gamma_{D_1} \oplus \gamma_{D_2})((f,h),(g,e)) = min(\gamma_{C_1}(f), \gamma_{C_1}(g), \gamma_{D_2}(h,e))$;

(e) $\forall (f,g) \in \mathscr{E}_1$ *and* $(h,e) \notin \mathscr{E}_2$,

(i) $(\alpha_{D_1} \oplus \alpha_{D_2})((f,h),(g,e)) = max(\alpha_{D_1}(f,g), \alpha_{C_2}(h), \alpha_{C_2}(e))$;

(ii) $(\beta_{D_1} \oplus \beta_{D_2})((f,h),(g,e)) = max(\beta_{D_1}(f,g), \beta_{C_2}(h), \beta_{C_2}(e))$;

(iii) $(\gamma_{D_1} \oplus \gamma_{D_2})((f,h),(g,e)) = min(\gamma_{D_1}(f,g), \gamma_{C_2}(h), \gamma_{C_2}(e))$.

Remark 3.15. *The strong product on PyCNGs is quite similar to the symmetric difference, if the conditions* (d) & (e) *of symmetric difference definition 3.14 are combined. With the same conditions* $(a),(b),(c)$ *of symmetric difference, the following condition is needed to define strong product on PyCNGs:*

(f) $\forall (f,g) \in \mathscr{E}_1$ *and* $(h,e) \in \mathscr{E}_2$,

(i) $(\alpha_{D_1} \oplus \alpha_{D_2})((f,h),(g,e)) = max(\alpha_{D_1}(f,g), \alpha_{D_2}(h,e))$;

(ii) $(\beta_{D_1} \oplus \beta_{D_2})((f,h),(g,e)) = max(\beta_{D_1}(f,g), \beta_{D_2}(h,e))$;

(iii) $(\gamma_{D_1} \oplus \gamma_{D_2})((f,h),(g,e)) = min(\gamma_{D_1}(f,g), \gamma_{D_2}(h,e))$.

Theorem 3.16. *Consider PyCNGs* Gr_1 *and* Gr_2 *of the graphs* $\mathscr{G}_1$ *and* $\mathscr{G}_2$*, respectively. Then symmetric difference* $Gr_1 \oplus Gr_2$ *of* Gr_1 *and* Gr_2 *is a PyCNG.*

Proof.

Let us take $Gr_1 = (C_1, D_1)$ and $Gr_2 = (C_2, D_2)$ to be PyCNGs of the graphs $\mathscr{G}_1 = (\mathscr{V}_1, \mathscr{E}_1)$ and $\mathscr{G}_2 = (\mathscr{V}_2, \mathscr{E}_2)$, respectively.

(i) Let $a_1 \in \mathscr{V}_1$ and $(b_1, b_2) \in \mathscr{E}_2$. Then,

$$\begin{aligned}(\alpha_{D_1} \oplus \alpha_{D_2})((a_1,b_1),(a_1,b_2)) &= max(\alpha_{C_1}(a_1), \alpha_{D_2}(b_1,b_2)) \\ &= max(\alpha_{C_1}(a_1), \alpha_{C_2}(b_1), \alpha_{C_2}(b_2)) \\ &= max(max(\alpha_{C_1}(a_1), \alpha_{C_2}(b_1)), max(\alpha_{C_1}(a_1), \alpha_{C_2}(b_2))) \\ &= max((\alpha_{C_1} \oplus \alpha_{C_2})(a_1,b_1), (\alpha_{C_1} \oplus \alpha_{C_2})(a_1,b_2)),\end{aligned}$$

$$\begin{aligned}(\beta_{D_1} \oplus \beta_{D_2})((a_1,b_1),(a_1,b_2)) &= max(\beta_{C_1}(a_1), \beta_{D_2}(b_1,b_2)) \\ &= max(\beta_{C_1}(a_1), \beta_{C_2}(b_1), \beta_{C_2}(b_2)) \\ &= max(max(\beta_{C_1}(a_1), \beta_{C_2}(b_1)), max(\beta_{C_1}(a_1), \beta_{C_2}(b_2))) \\ &= max((\beta_{C_1} \oplus \beta_{C_2})(a_1,b_1), (\beta_{C_1} \oplus \beta_{C_2})(a_1,b_2)),\end{aligned}$$

$$\begin{aligned}(\gamma_{D_1} \oplus \gamma_{D_2})((a_1, b_1), (a_1, b_2)) &= min(\gamma_{C_1}(a_1), \gamma_{D_2}(b_1, b_2)) \\ &= min(\gamma_{C_1}(a_1), \gamma_{C_2}(b_1), \gamma_{C_2}(b_2)) \\ &= min(min(\gamma_{C_1}(a_1), \gamma_{C_2}(b_1)), min(\gamma_{C_1}(a_1), \gamma_{C_2}(b_2))) \\ &= min((\gamma_{C_1} \oplus \gamma_{C_2})(a_1, b_1), (\gamma_{C_1} \oplus \gamma_{C_2})(a_1, b_2)).\end{aligned}$$

(ii) Let $(a_1, a_2) \in \mathscr{E}_1$ and $b_1 \in \mathscr{V}_2$. Then,

$$\begin{aligned}(\alpha_{D_1} \oplus \alpha_{D_2})((a_1, b_1), (a_2, b_1)) &= max(\alpha_{D_1}(a_1, a_2), \alpha_{C_2}(b_1)) \\ &= max(\alpha_{C_1}(a_1), \alpha_{C_1}(a_2), \alpha_{C_2}(b_1)) \\ &= max(max(\alpha_{C_1}(a_1), \alpha_{C_2}(b_1)), max(\alpha_{C_1}(a_2), \alpha_{C_2}(b_1))) \\ &= max((\alpha_{C_1} \oplus \alpha_{C_2})(a_1, b_1), (\alpha_{C_1} \oplus \alpha_{C_2})(a_2, b_1)),\end{aligned}$$

$$\begin{aligned}(\beta_{D_1} \oplus \beta_{D_2})((a_1, b_1), (a_2, b_1)) &= max(\beta_{D_1}(a_1, a_2), \beta_{C_2}(b_1)) \\ &= max(\beta_{C_1}(a_1), \beta_{C_1}(a_2), \beta_{C_2}(b_1)) \\ &= max(max(\beta_{C_1}(a_1), \beta_{C_2}(b_1), max(\beta_{C_1}(a_2), \beta_{C_2}(b_1))) \\ &= max((\beta_{C_1} \oplus \beta_{C_2})(a_1, b_1), (\beta_{C_1} \oplus \beta_{C_2})(a_2, b_1)),\end{aligned}$$

$$\begin{aligned}(\gamma_{D_1} \oplus \gamma_{D_2})((a_1, b_1), (a_2, b_1)) &= min(\gamma_{D_1}(a_1, a_2), \gamma_{C_2}(b_1)) \\ &= min(\gamma_{C_1}(a_1), \gamma_{C_1}(a_2), \gamma_{C_2}(b_1)) \\ &= min(min(\gamma_{C_1}(a_1), \gamma_{C_2}(b_1)), min(\gamma_{C_1}(a_2), \gamma_{C_2}(b_1))) \\ &= min((\gamma_{C_1} \oplus \gamma_{C_2})(a_1, b_1), (\gamma_{C_1} \oplus \gamma_{C_2})(a_2, b_1)).\end{aligned}$$

(iii) Let $(a_1, a_2) \notin \mathscr{E}_1$ and $(b_1, b_2) \in \mathscr{E}_2$. Then,

$$\begin{aligned}(\alpha_{D_1} \oplus \alpha_{D_2})((a_1, b_1), (a_2, b_2)) &= max(\alpha_{C_1}(a_1), \alpha_{C_1}(a_2), \alpha_{D_2}(b_1, b_2)) \\ &= max(\alpha_{C_1}(a_1), \alpha_{C_1}(a_2), \alpha_{C_2}(b_1), \alpha_{C_2}(b_2)) \\ &= max(\alpha_{C_1}(a_1), \alpha_{C_2}(b_1), \alpha_{C_1}(a_2), \alpha_{C_2}(b_2)) \\ &= max((\alpha_{C_1} \oplus \alpha_{C_2})(a_1, b_1), (\alpha_{C_1} \oplus \alpha_{C_2})(a_2, b_2)),\end{aligned}$$

$$\begin{aligned}(\beta_{D_1} \oplus \beta_{D_2})((a_1, b_1), (a_2, b_2)) &= max(\beta_{C_1}(a_1), \beta_{C_1}(a_2), \beta_{D_2}(b_1, b_2)) \\ &= max(\beta_{C_1}(a_1), \beta_{C_1}(a_2), \beta_{C_2}(b_1), \beta_{C_2}(b_2)) \\ &= max(\beta_{C_1}(a_1), \beta_{C_2}(b_1), \beta_{C_1}(a_2), \beta_{C_2}(b_2)) \\ &= max((\beta_{C_1} \oplus \beta_{C_2})(a_1, b_1), (\beta_{C_1} \oplus \beta_{C_2})(a_2, b_2)),\end{aligned}$$

$$\begin{aligned}(\gamma_{D_1} \oplus \gamma_{D_2})((a_1,b_1),(a_2,b_2)) &= min(\gamma_{C_1}(a_1),\gamma_{C_1}(a_2),\gamma_{D_2}(b_1,b_2))\\ &= min(\gamma_{C_1}(a_1),\gamma_{C_1}(a_2),\gamma_{C_2}(b_1),\gamma_{C_2}(b_2))\\ &= min(\gamma_{C_1}(a_1),\gamma_{C_2}(b_1),\gamma_{C_1}(a_2),\gamma_{C_2}(b_2))\\ &= min((\gamma_{C_1} \oplus \gamma_{C_2})(a_1,b_1),(\gamma_{C_1} \oplus \gamma_{C_2})(a_2,b_2)).\end{aligned}$$

(iv) Let $(a_1,a_2) \in \mathscr{E}_1$ and $(b_1,b_2) \notin \mathscr{E}_2$. Then,

$$\begin{aligned}(\alpha_{D_1} \oplus \alpha_{D_2})((a_1,b_1),(a_2,b_2)) &= max(\alpha_{D_1}(a_1,a_2),\alpha_{C_2}(b_1),\alpha_{C_2}(b_2))\\ &= max(\alpha_{C_1}(a_1),\alpha_{C_1}(a_2),\alpha_{C_2}(b_1),\alpha_{C_2}(b_2))\\ &= max(\alpha_{C_1}(a_1),\alpha_{C_2}(b_1),\alpha_{C_1}(a_2),\alpha_{C_2}(b_2))\\ &= max((\alpha_{C_1} \oplus \alpha_{C_2})(a_1,b_1),(\alpha_{C_1} \oplus \alpha_{C_2})(a_2,b_2)),\end{aligned}$$

$$\begin{aligned}(\beta_{D_1} \oplus \beta_{D_2})((a_1,b_1),(a_2,b_2)) &= max(\beta_{D_1}(a_1,a_2),\beta_{C_2}(b_1),\beta_{C_2}(b_2))\\ &= max(\beta_{C_1}(a_1),\beta_{C_1}(a_2),\beta_{C_2}(b_1),\beta_{C_2}(b_2))\\ &= max(\beta_{C_1}(a_1),\beta_{C_2}(b_1),\beta_{C_1}(a_2),\beta_{C_2}(b_2))\\ &= max((\beta_{C_1} \oplus \beta_{C_2})(a_1,b_1),(\beta_{C_1} \oplus \beta_{C_2})(a_2,b_2)),\end{aligned}$$

$$\begin{aligned}(\gamma_{D_1} \oplus \gamma_{D_2})((a_1,b_1),(a_2,b_2)) &= min(\gamma_{D_1}(a_1,a_2),\gamma_{C_2}(b_1),\gamma_{C_2}(b_2))\\ &= min(\gamma_{C_1}(a_1),\gamma_{C_1}(a_2),\gamma_{C_2}(b_1),\gamma_{C_2}(b_2))\\ &= min(\gamma_{C_1}(a_1),\gamma_{C_2}(b_1),\gamma_{C_1}(a_2),\gamma_{C_2}(b_2))\\ &= min((\gamma_{C_1} \oplus \gamma_{C_2})(a_1,b_1),(\gamma_{C_1} \oplus \gamma_{C_2})(a_2,b_2)).\end{aligned}$$

Hence the proof.

Definition 3.17. *(Degree of the symmetric difference on PyCNGs)*
Let us take $Gr_1 = (C_1, D_1)$ and $Gr_2 = (C_2, D_2)$ to be PyCNGs of the graphs $\mathscr{G}_1 = (\mathscr{V}_1, \mathscr{E}_1)$ and $\mathscr{G}_2 = (\mathscr{V}_2, \mathscr{E}_2)$, respectively. At any vertex $(a_1, a_2) \in \mathscr{V}_1 \times \mathscr{V}_2$:

$$\begin{aligned}(d_\alpha)_{Gr_1 \oplus Gr_2}(a_1,a_2) &= \sum_{((a_1,a_2),(b_1,b_2)) \in \mathscr{E}_1 \times \mathscr{E}_2} \alpha_{D_1} \oplus \alpha_{D_2}((a_1,a_2),(b_1,b_2))\\ &= \sum_{\substack{a_1=b_1 \in \mathscr{V}_1,\\ (a_2,b_2) \in \mathscr{E}_2}} max(\alpha_{C_1}(a_1),\alpha_{D_2}(a_2,b_2)) + \sum_{\substack{(a_1,b_1) \in \mathscr{E}_1,\\ a_2=b_2 \in \mathscr{V}_2}} max(\alpha_{D_1}(a_1,b_1),\alpha_{C_2}(b_1))\\ &\quad + \sum_{\substack{(a_1,b_1) \notin \mathscr{E}_1,\\ (a_2,b_2) \in \mathscr{E}_2}} max(\alpha_{C_1}(a_1),\alpha_{C_1}(b_1),\alpha_{D_2}(a_2,b_2))\\ &\quad + \sum_{\substack{(a_1,b_1) \in \mathscr{E}_1,\\ (a_2,b_2) \notin \mathscr{E}_2}} max(\alpha_{C_1}(a_1,b_1),\alpha_{C_2}(a_2),\alpha_{C_2}(b_2)),\end{aligned}$$

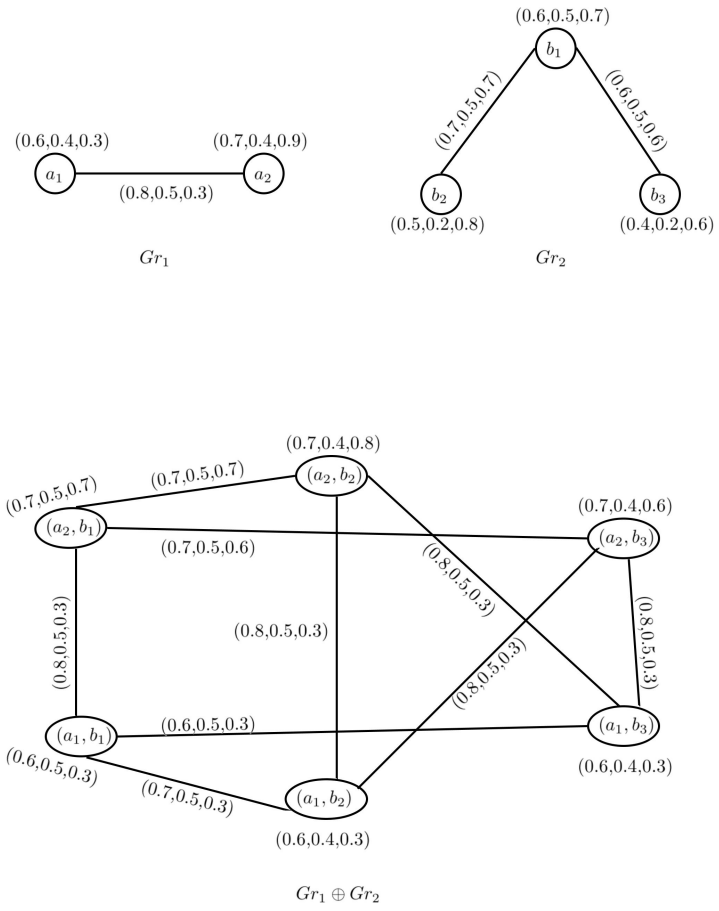

FIGURE 4. Gr_1 & Gr_2, Symmetric difference $Gr_1 \oplus Gr_2$

$$
\begin{aligned}
(d_\beta)_{Gr_1 \oplus Gr_2}(a_1, a_2) &= \sum_{((a_1,a_2),(b_1,b_2)) \in \mathscr{E}_1 \times \mathscr{E}_2} \beta_{D_1} \oplus \beta_{D_2}((a_1, a_2), (b_1, b_2)) \\
&= \sum_{\substack{a_1 = b_1 \in \mathscr{V}_1, \\ (a_2,b_2) \in \mathscr{E}_2}} max(\beta_{C_1}(a_1), \beta_{D_2}(a_2, b_2)) + \sum_{\substack{(a_1,b_1) \in \mathscr{E}_1, \\ a_2 = b_2 \in \mathscr{V}_2}} max(\beta_{D_1}(a_1, b_1), \beta_{C_2}(b_1)) \\
&\quad + \sum_{\substack{(a_1,b_1) \notin \mathscr{E}_1, \\ (a_2,b_2) \in \mathscr{E}_2}} max(\beta_{C_1}(a_1), \beta_{C_1}(b_1), \beta_{D_2}(a_2, b_2)) \\
&\quad + \sum_{\substack{(a_1,b_1) \in \mathscr{E}_1, \\ (a_2,b_2) \notin \mathscr{E}_2}} max(\beta_{C_1}(a_1, b_1), \beta_{C_2}(a_2), \beta_{C_2}(b_2)),
\end{aligned}
$$

$$
\begin{aligned}
(d_\gamma)_{Gr_1\oplus Gr_2}(a_1,a_2) &= \sum_{((a_1,a_2),(b_1,b_2))\in\mathscr{E}_1\times\mathscr{E}_2} \gamma_{D_1}\oplus\gamma_{D_2}((a_1,a_2),(b_1,b_2)) \\
&= \sum_{\substack{a_1=b_1\in\mathscr{V}_1,\\(a_2,b_2)\in\mathscr{E}_2}} min(\gamma_{C_1}(a_1),\gamma_{D_2}(a_2,b_2)) + \sum_{\substack{(a_1,b_1)\in\mathscr{E}_1,\\a_2=b_2\in\mathscr{V}_2}} min(\gamma_{D_1}(a_1,b_1),\gamma_{C_2}(b_1)) \\
&\quad + \sum_{\substack{(a_1,b_1)\notin\mathscr{E}_1,\\(a_2,b_2)\in\mathscr{E}_2}} min(\gamma_{C_1}(a_1),\gamma_{C_1}(b_1),\gamma_{D_2}(a_2,b_2)) \\
&\quad + \sum_{\substack{(a_1,b_1)\in\mathscr{E}_1,\\(a_2,b_2)\notin\mathscr{E}_2}} min(\gamma_{C_1}(a_1,b_1),\gamma_{C_2}(a_2),\gamma_{C_2}(b_2)).
\end{aligned}
$$

Definition 3.18. *(Total degree of the symmetric difference on PyCNGs)*
Consider PyCNGs $Gr_1 = (C_1, D_1)$ and $Gr_2 = (C_2, D_2)$ of the graphs $\mathscr{G}_1 = (\mathscr{V}_1, \mathscr{E}_1)$ and $\mathscr{G}_2 = (\mathscr{V}_2, \mathscr{E}_2)$, respectively. At any vertex $(a_1, a_2) \in \mathscr{V}_1 \times \mathscr{V}_2$:

$$
\begin{aligned}
(td_\alpha)_{Gr_1\oplus Gr_2}(a_1,a_2) &= \sum_{((a_1,a_2),(b_1,b_2))\in\mathscr{E}_1\times\mathscr{E}_2} \alpha_{D_1}\oplus\alpha_{D_2}((a_1,a_2),(b_1,b_2)) \\
&= \sum_{\substack{a_1=b_1\in\mathscr{V}_1,\\(a_2,b_2)\in\mathscr{E}_2}} max(\alpha_{C_1}(a_1),\alpha_{D_2}(a_2,b_2)) + \sum_{\substack{(a_1,b_1)\in\mathscr{E}_1,\\a_2=b_2\in\mathscr{V}_2}} max(\alpha_{D_1}(a_1,b_1),\alpha_{C_2}(b_1)) \\
&\quad + \sum_{\substack{(a_1,b_1)\notin\mathscr{E}_1,\\(a_2,b_2)\in\mathscr{E}_2}} max(\alpha_{C_1}(a_1),\alpha_{C_1}(b_1),\alpha_{D_2}(a_2,b_2)) \\
&\quad + \sum_{\substack{(a_1,b_1)\in\mathscr{E}_1,\\(a_2,b_2)\notin\mathscr{E}_2}} max(\alpha_{C_1}(a_1,b_1),\alpha_{C_2}(a_2),\alpha_{C_2}(b_2)) + max(\alpha_{C_1}(a_1),\alpha_{C_2}(a_2)),
\end{aligned}
$$

$$
\begin{aligned}
(td_\beta)_{Gr_1\oplus Gr_2}(a_1,a_2) &= \sum_{((a_1,a_2),(b_1,b_2))\in\mathscr{E}_1\times\mathscr{E}_2} \beta_{D_1}\oplus\beta_{D_2}((a_1,a_2),(b_1,b_2)) \\
&= \sum_{\substack{a_1=b_1\in\mathscr{V}_1,\\(a_2,b_2)\in\mathscr{E}_2}} max(\beta_{C_1}(a_1),\beta_{D_2}(a_2,b_2)) + \sum_{\substack{(a_1,b_1)\in\mathscr{E}_1,\\a_2=b_2\in\mathscr{V}_2}} max(\beta_{D_1}(a_1,b_1),\beta_{C_2}(b_1)) \\
&\quad + \sum_{\substack{(a_1,b_1)\notin\mathscr{E}_1,\\(a_2,b_2)\in\mathscr{E}_2}} max(\beta_{C_1}(a_1),\beta_{C_1}(b_1),\beta_{D_2}(a_2,b_2)) \\
&\quad + \sum_{\substack{(a_1,b_1)\in\mathscr{E}_1,\\(a_2,b_2)\notin\mathscr{E}_2}} max(\beta_{C_1}(a_1,b_1),\beta_{C_2}(a_2),\beta_{C_2}(b_2)) + max(\beta_{C_1}(a_1),\beta_{C_2}(a_2)),
\end{aligned}
$$

$$
\begin{aligned}
(td_\gamma)_{Gr_1\oplus Gr_2}(a_1,a_2) &= \sum_{((a_1,a_2),(b_1,b_2))\in\mathscr{E}_1\times\mathscr{E}_2} \gamma_{D_1}\oplus\gamma_{D_2}((a_1,a_2),(b_1,b_2)) \\
&= \sum_{\substack{a_1=b_1\in\mathscr{V}_1,\\(a_2,b_2)\in\mathscr{E}_2}} min(\gamma_{C_1}(a_1),\gamma_{D_2}(a_2,b_2)) + \sum_{\substack{(a_1,b_1)\in\mathscr{E}_1,\\a_2=b_2\in\mathscr{V}_2}} min(\gamma_{D_1}(a_1,b_1),\gamma_{C_2}(b_1)) \\
&\quad + \sum_{\substack{(a_1,b_1)\notin\mathscr{E}_1,\\(a_2,b_2)\in\mathscr{E}_2}} min(\gamma_{C_1}(a_1),\gamma_{C_1}(b_1),\gamma_{D_2}(a_2,b_2)) \\
&\quad + \sum_{\substack{(a_1,b_1)\in\mathscr{E}_1,\\(a_2,b_2)\notin\mathscr{E}_2}} min(\gamma_{C_1}(a_1,b_1),\gamma_{C_2}(a_2),\gamma_{C_2}(b_2)) + min(\gamma_{C_1}(a_1),\gamma_{C_2}(a_2)).
\end{aligned}
$$

Example 3.19.

As per Figure 4, examine the symmetric difference on PyCNGs. Then the vertex degree of (a_1,b_1) *is* $d_{Gr_1\oplus Gr_2}(a_1,b_1)=((d_\alpha)_{Gr_1\oplus Gr_2}(a_1,b_1),(d_\beta)_{Gr_1\oplus Gr_2}(a_1,b_1),(d_\gamma)_{Gr_1\oplus Gr_2}(a_1,b_1))=$ *(2.1,1.5,0.9) and the vertex total degree of* (a_1,b_1) *is* $td_{Gr_1\oplus Gr_2}(a_1,b_1)=((td_\alpha)_{Gr_1\oplus Gr_2}(a_1,b_1),(td_\beta)_{Gr_1\oplus Gr_2}(a_1,b_1),(td_\gamma)_{Gr_1\oplus Gr_2}(a_1,b_1))=$ *(2.7,2.0,1.2). Likewise, the vertex degree and vertex total degree of the balance vertices are obtained by* $d_{Gr_1\oplus Gr_2}(a_2,b_1)=$ *(2.2,1.5,1.6),* $td_{Gr_1\oplus Gr_2}(a_2,b_1)=$ *(2.9,2.0,2.3),* $d_{Gr_1\oplus Gr_2}(a_1,b_2)=$ *(2.3,1.5,0.9),* $td_{Gr_1\oplus Gr_2}(a_1,b_2)=$ *(2.9,1.9,1.2),* $d_{Gr_1\oplus Gr_2}(a_2,b_2)=$ *(2.3,1.5,1.3),* $td_{Gr_1\oplus Gr_2}(a_2,b_2)=$ *(3.0,1.9,2.1),* $d_{Gr_1\oplus Gr_2}(a_1,b_3)=$ *(2.2,1.5,0.9),* $td_{Gr_1\oplus Gr_2}(a_1,b_3)=$ *(2.8,1.9,1.2),* $d_{Gr_1\oplus Gr_2}(a_2,b_3)=$ *(2.3,1.5,1.2),* $td_{Gr_1\oplus Gr_2}(a_2,b_3)=$ *(3.0,1.9,1.8).*

4. Application of Product on PyCNG in Brain Network Analysis

The human brain is a complex structure of the nervous system, which controls many activities in our body. It comprises different brain regions which are interconnected by neural pathways to perform and regulate various functions like thinking, decision-making, breathing, etc. Graph theory is much useful to structure and demonstrate the brain regions and their interconnecting networks. Here, we consider a Pythagorean co-neutrosophic graphical environment to deal with brain network analysis, since the function of a particular region and the connecting neural path can be studied deeply with three membership functions and their individual weights.

(i) Let us consider the brain graphs $Gr=(V,E)$ of two autism patients with brain's functional regions like the sensory cortex, motor cortex, frontal lobe, parietal lobe, and temporal lobe, where vertex set V denotes the brain regions and edge set E denotes the effective connectivity between different brain regions. Since we are going to deal with Pythagorean co-neutrosophic graph, an explicit declaration about each membership of vertex and edge is essential. The existence, uncertain, and non-existence memberships of vertices denotes brain region's function, inconsistency in functioning, and failure in function, respectively. For edges,

the corresponding memberships may be considered as effective connectivity, inconsistency due to causal influences, and failure in connectivity. In general, kernels are used to define the similarity between a pair of elements. Here, we take the random walk graph kernel, which analyzes the communication network between two different brain network graphs and is used to measure the similarity in the number of random walks by comparing their corresponding random walk probability distributions. If a pair of Pythagorean co-neutrosophic graphs(PyCNGs) Gr_1 and Gr_2 are given, then the kernel executes the random walks on both graphs and compute the amount of matching walks, which will be equivalent to the performance of the random walk on their direct product graph. By using definitions 2.7 and 2.8, we can get the direct product of PyCNGs and the random walk graph kernel of graphs Gr_1 and Gr_2, where the weight matrix and decay factor must be found for each membership. Finally, the functional similarity and communications between these two autism patients will be analyzed by considering the output-direct product graph.

(ii) The shortest path graph kernel is another type of graph kernel, which measures the similarity between two PyCNGs by considering the shortest paths between their vertices. This kernel is generally suitable for graphs, where the distance between vertices is considered as road transport, social networks, molecular distance, etc. Here, the shortest path graph kernel will be used to measure the similarity by considering the shortest path between the neural elements. Also, the product of the wiener indices of two PyCNGs is equivalent to the shortest path kernel on graphs.

5. Conclusion

This paper deals with various products on Pythagorean co-neutrosophic graphs(PyCNGs), and some properties like degree, total degree are explained in the resultant PyCNG with examples, which give more flexible results than Pythagorean fuzzy graphs. Also, an application related to brain network analysis is given as an initiative to continue the progress in PyCNG.

Acknowledgments

The article has been written with the joint financial support of RUSA-Phase 2.0 grant sanctioned vide letter No.F.24-51/2014-U, Policy (TN Multi-Gen), Dept. of Edn. Govt. of India, Dt. 09.10.2018, UGC-SAP (DRS-I) vide letter No.F.510/8/DRS-I/2016(SAP-I) Dt. 23.08.2016 and DST (FST - level I) 657876570 vide letter No.SR/FIST/MS-I/2018/17 Dt. 20.12.2018.

References

[1] Ajay D, Chellamani P. Pythagorean neutrosophic fuzzy graphs. *International Journal of Neutrosophic Science.* 2020; 11(2): 108-114.

[2] Ajay D, Chellamani P, Rajchakit G, Boonsatit N, Hammachukiattikul P. Regularity of Pythagorean neutrosophic graphs with an illustration in MCDM. *AIMS Mathematics.* 2022; 7(5): 9424-9442.

[3] Ajay D, Karthiga S, Chellamani P. A Study on Labelling of Pythagorean Neutrosophic Fuzzy Graphs. *Journal of Computational Mathematica.* 2021; 5(1): 105-116.

[4] Ajay D, Chellamani P. Operations on Pythagorean neutrosophic graphs. *AIP Conference Proceedings.* 2022; 2516(1): 200028.

[5] Akram M, Akmal R. Intuitionistic Fuzzy Graph Structures. *Kragujevac Journal of Mathematics.* 2017; 41(2): 219-237.

[6] Akram M, Dar J.M, Naz S. Certain graphs under Pythagorean fuzzy environment. *Complex & Intelligent Systems.* 2019; 5(2): 127-144.

[7] Arindam Dey, Ranjan Kumar, Said Broumi, Pritam Bhowmik. Different Types of Operations on Neutrosophic Graphs. *International Journal of Neutrosophic Science.* 2022; 19(2): 87-94.

[8] Atanassov K.T. Intuitionistic fuzzy sets. *Fuzzy Sets and Systems.* 1986; 20(1): 87-96.

[9] Bhattacharya P. Some remarks on fuzzy graphs. *Pattern Recognition Letters.* 1987; 6(5): 297-302.

[10] Bhuttani K.R, Battou A. On M-strong fuzzy graphs. *Information Sciences.* 2003; 155(1-2): 103-109.

[11] Broumi S, Smarandache F, Talea M, Bakali A. Single Valued Neutrosophic Graphs: Degree, Order and Size. *IEEE International Conference on Fuzzy Systems(FUZZ).* 2016; 2444-2451.

[12] Dhavaseelan R, Jafari S, Farahani M. R, Broumi S. On single-valued co-neutrosophic graphs. *Neutrosophic Sets and Systems.* 2018; Vol. 22, 180-187.

[13] Kang U, Hanghang Tong, Jimeng Sun. Fast Random Walk Graph Kernel. *Proceedings of the 2012 SIAM International Conference on Data Mining(SDM).* 2012, 828-838.

[14] Kartick Mohanta, Arindam Dey, Anita Pal. A note on different types of product of neutrosophic graphs. *Complex & Intelligent Systems,* 2021; 2: 857-871.

[15] Kaufmann A. Introduction to the Theory of Fuzzy Subsets. *Academic Press: Cambridge, MA, USA.* 1975; 2.

[16] Meenakshi A, Mythreyi O. Applications of Neutrosophic Social Network Using Max Product Networks. *Journal of Intelligent & Fuzzy Systems.* 2023; 45(1): 407-420.

[17] Mordeson J.N, Peng C.S. Operations on fuzzy graphs. *Inf Sci.* 1994; 79(3): 159-170.

[18] Nagoor Gani A, Basheer Ahamed M. Order and Size in Fuzzy Graphs. *Bulletin of Pure and Applied Sciences.* 2003; 22E(1): 145-148.

[19] Nagoor Gani A, Radha K. On regular fuzzy graphs. *J. Phys. Sci.* 2008; 12: 33-40.

[20] Nagoor Gani A, Radha K. Conjunction of two fuzzy graphs. *International Review of Fuzzy Mathematics.* 2008; 3(1): 95-105.

[21] Nagoor Gani A, Rajalaxmi D (a) Subahashini. Properties of fuzzy labeling graph. *Applied Mathematical Sciences.* 2012; 6(70): 3461-3466.

[22] Nagoor Gani A, Rajalaxmi D (a) Subahashini. Fuzzy Labeling Tree. *International Journal of Pure and Applied Mathematics.* 2014; 90(2): 131-141.

[23] Nagoor Gani A, Shajitha Begum S. Degree, Order and Size in Intuitionistic Fuzzy Graphs. *International Journal of Algorithms, Computing and Mathematics.* 2010; 3(3): 11-16.

[24] Naz S, Ashraf S, Akram M. A Novel Approach to Decision-Making with Pythagorean Fuzzy Information. *Mathematics.* 2018; 6(6): 1-28.

[25] Parvathi R, Karunambigai M.G. Intuitionistic Fuzzy Graphs. *Computational Intelligence, Theory and Applications, International Conference in Germany* 2006; 139-150.

[26] Parvathi R, Karunambigai M.G, Atanassov K.T. Operations on intuitionistic Fuzzy Graphs. *In Proceedings of the 2009 IEEE International Conference on Fuzzy Systems, Jeju Island, Korea.* 2009; 51(5): 1396-1401.

[27] Radha K, Arumugam S. On maximal product of two fuzzy graphs. *International Journal of Current Research.* 2015; 7(1): 11508-11515.

[28] Radha K, Arumugam S. On residue product of two fuzzy graphs. *International Journal of Multidisciplinary Research and Development.* 2015; 2(11): 221-227.

[29] Rosenfeld A. Fuzzy graphs. *In Fuzzy Sets and Their Applications to Cognitive and Decision Processes; Elsevier: Amsterdam, The Netherlands.* 1975; 77-95.

[30] Sankar Sahoo, Madhumamgal Pal. Different types of products on intuitionistic fuzzy graphs. *Pacific Science Review A: Natural Science and Engineering.* 2015; 17(3): 87-96.

[31] Sasikala D, Divya B. A Newfangled Interpretation on Fermatean Neutrosophic Dombi Fuzzy Graphs. *Neutrosophic Systems With Applications.* 2023; 7: 36-53.

[32] Shovan Dogra. Different types of product of fuzzy graphs. *Progress in Nonlinear Dynamics and Chaos.* 2015; 3(1): 41-56.

[33] Smarandache F. Neutrosophic set- a generalization of the intuitionistic fuzzy set, *Granular Computing, IEEE International Conference.* 2006; 38-42.

[34] Smarandache F. A geometric interpretation of the neutrosophic set- A generalization of the intuitionistic fuzzy set. *Granular Computing, IEEE International Conference.* 2011; 602-606.

[35] Wang H, Smarandache F, Zhang Y, Sunderraman R. Single valued Neutrosophic Sets. *Multispace and Multistructure.* 2010; 410-413.

[36] Yager R.R. Pythagorean fuzzy subsets. *In: Proceedings of the Joint IFSA World Congress and NAFIPS Annual Meeting, Edmonton, Canada.* 57-61.

[37] Yager R.R, Abbasov A.M. Pythagorean membership grades, complex numbers, and decision making. *Int J Intell Syst.* 2013; 28(5): 436-452.

[38] Yager R.R. Pythagorean membership grades in multi-criteria decision making. *IEEE Trans Fuzzy Syst.* 2014; 22(4): 958-965.

[39] Zadeh L.A. Fuzzy sets. *Inf Control.* 1965; 8(3): 338-353.

[40] Zeng S, Muhammad Shoaib, Shahbaz Ali, Smarandache F, Hossein Rashmanlou, Farshid Mofidnakhaei. Certain properties of single-valued neutrosophic graph with application in food and agriculture organization. *International Journal of Computational Intelligence Systems.* 2021; 14(1): 1516-1540.

Received: April 03, 2024. **Accepted**: August 30, 2024.

NSS

Neutrosophic Sets and Systems, Vol. 72, 2024

University of New Mexico

Modified Non-Linear Triangular Neutrosophic Numbers: Theory and Applications in Integral Equation

A. Mohammed shapique[1,*] and E. Mathivadhana[2]

[1]IFET college of engineering, Villupuram, India; shapique@gmail.com

[2]IFET college of engineering, Villupuram, India; mathivadhana99@gmail.com

[*]Correspondence: shapique@gmail.com

Abstract. Existing methods for handling uncertainty and imprecision often fall short in addressing complex real-world problems. To overcome these limitations, this paper introduces a novel Generalized Non-Linear Triangular Neutrosophic Number (GNLTNN) that effectively captures uncertainty, indeterminacy, and falsity. By analysing GNLTNN through (α, β, γ)-cuts and defining arithmetic operations using the max-min principle, we provide a robust framework for handling neutrosophic information. The proposed neutrosophic Laplace transform method enables efficient solutions to integral equations involving non-linear neutrosophic numbers. The efficacy of our approach is demonstrated through graphical representations.

Keywords: Generalised neutrosophic number; Non-linearity; (α, β, γ)-cuts; Neutrosophic Laplace transform; Integral equation

1. Introduction

The inherent ambiguity and vagueness of real-world data often pose challenges for traditional mathematical modeling techniques. To address this limitation, Zadeh [31] introduced fuzzy set theory, a revolutionary approach that empowers the representation of imprecise and subjective information. By assigning membership degrees ranging from 0 to 1 , fuzzy sets provide a powerful framework for incorporating the nuances of human perception and subjective experiences into mathematical models. Over the past few decades, fuzzy sets and their applications have been extensively studied across various domains, playing crucial roles in fields like control and engineering [17], medical diagnosis [27], and computer vision [32]. In fuzzy set theory, the membership degree of an element ranges between 0 and 1, representing its degree of belongingness to the set. However, it's crucial to note that the non-membership degree is not always simply the complement of the membership degree. This deviation occurs due to

the presence of hesitation or uncertainty. Hesitation arises when there's doubt or ambiguity about an element's inclusion in the set, leading to a non-membership degree that may not directly correlate with its complement. Therefore, in fuzzy sets, non-membership degrees can deviate from being the exact inverse of membership degrees due to factors like uncertainty and hesitation.

Building upon this foundation, intuitionistic fuzzy set theory, proposed by Atanassov [4], expanded upon fuzzy set theory by introducing dual membership functions, capturing both membership and non-membership degrees. This dual representation enriched the characterization of uncertainty and ambiguity, offering researchers enhanced tools for modeling complex systems. Further advancing these concepts, neutrosophic set theory, developed by Smarandache [25], introduced a triadic membership structure accommodating truth, indeterminacy, and falsehood. This comprehensive framework enables neutrosophic sets to address a broader range of complexities and uncertainties, providing a versatile and robust approach for modeling and analyzing systems in the presence of indeterminacy, vagueness, and contradiction.

The significance of neutrosophic theory lies in its capacity to model and analyze systems characterized by ambiguity and inconsistency. Unlike traditional mathematical approaches, neutrosophic theory offers a more flexible and robust methodology for managing uncertainties, enabling researchers to develop accurate and reliable computational models. Wang et al. [30] proposed the notion of single-valued neutrosophic sets as a specific subset of neutrosophic sets tailored for applications in real-world economics and finance. Neutrosophic numbers find applications in various fields by providing a robust framework to handle uncertainty, vagueness, and imprecision. Recently Neutrosophic numbers are applied in solving neutrosophic data envelopment analysis model [16], multiple attribute decision-making problem [24], healthcare services [8], water management system [2], smart cities energy system [8], architecture selection for 5G-radio access network [23] and so on. For detailed studies on neutrosophic sets, see Peng [22] and Wang [29], and references therein.

Fuzzy integral equations constitute a significant branch of mathematics blending fuzzy set theory with integral equations, offering a powerful framework for modeling and solving problems involving uncertainty and imprecision prevalent in various real-world applications. Integrating fuzzy set theory into integral equations provides a flexible and robust approach to tackle problems where precise information is lacking or uncertain. Numerous studies have addressed the solution of fuzzy integral equations, including fuzzy Fredholm integral equations [1, 9] and fuzzy Volterra integral equations [3, 6, 11, 14, 21], as documented in various literature sources.

While linear membership functions have been a popular tool for solving differential and integral equations, a review of the literature reveals a potential gap in addressing non-linear

scenarios. Linear membership functions can be considered a special case of nonlinear membership functions. Mondal et al. [19] discussed various arithmetic operations using nonlinear triangular intuitionistic fuzzy numbers (NLTIFN) and solved integral equations with NLTIFN by applying the intuitionistic fuzzy Laplace transform method. Mullor and Molina [18] utilized NLNN to assess supply chain risk management within the automotive sector. Chakraborty et al. [5] discussed various forms of linear and non-linear neutrosophic numbers and applied the concept of NLNN to solve sequencing problems. From the literature survey, it is evident that only a few authors have discussed the concept of NLNN. This paper investigate a modified form of generalised nonlinear triangular neutrosophic number (GNLTNN). Further, we apply GNLTNN to solve Fredholm integral equations. The significance of the paper is as follows. A modified form of an GNLTNN is investigated. The (α, β, γ)-cuts of GNLTNN are obtained. Furthermore, arithmetic operations on GNLTNN are discussed. Neutrosophic valued function are also considered. By employing the neutrosophic Laplace transform method, we derive solutions to integral equations involving non-linear neutrosophic numbers. Finally, a graphical illustration of the solution is provided. This study contributes to the advancement of neutrosophic set theory and nonlinear membership functions, potentially opening new avenues for further research and application.

The remainder of the paper is structured as follows: Section 2 provides an overview of neutrosophic preliminaries and the properties of the neutrosophic Laplace transform. The concept of the modified GNLTNN is introduced in Section 3. Further, the $(\alpha,\ \beta,\ \gamma)$-cuts and its arithmetic operations are discussed. Section 4 presents the method of computing the values and ambiguities of NLTNN. Section 5 discusses the application of neutrosophic methods in solving linear Fredholm integral equations. Results discussion is presented in Section 6. Conclusions drawn from the research and potential areas for further investigation is presented in Section 7.

2. **Preliminaries**

Definition 1 [26] Let X denote a space of points. A neutrosophic set A in X is characterized by a truth $T_A(x)$, indeterminacy $I_A(x)$ and a falsity $F_A(x)$ membership function. These membership functions $T_A(x)$, $I_A(x)$ and $F_A(x)$ are real standard or non-standard subsets of $]0^-, 1^+[$ and satisfies $0^- \leqslant S(x) \leqslant 3^+$, where $S(x) = T_A(x) + I_A(x) + F_A(x)$.

In practical applications involving scientific and engineering problems, utilizing neutrosophic sets whose values are derived from real standard or non-standard subsets of $]0^-, 1^+[$ can be challenging. Consequently, the single-valued neutrosophic set (SVNS)is often preferred, as it confines its values to the interval $[0, 1]$. This simplification facilitates easier application and analysis in real-world scenarios.

Table 1. Comparison with the existing solution approach

Reference	Application	Uncertainty used	Methodology
[20]	Fredholm integral equation	Fuzzy	Integration theory of Fuzzy function
[1]	Fredholm integral equation	Fuzzy	Homotopy Perturbation Method
[10]	Fredholm integral equation	Fuzzy	Artificial neural networks
[19]	Fredholm integral equation	Non-linear Intuitionistic fuzzy number	(α, β)-cuts
Proposed	Fredholm integral equation	Modified non-linear neutrosophic number	(α, β, γ)-cuts

Definition 2 [30] Let X denote a set where each element $x \in X$ represents a point in space. A SVNS A in X is characterized by $T_A(x)$, $I_A(x)$, and $F_A(x)$. Each function assigns a value in the interval $[0, 1]$ to every element such that $0 \leqslant S(x) \leqslant 3$. Within the context of a SVNS A in X, an element x represented as $x = (T_x, F_x, I_x)$ is referred to as a SVNN.

Definition 3 [28] Let $x_1 = (T_{x_1}, F_{x_1}, I_{x_1})$ and $x_2 = (T_{x_2}, F_{x_2}, I_{x_2})$ be any two SVNNs. The operations for SVNNs is defined as follows:

(1) $x_1 \oplus x_2 = (T_{x_1} + T_{x_2} - T_{x_1} \times T_{x_2}, I_{x_1} \times I_{x_2}, F_{x_1} \times F_{x_2})$
(2) $x_1 \otimes x_2 = (T_{x_1} + T_{x_2}, I_{x_1} + I_{x_2} - I_{x_1} \times I_{x_2}, F_{x_1} + F_{x_2} - F_{x_1} \times F_{x_2})$
(3) $ax = (1 - (1 - T_x)^a, (I_x)^a, (F_x)^a)$, where $a > 0$

Definition 4 [15]A SVNN $\tilde{A} = \left(\underline{c}, c, \bar{c}; u_{\tilde{A}}, v_{\tilde{A}}, w_{\tilde{A}}\right)$ is termed as Single valued Triangular neutrosophic number (SVTNN)when its membership functions are linear.

$$T_{\tilde{A}}(x) = \begin{cases} \dfrac{(x - \underline{c})\, u_{\tilde{A}}}{c - \underline{c}}, & \text{if } \underline{c} \leqslant x < c \\ u_{\tilde{A}}, & \text{if } x = c \\ \dfrac{(\bar{c} - x)\, u_{\tilde{A}}}{\bar{c} - c}, & \text{if } c < x \leqslant \bar{c} \end{cases} \tag{2.1}$$

$$I_{\tilde{A}}(x) = \begin{cases} \dfrac{(c - x) + (x - \underline{c})\, v_{\tilde{A}}}{c - \underline{c}}, & \text{if } \underline{c} \leqslant x < c \\ v_{\tilde{A}}, & \text{if } x = c \\ \dfrac{(x - c) + (\bar{c} - x)\, v_{\tilde{A}}}{\bar{c} - c}, & \text{if } c < x \leqslant \bar{c} \\ 1, & \text{otherwise} \end{cases} \tag{2.2}$$

$$F_{\tilde{A}}(x) = \begin{cases} \dfrac{(c-x)+(x-\underline{c})\,w_{\tilde{A}}}{c-\underline{c}}, & \text{if } \underline{c} \leqslant x < c \\ w_{\tilde{A}}, & \text{if } x = c \\ \dfrac{(x-c)+(\bar{c}-x)\,w_{\tilde{A}}}{\bar{c}-c}, & \text{if } c < x \leqslant \bar{c} \\ 1, & \text{otherwise} \end{cases} \tag{2.3}$$

The graph of the above functions is presented in Figure 1.

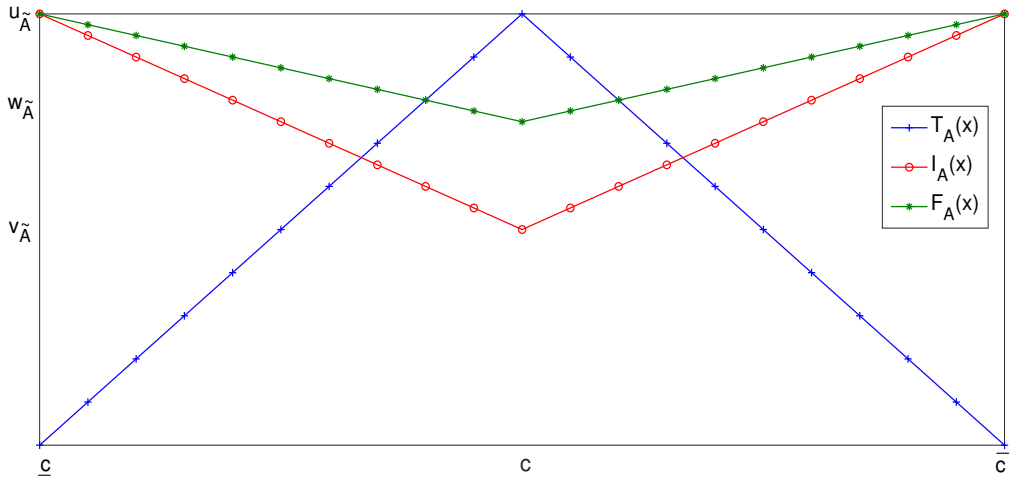

FIGURE 1. Graph of SVTNN

Definition 5 [15] Let $\tilde{A} = \left(\underline{c}, c, \bar{c}; u_{\tilde{A}}, v_{\tilde{A}}, w_{\tilde{A}}\right)$ represents SVTNN then the $(\alpha,\ \beta,\ \gamma)$-cut set is defined as:

$$\tilde{A}_{(\alpha,\beta,\gamma)} = \left\{\left\langle x, T_{\tilde{A}}(x) \geqslant \alpha, I_{\tilde{A}}(x) \leqslant \beta, F_{\tilde{A}}(x) \leqslant \gamma\right\rangle : x \in X\right\}, \tag{2.4}$$

satisfies

$$0 \leqslant \alpha \leqslant u_{\tilde{A}}; v_{\tilde{A}} \leqslant \beta \leqslant 1; w_{\tilde{A}} \leqslant \gamma \leqslant 1 \tag{2.5}$$

and

$$\alpha + \beta + \gamma \leqslant 3. \tag{2.6}$$

The $(\alpha,\ \beta,\ \gamma)$-cut set of SVTNN is represented as $\tilde{A}_{(\alpha,\beta,\gamma)} = \left\langle \tilde{A}_{(\alpha)}; \tilde{A}_{(\beta)}; \tilde{A}_{(\gamma)} \right\rangle$ which is a crisp subset of X. $\tilde{A}_{(\alpha)}$ represents the (α)-cut set of the SVTNN which is defined as follows.

$$\tilde{A}_{(\alpha)} = \left[T^L_{\tilde{A}}(\alpha), T^U_{\tilde{A}}(\alpha)\right].$$

Using Definition 4, the above set is expressed as

$$\tilde{A}_{(\alpha)} = \left[\underline{c}_{\tilde{A}} + \frac{\alpha\left(c_{\tilde{A}} - \underline{c}_{\tilde{A}}\right)}{u_{\tilde{A}}}, \bar{c}_{\tilde{A}} - \frac{\alpha\left(\bar{c}_{\tilde{A}} - c_{\tilde{A}}\right)}{u_{\tilde{A}}}\right]. \tag{2.7}$$

Similarly, the (β)-cut set and (γ)-cut set of the SVTNN are as follows

$$\begin{aligned}\tilde{A}_{(\beta)} &= \left[I_{\tilde{A}}^{L}(\beta), I_{\tilde{A}}^{U}(\beta)\right] \\ &= \left[\frac{c_{\tilde{A}} - v_{\tilde{A}}\underline{c}_{\tilde{A}} - \beta\left(c_{\tilde{A}} - \underline{c}_{\tilde{A}}\right)}{1 - v_{\tilde{A}}}, \frac{c_{\tilde{A}} - v_{\tilde{A}}\bar{c}_{\tilde{A}} + \beta\left(\bar{c}_{\tilde{A}} - c_{\tilde{A}}\right)}{1 - v_{\tilde{A}}}\right].\end{aligned} \tag{2.8}$$

$$\begin{aligned}\tilde{A}_{(\gamma)} &= \left[F_{\tilde{A}}^{L}(\gamma), F_{\tilde{A}}^{U}(\gamma)\right] \\ &= \left[\frac{c_{\tilde{A}} - w_{\tilde{A}}\underline{c}_{\tilde{A}} - \gamma\left(c_{\tilde{A}} - \underline{c}_{\tilde{A}}\right)}{1 - w_{\tilde{A}}}, \frac{c_{\tilde{A}} - w_{\tilde{A}}\bar{c}_{\tilde{A}} + \gamma\left(\bar{c}_{\tilde{A}} - c_{\tilde{A}}\right)}{1 - w_{\tilde{A}}}\right].\end{aligned} \tag{2.9}$$

Definition 6 [5] A SVNN $\tilde{A} = \left(\underline{c}, c, \bar{c}; u_{\tilde{A}}, v_{\tilde{A}}, w_{\tilde{A}}\right)$ is termed as NLTNN, when its membership functions are non-linear.

$$T_{\tilde{A}}(x) = \begin{cases} \left(\dfrac{x-a}{a-\underline{a}}\right)^{p_1}\omega & \text{if } \underline{a} \le x < a, \\ \omega & \text{if } x = a, \\ \left(\dfrac{\bar{a}-x}{\bar{a}-a}\right)^{p_2}\omega & \text{if } a < x \leqslant \bar{a}, \\ 0 & \text{otherwise} \end{cases} \tag{2.10}$$

$$I_{\tilde{A}}(x) = \begin{cases} \left(\dfrac{b-x}{b-\underline{b}}\right)^{q_1}\rho & \text{if } \underline{b} \leqslant x < b, \\ 0 & \text{if } x = b, \\ \left(\dfrac{x-\bar{b}}{\bar{b}-b}\right)^{q_2}\rho & \text{if } b < x \leqslant \bar{b}, \\ \rho & \text{otherwise} \end{cases} \tag{2.11}$$

$$F_{\tilde{A}}(x) = \begin{cases} \left(\dfrac{c-x}{c-\underline{c}}\right)^{r_1}\lambda & \text{if } \underline{c} \leqslant x < c, \\ 0 & \text{if } x = c, \\ \left(\dfrac{x-\bar{c}}{\bar{c}-c}\right)^{r_2}\lambda & \text{if } c < x \leqslant \bar{c}, \\ \lambda & \text{otherwise} \end{cases} \tag{2.12}$$

The above definition is derived from Chakraborty et al. [5]. These parameters, ω, ρ and λ scale the membership values in their respective functions.

Definition 7 The parametric form of neutrosophic valued function $f(t)$ is defined as follows :

$$[f(t)]_{(\alpha,\beta,\gamma)} = \left[\underline{f}(t,\alpha), \bar{f}(t,\alpha); \underline{f}(t,\beta), \bar{f}(t,\beta); \underline{f}(t,\gamma), \bar{f}(t,\gamma)\right] \tag{2.13}$$

Definition 8 If $f(t)$ is a neutrosophic valued function then the neutrosophic Laplace transform of $f(t)$ is defined as follows.

$$L\{f(t)\} = F(s) = \lim_{\kappa\to\infty} \int_0^{\kappa} e^{-st} \odot f(t)\, dt. \tag{2.14}$$

The lower and upper neutrosophic Laplace transform of the function $f(t)$ is as follows:

$$L\{f(t)\}_{(\alpha,\beta,\gamma)} = \left[\lim_{\kappa\to\infty} \int_0^{\kappa} e^{-st} \underline{f}_T(t,\alpha)dt, \quad \lim_{\kappa\to\infty} \int_0^{\kappa} e^{-st} \bar{f}_T(t,\alpha)dt; \lim_{\kappa\to\infty} \int_0^{\kappa} e^{-st} \underline{f}_I(t,\beta)dt, \right.$$
$$\left. \lim_{\kappa\to\infty} \int_0^{\kappa} e^{-st} \bar{f}_I(t,\beta)dt; \lim_{\kappa\to\infty} \int_0^{\kappa} e^{-st} \underline{f}_F(t,\gamma)dt, \quad \lim_{\kappa\to\infty} \int_0^{\kappa} e^{-st} \bar{f}_F(t,\gamma)dt \right].$$

Theorem 1 Let $f(t)$ be a continuous neutrosophic valued function defined on $[0,\infty)$ and exponential order p, then

(1) $L\{f'(t)\} = sF(s) \ominus f(0)$ if $f(t)$ is (i) differentiable
(2) $L\{f'(t)\} = -f(0) \ominus \{-sF(s)\}$ if $f(t)$ is (ii) differentiable

3. Modified form of generalized non-linear triangular neutrosophic number (GNLTNN)

Although Definition 6 outlines NLTNN, it lacks precision in representing NLTNN adequately. Specifically, the functions for indeterminacy-membership and falsity-membership do not associate parameters ρ and λ with their minimum values, but instead with their maximum values. We contend that this aspect hinders the accurate expression of the degree of indeterminacy and falsity within a decision-making framework. To refine the characterization of these functions, a modified form of NLNN is studied. This revised definition considers sets of parameters $p = (p_T, p_I, p_F)$ and $q = (q_T, q_I, q_F)$, where all elements fall within the range [1, ∞).

Definition 9 [18] Let $\tilde{A}_{(p,q)} = \left(\underline{c}, c, \bar{c}; u_{\tilde{A}}, v_{\tilde{A}}, w_{\tilde{A}}\right)$ be a generalised non-linear triangular neutrosophic number whose membership functions are as follows

$$T_{\tilde{A}}(x) = \begin{cases} u_{\tilde{A}}\left\{1 - \left(\dfrac{c-x}{c-\underline{c}}\right)^{p_T}\right\}, & \text{if } \underline{c} \leqslant x < c \\ u_{\tilde{A}}, & \text{if } x = c \\ u_{\tilde{A}}\left\{1 - \left(\dfrac{c-x}{c-\bar{c}}\right)^{q_T}\right\}, & \text{if } c < x \leqslant \bar{c} \\ 0, & \text{otherwise} \end{cases} \tag{3.1}$$

$$I_{\tilde{A}}(x)=\begin{cases} v_{\tilde{A}}+(1-v_{\tilde{A}})\left(\dfrac{c-x}{\underline{c}}\right)^{p_I}, & \text{if } \underline{c}\leqslant x<c \\ v_{\tilde{A}}, & \text{if } x=c \\ v_{\tilde{A}}+(1-v_{\tilde{A}})\left(\dfrac{c-x}{c-\bar{c}}\right)^{q_I}, & \text{if } c<x\leqslant \bar{c} \\ 1, & \text{otherwise} \end{cases} \tag{3.2}$$

$$F_{\tilde{A}}(x)=\begin{cases} w_{\tilde{A}}+(1-w_{\tilde{A}})\left(\dfrac{c-x}{\underline{c}}\right)^{p_F}, & \text{if } \underline{c}\leqslant x<c \\ w_{\tilde{A}}, & \text{if } x=c \\ w_{\tilde{A}}+(1-w_{\tilde{A}})\left(\dfrac{c-x}{c-\bar{c}}\right)^{q_F}, & \text{if } c<x\leqslant \bar{c} \\ 1, & \text{otherwise} \end{cases} \tag{3.3}$$

The above definition also suggests that the membership functions are centered on parameter c. This scenario appears reasonable within a context where uncertainty is articulated around a specific reference point. Figure 2 and 3 presents various forms of NLTNN.

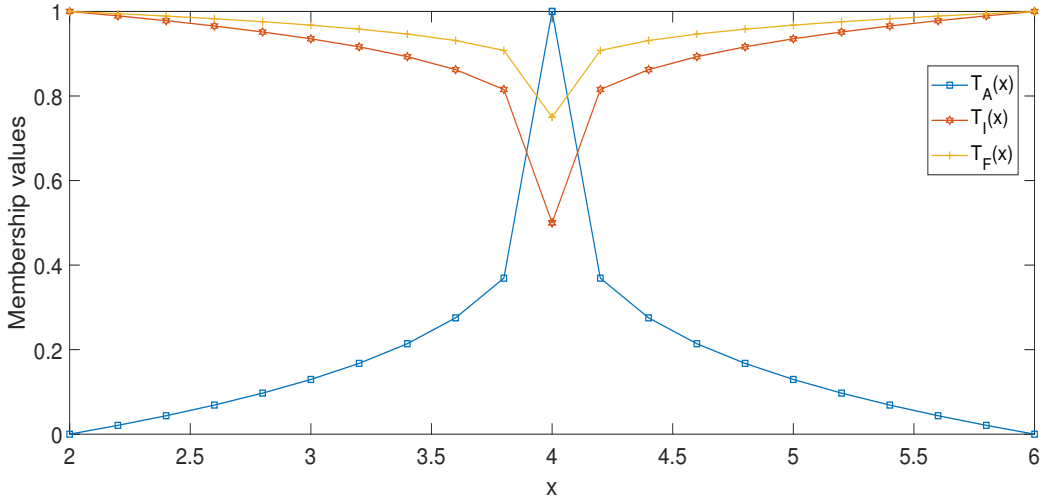

FIGURE 2. NLTNN with $p_T=p_I=p_F$=0.2, $q_T=q_I=q_F$=0.2

3.1. *(α, β, γ)-cuts of GNLTNN*

Definition 10 [18] For a GNLTNN $\tilde{A}_{(p.q)}=\left(\underline{c},c,\bar{c};u_{\tilde{A}},v_{\tilde{A}},w_{\tilde{A}}\right)$, the ($\alpha$, β, γ)-cut sets is defined as follows:

$$\tilde{A}_{(\alpha,\beta,\gamma)}=\left\{\left\langle x,T_{\tilde{A}}(x)\geqslant\alpha,I_{\tilde{A}}(x)\leqslant\beta,F_{\tilde{A}}(x)\leqslant\gamma\right\rangle:x\in X\right\} \tag{3.4}$$

and satisfies the conditions $0\leqslant\alpha\leqslant u_{\tilde{A}};v_{\tilde{A}}\leqslant\beta\leqslant 1;w_{\tilde{A}}\leqslant\gamma\leqslant 1$ and $\alpha+\beta+\gamma\leqslant 3$. The (α,β,γ) -cut sets of GNLTNN is represented as $\tilde{A}_{(p,q,\alpha,\beta,\gamma)}$ which is a crisp subset of X:

$$\tilde{A}_{(p,q,\alpha,\beta,\gamma)}=\left\langle\tilde{A}_{(p_T,q_T,\alpha)};\tilde{A}_{(p_I,q_I,\beta)};\tilde{A}_{(p_F,q_F,\gamma)}\right\rangle.$$

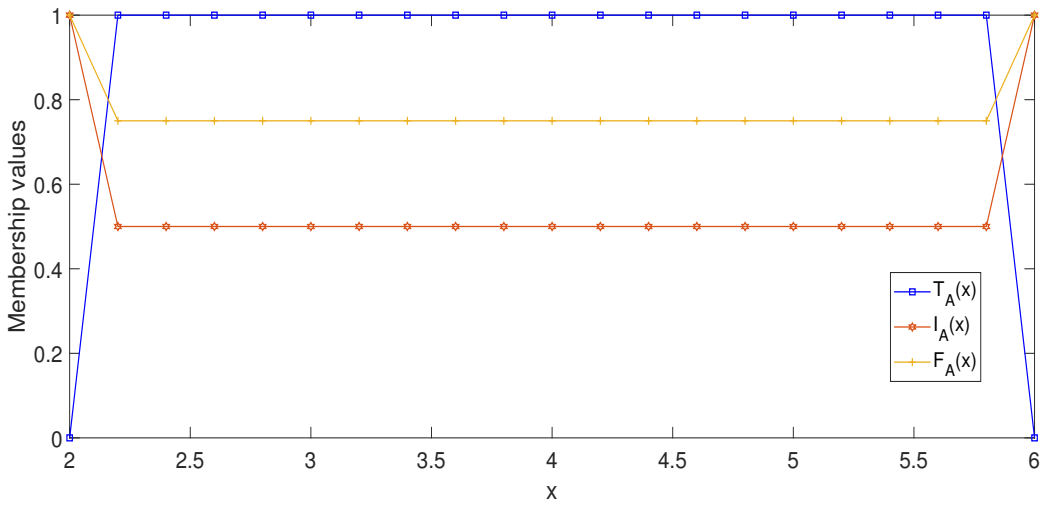

FIGURE 3. NLTNN with $p_T = p_I = p_F$=1000, $q_T = q_I = q_F$=1000

$\tilde{A}_{(p_T,q_T,\alpha)}$ represents the -cut set of the GNLTNN which is a closed interval defined as follows.

$$\tilde{A}_{(p_T,q_T,\alpha)} = \left[T^L_{\tilde{A}}(\alpha, p_T), T^U_{\tilde{A}}(\alpha, q_T)\right].$$

Using Definition 9, the above set is expressed as

$$\tilde{A}_{(p_T,q_T,\alpha)} = \left[c - (c-\underline{c})\left(1 - \frac{\alpha}{u_{\tilde{A}}}\right)^{\frac{1}{p_T}}, c - (c-\bar{c})\left(1 - \frac{\alpha}{u_{\tilde{A}}}\right)^{\frac{1}{q_T}}\right]. \tag{3.5}$$

Similarly,

$$\begin{aligned}\tilde{A}_{(p_I,q_I,\beta)} &= \left[I^L_{\tilde{A}}(\beta, p_I), I^U_{\tilde{A}}(\beta, q_I)\right] \\ &= \left[c - \underline{c}\left(\frac{\beta - v_{\tilde{A}}}{1 - v_{\tilde{A}}}\right)^{\frac{1}{p_I}}, c - (c-\bar{c})\left(\frac{\beta - v_{\tilde{A}}}{1 - v_{\tilde{A}}}\right)^{\frac{1}{q_I}}\right].\end{aligned} \tag{3.6}$$

$$\begin{aligned}\tilde{A}_{(p_F,q_F,\gamma)} &= \left[F^L_{\tilde{A}}(\gamma, p_F), F^U_{\tilde{A}}(\gamma, q_F)\right] \\ &= \left[c - \underline{c}\left(\frac{\gamma - w_{\tilde{A}}}{1 - w_{\tilde{A}}}\right)^{\frac{1}{p_F}}, c - (c-\bar{c})\left(\frac{\gamma - w_{\tilde{A}}}{1 - w_{\tilde{A}}}\right)^{\frac{1}{q_F}}\right].\end{aligned} \tag{3.7}$$

3.2. *Arithmetic operation on GNLTNN*

Let $\tilde{A}_{(p.q)} = (\underline{c}_1, c_1, \bar{c}_1; u_{\tilde{A}}, v_{\tilde{A}}, w_{\tilde{A}})$ and $\tilde{B}_{(p.q)} = (\underline{c}_2, c_2, \bar{c}_2; u_{\tilde{A}}, v_{\tilde{A}}, w_{\tilde{A}})$ be two GNLTNN with membership function as follows

$$T_{\tilde{A}}(x)=\begin{cases} u_{\tilde{A}}\left\{1-\left(\dfrac{c_1-x}{c_1-\underline{c}_1}\right)^{p_{T_1}}\right\}, & \text{if } \underline{c}_1 \leqslant x < c_1 \\ u_{\tilde{A}}, & \text{if } x = c_1 \\ u_{\tilde{A}}\left\{1-\left(\dfrac{c_1-x}{c_1-\bar{c}_1}\right)^{q_{T_1}}\right\}, & \text{if } c_1 < x \leqslant \bar{c}_1 \\ 0, & \text{otherwise} \end{cases} \tag{3.8}$$

$$I_{\tilde{A}}(x)=\begin{cases} v_{\tilde{A}}+(1-v_{\tilde{A}})\left(\dfrac{c_1-x}{\underline{c}_1}\right)^{p_{I_1}}, & \text{if } \underline{c}_1 \leqslant x < c_1 \\ v_{\tilde{A}}, & \text{if } x = c_1 \\ v_{\tilde{A}}+(1-v_{\tilde{A}})\left(\dfrac{c_1-x}{c_1-\bar{c}_1}\right)^{q_{I_1}}, & \text{if } c_1 < x \leqslant \bar{c}_1 \\ 1, & \text{otherwise} \end{cases} \tag{3.9}$$

$$F_{\tilde{A}}(x)=\begin{cases} w_{\tilde{A}}+(1-w_{\tilde{A}})\left(\dfrac{c_1-x}{\underline{c}_1}\right)^{p_{F_1}}, & \text{if } \underline{c}_1 \leqslant x < c_1 \\ w_{\tilde{A}}, & \text{if } x = c_1 \\ w_{\tilde{A}}+(1-w_{\tilde{A}})\left(\dfrac{c_1-x}{c_1-\bar{c}_1}\right)^{q_{F_1}}, & \text{if } c_1 < x \leqslant \bar{c}_1 \\ 1, & \text{otherwise} \end{cases} \tag{3.10}$$

and

$$T_{\tilde{B}}(x)=\begin{cases} u_{\tilde{A}}\left\{1-\left(\dfrac{c_2-x}{c_2-\underline{c}_2}\right)^{p_{T_2}}\right\}, & \text{if } \underline{c}_2 \leqslant x < c_2 \\ u_{\tilde{A}}, & \text{if } x = c_2 \\ u_{\tilde{A}}\left\{1-\left(\dfrac{c_2-x}{c_2-\bar{c}_2}\right)^{q_{T_2}}\right\}, & \text{if } c_2 \leqslant x \leqslant \bar{c}_2 \\ 0, & \text{otherwise} \end{cases} \tag{3.11}$$

$$I_{\tilde{B}}(x)=\begin{cases} v_{\tilde{A}}+(1-v_{\tilde{A}})\left(\dfrac{c_2-x}{\underline{c}_2}\right)^{p_{I_2}}, & \text{if } \underline{c}_2 \leqslant x \leqslant c_2 \\ v_{\tilde{A}}, & \text{if } x = c_2 \\ v_{\tilde{A}}+(1-v_{\tilde{A}})\left(\dfrac{c_2-x}{c_2-\bar{c}_2}\right)^{q_{I_2}}, & \text{if } c_2 \leqslant x \leqslant \bar{c}_2 \\ 1, & \text{otherwise} \end{cases} \tag{3.12}$$

$$F_{\tilde{B}}(x)=\begin{cases} w_{\tilde{A}}+(1-w_{\tilde{A}})\left(\dfrac{c_2-x}{\underline{c}_2}\right)^{p_{F_2}}, & \text{if } \underline{c}_2 \leqslant x \leqslant c_2 \\ w_{\tilde{A}}, & \text{if } x = c_2 \\ w_{\tilde{A}}+(1-w_{\tilde{A}})\left(\dfrac{c_2-x}{c_2-\bar{c}_1}\right)^{q_{F_2}}, & \text{if } c_2 \leqslant x \leqslant \bar{c}_2 \\ 1, & \text{otherwise} \end{cases} \tag{3.13}$$

The (α, β, γ)-cut is given by

$$\tilde{A}_{(p_1,q_1,\alpha,\beta,\gamma)} = \left[c_1 - (c_1 - \underline{c}_1)\left(1 - \frac{\alpha}{u_{\tilde{A}}}\right)^{\frac{1}{p_{T_1}}}, c_1 - (c_1 - \bar{c}_1)\left(1 - \frac{\alpha}{u_{\tilde{A}}}\right)^{\frac{1}{q_{T_1}}}; c_1 - \underline{c}_1\left(\frac{\beta - v_{\tilde{A}}}{1 - v_{\tilde{A}}}\right)^{\frac{1}{p_{I_1}}},\right.$$
$$\left. c_1 - (c_1 - \bar{c}_1)\left(\frac{\beta - v_{\tilde{A}}}{1 - v_{\tilde{A}}}\right)^{\frac{1}{q_{I_1}}}; c_1 - \underline{c}_1\left(\frac{\gamma - w_{\tilde{A}}}{1 - w_{\tilde{A}}}\right)^{\frac{1}{p_{F_1}}}, c_1 - (c_1 - \bar{c}_1)\left(\frac{\gamma - w_{\tilde{A}}}{1 - w_{\tilde{A}}}\right)^{\frac{1}{q_{F_1}}}\right] \tag{3.14}$$

and

$$\tilde{B}_{(p_2,q_2,\alpha,\beta,\gamma)} = \left[c_2 - (c_2 - \underline{c}_2)\left(1 - \frac{\alpha}{u_{\tilde{A}}}\right)^{\frac{1}{p_{T_2}}}, c_2 - (c_2 - \bar{c}_2)\left(1 - \frac{\alpha}{u_{\tilde{A}}}\right)^{\frac{1}{q_{T_2}}}; c_2 - \underline{c}_2\left(\frac{\beta - v_{\tilde{A}}}{1 - v_{\tilde{A}}}\right)^{\frac{1}{p_{I_2}}},\right.$$
$$\left. c_2 - (c_2 - \bar{c}_2)\left(\frac{\beta - v_{\tilde{A}}}{1 - v_{\tilde{A}}}\right)^{\frac{1}{q_{I_2}}}; c_2 - \underline{c}_2\left(\frac{\gamma - w_{\tilde{A}}}{1 - w_{\tilde{A}}}\right)^{\frac{1}{p_{F_2}}}, c_2 - (c_2 - \bar{c}_2)\left(\frac{\gamma - w_{\tilde{A}}}{1 - w_{\tilde{A}}}\right)^{\frac{1}{q_{F_2}}}\right] \tag{3.15}$$

3.2.1. *Addition of two GNLTNN*

This section presents addition of two NLTNN using (p,q,α,β,γ)-cut. For simplicity, we consider $p_{T_i} = q_{T_i} = n_1$, $p_{I_i} = q_{I_i} = n_2$, $q_{F_i} = q_{F_i} = n_3$, $i = 1, 2$. Let

$$C_{(p,q,\alpha,\beta,\gamma)} = A_{(p_1,q_1,\alpha,\beta,\gamma)} + B_{(p_2,q_2,\alpha,\beta,\gamma)} \tag{3.16}$$

Using Equations (3.14) and (3.15), we get

$$C_{(p,q,\alpha,\beta,\gamma)} = \left[\underline{\zeta}_1\left(1 - \frac{\alpha}{u_{\tilde{A}}}\right)^{\frac{1}{n_1}}, \bar{\zeta}_1\left(1 - \frac{\alpha}{u_{\tilde{A}}}\right)^{\frac{1}{n_1}}; \underline{\xi}_1\left(\frac{\beta - v_{\tilde{A}}}{1 - v_{\tilde{A}}}\right)^{\frac{1}{n_2}}, \bar{\zeta}_1\left(\frac{\beta - v_{\tilde{A}}}{1 - v_A}\right)^{\frac{1}{n_2}};\right.$$
$$\left. \underline{\xi}_1\left(\frac{\gamma - w_{\tilde{A}}}{1 - w_{\tilde{A}}}\right)^{\frac{1}{n_3}}, \bar{\zeta}_1\left(\frac{\gamma - w_{\tilde{A}}}{1 - w_{\tilde{A}}}\right)^{\frac{1}{n_3}}\right]. \tag{3.17}$$

The membership function of the above Equation (3.17) is as follows.

$$T_C(x) = \begin{cases} u_{\tilde{A}}\left\{1 - \left(\dfrac{x - c_1 - c_2}{\underline{\xi}_1}\right)^{n_1}\right\}, & \text{for } \underline{c}_1 + \underline{c}_2 \leqslant x < c_1 + c_2 \\ u_{\tilde{A}}, & \text{for } x = c_1 + c_2 \\ u_{\tilde{A}}\left\{1 - \left(\dfrac{x - c_1 + c_2}{\bar{\xi}_1}\right)^{n_1}\right\}, & \text{for } c_1 + c_2 < x \leqslant \bar{c}_1 + \bar{c}_2 \\ 0, & \text{otherwise} \end{cases} \tag{3.18}$$

$$I_C(x) = \begin{cases} v_{\tilde{A}} + (1 - v_{\tilde{A}})\left(\dfrac{c_1 + c_2 - x}{\underline{c}_1 + \underline{c}_2}\right)^{n_2}, & \text{for } \underline{c}_1 + \underline{c}_2 \leqslant x < c_1 + c_2 \\ 0, & \text{for } x = c_1 + c_2 \\ v_{\tilde{A}} + (1 - v_{\tilde{A}})\left(\dfrac{c_1 + c_2 - x}{\bar{\xi}_1}\right)^{n_2}, & \text{for } c_1 + c_2 < x \leqslant \bar{c}_1 + \bar{c}_2 \\ 1, & \text{otherwise} \end{cases} \tag{3.19}$$

$$F_C(x) = \begin{cases} w_{\tilde{A}} + (1 - w_{\tilde{A}}) \left(\dfrac{c_1 + c_2 - x}{\underline{c}_1 + \underline{c}_2} \right)^{n_3}, & \text{for } \underline{c}_1 + \underline{c}_2 \leqslant x < c_1 + c_2 \\ 0, & \text{for } x = c_1 + c_2 \\ w_{\tilde{A}} + (1 - w_{\tilde{A}}) \left(\dfrac{c_1 + c_2 - x}{\bar{\xi}_1} \right)^{n_3}, & \text{for } c_1 + c_2 < x \leqslant \bar{c}_1 + \bar{c}_2 \\ 1, & \text{otherwise} \end{cases} \tag{3.20}$$

where $\underline{\zeta}_1 = c_1 + c_2 - (c_1 + c_2 - \underline{c}_1 - \underline{c}_2)$, $\bar{\zeta}_1 = c_1 + c_2 - (c_1 + c_2 - \bar{c}_1 - \bar{c}_2)$, $\underline{\xi}_1 = c_1 + c_2 - (\underline{c}_1 + \underline{c}_2)$ and $\bar{\xi}_1 = c_1 + c_2 - (\bar{c}_1 + \bar{c}_2)$ Addition of two GNLTNN is illustrated in Example 1.

Example 1: If $\tilde{A} = (3, 5, 7; 1, 0.5, 0.75)$, $\tilde{B} = (4, 6, 8; 1, 0.5, 0.75)$ and $n_1 = n_2 = n_3 = 3$ then using Equation (3.17), we obtain

$$C_{(3,3,\alpha,\beta,\gamma)} = \Bigg[11 - 4(1-\alpha)^{\frac{1}{3}}, 11 + 4(1-\alpha)^{\frac{1}{3}}; 11 - 7\left(\frac{\beta - 0.5}{0.5}\right)^{\frac{1}{3}} 11 + 4\left(\frac{\beta - 0.5}{0.5}\right)^{\frac{1}{3}}; 11 - 7\left(\frac{\gamma - 0.75}{0.25}\right)^{\frac{1}{3}}, 11 + 4\left(\frac{\gamma - 0.75}{0.25}\right)^{\frac{1}{3}} \Bigg].$$

The graph of above equation is presented in Figure 4.

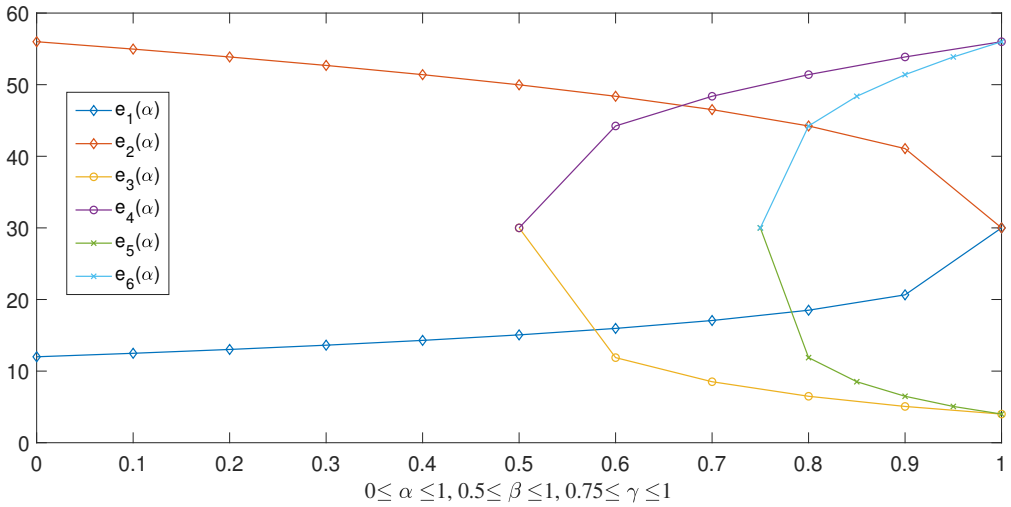

FIGURE 4. Addition of two GNLTNN

3.2.2. *Subtraction of two GNLTNN*

This section presents subtraction of two NLTNN using (p,q,α,β,γ)-cut. Let

$$C_{(p,q,\alpha,\beta,\gamma)} = A_{(p_1,q_1,\alpha,\beta,\gamma)} - B_{(p_2,q_2,\alpha,\beta,\gamma)}$$

Using Equations (3.14) and (3.15), we get

$$C_{(p,q,\alpha,\beta,\gamma)} = \left[\underline{\zeta}_2\left(1-\frac{\alpha}{u_{\tilde{A}}}\right)^{\frac{1}{n_1}}, \bar{\zeta}_2\left(1-\frac{\alpha}{u_{\tilde{A}}}\right)^{\frac{1}{n_1}}; \underline{\xi}_2\left(\frac{\beta-v_{\tilde{A}}}{1-v_{\tilde{A}}}\right)^{\frac{1}{n_2}}, \bar{\zeta}_2\left(\frac{\beta-v_{\tilde{A}}}{1-v_A}\right)^{\frac{1}{n_2}}; \underline{\xi}_2\left(\frac{\gamma-w_{\tilde{A}}}{1-w_{\tilde{A}}}\right)^{\frac{1}{n_3}}, \bar{\zeta}_2\left(\frac{\gamma-w_{\tilde{A}}}{1-w_{\tilde{A}}}\right)^{\frac{1}{n_3}}\right]. \tag{3.21}$$

The membership function of the above Equation is as follows.

$$T_C(x) = \begin{cases} u_{\tilde{A}}\left\{1- \quad \dfrac{x-c_1+c_2}{\underline{\xi}_2}\right)^{n_1}\right\}, & \text{for } \underline{c}_1-\underline{c}_2 \leqslant x < c_1-c_2 \\ u_{\tilde{A}}, \quad \text{for } x = c_1-c_2 \\ u_{\tilde{A}}\left\{1-\left(\dfrac{x-c_1+c_2}{\bar{\xi}_2}\right)^{n_1}\right\}, & \text{for } c_1-c_2 < x \leqslant \bar{c}_1-\bar{c}_2 \\ 0, \quad \text{otherwise} \end{cases} \tag{3.22}$$

$$I_C(x) = \begin{cases} v_{\tilde{A}}+\left(1-v_{\tilde{A}}\right)\left(\dfrac{c_1-c_2-x}{\underline{c}_1-\underline{c}_2}\right)^{n_2}, & \text{for } \underline{c}_1-\underline{c}_2 \leqslant x < c_1-c_2 \\ 0, \quad \text{for } x = c_1-c_2 \\ v_{\tilde{A}}+\left(1-v_{\tilde{A}}\right)\left(\dfrac{c_1-c_2-x}{\bar{\xi}_2}\right)^{n_2}, & \text{for } c_1-c_2 < x \leqslant \bar{c}_1-\bar{c}_2 \\ 1, \quad \text{otherwise} \end{cases} \tag{3.23}$$

$$F_C(x) = \begin{cases} w_{\tilde{A}}+\left(1-w_{\tilde{A}}\right)\left(\dfrac{c_1-c_2-x}{\underline{c}_1-\underline{c}_2}\right)^{n_3}, & \text{for } \underline{c}_1-\underline{c}_2 \leqslant x < c_1-c_2 \\ 0, \quad \text{for } x = c_1-c_2 \\ w_{\tilde{A}}+\left(1-w_{\tilde{A}}\right)\left(\dfrac{c_1-c_2-x}{\bar{\xi}_2}\right)^{n_3}, & \text{for } c_1-c_2 < x \leqslant \bar{c}_1-\bar{c}_2 \\ 1, \quad \text{otherwise} \end{cases} \tag{3.24}$$

where $\underline{\zeta}_2 = c_1-c_2-(c_1-c_2-\underline{c}_1+\underline{c}_2)$, $\bar{\zeta}_2 = c_1-c_2-(c_1-c_2-\bar{c}_1+\bar{c}_2)$, $\underline{\xi}_2 = c_1-c_2-(\underline{c}_1-\underline{c}_2)$ and $\bar{\xi}_2 = c_1-c_2-(\bar{c}_1-\bar{c}_2)$.

Subtraction of two GNLTNN is presented in Example 2.

Example 2: If $\tilde{A} = (1,2,3;1,0.5,0.75)$, $\tilde{B} = (4,6,8;1,0.5,0.75)$ and $n_1 = n_2 = n_3 = 3$ then using Equation (3.21), we get

$$C_{(3,3,\alpha,\beta,\gamma)} = \left[-4+(1-\alpha)^{\frac{1}{3}}, -4-(1-\alpha)^{\frac{1}{3}}; -4+3\left(\frac{\beta-0.5}{0.5}\right)^{\frac{1}{3}}, -4-\left(\frac{\beta-0.5}{0.5}\right)^{\frac{1}{3}}; -4+3\left(\frac{\gamma-0.75}{0.25}\right)^{\frac{1}{3}}, -4-\left(\frac{\gamma-0.75}{0.25}\right)^{\frac{1}{3}}\right].$$

The graph of above equation is presented in Figure 5.

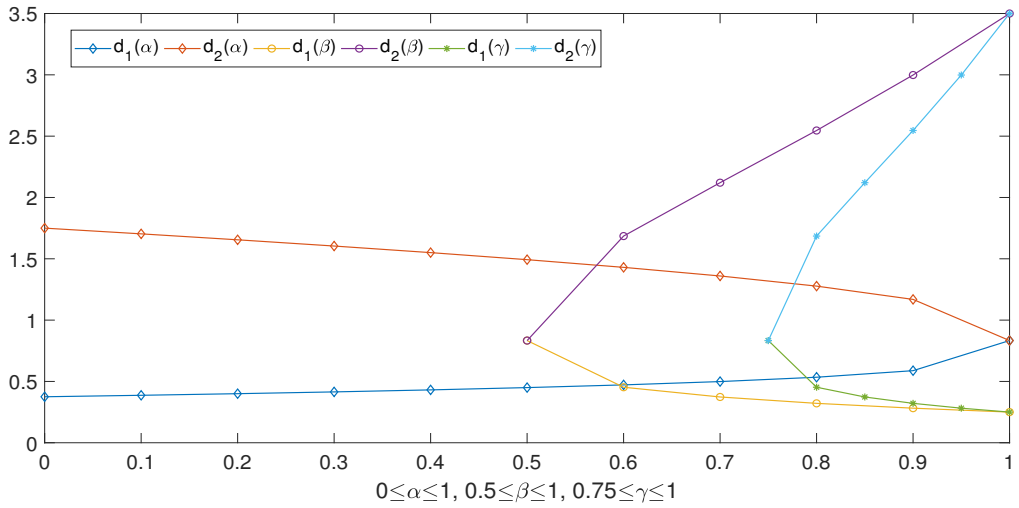

FIGURE 5. Subtraction of two NLTNN

3.2.3. *Multiplication and division of two GNLTNN*

This section presents the multiplication and division of two NLTNN using interval rule base method. Consider $[a_1, a_2]$ and $[a_3, a_4]$, where $a_i \neq 0, i = 1, 2, 3, 4$. Now $[a_1, a_2] . [a_3, a_4] = [\min\{a_1a_3, a_1a_4, a_2a_3, a_2a_4\}, \max\{a_1a_3, a_1a_4, a_2a_3, a_2a_4\}]$ and $\frac{[a_1,a_2]}{[a_3,a_4]} = \left[\min\left\{\frac{a_1}{a_3}, \frac{a_1}{a_4}, \frac{a_2}{a_3}, \frac{a_2}{a_4}\right\}, \max\left\{\frac{a_1}{a_3}, \frac{a_1}{a_4}, \frac{a_2}{a_3}, \frac{a_2}{a_4}\right\}\right]$. Using this technique, we can obtain the product of two NLTNN as follows.

For multiplication,

$$C_{\alpha,\beta,\gamma} = A_{\alpha,\beta,\gamma} * B_{\alpha,\beta,\gamma} = [e_1(\alpha), e_2(\alpha); e_1(\beta), e_2(\beta); e_1(\gamma), e_2(\gamma)], \tag{3.25}$$

where

$$e_i(\mathrm{J}) = \begin{cases} \min[A_1(j) \cdot B_1(j), A_1(j) \cdot B_2(\alpha), A_2(j) \cdot B_1(j), A_2(j) \cdot B_2(j)], \text{ for } i = 1, j = \alpha, \beta, \gamma \\ \max[A_1(j) \cdot B_1(j), A_1(j) \cdot B_2(j), A_2(j) \cdot B_1(j), A_2(j) \cdot B_2(j)], \text{ for } i = 2, j = \alpha, \beta, \gamma \end{cases}$$

For division,

$$C_{\alpha,\beta,\gamma} = \frac{A_{\alpha,\beta,\gamma}}{B_{\alpha,\beta,\gamma}} = [d_1(\alpha), d_2(\alpha); d_1(\beta), d_2(\beta); d_1(\gamma), d_2(\gamma)], \tag{3.26}$$

where

$$d_i(j) = \begin{cases} \min\left[\frac{A_1(j)}{B_1(j)}, \frac{A_1(j)}{B_2(j)}, \frac{A_2(j)}{B_1(j)}, \frac{A_2(j)}{B_2(j)}\right], \text{ for } i = 1, j = \alpha, \beta, \gamma \\ \max\left[\frac{A_1(j)}{B_1(j)}, \frac{A_1(j)}{B_2(j)}, \frac{A_2(j)}{B_1(j)}, \frac{A_2(j)}{B_2(j)}\right], \text{ for } i = 2, j = \alpha, \beta, \gamma \end{cases}$$

Example 3 If $\tilde{A} = (3, 5, 7; 1, 0.5, 0.75)$, $\tilde{B} = (4, 6, 8; 1, 0.5, 0.75)$ and $n_1 = n_2 = n_3 = 3$ then

$$A_{(3,3,\alpha,\beta,\gamma)} = \Bigg[5 - 2(1-\alpha)^{\frac{1}{3}}, 5 + 2(1-\alpha)^{\frac{1}{3}}, 5 - 3\left(\frac{\beta - 0.5}{0.5}\right)^{\frac{1}{3}}, 5 + 2\left(\frac{\beta - 0.5}{0.5}\right)^{\frac{1}{3}},$$
$$5 - 3\left(\frac{\gamma - 0.75}{0.25}\right)^{\frac{1}{3}}, 5 + 2\left(\frac{\gamma - 0.75}{0.25}\right)^{\frac{1}{3}}\Bigg].$$

$$B_{(3,3,\alpha,\beta,\gamma)} = \Bigg[6 - 2(1-\alpha)^{\frac{1}{3}}, 6 + 2(1-\alpha)^{\frac{1}{3}}, 6 - 4\left(\frac{\beta - 0.5}{0.5}\right)^{\frac{1}{3}}, 6 + 2\left(\frac{\beta - 0.5}{0.5}\right)^{\frac{1}{3}},$$
$$6 - 4\left(\frac{\gamma - 0.75}{0.25}\right)^{\frac{1}{3}}, 6 + 2\left(\frac{\gamma - 0.75}{0.25}\right)^{\frac{1}{3}}\Bigg].$$

$$e_i(\alpha) = \begin{cases} \min\ k_1(\alpha) & \text{if } i = 1 \\ \max\ k_1(\alpha) & \text{if } i = 2 \end{cases}$$

$$e_i(\beta) = \begin{cases} \min\ k_1(\beta) & \text{if } i = 1 \\ \max\ k_1(\beta) & \text{if } i = 2 \end{cases}$$

$$e_i(\gamma) = \begin{cases} \min\ k_1(\gamma) & \text{if } i = 1 \\ \max\ k_1(\gamma) & \text{if } i = 2 \end{cases}$$

where

$$k_1(\alpha) = \Big\{5 - 2(1-\alpha)^{\frac{1}{3}} \cdot 6 - 2(1-\alpha)^{\frac{1}{3}}, 5 + 2(1-\alpha)^{\frac{1}{3}} \cdot 6 - 2(1-\alpha)^{\frac{1}{3}},$$
$$5 - 2(1-\alpha)^{\frac{1}{3}} \cdot 6 + 2(1-\alpha)^{\frac{1}{3}}, 5 + 2(1-\alpha)^{\frac{1}{3}} \cdot 6 + 2(1-\alpha)^{\frac{1}{3}}\Big\},$$

$$k(\beta) = \Bigg\{5 - 3\left(\frac{\beta - 0.5}{0.5}\right)^{\frac{1}{3}} \cdot 6 - 4\left(\frac{\beta - 0.5}{0.5}\right)^{\frac{1}{3}}, 5 + 2\left(\frac{\beta - 0.5}{0.5}\right)^{\frac{1}{3}} \cdot 6 - 4\left(\frac{\beta - 0.5}{0.5}\right)^{\frac{1}{3}},$$
$$5 - 3\left(\frac{\beta - 0.5}{0.5}\right)^{\frac{1}{3}} \cdot 6 + 2\left(\frac{\beta - 0.5}{0.5}\right)^{\frac{1}{3}}, 5 + 2\left(\frac{\beta - 0.5}{0.5}\right)^{\frac{1}{3}} \cdot 6 + 2\left(\frac{\beta - 0.5}{0.5}\right)^{\frac{1}{3}}\Bigg\},$$

$$k(\gamma) = \Bigg\{5 - 3\left(\frac{\gamma - 0.75}{0.25}\right)^{\frac{1}{3}} \cdot 6 - 4\left(\frac{\gamma - 0.75}{0.25}\right)^{\frac{1}{3}}, 5 + 2\left(\frac{\gamma - 0.75}{0.25}\right)^{\frac{1}{3}} \cdot 6 - 4\left(\frac{\gamma - 0.75}{0.25}\right)^{\frac{1}{3}},$$
$$5 - 3\left(\frac{\gamma - 0.75}{0.25}\right)^{\frac{1}{3}} \cdot 6 + 2\left(\frac{\gamma - 0.75}{0.25}\right)^{\frac{1}{3}}, 5 + 2\left(\frac{\gamma - 0.75}{0.25}\right)^{\frac{1}{3}} \cdot 6 + 2\left(\frac{\gamma - 0.75}{0.25}\right)^{\frac{1}{3}}\Bigg\},$$

By varying the values of α, β and γ, it is observed that

$$e_1(\alpha) = \left(5 - 2(1-\alpha)^{\frac{1}{3}}\right) \cdot \left(6 - 2(1-\alpha)^{\frac{1}{3}}\right),$$
$$e_2(\alpha) = \left(5 + 2(1-\alpha)^{\frac{1}{3}}\right) \cdot \left(6 + 2(1-\alpha)^{\frac{1}{3}}\right),$$
$$e_1(\beta) = \left\{5 - 3\left(\frac{\beta - 0.5}{0.5}\right)^{\frac{1}{3}}\right\} \cdot \left\{6 - 4\left(\frac{\beta - 0.5}{0.5}\right)^{\frac{1}{3}}\right\},$$

$$e_2(\beta)=\left\{5+2\left(\frac{\beta-0.5}{0.5}\right)^{\frac{1}{3}}\right\}\cdot\left\{6+2\left(\frac{\beta-0.5}{0.5}\right)^{\frac{1}{3}}\right\},$$

$$e_1(\gamma)=\left\{5-3\left(\frac{\gamma-0.75}{0.25}\right)^{\frac{1}{3}}\right\}\cdot\left\{6-4\left(\frac{\gamma-0.75}{0.25}\right)^{\frac{1}{3}}\right\},$$

$$e_2(\gamma)=\left\{5+2\left(\frac{\gamma-0.75}{0.25}\right)^{\frac{1}{3}}\right\}\cdot\left\{6+2\left(\frac{\gamma-0.75}{0.25}\right)^{\frac{1}{3}}\right\}.$$

By interval rule base method, the $(\alpha.\ \beta,\ \gamma)$-cut of $\tilde{e}$ is given by

$$[\tilde{e}]_{(p,q,\alpha,\beta,\gamma)}=\Bigg[\left(5-2(1-\alpha)^{\frac{1}{3}}\right)\left(6-2(1-\alpha)^{\frac{1}{3}}\right),\left(5+2(1-\alpha)^{\frac{1}{3}}\right)\left(6+2(1-\alpha)^{\frac{1}{3}}\right);$$
$$\left\{5-3\left(\frac{\beta-0.5}{0.5}\right)^{\frac{1}{3}}\right\}\left\{6-4\left(\frac{\beta-0.5}{0.5}\right)^{\frac{1}{3}}\right\},\left\{5+2\left(\frac{\beta-0.5}{0.5}\right)^{\frac{1}{3}}\right\}\left\{6+2\left(\frac{\beta-0.5}{0.5}\right)^{\frac{1}{3}}\right\};$$
$$\left\{5-3\left(\frac{\gamma-0.75}{0.25}\right)^{\frac{1}{3}}\right\}\left\{6-4\left(\frac{\gamma-0.75}{0.25}\right)^{\frac{1}{3}}\right\},\left\{5+2\left(\frac{\gamma-0.75}{0.25}\right)^{\frac{1}{3}}\right\}\left\{6+2\left(\frac{\gamma-0.75}{0.25}\right)^{\frac{1}{3}}\right\}\Bigg].$$

The graph of above result is presented in Figure 6. Similarly,

$$d_i(\alpha)=\begin{cases}\min\ k_2(\alpha)\ \text{ if } i=1\\ \max\ k_2(\alpha)\ \text{ if } i=2\end{cases}$$

$$d_i(\beta)=\begin{cases}\min\ k_2(\beta)\ \text{ if } i=1\\ \max\ k_2(\beta)\ \text{ if } i=2\end{cases}$$

$$d_i(\gamma)=\begin{cases}\min\ k_2(\gamma)\ \text{ if } i=1\\ \max\ k_2(\gamma)\ \text{ if } i=2\end{cases}$$

where

$$k_2(\alpha)=\left\{\frac{5-2(1-\alpha)^{\frac{1}{3}}}{6-2(1-\alpha)^{\frac{1}{3}}},\frac{5+2(1-\alpha)^{\frac{1}{3}}}{6-2(1-\alpha)^{\frac{1}{3}}},\frac{5-2(1-\alpha)^{\frac{1}{3}}}{6+2(1-\alpha)^{\frac{1}{3}}},\frac{5+2(1-\alpha)^{\frac{1}{3}}}{6+2(1-\alpha)^{\frac{1}{3}}}\right\},$$

$$k_2(\beta)=\left\{\frac{5-3\left(\frac{\beta-0.5}{0.5}\right)^{\frac{1}{3}}}{6-4\left(\frac{\beta-0.5}{0.5}\right)^{\frac{1}{3}}},\frac{5+2\left(\frac{\beta-0.5}{0.5}\right)^{\frac{1}{3}}}{6-4\left(\frac{\beta-0.5}{0.5}\right)^{\frac{1}{3}}},\frac{5-3\left(\frac{\beta-0.5}{0.5}\right)^{\frac{1}{3}}}{6+2\left(\frac{\beta-0.5}{0.5}\right)^{\frac{1}{3}}},\frac{5+2\left(\frac{\beta-0.5}{0.5}\right)^{\frac{1}{3}}}{6+2\left(\frac{\beta-0.5}{0.5}\right)^{\frac{1}{3}}}\right\},$$

$$k_3(\gamma)=\left\{\frac{5-3\left(\frac{\gamma-0.75}{0.25}\right)^{\frac{1}{3}}}{6-4\left(\frac{\gamma-0.75}{0.25}\right)^{\frac{1}{3}}},\frac{5+2\left(\frac{\gamma-0.75}{0.25}\right)^{\frac{1}{3}}}{6-4\left(\frac{\gamma-0.75}{0.25}\right)^{\frac{1}{3}}},\frac{5-3\left(\frac{\gamma-0.75}{0.25}\right)^{\frac{1}{3}}}{6+2\left(\frac{\gamma-0.75}{0.25}\right)^{\frac{1}{3}}},\frac{5+2\left(\frac{\gamma-0.75}{0.25}\right)^{\frac{1}{3}}}{6+2\left(\frac{\gamma-0.75}{0.25}\right)^{\frac{1}{3}}}\right\}.$$

It is observed that

$$d_1(\alpha)=\frac{5+2(1-\alpha)^{\frac{1}{3}}}{6-2(1-\alpha)^{\frac{1}{3}}},\ d_2(\alpha)=\frac{5-2(1-\alpha)^{\frac{1}{3}}}{6+2(1-\alpha)^{\frac{1}{3}}},$$

$$d_1(\beta)=\frac{5+2\left(\frac{\beta-0.5}{0.5}\right)^{\frac{1}{3}}}{6-4\left(\frac{\beta-0.5}{0.5}\right)^{\frac{1}{3}}}, d_2(\beta)=\frac{5-3\left(\frac{\beta-0.5}{0.5}\right)^{\frac{1}{3}}}{6+2\left(\frac{\beta-0.5}{0.5}\right)^{\frac{1}{3}}},$$

$$d_1(\gamma)=\frac{5+2\left(\frac{\gamma-0.75}{0.25}\right)^{\frac{1}{3}}}{6-4\left(\frac{\gamma-0.75}{0.25}\right)^{\frac{1}{3}}}, d_2(\gamma)=\frac{5-3\left(\frac{\gamma-0.75}{0.25}\right)^{\frac{1}{3}}}{6+2\left(\frac{\gamma-0.75}{0.25}\right)^{\frac{1}{3}}},$$

By interval rule base method, the $(\alpha.\ \beta,\ \gamma)$-cut of $\tilde{d}$ is given by

$$[\tilde{d}]_{(3,3,\alpha,\beta,\gamma)}=\left\{\frac{5+2(1-\alpha)^{\frac{1}{3}}}{6-2(1-\alpha)^{\frac{1}{3}}}, \frac{5-2(1-\alpha)^{\frac{1}{3}}}{6+2(1-\alpha)^{\frac{1}{3}}}, \frac{5+2\left(\frac{\beta-0.5}{0.5}\right)^{\frac{1}{3}}}{6-4\left(\frac{\beta-0.5}{0.5}\right)^{\frac{1}{3}}}, \frac{5-3\left(\frac{\beta-0.5}{0.5}\right)^{\frac{1}{3}}}{6+2\left(\frac{\beta-0.5}{0.5}\right)^{\frac{1}{3}}}\right.$$

$$\left.\frac{5+2\left(\frac{\gamma-0.75}{0.25}\right)^{\frac{1}{3}}}{6-4\left(\frac{\gamma-0.75}{0.25}\right)^{\frac{1}{3}}}, \frac{5-3\left(\frac{\gamma-0.75}{0.25}\right)^{\frac{1}{3}}}{6+2\left(\frac{\gamma-0.75}{0.25}\right)^{\frac{1}{3}}}\right\}.$$

The graph of above result is presented in Figure 7.

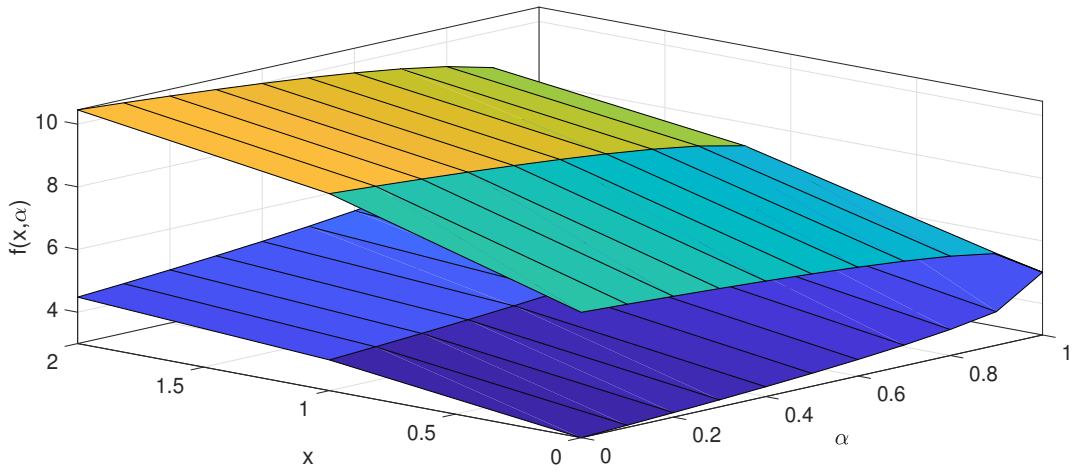

FIGURE 6. Multiplication of two NLTNN

3.3. *Neutrosophic valued function*

Let $\underline{H}(\alpha)$, $\overline{H}(\alpha)$, $\underline{H}(\beta)$, $\overline{H}(\beta)$, $\underline{H}(\gamma)$ and $\overline{H}(\gamma)$ are the continuous functions on the interval I. The set $\tilde{H}$ can be obtained by membership function as follows:

$$T_{\tilde{H}}(l(\alpha))=\begin{cases}\alpha, & l(\alpha)=\underline{H}(\alpha), 0\leqslant\alpha\leqslant 1\\ \alpha, & l(\alpha)=\bar{H}(\alpha), 0\leqslant\alpha\leqslant 1\\ 0, & \text{otherwise}\end{cases} \tag{3.27}$$

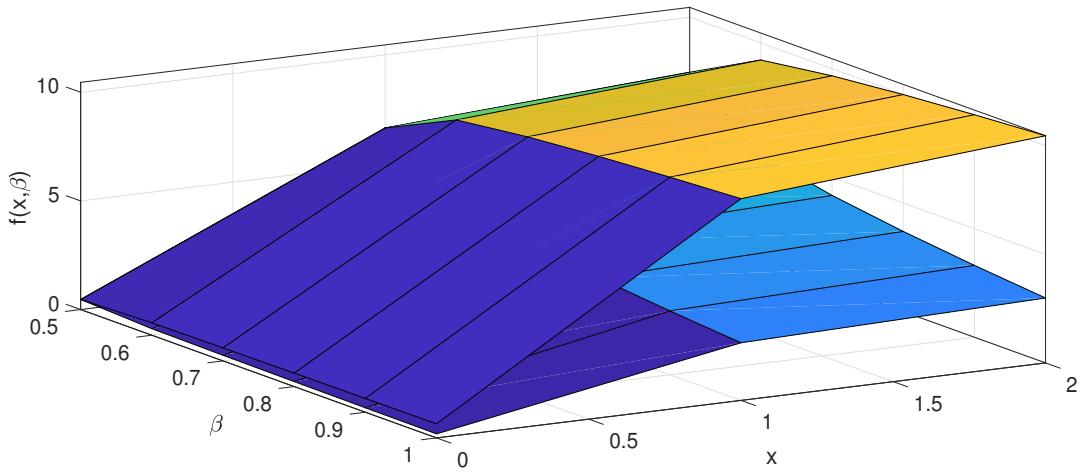

FIGURE 7. Division of two NLTNN

$$T_{\tilde{H}}\left(m\left(\beta\right)\right)=\begin{cases}\beta, & m\left(\beta\right)=\underline{H}\left(\beta\right),0\leqslant\beta\leqslant1\\ \beta, & m\left(\beta\right)=\bar{H}\left(\beta\right),0\leqslant\beta\leqslant1\\ 1, & \text{otherwise}\end{cases}\tag{3.28}$$

$$T_{\tilde{H}}\left(n\left(\gamma\right)\right)=\begin{cases}\gamma, & n\left(\gamma\right)=\underline{H}\left(\gamma\right),0\leqslant\gamma\leqslant1\\ \gamma, & n\left(\gamma\right)=\bar{H}\left(\gamma\right),0\leqslant\gamma\leqslant1\\ 1, & \text{otherwise}\end{cases}\tag{3.29}$$

The (α,β,γ)-cuts of neutrosophic valued function $\tilde{H}(t)$ is as follows:

$$[\tilde{H}(t)]_{(}\alpha,\beta,\gamma)=[\underline{H}(\alpha),\overline{H}(\alpha);\underline{H}(\beta),\overline{H}(\beta);\underline{H}(\gamma)\overline{H}(\gamma)].\tag{3.30}$$

Example 4: Consider a neutrosophic valued function $\tilde{F}(t)=at^2+t+1$, where a is a neutrosophic coefficient. Let $\tilde{H}(t)_{(}p,q)=(2,4,6,1,0.5,0.75)$, $p_i=q_i=4$ where $i=T,I,F$. Using equations $(3.5)-(3.7)$, we obtain

$$\begin{aligned}\tilde{F}\left(t\right)_{(4,4,\alpha,\beta,\gamma)}=\Bigg[&\left\{4-2(1-\alpha)^{\frac{1}{4}}\right\}t^2+t+1,\left\{4+2(1-\alpha)^{\frac{1}{4}}\right\}t^2+t+1;\\&\left\{4-2\left(\frac{\beta-0.5}{0.5}\right)^{\frac{1}{4}}\right\}t^2+t+1,\left\{4+2\left(\frac{\beta-0.5}{0.5}\right)^{\frac{1}{4}}\right\}t^2+t+1;\\&\left\{4-2\left(\frac{\gamma-0.75}{0.25}\right)^{\frac{1}{4}}\right\}t^2+t+1,\left\{4+2\left(\frac{\gamma-0.75}{0.25}\right)^{\frac{1}{4}}\right\}t^2+t+1\Bigg].\end{aligned}$$

The solution of the above equation is presented in Tables $2-4$

α	$t=0$		$t=1$		$t=2$		$t=3$	
	$\underline{F}(t,\alpha)$	$\bar{F}(t,\alpha)$	$\underline{F}(t,\alpha)$	$\bar{F}(t,\alpha)$	$\underline{F}(t,\alpha)$	$\bar{F}(t,\alpha)$	$\underline{F}(t,\alpha)$	$\bar{F}(t,\alpha)$
0	4.0000	8.0000	11.0000	27.0000	22.0000	58.0000	37.0000	101.0000
0.1	4.0520	7.9480	11.2080	26.7920	22.4679	57.5321	37.8319	100.1681
0.2	4.1085	7.8915	11.4341	26.5659	22.9767	57.0233	38.7363	99.2637
0.3	4.1706	7.8294	11.6825	26.3175	23.5356	56.4644	39.7299	98.2701
0.4	4.2398	7.7602	11.9591	26.0409	24.1580	55.8420	40.8364	97.1636
0.5	4.3182	7.6818	12.2728	25.7272	24.8639	55.1361	42.0913	95.9087
0.6	4.4095	7.5905	12.6378	25.3622	25.6851	54.3149	43.5513	94.4487
0.7	4.5198	7.4802	13.0793	24.9207	26.6785	53.3215	45.3174	92.6826
0.8	4.6625	7.3375	13.6501	24.3499	27.9627	52.0373	47.6003	90.3997
0.9	4.8753	7.1247	14.5013	23.4987	29.8779	50.1221	51.0051	86.9949
1	6.0000	6.0000	19.0000	19.0000	40.0000	40.0000	69.0000	69.0000

TABLE 2. Solution of the equation for various values of α and t..

β	$t=0$		$t=1$		$t=2$		$t=3$	
	$\underline{F}(t,\beta)$	$\bar{F}(t,\beta)$	$\underline{F}(t,\beta)$	$\bar{F}(t,\beta)$	$\underline{F}(t,\beta)$	$\bar{F}(t,\beta)$	$\underline{F}(t,\beta)$	$\bar{F}(t,\beta)$
0.5000	6.0000	6.0000	19.0000	19.0000	40.0000	40.0000	69.0000	69.0000
0.6000	4.6625	7.3375	13.6501	24.3499	27.9627	52.0373	47.6003	90.3997
0.7000	4.4095	7.5905	12.6378	25.3622	25.6851	54.3149	43.5513	94.4487
0.8000	4.2398	7.7602	11.9591	26.0409	24.1580	55.8420	40.8364	97.1636
0.9000	4.1085	7.8915	11.4341	26.5659	22.9767	57.0233	38.7363	99.2637
1.0000	4.0000	8.0000	11.0000	27.0000	22.0000	58.0000	37.0000	101.0000

TABLE 3. Solution of the equation for various values of β and t..

4. **Values and ambiguities of GNLTNN**

In this section, we aim to explore the values and ambiguities associated with GNLTNN. Let $\tilde{A}_{(p.q)}$ be GNLTNN. The values of GNLTNN for the $\alpha-$ cut , $\beta-$ cut and $\gamma-$ cut is denoted as $V_T(\tilde{A})$, $V_I(\tilde{A})$ and $V_F(\tilde{A})$ respectively. These values are defined as follows

$$V_T(\tilde{A}) = \int_0^{u_{\tilde{A}}} \left\{ T^L_{\tilde{A}}(\alpha, p_T) + T^R_{\tilde{A}}(\alpha, q_T) \right\} \phi_1(\alpha)\, d\alpha, \phi_1(\alpha) \in [0,1], \tag{4.1}$$

$$V_I(\tilde{A}) = \int_{v_{\tilde{A}}}^{1} \left\{ I^L_{\tilde{A}}(\beta, p_I) + I^R_{\tilde{A}}(\beta, q_I) \right\} \phi_2(\beta)\, d\beta, \phi_2(\beta) \in [0,1], \tag{4.2}$$

γ	$t=0$		$t=1$		$t=2$		$t=3$	
	$\underline{F}(t,\gamma)$	$\bar{F}(t,\gamma)$	$\underline{F}(t,\gamma)$	$\bar{F}(t,\gamma)$	$\underline{F}(t,\gamma)$	$\bar{F}(t,\gamma)$	$\underline{F}(t,\gamma)$	$\bar{F}(t,\gamma)$
0.75	6.0000	6.0000	19.0000	19.0000	40.0000	40.0000	69.0000	69.0000
0.80	4.6625	7.3375	13.6501	24.3499	27.9627	52.0373	47.6003	90.3997
0.85	4.4095	7.5905	12.6378	25.3622	25.6851	54.3149	43.5513	94.4487
0.90	4.2398	7.7602	11.9591	26.0409	24.1580	55.8420	40.8364	97.1636
0.95	4.1085	7.8915	11.4341	26.5659	22.9767	57.0233	38.7363	99.2637
1.00	4.0000	8.0000	11.0000	27.0000	22.0000	58.0000	37.0000	101.0000

TABLE 4. Solution of the equation for various values of γ and t

$$V_F(\tilde{A}) = \int_{w_{\tilde{A}}}^{1} \left\{ F_{\tilde{A}}^{L}(\gamma, p_F) + F_{\tilde{A}}^{R}(\gamma, q_F) \right\} \phi_3(\gamma)\, d\gamma, \phi_3(\gamma) \in [0,1], \tag{4.3}$$

where

- $\phi_1(\alpha)$ is monotonic and non-decreasing in the interval $\left[0, u_{\tilde{A}}\right]$ and $\phi_1(0) = 0$
- $\phi_2(\beta)$ is monotonic and non-increasing in the interval $\left[v_{\tilde{A}}, 1\right]$ and $\phi_2(1) = 0$
- $\phi_3(\gamma)$ is monotonic and non-increasing in the interval $\left[w_{\tilde{A}}, 1\right]$ and $\phi_3(1) = 0$

Without loss of generality, we assume $\phi_1(\alpha) = \alpha$, $\phi_2(\beta) = 1-\beta$ and $\phi_3(\gamma) = 1-\gamma$ Using Equations $(3.5) - (3.7)$ in Equations $(4.1) - (4.3)$ respectively, we get the following results

$$\begin{aligned} V_T(\tilde{A}) &= \int_{0}^{u_{\tilde{A}}} \left\{ 2c - \left(1 - \frac{\alpha}{u_{\tilde{A}}}\right)^{\frac{1}{n_1}} (2c - \underline{c} - \bar{c}) \right\} \alpha d\alpha \\ &= c u_{\tilde{A}} - \frac{(2c - \underline{c} - \bar{c}) \left(u_{\tilde{A}}\right)^2}{\left(\frac{1}{n_1} + 1\right)\left(\frac{1}{n_1} + 2\right)}, \end{aligned} \tag{4.4}$$

$$\begin{aligned} V_I(\tilde{A}) &= \int_{v_{\tilde{A}}}^{1} \left\{ 2c - \frac{\left(\underline{c} + c - \bar{c}\right)\left(\beta - v_{\tilde{A}}\right)^{\frac{1}{n_2}}}{\left(1 - v_{\tilde{A}}\right)^{\frac{1}{n_2}}} \right\} (1-\beta)\, d\beta \\ &= c\left(v_{\tilde{A}} - 1\right)^2 - \frac{{n_2}^2 \left({v_{\tilde{A}}}^2 - 2v_{\tilde{A}} + 1\right)(\underline{c} + c - \bar{c})}{(2{n_2}^2 + 3n_2 + 1)}, \end{aligned} \tag{4.5}$$

$$\begin{aligned} V_F(\tilde{A}) &= \int_{w_{\tilde{A}}}^{1} \left\{ 2c - \frac{\left(\underline{c} + c - \bar{c}\right)\left(\gamma - w_{\tilde{A}}\right)^{\frac{1}{n_3}}}{\left(1 - w_{\tilde{A}}\right)^{\frac{1}{n_3}}} \right\} (1-\gamma)\, d\gamma \\ &= c\left(w_{\tilde{A}} - 1\right)^2 - \frac{{n_3}^2 \left({w_{\tilde{A}}}^2 - 2w_{\tilde{A}} + 1\right)(\underline{c} + c - \bar{c})}{(2{n_3}^2 + 3n_3 + 1)}. \end{aligned} \tag{4.6}$$

Let $G_T(\tilde{A})$, $G_I(\tilde{A})$ and $G_F(\tilde{A})$ denotes the ambiguities of the GNLTNS for α, β and γ cut sets respectively, then

$$G_T(\tilde{A}) = \int_0^{u_{\tilde{A}}} \left\{ T^R_{\tilde{A}}(\alpha, q_T) - T^L_{\tilde{A}}(\alpha, p_T) \right\} \phi_1(\alpha)\, d\alpha, \phi_1(\alpha) \in [0,1] \tag{4.7}$$

$$G_I(\tilde{A}) = \int_{v_{\tilde{A}}}^{1} \left\{ I^R_{\tilde{A}}(\beta, q_F) - I^L_{\tilde{A}}(\beta, p_F) \right\} \phi_2(\beta)\, d\beta, \phi_2(\beta) \in [0,1] \tag{4.8}$$

$$G_F(\tilde{A}) = \int_{w_{\tilde{A}}}^{1} \left\{ F^R_{\tilde{A}}(\gamma, q_F) - F^L_{\tilde{A}}(\gamma, p_F) \right\} \phi_3(\gamma)\, d\gamma, \phi_3(\gamma) \in [0,1]\,. \tag{4.9}$$

Similarly, using Equations $(3.5) - (3.7)$ in Equations $(4.7) - (4.9)$, we get

$$G_T(\tilde{A}) = \frac{(\bar{c} - \underline{c}) \left(u_{\tilde{A}}\right)^2}{\left(\frac{1}{n_1} + 1\right)\left(\frac{1}{n_1} + 2\right)} \tag{4.10}$$

$$G_I(\tilde{A}) = \frac{{n_2}^2 (\underline{c} + \bar{c} - c) \left({v_{\tilde{A}}}^2 - 2v_{\tilde{A}} + 1\right)}{2{n_2}^2 + 3n_2 + 1} \tag{4.11}$$

$$G_F(\tilde{A}) = \frac{{n_3}^2 (\underline{c} + \bar{c} - c) \left({w_{\tilde{A}}}^2 - 2w_{\tilde{A}} + 1\right)}{2{n_3}^2 + 3n_3 + 1} \tag{4.12}$$

These values provide insights into the degree of truth, indeterminacy, and falsity associated with a GNLTNN within specific intervals defined by the cut sets. By analyzing these values, we can understand the distribution of uncertainty and ambiguity inherent in the GNLTNN.

5. **Linear Fredholm Integral Equation in Neutrosophic Environment**

This section delves into the realm of neutrosophic integral equations, a significant branch within integral equations. Such equations play a pivotal role in theoretical analysis, offering a robust framework for deriving analytical solutions, exploring the existence and uniqueness of solutions, and examining qualitative properties of various physical systems.

5.1. *Neutrosophic integral equation (NIE)*

We consider Fredholm integral equation of second kind

$$f(x) = g(x) + \lambda \int_a^b k(s,t)\, u(t)\, dt$$

The above Equation is said be NIE if

(1) $g(x)$ is neutrosophic valued function,

(2) $k(s,t)$ is neutrosophic valued function,

(3) Both $g(x)$ and $k(s,t)$ are neutrosophic valued functions.

5.2. *Condition for existence for solution of NIE*

Let the solution NIE be $\tilde{f}(x)$ and its (α,β,γ)- cuts be

$$\left[\tilde{f}(x)\right]_{(\alpha,\beta,\gamma)} = \left[\underline{f}(x,\alpha), \bar{f}(x,\alpha); \underline{f}(x,\beta), \bar{f}(x,\beta); \underline{f}(x,\gamma), \bar{f}(x,\gamma)\right].$$

The solution is said to be strong solution if

(1) $\frac{\partial \underline{f}(x,\alpha)}{\partial \alpha} > 0, \frac{\partial \bar{f}(x,\alpha)}{\partial \alpha} < 0 \quad \forall \alpha \in \left[0, u_{\tilde{A}}\right], \underline{f}(x,1) \leqslant \bar{f}(x,1)$

(2) $\frac{\partial \underline{f}(x,\beta)}{\partial \beta} < 0, \frac{\partial \bar{f}(x,\beta)}{\partial \beta} > 0 \quad \forall \beta \in \left[v_{\tilde{A}}, 1\right], \underline{f}(x,0) \leqslant \bar{f}(x,0)$

(3) $\frac{\partial \underline{u}(x,\gamma)}{\partial \gamma} < 0, \frac{\partial \bar{f}(x,\gamma)}{\partial \gamma} > 0 \quad \forall \gamma \in \left[w_{\tilde{A}}, 1\right], \underline{f}(x,0) \leqslant \bar{f}(x,0)$

The rest of the cases are weak solutions.

5.3. *Evaluation of NIE*

Consider the integral equation $f(x) = \bar{g}(x) + \lambda \int_a^b \bar{k}(s,t) f(t)\, dt$. Here we consider both $\bar{g}(x)$ and $\bar{k}(s,t)$ are neutrosophic valued function. Taking Laplace transform,, we get

$$L[f(x)) = L[\bar{g}(x)] + \lambda L[\bar{k}(x,t)] L[f(t)] \tag{5.1}$$

Case(i) When $k(x,t)$ is a positive function

$$\underline{f}(x,i) = \mathscr{L}^{-1}\left[\frac{\mathscr{L}\left\{\underline{g}(s,i)\right\}}{1-\lambda\mathscr{L}\left\{\underline{k}(s,i)\right\}}\right], i = \alpha,\beta,\gamma \tag{5.2}$$

$$\bar{f}(x,i) = \mathscr{L}^{-1}\left[\frac{\mathscr{L}\left\{\bar{g}(s,i)\right\}}{1-\lambda\mathscr{L}\left\{\bar{k}(s,i)\right\}}\right], i = \alpha,\beta,\gamma \tag{5.3}$$

Case(ii) When $k(x,t)$ is a negative function say $k(x,t) = -h(x,t)$ then

$$L[f(x)) = L[g(x)] + \lambda L[-h(x,t)] L[f(t)] \tag{5.4}$$

$$\underline{f}(x,i) = \mathscr{L}^{-1}\left[\frac{\lambda\mathscr{L}\left\{\underline{h}(x,t,i)\right\}\mathscr{L}\left\{\underline{g}(s,i)\right\}}{1-\lambda^2\mathscr{L}\left\{\underline{h}(x,t,i)\right\}\mathscr{L}\left\{\bar{h}(x,t,i)\right\}}\right], i = \alpha,\beta,\gamma \tag{5.5}$$

$$\bar{f}(x,i) = \mathscr{L}^{-1}\left[\frac{\lambda L\left\{\bar{h}(x,t,i)\right\}\mathscr{L}\left\{\bar{g}(s,i)\right\}}{1-\lambda^2\mathscr{L}\left\{\underline{h}(x,t,i)\right\}\mathscr{L}\left\{\bar{h}(x,t,i)\right\}}\right], i = \alpha,\beta,\gamma \tag{5.6}$$

Example 5: Consider a scenario of heat transfer in a one-dimensional rod. Let $f(x)$ represent the temperature distribution along the rod at position x, $g(x)$ represent the initial temperature distribution and $k(x,t)$ represent the thermal conductivity between two points x and t. The equation $f(x) = g(x) + \lambda \int_a^b k(x,t) f(t)\, dt$ describes how the temperature distribution evolves over time due to the heat flow between different points along the rod. let initial temperature distribution $g(x) = (3,5,7;1,0.5,0.75)e^{-x}$, proportionality constant $\lambda = 1$, length of the rod

a = 0,b = x, thermal conductivity $k(x,t) = \cos(x-t)$. Using Equations $(4.1)-(4.3)$, we can get the solution for the integral equation as follows

$$\underline{f}(x,\alpha) = \left(5 - 2(1-\alpha)^{\frac{1}{3}}\right) m(x), \bar{f}(x,\alpha) = \left(5 + 2(1-\alpha)^{\frac{1}{3}}\right) m(x),$$

$$\underline{f}(x,\beta) = \left\{5 - 3\left(\frac{\beta - 0.5}{0.5}\right)^{\frac{1}{3}}\right\} m(x), \bar{f}(x,\beta) = \left\{5 + 2\left(\frac{\beta - 0.5}{0.5}\right)^{\frac{1}{3}}\right\} m(x),$$

$$\underline{f}(x,\gamma) = \left\{5 - 3\left(\frac{\gamma - 0.75}{0.25}\right)^{\frac{1}{3}}\right\} m(x), \bar{f}(x,\gamma) = \left\{5 + 2\left(\frac{\gamma - 0.75}{0.25}\right)^{\frac{1}{3}}\right\} m(x),$$

where

$$m(x) = \left[\frac{e^{\frac{x}{2}}}{3} \quad \sqrt{3}\sin\frac{\sqrt{3}x}{2} + \cos\frac{\sqrt{3}x}{2}\right) + \frac{2e^{-x}}{3}\Bigg].$$

Graphical representation of the above result is presented in Figures $8-10$.

6. **Result discussion**

The conclusions drawn from Table $5-7$ offer valuable insights into the behavior of temperature distribution $f(x)$ in one-dimensional heat transfer modeling using NLTNN. From Table 5, it is observed that as α increases from 0 to 1, the values of $\underline{f}(x,\alpha)$ increase gradually, whereas the values of $\bar{f}(x,\alpha)$ decrease. From Table 6, it is observed that as β rises from 0.5 to 1, $\underline{f}(x,\beta)$ decreases gradually, whereas the values of $\bar{f}(x,\beta)$ increase. Table 7 behaves the same as Table 6. As γ increases from 0.75 to 1, $\underline{f}(x,\gamma)$ decreases gradually, whereas the values of $\bar{f}(x,\gamma)$ increase. The temperature distribution $\underline{f}(x)$ and $\bar{f}(x)$ are influenced by the parameter values, exhibiting distinct patterns based on the values of α, β, and γ.

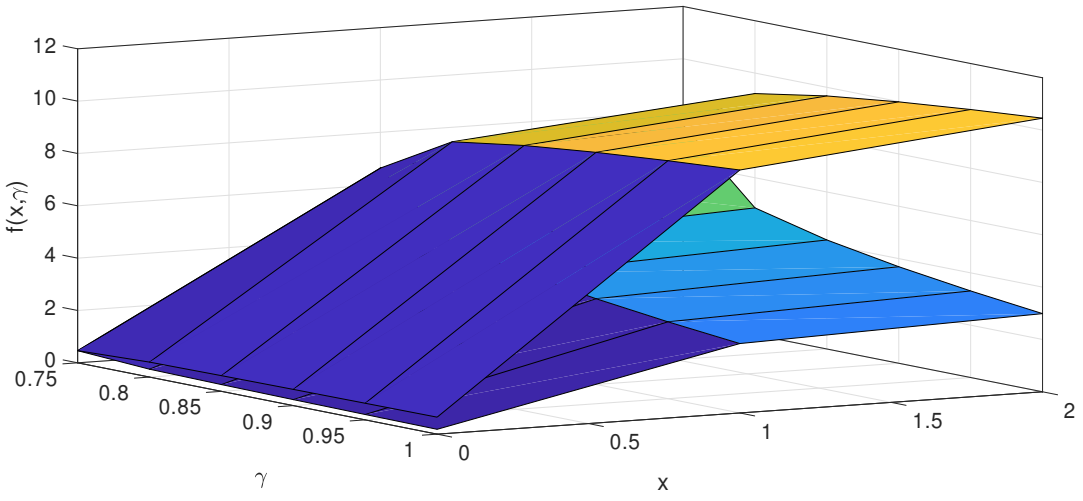

FIGURE 8. Solution of integral equation $f(x,\alpha)$

α	$x=0$		$x=1$		$x=2$	
	$\underline{f}(x,\alpha)$	$\bar{f}(x,\alpha)$	$\underline{f}(x,\alpha)$	$\bar{f}(x,\alpha)$	$\underline{f}(x,\alpha)$	$\bar{f}(x,\alpha)$
0.0	3.0000	7.0000	3.9792	9.2849	4.4814	10.4565
0.1	3.0690	6.9310	4.0708	9.1933	4.5845	10.3534
0.2	3.1434	6.8566	4.1694	9.0947	4.6955	10.2423
0.3	3.2242	6.7758	4.2766	8.9875	4.8162	10.1216
0.4	3.3131	6.6869	4.3946	8.8695	4.9491	9.9887
0.5	3.4126	6.5874	4.5265	8.7376	5.0977	9.8402
0.6	3.5264	6.4736	4.6774	8.5867	5.2677	9.6702
0.7	3.6611	6.3389	4.8562	8.4079	5.4689	9.4689
0.8	3.8304	6.1696	5.0807	8.1834	5.7218	9.2161
0.9	4.0717	5.9283	5.4007	7.8634	6.0822	8.8556
1.0	5.0000	5.0000	6.6321	6.6321	7.4689	7.4689

TABLE 5. Solution of the integral equation for various values of α and x.

β	$x=0$		$x=1$		$x=2$	
	$\underline{f}(x,\beta)$	$\bar{f}(x,\beta)$	$\underline{f}(x,\beta)$	$\bar{f}(x,\beta)$	$\underline{f}(x,\beta)$	$\bar{f}(x,\beta)$
0.5	5.0000	5.0000	6.6321	6.6321	7.4689	7.4689
0.6	3.2456	6.1696	4.3050	8.1834	4.8482	9.2161
0.7	2.7896	6.4736	3.7001	8.5867	4.1670	9.6702
0.8	2.4697	6.6869	3.2758	8.8695	3.6892	9.9887
0.9	2.2150	6.8566	2.9381	9.0947	3.3088	10.2423
1.0	2.0000	7.0000	2.6528	9.2849	2.9876	10.4565

TABLE 6. Solution of the integral equation for various values of β and x.

γ	$x=0$		$x=1$		$x=2$	
	$\underline{f}(x,\gamma)$	$\bar{f}(x,\gamma)$	$\underline{f}(x,\gamma)$	$\bar{f}(x,\gamma)$	$\underline{f}(x,\gamma)$	$\bar{f}(x,\gamma)$
0.75	5.0000	5.0000	6.6321	6.6321	7.4689	7.4689
0.8	3.2456	6.1696	4.3050	8.1834	4.8482	9.2161
0.85	2.7896	6.4736	3.7001	8.5867	4.1670	9.6702
0.9	2.4697	6.6869	3.2758	8.8695	3.6892	9.9887
0.9.5	2.2150	6.8566	2.9381	9.0947	3.3088	10.2423
1.0	2.0000	7.0000	2.6528	9.2849	2.9876	10.4565

TABLE 7. Solution of the integral equation for various values of γ and x.

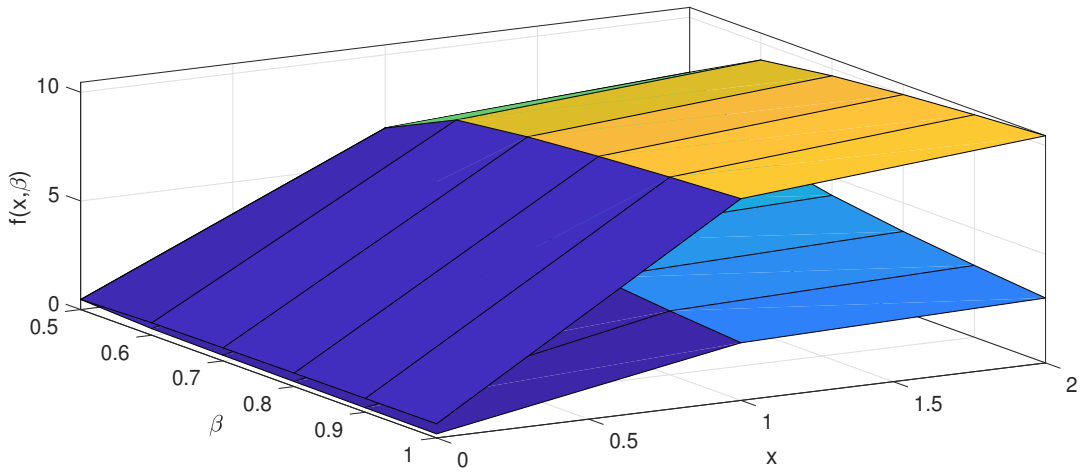

FIGURE 9. Solution of integral equation $f(x, \beta)$

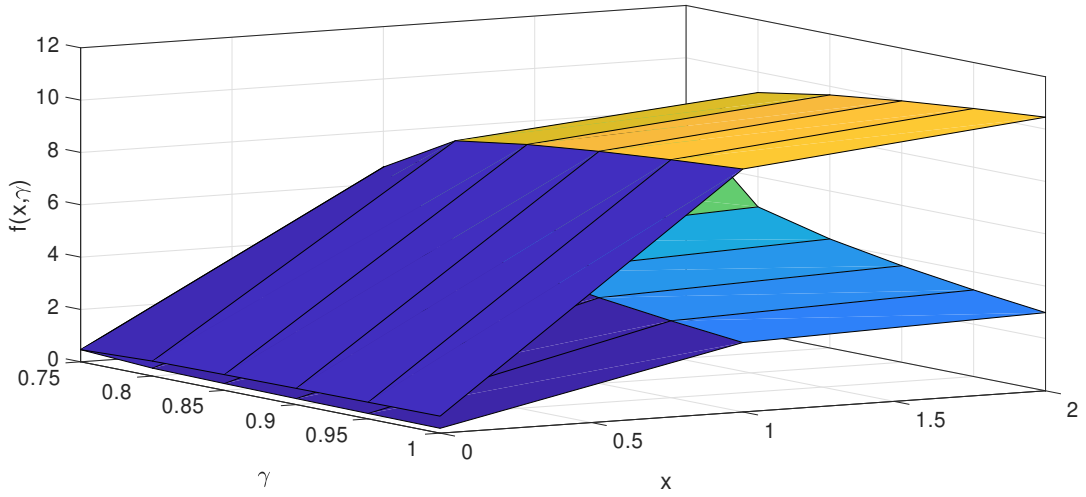

FIGURE 10. Solution of integral equation $f(x, \gamma)$

7. **Conclusion and future work**

In conclusion, this paper presents a refined version of GNLNN, which mitigates certain constraints observed in prior literature. We outline the fundamental properties of GNLNN, particularly emphasizing the notions of (α, β, γ). Moreover, we illustrate the application of this numerical framework in integral equations set within a neutrosophic context. This research paves the way for further exploration, offering avenues to tackle diverse categories of both differential and integral equations. Such endeavors hold promise for broadening the scope of mathematical modeling and analysis, thereby enhancing their utility and significance.

Conflict of Interest: The authors declare that they have no conflict of interest.

Authors Contribution: All the authors have equal contribution for preparing this article.

Acknowledgment: The authors express their gratitude to the anonymous reviewers for their thorough reading of the work and their insightful criticism, which helped to enhance the article's presentation.

References

[1] Alah, V. T., & Hashemzehi, S. (2008). The homotopy perturbation method for fuzzy Fredholm integral equations, 1-12.

[2] Abouhawwash, M., Jameel, M., & Askar, S. S. (2023). A Neutrosophic Framework for Assessment of Distributed Circular Water to Give Neighborhoods Analysis to Prepare for Unexpected Stressor Events. Neutrosophic Systems With Applications, 5, 27-35. https://doi.org/10.61356/j.nswa.2023.25

[3] Agarwal, R. P., O'Regan, D., & Lakshmikantham, V. (2004). Fuzzy Volterra integral equations: a stacking theorem approach. Applicable Analysis, 83(5), 521-532. https://doi.org/10.1080/00036810410001647117

[4] Atanassov, K. T., & Atanassov, K. T. (1999). Intuitionistic fuzzy sets (pp. 1-137). Physica-Verlag HD.

[5] Chakraborty, A., Mondal, S. P., Mahata, A., & Alam, S. (2021). Different linear and non-linear form of trapezoidal neutrosophic numbers, de-neutrosophication techniques and its application in time-cost optimization technique, sequencing problem. RAIRO-Operations Research, 55, S97-S118. https://doi.org/10.1051/ro/2019090

[6] Diamond, P. (2002). Theory and applications of fuzzy Volterra integral equations. IEEE Transactions on Fuzzy Systems, 10(1), 97-102. https://doi.org/10.1109/91.983284

[7] Elsayed, A., Arain, B., & Sallam, K. M. (2024). Exploring the Application of Digital Twin Technology in the Energy Sector using MEREC and MAIRCA Methods. Neutrosophic Systems With Applications, 19, 15-29. https://doi.org/10.61356/j.nswa.2024.19326

[8] Elsayed, A., & Arain, B. (2024). A Systematic Approach for Evaluating and Selecting Healthcare Waste Treatment Devices using OWCM-CODAS and Triangular Neutrosophic Sets. Neutrosophic Systems With Applications, 19, 67-79. https://doi.org/10.61356/j.nswa.2024.19325

[9] Friedman, M., Ming, M., & Kandel, A. (1999). On fuzzy integral equations. Fundamenta Informaticae, 37(1-2), 89-99. https://doi.org/10.3233/FI-1999-371205

[10] Fadravi, H. H., Buzhabadi, R., & Nik, H. S. (2014). Solving linear Fredholm fuzzy integral equations of the second kind by artificial neural networks. Alexandria Engineering Journal, 53(1), 249-257. https://doi.org/10.1016/j.aej.2013.12.002

[11] Hasan, S. Q., & Abdulqader, A. J. (2016). Numerical and analytic method for solving proposal fuzzy nonlinear volterra integral equation by using homotopy analysis method. American Journal of Applied Mathematics, 4(3), 142-157. https://doi.org/10.11648/j.ajam.

[12] Hussain, E. A., & Ali, A. W. (2013). Linear Volterra fuzzy integral equation solved by modified trapezoidal method. International Journal of Applied Mathematics & Statistical Sciences, 2(2), 43-54.

[13] Jahantigh, M., Allahviranloo, T., & Otadi, M. (2008). Numerical solution of fuzzy integral equation. Applied Mathematical Sciences, 2(1), 33-46.

[14] Jafarian, A., & Nia, S. M. (2012). Application of Taylor expansion method for the Volterra fuzzy integral equations system. Acta Universitatis Matthiae Belii, 20, 21-34.

[15] Khatter, K. (2020). Neutrosophic linear programming using possibilistic mean. Soft Computing, 24(22), 16847-16867. https://doi.org/10.1007/s00500-020-04980-y.

[16] Mohanta, K. K., & Sharanappa, D. S. (2023). A novel method for solving neutrosophic data envelopment analysis models based on single-valued trapezoidal neutrosophic numbers. Soft computing, 27(22), 17103-17119. https://doi.org/10.1007/s00500-023-08872-9.

[17] Mendel, J. M. (1995). Fuzzy logic systems for engineering: a tutorial. Proceedings of the IEEE, 83(3), 345-377. https://doi.org/10.1109/5.364485.

[18] Reig-Mullor, J., & Salas-Molina, F. (2022). Non-linear neutrosophic numbers and its application to multiple criteria performance assessment. International Journal of Fuzzy Systems, 24(6), 2889-2904. https://doi.org/10.1007/s40815-022-01295-y.

[19] Mondal, S. P., Goswami, A., & Kumar De, S. (2019). Nonlinear triangular intuitionistic fuzzy number and its application in linear integral equation. Advances in Fuzzy Systems, 2019(1), 4142382. https://doi.org/10.1155/2019/4142382.

[20] Mordeson, J., & Newman, W. (1995). Fuzzy integral equations. Information Sciences, 87(4), 215-229. https://doi.org/10.1016/0020-0255(95)00126-3.

[21] Narayanamoorthy, S., & Sathiyapriya, S. P. (2016). Homotopy perturbation method: a versatile tool to evaluate linear and nonlinear fuzzy Volterra integral equations of the second kind. SpringerPlus, 5, 1-16. https://doi.org/10.1186/s40064-016-2038-3.

[22] Peng, X., & Dai, J. (2020). A bibliometric analysis of neutrosophic set: two decades review from 1998 to 2017. Artificial Intelligence Review, 53(1), 199-255. https://doi.org/10.1007/s10462-018-9652-0.

[23] Sharaf, I. M., Alamoodi, A. H., Albahri, O. S., Deveci, M., Talal, M., Albahri, A. S., & Pedrycz, W. (2024). Architecture selection for 5G-radio access network using type-2 neutrosophic numbers based decision making model. Expert Systems with Applications, 237, 121420. https://doi.org/10.1016/j.eswa.2023.121420.

[24] Senapati, T. (2024). An Aczel-Alsina aggregation-based outranking method for multiple attribute decision-making using single-valued neutrosophic numbers. Complex & Intelligent Systems, 10(1), 1185-1199. https://doi.org/10.1007/s40747-023-01215-z.

[25] Smarandache, F. (1998). Neutrosophy: neutrosophic probability, set, and logic: analytic synthesis & synthetic analysis.

[26] Smarandache, F. (2005). Neutrosophic set-a generalization of the intuitionistic fuzzy set. International journal of pure and applied mathematics, 24(3), 287.

[27] Szmidt, E., & Kacprzyk, J. (2004). Medical diagnostic reasoning using a similarity measure for intuitionistic fuzzy sets. Note IFS, 10(4), 61-69.

[28] Tey, D. J. Y., Gan, Y. F., Selvachandran, G., Quek, S. G., Smarandache, F., Abdel-Basset, M., & Long, H. V. (2019). A novel neutrosophic data analytic hierarchy process for multi-criteria decision making method: A case study in kuala lumpur stock exchange. IEEE access, 7, 53687-53697. https://doi.org/10.1109/ACCESS.2019.2912913.

[29] Wang, H., Smarandache, F., Sunderraman, R., & Zhang, Y. Q. (2005). interval neutrosophic sets and logic: theory and applications in computing: Theory and applications in computing (Vol. 5). Infinite Study.

[30] Wang, H., Smarandache, F., Zhang, Y., & Sunderraman, R. (2010). Single valued neutrosophic sets. Infinite study.

[31] Zadeh, L. A. (1965). Fuzzy sets. Information and control, 8(3). 338-353.https://doi.org/10.1016/S0019-9958(65)90241-X.

[32] Zimmermann, H. J. (2011). Fuzzy set theory—and its applications. Springer Science & Business Media.

Received: April 05, 2024. **Accepted**: August 30, 2024.

A Novel Medical Image Segmentation Using Neutrosophic Sets With Slope Variation

Sangeeta K Siri[1], S Pramod Kumar[2], Mrityunjaya V. Latte[3]
[1]Global Academy of Technology. Bengaluru, Karnataka, India, sangeetamk28@gmail.com
[2]Jawaharlal Nehru National College of Engineering, Shivamogga, India.
[3]East Point College of Engineering, Bengaluru, Karnataka, India.

Abstract: Computer-Aided Diagnostic methods demand the precise segmentation of medical images. The important stage in diagnosis is the extraction of the Region of Interest (ROI). Illustration of the image in a more meaningful way is the aim of segmentation. Segmentation finds extensive use in computer vision, object recognition, image recovery based on the content, etc. In the proposed model, Slope Variation Scatter (SVS) plot of image is obtained to compute vertices of Neutrosophic Gaussian Function (NGF). The SVS describes global variation rate of image histogram. In this, the crests represent local mean of pixels/ certainty mean and valleys represents uncertainty mean. A novel NGF is membership function designed to convert abdominal Computed Tomography (CT) to Neutrosophic Subsets (NS). The NS comprises of object, nonobject and edge subsets. The Object Subset (OS) represents liver or kidney, Nonobject Subset (NOS) represents background of liver/kidney and Edge Subset (ES) represents edges of liver or kidney. The proposed model is experimented on 106 abdominal CT images to segment the liver and kidney accurately. The experimental outcomes are compared with Fuzzy C Means algorithm (FCM), show that the anticipated framework is proficient of segmenting an intended organ automatically and precisely. The proposed model achieves average accuracy, Relative Volume Difference (RVD) and Dice Similarity Factor (DSF) for liver are 91.01%, 8.23% and 89.61% respectively. The average accuracy, RVD and DSF for kidney are 91.11%, 5.96% and 91.45% respectively.

Keywords: Neutrosophic Set, Slope Variation Scatter plot, Segmentation, Neutrosophic Gaussian Function, Computed Tomography, liver segmentation, kidney segmentation.

1. Introduction

An essential stage in image processing is image segmentation, which separates an image into distinct areas having similar attributes such as colour, texture, pixel intensity, edges, etc and confiscates objects of interest that usually is called Region of Interest (ROI) [1, 2]. As a result, the process of image segmentation is adopted to fix the boundaries to objects. It results in each pixel in an image being given a unique label [2]. The image is renewed into identifiable data structure through image segmentation. It also targets feature extraction and

parameter measurement, which simplifies advance image analysis. The advance image analysis is essential in the many more fields like military [8], remote sensing [6], industrial automation [9], transportation [3, 4], medicine [5], communication [7], military [8], etc.

In medical field, segmentation has grabbed lot of attention since they are used in treatment planning, lesion location, anatomical structural research, estimating disease likelihood, disease diagnosis, surgery planning, carry out virtual surgical simulations, organ development study, functional mapping, clinical measurement [14], etc. Image segmentation reduces redundant information and facilitates object visibility [10]. The image analysis is straightway impacted by superiority of image segmentation [11]. To diagnose and to choose appropriate therapy, image segmentation has proven to be one of the most useful technologies available to medical practitioners. It is anticipated that adaptive algorithms will support and ease the process of making medical decisions.

In the last forty years, various image segmentation algorithms/models were designed. But still the topic is open for obtaining a single segmentation algorithm/ model which can be applied on all types of images to achieve accurate segmentation. It is sometimes hard to predict which segmentation algorithm is better for a specific object segmentation. This is due to different imaging characteristics, variances in the patients under consideration, small differences in the task being addressed, and variations in the validation metric [12]. Medical segmentation is the complex field in image processing because variations in light and distance are two irregular circumstances that might be present in medical images while acquiring the image. Additionally, the resolution of the images may be low, which complicate the identification of minor lesions [11]. Medical images may also include hair, reflections, and shadows, all of which might make it difficult to distinguish and analyze lesions. In addition, in medical images, variations in brightness, illumination, movement of patient in capturing the images, etc. make image unclear. Also, biomedical images may be blurry because of inheritance characteristic of image acquisition device and due to movement of patient, which affect the quality of image [13]. Since biomedical images are fuzzy, edges are not crispy, tissues are soft and have the same pixel intensity, etc. make the segmentation process very complex. Because of these issues and variations in tissue distribution among the human population, segmentation findings need to be interpreted with some degree of ambiguity. As a result, medical image segmentation can be thought of as an unsolved problem.

The automatic segmentation techniques can be classified as supervised and unsupervised. Supervised techniques are one which require the contribution of an operator throughout the process of segmentation while unsupervised techniques usually operator contribution only after accomplishment of segmentation process. Unsupervised techniques are desired to produce replicable outcomes. Whilst operator contribution is still necessary for error rectification in the incident of an unsatisfactory outcome.

A Fuzzy Set (FS) defines only two values, “true” and “false” which is sometime difficult to handle real life difficulties [16]. The extension/generalized form of Intuitionistic Fuzzy Set is Neutrosophic Set (NS) which is a burgeoning tool to handle real life problems like human thoughts [16], medical image analysis [15], etc. The NS deals with ambiguity, inconsistency, and uncertainty for computation and decision making. The NS consists of three membership function named as Object Subset (OS) or true subset, nonobject subset (NOS) or false subset and indeterminacy subset or Edge Subset (ES) which are independent entities. For all real-life decision-making problems, NS is more flexible and efficient since it assigns the same weight to the indeterminacy subset as it does to OS and NOS. NS is also versatile because in addition truth components, it can accommodate indeterminacy and false components, whereas FS cannot handle with all these. Because of all these reasons, NS has many practical applications in various fields like image processing, decision making, data mining, block chain, marketing, medicine, strategic planning, etc [17].

Transforming the image pixearevalues into NS using neutrosophic functions or membership functions (MFs) is called as neutrophication process, predominantly considering indeterminacy values that result from nebulousness. It has become customary to confine the MFs to well-known formats such as sigmoid, standard Gaussian, trapezoidal, and triangle forms [17]. Developing MFs is a crucial effort for Neutrophication process as the MFs determine the success of an approach. The method in which ambiguity and vagueness are handled in software metrics is aided by the theory of neutrosophic system. Using MFs in an expert system inside a neutrosophic environment definitely answer the problem's uncertainty. Commonly used MFs in real time are S/Z-shaped, trapezoid, triangle, gauss, and bell-shaped. Chosing proper MF for specific application is tricky and deciding factor for success of neutrophication process.Neutrosophic Gaussian Function (NGF) provides low computational complexity. For this reason, a novel NGF is designed to convert CT images to its NS domain. The NGF parameters play key role in defining the MF and accuracy of transformation.

we are exploiting Slope Variation Scattering plot of image which directly describes the pixel variation rate of image histogram. The crests represent the mean/certainty level of local pixels and valleys symbolizes uncertainty mean. The valleys can be taken as thresholds to eliminate background or crests values can be taken to separate objects from the background.

Segmenting spleen, kidney, liver, etc. from abdominal CT scan is most demanding as well as complex task job in Computer Aided Diagnostics system since organs are complex in shape, organs are close to each other, have same pixel intensity level, etc. Because of these reasons many segmentation algorithms fail to segment precisely. This motivated us to propose a novel model based on SVS and NS theory which accurately segments the intended organ from abdominal CT scan automatically and precisely.

The article is organized as follows. Section 2 describes literature survey, section 3 explains proposed model, section 4 illustrates experimental results, section 5 depicts quantitative analysis and last section is about conclusions.

2. Literature Survey

Panimalar et al [18] used haar wavelet transform on NS to denoise the image. The level of indeterminacy of image is obtained using NS entropy. The proposed method is compared with commonly used denoising methods like median and wiener filter, providing better quality image. Thanikachalam V [19] et al proposed accurate NS segmentation with Optimal Deep Brief Network Model for diagnosis of Diabetic Retinopathy (DR). The DR dataset was utilized for experimentation, providing promising outcome compared to existing technique. The NS theory provides indeterminacy present in image with high efficacy. This property was utilized by Talouki AG et al [20] for image completion to fill holes and decrease intensity ambiguity in the image. The dental radiographic image was mapped to NS domain by Datta S [21] et al to acquire initial segmentation of ROI. The ROI was amended by FCM algorithm to obtain accurate outcomes. The model has been evaluated on publically available dataset with the accuracy of 93.2%. Ziyun Wang et al [22] proposed U-NET which includes expectation maximization attention mechanism to segment kidney and its tumour. This model is implemented on kits19 dataset reaching dice coefficient of 0.95 and 0.83 for kidney and tumour segmentation respectively.

Liver is one of the difficult organs to separate from the abdominal CT scan because edges are not clear. Sangeeta et al. [23] converted CT image to NS and morphological operations are utilized to detach liver image from CT scan and Fast Marching Method

(FMM) is exploited to mark edge of liver. Sangeeta et al. [24] combined advantages of NS domain of abdominal CT scan image and Chan-Vase algorithm to acquire specific liver image. Sangeeta et al. [25] proposed accurate liver segmentation algorithm using Expectation-Maximization (EM) with optimal quantity of clusters (K). The K value is accomplished by finding mean of all local peaks which delivers minimum and maximum thresholds to detach liver from CT scan using threshold-based segmentation. Statistics of pixel intensity distribution was studied to obtain threshold values to isolate liver from CT scan by Sangeeta et al [26]. The liver edges are corrected by improved chain code and Bresenham pixel interconnection approaches. This delivered an exact liver image. Wang Z [27] proposed new model based on Slope Difference Distribution (SDD) of image to find the thresholds to separate two or more objects in the image. The maximum True Positive computation for cells as 93.4%. Wang Z et al. [28] anticipated novel segmentation model based on non-iterative clustering approach. The model was applied on fuzzy image to isolate fuzzy object unerringly. Wang Z [29] et al. achieves shape features of object as sparse characteristics using SDD. In this paper, minimum distances between SDD are utilized to recognize the object. Sangeeta et al. [30] achieves accurate threshold values by SDD features of liver image. By applying these, liver image is separated from CT scans precisely. Subsequently FMM is used to put outline for liver image in CT scan image. Nayantara et al [31] proposed Deep Learning framework in combination of leaky ReLU layers and SegNet to extract intact precise liver image from CT scan dataset. This framework achieves Dice Coefficient of 96%. Zhang et al [32] anticipated a novel Deep Learning model which extracts circular regions to detect hepatic steatosis to obtain exact liver image from abdominal CT scan with 95% confidence interval. Leube et al [33] anticipated automated kidney segmentation from CT images. In this, two types of segmentation are performed initially. First segmentation is performed on CT images and is called as detail segmentation; second segmentation is performed on PET images, and it is called as coarse segmentation. Subsequently, 5 different UNET is implemented to obtain final kidney segmentation. The framework is performed on 20 different patients. Cao et al [34] designed automatic kidney segmentation network based on deep neural network. This integrates decoding module and multi-scale spatial perception module. This achieves precision of 98.52%. Prashanta et al [35] proposed modified breadth first algorithm for finding shortest path (SP) for connected networks in neutrosophic environment. In this article, neutrosophic edge length is transformed to crisp edge lengths to find SP. Rajesh et al [36] suggested a model to handle

multiple criteria and ambiguous data. To implement this, Pythagorean NS Theory is designed to provide beneficial tool for decision-making in selecting a partner. Ivan et al [37] utilized neutrosophic logic in decision making for disease prevention program and health promotion. The aim of the proposed model is to use neutrosophic logic in resource allocation effectively in ambiguous condition in the field of public health. Srinivasan S et al [38] designed combined endeavour of multidimensional Convolutional Neural Network (CNN) and UNET. This framework is implemented on dermoscopy images to segment skin lesions. The proposed model shows better performance compared to traditional UNET. Shahat et al[39] proposed combined venture of NS theory and optimization algorithms to segment brain CT images. Neutrosophication operation is performed using S membership function providing precise segmentation results. Mostafa et al [40] addressed noise and ambiguity present in medical images. The authors have designed different types of filters based on NS theory to remove noise in X-ray images.

3. Proposed Model

The proposed model is presented in two parts. In part 3(a), calculation of Slope Variation Scatter (SVS) of the object image is obtained to formulate parameters of NGF and in part 3(b), CT scan image is transformed to NS domain to acquire accurate segmentation of an object image from the source image.

3(a) Formulation of parameters of NGF from SVS of image.

The SVS was first defined in [43] by Wang Z to obtain threshold to segment the laser line. The SVS describes global variation rate of image histogram. The crests represent the local mean/ certainty mean of pixels and valleys represents uncertainty mean. The valleys can be taken as thresholds to eliminate background or crests values can be taken to separate objects from the background. The SVS of object histogram is defined as rate of variation of pixel scattering and is designed as follows.

Step 1: The abdominal CT scan image is converted to grey scale and resized to 512X512 and assumed to be having Gaussian distribution.

Step 2: Crop small part of object (may be liver/ kidney/ spleen) to find its SVS.

Step 3: Compute normalized histogram scattering $P_N(x)$ by following formula.

$$P_N(x = i) = \frac{n_i}{n_j}, i = 0.....255 \quad (1)$$

Where n_i represents the frequency of the pixel value i, and highest frequency that ensues at j in the interval [0 to 255] is indicated by n_j.

Step 4: A noise-removal filter based on the Discrete Fourier Transform (DFT) is utilized.

(a) The normalized histogram scattering is converted into frequency domain by the DFT as follows.

$$F(H)=\sum_{x=0}^{255}P(x)e^{\frac{-j2\Pi Hx}{255}}, \qquad H=0,.....255 \tag{2}$$

Where F(H) (H=0……255) corresponds Fourier Transformation (FT) of the normalized histogram scattering $P_N(x)$.

(b) The high frequency components from 20 to 255 are eliminated and low frequency components are retained as follows.

$$F'(H)=\begin{cases} F(H); H=0,1,.....19 \\ F(H); H=235,...255 \\ F(H); H=20,21,.....234 \end{cases} \tag{3}$$

Where F' (H) (H=0…….255) represents the filtered FT of P(x) by applying Low Pass filter of bandwidth (BW) of 20. The trial-and-error analysis is performed on large CT scan dataset yielded BW=20.

(c) Subsequently, frequency domain of an image F' (H) is converted to spatial domain by using equation (4).

$$P_N^{'}(x)=\frac{1}{T}\sum_{H=0}^{255}F^{'}(H)\ e^{\frac{j2\Pi Hx}{255}} \qquad x=0…….255 \tag{4}$$

$P_N^{'}(x)$ is smoothed histogram scattering.

Step 5: Every point on $P_N^{'}(x)$, two slopes are computed: one on the left and second on the right to compute Slope Variation (SV). The N adjacent points on each side are fitted into a line model to calculate slope values as follows.

$$y_i=ax_i+b; \qquad i=1,2…….N \tag{5}$$

Where a and b are coefficients of fitted line and they are calculated by following equation.

$$[a,b]^T=(C^TC)^{-1}C^TY \tag{6}$$

C and Y in equation (6) is obtained by following equation (7) and (8).

Where $$C=\begin{bmatrix} x(1) & 1 \\ x(2) & 1 \\ . & . \\ x(N) & 1 \end{bmatrix} \tag{7}$$

$$Y=[y_1,y_2,.....y_n]^T \tag{8}$$

where (x_i, y_i); i = 1, 2, . . ., N is the coordinate of the i^{th} point on the filtered data. In this article, the value of N is chosen as 20.

Let $a_1(i)$ and $a_2(i)$ are two slopes at i[th] point on right-hand and left-hand side respectively. The Slope Variation (SV) at i[th] point as computed as follows.

$$SV(i) = a_2(i) - a_1(i).....where \quad i = N+1..... \quad 255 \tag{9}$$

Here SV (i) indicates SVS of object. The crests and valleys are computed by equating the derivative of SV (i) to 0. The crests C_i where i=1……n_c and valleys V_i where i=1……n_v, with largest local variation in SVS are obtained. The crests symbolize to certainty of pixels values in the object and valleys symbolize to uncertainty pixel values in the object region.

Step 6: Find pixel values which is having highest crest which corresponds to centre (*cen*t) of NGF. Consider two pixel values whose crests are placed on left-hand side of *cent* named as x_1 and x_2 and two pixel values whose crests are positioned on right-hand side x_3 and x_4. Now, (x_1, x_2, cent, x_3, x_4) are parameters of NGF to convert the image to the NS domain. The NGF and its parameters are described in figure 1.

3.2 NS framework:

The word "Neutrosophic" is combination of two Latin words, "neuter" means "neutral" and "sophia" means "wisdom". This theory wisely and accurately finds indeterminacy in fuzzy images. NS theory was introduced by Smarandache F in 1999 [42,45] which is commonly used in decision making process [46] in real world problems. In recent days, NS theory is utilized in fault detection, optimum design, medical diagnosis, decision making, image processing, computational intelligence, etc. NS has wide range of applications which covers most of the areas since it deals with vagueness and indeterminacy [46]. Any image in NS theory consists of three subsets named as (i) Object Subset (OS) or true Subset (ii) Non-Object Subset (NOS) or false subset and (iii) Edge Subset (ES) or indeterminacy subset. The given image is transformed to NS domain utilizing NGF as follows.

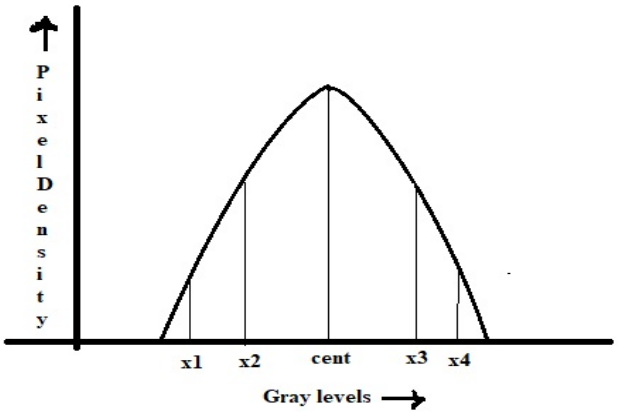

Figure 1: NGF Graph

Step 1: Compute Object Subset (OS) and Non-Object Subset (NOS) using novel SMF as follows.

$$OS(x,y) = \Pi(A_{xy}, x_1, x_2, cent, x_3, x_4) = \begin{cases} 0 & A_{xy} < x_1 \\ \frac{(A_{xy}-x_1)^2}{(x_4-x_1)^2} & x_1 \le A_{xy} < x_2 \\ 1-\frac{(A_{xy}-x_2)}{(x_4-x_2)} & x_2 \le A_{xy} < cent \\ 1-\frac{A_{xy}-x_3}{(x_4-x_3)} & cent \le A_{xy} < x_3 \\ \frac{(A_{xy}-x_4)^2}{(x_4-x_3)} & x_3 \le A_{xy} < x_4 \\ 0 & A_{xy} > x_4 \end{cases} \quad (10)$$

$$NOS(x,y) = 1 - OS(x,y) \quad (11)$$

OS represents the degree of being object pixels, and NOS presents the degree of background pixels.

Step 2: Edge subset is obtained as follows.

(a)Let A (x, y) be pixel intensity value at (x, y) and $\hat{A}(x,y)$ represents local mean.

$$\hat{A}(x,y) = \frac{1}{T}\sum_{m=i-w/2}^{m=i+w/2}\sum_{n=i-w/2}^{n=i+w/2} A(m,n) \quad (12)$$

Where w is size of sliding window. Le e(x, y) as absolute value of pixel intensity at A (x, y) and its local mean $\hat{A}(x,y)$. Let e_{min} and e_{max} be lowest and highest value of e(x, y) in whole object image.

(b)Then edge subset (ES) is formulated using equation (13).

$$ES(x,y) = \frac{e(x,y)-e_{min}}{emax_{max}} \quad (13)$$

Step 3: Convert image OS, NOS and ES into binary image.

Image segmentation is charactered by homogeneousness of local region. The homogeneity characteristic of image is obtained by discontinuity of intensity corresponds to the variations in grey levels and Standard Deviation (SD) which describes dissimilarity within local region. The homogeneousness is characteristics of foreground and background, while hazy boundaries are slowly varying from foreground to background. The homogeneousness value

of boundary is lesser than foreground and background. The window size of DXD cantered at (x, y) is used for calculating the SD of pixel A (i, j).

$$SD(x,y) = \sqrt{\frac{\sum_{m=x-(D-1)/2}^{x+(D-1)/2} \sum_{n=y-(D-1)/2}^{y+(D-1)/2} (A_{mn} - mu_{xy})^2}{D^2}} \quad (14)$$

Where mu_{xy} average of intensity is values within window and determined by equation (15).

$$mu_{xy} = \frac{\sum_{p=x-(D-1)/2}^{x+(D-1)/2} \sum_{q=y-(D-1)/2}^{y-(D-1)/2} A_{pq}}{D^2} \quad (15)$$

The edge values are obtained by discontinuity of pixel A (i, j) which is calculated by Sobel operator.

$$E_g(x,y) = \sqrt{A_x^2 + A_y^2} \quad (16)$$

Where A_x corresponds to horizontal derivative and A_y corresponds to vertical derivative. Now, homogeneousness characteristic can be defined by equation (17).

$$HO(x,y) = 1 - \frac{SD(x,y)}{SD_{max}} \frac{E_g(x,y)}{E_{g_{max}}} \quad (17)$$

Where SD_{max}=max {SD (x, y)} and E_{gmax}=max {E_g(x, y)}. The Edge subset ES (x, y) is represented as

$$ES(x,y) = 1 - HO(x,y) \quad (18)$$

The value of ES (x, y) has a range of 0 to 1

Step 5: Method to compute value of α

(i) (a) mini = smallest {largest values of every column in Edge Subset (ES)≠0}

(b) α will take any number which is any value less than or equal to mini.

(ii) NS of image is converted to binary i.e.

The NS of image is converted to binary. O (x, y) is binary form of OS (x, y), E (x, y) is binary form of ES (x, y) and B (x, y) is binary form NOS (x, y) and these are obtained by equation (19), (20) and (21) respectively.

$$O(x,y) = \begin{cases} 1 & OS(x,y) \geq OS_{th}, ES(x,y) < \alpha \\ 0 & others \end{cases} \quad (19)$$

$$E(x,y) = \begin{cases} 1 & OS(x,y) < OS_{th} \vee NOS < NOS_{th}, ES(x,y) \geq \alpha \\ 0 & others \end{cases} \quad (20)$$

$$B(x,y) = \begin{cases} 1 & NOS(x,y) \geq NOS_{th}, \quad ES(x,y) < \alpha \\ 0 & others \end{cases} \quad (21)$$

Figure 3: Demonstration of Slope Variation Scatter (SVS); (a) Cropping random section of liver; (b) SVS of liver image; (c) Cropping arbitrary section of kidney image; (d) SVS of kidney image.

Perform morphological operation on edge image to achieve exact output. The framework of proposed model which is combined endeavour of SVS and NS theory to separate intended object from CT scan images is shown in figure 3.

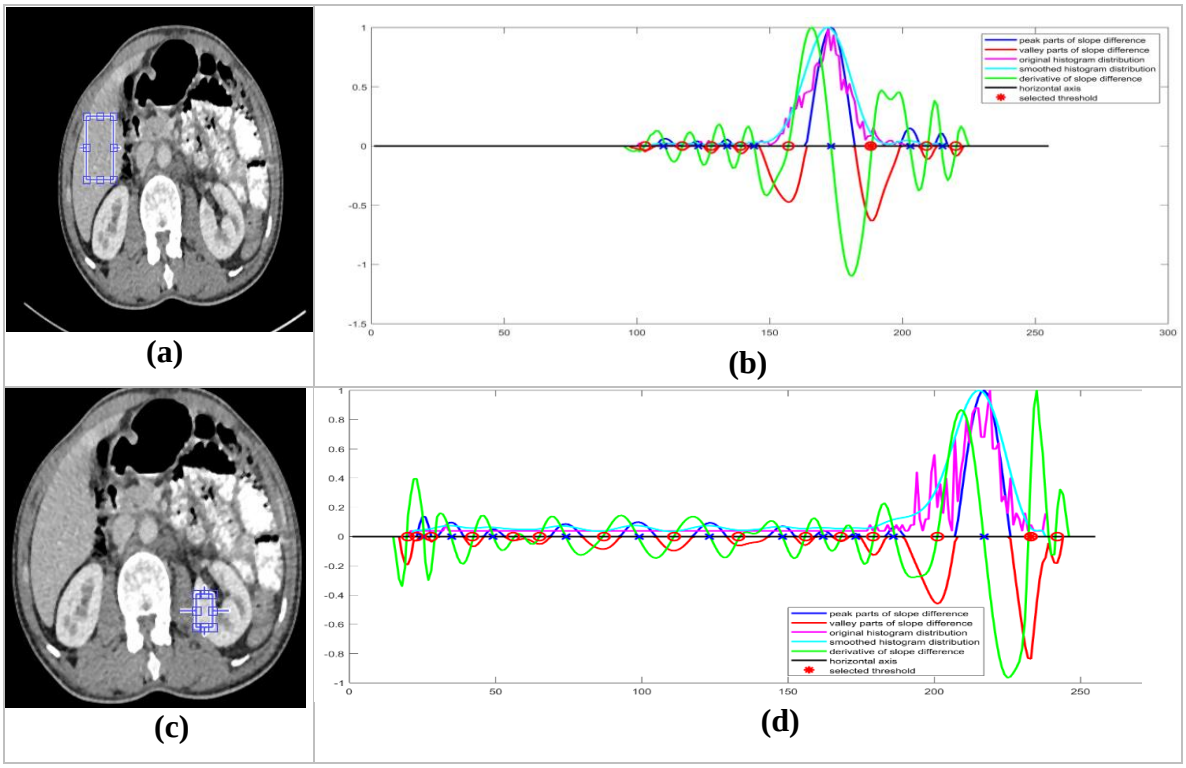

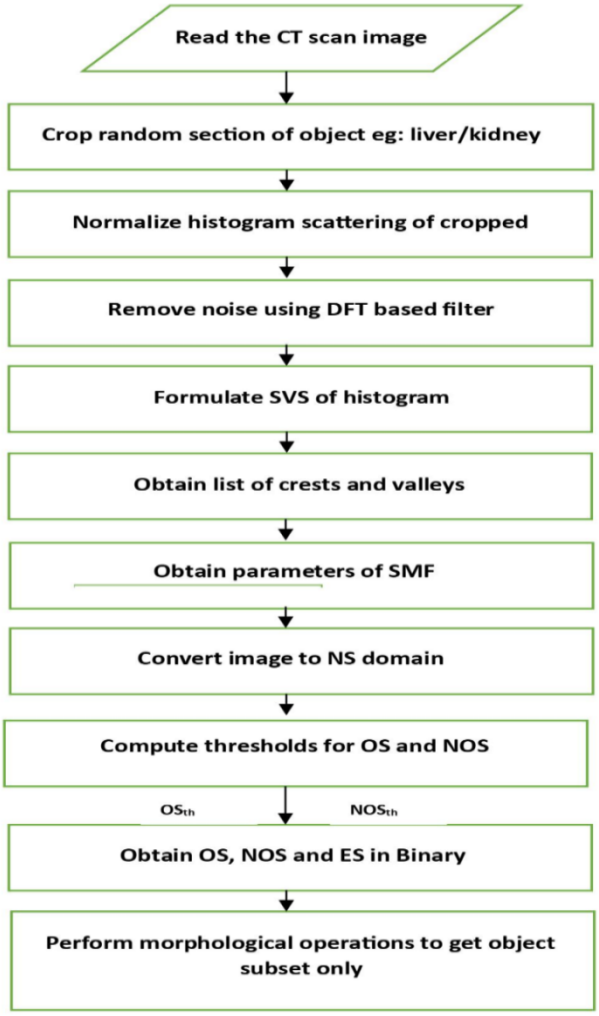

Figure 3: Framework of proposed model

4. Experimental Results

The database for trial and testing contains 106 patients CT scan images collected from M/s Hubli scan centre, Karnataka, India. The images are in colour format of size 1019 x 682. Figure 2 illustrates SVS of randomly cropped liver and kidney image from which NGF parameters are decided. Figure 2(a) and (b) illustrate cropping liver and kidney image from CT scan respectively. Figure (b) and (d) describe SVS plot of liver and kidney respectively. In figure 2(b) and (d), x-axis represents pixel value from 0 to 255; y axis represents normalized pixel density, lilac describes original histogram; whereas sky-blue represents smoothed histogram; Persian Blue exemplifies SVS, the Persian Blue cross corresponds to crest values, red circles on x-axis represents valley value; green indications derivation of SVS.

Figure 4 illustrates experimental results on CT scan to segment the liver. Figure 4(a1),(a2) and (a3) represent CT scan images, 4(a4),(a5) and (a6) demonstrate cropping arbitrary section of liver, 4(a7),(a8) and (a9) show SVS of object image; 4(a10),(a11) and (a12) show OS of image; 4(a13),(a14) and (a15) illustrate NOS of image; 4(a16),(a17) and (a18) show ES of image; 4(a19),(a20) and (a21) represent segmented liver image from abdominal CT scan; 4(a22),(a23) and (a24) show outline marking to liver in CT scan image; 4(a25),(a26) and (a27) show segmentation results of FCM.

Figure 5 illustrates experimental results on CT scan to segment the kidney. Figure 5(b1),(b2) and (b3) represent CT scan images, 5(b4),(b5) and (b6) demonstrate cropping arbitrary section of kidney, 5(b7),(b8) and (b9) show SVS of object image; 5(b10),(b11) and (b12) show OS of image; 5(b13),(b14) and (b15) illustrate NOS of image; 5(b16),(b17) and (b18) show ES of image; 5(b19),(b20) and (b21) represent segmented kidney image from abdominal CT scan; 5(b22),(b23) and (b24) show outline marking to kidney in CT scan image; 5(b25),(b26) and (b27) show segmentation results of FCM.

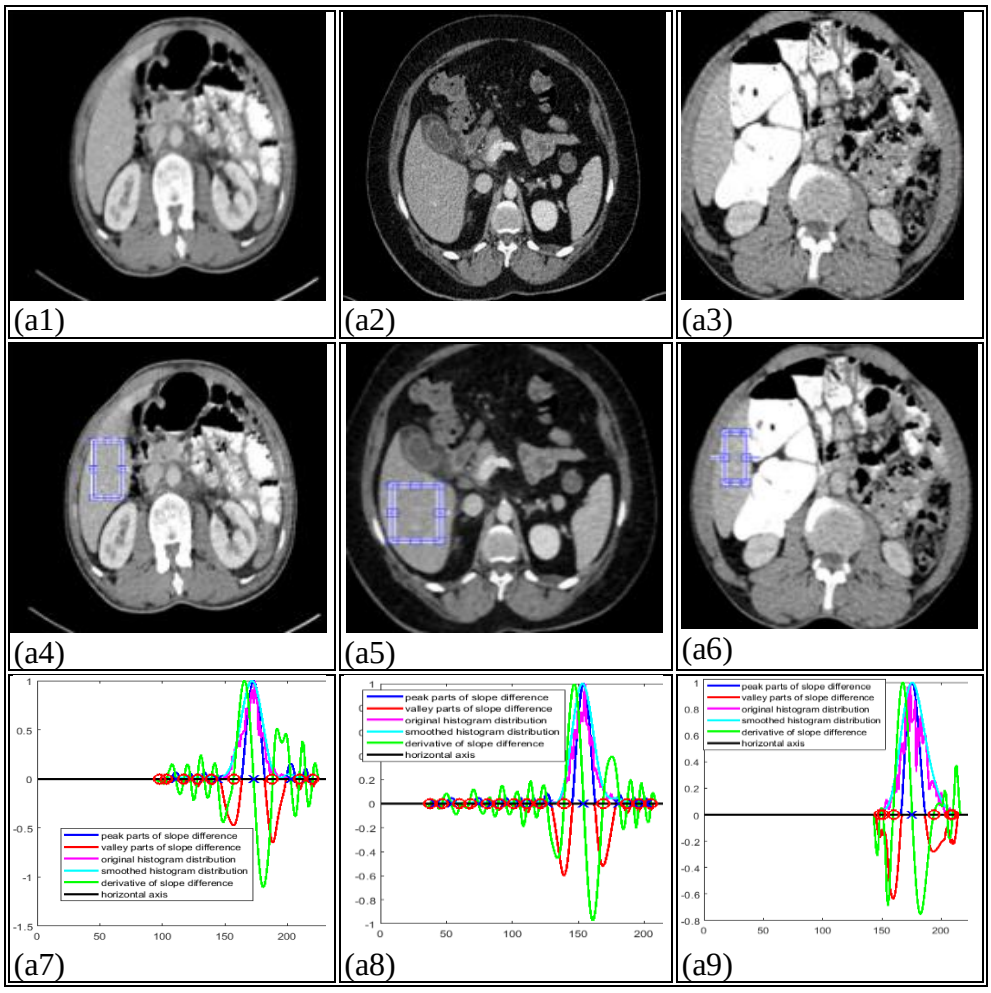

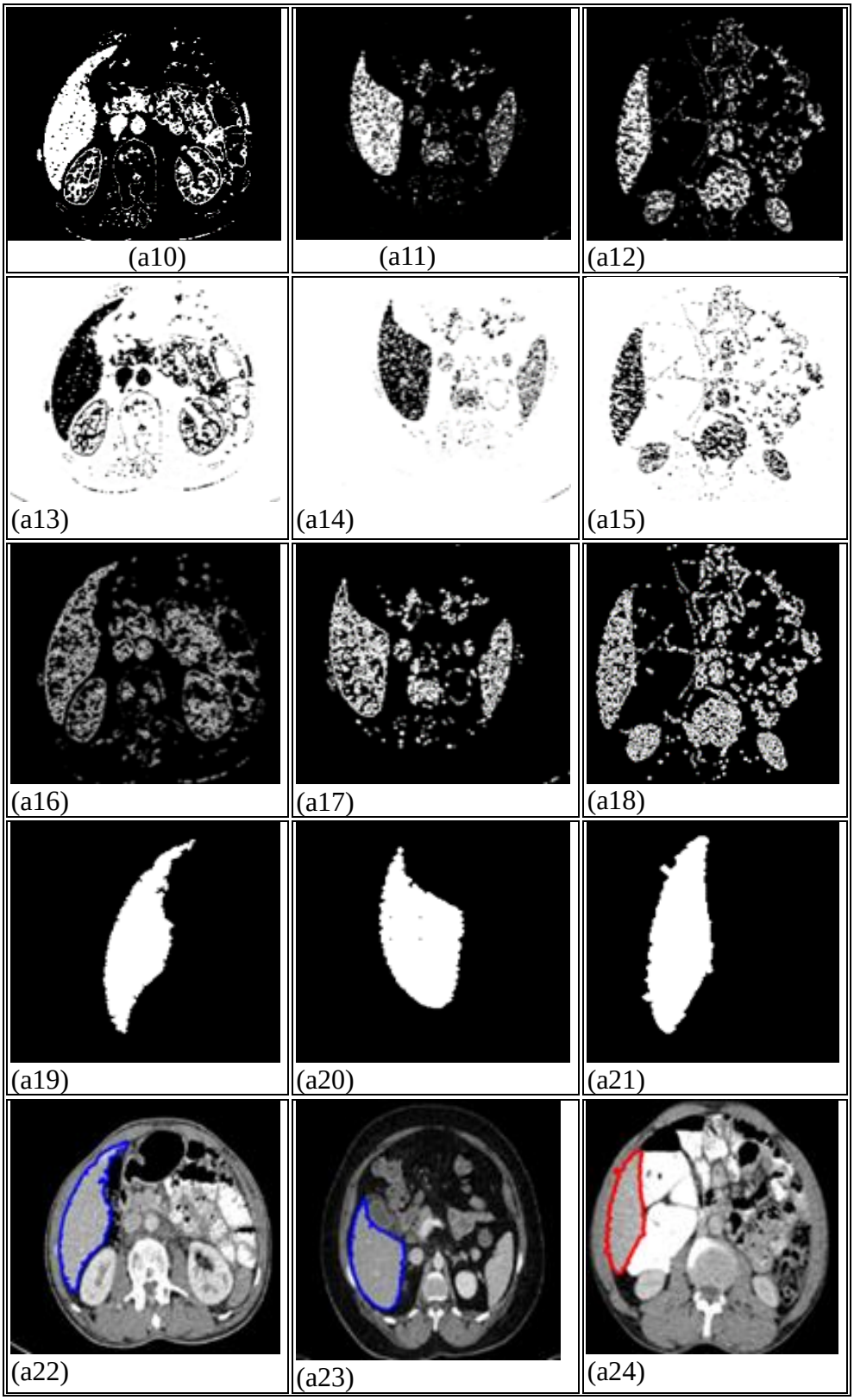

(a10) (a11) (a12)

(a13) (a14) (a15)

(a16) (a17) (a18)

(a19) (a20) (a21)

(a22) (a23) (a24)

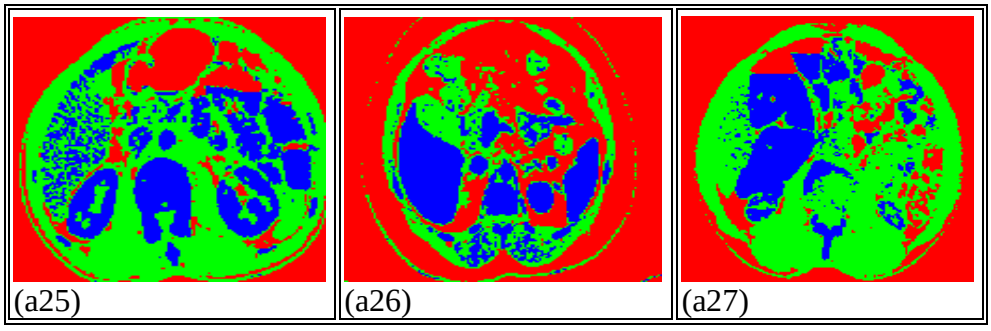

Figure 4: Experimental results of proposed framework for liver segmentation from abdominal CT scan (a1),(a2) and (a3) represent CT scan images, (a4),(a5) and (a6) demonstrate cropping arbitrary section of liver, (a7),(a8) and (a9) show SVS of object image; (a10),(a11) and (a12) show OS of image; (a13),(a14) and (a15) illustrate NOS of image; (a16),(a17) and (a18) show ES of image; (a19),(a20) and (a21) represent segmented liver image from abdominal CT scan; (a22),(a23) and (a24) show outline marking to liver in CT scan image; (a25),(a26) and (a27) show segmentation results of FCM.

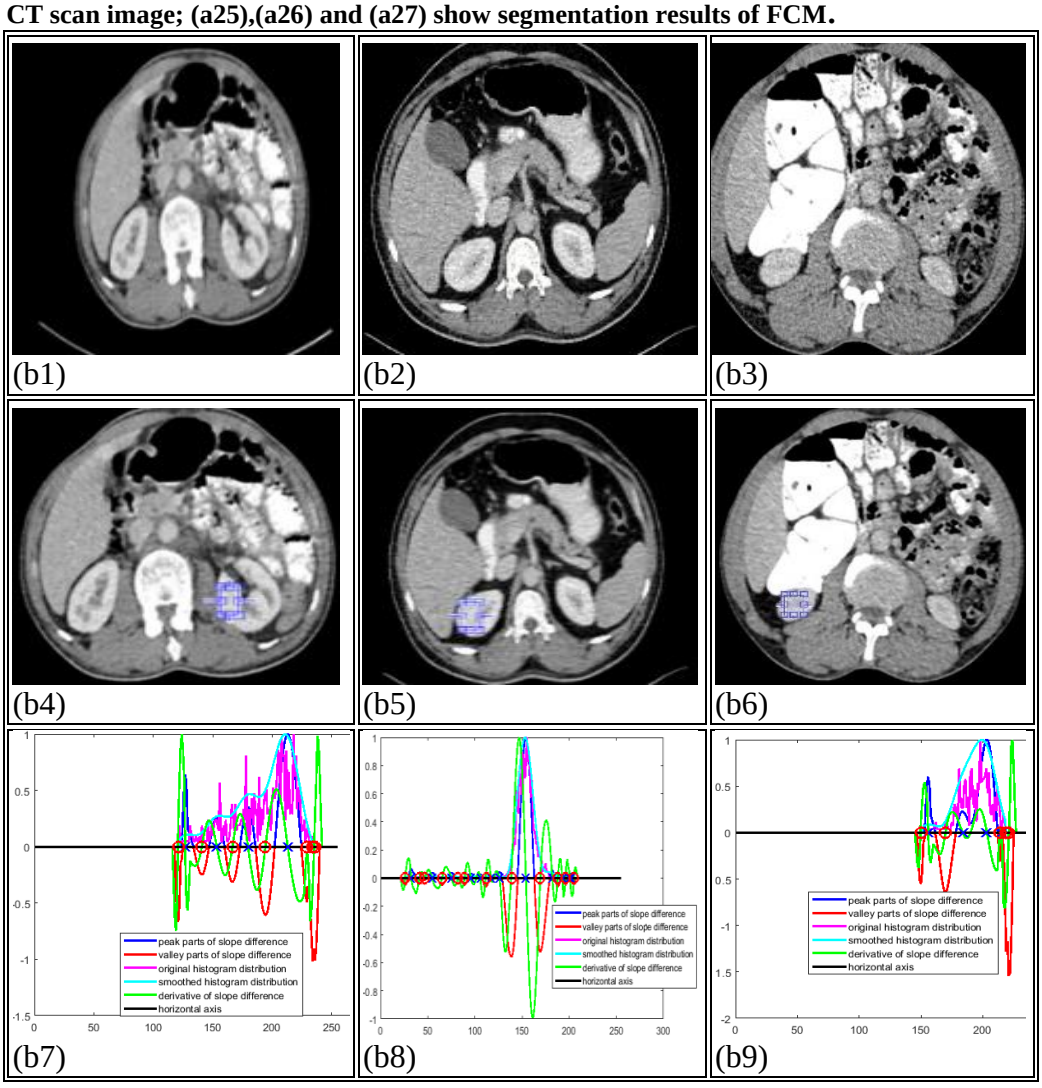

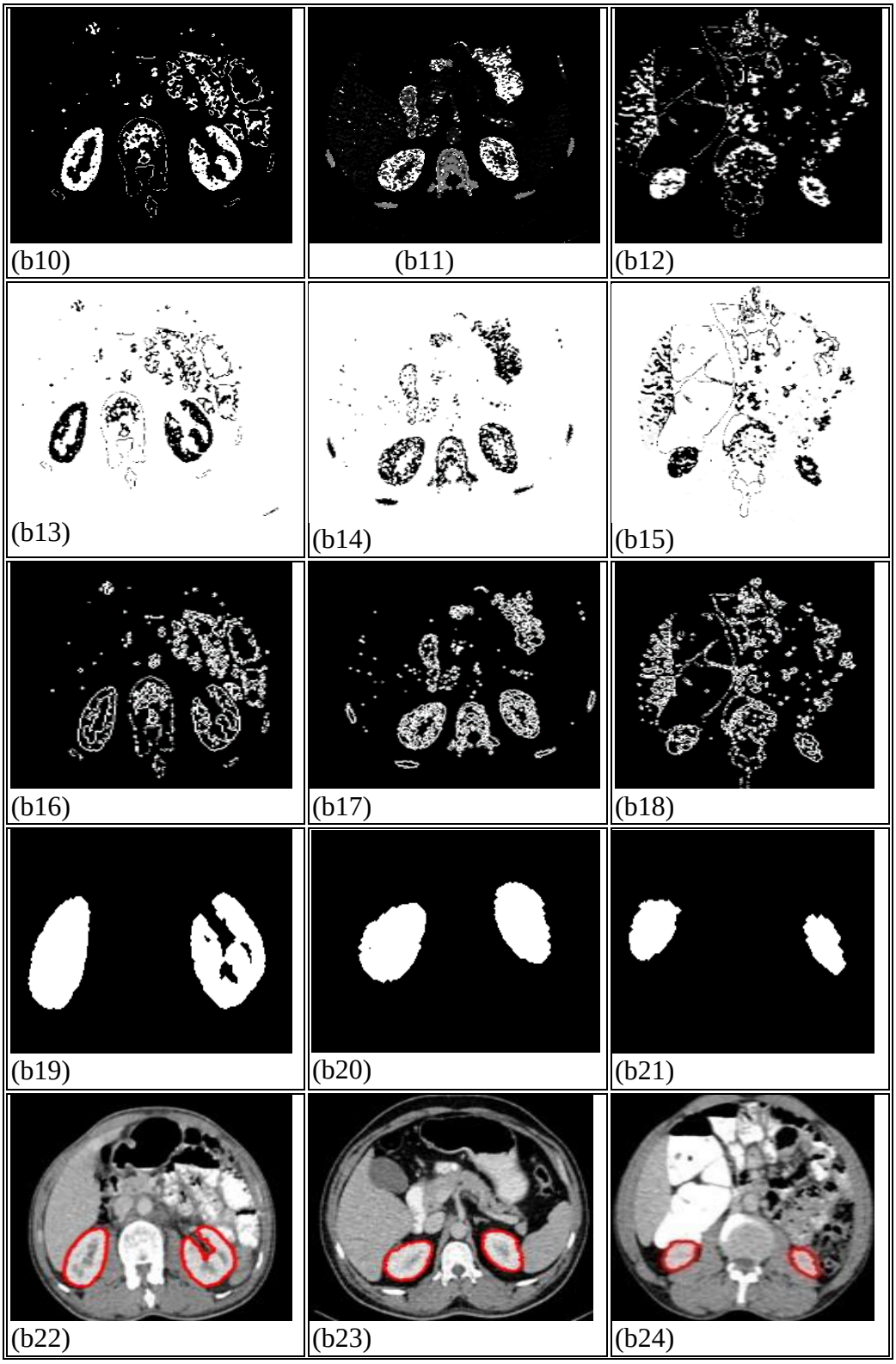
(b10)
(b11)
(b12)
(b13)
(b14)
(b15)
(b16)
(b17)
(b18)
(b19)
(b20)
(b21)
(b22)
(b23)
(b24)

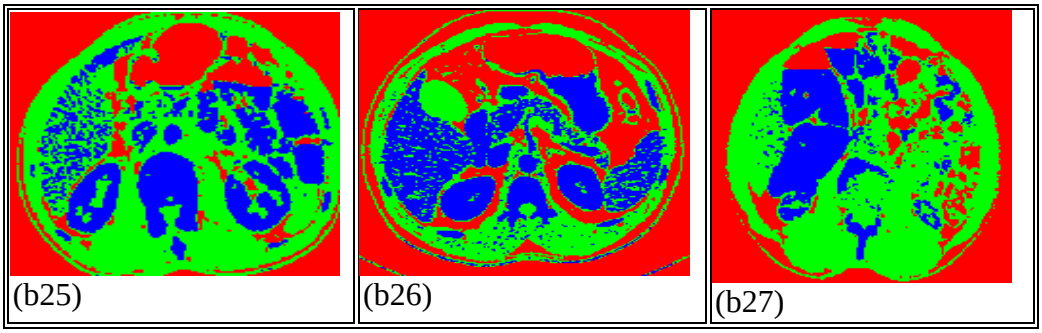

Figure 5: Experimental results of proposed framework for kidney segmentation from abdominal CT scan (b1),(b2) and (b3) represent CT scan images, (b4),(b5) and (b6) demonstrate cropping arbitrary section of kidney, (b7),(b8) and (b9) show SVS of object image; (b10),(b11) and (b12) show OS of image; (b13),(b14) and (b15) illustrate NOS of image; (b16),(b17) and (b18) show ES of image; (b19),(b20) and (b21) represent segmented kidney image from abdominal CT scan; (b22),(b23) and (b24) show outline marking to kidney in CT scan image; (b25),(b26) and (b27) show segmentation results of FCM.

5.Quantitative analysis

The segmentation model with high efficiency and minimal bias are key objectives in surgical planning which will directly impact the results. Hence quantitative estimation of image segmentation model is crucial.

5.1 Accuracy (Acc)

Segmentation accuracy analyses the deviation between annotated image and segmentation predicted image. In this paper, annotated image is approved with the manual segmentation image under supervision of medical practitioner [43]. The similarity between an annotated image and algorithm predicted image reflects the accuracy (Acc). The accuracy measure is calculated as shown in Eq. (22) [48]. The accuracy for liver and kidney for proposed model and FCM is shown in figure 6 and 7 respectively. Acc will be *one* if segmentation is perfect. As Acc moves away from *one* denotes deviation of segmentation.

$$Acc = \frac{correctly\ classified\ \ pixels}{Total\ number\ of\ pixels} * 100 \quad (22)$$

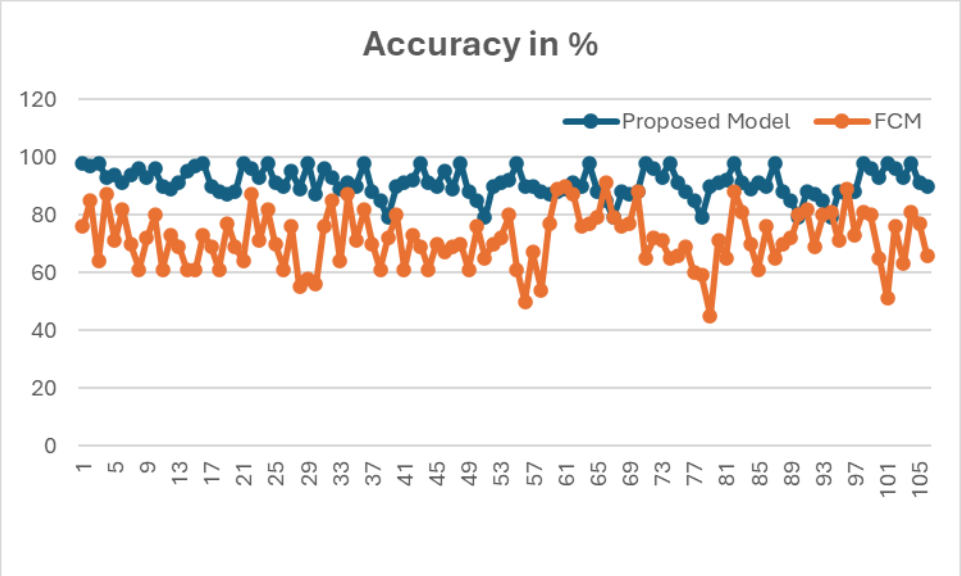

Figure 6: Evaluation of proposed framework and FCM for liver segmentation using Acc.

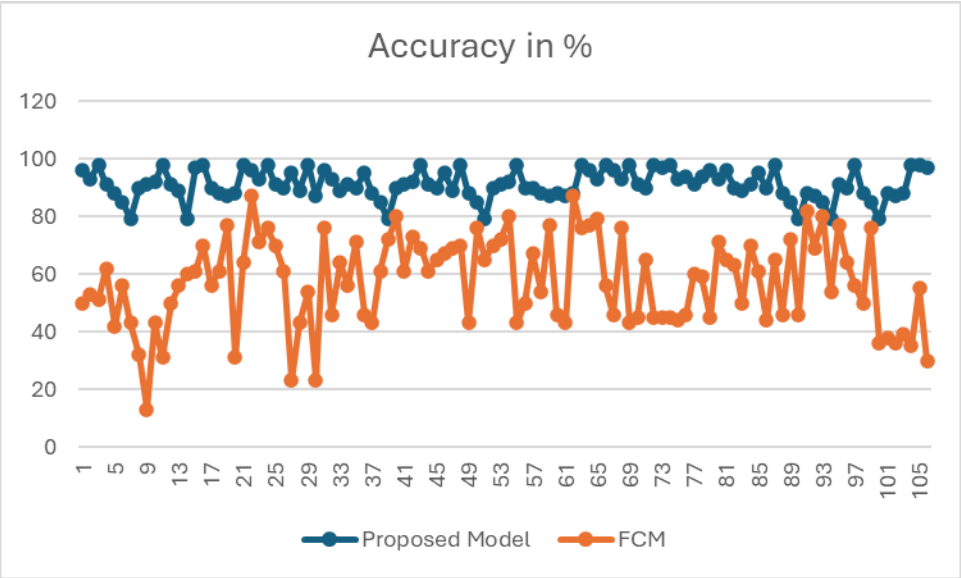

Figure 7: Evaluation of proposed framework and FCM for kidney segmentation using Acc.

5.2 Relative Volume Disagreement (RVD)

The specific RVD exists between 2 images SEG_{ALG} and SEG_{GT} is given in per cent and defined as.

$$RVD=100*(|SEG_{ALG}-SEG_{GT}|)/SEG_{GT} \quad (23)$$

with SEG_{ALG} as image segmented by proposed algorithm and SEG_{GT} as ground truth image [37]. A score of 0% indicates that the two areas completely overlap. A comparison of the suggested model with FCM algorithm using RVD for liver and kidney is shown in figure 8 and 9 respectively.

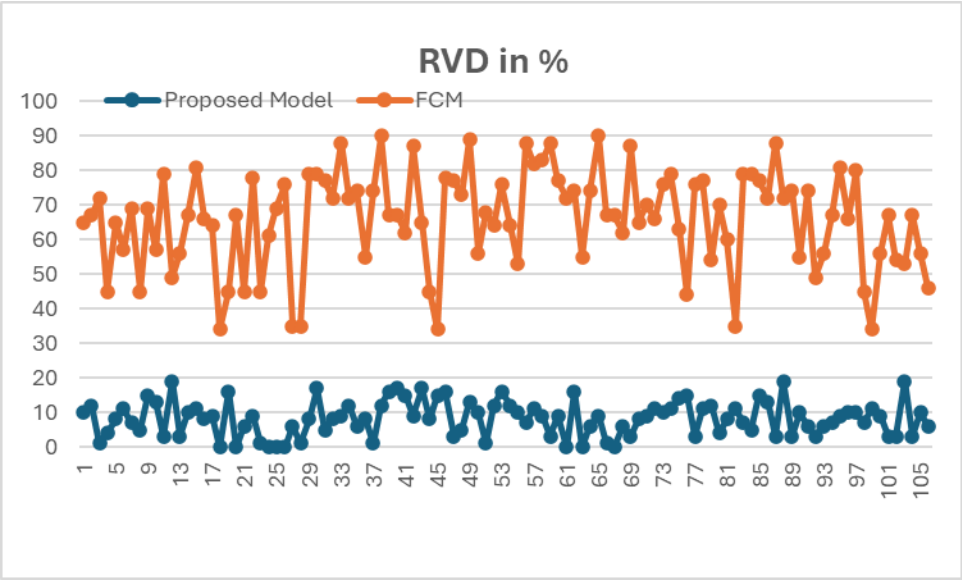

Figure 8: Evaluation of proposed framework and FCM for liver segmentation using RVD.

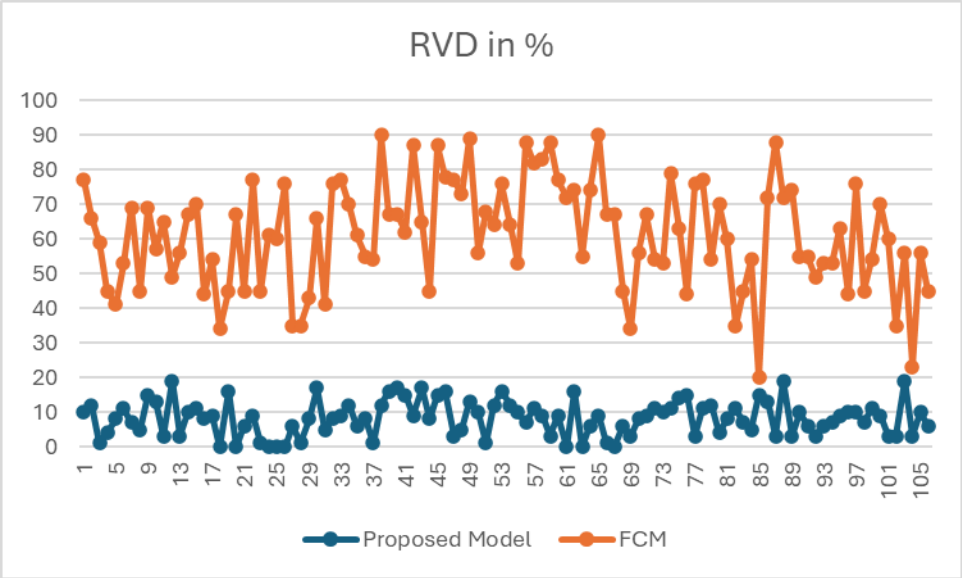

Figure 9: Evaluation of proposed framework and FCM for kidney segmentation using RVD.

5.3 Dice Similarity Factor (DSF)

The similarity of two objects is also evaluated by DSF. In this evaluation technique, Dice's coefficient needs to be calculated to evaluate similarities [47]. DSF is defined as

$$DSF = 2 * [SEG_{ALG} \cap SEG_{GT}]/[SEG_{ALG} - SEG_{GT}]*100 \quad (24)$$

where SEG_{ALG} and SEG_{GT} are the segmented and ground truth, respectively. The DSF values are in the 0–100% range. When the value is near 0%, it represents less or no similarity between the segmented and ground truth regions. If the DSF value is near 100%, then the segmented and ground truth regions are more similar. The DSF for liver and kidney for proposed model and FCM is shown in figure 10 and 11 respectively. The tabulation of average accuracy, RVD and DSF for liver and kidney is shown in table 1.

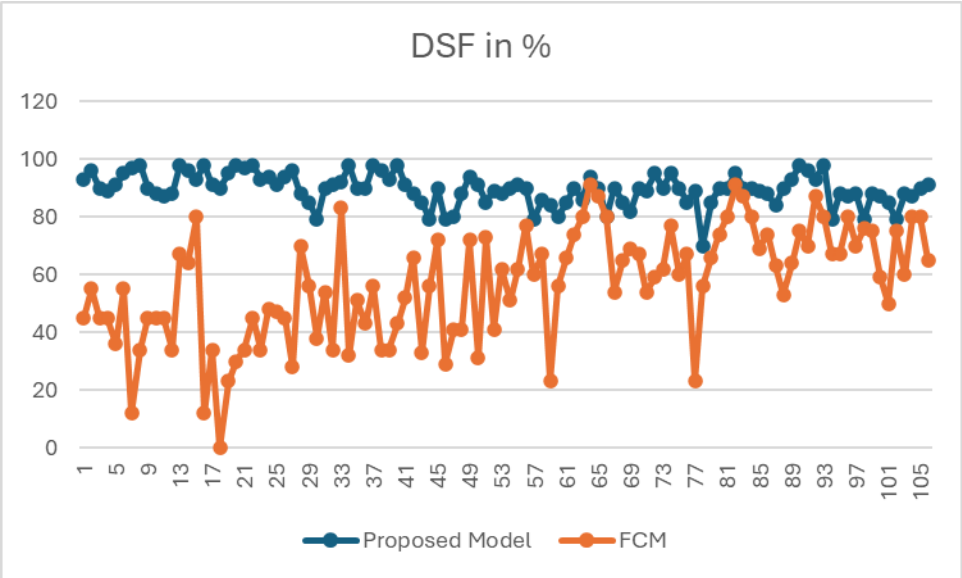

Figure 10: Evaluation of proposed framework and FCM for liver segmentation using DSF.

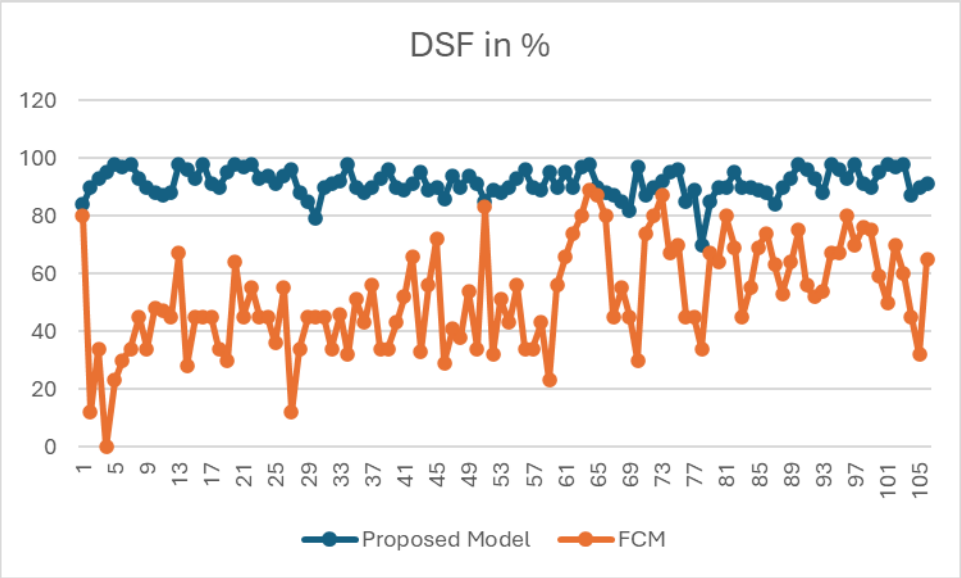

Figure 11: Evaluation of proposed framework and FCM for kidney segmentation using DSF

Table 1: Comparison of average accuracy, RVD and DSF for liver and kidney of proposed model and FCM

Evaluation Metric	Acc	RVD	DSF
	Proposed Model		
Liver	91.01%	8.23	89.61
Kidney	91.11%	5.96	91.45
	FCM		
Liver	71.58	66	57.02
Kidney	57.13	61.11	52.02

Conclusions

In this paper, the combined endeavour of two mathematical tools is used to obtain the accurate biomedical object segmentation. The first mathematical tool is Slope Variation Scatter plot of intensity variation of object image is obtained. The crests in the SVS provide mean pixel values in the objects. Using Crests present in the SVS, a novel NGF is proposed which converts medical image to NS domain. The NS is a dreadful mathematical tool that illustrates degree of truth, false and indefinity that must be considered as independent event in real time. The proposed model is experimented to separate liver and kidney from the CT scan image accurately. It is observed that results using anticipated framework is far better that Fuzzy-C-Means algorithm.

References

[1] S. Broumi, Bipolar Neutrosophic Minimum Spanning Tree, Smart Application and Data Analysis for Smart Cities, 201–206, 2018. doi: 10.2139/ssrn.3127519.
[2] Jha S, Kumar R, Priyadarshini I, Smarandache F, Long HV. Neutrosophic image segmentation with dice coefficients. Measurement. 2019 Feb 1;134:762-72.
[3] Zhao J, Wang X, Li M. A novel Neutrosophic image segmentation based on improved fuzzy C-means algorithm (NIS-IFCM). International Journal of Pattern Recognition and Artificial Intelligence. 2020 May 26;34(05):2055011.

[4] Zhao J, Wang X, Li M. A novel Neutrosophic image segmentation based on improved fuzzy C-means algorithm (NIS-IFCM). International Journal of Pattern Recognition and Artificial Intelligence. 2020 May 26;34(05):2055011.
[5] H. D. Cheng et al., Color image segmentation: Advances and prospects, Patt. Recogn. 34(12) (2001) 2259–2281.
[6] W. Chunyan et al., High resolution remote sensing image segmentation based on the interval type-2 fuzzy model, Chin. J. Sci. Instr. 37(3) (2016) 658–666.
[7] M. Cucuringu et al., Detection of core - periphery structure in networks using spectral methods and geodesic paths, Eur. J. Appl. Math. 27(6) (2016) 846–887.
[8] J. Zhao et al., Side scan sonar image segmentation based on neutrosophic set and quantum-behaved particle swarm optimization algorithm, Marine Geophys. Res. 37(3) (2016) 229–241.
[9] X. Wu et al., Study on industrial automation with SCARA robot vision system design, Adv. Mater. Res. 675 (2013) 72–76.
[10] Luo D, Zhang Y, Li J. Research on Several Key Problems of Medical Image Segmentation and Virtual Surgery. Contrast Media & Molecular Imaging. 2022 Apr 11;2022.
[11] Deheyab AO, Alwan MH, Rezzaqe IK, Mahmood OA, Hammadi YI, Kareem AN, Ibrahim M. An Overview of Challenges In Medical Image Processing. InProceedings of the 6th International Conference on Future Networks & Distributed Systems 2022 Dec 15 (pp. 511-516).
[12] Weese J, Lorenz C. Four challenges in medical image analysis from an industrial perspective. Medical image analysis. 2016 Oct 1;33:44-9.
[13] Oliveira, R. B., Marranghello, N., Pereira, A. S., & Tavares, J. M. R. "A computational approach for detecting pigmented skin lesions in macroscopic images". Expert Systems with Applications, vol.61, pp.53-63, 2016.
[14] Broumi S, Nagarajan D, Bakali A, Talea M, Smarandache F, Lathamaheswari M, Kavikumar J. Implementation of neutrosophic function memberships using MATLAB program. Infinite Study. 2019.
[15] Smarandache, F., 2019. Neutrosophic set is a generalization of intuitionistic fuzzy set, inconsistent intuitionistic fuzzy set (picture fuzzy set, ternary fuzzy set), pythagorean fuzzy set, spherical fuzzy set, and q-rung orthopair fuzzy set, while neutrosophication is a generalization of regret theory, grey system theory, and three-ways decision (revisited). Journal of new theory, (29), pp.1-31.
[16] Das S, Roy BK, Kar MB, Kar S, Pamučar D. Neutrosophic fuzzy set and its application in decision making. Journal of Ambient Intelligence and Humanized Computing. 2020 Nov;11:5017-29.
[17] Norouzi A, Rahim MS, Altameem A, Saba T, Rad AE, Rehman A, Uddin M. Medical image segmentation methods, algorithms, and applications. IETE Technical Review. 2014 May 4;31(3):199-213.
[18] Panimalar, A., Aarthi, D., Kumar, S.S. *et al.* Analysing Medical Image with Discrete Wavelet Transform Under Uncertainty. *Int. J. Appl. Comput. Math* 9, 114 (2023). https://doi.org/10.1007/s40819-023-01566-8
[19] Thanikachalam V, Kavitha MG, Sivamurugan V. Diabetic Retinopathy Diagnosis Using Interval Neutrosophic Segmentation with Deep Learning Model. Computer Systems Science & Engineering. 2023 Mar 1;44(3).
[20] Talouki AG, Koochari A, Edalatpanah SA. Image completion based on segmentation using neutrosophic sets. Expert Systems with Applications. 2024 Mar 15;238:121769.

[21] Datta S, Chaki N, Modak B. A novel technique for dental radiographic image segmentation based on neutrosophic logic. Decision Analytics Journal. 2023 Jun 1;7:100223.
[22] Wang Z, Chen Y, Yin J. Application of Improved U-Net with Feature Fusion and Expectation-Maximization Attention in Kidney Tumor Segmentation of CT Images. In Proceedings of the 2024 4th International Conference on Bioinformatics and Intelligent Computing 2024 Jan 26 (pp. 113-118)..
[23] Siri, Sangeeta K. and Latte, Mrityunjaya V.. "A Novel Approach to Extract Exact Liver Image Boundary from Abdominal CT Scan using Neutrosophic Set and Fast Marching Method" *Journal of Intelligent Systems*, vol. 28, no. 4, 2019, pp. 517-532. https://doi.org/10.1515/jisys-2017-0144
[24] Siri SK, Latte MV. Combined endeavor of Neutrosophic Set and Chan-Vese model to extract accurate liver image from CT scan. Computer methods and programs in biomedicine. 2017 Nov 1;151:101-9.
[25] Siri SK, Kumar S P, V. Latte M. An improved expectation-maximization algorithm to detect liver image boundary in ct scan images. IETE Journal of Research. 2023 Oct 31;69(10):6846-54.
[267] Siri SK, Pramod Kumar S, Latte MV. Accurate Liver Border Identification Model in CT Scan Images. International Journal of Image and Graphics. 2021 Jul 30;21(03):2150039.
[27] Wang Z. A new approach for segmentation and quantification of cells or nanoparticles. IEEE Transactions on Industrial Informatics. 2016 Mar 14;12(3):962-71.
[28] Wang Z, Yang Y. A non-iterative clustering based soft segmentation approach for a class of fuzzy images. Applied Soft Computing. 2018 Sep 1;70:988-99.
[29] Wang Z. Recognition of occluded objects by slope difference distribution features. Applied Soft Computing. 2022 May 1;120:108622.
[30] Sangeeta K. Siri, S. Pramod Kumar & Mrityunjaya V Latte (2022) Threshold-Based New Segmentation Model to Separate the Liver from CT Scan Images, IETE Journal of Research, 68:6, 4468-4475, DOI: 10.1080/03772063.2020.1795938.
[31] Nayantara, P.V., Kamath, S., Kadavigere, R. et al. Automatic Liver Segmentation from Multiphase CT Using Modified SegNet and ASPP Module. SN COMPUT. SCI. 5, 377 (2024). https://doi.org/10.1007/s42979-024-02719-2.
[32] Zhang, Z., Li, G., Wang, Z. et al. Deep-learning segmentation to select liver parenchyma for categorizing hepatic steatosis on multinational chest CT. Sci Rep 14, 11987 (2024). https://doi.org/10.1038/s41598-024-62887-2.
[33] Leube J, Horn M, Hartrampf PE, Buck AK, Lassmann M, Tran-Gia J. PSMA-PET improves deep learning-based automated CT kidney segmentation. Zeitschrift Für Medizinische Physik. 2024 May 1;34(2):231-41.
[34] Cao G, Sun Z, Wang C, Geng H, Fu H, Yin Z, Pan M. RASNet: Renal automatic segmentation using an improved U-Net with multi-scale perception and attention unit. Pattern Recognition. 2024 Jun 1;150:110336.
[35] Raut PK, Behera SP, Broumi S, Baral A. Evaluation of Shortest Path by using Breadth-First Algorithm under Neutrosophic Environment. HyperSoft Set Methods in Engineering. 2024 Jan 17;1:34-45.
[36] Saini RK, Ahirwar A, Smarandache F, Kushwaha M. Multi-Criteria Group Decision-Making with ELECTRE-III Method for Selection of Female Spouse in Pythagorean Neutrosophic Environment. Plithogenic Logic and Computation. 2024 Jan 25;1:36-53.

[37] Concepción IP, Almendariz KA, Valdiviezo WV. Neutrosophic Evaluation of Health Promotion Programs for Resource Allocation. Neutrosophic Optimization and Intelligent Systems. 2024 Jan 28;1:57-66.
[38] Srinivasan S, Durairaju K, Deeba K, Mathivanan SK, Karthikeyan P, Shah MA. Multimodal Biomedical Image Segmentation using Multi-Dimensional U-Convolutional Neural Network. BMC Medical Imaging. 2024 Feb 8;24(1):38.
[39] El-Shahat D, Talal N, Ye J, Cui WH. CT Image Segmentation Using Optimization Techniques under Neutrosophic Domain. Neutrosophic Systems with Applications. 2024 Apr 1;16:1-1.
[40] Mostafa NN, Kumar AK, Ali Y. A Comparative Study on X-Ray image Enhancement Based on Neutrosophic Set. Sustainable Machine Intelligence Journal. 2024 Apr 21;7:2-1.
[41] Wang Z, Monitoring of GMAW weld pool from the reflected laser lines for real times control, IEEE Trans. Ind. 10(4), (2014) 2073-2083
[42] Smarandache F. A Unifying Field in Logics: Neutrosophic Logic. Neutrosophy, Neutrosophic Set, Neutrosophic Probability: Neutrosophic Logic. Neutrosophy, Neutrosophic Set, Neutrosophic Probability. Infinite Study; 2005.
[43] Abdel-Basset, M., Smarandache, F. & Ye, J. Special issue on "Applications of neutrosophic theory in decision making-recent advances and future trends". *Complex Intell. Syst.* 5, 363–364 (2019). https://doi.org/10.1007/s40747-019-00127-1
[44] AboElHamd E, Shamma HM, Saleh M, El-Khodary I. Neutrosophic logic theory and applications. Neutrosophic sets and systems. 2021 Mar 31;41:30-51.
[45] C. Graaf, A. Koster, K. Vincken, and M. Viergever, "Validation of the interleaved pyramid for the segmentation of 3D vector images, " Pattern Recognition Letters, vol. 15, no. 5, pp. 467–475, 1994.
[46] Elmasry WH, Moftah HM, El-Bendary N, Hassanien AE. Performance evaluation of computed tomography liver image segmentation approaches. In2012 12th International Conference on Hybrid Intelligent Systems (HIS) 2012 Dec 4 (pp. 109-114). IEEE.
[47] Jaesik Min, Mark Powell, Kevin W. Bowyer, ―Automated Performance Evaluation of Range Image Segmentation Algorithms‖, IEEE Transactions on Systems, Man, and Cybernetics—Part B: Cybernetics, vol. 34, no. 1, February 2004, pp-263-271.
[48] Kumar SP, Latte MV. Fully automated segmentation of lung parenchyma using break and repair strategy. Journal of Intelligent Systems. 2019 Apr 24;28(2):275-89.

Received: April 20, 2024. Accepted: Aug 22, 2024

NSS
Neutrosophic Sets and Systems, Vol. 72, 2024
University of New Mexico

Neutrosophic Log-Gamma Distribution and its Applications to Industrial Growth

Fuad S. Al-Duais[1,2]

[1] Department of Mathematics, College of Science and Humanities in Al-Kharj, Prince Sattam Bin Abdulaziz University 11942 Al-Kharj, Saudi Arabia
[2] Business Administration Department, Administrative Science College, Thamar University, Thamar, Yemen

* Correspondence: f.alduais@psau.edu.sa

Abstract: This study suggests a novel statistical distribution known as the neutrosophic log-gamma distribution (NLGD) for analyzing the interval value data. The proposed distribution is derived from the transformation method, utilizing the approach of neutrosophic logic. The statistical characteristics of the proposed are studied within a neutrosophic framework. Basic statistical properties such as moments of origin, mode, mean deviation, and other related functions that are commonly employed in statistical applications are derived. In addition to the basic properties of the model, the estimation approach of maximum likelihood is also studied. The derived estimators of the proposed model are further assessed by the simulation method. Comparative research using real-world examples shows that NLGD does a better job of modelling complicated industrial growth and production measures than standard distribution. Application of the proposed model improves our understanding of the theoretical component and our ability to forecast outcomes in statistical applications. This, in turn, leads to improved decision-making and operational efficiency in many industrial sectors.

Keywords: Neutrosophic model, descriptive statistics, uncertainty measures, estimation, simulation.

1. Introduction

The distribution of income size is crucial for all economies when it comes to making decisions on social and economic policies [1] . The distribution of income plays a crucial role in economic and social statistics, serving as the foundation for concentration and Lorenz curves [2], [3] . These curves are essential for measuring inequality and evaluating overall social welfare. Market demand and elasticity are influenced by income distribution, which in turn impacts how firms behave and ultimately affects market equilibrium [4]. Income distribution plays a crucial role in shaping the level of savings within a society, as well as impacting the productive efforts of different societal groups. Understanding the distribution of firm sizes is crucial for economists specializing in industrial organization, government regulators, and courts [5] . In antitrust cases, courts rely on market share data from firms and industries to make informed decisions. Pareto's laws of income distribution laid the foundation for statistical studies on personal income distributions [6]. There

are many statistical distributions used to model income size[6], [7], [8] . One of such distributions is gamma distribution [9], [10]. The Pearson type III distribution, also known as the gamma distribution, is widely utilized in applied statistics for modeling unimodal and positive data. It is commonly employed in analyzing waiting times, income levels, insurance claims, and rainfall patterns.

If the exponential function applied to gamma distribution we obtained the log-gamma distribution which also has very important applications in economics [11-13] . Mathematically, if random variable Y follows gamma distribution with two parameters, then $X = exp(Y)$ follows the log-gamma distribution with probability density function (PDF) given below:

$$f(\mathrm{y}) = \frac{b^p}{\Gamma(p)} \mathrm{y}^{b-1} (\log(\mathrm{y}))^{p-1}, \mathrm{y} \geq 1, \mathrm{p}, \mathrm{b} > 0 \quad (1)$$

where p, and b are both shape parameters of the distribution.

The classical structure of log-gamma distribution is shown in Figure 1.

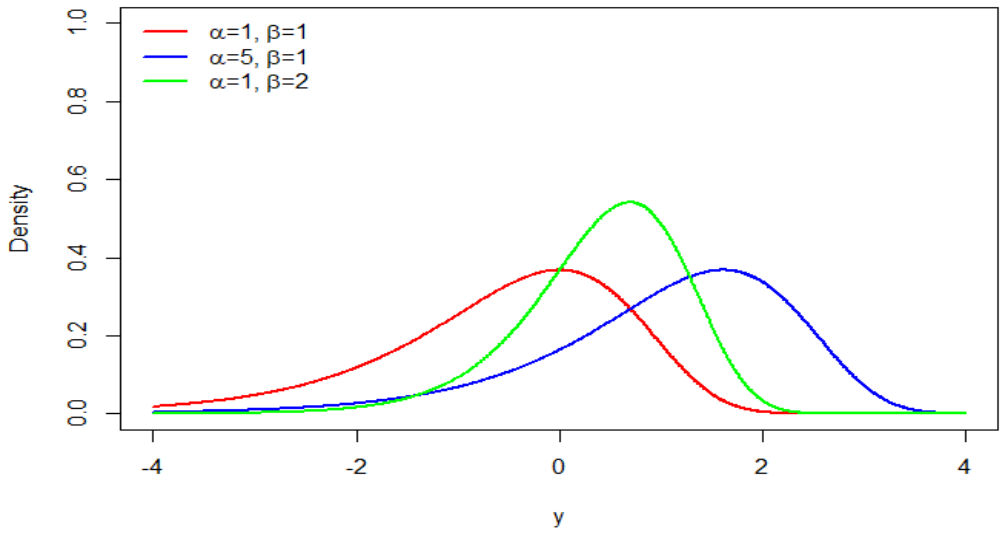

Figure 1: Density plots of the log-gamma distribution

The log gamma distribution is very versatile and can be viewed as the generalized form of the Pareto distribution. Particularly with parameter p = 1, it reduces to the Pareto distribution of type-I. Unlike the Pareto type I distribution, which always has a decreasing density, the log-gamma distribution can have unimodal densities, making it more flexible. The shape of the classical. There are several reasons that log-gamma distribution is very important in statistical applications for business data, finance and engineering studies. The log-gamma distribution is well suited for modelling skewed data. Many real data sets exhibit skewness and log-gamma provides adequate fit compared to other symmetric distributions. In terms of scale and shape parameters log-gamma distribution is symmetric for modeling variety of real data sets and its versatile behaviors [14]. It has a key application in modelling financial data such as profit, loss asset returns, especially when applications exhibit skewness and heavy tails problems. In reliability studies, it is commonly employed to model the lifetime of systems and products. It is highly useful in studying the survival time and in planning maintenance schedules. This also frequently used in medical research for modelling survival data which are often skewed. The log-gamma distribution is also used as prior distribution for many parameters in Bayesian studies. To model extreme events, it is also used in extreme value theory. This helps in understanding risk assessment and mitigation.

Although the log-gamma distribution is useful for skewed and heavy-tailed data, it struggles with imprecise data. Neutrosophic distributions, on the other hand, are tailored to handle uncertainty and imprecision commonly found in real-world situations [15-17]. Neutrosophic collections provide a more thorough approach compared to the traditional collection notion when dealing with ambiguous, vague, and irregular information [18]. The subscription features, namely truth-membership, indeterminacy-membership, and falsity-membership, provide a precise understanding of whether a component belongs to the collection, is uncertain, or does not belong to the collection. This structure also incorporates relevant data and probability distributions to further enhance its efficiency in handling intricate information [19-22]. Neutrosophic statistics, together with possibility distributions, offer valuable methods for analyzing data or uncertainty that is characterized by neutrosophic sets [23-25]. Neutrosophic probability distributions are used to determine the likelihood of events or outcomes in situations where there is ambiguity. They specifically focus on measures such as central tendency, dispersion, and other properties of neutrosophic data [26].

To develop a more adaptable distribution term the NLGD is the primary aim of this study. This neutrosophic model effectively manages the fuzzy applications. The core motivation behind this study is to handle the ambiguous data and enhancing its ability to analyze and interpret such vague information.

This study is organized as follows: Section2 describes the classical model and its extension to neutrosophic model. Section 3 discusses the quantile function and simulation analysis of the NLGD. Section4 examines the estimation strategy for unknown parameters. Section 5 conducts a real data analysis to explain the theoretical part of the proposed model. Finally, Section 6 concludes major findings.

2. Proposed Model

In the neutrosophic framework, the parameters p and b are not fixed numbers rather than belonging to intervals or fuzzy sets. This reflecting the imprecision and uncertainty in the model and can be defined as:

$$f(z;\beta_N,p_N)=\frac{\beta_N^{p_N}}{\Gamma(p_N)}z^{\beta_N-1}(\log z)^{p_N-1},\quad z\geq 1,\ p_N>0,\ \beta_N>0 \tag{2}$$

where $p_N\epsilon[p_l,p_u]$ and $\beta_N\epsilon[\beta_l,\beta_u]$ are two imprecise shape parameters of the proposed NLGD.

The conversion of log-gamma distribution into neutrosophic structure enhanced the capability of the distribution to manage uncertain and imprecise data. The neutrosophic form provide more realistic and flexible data modelling, making it more valuable distribution for handling applications involving ambiguous information. The structure of imprecise distribution can be seen in Figure 2.

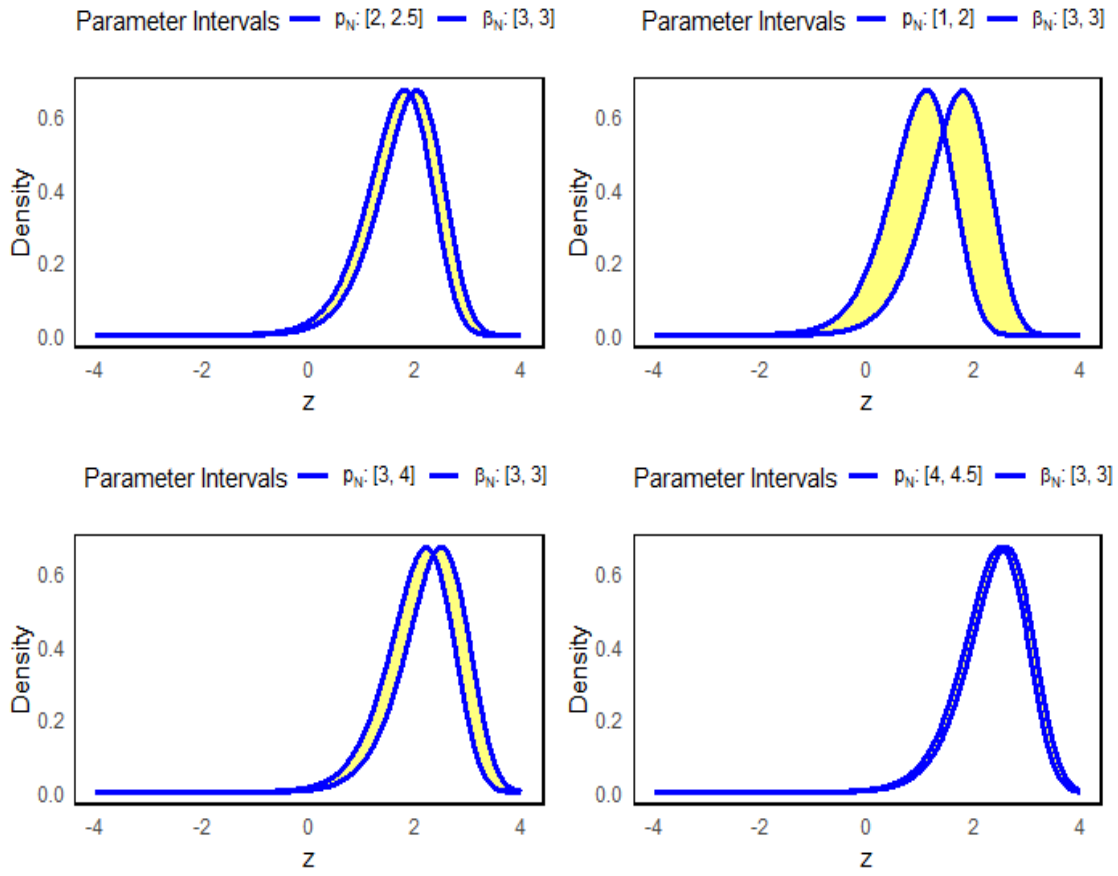

Figure 2: PDF plot of the NLGD for different imprecise parameters setting

Figure 2 visualize the PDF plot of NLGD assuming that shape parameter P_N is imprecise while the β_N is crisp value. Due to not precisely unknown value of shape parameter P_N , uncertainty in the PDF is shown with yellow shaded color each plot. This representation indicates more comprehensive understanding of possible shape of the distribution can take. Neutrosophic PDF helps in visualizing how parametric imprecision affects the distribution, allowing better decision making under uncertain environment. The neutrosophic PDF can have numerous benefits, for example it allows actuaries to view the potential variability in loss distributions that may lead to setting reserves and premiums. Similarly, it also guides the economists to count for uncertainties in economic indicators resulting in more robust forecasting models. Similar to PDF function another associated function is the cumulative distribution function. The neutrosophic CDF function of NLGD can be determined as follows:

$$H(z) = \int_1^z \frac{\beta_N^{p_N}}{\Gamma(p_N)} z^{\beta_N - 1} (\log z)^{p_N - 1} dz \tag{3}$$

Further simplification of (3) yielded:

$$H(z) = \frac{\gamma\left(p_N, \frac{log(z)}{\beta_N}\right)}{Gamma(p_N)} \tag{4}$$

where $\gamma(.)$ representing the incomplete gamma distribution.

The shape of the neutrosophic CD function is depicted in Figure 3.

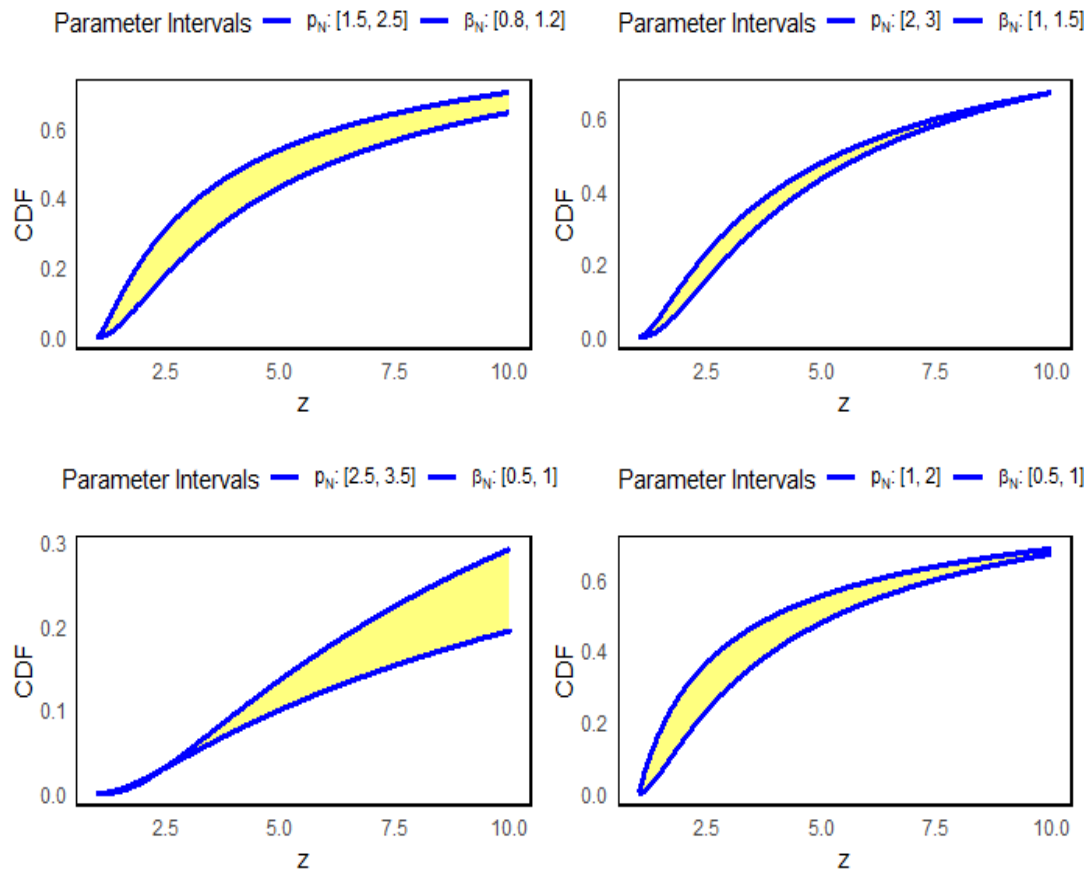

Figure 3: CDF curves of the NLGD with various imprecise parameters.

Figure 3 shows the CDF of the NLGD indicates the cumulative probability of random variable being less than or equal to some particular value. Figure 3 indicates that similar to classic structure plot starts at zero and increases to one with non-decreasing feature. This plot provides a complete description of the NLGD. The yellow area in each plot indicates indeterminacy in the parameters of the distribution. The yellow bounded area encapsulates the possible variations in the CD function due to imprecision in the studied parameters. By plotting the lower and upper bound of the distribution plot, users can assess the potential variability in the cumulative probabilities which quite significant for knowing the behavior of the model over its entire domain.

The other important function related to CDF is the survival function. Survival function is critical concepts used in reliability theory, risk management and survival analysis. This function is important because it provides information about the failure rates or longevity of systems or processes. Mathematically the survival function can easily be established for the NLGD as:

$$S(z) = 1 - H(z) = 1 - \frac{\gamma\left(p_N, \frac{log(z)}{\beta_N}\right)}{Gamma(p_N)} \tag{5}$$

For imprecise values of neutrosophic parameters, the survival function of the NLGD can be depicted in Figure 4.

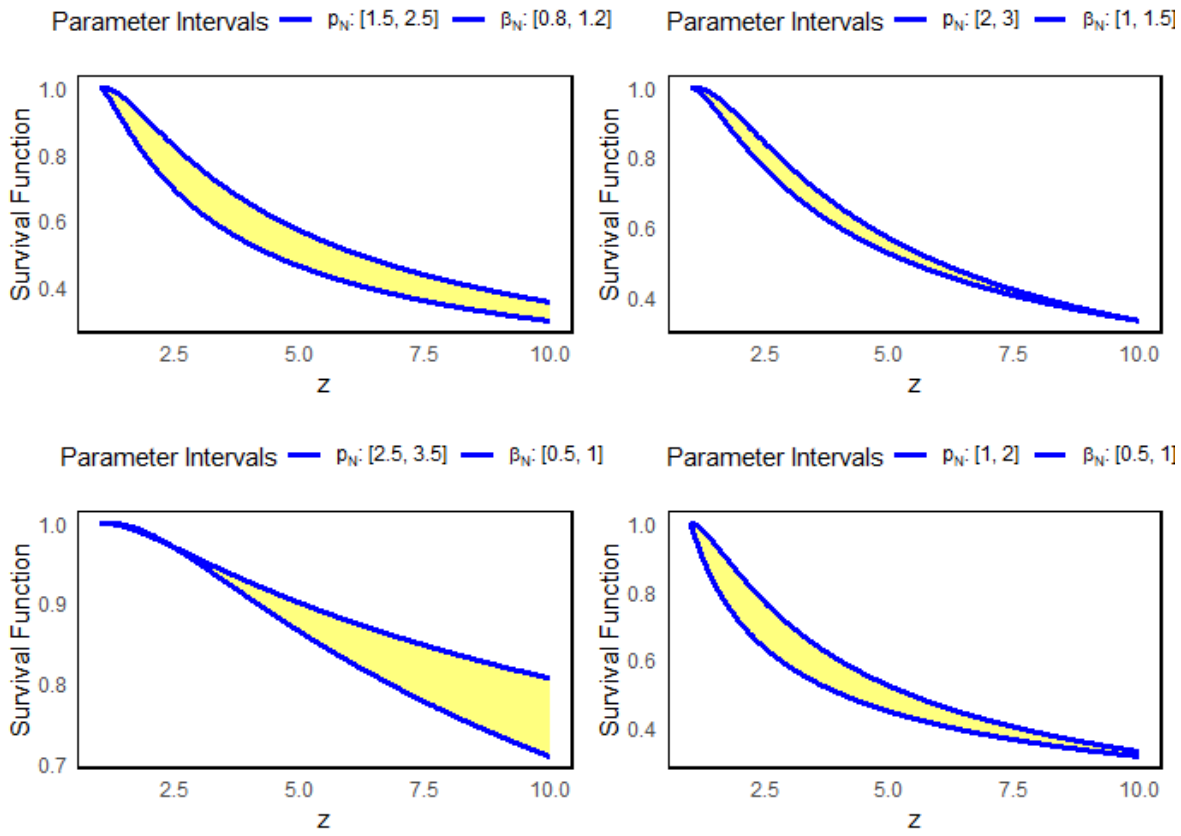

Figure 4: Survival function of the NLGD

As shown in Figure 4, survival function is time dependent function which provides information about the likelihood of systems or component to survival behind the time period t. It is essential information because this information is used in reliability analysis to improve the durability of the products. It helps in making data-driven decisions about warranties of the products and better understanding about the distribution of lifetimes. The ratio between PDF and survival functions provides the hazard function. The hazard function of the NLGD is given by:

$$h(z;\beta_N,p_N)=\frac{\frac{\beta_N^{p_N}}{\Gamma(p_N)}z^{\beta_N-1}(\log z)^{p_N-1}}{1-\frac{\gamma\left(p_N,\frac{\log(z)}{\beta_N}\right)}{\Gamma(p_N)}};\ z\geq 1,\ p_N>0,\ \beta_N>0. \tag{6}$$

Hazard function provides the instantaneous failure rate of component or system at any specific time. It represents the likelihood of death or failure occurring at particular time t given that system or component has been survived up to that time. The hazard function for different values of neutrosophic parameters are shown in Figure 5.

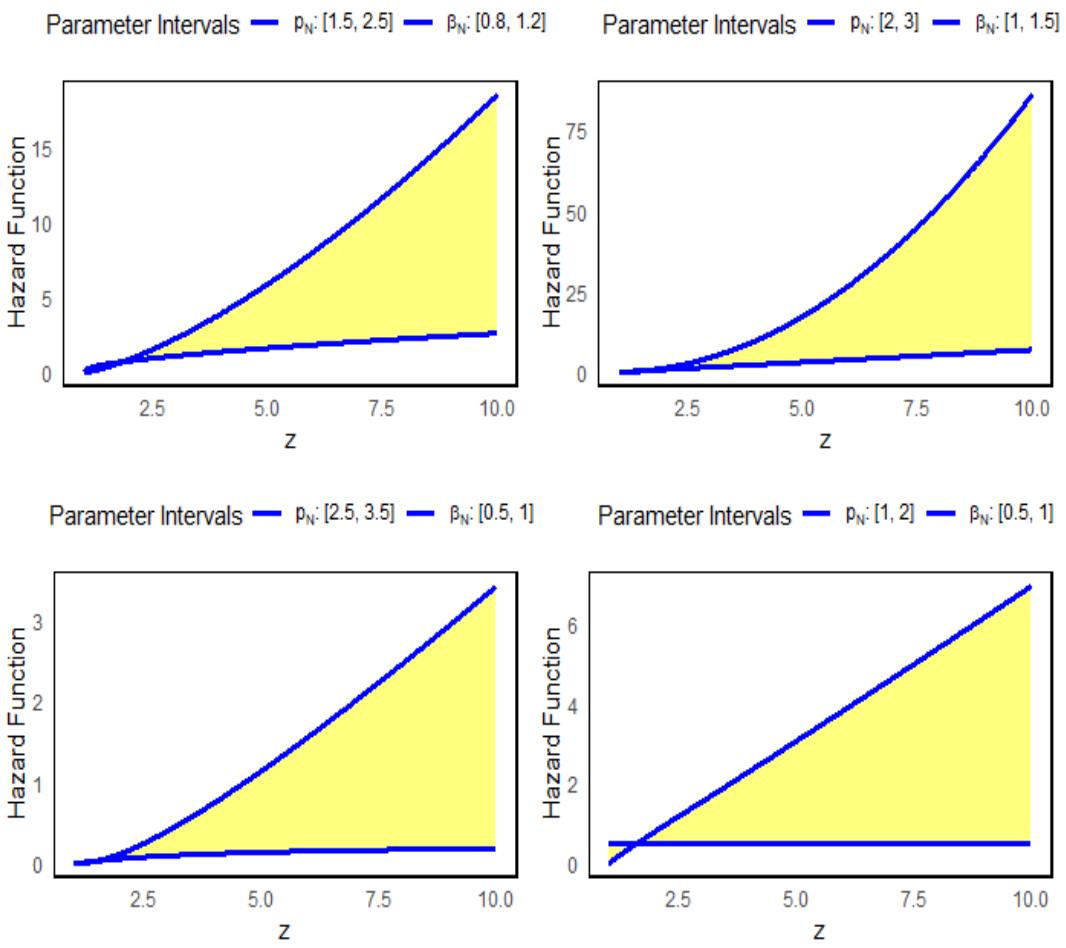

Figure 5: Hazard function of the NLGD for different imprecise parameters setting

As shown in Figure 5, neutrosophic hazard function is different from the classical concept of hazard function. It is represented by a sturdy curve and able to handle vagueness, indeterminacy and uncertainty. This sturdy structure reflects the inherent variability in due to assuming the imprecise values of the distributional parameters.

The kth moment of the NLGD can be written as follows:

$$E(Z^k) = \left(\frac{\beta_N}{\beta_N - k}\right)^{p_N}, \quad k < \beta_N \tag{7}$$

In neutrosophic framework (7) can be derived as follows:

$$E(Z^k) = \int_1^{\infty} z^k f(z; \beta_N, p_N)\, dz \tag{8}$$

Equation (8) can be further simplified as:

$$E(Z^k) = \int_1^{\infty} z^k \frac{\beta_N^{p_N}}{\Gamma(p_N)} z^{\beta_N - 1} (\log z)^{p_N - 1}\, dz \tag{9}$$

Solving (9) yielded:

$$E(Z^k) = \frac{\beta_N^{p_N}}{\Gamma(p_N)} \frac{\Gamma(p_N)}{(\beta_N - k)^{p_N}} \tag{10}$$

Hence simplification of (10) provided

$$E(Z^k) = \left(\frac{\beta_N}{\beta_N - k}\right)^{p_N} \tag{11}$$

which is required result.

Now assuming the different of values of k mean and variance can easily be derived.

Thus, the mean of the NLGD is given by:

$$mean = E(Z) = \left(\frac{\beta_N}{\beta_N - 1}\right)^{p_N} \tag{12}$$

Similarly, variance from (11) can be written as:

$$\text{var}(Z) = \left(\frac{\beta_N}{\beta_N - 2}\right)^{p_N} - \left(\frac{\beta_N}{\beta_N - 1}\right)^{2p_N}, \quad \beta_N > 2 \tag{13}$$

Utilizing mean and variance coefficient of variation of the NLGD can be written as:

$$\text{CV} = \frac{\sqrt{\left(\frac{\beta_N}{\beta_N - 2}\right)^{p_N} - \left(\left(\frac{\beta_N}{\beta_N - 1}\right)^{p_N}\right)^2}}{\left(\frac{\beta_N}{\beta_N - 1}\right)^{p_N}} \tag{14}$$

Similarly, mode of the NLGD can be expressed as:

$$z_{\text{mode}} = \exp\left(\frac{p_N - 1}{\beta_N + 1}\right) \tag{15}$$

To derive the mode of the NLGD, we need to differentiate the PDF with respect to z and setting it to zero.

i.e.,

$$\frac{d}{dz} f(z) = \frac{\beta_N^{p_N}}{\Gamma(p_N)} \left[(\beta_N - 1) z^{\beta_N - 2} (\log z)^{p_N - 1} + z^{\beta_N - 2} (p_N - 1)(\log z)^{p_N - 2}\right] = 0 \tag{16}$$

Simplification of (16) leads to:

$$(\beta_N - 1) \log z + (p_N - 1) = 0 \tag{17}$$

Further simplification yielded:

$$z_{\text{mode}} = \exp\left(\frac{p_N - 1}{\beta_N + 1}\right) \tag{18}$$

which is required result.

Utilizing (11) , third and fourth moments respectively can be written as:

$$E(Z^3) = \left(\frac{\beta_N}{\beta_N - 3}\right)^{p_N} \tag{19}$$

$$E(Z^4) = \left(\frac{\beta_N}{\beta_N - 4}\right)^{p_N} \tag{20}$$

Using (19) and (20), coefficients of skewness and kurtosis can be written as:

$$\gamma_1 = \frac{\left(\frac{\beta_N}{\beta_N - 3}\right)^{p_N} - 3\left(\frac{\beta_N}{\beta_N - 1}\right)^{p_N} \sigma^2 - \left(\left(\frac{\beta_N}{\beta_N - 1}\right)^{p_N}\right)^3}{\sigma^3} \tag{21}$$

$$\gamma_2 = \frac{\left(\frac{\beta_N}{\beta_N - 4}\right)^{p_N} - 4\left(\frac{\beta_N}{\beta_N - 1}\right)^{p_N}\left(\frac{\beta_N}{\beta_N - 3}\right)^{p_N} + 6\left(\left(\frac{\beta_N}{\beta_N - 1}\right)^{p_N}\right)^2 \left(\frac{\beta_N}{\beta_N - 2}\right)^{p_N} - 3\left(\left(\frac{\beta_N}{\beta_N - 1}\right)^{p_N}\right)^4}{\left(\left(\frac{\beta_N}{\beta_N - 2}\right)^{p_N} - \left(\left(\frac{\beta_N}{\beta_N - 1}\right)^{p_N}\right)^2\right)^2} \tag{22}$$

Likewise other important functions and key statistical properties can be established in the neutrosophic framework. Table 1 shows some basic suggested model based on neutrosophic parameters.

Table 1: Computation of basic properties of proposed model

β_N	p_N	Mean	variance	CV
[2.5,3.5]	[1, 2]	[1,5.44]	[0,48]	[0,6.92]
[3.1,4.0]	[2,4]	[1.06,13.16]	[0,173.73]	[0,12.34]
[4,4.5]	[3,4]	[1.42,5.06]	[0,23.40]	[0,3.24]
[5,5.5]	[4,5]	[1.52, 4.91]	[0,18.38]	[0,2.81]
[6,6.5]	[5, 6]	[1.54, 4.82]	[0,16.02]	[0,2.5]
[7, 7.5]	[7, 8]	[1.67,5.96]	[0, 22.8]	[0,2.84]

Table1 indicates the values in intervals, reflecting the imprecision and vagueness existed in the distribution parameters. Some intervals particularly related to variance and CV include zero, indicating that the distribution can be perfectly predictable in some cases. Generally, CV tends to decrease as values of the parameters increase.

3. Quantile Function

The quantile function of the NLGD can be calculated easily by inversing the CDF function. However, the quantile function of the NLGD does not have no closed form expression that makes it difficult to solve it analytically. Instead, some numerical solution will be applicable to find random numbers generation from the NLGD. Finding the quantile function via inverse CDF method is a fundamental concept in statistical applications and used essentially for generating random samples from the NLGD. Using quantile function on uniform numbers, one can generate random samples from the target model.

In the neutrosophic framework the quantile function can be written as :

$$Q(u) = [Q_L(u), Q_U(u)] \tag{23}$$

The exact expression for (23) is not straightforward and may be expressed as:

$$Q(u) = \left[{Q_L}^{-1}(u), {Q_U}^{-1}(u)\right] \tag{24}$$

To find the numerical solution of (24), the Newton Raphson method may be used. It is an iterative procedure to find successively better approximation to the root of real value function. Given the $F(z)$, the iteratively updates the estimate z_n as follows:

$$z_{n+1} = z_n - \frac{F(z_n)-u}{F(\acute{z}_n)} \tag{25}$$

where $F(\acute{z}_n)$ is the derivative of $F(z_n)$. This method needs the derivative of CDF which is an essential component of the fundamental equation. The used of Newton Raphson method is most effective in initial guess is chosen closer to true value. To find the random samples from the NLGD, a program written in R has been utilized. Let we assume that the proposed model with $\beta_N = [2.5, 3.5\ ]$ and $p_N = [1, 2]$. The random generated samples with some specific seed setting, are shown in Table 2.

Table 2: Random samples generation from the NLGD.

Random Samples				
[1.31, 1.49]	[1.72, 1.84]	[1.42, 1.58]	[1.81,1.93]	[1.90, 2.00]
[0.88, 1.14]	[1.51, 1.66]	[1.82, 1.94]	[1.53, 1.68]	1.45, 1.62]
[1.93, 2.03]	[1.45, 1.62]	[1.62, 1.76]	[1.54, 1.69]	[1.05, 1.28]

Table 2 show 15 random samples generated through computer program written in R. The R package "VGAM" has been utilized for random samples generation of the NLGD. Table 2 indicates that values are in intervals due to assumed vagueness in the parameters of the proposed model.

4. Estimation Procedure

In this section, analytical results of the NLD for moments, skewness, and kurtosis have been validated using the Monte Carlo simulation. The NLD can be readily simulated in R software to assess the validity of theory-based results.

To estimate the parameters of the NLGD, we can focus on the commonly used method of maximizing the log-likelihood function of the NLGD. This method is well known in statistical analysis and commonly used known as maximum likelihood estimation. In this procedure we try to find the best fit parameters of shape and scale parameters that maximize the likelihood of the observed sample. Let for the data values $Z = z_1, z_2, \dots z_n$ assume to follow the NLGD then the log-likehood function can be written as:

$$\mathcal{L}(\beta_N, p_N; \{z_i\}) = \sum_{i=1}^{n} \left[\log\left(\frac{\beta_N^{p_N}}{\Gamma(p_N)} \right) + (\beta_N - 1) \log z_i + (p_N - 1) \log(\log z_i) \right] \quad (26)$$

Further simplification of (26) yielded:

$$\mathcal{L}(\beta_N, p_N; \{z_i\}) = n \log\left(\frac{\beta_N^{p_N}}{\Gamma(p_N)} \right) + (\beta_N - 1) \sum_{i=1}^{n} \log z_i + (p_N - 1) \sum_{i=1}^{n} \log(\log z_i) \quad (27)$$

Partial derivatives of (27) with respect to β_N and p_N resulted in respectively:

$$\frac{\partial \mathcal{L}}{\partial \beta_N} = n \frac{p_N}{\beta_N} + \sum_{i=1}^{n} \log z_i \quad (28)$$

$$\frac{\partial \mathcal{L}}{\partial p_N} = n \left(\log \beta_N - \frac{\Gamma'(p_N)}{\Gamma(p_N)} \right) + \sum_{i=1}^{n} \log(\log z_i) \quad (29)$$

Now it is evident that analytical solution of (28) and (29) are not possible, instead some numerical approach would be used to find the optimum values of β_N and p_N. We have utilized BFGS optimization method to find the values of β_N and p_N. A program written in R has been utilized to find the optimum values of shape and scale parameters of the NLGD. The objective of this simulation program is to find the optimum estimates and the calculate the corresponding mean squared error (MSE) at various sample sizes. Random sample of sizes $\{n = 25, 50, 75, \ 100 \ and \ 120\}$

are drawn from the NLGD with $p_N = [1,1]$ and $\beta_N = [2.5,3.5]$. To ensure sufficient statistical power each sample size is simulated 1000 times to find the estimates and corresponding MSE. Results from this simulation are shown in Table 3.

Table 3: Estimated parameters of the NLGD with MSE using simulated data

Sample Size	Estimated (β_N)	Estimated (p_N)	MSE (β_N)	MSE (p_N)
25	[2.54, 4.01]	[2.41, 3.91]	[0.85, 2.58]	[2.16,11.49]
50	[3.75, 3.75]	[1.01, 4.21]	[0.32, 1.30]	[1.12, 6.55]
75	[2.15, 4.09]	[1.76, 4.83]	[0.24, 1.03]	[0.92, 5.19]
100	[1.97, 3.49]	[1.68, 4.21]	[0.22, 0.97]	[0.84, 4.83]
120	[2.11, 2.59]	[1.92, 3.07]	[0.20, 1.00]	[0.83, 4.41]

Table 3 shows the results from the simulation data, where each dataset is simulated for specified sample size. The estimated parameters and their MSE(s) are given in ranges due to assumed indeterminacy in the parameters of underlying model. Results show that as the sample size increases, the estimated values of parameters tend to narrow, indicating precise estimation with larger sample sizes. Overall MSE of the estimated values decrease with increasing sample size. This indicates that more reliable and accurate results are expected with larger sample sizes.

5 Real Data Application

In this section, we have utilized the suggested distribution model on actual carbon dioxide (CO2) data obtained from the World Bank for Saudi Arabia [27]. The release of CO2 has a notable effect on a country's climate. To do high emissions of CO2, air quality in urban areas of Kingdom is highly compromised because of industrial activities. This climate indicator is a focal point of research globally and plays a crucial role in the ongoing changes to the world's climate. The primary cause of carbon emissions stems from the combustion of fossil fuels during industrial activities and deforestation. The Kingdom of Saudi Arabia holds a prominent position in the global oil market, presenting both distinct challenges and opportunities when it comes to managing carbon emissions. It is crucial to study the effects of CO2 on public health and take measures to reduce its emission on a smaller scale. The Kingdom, known for its desert and arid environment, is especially at risk from climate change. The changes in the climate have a profound impact not only on the country's weather patterns but also contribute significantly to heatwaves, global warming, and harsh weather conditions. As a result, these weather phenomena have repercussions on natural resources like water availability, shifts in climate patterns, and affect agricultural productivity. On the other hand,

due to major supplier oil, Kingdom highly depends on fossile export. Transitioning to renewable energy sources particularly solar power can help decrease carbon emissions. Utilization of country vast desert zone and solar industry can provide healthy environment. Due to environmental and instrumental factors, carbon emissions values are not always precise and can vary. In order to determine the significance of a proposed method, exact carbon emission values are transformed into interval values using a procedural methodology [28]. The carbon emission values in time span of 2005 to 2020 are given in Table 4.

Table 4: Carbon emission values for Saudi Arabia time period 2005-2020

Carbon emission values				
[12.63,13.21]	[12.42, 14.00]	[13.02,13.84]	[13.32, 15.08]	[13.33, 15.21]
[15.12, 15.21]	[14.85, 15.90]	[15.08, 16.87]	[15.43, 16.53]	[16.36,17.28]
[16.30, 18.21]	[16.34, 17.24]	[15.40, 16.75]	[14.49, 16.63]	[14.60, 14.80]

Interval values in Table 4 show that imprecise values are available for analysis due to technical malfunctions and limitations of measuring devices or sensors. Carbon emissions are usually measured by air sampling procedures or gas emission at specific points. Thus, due limitations of these procedures, collected samples can be considered compromised and not available in exact numbers. If we fit the conventional model of log-gamma distribution on carbon emission values, fitting graph can be seen in Figure 6.

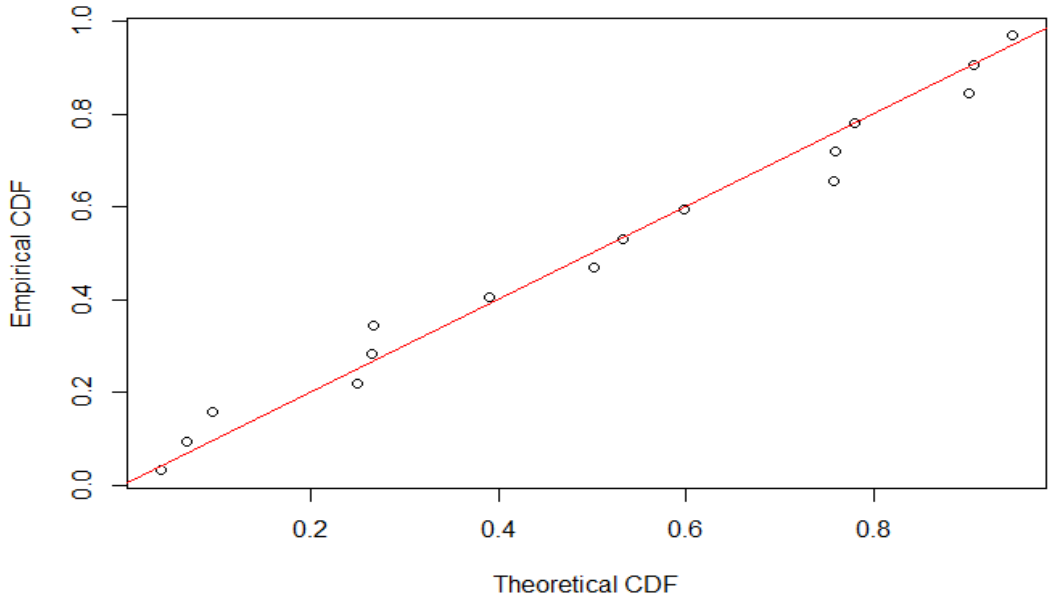

Figure 6: Fitting plot of log-gamma distribution on carbon emissions data

Figure 6 shows that log-gamma distribution is better fit model the carbon emissions data. However, the existing log-gamma distribution could not be used to analysis imprecise data given in Table 4. A statistical description of the data in terms of estimated parameters of the NLGD are given in Table 5.

Table 5: Estimated parameters of the NLGD for carbon emissions data

Statistical measures	Computed values
Estimated (β_N)	[7.49, 8.48]
Estimated (p_N)	[123.75, 123.91]

Results in Table 5 show that estimated values of the parameters are in interval forms due to vagueness in the underlying data. These imprecise estimated values can be used to find the statistical characteristics of the carbon emissions data. The neutrosophic model in this way is more generic as compared to existing model.

6 Conclusions

In this study, a novel distribution called NLGD has been introduced for analyzing neutrosophic data. The NLGD distribution shows great efficacy in analyzing data with interval values. By employing the neutrosophic logic, the suggested distribution has established a statistical model for describing interval characteristics such as mean, mode, variance, and shape coefficients. Key functions like the reliability function and hazard function have been devloped due to the widespread use of the proposed model in reliability analysis. These functions are essential for understanding and analyzing the model utility in survival analysis. The MLE method has been used to estimate the parameters of the proposed model under an indeterminate environment. A simulation has been conducted to evaluate the accuracy of the established model and examine the impact of sample size on the results. Based on the simulation results, it can be concluded that larger sample sizes lead to more precise estimation. At long last, a genuine data set on carbon emissions has been employed to analyze both the theoretical framework of the study and the practical implementation of the proposed model.

Acknowledgement:

The authors extend their appreciation to Prince Sattam bin Abdulaziz University for funding this research work through the project number (PSAU/2024/01/28229)

References

1. Y. Atikankul, A. Thongteeraparp, W. Bodhisuwan, and A. Volodin, "The Length-Biased Weighted Lindley Distribution with Applications," Lobachevskii Journal of Mathematics, 41(3), 2020.
2. T. Sitthiyot and K. Holasut, "A simple method for estimating the Lorenz curve," Humanities and Social Sciences Communications, 8(1), 2021.
3. M. Fajar, S. Setiawan, and N. Iriawan, "The New Measures of Lorenz Curve Asymmetry: Formulation and Hypothesis Testing," Decision Making: Applications in Management and Engineering, 7(1), 2024.
4. C. Kroer, A. Peysakhovich, E. Sodomka, and N. E. Stier-Moses, "Computing Large Market Equilibria Using Abstractions," Operational Research, 70(1), 2022.
5. G. Issayeva et al., "The Relationship between Renewable Energy Consumption, CO2 Emissions, Economic Growth, and Industrial Production Index: The Case of Kazakhstan," International Journal of Energy Economics and Policy, 13(6), 2023.
6. Y. Bilan, H. Mishchuk, N. Samoliuk, and H. Yurchyk, "Impact of Income Distribution on Social and Economic Well-Being of the State," Sustainability (Switzerland), 12(1), 2020.
7. C. Panico, A. Pinto, and M. P. Anyul, "Income distribution and the size of the financial sector: A Sraffian analysis," Cambridge Journal of Economics, 36(6), 2012.
8. R. Becerril-Arreola, R. E. Bucklin, and R. Thomadsen, "Effects of income distribution changes on assortment size in the mainstream grocery channel," Management Science, 67(9) 2021.
9. X. Ke, S. Wang, M. Zhou, and H. Ye, "New Approaches on Parameter Estimation of the Gamma Distribution," Mathematics, 11(4), 2023.
10. H. S. Klakattawi, "The Weibull-Gamma distribution: Properties and applications," Entropy, 21(5), 2019.
11. L. J. Halliwell, "The Log-Gamma Distribution and Non-Normal Error," Variance (ISSN 1940-6452), 2017.
12. A. M. M. Ibrahim and Z. Khan, "Neutrosophic Laplace Distribution with Properties and Applications in Decision Making," International Journal of Neutrosophic Science, vol. 23(1), 2024.
13. H. Y. A. Shihabeldeen and Z. Khan, "Neutrosophic Structure of the Log-logistic Model with Applications to Medical Data," International Journal of Neutrosophic Science, vol. 23(1), 2024.
14. M. N. Shahzad and Z. Asghar, "Parameter Estimation of Singh Maddala Distribution by Moments," International Journal of Advanced Statistics and Probability, 1(3), 2013.
15. Smarandache, F. Neutrosophic set-a generalization of the intuitionistic fuzzy set. International Journal of Pure and Applied Mathematics, 24(3), 287, 2005.
16. Broumi, S., Sundareswaran, R., Shanmugapriya, M. ., Nordo, G., Talea, M. ., Bakali, A., and Smarandache, F. Interval- valued fermatean neutrosophic graphs, Decision Making: Applications in Management and Engineering, Collected Papers, 5(2), 176–200, 2022. https://doi.org/10.31181/dmame0311072022b
17. F. Smarandache, X. Zhang, and M. Ali, Algebraic Structures of Neutrosophic Triplets, Neutrosophic Duplets, or Neutrosophic Multisets, Symmetry 2019,11(2), p. 171, 2019
18. Khan, Z., Gulistan, M., Hashim, R., Yaqoob, N., & Chammam, W. Design of S-control chart for neutrosophic data: An application to manufacturing industry. Journal of Intelligent & Fuzzy Systems, 38(4), 4743–4751, 2020.
19. Smarandache, F. A unifying field in logics: neutrosophic logic. Neutrosophy, neutrosophic set, neutrosophic probability: neutrosophic logic. Neutrosophy, neutrosophic set, neutrosophic probability. Infinite Study, 2005.
20. Smarandache, F., Introduction to Neutrosophic Statistics, Sitech & Education Publishing, Craiova, 2014, 124 p.
21. Z. Khan, A. Al-Bossly, M. M. A. Almazah, and F. S. Alduais, On Statistical Development of Neutrosophic Gamma Distribution with Applications to Complex Data Analysis, Complexity, vol. 2021, pp. 1-8, 2021.
22. U. Rivieccio, Neutrosophic logics: Prospects and problems, Fuzzy Sets and Systems, vol. 159(4), pp. 1860–1868, Jul. 2008.

23. S. Broumi and F. Smarandache, Several similarity measures of neutrosophic sets, Infinite Study, 410(1), 2013.
24. A. M. M. Ibrahim and Z. Khan, Neutrosophic Laplace Distribution with Properties and Applications in Decision Making, International Journal of Neutrosophic Science, 23(1), 2024
25. H. Y. A. Shihabeldeen and Z. Khan, Neutrosophic Structure of the Log-logistic Model with Applications to Medical Data, International Journal of Neutrosophic Science, vol. 23, no. 1, 2024.
26. F. Smarandache et al., Introduction to neutrosophy and neutrosophic environment, Neutrosophic Set in Medical Image Analysis, pp. 3–29, 2019.
27. World bank data (https://data.worldbank.org/)
28. Khan, Z., Gulistan, M., Chammam, W., Kadry, S., & Nam, Y. A new dispersion control chart for handling neutrosophic data. IEEE Access, 8, 96006-96015, 2020.

Received: April 26, 2024. Accepted: August 25, 2024.

Neutrosophic Sets and Systems, Vol. 72, 2024
University of New Mexico

Hybrid Neutrosophic Deep Learning Model for Enhanced Arabic Handwriting Recognition

Mohamed G. Mahdi[1, 2, *], Ahmed Sleem[3], Ibrahim M. Elhenawy[4], Soha Safwat[5]

[1] Department of Information Technology, Faculty of Information Technology and Computer Science, Sinai University, Qantara Branch., Ismailia, Egypt (mohamedgresha@hotmail.com)
[2] Department of Computer Science, Faculty of Computers and Informatics, Zagazig University, Zagazig, Sharqiyah, Egypt (m.gresha@fci.zu.edu.eg)
[3] Department of Computer Science, Faculty of Computers and Informatics, Tanta University, Tanta, Egypt (Ahmed.selim@ics.tanta.edu.eg)
[4] Department of Computer Science, Faculty of Computers and Informatics, Zagazig University, Zagazig, Sharqiyah, Egypt (ielhenawy@zu.edu.eg)
[5] Department of Computer Science, Faculty of Computers and Information Systems, Egyptian Chinese University, Cairo, Egypt (ssafwat@ecu.edu.eg)
* Correspondence: m.gresha@fci.zu.edu.eg ; mohamedgresha@hotmail.com

Abstract: Recognizing handwritten Arabic characters poses a significant challenge due to the complexities of the cursive script and the visual similarities between characters. While deep learning techniques have shown substantial promise, advancements in model architectures are essential to further enhance performance. Neutrosophic Sets (NS) have demonstrated their potential in improving classification models by effectively handling indeterminate and inconsistent data. This paper introduces a novel approach that integrates Neutrosophic Sets with a hybrid deep learning model, combining Convolutional Neural Networks (CNNs) with Bidirectional Recurrent Neural Networks (Bi-LSTM and Bi-GRU). This integration allows for the extraction of spatial features and modeling of temporal dynamics in handwritten Arabic text. Experiments conducted on the Hijjaa and AHCD datasets revealed that the NS_CNN_Bi-LSTM model achieved an accuracy of 92.38% on the Hijjaa dataset, while the NS_CNN_Bi-GRU model attained 97.38% accuracy on the AHCD dataset, outperforming previous deep learning approaches. These results highlight the significant performance improvements achieved through advanced temporal modeling and contextual representation, without the need for explicit segmentation. The findings contribute to the ongoing development of highly accurate and sophisticated deep learning systems for Arabic handwriting recognition, with broad applications in areas requiring efficient extraction of text from handwritten documents.

Keywords: Handwritten Character Recognition; Deep Learning; Arabic Natural Language Processing; Optical Character Recognition; Neutrosophic Sets.

1. Introduction

Handwriting recognition, a key area within Optical Character Recognition (OCR), is crucial in various sectors like industry, education, government, and healthcare. Arabic handwriting recognition, in particular, is a challenging but promising research area due to its complex, cursive nature and the variability in individual handwriting styles [1,2]. Despite these challenges, recent advancements have improved the accuracy of Arabic handwriting recognition systems.

Deep learning, particularly through Recurrent Neural Networks (RNNs) and Long Short-Term Memory (LSTM) networks, has revolutionized handwriting recognition. RNNs, despite initial training difficulties, benefit from LSTM networks that handle contextual information better. To address challenges in offline handwriting recognition, images can be converted into 1D sequences and processed bidirectionally with LSTM networks. Integrating Convolutional Neural Networks

(CNNs) with RNNs has further enhanced the ability to recognize and process handwritten characters effectively [3].

Neutrosophic Sets (NS) and Neutrosophic Numbers (NN) provide a robust mathematical framework, finding applications in various fields, including Decision-Making, Image Processing, and Information Systems. These frameworks are particularly relevant in contexts involving indeterminate, inconsistent, or incomplete information [4–9]. By extending classical and fuzzy set theories to include the indeterminacy component, neutrosophic sets offer a flexible, generalized tool that more accurately reflects the complexities of real-world scenarios, making them particularly useful where traditional approaches may be inadequate.

This study aims to develop an advanced system for offline Arabic handwriting recognition by harnessing the capabilities of CNNs, Bidirectional Long Short-Term Memory (Bi-LSTM) networks, and Bidirectional Gated Recurrent Units (Bi-GRU), while also incorporating Neutrosophic Sets (NS) and Neutrosophic Numbers (NN) into existing models. The proposed system is specifically engineered to tackle the unique challenges inherent in Arabic handwriting recognition.

The primary contributions of this research are as follows:

- Examination of Neutrosophic Sets and Neutrosophic Numbers, including their applications across different domains.
- Development and implementation of innovative novel models designed to enhance recognition accuracy.
- Evaluation and comparison of the proposed models with state-of-the-art approaches and previous studies.

The paper is structured as follows: Section 2 presents a comprehensive survey of the current advancements in Arabic handwriting recognition. Section 3 provides an overview of Neutrosophic Sets and Neutrosophic Numbers. Section 4 outlines the details of our proposed system. In Section 5, we report the results of our experiments. Section 6 offers an in-depth discussion and a systematic evaluation of the system's performance. Section 7 summarizes our key findings and suggests potential avenues for future research. Finally, Section 8 revisits and elaborates on these proposed directions for future investigation in this field.

2. Related work

This research represents the first application of Neutrosophic Sets and Neutrosophic Numbers in the field of Recognition of Handwritten Arabic Characters. Consequently, this section is divided into two parts: The first part reviews a thorough examination of the existing literature, encompassing a wide range of methodologies that utilize machine learning and deep learning techniques for the Recognition of Handwritten Arabic Characters. The second part examines the latest research on Neutrosophic Sets and Neutrosophic Numbers with a focus on Image Classification. The reviewed studies primarily focus on introducing various approaches to tackle this challenging task.

2.1. Recognition of Handwritten Arabic Characters

In 2017, El-Sawy et al. [10] presented a novel CNN model that was trained and tested using their proprietary dataset called AHCD. The dataset consisted of 16,800 handwritten Arabic characters from 60 individuals aged 19 to 40, divided into 28 classes. Their model achieved an impressive accuracy of 94.9% on this dataset.

In a 2020 study conducted by Altwaijry et al. [11], the focus shifted towards recognizing Arabic letters in children's handwriting. The researchers created a special dataset called Hijja, consisting of 47,434 distinct and linked Arabic characters written by youngsters aged 7 to 12. They developed a CNN-based model to assess its performance on the dataset. A comparison was made with the model proposed by El-Sawy [10] using both the Hijja and AHCD datasets. The experimental findings demonstrated that their model outperformed the compared model, achieving accuracy rates of 88% and 97% on the Hijja and AHCD datasets, respectively.

Nayef et al. [12] presented a study focusing on CNN models for recognizing handwritten Arabic characters while incorporating an improved Leaky-ReLU activation function. Four datasets were used to evaluate their models: AHCD, HIJJA, MNIST, and their own dataset containing 38,100 handwritten Arabic characters. The proposed CNN model, employing Leaky-ReLU optimization, surpassed the model mentioned in [12], achieving accuracy rates of 99%, 95%, and 90% on AHCD, the researchers' dataset, and Hijja, respectively.

2.2. Neutrosophic in Image Classification

In recent years, Neutrosophic has attracted considerable attention within the scientific community. In [13], the authors proposed a membership-based neutrosophic approach for supervised fingerprint image classification. The model applies neutrosophic logic to handle uncertainty in fingerprint features, enhancing classification accuracy. The study evaluated the approach using standard datasets and reported improved performance compared to traditional techniques. The method effectively handled noise and ambiguous data, proving its robustness for fingerprint image analysis.

Elatawy et al.[14] developed a system to recognize alphabet Arabic sign language using neutrosophic techniques and fuzzy c-means. The system enhances input images with a Gaussian filter, then converts them to a neutrosophic domain for feature extraction. This leads to the classification of corresponding letters, with a reported accuracy of 91%. The combination of neutrosophic image processing and fuzzy clustering effectively improves sign language recognition accuracy.

In 2023, the authors proposed a deep learning model combining Neutrosophic and CNN for image and text classification. They used a neutrosophic approach to preprocess input data, enhancing feature extraction and noise reduction. The model was evaluated on multiple datasets and achieved notable improvements in accuracy compared to traditional methods. Data augmentation techniques, such as rotation and flipping, were applied to improve generalization. The authors also experimented with various optimizers, with the Adam optimizer showing the best results. Their model demonstrated its robustness in handling complex classification tasks[4].

3. Neutrosophic Sets and Neutrosophic Numbers

Neutrosophic Sets (NS), introduced by Florentin Smarandache in 1998[15], represent a significant extension of classical set theory and fuzzy set theory. The core idea behind neutrosophic sets is to handle the uncertainty, imprecision, incompleteness, and inconsistency that often arise in real-world situations. While classical set theory strictly dichotomizes elements into members and non-members, and fuzzy set theory introduces the notion of partial membership, neutrosophic sets allow for a more nuanced representation by incorporating three independent components: truth-membership (T), indeterminacy-membership (I), and falsity-membership (F)[15–17].

3.1. Formal Definition of Neutrosophic Sets

A Neutrosophic Set (NS) can be characterized as a three-part structure:

- T: The degree of truth.
- I: The degree of indeterminacy.
- F: The degree of falsity.

Each element in the neutrosophic set is represented by a triplet $x(T, I, F)$. And Formally, a Neutrosophic Set A in a universe of discourse U is defined as:

$$A = \{\langle x, T_A(x), I_A(x), F_A(x)\rangle : x \in U\}, \quad (1)$$

where:

- $T(x) \in [0,1]$ is the truth-membership degree of the element x.
- $I(x) \in [0,1]$ is the indeterminacy-membership degree of x.

- $F(x) \in [0,1]$ is the falsity-membership degree of x.

Unlike in Fuzzy Sets, where $T_A(x) + F_A(x) = 1$, Neutrosophic Sets allow the sum $T_A(x) + I_A(x) + F_A(x)$ to take any value in the real number space, thus offering flexibility in modeling situations where the information is incomplete or conflicting.

For example, if we consider an element x in a Neutrosophic Set A, the membership degrees might be:

$$T_A(x) = 0.6, I_A(x) = 0.3, F_A(x) = 0.2$$

In this case, $T_A(x) + I_A(x) + F_A(x) = 1.1$, indicating that the sum of the three components is not necessarily constrained to 1, unlike in classical or Fuzzy Sets. This ability to model indeterminacy $I_A(x)$ independently of the truth $T_A(x)$ and falsity $F_A(x)$ components make Neutrosophic Sets particularly powerful in contexts where uncertainty is a dominant factor.

Building on the concept of Neutrosophic Sets, Neutrosophic Numbers (NN) have been developed to represent uncertain quantities in mathematical and engineering contexts. A Neutrosophic Number N is defined as a triplet:

$$N = \langle T_N, I_N, F_N \rangle, \quad (2)$$

where T_N , I_N , and F_N are the truth, indeterminacy, and falsity components, respectively. These components are often intervals or real numbers, reflecting the uncertainty and vagueness associated with the quantity.

Neutrosophic Numbers can be used in Arithmetic Operations, Decision-Making processes, and various Engineering Applications where conventional numbers fail to capture the complexity of the situation.

3.2. Types of Neutrosophic Sets

There are several variations of neutrosophic sets, designed to capture different aspects of uncertainty:

3.2.1. Single-Valued Neutrosophic Sets (SVNS)

A **Single-Valued Neutrosophic Set (SVNS)** is an extension of the traditional Fuzzy Set, designed to handle uncertainty, vagueness, and indeterminacy[18]. Each element x in a Neutrosophic Set is characterized by three independent membership functions:

- **Truth Membership** $T(x)$, which measures the degree of truth.
- **Indeterminacy Membership** $I(x)$, which quantifies the level of indeterminacy or uncertainty about the element's membership.
- **Falsity Membership** $F(x)$, which measures the degree of falsity.

Mathematically, for a given element x, we have:

$$T(x), I(x), F(x) \in [0,1], \quad (3)$$

These values represent the truth, indeterminacy, and falsity respectively, with the constraint:

$$0 \leq T(x) + I(x) + F(x) \leq 3, \quad (4)$$

An SVNS provides a flexible way to express uncertainty in data, where each of the three values reflects different aspects of the element's membership in the set. SVNS are especially useful in problems like Image Processing, Decision-Making, and Classification, where managing imprecise or noisy data is crucial.

3.2.2. Interval-Valued Neutrosophic Sets (IVNS)

Interval-Valued Neutrosophic Sets (IVNS) further extend the SVNS by allowing the membership functions—truth, indeterminacy, and falsity—to take interval values instead of single

values. This reflects greater uncertainty, as each membership is now an interval rather than a precise number[19].

For an element x, the truth membership $T(x)$, indeterminacy membership $I(x)$, and falsity membership $F(x)$ are intervals defined as:

$$T(x) \in [T_{\min}, T_{\max}],\ I(x) \in [I_{\min}, I_{\max}],\ F(x) \in [F_{\min}, F_{\max}], \tag{5}$$

with the condition that:

$$T_{\min}, I_{\min}, F_{\min} \geq 0,\ T_{\max}, I_{\max}, F_{\max} \leq 1, \tag{6}$$

and:

$$0 \leq T_{\max} + I_{\max} + F_{\max} \leq 3, \tag{7}$$

This representation allows the model to capture a range of possible values for each membership, reflecting uncertainty or variability in the data more effectively than a single value. IVNS are useful in cases where the data itself is inherently imprecise, such as Expert Decision-Making with vague or uncertain information.

3.2.3. Multi-Valued Neutrosophic Sets

In **Multi-Valued Neutrosophic Sets**, the membership values for truth, indeterminacy, and falsity are drawn from a discrete set rather than a continuous interval[20]. For an element $\boldsymbol{x}$, we have:

$$T(x) \in \{t_1, t_2, \dots, t_n\},\ I(x) \in \{i_1, i_2, \dots, i_m\},\ F(x) \in \{f_1, f_2, \dots, f_p\}, \tag{8}$$

where $\boldsymbol{t_i}$, $\boldsymbol{i_j}$, and $\boldsymbol{f_k}$ are discrete values typically chosen from a finite set of real numbers. This framework is appropriate for problems where the degree of truth, falsity, and indeterminacy must take on specific predefined values rather than being continuous. For instance, multi-valued neutrosophic sets are useful in Logical Systems or Decision Models where categorical values are required.

3.2.4. Generalized Neutrosophic Sets

Generalized Neutrosophic Sets extend the neutrosophic model by allowing the truth, indeterminacy, and falsity membership functions to take values outside the traditional interval [0, 1] [21]. For an element x, the memberships are defined as:

$$T(x), I(x), F(x) \in \mathbb{R}, \quad \text{with no restrictions,} \tag{9}$$

This type of set allows membership values to exceed 1 or be negative, which can represent extreme certainty or extreme falsity, respectively. Generalized Neutrosophic Sets are more abstract and are used in cases where a wider range of membership values is necessary, often in philosophical or highly theoretical applications.

3.2.5. Refined Neutrosophic Sets

Refined Neutrosophic Sets provide a more granular view of the truth, indeterminacy, and falsity memberships by dividing each of these components into sub-components[22]. For example, truth membership could be refined into positive truth and negative truth, capturing more subtle nuances of the element's relationship with the set. For an element $\boldsymbol{x}$, the truth membership could be defined as:

$$\boldsymbol{T(x) = T_1(x) + T_2(x)},\ \text{where}\ \ \boldsymbol{T_1(x)}\ \text{is positive truth, and}\ \boldsymbol{T_2(x)}\ \text{is negative truth.}, \tag{10}$$

This allows for a more detailed representation of uncertainty and is useful in complex Decision-Making problems where the fine-grained nature of the data is important.

In summary, **SVNS** are simpler and computationally efficient but less flexible in representing complex uncertainty compared to **IVNS**, **Generalized**, or **Refined Neutrosophic Sets**, which provide more nuanced and detailed representations of uncertainty at the cost of computational complexity.

4. Research Methodology

In this research, we employ the most utilized strategies and techniques, specifically in the field of NLP, for Arabic Recognition of Handwritten Characters. We present and discuss these strategies, methods, and their implementation plan in the research, supported by links on GitHub and Kaggle. This is aimed at sharing our findings with researchers worldwide who are interested in this specialization, to support scientific collaboration and validate the results of our research, ensuring that no one can claim the results are inaccurate.

4.1. Datasets Description

For all experiments conducted in this paper, we utilized publicly available datasets comprising of Hijjaa Data set, Arabic Handwritten Characters Data set (AHCD).

The Hijjaa dataset[1], created by Saudi Arabian schoolchildren [11], comprises 47,434 images of 108 Arabic letters in various word positions. Despite initial issues with letter placement and alignment, the dataset was resized to 32x32 pixels, balanced for letter representation, and organized into 29 folders without vocalization diacritics. In contrast, the Arabic Handwritten Characters Dataset[2] (AHCD) includes 16,800 characters written by 60 participants, scanned at 300 dpi, and divided into training and test sets [10]. The AHCD dataset's pre-processing involved converting images to grayscale and applying filters to handle variations in writing styles and character shapes.

4.2. Proposed Models

The final models represent a sophisticated Deep Learning model architecture designed to incorporate Neutrosophic Logic principles into a CNNs structure, followed by a series of (Bi-LSTM/Bi-GRU) layers. The model leverages the unique capabilities of both CNNs and (LSTM/GRU) to capture spatial features and temporal dependencies, making it suitable for complex tasks such as Image Recognition, where uncertainty and imprecision are inherent.

4.2.1. Neutrosophic Transformation and Layer

In neutrosophic image processing, we aim to represent an image in terms of **truth** (T), **indeterminacy** (I), and **falsity** (F), which provide a more nuanced interpretation of image characteristics compared to classical binary or fuzzy representations. Below is a detailed explanation of each step in the conversion of an image into a neutrosophic representation, including the relevant equations.

4.2.1.1. Preprocessing the Input Image

The input is a grayscale image, where pixel values range from 0 to 255. The first step in converting the image into a neutrosophic image involves normalizing these pixel intensities to a scale between 0 and 1. This normalization makes the subsequent calculations easier to handle numerically.

$$N(x,y) = \frac{I(x,y)}{255}, \tag{11}$$

Where:

- $N(x,y)$is the normalized pixel intensity at position (x,y).

[1] https://github.com/israksu/Hijja2

[2] https://www.kaggle.com/datasets/mloey1/ahcd1

- $I(x, y)$ is the original intensity of the pixel at position (x, y), which lies between 0 and 255.

4.2.1.2. Calculation of Local Mean Intensity

To assess the **local intensity** around each pixel, we compute the local mean of pixel values in a neighborhood window (usually a 3x3 or 5x5 window) around the pixel (x, y).

The local mean $\mu(x, y)$ is given by:

$$\mu(x, y) = \frac{1}{|W|} \sum_{(x', y') \in W} N(x', y'), \quad (12)$$

Where:

- $\mu(x, y)$ is the local mean intensity around the pixel (x, y).
- W is the neighborhood window centered around (x, y).
- $|W|$ is the number of pixels in the neighborhood window.

4.2.1.3. Calculation of Local Standard Deviation

Next, we compute the **local standard deviation** $\sigma(x, y)$ in the same neighborhood. The local standard deviation measures the variation in pixel intensities within the neighborhood window. It provides insight into how homogeneous or inhomogeneous the local region is.

$$\sigma(x, y) = \sqrt{\frac{1}{|W|} \sum_{(x', y') \in W} (N(x', y') - \mu(x, y))^2}, \quad (13)$$

Where:

- $\sigma(x, y)$ is the local standard deviation at pixel (x, y).
- $\mu(x, y)$ is the local mean intensity computed in Step 2.
- W is the neighborhood window.

4.2.1.4. Calculation of Truth Membership (T)

The **truth membership** (T) evaluates how similar the intensity of a pixel is to its surrounding neighborhood. A pixel whose intensity is close to the local mean will have a high truth value, indicating that it likely belongs to the background or a homogenous region.

The truth membership is defined as:

$$T(x, y) = \frac{N(x,y) - min(N)}{max(N) - min(N)}, \quad (14)$$

Where:

- $T(x, y)$ is the truth membership of the pixel at position (x, y).
- $N(x, y)$ is the normalized intensity of the pixel.
- $min(N)$ and $max(N)$ are the minimum and maximum intensity values in the neighborhood window W.

This normalization ensures that truth values are scaled between 0 and 1.

4.2.1.5. **Calculation of Indeterminacy Membership** (I)

The **indeterminacy membership** (I) quantifies the uncertainty associated with a pixel's intensity. In regions where there is high variance in intensity (e.g., edges or noisy areas), the indeterminacy will be high.

The indeterminacy membership is calculated using the local standard deviation:

$$I(x,y) = 1 - \exp\left(-\frac{\sigma(x,y)^2}{2}\right), \quad (15)$$

Where:

- $I(x,y)$ is the indeterminacy membership of the pixel at position (x,y).
- $\sigma(x,y)$ is the local standard deviation calculated in Step 3.

This formula ensures that indeterminacy increases as the standard deviation (and hence the local variation in pixel intensities) increases.

4.2.1.6. **Calculation of Falsity Membership** (F)

The **falsity membership** (F) is the complement of the truth membership. It indicates how different a pixel's intensity is from its neighbors, potentially identifying regions that do not belong to the background or homogeneous areas.

$$F(x,y) = 1 - T(x,y), \quad (16)$$

Where:

- $F(x,y)$ is the falsity membership of the pixel at position (x,y).
- $T(x,y)$ is the truth membership calculated in Step 4.

4.2.1.7. **Construction of the Neutrosophic Image**

Finally, the image is represented in a **Neutrosophic Set** by combining the truth (T), indeterminacy (I), and falsity (F) memberships for each pixel. Thus, each pixel in the image is represented as a triplet $(\boldsymbol{T}, \boldsymbol{I}, \boldsymbol{F})$, where:

- $T(x,y)$ captures how similar the pixel is to the local region.
- $I(x,y)$ captures the uncertainty or indeterminacy about the pixel.
- $F(x,y)$ captures how different the pixel is from the local region.

Final Output

The output is a **Neutrosophic Image**, where each pixel is represented as:

$$\text{Neutrosophic Image} = \{(T(x,y), I(x,y), F(x,y)) \mid x,y \in \text{Image Dimensions}\}, \quad (17)$$

This representation provides more information than classical pixel intensities by accounting for local homogeneity (truth), uncertainty (indeterminacy), and differences (falsity) within the image.

This step-by-step process allows for a comprehensive analysis of the image in terms of local features and uncertainties, making it a powerful tool for image processing tasks such as denoising, edge detection, and segmentation.

4.2.2. Convolutional Layers

Next, the model employs multiple convolutional layers to extract spatial features from the transformed input. Convolutional layers apply filters to the input tensor to detect local patterns such as edges or textures, which are crucial for understanding image content. Each convolutional operation can be represented as:

$$X_{\text{conv}}^{(l)} = \sigma(W^{(l)} * X_{\text{conv}}^{(l-1)} + b^{(l)}), \quad (18)$$

where $X_{\text{conv}}^{(l)}$ is the output of the l-th convolutional layer, $W^{(l)}$ are the filters, $*$ denotes the convolution operation, $b^{(l)}$ is the bias term, and σ is an activation function, typically ReLU.

MaxPooling layers follow some convolutional layers, downsampling the feature maps to reduce computational complexity and to focus on the most prominent features. Batch normalization is applied to stabilize and accelerate training by normalizing the input to each layer, ensuring that it has a mean of zero and a standard deviation of one.

4.2.3. Reshaping and Bidirectional recurrent neural network Layers

After the convolutional layers, the 3D tensor X_{conv} is reshaped to a 2D tensor in preparation for the GRU layers. Specifically, the tensor is reshaped from dimensions (H', W', C') to $(H' \times W', C')$, where $H' \times W'$ is treated as the sequence length, and C' represents the features at each timestep. This operation is mathematically described as:

$$X_{\text{reshape}} = \text{Reshape}(X_{\text{conv}}) = (H' \times W', C'), \tag{19}$$

4.2.3.1. Bi-LSTM

The Bi-LSTM layers then process this reshaped tensor. LSTMs (Long Short-Term Memory networks) are a type of Recurrent Neural Network (RNN) that can capture temporal dependencies by maintaining a hidden state that evolves over the sequence while also incorporating mechanisms to learn when to forget or remember certain information. The bidirectional nature of the LSTM means that it processes the input sequence in both forward and backward directions, capturing context from both past and future states. The output from each LSTM layer is:

$$H_t^{\text{Bi-LSTM}} = \text{LSTM}_{\text{fwd}}(X_{\text{reshape},t}) \oplus \text{LSTM}_{\text{bwd}}(X_{\text{reshape},t}), \tag{20}$$

where $\oplus$ denotes concatenation, LSTM_{fwd} and LSTM_{bwd} are the forward and backward LSTMs, and $\boldsymbol{H_t^{\text{Bi-LSTM}}}$ is the hidden state at time step $\boldsymbol{t}$.

4.2.3.2. Bi-GRU

The Bi-GRU layers then process this reshaped tensor. GRUs are a type of Recurrent Neural Network (RNN) that can capture temporal dependencies by maintaining a hidden state that evolves over the sequence. The bidirectional nature of the GRU means that it processes the input sequence in both forward and backward directions, capturing context from both past and future states. The output from each GRU layer is:

$$H_t^{\text{Bi-GRU}} = \text{GRU}_{\text{fwd}}(X_{\text{reshape},t}) \oplus \text{GRU}_{\text{bwd}}(X_{\text{reshape},t}), \tag{21}$$

where $\oplus$ denotes concatenation, GRU_{fwd} and GRU_{bwd} are the forward and backward GRUs, and $\boldsymbol{H_t^{\text{Bi-GRU}}}$ is the hidden state at time step $\boldsymbol{t}$.

4.2.3. Fully Connected Layers and Output

Finally, the output of the last RNN layer is flattened into a vector and passed through several dense (fully connected) layers. These layers perform non-linear transformations on the high-level features extracted by the convolutional and RNN layers, enabling the model to make predictions. The final layer applies a SoftMax activation function to produce a probability distribution over the target classes:

$$\hat{y} = \text{SoftMax}(W_{\text{out}} X_{\text{dense}} + b_{\text{out}}), \tag{22}$$

where $\hat{y}$ is the predicted output, W_{out} and b_{out} are the weights and bias of the output layer, and X_{dense} is the output of the last dense layer.

This architecture allows the model to capture both the spatial features and temporal dependencies in the data while explicitly accounting for uncertainty through neutrosophic logic. This

makes it particularly well-suited for complex tasks such as image recognition in environments where data uncertainty is a significant factor.

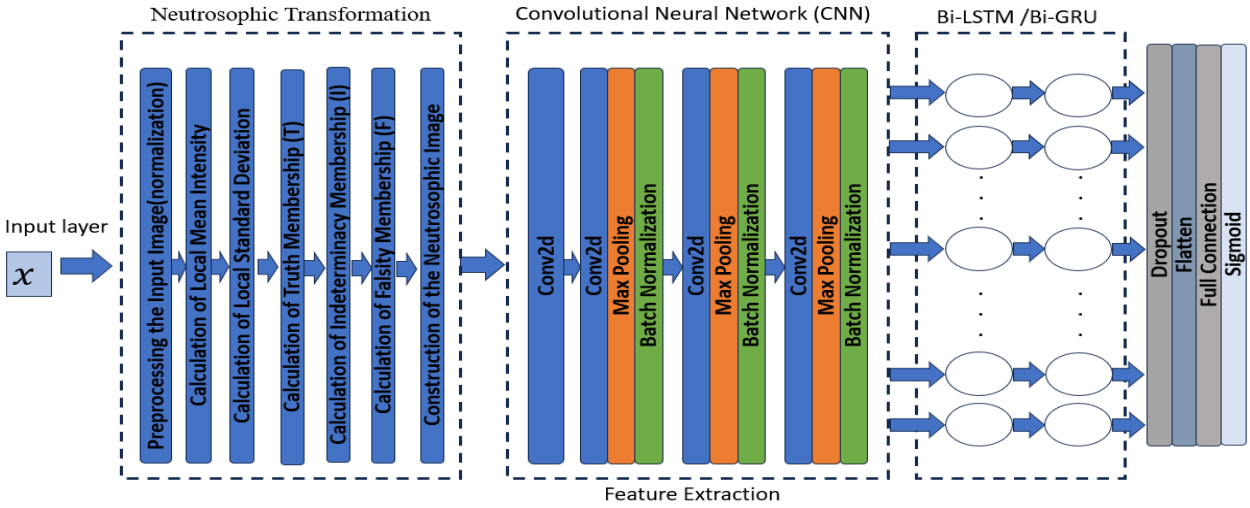

Figure 1. NS_CNN_Bi-LSTM/Bi-GRU architecture.

5. Experiments

5.1. Evaluation Phase

These evaluation metrics are employed to assess and compare the performance of classification models. Precision, recall, and F1-score provide insights into specific characteristics, such as the balance between True Positives (TP), True Negatives (TN), False Positives (FP), and False Negatives (FN), while accuracy offers a general performance overview. When interpreting and applying these metrics, it is essential to consider the problem's specific requirements and context.

1- Accuracy:

$$\textbf{Accuracy} = \frac{TP + TN}{TP + FP + FN + TN} \tag{23}$$

2- Recall:

$$\textbf{Recall} = \frac{TP}{TP + FN} \tag{24}$$

3- Precision:

$$\textbf{Precision} = \frac{TP}{TP + FP} \tag{25}$$

4- F1-score:

$$\textbf{F1} - \textbf{score} = \frac{2(\text{Recall} * \text{ Precision})}{\text{Recall} + \text{Precision}} \tag{26}$$

5.2. Experimental Setup

We conducted experiments in the Kaggle environment using a Dell G5 15 laptop, featuring an 8th generation Intel Core i7 processor with a base frequency of 2.20 GHz and a maximum frequency of 2.21 GHz. The system is equipped with an NVIDIA GeForce GTX graphics card (6 GB VRAM) and 16 GB of RAM, with settings adjusted to utilize NVIDIA TESLA P100 GPUs for all trials. While some

processes, such as those involving Pandas and Scikit-learn libraries, do not benefit from GPU acceleration, these GPUs are highly advantageous for training deep learning models.

5.3. Experimental Design

In this study, The models were compiled with a categorical cross-entropy loss function and the Adam optimizer, with accuracy as the evaluation metric. The training process involved a dataset of images and their corresponding labels. For training, a batch size of 128 was used, and the model underwent 200 epochs of training to learn from the data. A separate validation dataset, comprising images and their corresponding labels, was used to evaluate the model's capacity to generalize to previously unseen data. During training, the model's weights were adjusted according to the loss function and optimizer to minimize the loss and enhance prediction accuracy. To ensure robust performance and avoid overfitting, the validation data was continuously monitored, allowing for adjustments to the training process as needed.

6. Results and Discussion

In this study, we proposed four novel deep learning models, **CNN_Bi-LSTM, CNN_Bi-GRU, NS_CNN_Bi-LSTM, and NS_CNN_Bi-GRU**, for the task of Arabic handwritten character recognition. Our research aimed to utilize existing deep learning techniques and enhance the accuracy of Arabic handwriting recognition. To evaluate the performance of our proposed models, we utilized two datasets: AHCD and Hijjaa.

In Experiment 1, the performance of four models—CNN_Bi-LSTM, CNN_Bi-GRU, NS_CNN_Bi-LSTM, and NS_CNN_Bi-GRU—was tested on the AHCD dataset. The NS_CNN_Bi-GRU model outperformed all others, achieving 97.38% accuracy on the testing set and 99.90% on the training set, with the lowest loss values (0.0034 for training and 0.2364 for testing). High training accuracies (ranging from 99.37% to 99.99%) indicate strong learning capabilities across all models, with the NS-enhanced versions performing slightly better. Test accuracies and loss metrics further confirmed the NS_CNN_Bi-GRU's superior generalization to unseen data, highlighting the impact of the NS component in improving model performance.

The models maintained consistently high macro and weighted averages for precision, recall, and F1-scores (0.96 to 0.97), demonstrating balanced performance across all character classes. Characters like ج ,ب ,ا, and س had near-perfect F1-scores, while a few, including ر ,ذ ,ت, and ظ, showed slightly lower F1-scores (0.92 to 0.96), likely due to structural similarities. Overall, the NS-enhanced models, particularly NS_CNN_Bi-GRU, exhibited better accuracy and lower losses, suggesting that GRU units may be more effective than LSTM units in character recognition tasks.

In Experiment 2, the proposed models were tested on the Hijjaa dataset, with the NS_CNN_Bi-LSTM model outperforming all others. It achieved a 92.38% accuracy on the testing set and 99.38% on the training set. The NS_CNN_Bi-LSTM also recorded the lowest loss value of 0.0206 during training, with a test loss of 0.5159, indicating its strong performance. Comparatively, CNN_Bi-LSTM, CNN_Bi-GRU, and NS_CNN_Bi-GRU had slightly lower test accuracies (ranging from 90.23% to 91.78%) and higher loss values, reflecting stable but slightly inferior generalization compared to NS_CNN_Bi-LSTM.

Class-wise, characters such as ش ,ا, and ي consistently achieved high F1-scores, indicating the models' strong ability to recognize these characters. However, characters like ذ ,د, and ء proved more challenging, particularly for CNN_Bi-LSTM and CNN_Bi-GRU models. The NS-enhanced models, especially NS_CNN_Bi-LSTM, demonstrated better performance in recognizing these difficult characters. Across all models, macro and weighted average precision, recall, and F1-scores hovered around 0.90, with NS_CNN_Bi-LSTM showing a marginally better balance and higher overall averages, suggesting its superiority in handling diverse character classes.

In summary, the results show that integrating the NS component with CNN and Bidirectional Recurrent Layers (LSTM/GRU) significantly enhances the accuracy and reduces the loss of models

for Arabic handwritten character recognition across different datasets. The NS_CNN_Bi-GRU model performs best on the AHCD dataset, achieving a strong balance between accuracy and loss, while the NS_CNN_Bi-LSTM model stands out on the Hijjaa dataset with superior accuracy and lower loss during both training and testing. Overall, the NS-enhanced models demonstrate robust performance, especially in handling difficult character classes, proving to be valuable in advancing the field of Arabic handwritten character recognition.

Table 1. The results of proposed Models on AHCD Dataset.

Model		**CNN_Bi-LSTM**			**CNN_Bi-GRU**			**NS_CNN_Bi-LSTM**			**NS_CNN_Bi-GRU**		
Char.	**Class #**	**Precision**	**Recall**	**F1-score**	**Precision**	**Recall**	**F1-score**	**Precision**	**Recall**	**F1-score**	**Precision**	**Recall**	**F1-score**
ا	1	0.98	0.99	0.98	0.98	0.99	0.99	0.95	1	0.98	1	0.99	1
ب	2	0.98	0.98	0.98	1	0.99	1	1	0.97	0.99	0.98	0.98	0.98
ت	3	0.91	0.93	0.92	0.91	0.97	0.94	0.94	0.98	0.96	0.97	0.94	0.95
ث	4	0.93	0.95	0.94	0.96	0.97	0.97	0.97	0.98	0.98	0.98	0.99	0.98
ج	5	0.98	0.95	0.97	0.99	0.97	0.98	1	0.98	0.99	1	0.99	1
ح	6	0.94	0.98	0.96	0.94	0.99	0.97	0.94	0.97	0.96	0.94	1	0.97
خ	7	0.95	0.97	0.96	1	0.97	0.98	0.94	0.94	0.94	0.99	0.95	0.97
د	8	0.92	0.97	0.95	0.94	0.96	0.95	0.97	0.97	0.97	0.93	0.95	0.94
ذ	9	0.94	0.94	0.94	0.97	0.9	0.94	0.97	0.97	0.97	0.97	0.95	0.96
ر	10	0.97	0.94	0.95	0.91	0.99	0.95	0.94	0.99	0.97	0.91	0.98	0.95
ز	11	0.97	0.91	0.94	0.97	0.94	0.96	0.99	0.93	0.96	0.98	0.93	0.96
س	12	0.99	0.98	0.99	0.98	0.98	0.98	1	0.98	0.99	0.95	1	0.98
ش	13	0.99	0.97	0.98	0.98	0.98	0.98	0.98	0.98	0.98	0.99	0.99	0.99
ص	14	0.97	0.98	0.98	0.94	0.99	0.97	0.96	0.98	0.97	0.98	0.98	0.98
ض	15	0.96	0.97	0.96	0.99	0.93	0.96	0.99	0.93	0.96	1	0.97	0.98
ط	16	0.94	0.98	0.96	0.94	0.99	0.96	0.94	0.99	0.96	0.94	1	0.97
ظ	17	0.97	0.95	0.96	0.99	0.94	0.97	0.98	0.93	0.95	1	0.94	0.97
ع	18	0.98	0.93	0.96	0.99	0.99	0.99	0.96	0.97	0.97	0.99	0.97	0.98
غ	19	0.98	0.95	0.97	1	1	1	0.97	0.97	0.97	0.99	0.98	0.99
ف	20	0.93	0.97	0.95	0.94	0.97	0.96	0.94	0.98	0.96	0.97	0.97	0.97
ق	21	0.97	0.94	0.95	0.97	0.94	0.96	0.98	0.96	0.97	0.97	0.96	0.97
ك	22	0.94	0.97	0.95	1	0.95	0.97	0.99	0.98	0.99	0.98	0.97	0.97
ل	23	0.99	0.99	0.99	0.99	0.99	0.99	0.99	1	1	0.99	0.99	0.99
م	24	0.97	0.98	0.98	0.97	1	0.98	0.99	0.97	0.98	0.98	0.99	0.99
ن	25	0.96	0.9	0.93	0.97	0.93	0.95	0.99	0.94	0.97	0.94	0.96	0.95
ه	26	0.99	0.97	0.98	0.98	0.97	0.97	0.97	0.98	0.98	0.97	0.97	0.97
و	27	0.96	0.97	0.96	0.96	0.96	0.96	0.97	0.97	0.97	0.97	0.97	0.97
ي	28	0.97	0.97	0.97	0.99	1	1	0.99	0.98	0.99	1	0.99	1
Accuracy (train)				0.9937			0.9978			0.9999			**0.999**
Accuracy (test)				0.9616			0.9705			0.9714			**0.9738**

Loss (train)			0.023			0.0058			**0.0034**			0.0046
Loss (test)			0.2369			0.2495			**0.2364**			0.2406
Macro avg	0.96	0.96	0.96	0.97	0.97	0.97	0.97	0.97	0.97	0.97	0.97	0.97
Weighted avg	0.96	0.96	0.96	0.97	0.97	0.97	0.97	0.97	0.97	0.97	0.97	0.97

Table 2. The results of proposed Models on Hijjaa Dataset.

Model		**CNN_Bi-LSTM**			**CNN_Bi-GRU**			**NS_CNN_Bi-LSTM**			**NS_CNN_Bi-GRU**		
Char.	**Class #**	**Precision**	**Recall**	**F1-score**	**Precision**	**Recall**	**F1-score**	**Precision**	**Recall**	**F1-score**	**Precision**	**Recall**	**F1-score**
ا	1	0.99	0.98	0.98	0.99	0.98	0.98	0.99	0.99	0.99	0.99	0.96	0.98
ب	2	0.93	0.97	0.95	0.92	0.95	0.94	0.93	0.94	0.93	0.94	0.94	0.94
ت	3	0.84	0.93	0.88	0.9	0.89	0.9	0.91	0.89	0.9	0.86	0.88	0.87
ث	4	0.94	0.86	0.9	0.93	0.91	0.92	0.93	0.92	0.92	0.9	0.88	0.89
ج	5	0.96	0.91	0.94	0.95	0.93	0.94	0.95	0.94	0.95	0.91	0.94	0.92
ح	6	0.85	0.89	0.87	0.84	0.9	0.87	0.88	0.89	0.89	0.85	0.84	0.84
خ	7	0.91	0.87	0.89	0.87	0.91	0.89	0.89	0.91	0.9	0.89	0.88	0.88
د	8	0.77	0.77	0.77	0.8	0.74	0.77	0.78	0.72	0.75	0.83	0.71	0.77
ذ	9	0.71	0.75	0.73	0.8	0.73	0.76	0.83	0.72	0.77	0.84	0.73	0.78
ر	10	0.87	0.89	0.88	0.86	0.91	0.88	0.95	0.88	0.91	0.88	0.89	0.89
ز	11	0.93	0.88	0.9	0.89	0.89	0.89	0.89	0.91	0.9	0.9	0.94	0.92
س	12	0.93	0.98	0.96	0.95	0.95	0.95	0.97	0.92	0.94	0.94	0.92	0.93
ش	13	0.96	0.94	0.95	0.98	0.94	0.96	0.98	0.96	0.97	0.96	0.96	0.96
ص	14	0.93	0.86	0.89	0.91	0.9	0.9	0.85	0.94	0.9	0.83	0.9	0.86
ض	15	0.95	0.87	0.91	0.92	0.9	0.91	0.91	0.91	0.91	0.92	0.86	0.89
ط	16	0.93	0.93	0.93	0.9	0.94	0.92	0.92	0.93	0.92	0.88	0.92	0.9
ظ	17	0.95	0.94	0.94	0.97	0.9	0.93	0.96	0.93	0.94	0.93	0.91	0.92
ع	18	0.81	0.88	0.84	0.88	0.85	0.87	0.86	0.9	0.88	0.81	0.84	0.82
غ	19	0.88	0.87	0.87	0.91	0.84	0.87	0.91	0.89	0.9	0.92	0.82	0.87
ف	20	0.83	0.87	0.85	0.83	0.87	0.85	0.85	0.87	0.86	0.78	0.87	0.82
ق	21	0.91	0.9	0.9	0.94	0.9	0.92	0.95	0.89	0.92	0.85	0.92	0.88
ك	22	0.87	0.91	0.89	0.91	0.89	0.9	0.92	0.92	0.92	0.9	0.89	0.9
ل	23	0.9	0.93	0.91	0.89	0.91	0.9	0.88	0.94	0.91	0.91	0.91	0.91
م	24	0.92	0.95	0.93	0.88	0.96	0.92	0.93	0.94	0.94	0.89	0.89	0.89
ن	25	0.8	0.86	0.83	0.78	0.88	0.82	0.83	0.89	0.86	0.85	0.81	0.83
ه	26	0.94	0.88	0.91	0.91	0.87	0.89	0.89	0.94	0.91	0.87	0.89	0.88
و	27	0.96	0.9	0.93	0.94	0.91	0.92	0.97	0.9	0.93	0.91	0.93	0.92
ي	28	0.96	0.94	0.95	0.93	0.93	0.93	0.95	0.95	0.95	0.94	0.93	0.93
ء	29	0.9	0.85	0.87	0.87	0.85	0.86	0.9	0.86	0.88	0.83	0.87	0.85
Accuracy (train)				0.9883			0.9911			**0.9938**			0.9666
Accuracy (test)				0.9178			0.9023			**0.9238**			0.9064

Loss (train)			0.0369			0.0273			**0.0206**			0.0935
Loss (test)			**0.4983**			0.5281			0.5801			0.5159
Macro avg	0.9	0.89	0.9	0.9	0.89	0.9	0.92	0.91	0.91	0.89	0.88	0.88
Weighted avg	0.9	0.9	0.9	0.9	0.9	0.9	0.92	0.92	0.92	0.89	0.89	0.89

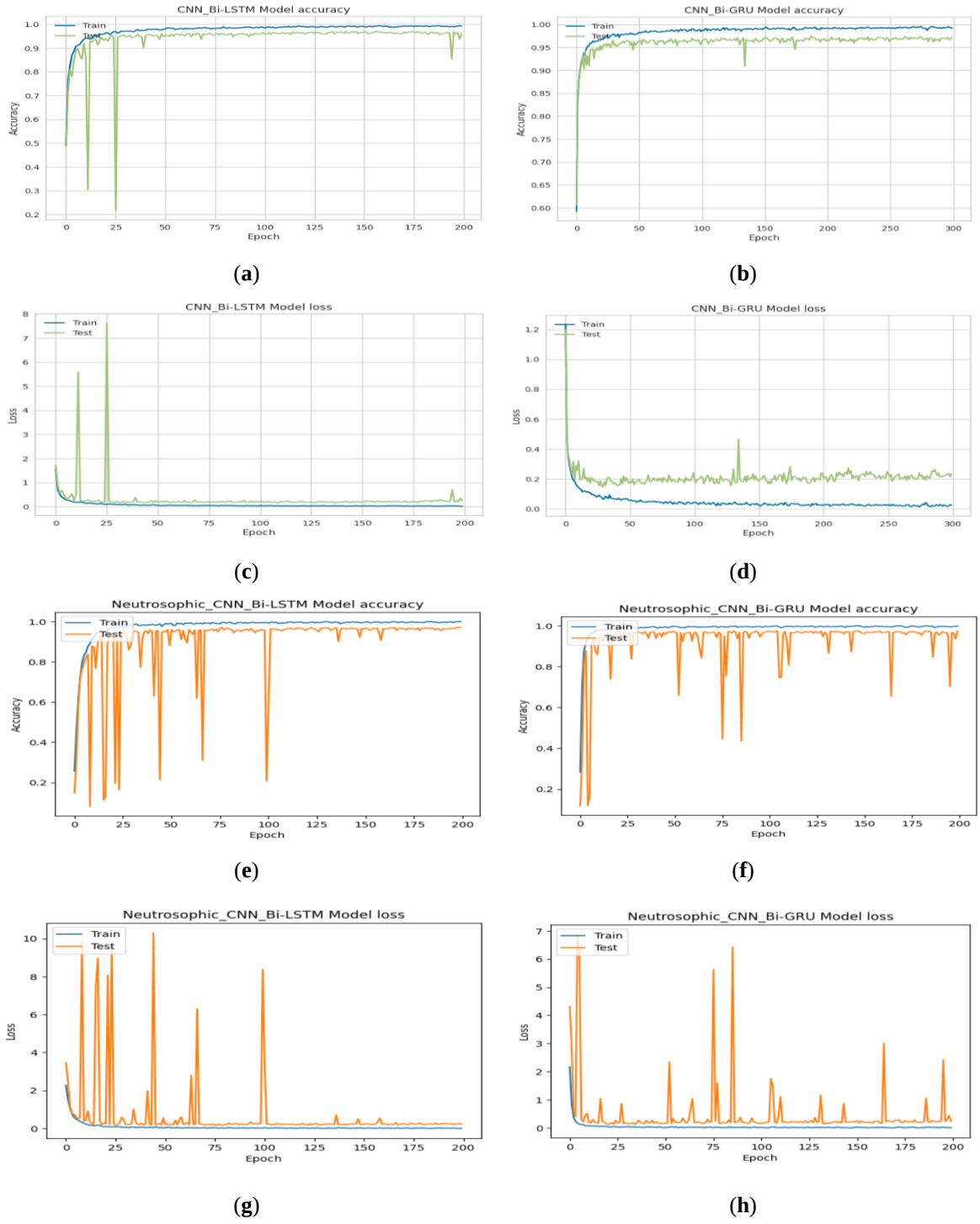

Figure 2. Model performance on the AHCL dataset: (a) Accuracy curves for CNN_Bi-LSTM during training and testing; (b) Accuracy curves for CNN_Bi-GRU during training and testing; (c) Loss curves for CNN_Bi-LSTM during

training and testing; (d) Loss curves for CNN_Bi-GRU during training and testing; (e) Accuracy curves for NS_CNN_Bi-LSTM during training and testing; (f) Accuracy curves for NS_CNN_Bi-GRU during training and testing; (g) Loss curves for NS_CNN_Bi-LSTM during training and testing; (h) Loss curves for NS_CNN_Bi-GRU during training and testing.

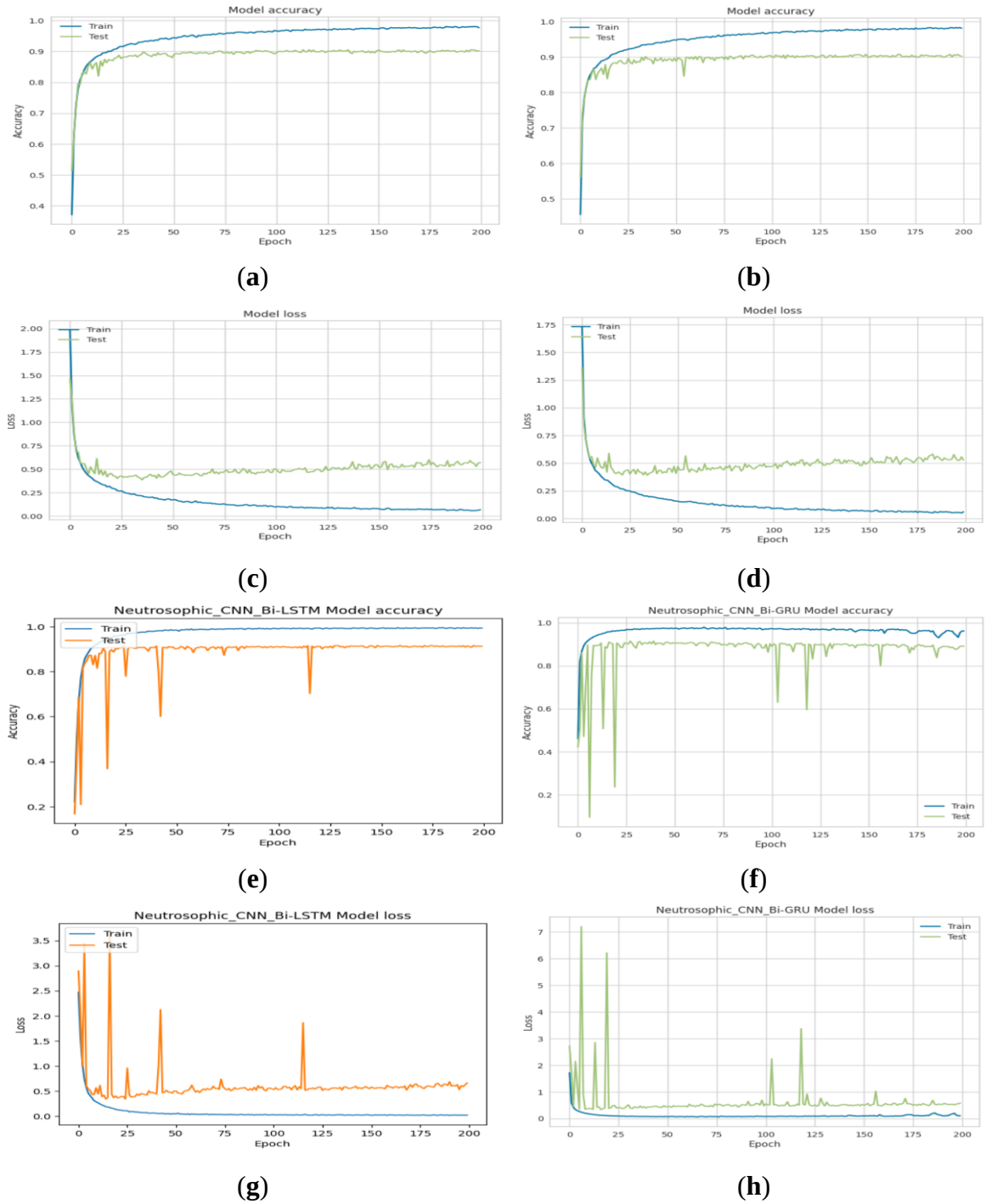

Figure 3. Model performance on the Hijjaa dataset: (a) Accuracy curves for CNN_Bi-LSTM during training and testing; (b) Accuracy curves for CNN_Bi-GRU during training and testing; (c) Loss curves for CNN_Bi-LSTM during

training and testing; (d) Loss curves for CNN_Bi-GRU during training and testing; (e) Accuracy curves for NS_CNN_Bi-LSTM during training and testing; (f) Accuracy curves for NS_CNN_Bi-GRU during training and testing; (g) Loss curves for NS_CNN_Bi-LSTM during training and testing; (h) Loss curves for NS_CNN_Bi-GRU during training and testing.

Table 3 compares the performance of the proposed CNN_Bi-LSTM, CNN_Bi-GRU, NS_CNN_Bi-LSTM, and NS_CNN_Bi-GRU models with other models in the literature on the Hijjaa and AHCD datasets. The NS_CNN_Bi-LSTM model achieves the highest accuracy on the Hijjaa dataset, with 99.38% during training and 92.38% on testing, outperforming most existing models. Similarly, the NS_CNN_Bi-GRU model excels on the AHCD dataset, achieving 99.90% training accuracy and 97.38% testing accuracy, demonstrating its superiority in both datasets. These models consistently deliver strong precision, recall, and F1-scores, making them highly effective for Arabic handwritten character recognition tasks.

Table 3. Performance comparison with models from the literature

References	Datasets		Accuracy	Precision	Recall	F1-Score
Altwaijry et al. [11]	Hijjaa		88%	88%	88%	88%
Nayef et al., [12]	Hijjaa		90%	-	-	-
Bin Durayhim et al. [23]	Hijjaa	Train	99.5%	99%	99%	99%
		Test	86.3%	85%	86%	85%
M.G. Mahdi et al. (LSTM[24]	Hijjaa	Train	96.2%	96%	96%	96%
		Test	84.6%	85%	84%	84%
M.G. Mahdi et al. (GRU)[24]	Hijjaa	Train	92.7%	92%	92%	92%
		Test	81.5%	82%	81%	81%
M.G. Mahdi et al. (Bi-LSTM) [24]	Hijjaa	Train	98.3%	98%	98%	98%
		Test	85%	85%	84%	84%
M.G. Mahdi et al. (Bi-GRU) [24]	Hijjaa	Train	97.3%	97%	97%	97%
		Test	84.6%	85%	85%	85%
CNN_Bi-LSTM	Hijjaa	Train	98.83%	98%	98%	98%
		Test	91.78%	91%	91%	91%
CNN_Bi-GRU	Hijjaa	Train	99.11%	99%	99%	99%
		Test	90.23%	90%	90%	90%
Proposed NS_CNN_Bi-LSTM	Hijjaa	Train	**99.38**	**99%**	**99%**	**99%**
		Test	**92.38%**	**92%**	**92%**	**92%**
Proposed NS_CNN_Bi-GRU	Hijjaa	Train	96.66%	96%	96%	96%
		Test	90.64%	90%	90%	90%
Altwaijry et al. [11]	AHCD		97%	97%	97%	97%
El-Sawy et al. [10]	AHCD		94.9%	-	-	-
Nayef et al., [12]	AHCD		99%	-	-	-
Bin Durayhim et al. [23]	AHCD	Train	98%	99%	99%	99%
		Test	95.5%	95%	95%	95%
M.G. Mahdi et al. (LSTM[24]	AHCD	Train	99.7%	99%	99%	99%

M.G. Mahdi et al. (GRU)[24]	AHCD	Test	94.9%	95%	95%	95%
		Train	99.8%	99%	99%	99%
		Test	93.1%	93%	93%	93%
M.G. Mahdi et al. (Bi-LSTM) [24]	AHCD	Train	99.8%	99%	99%	99%
		Test	94.9%	95%	95%	95%
M.G. Mahdi et al. (Bi-GRU) [24]	AHCD	Train	99.9%	99%	99%	99%
		Test	95.7%	96%	96%	96%
CNN_Bi-LSTM	AHCD	Train	99.37%	99%	99%	99%
		Test	96.16%	96%	96%	96%
CNN_Bi-GRU	AHCD	Train	99.78%	99%	99%	99%
		Test	97.05%	97%	97%	97%
Proposed NS_CNN_Bi-LSTM	AHCD	Train	99.99%	99%	99%	99%
		Test	97.14%	97%	97%	97%
Proposed NS_CNN_Bi-GRU	AHCD	Train	**99.9%**	**99%**	**99%**	**99%**
		Test	**97.38%**	**97%**	**97%**	**97%**

7. Conclusions

This research article introduces and evaluates two new deep learning models for Arabic handwriting recognition: CNN_Bi-LSTM and CNN_Bi-GRU. Additionally, the models were enhanced by integrating Neutrosophic sets (NS), resulting in two more models: NS_CNN_Bi-LSTM and NS_CNN_Bi-GRU. The models were designed to classify Arabic letters into 28 and 29 classes, with evaluations conducted using two datasets: AHCD and Hijjaa. The performance of the four models was compared among themselves and against existing methods in the literature.

The experimental results demonstrate the effectiveness of the proposed hybrid deep learning models in Arabic handwriting recognition. The NS_CNN_Bi-GRU model achieved a state-of-the-art accuracy of 97.38% on the AHCD dataset, while the NS_CNN_Bi-LSTM model reached 92.38% accuracy on the Hijjaa dataset, surpassing previous techniques. These results underscore the advantage of combining convolutional and bidirectional recurrent networks for capturing both spatial and temporal features in Arabic handwriting.

8. Limitation and Future work

The limitations of this research include the need for further improvements in the recognition accuracy of the hybrid models, particularly when handling noisy or complex Arabic handwriting. The models were only tested on two datasets (AHCD and Hijjaa), limiting the understanding of their generalization across more diverse datasets or real-world applications. Additionally, the focus was on overall accuracy, with little analysis of errors, failure cases, or the interpretability of the models' decisions.

To address these limitations, future research should explore alternative architectures, such as attention mechanisms or transformers, to enhance accuracy and robustness. More detailed component analysis, advanced data augmentation techniques, and evaluations on broader datasets could improve generalization. Real-world application testing in document processing and transfer learning to other languages or handwriting styles should also be considered. Efforts to optimize computational efficiency, model size, and inference speed would enable deployment in resource-constrained environments. Enhancing interpretability and expanding the scope to other Arabic language processing tasks could further extend the models' practical utility.

Conflicts of Interest: The author declares that they have no conflict of interest.

Funding: This research received no external funding.

Code Availability Statement: The implementation used in this article were be in GitHub. For details, please refer to https://github.com/MohamedGresha/deep-learning-methods-on-Optical-Character-Recognition-Arabic-text/tree/main .

References

1. Alghyaline, S. Arabic Optical Character Recognition: A Review. *CMES - Computer Modeling in Engineering and Sciences* 2023, *135*, 1825–1861.
2. Mahdi, M.G.; Sleem, A.; Elhenawy, I. Deep Learning Algorithms for Arabic Optical Character Recognition: A Survey. *Multicriteria Algorithms with Applications* **2024**, *2*, 65–79, doi:10.61356/J.MAWA.2024.26861.
3. Ghanim, T.M.; Khalil, M.I.; Abbas, H.M. Comparative Study on Deep Convolution Neural Networks DCNN-Based Offline Arabic Handwriting Recognition. *IEEE Access* **2020**, *8*, 95465–95482, doi:10.1109/ACCESS.2020.2994290.
4. Wajid, M.A.; Zafar, A.; Wajid, M.S. A Deep Learning Approach for Image and Text Classification Using Neutrosophy. *International Journal of Information Technology* **2024**, *16*, 853–859, doi:10.1007/s41870-023-01529-8.
5. Alanazi, A.A.; Abaker, A.O.I.; Abdel-Khalek, S.; Alhomayani, F.M.; Aripov, M. Neutrosophic Logic Empowered Machine Learning Algorithm with Salp Swarm Optimization for Biomedical Image Analysis. *International Journal of Neutrosophic Science* **2024**, *23*, 104–116, doi:10.54216/IJNS.230408.
6. Hassen, O.A.; Mashhadani, S.; Alhakam, I.; Darwish, S.M. A New Paradigm for Decision Making under Uncertainty in Signature Forensics Applications Based on Neutrosophic Rule Engine. *International Journal of Neutrosophic Science* **2024**, *24*, 267–282, doi:10.54216/IJNS.240224.
7. Ebtesam, E.; Al-Mansor, E. Al Leveraging Bat Algorithm with Rough Neutrosophic Soft Set for Enhanced Oral Cancer Detection and Classification. *International Journal of Neutrosophic Science* **2024**, *24*, 71–81, doi:10.54216/IJNS.240405.
8. A., A.; Sugapriya, P.; .. D.; .. S.S.; .. K.; Irudayam, F.N. Enhanced Brain Tumor Diagnosis Through Differential and Canonical Quadri –Partitioned Neutrosophic Set Classification Methods:A Comparative Study. *International Journal of Neutrosophic Science* **2024**, *24*, 277–292, doi:10.54216/IJNS.240420.
9. Straub, J.; Mohammed, H.; Kabir, D.; Alam, S.B.; Mondal, S.K.; Al-Saidi, M.; Ballagi, Á.; Hassen, O.A.; Saad, S.M. Cognitive Classifier of Hand Gesture Images for Automated Sign Language Recognition: Soft Robot Assistance Based on Neutrosophic Markov Chain Paradigm. *Computers 2024, Vol. 13, Page 106* **2024**, *13*, 106, doi:10.3390/COMPUTERS13040106.
10. El-Sawy, A.; Loey, M.; El-Bakry, H. Arabic Handwritten Characters Recognition Using Convolutional Neural Network. *WSEAS Transactions on Computer Research* **2017**, *5*, 11–19.

11. Altwaijry, N.; Al-Turaiki, I. Arabic Handwriting Recognition System Using Convolutional Neural Network. *Neural Comput Appl* **2021**, *33*, 2249–2261, doi:10.1007/s00521-020-05070-8.
12. Nayef, B.H.; Abdullah, S.N.H.S.; Sulaiman, R.; Alyasseri, Z.A.A. Optimized Leaky ReLU for Handwritten Arabic Character Recognition Using Convolution Neural Networks. *Multimed Tools Appl* **2022**, *81*, 2065–2094, doi:10.1007/s11042-021-11593-6.
13. Vinoth, D.; Devarasan, E. A Membership Based Neutrosophic Approach for Supervised Fingerprint Image Classification. *Neutrosophic Sets and Systems* **2023**, *60*, 420–445, doi:10.5281/ZENODO.10224226.
14. Elatawy, S.M.; Hawa, D.M.; Ewees, A.A.; Saad, A.M. Recognition System for Alphabet Arabic Sign Language Using Neutrosophic and Fuzzy C-Means. *Educ Inf Technol (Dordr)* **2020**, *25*, 5601–5616, doi:10.1007/S10639-020-10184-6/TABLES/3.
15. Smarandache, F. *Neutrosophy: Neutrosophic Probability, Set, and Logic: Analytic Synthesis & Synthetic Analysis*; American Research Press, 1998;
16. Ali, M.; Smarandache, F.; Vladareanu, L. Neutrosophic Sets and Logic. In *Emerging Research on Applied Fuzzy Sets and Intuitionistic Fuzzy Matrices*; Adak, A.K., Manna, D., Bhowmik, M., Eds.; IGI Global: Hershey, PA, USA, 2017; pp. 18–63 ISBN 9781522509141.
17. Zhang, X.; Li, M.; Lei, T. On Neutrosophic Crisp Sets and Neutrosophic Crisp Mathematical Morphology. *Neutrosophic Sets and Systems* **2021**, *43*, 1–11.
18. Borah, G.; Dutta, P. Fuzzy Risk Analysis in Crop Selection Using Information Measures on Quadripartitioned Single-Valued Neutrosophic Sets. *Expert Syst Appl* **2024**, *255*, 124750, doi:https://doi.org/10.1016/j.eswa.2024.124750.
19. Khatun, M.; Basu, T.M.; Manna, S.; Mondal, S.K. Extended Dombi–Hamy Mean Operator and Gaussian Likelihood-Based Ranking Approach for Solving MCDM Problems in Interval-Valued Neutrosophic Environment. *Expert Syst Appl* **2024**, *253*, 124272, doi:https://doi.org/10.1016/j.eswa.2024.124272.
20. Mahmood, A.; Abbas, M.; Murtaza, G. Multi-Valued Multi-Polar Neutrosophic Sets with an Application in Multi-Criteria Decision-Making. *Neutrosophic Sets and Systems* **2023**, *53*, 530–561, doi:10.5281/ZENODO.7536084.
21. Al-Hijjawi, S.; Ahmad, A.G.; Alkhazaleh, S.; Al-Hijjawi, S.; Ahmad, A.G.; Alkhazaleh, S. A Generalized Effective Neurosophic Soft Set and Its Applications. *AIMS Mathematics 2023 12:29628* **2023**, *18*, 29628–29666, doi:10.3934/MATH.20231517.
22. Sharma, M.; Kandasamy, I.; Vasantha, W.B. Emotion Quantification and Classification Using the Neutrosophic Approach to Deep Learning. *Appl Soft Comput* **2023**, *148*, 110896, doi:10.1016/J.ASOC.2023.110896.

23. Bin Durayhim, A.; Al-Ajlan, A.; Al-Turaiki, I.; Altwaijry, N. Towards Accurate Children's Arabic Handwriting Recognition via Deep Learning. *Applied Sciences 2023, Vol. 13, Page 1692* **2023**, *13*, 1692, doi:10.3390/APP13031692.
24. Mahdi, M.G.; Sleem, A.; Elhenawy, I.; Safwat, S. Advancing Arabic Handwriting Recognition with Convolutional and Recurrent Neural Network Ensembles. *Information Sciences with Applications* **2024**, *3*, 43–63, doi:10.61356/J.ISWA.2024.3294.

Received: May 10, 2024. Accepted: Sep 13, 2024.

Neutrosophic Sets and Systems (NSS) is an academic journal, published quarterly online and on paper, that has been created for publications of advanced studies in neutrosophy, neutrosophic set, neutrosophic logic, neutrosophic probability, neutrosophic statistics etc. and their applications in any field.

All submitted papers should be professional, in good English, containing a brief review of a problem and obtained results.

It is an open access journal distributed under the Creative Commons Attribution License that permits unrestricted use, distribution, and reproduction in any medium, provided the original work is properly cited.

ISSN (print): 2331-6055, ISSN (online): 2331-608X
Impact Factor: 1.739

NSS has been accepted by SCOPUS. Starting with Vol. 19, 2018, all NSS articles are indexed in Scopus.

NSS is also indexed by Google Scholar, Google Plus, Google Books, EBSCO, Cengage Thompson Gale (USA), Cengage Learning, ProQuest, Amazon Kindle, DOAJ (Sweden), University Grants Commission (UGC) - India, International Society for Research Activity (ISRA), Scientific Index Services (SIS), Academic Research Index (ResearchBib), Index Copernicus (European Union),CNKI (Tongfang Knowledge Network Technology Co., Beijing, China), etc.

Google Dictionary has translated the neologisms "neutrosophy" (1) and "neutrosophic" (2), coined in 1995 for the first time, into about 100 languages.

FOLDOC Dictionary of Computing (1, 2), Webster Dictionary (1, 2), Wordnik (1), Dictionary.com, The Free Dictionary (1),Wiktionary (2), YourDictionary (1, 2), OneLook Dictionary (1, 2), Dictionary / Thesaurus (1), Online Medical Dictionary (1, 2), and Encyclopedia (1, 2) have included these scientific neologisms.

DOI numbers are assigned to all published articles.

Registered by the Library of Congress, Washington DC, United States, https://lccn.loc.gov/2013203857.

Recently, NSS was also approved for Emerging Sources Citation Index (ESCI) available on the Web of Science platform, starting with Vol. 15, 2017.

Editors-in-Chief:

Prof. Dr. Florentin Smarandache, Postdoc, Department of Mathematics, University of New Mexico, Gallup, NM 87301, USA, Email: smarand@unm.edu.
Dr. Mohamed Abdel-Basset, Faculty of Computers and Informatics, Zagazig University, Egypt, Email: mohamed.abdelbasset@fci.zu.edu.eg.
Dr. Said Broumi, Laboratory of Information Processing, Faculty of Science Ben M'Sik, University of Hassan II, Casablanca, Morocco, Email: s.broumi@flbenmsik.ma.

23316055

$39.95